



<https://theses.gla.ac.uk/>

Theses Digitisation:

<https://www.gla.ac.uk/myglasgow/research/enlighten/theses/digitisation/>

This is a digitised version of the original print thesis.

Copyright and moral rights for this work are retained by the author

A copy can be downloaded for personal non-commercial research or study,
without prior permission or charge

This work cannot be reproduced or quoted extensively from without first
obtaining permission in writing from the author

The content must not be changed in any way or sold commercially in any
format or medium without the formal permission of the author

When referring to this work, full bibliographic details including the author,
title, awarding institution and date of the thesis must be given

Enlighten: Theses

<https://theses.gla.ac.uk/>
research-enlighten@glasgow.ac.uk

**THE WEATHERING OF SANDSTONE ON
HISTORIC BUILDINGS: CULZEAN
CASTLE, A CASE STUDY**

A thesis submitted for the degree of Doctor of Philosophy

© **Carolyn Susan Hayles**

Bsc Hons. Keele University, England

Department of Geology & Applied Geology
University of Glasgow

November 1998

ProQuest Number: 10904954

All rights reserved

INFORMATION TO ALL USERS

The quality of this reproduction is dependent upon the quality of the copy submitted.

In the unlikely event that the author did not send a complete manuscript and there are missing pages, these will be noted. Also, if material had to be removed, a note will indicate the deletion.



ProQuest 10904954

Published by ProQuest LLC (2018). Copyright of the Dissertation is held by the Author.

All rights reserved.

This work is protected against unauthorized copying under Title 17, United States Code
Microform Edition © ProQuest LLC.

ProQuest LLC.
789 East Eisenhower Parkway
P.O. Box 1346
Ann Arbor, MI 48106 – 1346

GLASGOW
UNIVERSITY
LIBRARY

11609

(copy 1)

Acknowledgements

This research project was funded by the Getty Grant Programme under the supervision of the National Trust for Scotland.

I would like to thank the following people for their assistance, support and encouragement during the completion of this thesis:

- staff, technicians and students in the Department of Geology & Applied Geology, Glasgow University ;
- staff at Culzean Castle and the National Trust for Scotland;
- staff at the Department of Civil Engineering, University of Paisley;
- my Colleagues at the Building Research Establishment Scotlab & Garston;
- the Department of Earth Sciences, University of Keele;
- the Department of Agricultural Chemistry, University of Glasgow; and
- the Department of Civil Engineering, Napier University .

To my friends and family who have motivated and comforted me throughout.

Thank you.

Abstract

Culzean Castle is located 45 miles south of Glasgow on the West Coast of Scotland. It is a fine example of the work of architect Robert Adam. The castle is currently owned by the National Trust for Scotland, and is one of Scotland's most popular tourist attractions. The stonework has suffered through prolonged exposure in the castle's cliff-top position overlooking the Firth of Clyde. As a result some of the stonework was replaced in the 1970s, and current with this research, more stonework needs to be replaced.

The castle was constructed from local sandstones, specifically volcanigenic lithic arenites (quartz-rich sandstones containing feldspars, lithic fragments, clays and micas, cemented together with calcium carbonate).

Culzean was built during three periods using local stone. The original Late-Medieval castle was constructed from what has proved to be 'durable sandstone' (OB) which shows little evidence of deterioration in its more sheltered location as the foundations of the current building.

During the eighteenth century, Robert Adam designed additions to the castle using another local sandstone (AB). This stone has undergone considerable deterioration (e.g. spalling, contour scaling and surface pitting), and in some instances has failed, with surface material falling from the building. The majority of the AB stones, particularly on the Drum Tower balcony need to be cut back or replaced right away.

Finally during the late 1800s a west wing was added to the castle, of redder sandstone from Maybole (VB), which currently exhibits some surface deterioration (mainly contour scaling), but not on the same scale as the AB stone.

Research was undertaken to examine the differences between these stones, particularly to determine the characteristics of the AB stone which allow it to weather more rapidly than the others.

Cores samples of 75 mm diameter, 150 mm depth were taken from the building using a dry drilling method to prevent chemical alteration. A number of analytical techniques including ion chromatography, x-ray fluorescence, x-ray diffraction, scanning electron microscopy and cathodoluminescence microscopy were used to examine the geochemistry and mineralogy of the stone. The role of externally derived soluble salts and the potential for physical change were then determined.

Petrographic analysis highlighted a number of characteristic processes. The rock forming minerals, specifically the quartz, feldspars and micas showed similar mechanisms of deterioration in the three sandstones. These mechanisms

included dissolution, particularly along lines of weakness and compositional variation, with ionic exchange at mineral edges.

Clay minerals were found in abundance in the Culzean sandstones. Of greatest importance were the clays which absorb water, found in the AB stones (combinations of illite/smectite/chlorite species) which with access to ingressing solution and under confining pressures are particularly destructive for their size. There was also evidence for calcium carbonate cement dissolution and reprecipitation.

The pore structure of the stones was of fundamental importance, as interconnecting pore channels increased permeability. The AB samples were found to have micro-porosity ($< 5\mu$), created by cement and mineral dissolution, and interconnecting pore-space structures.

Geochemical analysis identified the presence of soluble salts in the stone. Halite, gypsum and thenardite were present in abundance, particularly the AB samples. The occurrence of soluble salts at depth in the stone provided important information on the composition of the solutions driven into the stone at Culzean and the depths to which they could penetrate according to porosity and permeability. It also highlighted the presence of moisture at depth allowing salt crystallisation/hydration cycles and chemical reactions to take place.

Analysis of the bulk chemistry of these three stones showed that overall the chemical make-up of each individual stone sampled was complicated and unique. There was no evidence for greater movement of specific elements through the stone profiles of the Adam's building stone when compared with the other two. Such was the natural chemical variation found in each of the stone profiles examined.

The roles of temperature and humidity, controlling all aspects of moisture movement within the stone were also examined. These factors affected the ability of the stone to dry out and thus where the zone of maximum moisture content was situated and consequently where soluble salt crystallisation/hydration was heightened.

There was surface evaporation of the exterior of the stone, behind which a wetting/drying zone allowed soluble salts to crystallise/dissolve. This salt crystallisation/solution zone moved in and out of the stone at depths of 10 – 40 mm, the zone of maximum moisture content. This resulted in the breakdown of the stone as its exterior surface spalled by the action of contour scaling.

The results of this investigation have been used to produce a model for stone decay controlled by the ingress of salts in solution into the stone, and the ineffectual drying out of the stone.

Abbreviations

Listed below are abbreviations used in the text.

AA	Atomic Absorption
AB	Adam's Building Stone
AE	Atomic Emission
BGS	British Geological Survey
BRE	Building Research Establishment
BSE	Back Scattered Electrons
CL	Cathodoluminescence Microscopy
HPLC	High Performance Liquid Chromatography (<i>bidistilled water</i>)
IC	Ion Chromatography
LORS	Lower Old Red Sandstone
NTS	National Trust for Scotland
OB	Original Building Stone
OQ	Original Quarry Stone
ORS	Old Red Sandstone
OS	Ordnance Survey
PC	Point Counting
PPL	Plain Polarised Light
PPM	Parts Per Million
REE	Rare Earth Elements
RGU	Robert Gordon University
SEM	Scanning Electron Microscopy
VB	Victorian Building Stone
VQ	Victorian Quarry Stone
XPL	Crossed Polarised Light
XRD	X-ray Diffraction
XRF	X-ray Fluorescence

Table of Contents

Title Page	i
Declaration	ii
Acknowledgements	iii
Abstract	iv
Abbreviations	vi
Table of Contents	vii
List of Figures	xii
List of Tables	xvi

Chapter One: Introduction

1.1 Rationale for project	1
1.1.1 Aims and Objectives	1
1.1.2 Thesis Structure.....	3
1.2 The Culzean Problem.....	6
1.2.1 Culzean in its historical context.....	6
1.2.2 Geological and geographical location.....	7
1.2.3 Responses to weathering problem.....	9
1.3 Building stone as a material	12
1.3.1 Classification of building stones.....	12
1.3.2 Sandstones.....	15
1.3.3 Sedimentary rocks as building stone.....	17
1.4 Basic principles of weathering and factors involved	19
1.4.1 Introduction to the weathering processes.....	19
1.4.2 Physical weathering	19
1.4.3 Chemical weathering.....	21
1.4.4 Organic processes.....	23
1.5 Stone decay	24
1.6 An overview of weathering research.....	25
1.6.1 Introduction to weathering research.....	26
1.6.2 Weathering processes and products	29
1.6.3 Salt weathering.....	29
1.6.4 Clay	35
1.6.5 Weathering simulation	37
1.6.6 Applied weathering studies	40
1.6.7 Soluble salts and building stone decay	41
1.6.8 Air pollution.....	44
1.6.9 Cleaning	51
1.6.10 Microbiology.....	52
1.7 Weathering models.....	54
1.8 Factors influencing the decay of sandstone at Culzean	61

Table of Contents continued

Chapter Two: Fieldwork investigations and sampling	
2.1	Sampling 63
2.2	Sampling strategy 64
2.2.1	Constraints to adopting a statistically valid sampling scheme 64
2.2.2	Adopted strategy 66
2.3	Sampling method 67
2.4	The recording of weathering features 68
2.4.1	Classification methods 68
2.4.2	Classification of weathering patterns at Culzean 70
2.5	Sites on the building sampled and their state of decay 72
2.5.1	Adam's Balcony - stone from the Drum Tower 72
2.5.2	The west wing of the castle constructed in 1879 75
2.5.3	Original Building -The Late Medieval foundations of the 13 th C 77
2.6	The Quarries and their Locations 77
2.6.1	The Ballochnie Quarry 78
2.6.2	The Quarry used in 1879: St Murray's, Maybole 80
2.6.3	Home Farm, Culzean Estate 82
2.7	Sampling summary 84
Chapter Three: Analytical methods	
3.1	Introduction to analytical methods 86
3.2	Investigative strategy for laboratory work 86
3.2.1	Previous Work 86
3.2.2	Proposed analysis of the Culzean Stone 88
3.3	Sub-sampling methodology 89
3.4	Instrumentation 90
3.4.1	XRD techniques 91
3.4.2	Scanning Electron and Cathodoluminescence Microscopy 94
3.4.3	Optical Microscopy - Point counting 98
3.4.4	X-ray Fluorescence 99
3.4.5	Ion Chromatography 103
3.4.6	Atomic Absorption and Emission Spectrophotometry 106

Table of Contents continued

Chapter Four: The properties of the Culzean stones	
4.1 Introduction.....	109
4.2 Physical characteristics of sandstone.....	111
4.3 The ORS and characterisation of the stone.....	113
4.4 Mineralogical characteristics of the stones examined.....	116
4.4.1 Building Stone used by Adam between 1777 and 1792 (AB).....	117
4.4.2 The Building Stone of 1879 (VB).....	118
4.4.3 Stone from the quarry used in 1879 (VQ).....	118
4.4.4 Building Stone used in 1200s for the original castle (OB).....	119
4.4.5 Stone from the quarry used in 1200s for the original castle (OQ).....	119
4.5 The alteration of rock forming minerals.....	125
4.5.1 Quartz.....	126
4.5.2 Feldspars.....	127
4.5.3 Lithic fragments.....	128
4.5.4 Micas.....	128
4.5.5 Pore Spaces.....	129
4.5.6 Overview of mineral weathering.....	132
4.6 Clay content composition and distribution.....	133
4.7 Cement composition and distribution.....	138
4.7.1 Carbonate composition.....	138
4.7.2 The pore-infill cement.....	140
4.7.3 Carbonate grains and mineral replacement.....	144
4.7.4 Diagenetic nodules and concretions.....	145
4.8 Soluble salts.....	145
4.8.1 Soluble salts present.....	145
4.8.2 Preliminary profiling of soluble salt content in core samples.....	147
4.8.3 Soluble salt crystallisation, hydration and hygroscopy.....	148
4.9 Engineering Tests.....	149
4.9.1 Dry Mass Density.....	150
4.9.2 Absorption and Porosity.....	150
4.9.3 Sodium Sulphate Test.....	152
4.9.4 Point-Load Strength.....	153
4.10 Conclusions drawn from engineering tests.....	153
4.11 Conclusions drawn from petrographic & mineralogical data.....	154

Table of Contents continued

Chapter Five: Chemical profiling of the Culzean stones	
5.1	Introduction to chemical profiling 157
Section 1	Leaching experiments on stone cores 159
5.2	Anion and cation activity 159
5.2.1	Experimental approach to the leaching of ions 159
5.2.2	Sodium and chloride ions 162
5.2.3	Calcium and sulphate ions 164
5.2.4	Magnesium, potassium and aluminium ions 166
5.2.5	Fluoride, nitrate, nitrite and phosphate ions 167
5.3	Section 1 summary and discussion 168
Section 2	Chemical profiling of stone cores 170
5.4	Chemical weathering and compositional changes 170
5.4.1	The chemical composition of the stone in relation to mineralogy 170
5.4.2	Products of weathering 171
5.5	Chemical profiling of Major elements by XRF and IC 172
5.5.1	AB profiles 175
5.5.2	Summary of cation & anion distribution through AB Profiles 182
5.5.3	Comparisons with VB, VQ, OB & OQ 185
5.5.4	Trace elements 186
5.6	Section 2 summary 189
5.7	Chapter 5 summary 191
Chapter Six: Climate and the effect of temperature and humidity variations	
6.1	Introduction to Chapter 6 194
6.2	Previous research 194
6.3	The climate at Culzean 207
6.4	Temperature & humidity recordings from Culzean stone 209
6.4.1	Surface temperatures 209
6.4.2	Surface and subsurface temperature and humidity 213
6.4.3	Relative humidity and moisture retention 216
6.4.4	Temperature variations 217
6.4.5	Infrared video of the castle and its outbuildings 218
6.5	Summary of temperature, humidity and climate data 219
6.6	Analytical shortcomings 221

Table of Contents continued

Chapter Seven: Discussion, conclusions and recommendations for the future	
7.1 Aims of research and hypotheses tested	223
7.1.1 Research Aims.....	223
7.2 The variations in the character of the three stones.....	225
7.2.1 Adam's building stone	225
7.2.2 Building stone used in 1879 for the west wing.....	228
7.2.3 Original Building Stone	230
7.2.4 Quarry stone used in 1879.....	232
7.2.5 Original Quarry	232
7.2.6 Principal variations between the stones examined.....	232
7.3 The key processes driving the variations examined.....	235
7.3.1 Exogenous Factors: Environment/ Physical processes	235
7.3.2 Endogenous factors: Lithology	236
7.3.3 Key chemical weathering processes.....	236
7.3.4 Summary of chemical weathering processes	241
7.4 Formulation of model.....	243
7.5 Models.....	245
7.5.1 Moisture movement models.....	245
7.5.2 Culzean sandstone models	249
7.5.3 The <i>Egm</i> of the AB sandstone.....	253
7.5.4 The <i>Egm</i> of the OB sandstone.....	255
7.5.5 The <i>Egm</i> of the VB sandstone.....	255
7.6 Recommendations for the future.....	256
References.....	259
Appendices.....	
1 XRF & AA calibration & detection limits and raw data from geochemical analyses	
2 Paper from III International Symposium on the Conservation of Monuments in the Mediterranean Basin	
3 Paper from the 1995 LCP Congress on the Preservation and Restoration of Cultural Heritage	
4 Microbiological examination of sandstone construction material	
Plates.....	back pocket

List of Figures

Chapter One: Introduction

- 1.1 Location map of Scotland to show position of Culzean
- 1.2 Simplified geological map of Ayrshire Coast, Culzean and Maybole
- 1.3 A hypothetical cycle in the degrading of sandstone (after B J Bluck, 1992)
- 1.4 Proposed model for the weathering of sandstone

Chapter Two: Fieldwork investigations and sampling

- 2.1 Culzean Castle from the seaward aspect to show core sample location
- 2.2 Plan of Culzean Castle and coring sites

Chapter Three: Analytical methods

- 3.1 An example of SEM BSE Imaging

Chapter Four: The properties of the Culzean stones

- 4.1 Triangular plot to show compositional variations of AB, VB and OB
 - 4.1.1 Folk (1968)
 - 4.1.2 McBride (1963)
- 4.2 Mineralogical compositional profiles by SEM Atomic Number Contrast Imaging
 - 4.2.1 Compositional variation through AB1
 - 4.2.2 Compositional variation through AB2
 - 4.2.3 Compositional variation through AB3
 - 4.2.4 Compositional variation through AB4
 - 4.2.5 Compositional variation through AB5
 - 4.2.6 Compositional variation through AB6
 - 4.2.7 Compositional variation through AB7
 - 4.2.8 Compositional variation through AB8
 - 4.2.9 Compositional variation through AB9
 - 4.2.10 Compositional variation through AB10
 - 4.2.11 Compositional variation through AB11
 - 4.2.12 Compositional variation through AB12
- 4.3 Mineralogical compositional profiles by SEM Atomic Number Contrast Imaging
 - 4.3.1 Compositional variation through VB1
 - 4.3.2 Compositional variation through VB2
 - 4.3.3 Compositional variation through VB3
 - 4.3.4 Compositional variation through VQ1
 - 4.3.5 Compositional variation through VQ2
 - 4.3.6 Compositional variation through VQ3
- 4.4 Mineralogical compositional profiles by SEM Atomic Number Contrast Imaging
 - 4.4.1 Compositional variation through OB1
 - 4.4.2 Compositional variation through OB2
 - 4.4.3 Compositional variation through OB3
 - 4.4.4 Compositional variation through OQ1
 - 4.4.5 Compositional variation through OQ2
 - 4.4.6 Compositional variation through OQ3

List of Figures Continued

- 4.5 Diagrammatic representation of the succession of layers in some of the clay minerals present in AB, VB, and OB
- 4.6 Graph to show variation in soluble salt and carbonate content by % weight of sample
- 4.7 Graph to show the results from saturated sodium sulphate testing on selected AB, OB and VB samples

Chapter Five: Chemical profiling of the Culzean stones

- 5.1 AA & AE: Results from water extraction experiments
 - 5.1.1 Water extraction of calcium analysed by AA
 - 5.1.2 Water extraction of sodium analysed by AE
 - 5.1.3 Water extraction of potassium analysed by AE
 - 5.1.4 Water extraction of aluminium analysed by AA
 - 5.1.5 Water extraction of magnesium analysed by AA
 - 5.1.6 Water extraction of calcium from VB samples analysed by AA
 - 5.1.7 Water extraction of sodium from VB samples analysed by AE
 - 5.1.8 Water extraction of calcium from OB samples analysed by AA
 - 5.1.9 Water extraction of sodium from OB samples analysed by AE
- 5.2 Ion chromatography: Results from water extraction experiments
 - 5.2.1 Water extraction of chloride analysed by IC
 - 5.2.2 Water extraction of sulphate analysed by IC
 - 5.2.3 Water extraction of fluoride analysed by IC
 - 5.2.4 Water extraction of chloride in VB samples analysed by IC
 - 5.2.5 Water extraction of sulphate in VB samples analysed by IC
 - 5.2.6 Water extraction of chloride in OB samples analysed by IC
 - 5.2.7 Water extraction of sulphate in OB samples analysed by IC
 - 5.2.8 Scatter graph to show the relationship between soluble sodium and chloride
 - 5.2.9 Scatter graph to show the relationship between soluble calcium and sulphate
 - 5.2.10 Scatter graph to show the relationship between soluble sodium + magnesium and chloride
 - 5.2.11 Scatter graph to show the relationship between soluble magnesium and chloride
- 5.3 Ion chromatography: Results for AB core samples
 - 5.3.1 Distribution of chloride through AB1
 - 5.3.2 Distribution of chloride through AB6
 - 5.3.3 Distribution of chloride through AB9
 - 5.3.4 Distribution of chloride through AB12
 - 5.3.5 Distribution of sulphate through AB1
 - 5.3.6 Distribution of sulphate through AB6
 - 5.3.7 Distribution of sulphate through AB9
 - 5.3.8 Distribution of sulphate through AB12
 - 5.3.9 Distribution of fluoride through AB1
 - 5.3.10 Distribution of fluoride through AB6
 - 5.3.11 Distribution of fluoride through AB9
 - 5.3.12 Distribution of fluoride through AB12
 - 5.3.13 Distribution of nitrate through AB1
 - 5.3.14 Distribution of nitrate through AB6

List of Figures Continued

- 5.4 Ion chromatography: Results for OB and OQ core samples
 - 5.4.1 Distribution of sulphate through OB1
 - 5.4.2 Distribution of sulphate through OB3
 - 5.4.3 Distribution of sulphate through OQ1
 - 5.4.4 Distribution of sulphate through OQ2
 - 5.4.5 Distribution of chloride through OB1
 - 5.4.6 Distribution of chloride through OB3
 - 5.4.7 Distribution of chloride through OQ1
 - 5.4.8 Distribution of chloride through OQ2
 - 5.4.9 Distribution of fluoride through OB1
 - 5.4.10 Distribution of fluoride through OB3
 - 5.4.11 Distribution of fluoride through OQ1
 - 5.4.12 Distribution of fluoride through OQ2
- 5.5 Ion chromatography: Results for VB and VQ core samples
 - 5.5.1 Distribution of sulphate through VB1
 - 5.5.2 Distribution of chloride through VB1
 - 5.5.3 Distribution of fluoride through VB1
- 5.6 XRF Major elements: Results from AB core samples
 - 5.6.1 Major elemental profiles for AB1 plotted against silica
 - 5.6.2 Major elemental profiles for AB2 plotted against silica
 - 5.6.3 Major elemental profiles for AB3 plotted against silica
 - 5.6.4 Major elemental profiles for AB4 plotted against silica
 - 5.6.5 Major elemental profiles for AB5 plotted against silica
 - 5.6.6 Major elemental profiles for AB6 plotted against silica
 - 5.6.7 Major elemental profiles for AB7 plotted against silica
 - 5.6.8 Major elemental profiles for AB8 plotted against silica
 - 5.6.9 Major elemental profiles for AB9 plotted against silica
 - 5.6.10 Major elemental profiles for AB10 plotted against silica
 - 5.6.11 Major elemental profiles for AB11 plotted against silica
 - 5.6.12 Major elemental profiles for AB12 plotted against silica
- 5.7 XRF Trace elements
 - 5.7.1 Sr concentrations through AB4, AB5 and AB11
 - 5.7.2 Co, Cu and Ni concentrations through core AB4

Chapter Six: Climate and the effect of temperature and humidity variations on building stone

- 6.1 Maximum and minimum air temperature variations at Culzean during May and November 1993
 - 6.1.1 May 1993
 - 6.1.2 November 1993
- 6.2 Plan of Drum Tower Balcony to show where the recordings of surface temperature were undertaken
- 6.3 Graph to compare Midday surface temperature variations of stone blocks around the balcony from North-to-West-to-South
- 6.4 A plan of the Drum Tower Balcony to show location of plugged boreholes where temperature and humidity measurements were undertaken

List of Figures Continued

- 6.5 Scatter graphs to show relationships between air relative humidity (RH), stone surface RH, and the RH of the inside of the bore holes
 - 6.5.1 North facing portion of the balcony
 - 6.5.2 West facing portion of the balcony
 - 6.5.3 South facing portion of the balcony
- 6.6 Scatter graphs to show relationships between air temperature, stone surface temperature and the temperature of the inside of the boreholes for the North-facing portion of the balcony
 - 6.6.1 Surface, interior & air
 - 6.6.2 Surface & interior
 - 6.6.3 Air & surface
 - 6.6.4 Interior & air
- 6.7 Scatter graphs to show relationships between air temperature, stone surface temperature and the temperature of the inside of the boreholes for the West-facing portion of the balcony
 - 6.7.1 Surface, interior & air
 - 6.7.2 Air & surface
 - 6.7.3 Surface & interior
 - 6.7.4 Interior & air
- 6.8 Scatter graphs to show relationships between air temperature, stone surface temperature and the temperature of the inside of the bore holes for the South-facing portion of the balcony
 - 6.8.1 Air, surface & interior
 - 6.8.2 Air & surface
 - 6.8.3 Surface & interior
 - 6.8.4 Interior & air
- 6.9 Stills from the infrared video of the castle and its outbuildings
 - 6.9.1 View of balcony West, high up
 - 6.9.2 Wall adjacent to balcony North
 - 6.9.3 Residential west wing, landward facing
 - 6.9.4 Far view of the castle from the cliffs
 - 6.9.5 Balcony south
 - 6.9.6 Residential west wing
 - 6.9.7 General view of the whole castle
 - 6.9.8 View of the North face of the balcony North
 - 6.9.9 The balcony North

Chapter 7: Discussion, conclusions and recommendations for the future

- 7.1 Moisture movement
 - 7.1.1 Drying stage I
 - 7.1.2 Sorption curve
- 7.2 Diagram to show moisture ingress and egress and the mechanisms that drive them
- 7.3 AB stone: Development of current deterioration
- 7.4 Primary and secondary drivers on the AB stone
- 7.5 Comparison of visible stages of deterioration for the three Culzean stones

List of Tables

Chapter Two: Fieldwork investigations and sampling

- 2.1 Classification of weathering forms based on Fitzner et al. (1995)
- 2.2 Classification of weathering forms from AB samples
- 2.3 Classification of weathering forms from VB and VQ samples
- 2.4 Classification of weathering forms from OB and OQ samples

Chapter Three: Analytical methods

- 3.1 Division of cores for geochemical analysis

Chapter Four: The properties of the Culzean stones

- 4.1 Mean and median point counting values
- 4.2 AB Samples: SEM atomic number contrast BSE Imaging
- 4.3 VB & VQ Samples: SEM atomic number contrast BSE Imaging
- 4.4 OB & OQ Samples: SEM atomic number contrast BSE Imaging
- 4.5 AB Samples: To show compositional variation of calcium carbonate cement
- 4.6 OB & OQ Samples: To show compositional variation of calcium carbonate cement
- 4.7 VB & VQ Samples: To show compositional variation of calcium carbonate cement

Chapter Five: Chemical Profiling of the Culzean stones

- 5.1 Comparative data for leaching experiments
- 5.2 Mean values for anion and cation contents of HPLC and rainwater
- 5.3 Classification of weathering forms from AB, VB and OB samples

Chapter Seven: Discussions, conclusions and recommendations for future research

- 7.1 A summary of the classification of weathering forms from AB samples
- 7.2 A summary of the classification of weathering forms from VB samples
- 7.3 A summary of the classification of weathering forms from OB samples

Appendix 1

- 1 XRF calibration and detection limits for major elements
- 2 XRF calibration and detection limits for trace elements
- 3 AA & AE calibration and detection limits-instrument conditions
- 4 AA & AE calibration and detection limits-standards & calibration statistics
- 5 XRD Results from clay analyses
- 6 AA & AE: Results from water extraction experiments
- 7 Ion chromatography: Results from water extraction experiments
- 8 Ion chromatography: Results for AB core samples
- 9 Ion chromatography: Results for OB and OQ core samples
- 10 Ion chromatography: Results for VB and VQ core samples
- 11 XRF Major elements: Results from AB core samples
- 12 XRF Trace elements: Results from AB core samples
- 13 XRF Major elements: Results from OB and OQ core samples
- 14 XRF Trace elements: Results from OB and OQ core samples
- 15 XRF Major elements: Results from VB and VQ core samples
- 16 XRF Trace elements: Results from VB and VQ core samples
- 17 Dry mass density, absorption, porosity, saturated sodium sulphate crystallisation and point-load strength tests
- 18 Dry mass density, absorption, porosity, saturated sodium sulphate crystallisation and point-load strength tests for Lower Carboniferous, Permian & ORS rocks
- 19 Monthly climatic data from Culzean
- 20 Culzean meteorological recordings at 0900 GMT for May & November 1993
- 21 Wind and rain recordings on the Adam's Balcony
- 22 Monthly relative humidity as a percentage
- 23 Midday temperature in degrees centigrade

Chapter One

Introduction

1.1 Rationale for project

1.1.1 Aims and Objectives

The causes of stone decay are complicated and therefore require detailed study using a number of different techniques to obtain an understanding of the wealth of reactions and processes taking place (Feilden, 1994). There is the need to develop understanding of the alteration of stone properties under particular conditions of exposure. An approach that envelops a number of diverse angles and disciplines, examining them and bringing them together as a working, genetic model.

In this thesis a new approach has been attempted, examining stone which is unaffected by cleaning or extreme pollution. Therefore 'natural' processes have to be ascertained prior to anthropogenic treatments.

By concentrating on geochemical analysis, yet trying to consider all contributing factors at every juncture, the intention has been to:

- typify the inherent characteristics of each sandstone used;
- profile a pattern of weathering through the building stones;
- build up a genetic model of natural (salt water induced) stone decay; and

- produce a model to be used to predict the fate of other buildings constructed of similar stone.

This research project has a number of goals. These can be broken down into general aims and a number of specific objectives as detailed below.

1.1.1.1 General Aims

- to determine the physical and chemical characteristics of the Culzean building stones in their fresh and weathered states, and to establish the factors causing stone decay;
- to consider the interrelationship between geological, environmental and time controls on decay, and the wider implications of this for building stones and weathering studies;
- to deduce, in the light of a simple model of aqueous ingress-egress, the physical and chemical weathering processes causing decay of the Culzean stones, and the relative tendencies of these stones to decay in the Culzean setting; and
- in the light of these findings, to advise the building owners on future conservation measures, including predictions of further decay patterns on existing stone and the choice of suitable stone for replacement.

1.1.1.2 Specific Objectives

- to establish the mineralogical and textural characteristics of the various Culzean stones in their unweathered state;
- to determine the physical patterns of decay in relation to stone type and aspect in both 'natural' and man-made environments;
- to measure the microclimatological parameters at the stone face and within the stone;
- to summarise the physical (engineering) properties of the Culzean stones;
- to describe the mineralogical, textural and chemical changes in the stone in the transition from unweathered to weathered material; and
- to undertake experiments to determine the reactivity of the stone under simulated natural conditions, and hence to deduce some of the chemical processes causing decay.

1.1.2 Thesis Structure

It is necessary briefly to explain the structure of the thesis, especially in relation to the ultimate formulation of a conceptual model for stone decay at Culzean.

This introductory chapter identifies the overall aims and specific objectives of the research. Following this there is a description of Culzean Castle, the building

under examination, including its location, architectural history, importance in Scottish heritage terms, and the present condition of its stonework. The chapter then describes the physical properties of sandstone, with which the castle was built. Thereafter, a discussion of the basic principles of weathering is given, before a critique of previous research undertaken including a summary of models previously produced on the weathering of building stones.

Chapter Two provides an overview of the fieldwork investigation and sampling strategy adopted for the purposes of this research. It outlines of the sampling techniques used, the constraints on sampling and how a method appropriate to sampling a historic building was developed. It provides a description of the various sources of stone from around the castle and its associated quarries. It also details a proposed classification system characterising the samples acquired for analysis.

Chapter Three describes in detail the analytical techniques used in the study of the geochemistry and mineralogy of the stone. It provides a summary of the investigative strategy for the laboratory work undertaken and a description of subsequent analytical methods used to study the core samples, described in the previous chapter.

Chapter Four describes the petrography and mineralogy of the stone and where this has influenced the weathering processes taking place. This chapter provides a description of the mineralogical properties of the different sandstones used to build Culzean before highlighting specific chemical and physical properties which have

resulted in weakness, alteration, dissolution, redistribution, and the precipitation of new minerals within the stone.

Chemical alteration and the mobility of ions are examined and discussed in Chapter Five. The chapter has been divided into two sections, monitoring the solubility and extraction of material from the stone and profiling the chemistry of the stone, both using geochemical analytical techniques.

Chapter Six is a short chapter to discuss environmental controls and the detailed parameters of microclimate that affect decay. This includes some preliminary temperature and humidity data recordings undertaken whilst researching the weathering of the stone at Culzean. A description of the shortcomings of the test methods and measurements has been provided at the end of the chapter with recommendations for future research.

The final chapter draws this information together by proposing a conceptual model of stone decay relating to earlier research, previously published models and the outcomes of this current research project. In this final chapter a working physio-chemical model for weathering is presented which can be applied to Culzean as well as other buildings undergoing the same weathering processes.

1.2 *The Culzean Problem*

1.2.1 Culzean in its historical context

In Late Georgian architecture, Robert Adam (1728-92) is the outstanding name from the 1760s onwards. The most famous of the Adam brothers, Robert Adam has been hailed 'Scotland's greatest architect' (Wilson, 1992); the 'father of classical revival' (West, 1979), he is one of the few architects in history whose name is synonymous with a particular style. His work evokes images of elegance and grandeur, as seen in great private houses such as Culzean, which is one of the most visited tourist attractions in Scotland.

Despite this fact, Adam's most original work was done on his interiors, the Roman plaster technique of hard stucco that he revived and his characteristic ceilings. In addition, his influence affected a great deal of the art-work produced in the last 30 years of the Eighteenth Century, including Sheraton furniture, Wedgwood pottery and silverware (West, 1979).

Culzean Castle (Plate 2) is the best known of the Adams' castles, and is an old house (Late Medieval) rebuilt. Originally the dwelling was constructed using stone quarried from the cliffs beneath what is now Home Farm. Adam designed his castle using the medieval foundations for the Tenth Earl of Cassillis in four stages over a period of fifteen years (1777-1792). Therefore Culzean's history stretches back prior to Adam's involvement.

Adam's country house plans were often complex, and Culzean is no exception. Constructed from the Lower Old Red Sandstone (LORS) quarried locally, Adam

used material contrasting in colour and texture, from purple to greenish-grey. The skyline is deliberately made up of the contrast between square and circular towers, and the turrets (Plate 1) accentuate the lower blocks. The long side of the castle looks over the Firth of Clyde; the entrance is on the narrow side, approached over the viaduct (Rykwert & Rykwert, 1950).

Adam is believed to have compromised by choosing cheaper building materials so that he could build extravagant structures, like those seen at Culzean, within budget. Other great Scottish architects such as Alexander 'Greek' Thompson and Charles Rennie Macintosh were also offenders!

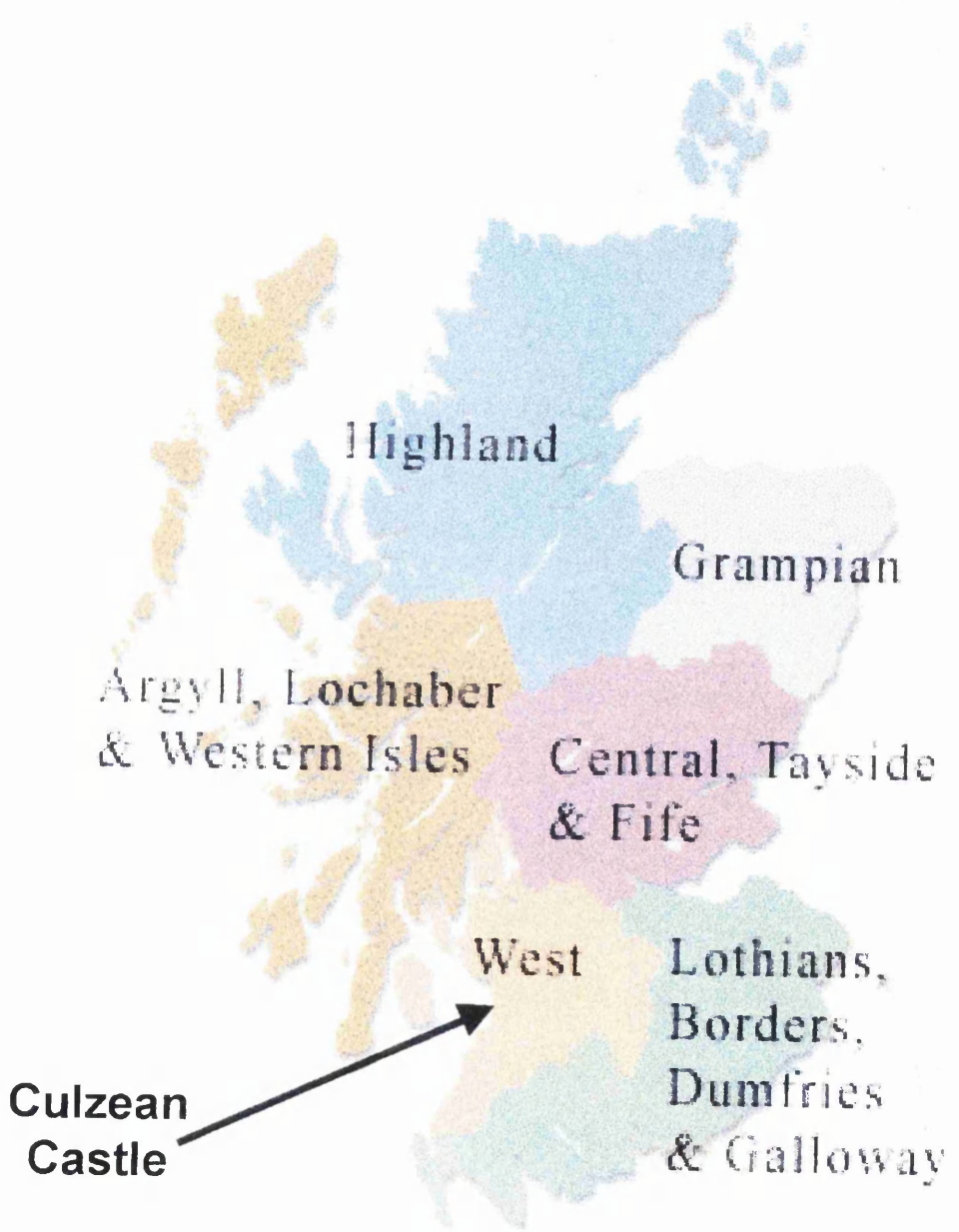
Culzean Castle as it is today was not completed until the nineteenth century, when additional rooms were added (the 'West Wing' of the castle). The architect at this time chose a red-brown micaceous stone, different in colour from that used by Adam.

Culzean was taken over by the National Trust for Scotland (NTS) in 1945 and is their 'flagship' property. It is the second most visited tourist attraction in Scotland after Edinburgh Castle.

1.2.2 Geological and geographical location

Culzean Castle, lies approximately 45 miles South West of Glasgow, on the Ayrshire Coast overlooking the Firth of Clyde and Arran (Figure 1.1). The Castle is exposed to severe Westerly winds in its West-facing cliff top position. Rain and sea spray penetration of the building stone are likely to have played an important role in

Figure 1.1 **Location map of Scotland**
To show position of Culzean



the weathering process. The influence of climate on the weathering patterns at Culzean is discussed in *Chapter 6*.

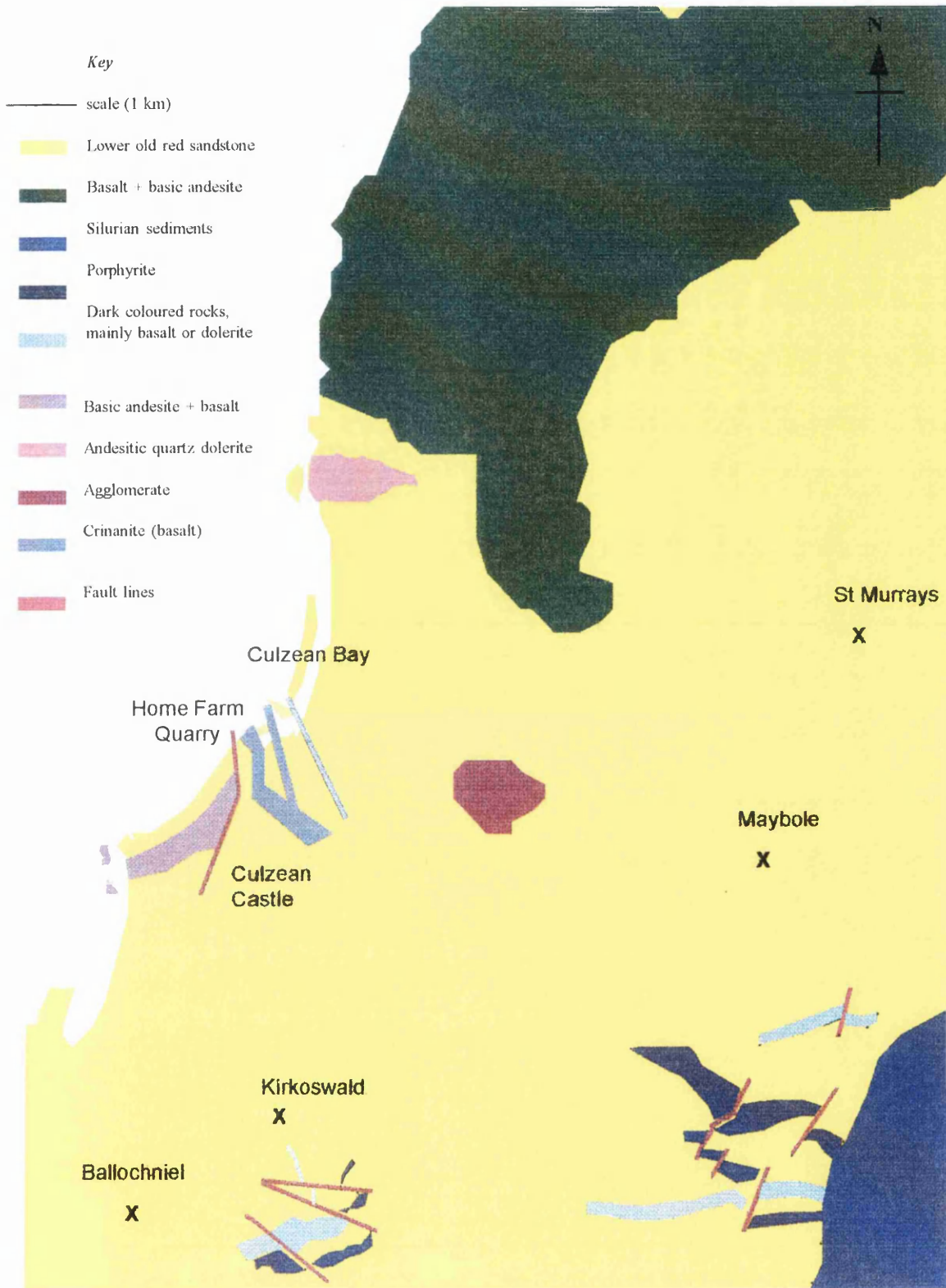
Culzean stands on lavas and sills of Old Red Sandstone (ORS) formed 345-395 thousand years ago and has, a little to the North, a boundary with olive-brown sandstones (lithic arenites). This is a large area of Devonian Lower Old Red Sandstone (LORS), with some volcanic lavas exposed. Culzean itself is built from this local sandstone whilst sitting on some of these lavas (Figure 1.2).

The sandstones, shales and conglomerates of the LORS period were laid down in lacustrine and fluvial environments, with a marked unconformity over a majority of the Silurian and Ordovician rocks. Deposition of these sediments was interrupted by igneous activity, whereby thick sequences of basaltic and andesitic lavas were deposited, and sills and dykes intruded. After this period of volcanic activity there was further subsidence, resulting in the deposition of more sandstones and conglomerates containing igneous pebbles indicative of local uplift and erosion (Eyles *et al.*, 1949).

Thus the LORS locally comprises of successions of conglomerates, sandstones, and siltstones (Anderton *et al.*, 1987). In the Culzean area it is mainly sandstones, although there are occasional bands of conglomerate and variously coloured marls. There are some bands of tuffaceous sandstone towards the top of the succession (at least 425m thick) in the Maybole District.

The sandstones from which Culzean was built can be flaggy or false-bedded red, yellow, greenish, or purplish-grey sandstones (British Geological Survey, 1867). Those used during the late Medieval period (1200s) are mottled greenish and

Figure 1.2 Simplified geological map of the Ayrshire Coast, Culzean and Maybole



purplish-grey; green-grey and red-brown during the Georgian period (1777-1792); red and purplish-red stones were used in the late 1800s. They are all mottled lithic arenite sandstones where the feldspars were frequently kaolonised into a white powder. Large flakes of white mica were present as a result of their fluvial deposition.

Research was initially undertaken by Bob Heath (the architect employed by the NTS at Culzean), to locate the quarries used over the years to build Culzean. The quarry used for the original building was located on the shore beneath Home Farm on the Culzean Estate. The quarry used by the Victorians was located just outside the town of Maybole, where many of the civic and residential buildings of this town were built at the same time using the same material. However despite visiting a large number of other local former quarries, the quarry or quarries utilised to build Adam's Culzean has not been located. A quarry at Ballochnie, believed to be the most likely (and not far from the estate) was examined along with others further afield, but no matching stone type was found. The records for the estate are held in the estate office for the Earl of Cassillis, however access to these records was not granted.

1.2.3 Responses to weathering problem

Over recent years some stonework at Culzean has deteriorated to unacceptable levels, with a risk of injury to visitors and staff from stone falling off the Drum Tower. Types of surface decay include pitting, blistering, spalling, cracking, and cavity decay (Bell, 1993). Examples of these can be seen in Plates 3 - 7. The decay

results from 'weathering' i.e. reaction of the stone and mortar with the atmosphere. Wind, rain, sea spray, runoff, and ground moisture have enabled solutions to enter the exposed stone surfaces of this multi-faceted and permeable structure.

The complex shape of the building and its intricate architectural detailing results in a great variety of microclimates, so that small portions of the building have their own characteristic decay patterns. The outcome of such diversity is the inconsistency of the building's decay. It is the relationship between stone and environment that is the central issue throughout the thesis.

Additionally, the variable nature of the stones adds to the diverse forms of decay. At Culzean, like many other historic buildings, the building stones have been taken from quarry locations with different inherent characteristics both between and within the relevant quarries, contributing to the present difficulties. Although all the building stones used have been taken from locally quarried LORS, the variations within this unit are great and the overall nature of the stone can vary in a single quarry face (see *Chapter 5*).

In the 1960s a decision was made to replace nearly all the stone at the front of the castle as a partial replacement involving only the most severely deteriorated stone would have given the castle a patchwork appearance (Learmont, 1992). The repairs took place to improve the aesthetics of the front of the building, as it was the surface features of the stone that were, in the eyes of the NTS, becoming unsightly. Thus the outer skin of the stone was replaced giving the appearance of a new castle (Plate 1). The original quarries, all within 5 miles of Culzean, have since been

closed. The stone chosen came from Springwell, Northumberland. This is a fawn, Carboniferous sandstone of fine-medium grain.

More recent repair work around the castle has been undertaken using Stanton Moore stone from Derbyshire. These particular quarry sources were used as they have been used extensively for repair work by conservation bodies in Scotland. The stones are readily available, workable, and perceived to be a reasonable colour match. Additionally, there are currently no quarries in Scotland producing a stone that directly matches the stone used by Adam to build Culzean. No consideration was taken into account of the stones' durability or matching the stone properties to those already in place or indeed the colour match of the stone once it had been placed on the building and allowed to season.

At the time of this research, the NTS was concerned with conserving and/or restoring the badly eroded seaward elevation, specifically Adam's Drum Tower (Plate 2). Temporary repairs had been made to the balcony of the Drum Tower because the NTS were concerned about the aesthetics of this side of the building. A number of the stone faces were coated with a cement mortar during the 1970s. This had proved detrimental to the stone in the long term; Plate 9 exemplifies the increased spalling effect. This was also becoming a safety concern as the patina spalling off could cause injury. To replace whole stones on a massive scale might detract from the aesthetic appearance of the building and destroy too much of the original fabric. The NTS were interested in matching and quarrying the stone locally if possible. It was this fact that prompted this research on stone decay, and specifically the mechanics of deterioration at Culzean.

It was clearly vital to develop an understanding of how and why the stone used (particularly that used by Adam) decays, how it behaves on the existing building, and hence to assess the durability of the LORS for building purposes. These results could then influence the choice of stone used to repair and replace the Culzean stone, address issues regarding the re-opening of a former quarry, and influence future decisions made by the NTS with respect to sandstone building restoration.

1.3 Building stone as a material

1.3.1 Classification of building stones

Natural stone is the basic material of the Earth's crust and therefore one of the most widely accessible building materials available.

Rocks are aggregates of minerals, and as such, all rocks (stone if fabricated) are composed of one or more kinds of minerals which help determine the physical and chemical properties of rocks (Winkler, 1975). The most important mineral components are either silicate or carbonate crystalline solids. All silicates except quartz have variable chemical compositions, which can be characterised within limits. Silicates fall into four main groups. Most important to the study of sandstone are the framework structures including quartz, feldspars and feldspathoids, and the sheet structures which include the clay and mica groups. The carbonates can be the main constituent of some rocks as minerals and as a cementing agent for the mineral grains.

As natural materials, rocks are variable in composition and properties and are not as readily characterised in the same way as synthetic construction materials such as

concrete or ceramics. Rocks are classified into three major groups based on their origin: igneous, metamorphic and sedimentary.

1.3.1.1 Igneous rocks

Igneous rocks are formed by the crystallisation of magma or lava, a complex silicate melt occurring in a variety of environments in and on the Earth's crust. The way magma is injected into the crust determines many of the features of the resulting solid rock, especially size and texture. Grain size and chemistry/mineralogical compositions are the two main criteria used for identifying and classifying igneous rocks. Examples of igneous rocks include granite, basalt, and gabbro.

1.3.1.2 Metamorphic rocks

Metamorphism involves the alteration of pre-formed rocks by temperature, pressure, and migrating fluids, often in environments deep in the Earth's crust. New characteristics reflecting these conditions are 'printed' over the existing features of the rock. The severe conditions to which the rock is subjected allow the minerals with which they are originally made to become unstable and change to maintain equilibrium with the new environment. Examples of metamorphic rocks include marble, schist, gneiss, and slate.

1.3.1.3 Sedimentary rocks

Sedimentary rocks are those formed on the Earth's surface. Their formation is more readily comprehended than that of igneous or metamorphic rocks formed at great depths in the crust (Pellant, 1990). Sedimentary rocks are characterised by bedding planes or stratification. This feature is a series of roughly parallel plane surfaces representing the original surfaces on which the sediment was deposited. Most of the sediments preserved as rocks were formed in marine environments, though there is also deltaic and desert sediment. Sedimentary rocks are secondary, in that they contain grains derived from igneous, metamorphic, and possibly earlier sedimentary rocks which have undergone weathering, erosion, transportation, and deposition. This can take place in rivers, glaciers and aeolian environments. After the sediment has been deposited, it can be subjected to a variety of 'diagenetic' processes, which convert the loose particles into solid rock. Diagenetic processes take place at relatively low temperatures and pressures near the Earth's surface. At increasing depth, metamorphism takes over. Compaction and cementation are two of the most important diagenetic events. Compaction removes pore fluid and the grains are arranged with closer packing. The weight of overlying strata has a considerable effect on compaction. Cementation involves the formation of secondary minerals around the grains, often quartz, calcite, or iron oxides. There are three main groups of sedimentary rocks: detrital sediments (conglomerates, sandstones, and shales); organic (some limestones, coals and bone beds), and the chemically formed sediments (some limestones and the evaporites).

Detrital sediments are made of particles worn from pre-formed rocks i.e. as a result of the processes of weathering, erosion, transportation and deposition. The detailed

chemistry and grain size of the detrital sediments depends on the nature of the original source material, the environment of deposition and post-deposition processes, which convert the sedimentary particles into solid rock. All these factors interplay in a variety of ways, which lead to the great diversity of detrital sediments.

Detrital sediments accumulate in vast thicknesses, especially in some marine environments such as on continental shelves, at the mouths of large river systems, and in ocean trenches. All these sediments have various structures related to the processes that have formed them. Bedding or stratification is the most obvious of these and originally this layering is quite flat. It may be picked out by changes in grain size and sediment chemistry. Sedimentary particles which are deposited in a moving current of water or wind exhibit a structure called cross or current bedding. In certain environments where sediments of different grain sizes are allowed to settle through the water column, graded bedding will occur with the coarser grains lower in each bed than the finer particles. As a general rule, the coarser sediment is found in shallower waters, beaches and screes, whilst the fine-grained clays are found far out to sea.

1.3.2 Sandstones

The chemical composition of sandstones is related to the rocks in the source area and to the chemical environments where the rocks are deposited and hardened.

In general terms these rocks have a 'simple' chemistry because the number of minerals surviving weathering cycles and accumulation are relatively few in number.

Quartz is the most common detrital mineral since it is a chemically stable and mechanically resistant mineral under almost all conditions and thus often forms vast thicknesses of sandstone. Feldspars are also common but not all feldspars survive the weathering processes. Feldspars are chemically less stable than quartz, and respond strongly to hydrolysis and hydration, when the atomic lattice is destroyed and the ions are freed to combine as new minerals. Calcium-bearing varieties are prone to relatively rapid decay and go into solution as carbonates and chlorides. Albite, orthoclase and microcline species are the most stable and thus more commonly found. This in turn indicates instability in the chemistry of the building stone, as feldspar decays into clays.

Clay minerals are extremely important and are hydrous aluminosilicates formed through the deterioration of feldspars. They have a layered atomic structure, which results in the development of a platy/flaky habit. The presence of exchangeable ions such as potassium (K^+), sodium (Na^+), magnesium (Mg^{2+}), calcium (Ca^{2+}) and hydrogen (H^+) allows considerable base exchange and such reactions in clay masses results in many different species of clay minerals being formed. The structure of clays allows them to absorb water, sometimes in great quantities depending on their atomic structure. Aggregates of previous rocks (lithic fragments) can also be found in sandstones. Ferromagnesian minerals, mainly silicates, are easily weathered and like feldspars they decay into clays with their secondary products going into solution. Mica is common in sandstones except those where wind action has been

involved, as it is easily blown away. Other stable minerals include tourmaline, rutile, zircon, monazite and muscovite, but these generally only form a small percentage of sandstones. These minerals are bound together by a 'cement', which originates during diagenesis. This is the most widespread form of final lithification when a cement is introduced from outside in aqueous solution, or from the solution of materials from within the sediment, and its redeposition. Common cements are silica, iron oxides and iron hydroxides, calcium and magnesium carbonate and iron sulphides and carbonates (Simpson, 1983).

The texture of sandstone is important for determining some of its physical properties such as porosity, permeability, and strength. Despite lithification, during which time pressures result in the expulsion of a large amount of water where pore spaces are continually reduced and compaction and hardening ensues, sandstones are still porous in nature. It is this porosity, determined by the sorting (particle size and shape), packing and cementing of grains that determines the permeability, strength and reactivity of the rock.

1.3.3 Sedimentary rocks as building stone

In addition to cost, appearance and strength, there are two other important things to consider when choosing a rock-type for building purposes:

- properties of the stone that determine responses to weathering processes; and
- those properties that are significantly changed by the weathering process.

When considering the former, rock type and in particular mineral composition are the primary concerns. Igneous rocks such as granite and some of the metamorphic rocks are good stones for building as their chemistry or mineral susceptibility is more stable than sedimentary rocks. Their crystallinity and particle size tend to reduce porosity and consequently permeability.

The sedimentary rocks tend to be less chemically stable and have higher porosities when compared with igneous and metamorphic rocks. The ability of water and solutions to penetrate a rock affects its resistance to most weathering processes and is determined by its porosity and permeability. However, sedimentary rocks are more readily quarried, cut, and sculpted, and are therefore more cost effective; and importantly, they were an easy material to access and build with in the past, when tools were more primitive.

Resistance to decomposition processes, in addition to being related to porosity and pore structure, permeability and mineral composition, involves many other variables such as the crystal structure and shape of minerals, grain texture, planes of weakness, cracks, bedding planes, and the nature of salts in the rock.

Those properties that are significantly changed by weathering processes include tensile strength, compressive and shear strengths, colour, texture, and particle size, permeability, infiltration capacity, erodability, bulk density, consolidation, bearing capacity, and many others. The physical properties of the stone change over time as a result of weathering. The changes can, in some circumstances, lead to thresholds of failure being crossed.

1.4 Basic principles of weathering and factors involved

1.4.1 Introduction to the weathering processes

Weathering is part of the process of the adjustment of minerals and rocks to an environment different from the one in which they were formed (Simpson & Horrobin, 1984).

There are two main categories of weathering processes, disintegration and decomposition. The former causes rock breakdown without significant mineral alteration and the latter causes chemical changes to the rock. Much discussion in the literature on weathering in general concentrates on individual processes; often examined separately in controlled environments. It is necessary to emphasise that these two groups of processes occur together and the resultant 'weathering pattern' will reflect the combined effects of several different processes.

1.4.2 Physical weathering

There are a number of different ways in which disintegration can occur. One of the most important where stone weathering is concerned is differential thermal expansion and temperature variation. The repeated heating and cooling of rock by diurnal and seasonal temperature variations have long been considered an important factor in the mechanical breakdown of rocks or exfoliation. A zone of stress develops between the heated and unheated rock, which may eventually result in fracture parallel to the surface.

All minerals, other than those of the cubic habit or system, have varying thermal expansions in different crystallographic directions. [The 'habit' of a crystal refers to the characteristic shape a crystal commonly assumes. This may be a cube, octahedron, rhombohedron, scalenohedron, etc. or a combination of these habits. The nature of the cubic system allows each of the faces to expand equally and thus differently from the other crystal habits with irregular faces (Simpson, 1983).]

In any rock mass or stone, the matrix of crystals lie at random in respect of their crystallographic orientation. On heating a stone or rock, differential stresses will be set up at the interface of the matrix of minerals. Such stress can be relieved by the granular disintegration of the rock.

The differential thermal expansion and temperature variation processes are aided by the presence of water. When water combines chemically with the more susceptible minerals in a rock (e.g. salts, see below), they can swell. This produces an increase in volume, which causes the outer layers of rock to be lifted off as concentric shells (exfoliation). Therefore, some weathering that used to be attributed to insolation may now be attributed to chemical changes produced by moisture.

1.4.2.1 Disintegration by frost

Frost weathering of rock tends to fracture the material into coarse, angular fragments. The mechanism may partly be the result of the volume change that takes place when water freezes, but there is also a substantial force exerted by the growth of ice crystals. As a saturated porous material freezes, the crystals begin to form in

the larger pores and continue to grow by withdrawing water from smaller pores; mechanical disruption or frost shattering may accompany such crystal growth (Small, 1987).

1.4.2.2 Disintegration by salts

Salts break up rocks in a number of ways which have traditionally been divided into two main groups, those involving predominantly physical changes in the state of the material and those involving some change in the chemical state of the material (Goudie & Viles, 1997). The most cited cause of salt weathering is salt crystal growth. Salt crystal growth can be triggered by a number of mechanisms for example a fall in temperature, which reduce their solubility, or a change in air humidity. Similarly salt hydration, the absorption of water, which increases the volume of the salt, can have a disintegration effect as it places pressure on the pore walls. This is particularly the case with hygroscopic salts e.g. halite, which attract water from the atmosphere. The pressures produced both by salt crystallisation and by salt hydration appear to exceed comfortably the tensile strengths of most rocks (Goudie & Viles, 1997). The mechanisms of salt weathering will be dealt with in greater detail in Sections 1.6.3 and 1.6.7.

1.4.3 Chemical weathering

Decomposition processes promote changes in both the physical and chemical characteristics of rocks and minerals.

The essential processes in decomposition are hydrolysis, hydration, oxidation, reduction, carbonation and solution:

- hydrolysis occurs when the salt of a strong base and a weak acid is dissolved in water. Water is the single most important agent of change. Water dissociates to a small degree into H^+ and OH^- (hydroxide) ions, which together with dissolved ions of other substances, such as Na^+ and K^+ , make the solution a reactive agent of change. The electrically charged atoms (ions) in the solution can combine with material in the rock or stone to produce more stable assemblages. This is common in the feldspars, for example orthoclase feldspar can react to form kaolinite, a clay mineral;
- hydration involves the chemical addition of water (hydroxyl molecule) to minerals (atomic structure). New minerals such as hydrous silicates and hydrous oxides are formed. There are often changes in volume involved, for example the decomposition of plagioclase feldspar (albite) to produce clay (kaolinite) by hydration, and sodium carbonate by carbonation;
- oxidation is almost always associated with hydration. Oxidation is the addition of oxygen, and most widely occurs in iron compounds. The oxidation of iron pyrite in the presence of water produces ferrous sulphate and sulphuric acid. The colour of stone is attributed to iron compounds;
- carbonation is the reaction of minerals and rocks containing Ca^{2+} , Mg^{2+} , Na^+ and K^+ ions with water which contains CO_2 (carbon dioxide) i.e. weak carbonic acid. These ions may all be removed and redeposited elsewhere. This is one of

the most important processes in rock decomposition, particularly in carbonate rocks; and

- solution is prevalent because most minerals are slightly soluble in water. Minerals such as Na^+ , K^+ and Mg^{2+} chlorides are most likely to enter solution. Chlorides and sulphates of iron are also soluble. Solutions may become increasingly acidic/alkali improving their solvency. Carbonate rocks are more readily attacked and secondary products of decomposition processes removed.

The principle mechanisms by which a rock or stone weathers have been outlined above to provide the reader with a clearer understanding of the complex processes involved. They also provide an understanding of the difficulties of pinpointing, particularly where decomposition processes are involved, the many complicated reactions taking place, and their role in the overall breakdown of the material (Small, 1987).

1.4.4 Organic processes

Organic processes or biological action can also play a role in rock weathering and include processes such as root wedging from larger matter, colloidal plucking as individual grains are removed, and lichen growth. The latter result in the blistering and sloughing of rock surfaces, which produce erosion pits. In addition, fungi can physically penetrate the stone advancing the chelation process; a chemical reaction where the organic acids attract metal ions from the rock's mineral constituents.

Mosses and algae encourage moisture retention and so lengthen the time period over which the rock remains damp.

1.5 Stone decay

Academic research into stone decay has taken place for many years. Schaffer published his book on "The weathering of building stones" in 1932, and in Scotland, Laurie & Milne wrote a paper on, "The evaporation of water and salt solutions from surfaces of stone, brick, and mortar" for The Proceedings of the Royal Society of Edinburgh session of 1926-1927. "Stone: Properties, Durability in Man's Environment", by Winkler was first published in 1973, to provide an 'overall understanding of the basics'.

Indeed, the building industry has long been concerned with weathering processes of natural and artificial materials, understanding and preventing accelerated deterioration.

There are a number of reasons why research in the decay of historic buildings, for example, is so inadequate. Although there has always been a widespread interest, one of the major problems is the limited cross-fertilisation of ideas between disciplines. As such, basic understanding of previous work cannot be restricted to building stone-specific research, but must embrace work undertaken in the areas of weathering, landforms and soils.

It is difficult to comprehensively review applied studies in stone weathering because the information is disseminated amongst so many disparate groups. There are many publications in diverse journals and a proliferation of unpublished reports.

In Britain, national research in this area has been organised by public agencies such as the Building Research Establishment (privatised in 1997), English Heritage, and Historic Scotland. Only recently has collaboration between them increased and included other bodies. Despite the number of buildings in Britain of international interest and the adverse climate and pollution, little research has been initiated in comparison with countries such as Italy, Germany, Portugal and Spain. However, it has since been recognised that there is the need for a new multidisciplinary approach in building material research.

The stone cleaning industry boom of the 1980's has led the new wave of research particularly in Scotland. A number of the methods used, although cleaning the stone, have resulted in irreparable damage to the 'fresh' stone beneath. Methods used on the limestones of the South of England were brought to the North, without taking into account the differences in the make-up of the stone.

1.6 An overview of weathering research

Natural stone is one of, if not the oldest building materials used by man. The most extensive use of stone began in the middle of the eighteenth century until the late nineteenth century, when the wealth of Europe and North America expressed itself in grandiose public buildings and private houses and mansions (Prentice, 1990).

1.6.1 Introduction to weathering research

It is the recent, yet rapid, deterioration of stone that has prompted concern. Interest in stone architecture and its preservation has at the same time increased. Stone has become a symbol of prestige, conveying a building's sense of permanence and solidity. It is the deterioration of this material, often irreplaceable (quarrying of direct replacements for the stone being impractical and uneconomical) that has prompted the funding of research in the weathering of building stone.

The principal variables controlling the nature and rate of weathering have long been recognised in the development of soil:

- the composition and structure of the parent rock;
- the nature of the climate; and
- the length of time over which the weathering has occurred.

The same principles can be applied in the weathering of building stone.

However, there are still many questions to be answered. It is not known precisely how different processes achieve rock breakdown, and why weathering varies greatly on different rocks and in different climates.

The study of weathering processes has always posed difficulties because most act over long time spans. The processes can be difficult to observe in action in the field except over a period of many years or decades. Many researchers have resorted to laboratory experiments. It is hard to satisfactorily simulate weathering mechanisms

in the laboratory without acceleration. This can affect the mechanisms of decay and thus the validity of the results.

In their natural environment, unweathered and weathered rock will occur in close juxtaposition. This phenomenon is also seen on buildings. In both cases it is difficult to ascertain which weathering processes have transformed the one into the other, because different processes can produce identical or similar results. The problems of interpretation of rock weathering in situ are further complicated by past climatic changes, from the effects of frost to pollution (Robinson & Williams, 1994).

Despite its importance to geomorphology, experimental research into the fundamental mechanisms of weathering has until quite recently been badly neglected. Many geologists and geomorphologists in the past believed rock weathering was such an obvious phenomenon, and the nature of the different processes so self evident, that detailed research was unnecessary as it was not of great concern.

Before 1950, only a few geologists and geomorphologists undertook experiments to discover how the different weathering processes worked. The most famous of these was Griggs (1936) whose experiments, although seriously flawed, were quoted for decades as proof that temperature changes ($> 0^{\circ}\text{C}$) are almost totally ineffective in causing rock breakdown except in the presence of water.

The absence of research directly related to building encouraged architects and engineers who were concerned about the strength and durability of building stones, concrete and other construction materials, to initiate research. The well-studied

texts of Schaffer (1932), Honeyborne & Harris (1958), and Winkler (1973) provide examples of work undertaken directly relating to rock weathering in the built environment.

From the 1960s onwards, geomorphologists and pedologists undertook more work in which attempts were made to establish the processes and products of weathering.

Texts published at this time include:

- Loughnan's "chemical weathering of the silicate minerals" (1969);
- "The formation of soil material" (Paton, 1978);
- The Soil Science Society of America's "Minerals in soil environments" (1977);
and
- pioneering work undertaken by Battle (Battle, 1936; Whalley & McGreevy, 1991).

Towards the late 1980s, there has been an increase in work, which has attempted to explain the processes and products of weathering. Substantive geomorphological texts include Trudgill (1984); Ollier, (1984); and Cooke & Doornkamp (1989). Research papers were also being produced highlighting specific weathering features and processes. The lead for this work was taken by researchers in the UK and include work by: Smith, Magee and Whalley (1994), McGreevy & Smith (1984; 1985), Smith & McGreevy (1987), McGreevy (1982, 1985), Cooke (1979), Goudie (1974, 1977), and Whalley, Smith, & Magee (1992) (see below).

1.6.2 Weathering processes and products

A number of studies have been undertaken since the 1980s to look at weathering forms (contour scaling, honeycombing, spalling, etc.) and the mechanisms driving their formation. The key mechanisms documented have been the presence of water and soluble salts. A number of papers have been written which isolate key factors in the deterioration process from specific experimental work.

1.6.3 Salt weathering

The most cited cause of salt weathering is generally the process of salt crystal growth from solutions in rock pores and cracks (Evans, 1970). Various mechanisms can cause crystal growth to occur. Goudie & Viles (1997) have produced an overview of the mechanisms of salt crystallisation and hydration, the majority of which are interrelated and it is therefore unrealistic to isolate them as individual processes. These have been summarised below alongside examples of experimental work undertaken to determine the appropriate mechanisms.

The properties of the rock are of utmost importance in determining their susceptibility to salt weathering. The porosity of the rock is a highly important parameter in determining the quantity and position of soluble salts within that rock. Porosity determines the rock's permeability according to whether it has an open or closed pore system. Porosity affects salt weathering in two main ways:

- how water moves in and out of the material through inflow, capillarity and evaporation; and

- where the major foci of salt crystallisation is.

A number of equations have been produced to calculate crystallisation pressures including Corren (1949), Winkler & Singer (1972) and Fitzner & Sneath (1982). Fitzner & Sneath (1982) developed an equation which considers crystallisation pressures in relation to porous materials. Following work done by Everett (1961), they approach the theoretical problem of crystallisation pressures in porous media in terms of an analogy with the thermodynamics of freezing of solutions in porous materials: $P = 2\sigma(1/rR)$

P crystallisation pressure

σ ionic interfacial tension of the salt solution

r radii of small pores

R radii of large pores

According to their theoretical approach, crystallisation occurs first in large pores and only moves into small pores once the larger ones are full. Until that point, small pores act as supply reservoirs for salt solutions. Stones with a high volume of large pores and a higher volume of smaller pores are seen to be particularly sensitive to salt weathering and frost weathering.

Certain common salts hydrate and dehydrate relatively easily in response to changes in temperature and humidity. This is particularly true of sodium sulphate, sodium carbonate, magnesium sulphate and sodium nitrate, though not to the same degree of calcium sulphate and sodium chloride. As a change of phase takes place to the hydrated form, water is absorbed. This increases the volumes of the salt and thus develops pressure against pore walls. For example sodium carbonate and sodium

sulphate both undergo a volume change in excess of 300% as they hydrate (Goudie & Viles, 1997).

Following on from this, some salts rapidly decrease in solubility as temperatures fall. Nocturnal cooling can therefore cause salt crystallisation to occur.

Evaporation helps to create saturated solutions from which crystallisation can occur, and when this happens, highly soluble salts will produce large volumes of crystals. Consequently, air humidity is a highly important control of the effectiveness of salt crystallisation. A salt can crystallise only when the ambient relative humidity is lower than the equilibrium relative humidity of the saturated salt solution. If that is the case on a rock surface, then the salt will crystallise and cause decay.

Sperling and Cooke (1985) looked at the differentiation between the forces of crystal growth and hydration in salt weathering, using a single salt-hydrate system (sodium sulphate). Results showed that the hydration of sodium sulphate is an effective mechanism of rock disintegration but that it is significantly less destructive than crystal growth pressure. The crystallisation of thenardite (Na_2SO_4) is, in turn, more effective in rock weathering than the crystal growth of mirabilite ($\text{Na}_2\text{SO}_4 \cdot 10\text{H}_2\text{O}$). They found that rates of disintegration were most rapid where the diurnal temperature range was extreme and relative humidity lowest.

Cooke & Smalley (1968) proposed that the disruption of rock may take place because certain salts have higher coefficients of expansion than the minerals of the rock in whose pores they occur. Hygroscopic salts are particularly disruptive because they have the ability to absorb water vapour from the atmosphere and to yield a saturated solution. Halite is hygroscopic and attracts moisture from the

atmosphere. One of the earliest discussions of the importance of sodium chloride deliquescence was that by Wallace (1916) who noticed the effects of brine springs that issued from Devonian limestone and dolomites at the foot of the Manitoba escarpment in Canada.

Under these conditions the deliquescent salt will absorb water vapour from the air to form a solution. The water absorption will stop and equilibrium will be reached when the water vapour pressure of the saturated solution is equal to the vapour pressure in the atmosphere.

Sources of moisture for salt weathering can either provide a source of salt or a means by which salts can be mobilised and deposited in pores and cracks. Dew, fog, rain and groundwater will all be sources of moisture.

McGreevy (1985) undertook a preliminary Scanning Electron Microscope (SEM) study of honeycomb weathering (the gouging out of circular surface pits to look like a honeycomb) of sandstone in a coastal environment. McGreevy observed that both disintegration and decomposition processes were at work to produce this phenomenon. He observed that salt crystallisation in the sandstone's pore spaces were dislodging quartz grains to accelerate the effects of granular disintegration. SEM analysis additionally pinpointed the etching of quartz grains by the solvent action of sea spray entering the rock. Despite its coastal position little halite (NaCl) was found on the surface of the rock or in near surface regions. Gypsum was found in abundance as a result of a chemical reaction between the sea spray and the rock. However, the causes of the honeycomb pattern were not determined. Overall observations showed that the solutional activity complements the physical breakdown mechanisms in weakening individual grains. Therefore, as well as the largely physical processes of decay involved in salt crystallisation and hydration,

salt solutions may have a series of chemical effects on materials. Salt solutions possess a wide range of pH values and may produce etching and the transformation of a range of minerals.

McGreevy and Smith (1985) also looked at the spalling of quartz overgrowth and observed that salt solutions can penetrate gaps between overgrowths and host grains, detaching the overgrowths by salt weathering mechanisms. It was noticed that the pore spaces in the rock were completely filled with microcrystalline salt. In this instance the importance of pore spaces is emphasised, as in much other work on this subject.

The crystallisation of salts in pore spaces could result in weathering/breakdown by:

- the bridging across and enlargement of pores by crystals of salt growing out of solution during the heating phase of the experimental cycle;
- an increase in volume of salts filling pore spaces due to hydration during the cooling and/or wetting phase of the experimental cycle; and
- differential thermal expansion of crystallised salt relative to the enclosing quartz during the heating phase.

McGreevy (1985) also suggested that the pressure exerted by salt crystal growth in confined spaces was directly related to temperature. It was argued that the rates and amounts of rock disintegration by salt crystallisation increased with the maximum temperatures to which rocks are subjected. McGreevy also contended that a dark coloured surface combined with a low specific heat capacity and thermal

conductivity should be more conducive to high surface temperature than if a rock possesses only one or two of these characteristics.

There is controversy amongst researchers as to whether the presence of salts accelerates the rate at which frost action operates and if it does, why this should be. Williams & Robinson (1991) have produced a review of some of the mechanisms that might explain why under some conditions salts could accelerate frost weathering. These include surface sealing, the combined growth of salt and ice crystals and greater saturation. Surface sealing is where salts have accumulated on the outer layers of a rock surface as a result of surface evaporation, which could block pores and seal the surface. The combined action of salt crystal growth and frost action might be greater than they would be individually and as salt crystals form they might tend to reduce the amount of pore space available for ice formation. The hygroscopic nature of some salts allows some rocks to take up more moisture from the atmosphere than rocks that do not contain saline solutions. The presence of greater amounts of moisture in the rock pores could make them more susceptible to frost weathering (Williams & Robinson, 1991).

Robinson & Williams (1982) undertook an important experiment applicable to the weathering of architectural stone on rock specimens. Robinson & Williams subjected sandstones of different shapes to weathering by sodium sulphate (Na_2SO_4). They found that shape is an important factor controlling the rate of rock breakdown, and that the total edge length of specimens may be more significant than relative surface area. They also found that the orientation of bedding within the sandstone shape had no significant effect on the weathering rate.

A common misconception about weathering processes is that they are always destructive. In reality they may strengthen rocks particularly sandstone, through the formation of a patina or surface crust. This patina can help to strengthen and even waterproof the stone. Robinson & Williams (1987), in their work on surface crusting of sandstones in Southern England and Northern France, found the crust/patina to exert a profound control on the morphology of natural outcrops of the sandstones and upon the origin and distribution of micro-weathering features that they exhibit. The deposition of silica in the crusts 'weatherproofs' the rock by reducing water ingress and strengthens the rock by increasing the cementation and interlocking between grains. Their preliminary studies of soft and porous sandstone in Britain such as the Ashdown Sandstone suggest silica crusting to be commonplace. However, they found that although ORS also develop crusts, they are of a rather different character, because of lower water ingress.

1.6.4 Clay

Scientists looking at the weathering of soils have studied the formation and alteration of clays by the weathering of aluminosilicate minerals (Potter & Rossman, 1977; Singer, 1993). These reactions are well investigated and documented, and examples include:

- the formation of smectite from mica, ultimately resulting in the formation of kaolinite (Banfield & Eggleton, 1988; Stoch & Sikora, 1976);

- the transformation of chlorite to vermiculite by dissolution Mg^{2+} and iron (Fe^{2+}) (Proust *et al.*, 1986), and oxidation of Fe^{2+} (Ross & Kodama, 1976);
- smectite and kaolinite dissolution (Senkai *et al.*, 1981; Carroll-Webb & Walther, 1988);
- the formation of halloysite and kaolinite in soils (Steeffel & Van Cappellen, 1990); and
- the transformation of vermiculites and smectites to secondary aluminium (Al^{3+}) chlorites (Tamura, 1955; Swaney, 1960; Barnhisel, 1982).

However, clay is also considered when looking at the strength and durability of rocks. For example Sasaki, Kinoshita & Isgijima (1981), demonstrate the importance of expansive clay minerals within argillaceous rocks in controlling their moisture sensitivity. They highlighted the importance of clay softening in the presence of water as a control of moisture related reduction in cement.

Hawkins & McConnell in their paper on "Sensitivity of sandstone strength and deformability to changes in moisture content" (1992) also look at changes in strength and relate it to the softening and possible expansion of clay minerals. By studying a range of sandstones, they found the degree of sensitivity of a sandstone to moisture content was controlled by the proportions of quartz and clay minerals present and to a lesser extent by the rock micro-fabric. Their research indicates that the development of pore pressure during loading is negligible especially in pure sandstones and does not play a significant role in moisture related strength reduction. Their work shows that there is a large variation in the sensitivity of

sandstones to moisture content, and an increase in moisture content of as little as 1% from the dry state can have a marked effect on both strength and deformability.

1.6.5 Weathering simulation

A whole range of testing techniques have and will continue to be used to examine the state of weathering of rocks. A major problem common to many experimental weathering studies is how to measure the weakening of rock without further weakening them or causing premature breakdown.

It has been common to simulate rock weathering in an attempt to understand the weathering processes taking place. Goudie (1974) used deep-freeze chambers and ovens with temperature cycling devices to simulate weathering conditions. He did this to assess the importance of salt crystallisation and other mechanical weathering processes. He looked at the effects of thermal expansion of salts for the first time.

Leading on from this, Smith and McGreevy (1988) undertook a laboratory study to investigate the relationships between salt and contour scaling under simulated hot desert conditions. Blocks of sandstone were treated with ten percent solutions of Na_2SO_4 and MgSO_4 daily for a period of sixty days, and were subjected to desert temperatures. They found that a critical moisture content could be reached within the rock, below which the transport of liquid water to the surface was no longer possible, and only the less efficient vapour diffusion mechanisms remained available (Amoroso & Fassina, 1983). Thus salt was not brought to the surface but remained at depth within the rock, to be added to during the next wetting phase.

The repetition of this process concentrated the salts in a layer within the rock whilst ensuring that some salts continued to crystallise at the surface at the end of each cycle. Surface disintegration and essentially surface-parallel cracks were produced in the sandstone blocks.

During weathering simulations in the past, researchers have tended to record changes made to temperature conditions and to the initial degree of saturation of their specimens. In doing this they often fail to monitor the fluctuation of temperatures and humidity levels within their rock samples. The results of the experiments are therefore difficult to interpret. More recently Feiden (1994) and Goudie & Viles (1995) have addressed this.

Goudie & Viles (1995) produced a paper on the laboratory simulation of salt weathering which was used to ascertain the effects of sodium sulphate and sodium carbonate under 'Negev' conditions using a single immersion technique.

'Negev' conditions are set on a 24 hour cycle, based on actual observations of ground surface temperature and humidity on 26-27 September 1967 at Ardat in the Negev desert of Israel (Orshan, 1986).

They found that the amount of debris liberated by simulated salt weathering, with a single immersion technique under 'Negev' conditions, is closely related to the water absorption capacities and the salt uptakes of the rocks. For five of the six rock types examined, the amount of weathering achieved by sodium sulphate was greater than that by sodium carbonate. They found salt weathering to produce blistering on rock surfaces in addition to granular disintegration and splitting.

SEM examination of weathered blocks showed salt crystallising in pores and widespread cracking on vulnerable rocks. They also found that diurnal cycles of temperature and humidity change caused continued weathering long after the initial input of salt to the rock had taken place (Goudie & Viles, 1995).

Feiden (1994) who looked at the thermal expansion and the action of moisture listing the stresses induced, published research on temperature and relative humidity.

Feiden (1994) summarised that the stresses induced in building materials by temperature changes were dependent on five factors:

- the magnitude of absolute dimensional change in the material, which is the product of its dimensions multiplied by the coefficient of expansion and temperature differential and the effects of changes in relative humidity;
- the elasticity of the material;
- the capacity of the material to creep or flow under load;
- the degree of restraint to the movement of the material by its connection to other elements of the structure; and
- the change in moisture content by evaporation.

It is essential to know how the temperatures and moisture levels vary inside the samples if the weathering processes at work are to be interpreted correctly. Rock materials differ in their specific heat and conductivity. Consequently the

temperature and humidity fluctuations in rocks never correspond precisely with the changes recorded in the surrounding environment. Temperature and humidity levels will vary from rock to rock and from stone to stone. This is an area that is relatively unexplored at present.

1.6.6 Applied weathering studies

In the last twenty years there has been a move towards applied weathering studies and this research has included the weathering of buildings constructed of stone. Following the lead given by architects and engineers to apply studies on the weathering of rocks in situ to buildings, geomorphologists have become increasingly interested in the deterioration of building stone. There has been a bias towards the study of major culturally important sites (Smith, Magee, & Whalley, 1992, 1994), where researchers have applied their geomorphological approach to assessments of building stone decay.

In this applied research there has also been a bias towards the weathering of calcareous building stone (e.g. Lal Gauri, 1978; Honeyborne *et al.*, 1982; Bell, 1993), and until recently, carbonate dissolution was thought to be the only geochemical process operating in combination with physical processes (Mausfeld & Grassegger, 1994).

This bias towards research on calcareous building stones has meant that few researcher have looked at the role that clays play in the deterioration of building stone. German researchers working on the changing environments of pore solutions

have looked at clay mineral reactions and found a profile of clay alteration (Mausfeld & Grassegger, 1994). They found that towards the surface of the stone, Al-hydroxides were mobilised by low pH mineral dissolution, and consequently chlorite/smectite clays were transported within the stone. With increasing pH of the pore solutions these Al-hydroxides were found to be fixed in the inter-layers of the friable zone, thus resulting in the formation of chlorite rich disordered chlorite/smectite and finally Al-chlorite (sудоite).

They found that the clay mineral composition of the deeper unweathered parts of the building stone was constant. The changes in the outer 30mm of the block were attributed to weathering processes. The changes in the leaching state of feldspars indicated values of $\text{pH} < 4$ in the pore solutions. Therefore the changes in composition of the first 30mm were interpreted as reactions with low pH solutions (Mausfeld & Grassegger, 1994).

1.6.7 Soluble salts and building stone decay

Numerous studies involving direct observations have established that salt crystallisation leads to structural decay in buildings, and has been a serious concern in the conservation world from the early 1970s. Examples include:

- Winkler & Wihelm's study of salt burst by hydration in architectural stone (1970);
- Winkler & Singer (1972) "Crystallisation pressure of salts in stone and concrete"; and

- Arnold's "Behaviour of some soluble salts in stone deterioration (1976), who made one of the first attempts to characterise the different soluble salts found in building stone.

However, agreement among investigators regarding the nature of the process has still not been achieved. For example, the source of the internal crystallisation pressure and the dependence upon pore size distribution in porous stone is disputed (Ginell, 1994). Lewin (1982) in his paper, "The mechanisms of masonry decay through crystallisation" proposed that the crystallisation pressure results from the sudden release of free energy accompanying salt crystallisation from supersaturated solution. Lewin suggests that salts capable of forming supersaturated solutions, e.g. MgCl_2 , NaCl , and Na_2NO_3 , should be effective in inducing decay.

He proposes that salts will crystallise in pores, channels and cracks at and near exposed surfaces and that liquid water deposits dissolved matter wherever evaporation occurs. The site of this crystallisation is determined by the dynamic balance between the rate of escape of water from the surface and the rate of re-supplying of solution to that site. The former is a function of temperature, air humidity and local air currents. The latter is controlled by surface tension, pore radii, viscosity and the path length from the source of the solution to the site of the evaporation.

Lewin (1982) presented work to demonstrate that the mechanisms of salt decay of exposed stone and masonry consists in the deposition of solutes from solution within the pores of the solid close to the surface. This is characteristically

manifested in the form of a thin layer of the surface that lifts up in the form of a blister, peels outward as a spall, flakes off or powders away.

The initial thickness of this surface decay is of the order of a mm. When this thickness of surface has separated, the decay process may be initiated again in the underlying, still sound stone, resulting in a second such decay layer under the first. The process can then proceed again beneath these layers.

Experimental observations established that the deposition from solution of a simple, non-hydrated salt, such as NaCl, in the pores at the surface of a stone generates pressures sufficient to break down the stone.

Another mechanism (McMahon *et al.*, 1992) relates to the rapid crystallisation and increase in volume on conversion of anhydrous Na_2SO_4 to the hydrated form (thenardite to mirabolite). At temperatures above 32.4°C the anhydrous salt thenardite dissolves to form a supersaturated solution of the hydrated form, mirabolite, which can then crystallise rapidly. This process also results in free energy release and is similar to the freezing of water, which can generate high internal pressures and disruptive stresses in porous materials.

The susceptibility of porous materials to salt crystallisation damage, as outlined in the sections 1.6.2 and 1.6.3, appears to be related to pore size distribution and total pore volume of the material. Rossi-Manareai & Tucci (1991) in their paper "Pore structure and the disruptive or cementing effect of salt crystallisation in various types of stone" make quantitative crystallisation pressure estimates for a variety of naturally occurring, salt-damaged materials including calcareous and calcitic sandstones. The importance of pore structure is emphasised in their estimates,

which are made on the basis of the liquid-solid surface tension and the pore size distribution in these materials. They found that for sandstone, in the surface regions of high porosity, the crystallisation pressures were low, i.e. not sufficient to lead to mechanical failure, therefore salt crystallisation was causing surface hardening and not disintegration. Additionally sandstones, including the surface crust, showed a high crystallisation pressure because of the high percentage of small pores in the crust. This, they believe, can be responsible for the exfoliation and crumbling of the surface crust. Their conclusion was that the presence of soluble salts will only aggravate stone decay in the case of particular pore structures, and that before assuming the presence of soluble salts to be harmful, the pore structure of the stone should be examined.

Fitzner & Snethlage (1982) and Snethlage & Wendler (1997) have undertaken additional work on the crystallisation of soluble salts and their role in the deterioration of building stone. This is referred to in Section 1.7, as they propose a model for sandstone degradation based on this work.

1.6.8 Air pollution

A number of studies have been undertaken which look at soluble salts and the deterioration of building stone with respect to atmospheric pollution. This is where the presence of pollutants in the atmosphere activates and accelerates sulphation, solution and salt weathering processes.

Air in urban areas typically contains higher concentrations of the 'acid' gases, SO_2 and NO_x , than air in rural locations due to fossil fuel burning. The sulphur compounds contained in coals and oils are converted into SO_2 during combustion. Nitrogen oxides (NO_x) are formed when fossil fuels are burnt, including natural gas that is free of sulphur. The main urban source of NO_x is from motor vehicles. Another impurity in UK coal is chlorine, which is converted during combustion to hydrochloric acid gas. Chlorine can dissolve readily in water to form a strong acid. This may have been a significant contributor to building damage in the past, when homes used coal for heating, cooking and the amount of coal burnt was greater (Cooke & Gibbs, 1994).

Weathering is principally accelerated by modifying the composition of the 'boundary layer' of the atmosphere with SO_2 and NO_x gases. This activates and accelerates sulphation, solution, and salt weathering processes. CO_2 , found in higher concentrations in urban areas, under certain circumstances can also accelerate urban weathering.

Much work has been attempted to look at the cause and effect of air pollution on building stone. Researchers in Venice, most notably Amoroso, Fassina and Camuffo, were among the first to undertake this research from the 1970s onwards (Fassina, 1978, 1988; Amoroso & Fassina, 1983; Camuffo, *et al.*, 1982, 1983, 1984, 1993; Guidobaldi, *et al.*, 1981, 1985, 1988; Del Monte & Vittori, 1985; Pallecchi & Pinn, 1988; Sabbioni & Zappia, 1992). The Italians looked at gypsum crusts on decaying buildings in several cities in Northern Italy. They discovered that carbonaceous particles were found consistently and in high concentrations inside the gypsum. It was proposed that these particles, which originated from oil burning,

act as a catalyst for the production of gypsum, the dominant decay process (The science of the total environment, No. 36, 1984). The studies of Amoroso & Fassina began in 1971, when daily measurements of the concentrations of some atmospheric pollutants were determined. Aerosol acidity, sulphate particulate matter, and sulphur dioxide concentrations showed a seasonal trend. Microscopic and microchemical analysis showed surface cracking caused by gypsum formation (calcium sulphate). There was believed to be a 'wetting phase' during which solutions containing sulphuric acid and sodium chloride penetrated the stone. The crystallisation of soluble salts, during the drying phase, resulted in the mechanical breakdown of the stone (Fassina, 1978).

Camuffo, *et al.* (1983) looked at the origin and growth mechanisms of sulphated crusts on urban limestones and marbles. They studied gypsum crusts and found that the distribution of soluble salts decreases exponentially from the surface towards the inside of the rock. Their work suggests that besides the effects due to the crystallisation, the differences in thermal expansion of the salts entrapped in the pores of the surface layer of the rock may favour the disruption of the face of the monuments where the thermal shock is maximal. The consequence of the differences in thermal expansion becomes dramatic in the case of gypsum wedges with respect to calcite, which may lead to pieces breaking off from the original stone.

Their observations and particularly the presence of gypsum crystals over metallic surfaces gave rise to the hypothesis that a fraction of the gypsum observed on carbonatic surfaces was originally airborne and therefore deposited on the actual

surfaces when they were wet. Thus, besides the growth mechanism, there is also a less intense growth due to deposit of gypsum transported by the wind or by percolation from neighbouring deterioration layers. The analysis of atmospheric aerosols lead to part of the gypsum observed in deterioration layers being deposited by some carbonaceous particles on the wet surface and therefore recrystallised on it together with the local gypsum due to the transformation of the limestone.

Camuffo and co-workers stress the importance of daily and seasonal meteorological factors. They studied a large variety of deterioration mechanisms, many of which they related not just to the composition of atmospheric pollutants but to the action of water supplied by the environment and to the property of the material. They concluded that deterioration occurs where the stone is porous enough to retain water and allow movement of salt solutions. This is heightened when the stone is subjected to chemico-physical reactions in the presence of water or of aggressive solutions where water combines with environmental pollutants or catalysts (Camuffo, 1984). Undertaking a number of case studies on monuments including the Trajan Column and Sistene Chapel (1989; 1993) and the Orvieto Cathedral (1988), Camuffo and Bernardi looked at variations in damage type across these monuments. They conclude that the principle types of deterioration critically depend on the way the surface of the stone is wetted by rain (Camuffo et al., 1982). The problem of surface moisture and condensation, wet and dry deposition, depends on the chemico-physical characteristics of both atmosphere and the building.

Researchers are currently attempting to find different ways of recording the patterns of damage and calculating 'factors of enrichment' in relation to sandstone and crustal rock composition, to point out the components present as a result of

atmospheric deposition (Sabbioni & Zappia, 1992). [Indeed, recently, a number of papers have been published specifically documenting the nature of black crusts (Whalley *et al.*, 1992; Fobe *et al.*, 1993; Pavia Santamaria *et al.*, 1994).]

At the same time, Charola *et al.*, at the Metropolitan Museum of Art, New York, and Reddy and co-workers with the United States Geological Survey, were researching acid rain damage, specifically with respect to carbonate stone. Charola produced overview papers outlining the processes of calcite dissolution and soluble salt formation i.e. gypsum, believed to be of greatest significance (Charola & Lewin, 1979 & 1979a; Charola, 1987). Whilst Reddy undertook an *in situ* experimental procedure, which was used to identify and quantify acid rain damage to carbonate stone based on the change in rain runoff chemical composition. Results showed that surface recession was directly proportional to the quantity of hydrogen ion loading from rainfall on the stone surface. The preliminary study to estimate the influence of sulphur dioxide deposition suggested that damage to the stone by sulphur dioxide was not significant (Reddy, 1988).

In the late 1980s, British researchers began looking at the damage being done to buildings by 'acid rain'. Research at the Building Research Establishment (BRE) showed that it was the combined effect of sulphur dioxide and acid rain (rainwater containing sulphate, nitrogen oxides, nitrates, and chlorides) which resulted in the formation of gypsum in the pores of both sandstone and limestone. A study of twenty-five sites in Southeast England showed that damage to stone samples was greater when there was more SO₂ in the atmosphere (Jaynes & Cooke, 1987). Concentrations of SO₂ in urban areas were twice as high as in rural sites, but weathering was only a quarter greater by comparison, because of the action of acid

rain. Monitoring sites were set up by BRE at Bolsover Castle, Derbyshire, Lincoln Cathedral, and Wells Cathedral, Somerset. An eight-year national programme of monitoring in collaboration with the former CEEB, British Coal Corporation, National Physics Laboratory, English Heritage, and Warren Springs Laboratories was begun. The setting up of this monitoring programme is well-documented (Pearce, 1985; Yates, Coote & Butlin, 1988). However, results have not been published and only a general paper on the effects of air pollution on buildings and materials was given as a keynote conference paper in 1990 and published in the Proceedings of the Royal Society of Edinburgh (Butlin, 1991). In associated work at BRE, samples of Portland limestone and White Mansfield dolomitic sandstone were being subjected to a simulated SO₂ polluted atmosphere using an atmospheric flow chamber (Lewry *et al.*, 1994). This technique was to be improved to investigate the effects of humidity and pollutants on stone, specifically to investigate the effects of relative humidity on the dry deposition of SO₂ onto dry and wet surface. Results from this subsequent work have not been published.

Lipfert (1989) has researched the effects of dry deposition (and their velocities) on different sandstones. German workers have also shown interest in this field with workers such as and Wittenburg and Dannecker (1992), whose findings document sulphate particle deposition of 5-10% for vertical surface of sandstone buildings depending on the atmospheric conditions.

More recently, an EEC project was launched in 1994 with the title "Marine spray and polluted atmosphere as factors of damage to monuments in the Mediterranean coastal environment". The aim of this research was to make a scientific study of the processes of weathering on monuments with particular reference to the

Mediterranean coastal areas of Southern Europe. The two factors which were believed to act together to cause stone decay are sea spray and pollution. The initial programme involved the following:

- monitoring environmental and micro-environmental parameters;
- systematic mineralogical, petrographical and chemical examination of the stone;
and
- analysis of the physical and mechanical characteristics of the weathered surfaces.

These were undertaken to evaluate the state of conservation and recommendations for conservative intervention on the monuments exposed to sea spray and pollution.

Zeza & Macri (1995) in their paper 'Marine aerosol and stone decay' reported on the first results from this work. They found that salts from both sea spray and pollution, from wet and dry deposition, both chlorides and sulphates, generally acted together to cause decay.

Widespread salt precipitation was found not only to take place at the surface of the stone, but also within micro-fractures in the stone blocks causing severe decay and the detachment of large stone chips. For example, halite was found to have a disaggregating action both directly on the surface of the stone and by infiltrating the micro-fissures of the stone, to produce deep chipping.

In their summary of this interim report they conclude that at this stage generalisations cannot be made regarding the effect of the marine aerosol on stone decay. The first studies of wet and dry deposition show that their effects are related to a series of important parameters such as the geomorphological conditions, the

different ways in which the coasts are exposed to winds and storms, the distance from the sea and the height above sea level. They found that the effects of marine aerosol are not only limited to the external parts of monuments and it has been shown that condensation waters, enriched by ions of marine origin, are able to provoke an intense state of decay at depth in the stone too (Zezza & Macri, 1995).

1.6.9 Cleaning

Research into the effect of cleaning increased in the 1980s. There was greater interest in the UK and particularly Scotland, where techniques used to clean limestone and marble were adopted for sandstone, sometimes with unexpected and undesirable results. Further to the discolouration the chemical cleaning methods often afforded, there was concern that both the chemical and abrasive methods led to the removal of the surface patina, which was providing a protective coating for the building (Bluck & Porter, 1992).

This prompted a number of conservation bodies to concentrate research in this area. The Masonry Conservation Research Group at Robert Gordon University (RGU) undertook important work in the UK for Historic Scotland. This work outlines the nature of sandstone and its propensity to soiling in an urban environment before discussing specific case studies of buildings cleaned in Scotland. Their experimental research characterises different cleaning regimes and their propensity to accelerate decay. RGU's report for Historic Scotland was published in 1991. An international conference on stone cleaning was held in Scotland in 1992. A book

was subsequently produced "Stone cleaning and the nature, soiling and decay mechanisms of stone" (Webster, 1992). This provided a comprehensive textbook documenting work undertaken by UK researchers from different research fields on the subject of stone conservation.

1.6.10 Microbiology

It is important to note at this point that microbial growth on buildings has become a major research interest to microbiologists although this is not within the scope of this thesis.

The presence of organisms, whether active or decayed, will trap moisture by clogging pores and consequently reducing the rate of run-off and promoting further growth. As a result, nearly saturated areas support the most prolific biological growths, including colonies of algae with associated bacteria, fungi, and small plants and mosses.

W. E. Krumbein has led research in this field for many years. He first published in 1952 when he undertook his PhD on "The microbial weathering of building stones" (Van Der Molen *et al.*, 1980). Krumbein is still a key contributor to this field and is currently looking at marbles exposed to natural and anthropogenic influences in Northern and Southern climates for the EU 496 EUROMARBLE project, as part of the EUREKA-EUROCARE umbrella project (EU 140).

Microbial growths such as algae, lichens, mosses or higher plants like liverworts can be used to indicate the state of the stone, how much moisture is being retained and its likely decay patterns.

Researchers in this discipline have tended to concentrate on particular species of organisms and their effects on specific building stone types. RGU have however undertaken a comprehensive literature review on the microbiological deterioration of stonework, as part of a project for Historic Scotland. This included "Biological growths, biocide treatment, soiling and decay of sandstone buildings and monuments in Scotland" (RGU Masonry Conservation Research Group, 1995). This is a comprehensive study, yet to be published. It is believed that microbiologists will continue to contribute advances in the understanding of rock weathering processes over the next few years (Robinson & Williams, 1994).

It should be noted that, in addition to the damage micro-organisms themselves achieve in the form of biodeterioration, there are a number of knock-on effects of organic growth on buildings which can change the chemical and physical make-up of the stone. The presence of algae may encourage freeze-thaw processes due to water entrapment. This may result in physical damage to the stone surface. Cell secretions may clog pores trapping moisture enhancing this process. Micro-organisms may provide an initial etching of a surface, which then opens the way for salt attack. Also algal growth encourages other organisms to colonise including fungi and bacteria which can speed up the chemical decay of the stone. Warscheid *et al.* (1988, 1990, and 1992), suggest that feldspar and clay-rich sandstone provides the best conditions for bacterial growth and biodeterioration since there is a good supply of extractable minerals and enlargeable porosity.

Also bacteria, which are the largest group of micro-organisms (of which only a small percentage are actually known), can produce acids which are damaging to the stone. For example hydrogen-reducing bacteria, sulphur-oxidising and sulphur-reducing bacteria, iron-oxidising bacteria, nitrifying bacteria and denitrifying

bacteria, which can all have a detrimental effect on the stone (Wakefield & Jones, 1998).

1.7 Weathering models

Some researchers have attempted to produce models for stone weathering. Schiavon (1992) suggested a decay model for limestones in an urban area (King's College Chapel, Cambridge and St Luke's Church, London) in which two mechanisms dominated; the absorption of atmospheric pollutants on the stone's surface and sulphation allowing the calcite to be replaced by gypsum. His model is described as follows:

- adsorption of atmospheric pollutants, namely SO_2 , either by dry or wet deposition (the high degree of alteration in areas sheltered from rain favours a dry deposition process);
- sulphation as a result of the wetting of the stone;
- gypsum replacement of calcite;
- penetration of weathering solutions through cracks, cleavages and intercrystalline boundary planes; and
- crystallisation pressures, although present, do not appear to be causing any serious damage.

At this stage, Schiavon found that differences in microtexture lead to different decay patterns (and thus possibly two different models). For example the oolitic

grains in the oosparite (St Luke's Church, London) are preferentially replaced with respect to the cement by dissolution of the calcite followed by precipitation of gypsum in the created void, or slower atomic replacement through a thin film mechanism. Schiavon shows that the calcite fragments found in the crusts are not soil, dust or recrystallised calcite, but remnants from the cement itself.

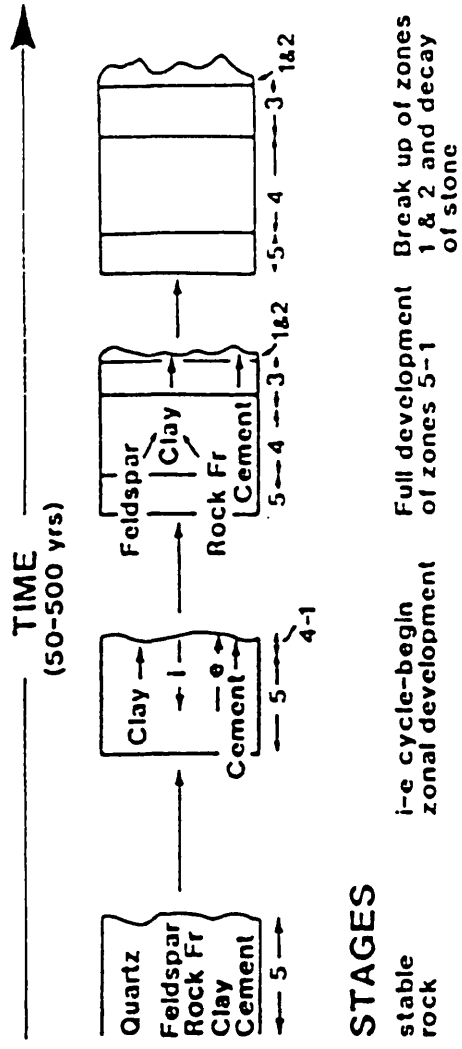
In the case of the oomicrite (King's College Chapel, Cambridge), most oolitic grains are still calcitic whereas the micritic cement, despite its low porosity, is almost totally replaced by gypsum. This replacement process, Schiavon believes, is likely to have been predated by dissolution of the calcite cement, as suggested by the presence of many intergranular microcavities in areas not yet subjected to calcium precipitation. This may reflect the lower degree of pollution in Cambridge; the dissolution/replacement of the micritic cement probably occurring at a fairly early stage in the decay process, further decay allowing the replacement to occur as seen at St Luke's.

A model like this cannot be directly related to sandstone deterioration mechanisms. Sulphation will be far less prevalent, even in sandstones with carbonate cement. However the model provides essential information on the processes involved in the dissolution of cementing agents and the production of crusts and their mineral constituents.

Bluck (1992) produced a hypothetical cycle for the degradation of sandstone. He showed the progress of a sandstone from fresh rock to a building stone decayed by the action of cleaning, identifying five zones (Figure 1.3):

1. surface soiling;

Figure 1.3 A hypothetical cycle in the degrading of sandstone (after B J Bluck, 1992)



2. re-precipitation of dissolved mineral cements;
3. gradation to zone *two* (with colour change);
4. depletion of mineral cement; and
5. original rock.

The model shows the importance of water ingress-egress in the production of a profile of stone weathering, as confirmed below by Mausfield & Grassegger (1994). Of importance in this cycle was the enrichment of clays in zones *two*, *three* and *four*, and a corresponding reduction in feldspars when compared with the feldspar-clay ratios of the fresh rock in zone *five*. Bluck suggests that sandstones may acquire more clay by the breakdown of feldspars during weathering processes, which allows for the transportation and reprecipitation of these elements as clay minerals towards the surface of the stone. It is proposed that in the outer zones *one* and *two*, increased moisture retention time will allow clays to expand and aid other factors such as frost action to break up the stone.

However, similar research has been undertaken in Germany by Mausfield & Grassegger (1994), who proposed a model based on solution-mineral interactions, stressing the importance of pore water transport, dominated by wetting-drying cycles.

They proposed that the initial acid pore solution entering a building stone during rainfall is increasingly neutralised with time and depth, and may even become alkaline with depth. Thus mineral dissolution features dominate near the surface of the building stones or in the near surface friable zone beneath spalling-off layers,

where rock-water contact is most intensive. At increasing depth the intensity of dissolution decreased. They found in studying clay mineral reactions at St Vitus Cathedral, S. W. Germany, that clay mineral precipitation reactions may dominate the deeper parts of the weathered zone. They found Al-hydroxides fixed in the inter-layers of the friable zone, resulting in the formation of chlorite rich disordered chlorite/smectite and Al-chlorite (sудоite).

Mausfield & Grassegger state that the actual depth of dissolution domination depends on the aspect of the stone, the amount of acid immission, the buffering potential of the rock, the corresponding pH value of the decay reaction, and the pore water transport. These factors are strongly influenced by pore size distribution.

Interaction and interdependencies of factors influencing dissolution/precipitation reactions in a multi mineral system with complex pore water transport tend to obscure the reaction controlling parameters. Feedbacks of the geochemical system to the physical weathering processes, e.g. porosity modification or weakening of grain bonds by dissolution, result in extremely complex system architecture.

For decay processes of one mineral the reaction path may be modelled but for more complex problems these systems can only be accessed by computer aided modelling. There have been three different attempts at computer modelling on this scale; Cooper *et al.* (1989), who tried to produce an expert system, Haag & Grassegger (1994) who suggest the use of neural networks to evaluate complex interactions, and Massey (1992) who modelled one part of the weathering effects.

This research by Mausfield & Grassegger is valuable for putting together a hypothetical model for sandstone decay because it emphasises the importance of porosity/permeability and identifies a profile of weathering through the stone.

In addition, researchers at Wolverhampton University have produced a model by undertaking a microcatchment study to examine all aspects of stone decay on Mottled Hollington Sandstone.

Halsey *et al.* (1995) believes the dominant deterioration mechanism affecting Hollington Sandstone to be the formation and detachment of surface crusts. Results highlight that crusts may form due to the blocking of pores by atmospheric particulates and algae. Additionally, pores may be blocked by salts especially gypsum and possibly halite. It is believed that both these processes occur concurrently and probably complement each other, with gypsum crystals growing around particulates and algae, hence trapping them within the sandstone pores. Gypsum accumulation is seen to take place from calcium contained within the sandstone and, in this study, no conclusive evidence exists for the atmospheric deposition of calcium.

The results suggest that crust detachment may be aided by gypsum and possibly halite exerting underlying pressures due to changes in temperature and moisture availability in the pores of the stone. Detachment could also be aided by a weakening of the sandstone below the crust, due to the loss of calcium carbonate cement. They believe that further weakening could be caused by the weathering of orthoclase to form kaolinite. The trapping of moisture behind the crust may

increase the rate of kaolinite formation in this zone, which could aid crustal detachment (Halsey *et al.*, 1995).

There is no indication of the mineralogical make-up of the stone; the presence of calcium carbonate, orthoclase feldspar and kaolinite is referred to, but there is no indication of mineral proportions. However the processes described which result in the detachment of the surface crusts are important and must be considered when proposing a model for the weathering of the Culzean sandstone.

Snethlage & Wendler (1997) have undertaken experiments and subsequently produced a model for moisture cycles and sandstone degradation. They suggest that both the mechanisms of wetting and drying, and freezing and thawing cause the displacement of grains relative to each other and contribute to the loosening of the grain structure.

Their experiments showed that lots of gypsum was found below scales, flakes and exfoliation, particularly on clay-rich sandstones. The conclusion that they draw is the gypsum not only enhances the decay, but even causes the detachment of the scales as a result of its crystallisation pressure.

They undertook hygric dilation experiments in the presence of NaCl, MgSO₄ and CaNO₃(nitrate) and found that salt free stone expands during wetting and contracts during drying. The salt-contaminated stone reacts in the opposite way, it contracts during wetting and expands during drying. In the latter, dilation is not reversible and the amount of dilation increases from cycle to cycle.

They found that grain-to-grain distances in salt-contaminated stone are smaller in the wet state than in the dry state. Both states they suggest, however, represent some kind of equilibrium state of the grain structure, so that during the wetting and drying cycles, the volume of the stone moves between these two limits.

They propose a model in which dilation and contraction i.e. the displacement of grains relative to each other, under the influence of moisture and dissolved ionic species, is the only process needed to explain the deterioration of stones. This process provides the open spaces in the grain structure, as suggested by Pühringer *et al.* (1985). They propose that it is most probable that salt crystallisation pressure occurs only in strongly salt-enriched stones where the coarse pores can be filled up with salt crystals (Fitzner & Sneath, 1982). They suggest that the idea of a crystallisation and hydration pressure should still be questioned.

The model they propose states that during the drying process, salts migrate into the part of a pore system that is still wet (not necessarily to the surface). They are enriched in the rest of the pore liquid and precipitate when all the remaining liquid has evaporated. Damage happens in the zone of the maximum moisture content, which is necessarily the zone of the salt precipitation. The actual location depends on the moisture transport coefficient of the stone and on the transition coefficient of the stone i.e. on the conditions of the building. (They use computer calculations to demonstrate that the mean moisture distribution in porous materials shows a clear 'maximum' whose position is determined by the water transport parameters of the material itself and the surrounding drying conditions.)

The model proposes that it is the periodic moisture cycles to which stone is subjected that cause the deterioration of natural stone. The location of the maximum in the mean moisture distribution curve determines the site of damage. They demonstrate the effect of salts on the intensification of the moisture cycles by colloid chemistry models.

Therefore they propose that the final pore solutions, which are enriched in salts, have been found to evaporate at the place where the maximum is situated. At this site, salts precipitate; the type of damage that will occur is determined by the position of the maximum relative to the surface. Damage types e.g. contour scaling, flaking, exfoliation, sanding off, and the detachment of black crusts, can be explained by the different depths of this maximum in the stone. For example, contour scales will form when the maximum is situated in the interior of the stone; sanding off will occur when the maximum is near the surface of the stone. Sneathlage & Wendler (1997) propose that other decay phenomena can be explained as intermediate forms of these two extremes.

1.8 Factors influencing the decay of sandstone at Culzean

It is proposed that for sandstone weathering in a coastal environment the following are paramount:

- the overall climate;
- exposure to wind, rain & sea spray;

- exposure to pollution;
- variations in the temperature and humidity of the stone;
- ingress and egress of moisture;
- chemical composition of the pore fluids;
- mineralogy and chemistry of the stone; and
- pore structure and permeability.

These are all identified in the flow diagram produced in Figure 1.4. The importance of the environment and lithology are emphasised by Figure 1.4. This has been produced to structure what is known about the nature of sandstone weathering, to tie together information gathered in reviewing the multi-disciplinary research and ultimately demonstrate the *weathering system* as it is understood at present.

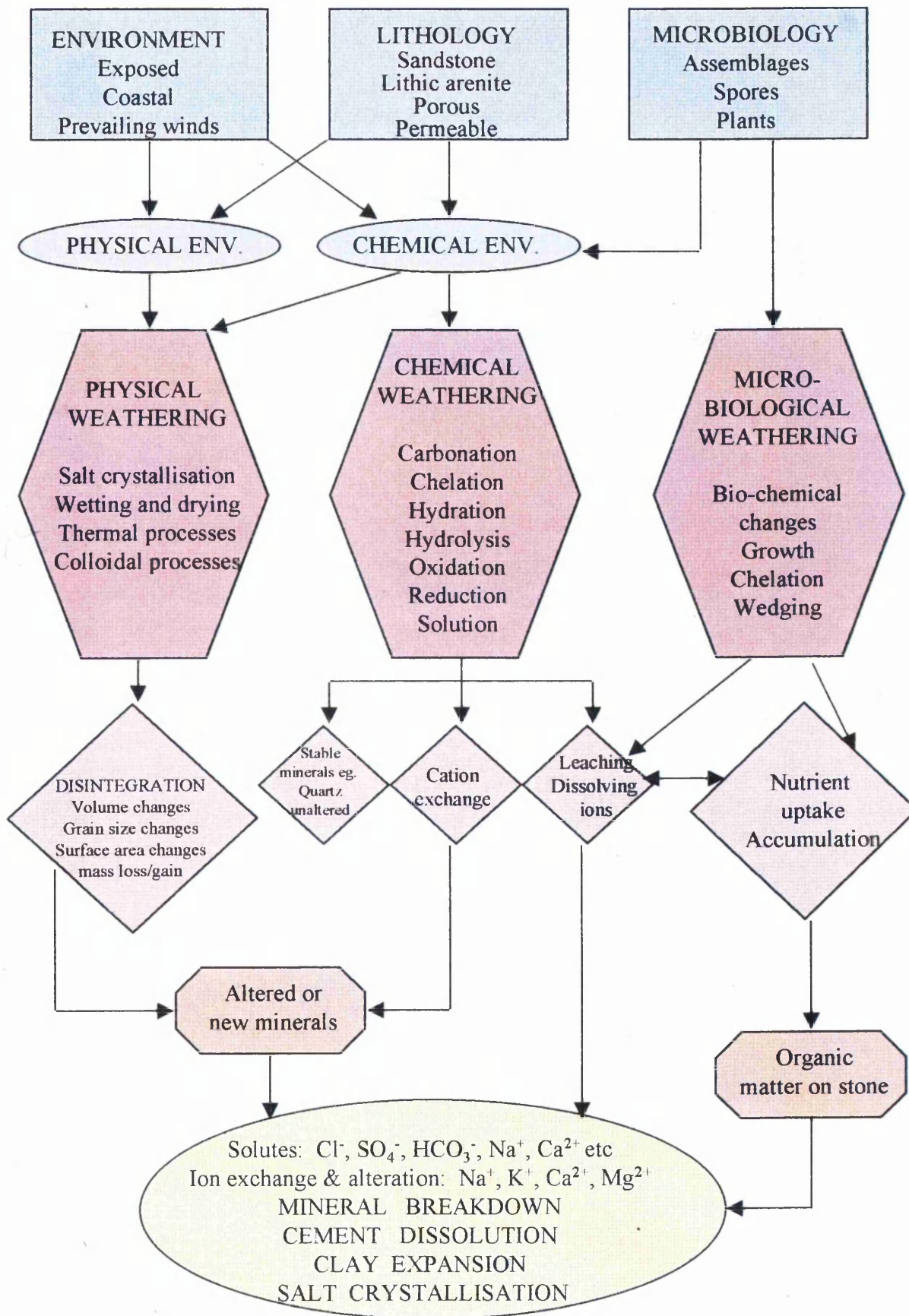
From the research discussed in this thesis, a conceptual model will be produced. This will relate to previously published models, and tie together this current research with earlier work to identify the weathering processes and products within the stone and establish the key mechanisms at work within the *weathering system* set out above.

Figure 1.4 Proposed model for the weathering of sandstone

P
R
E
V
A
I
L
A
N
T
S

P
O
S
S
I
B
I
L
I
T
I
E
S

O
U
T
C
O
M
E
S



Chapter Two

Fieldwork investigations and sampling

2.1 Sampling

Before discussing the design of the sampling strategy adopted for this work, it is useful to consolidate the aims of the research and highlight the two principal objectives:

- to determine what it was about the character of the Adam's building stone used between 1777 and 1792 (AB) that made it so susceptible to decay. How and why the AB stone was deteriorating more quickly than the stone used for the original building in the 13th century (OB) and the stone used in 1879 by Wardrop and Reid (VB); and
- to test the working model for sandstone weathering proposed in *Chapter 1*, based on visual evidence of the weathering of the stone at Culzean, particularly the AB stone.

With this in mind, it was essential to compare the different sandstones used on the building. This was done by sampling the three building stones to determine the

physical and chemical variations, both between and within the three sandstones (including differences between the surface material and the stone at depth).

Both quantitative and qualitative analytical methods were required to provide data that could differentiate between weathered and unweathered samples and demonstrate what it was about the character of AB that made it so susceptible to decay.

This chapter outlines the sampling techniques used, the constraints on sampling and how a method appropriate to sampling a historic building was developed. It provides a description of the various sources of stone from around the castle and its associated quarries. It also details a proposed classification system characterising the samples acquired for analysis.

2.2 Sampling strategy

The National Trust for Scotland (NTS) were sympathetic to the requirements of such a research project, but imposed constraints on sampling due to the building's architectural importance.

2.2.1 Constraints to adopting a statistically valid sampling scheme

A decision was made to take cores from the building as this was perceived to be the least visually disruptive way to obtain consistent and comparable samples, and to

compare the weathered surface with the unweathered stone at depth. Additional sandstone cores could be drilled and slotted into the cavities left by the sampling, and sealed with a lime mortar.

It was determined at the outset that the number of cores required for a statistically significant sample was never going to be agreed. Ideally a random or systematic sample size would have been used. These can be defined as:

- *random sampling* is where any one individual measurement or count in a 'population' is as likely to be included as any other and achieved by dividing the area to be covered into a grid and using random numbers to choose the samples to be analysed (Alder & Roessler, 1964); and
- *systematic sampling* is where selection is made from the population at regular intervals generally by setting up a grid to cover the sample area and for example choosing every tenth stone to be analysed (Hammond & McCullagh, 1986).

Either of these two methods could provide an unbiased representation of the quantities and variations of the different weathering features recognised at Culzean. However the quantity and often inaccessibility of the samples that would be required to obtain an ideal random or systematic sample made it unacceptable. There were restrictions imposed both on the number and the position of the cores, especially with relation to height. However the opportunity to work on this very important building, both architecturally and historically, was given, and it was necessary to

accept these constraints. Particularly as the research funding was gained for the sole purpose of studying the Culzean stone.

Ultimately it was agreed that a small number, a representative sample from each site and of each weathering style at that site, could be cored. In addition any material falling off the surface of the stone could be removed and used for analysis. These samples are detailed below.

2.2.2 Adopted strategy

Initial experimental work was undertaken using the friable and easily accessed material from the surface of samples on the balcony of the Drum Tower at Culzean (Plates 21 and 23).

A compromise was reached with the NTS to provide the most representative sample possible with least disruption to the building. Coring was concentrated on the balcony of the castle. It was in this area that the greatest deterioration was occurring and it was also an area not in the direct view of the public. In total twelve cores were taken from the balcony, three from the original building constructed in the 13th century and three from the west wing built in 1879. The cores were 75 mm in diameter and 150 mm in depth. A sampling strategy was devised in which the following were all carefully considered:

- stone type;

- aspect;
- microclimate;
- sampling size;
- stone type variation;
- surface colouring; and
- the spectrum of weathering styles.

An attempt was made to account for all these variations in the final agreement.

No access was given to the front of the castle or the restored visitors' entrance, both of which had been repaired in the 1970s. As such no comparison could be made with the replacement stone for compatibility.

2.3 Sampling method

In order to attain a maximum of information from the stone a slow, dry drilling method was used. This was to prevent any contamination that might have taken place if a lubricant had been used and to avoid any changes to porosity and permeability, chemical alteration and/or the removal of salts by the flushing of

fluids. This technique is the same as that adopted by the Masonry Conservation Research Group at the Robert Gordon University, Aberdeen (1991).

A hand-held diamond drill connected to a portable generator allowed coring of quarry faces in addition to the building. The cores, 75 mm in diameter were drilled to a depth of 150 mm where possible, although for the more resistant material this depth was unobtainable. The drill was worked at a low power to stop the drill bit from heating up and to prevent alteration of the sample by high frictional heat during drilling (Plate 24). The drilling of some samples dislodged the outer surface of the stone from the remainder of the core. All material was collected, recorded and retained for analysis.

2.4 The recording of weathering features

2.4.1 Classification methods

Simple studies have been undertaken (Leary, 1983; Rodriguez-Navarro *et al.*, 1994) to characterise stone according to its location on a building and susceptibility to decay. However, other researchers have attempted to produce maps identifying individual decay features. These have been examined so that an appropriate method could be adopted to characterise the Culzean stone.

The Norwegian centre for natural stone research has produced stone type maps and decay maps for the soapstones on the Nidaros Cathedral, Trondheim (Steinforsk,

1993). The legend gives a scale of one to seventeen for decay type (including black crusts, algae and salt efflorescence) and one to fourteen for stone type. Each decay/stone type has a symbol, pattern or colour; depending on the type of 'map' being produced, one of these descriptive criteria is used. This is a straightforward method and, in the case of a decay map, allows large areas of the building to be characterised in detail.

A number of researchers have produced papers outlining their proposals for the classification and mapping of weathering forms. Smith *et al.* (1992) produced a checklist for visual assessment as part of a geomorphological approach. They used a number of broad process categories for different weathering features. These were as follows:

- mechanical breakdown;

- solution;

- surface alteration and/or deposition;

- biological action; and

- human damage/change.

In each category there are ranges of individual features, each with their own code for easy recognition. This method can provide an overall summary of the site to be studied or as a checklist for individual stones.

Fitzner *et al.* (1995) produced a detailed classification scheme of weathering forms.

The scheme comprises three groups of weathering forms:

- loss of material/fissuration;

- discolouration/deposits on the stone surface; and

- detachment of material.

The next and more precise level for the state description is obtained by differentiating these three groups. Nineteen main weathering forms are produced. They produced two maps, one for weathering form and one for damage category which takes the information from all the other categories and classifies it as either very slightly damaged, slightly damaged, moderately damaged, severe damage, or very severe damage.

2.4.2 Classification of weathering patterns at Culzean

A classification system was required to properly assess the material to be removed from the quarries and castle for analysis. Fitzner *et al.* (1995) was perceived to be a useful method on which to base a classification of the weathering features present at Culzean.

However, in order to characterise the stone at Culzean a simplified version of this classification system has been adopted and in particular three main detachment features have been identified from the list produced by Fitzner *et al.* (1995).

Table 2.1 Classification of weathering forms based on Fitzner *et al.* (1995)

1	2	3
LOSS OF MATERIAL OR FISSURATION	DISCOLOURATION OR DEPOSITS	DETACHMENT OF MATERIAL
Unweathered (U)	Discolouration (D)	Patina spalling (PS)
Fissures (FS)	Colouration reddy brown (RD)	Exfoliation or Contour Scaling (S)
Back weathering (W)	Colouration green-grey (GD)	Granular disintegration (G)
Outbursts (O)	Colonisation (B)	Scales to granular disintegration (SG) Spalling to contour scaling (SP)

Each of the categories outlined in Table 2.1 can be mapped out using shading (1), a colour (2), and a number (3). The results can be combined with a damage category. Individual samples were pinpointed for analysis and these have been characterised according to the method described above in Tables 2.2- 2.4 and Figure 2.4, which will be discussed in more detail below.

2.5 Sites on the building sampled and their state of decay

From visual evidence it was known that the building stone used by Robert Adam (especially on the Drum Tower balcony) was deteriorating more quickly than the original building stone (the foundations of the castle built in the 13th century) and the building stone used in 1879 to construct the West Wing of the castle. On this basis, three sampling sites were chosen on consultation with the NTS. Figure 2.1 and 2.2 provide a photographic elevation and plan of the castle and its grounds to show the locations of the three sampling sites:

- Adam's 'Drum Tower' balcony;
- Late Medieval seaward facing foundations of the castle; and
- the base of the West Wing constructed in 1879.

At each site, as great variability in aspect was sampled as the site permitted (Plates 17 and 18).

2.5.1 Adam's Balcony - stone from the Drum Tower

The Drum Tower balcony is a semi-circular seaward structure accessed from the music room by window. A wall about 1 m in height surrounds the balcony (Plate

Figure 2.1 Culzean Castle from the seaward aspect to show core sample location

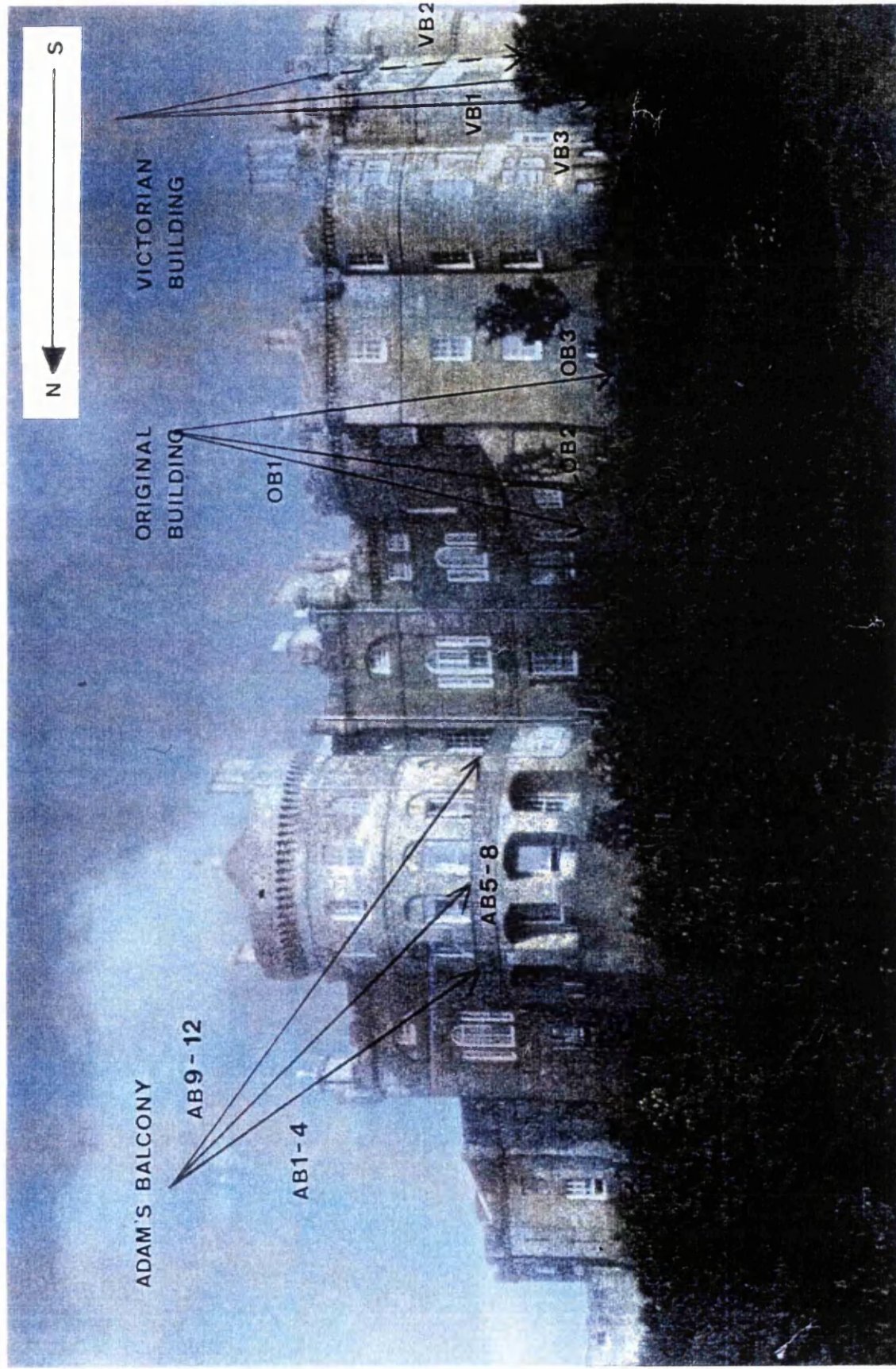
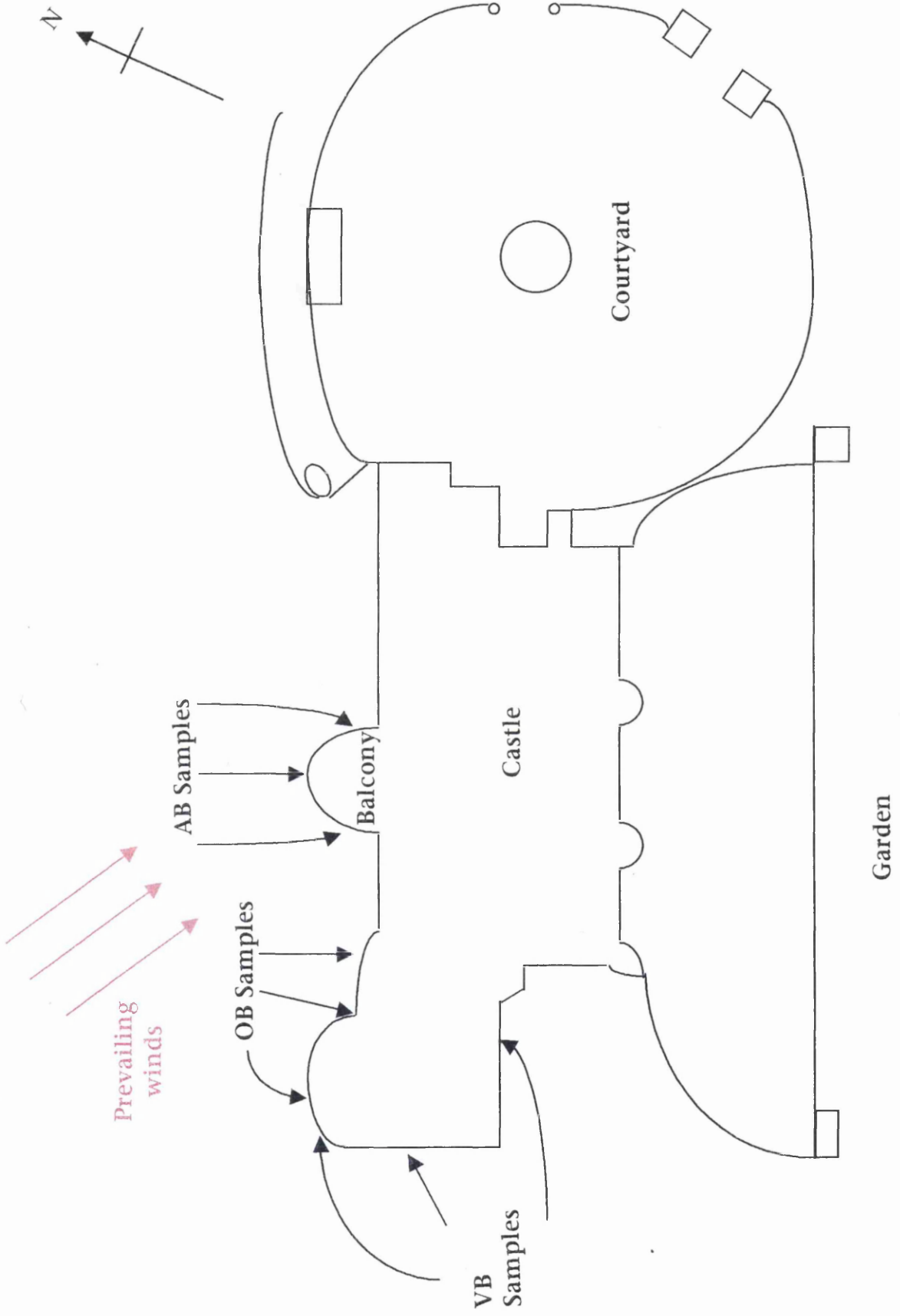


Figure 2.2 Sketch plan of Culzean Castle and coring sites



2). The stone above the balcony was the most decayed stone of the entire building, and thus in greatest need of restoration. The stones here are directly subjected to the prevailing South Westerly winds at a height of 10 m above sea level. The location of the cores drilled from the balcony can be seen in Figure 2.3.

These stones illustrated the maximum effects of, and the greatest differences in weathering at Culzean (Plates 12 & 13). For these reasons the NTS expressed the wish that research was concentrated on these samples.

The balcony stones chosen for sampling have been categorised according to Fitzner's mapping technique described above in Section 2.4. In addition, a simple descriptive classification system has also been adopted to highlight the principal decay feature identified and thus clearly differentiate between the samples. The results of this categorisation have been added to the Fitzner-style weathering classification system shown in Tables 2.2-2.4. This classification system divides the samples into three distinct categories:

- F_1 (**Fresh**) - The stone showed no external visible weathering. It retained its original tooling;
- P_2 (**Patina**) - The stone exhibited a patina, which may have been in the process of spalling and exhibit signs of exfoliation beneath; and
- C_3 (**Contour Scaling**) - The stone had lost its original surface and clearly exhibited a surface of contour scaling where layers of the stone, only mm in

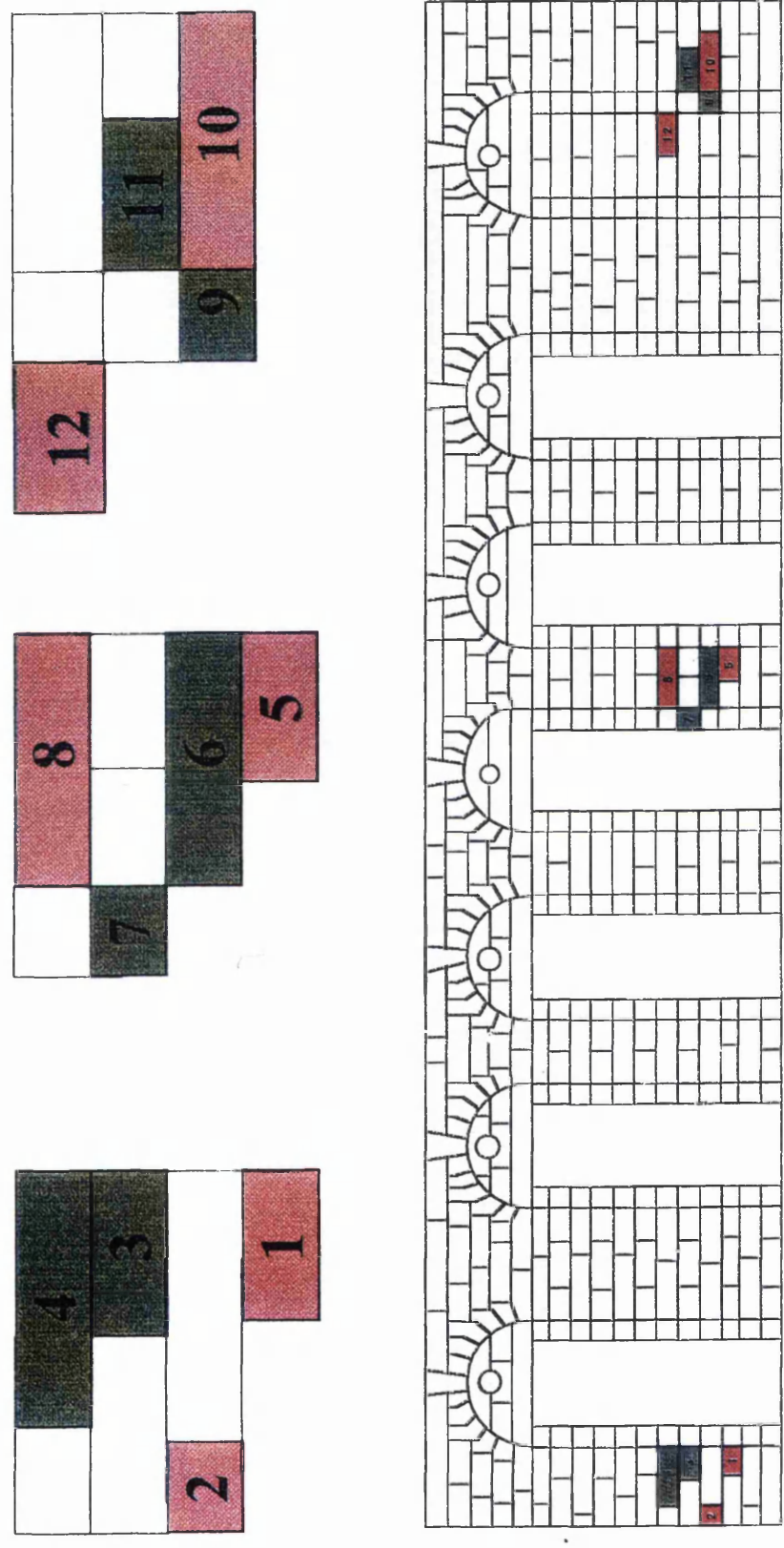
Table 2.2

Classification of weathering forms from AB samples

ASPECT	AB1	AB2	AB3	AB4	AB5	AB6	AB7	AB8	AB9	AB10	AB11	AB12
NORTH	X	X	X	X	X	X	X	X	X	X		
WEST												
SOUTH											X	X
DESCRIPTIVE CLASSIFICATION												
FRESH (F1)					X	X		X		X		X
PATINA (P2)												
SCALING (C3)	X	X	X	X		X	CEMENT		X		CEMENT	
FISSURATION												
U					X			X		X		X
FS		X		X			X		X		X	
W	X	X		X		X	X		X		X	
O			X			X						
DISCOLOURATION												
D	X	X		X	X	X	X	X	X	X	X	X
RD	X	X			X	X	X	X	X	X	X	X
GD												
B					X	X	X	X	X			X
DETACHMENT												
PS	X	X	X	X		X	X	X			X	
S	X	X		X	X	X		X	X	X		X
G	X	X		X		X		X	X	X		X
SG	X	X		X		X		X	X	X		X
SP			X			X			X			

Figure 2.3

Elevation of the Drum Tower Balcony to show position of stone blocks classified according to weathering criteria and from which cores were taken for analysis

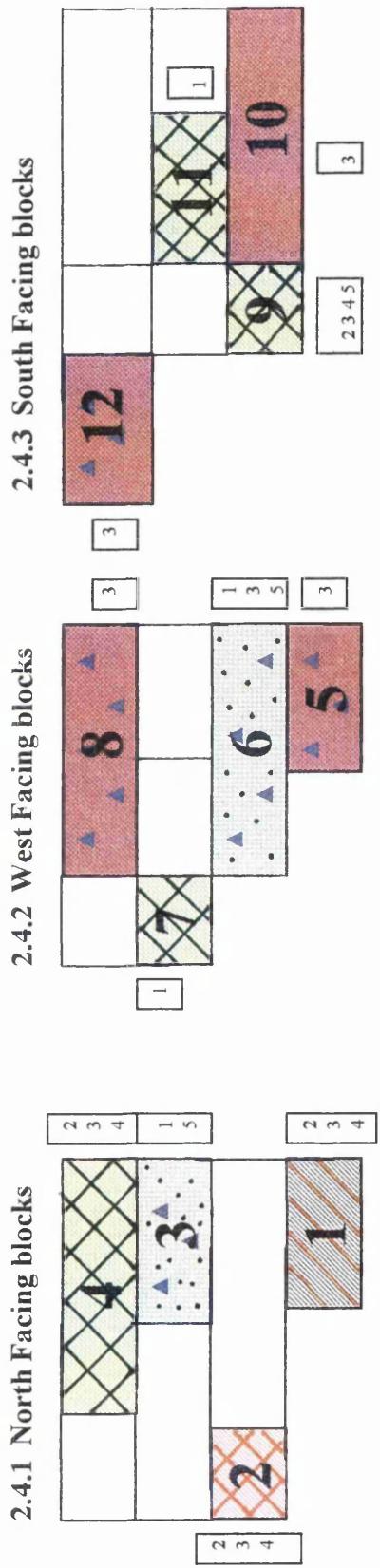


thickness, were falling away from the wall. There were numerous similar surfaces that lay parallel with the stone surface. There was an indicative increase in porosity due to loss of the stone's cementing material.

Some stone blocks were rendered with a cement mortar. Often the cement was seen spalling off with the patina attached. The condition of the material from which the balcony was made varied from completely exfoliated blocks to blocks still intact.

A distinct variation that could be seen in the stone on the balcony was its colour. The extent of variations in the LORS has already been described and this is an example of material removed from what is believed to be the same quarry and from different horizons within that quarry. The stones' surface colours could be split into two categories of a green-grey and a red-brown. These were believed to be surface weathering colour changes but were quite significant and readily differentiated on the building. The two colour ranges were assessed using the Munsell book of colour. The first ranged from an *olive-drab*(10) to *old-ivory*(8) (green-grey). The second was a *tan-sand* (6) to *ivory-straw* (8) (red-brown), possibly an expression of the state of the iron in the stone. It is possible that some of these were colour changes that had occurred since the stone had been emplaced on the building. This is of importance because visually the green-grey blocks were more decayed than the red-brown blocks. This may have far-reaching effects on the significance of colour and whether this alteration pre- or post-dates emplacement in the building. Colour variation existed through the cores and was not just a surface phenomenon, although the colour differential was more pronounced here.

Figure 2.4 Mapping of weathering classification on AB samples



Key

- | | | |
|-----------------------|--------------------------------------|--|
| Fissuration | U Unweathered | |
| | FS Fissures | |
| | W Back weathering | |
| | O Outbursts | |
| Discolouration | D Discolouration | |
| | RD Reddy - brown | |
| | GD Green - grey | |
| | B Coloured by organisms | |
| Detachment | PS Patina spalling | |
| | S Exfoliation/contour scaling | |
| | G Granular disintegration | |
| | SG Scales to granular disintegration | |
| | SP Spalling to contour scaling | |

Therefore, in order to make maximum use of the stone available for analysis, twelve stones were sampled from the balcony, varying in aspect, decay (surface properties) and surface colour. A detailed classification of their characteristics can be seen in Table 2.2 which includes the overall damage classification, and Figure 2.4 which makes the distinction between the stone's sampled. From Figure 2.4 it is apparent that a greater number of weathering features are observed on the stones from the North and West of the balcony than from the South, and the reddy-brown samples display surface weathering features, not exhibited by the South facing blocks. The green-grey samples exhibited weathering features throughout but there was less variation in the weathering styles of the samples taken from the South facing blocks. A large number of the samples exhibited more than one surface weathering style which is why the distinction between F1, P2 and C3 was made to simplify the weathering classification and provide a distinction between what appeared to be the three principal stages of deterioration.

2.5.2 The west wing of the castle constructed in 1879

The stone used by Wardrop and Reid to build the west wing of the castle did not vary in colour or degree of deterioration to nearly the same extent as those used by Adam (Plates 16 and 17). This was a much deeper red-brown sandstone, *tan buff* (6) - *wild rose* (2) (Munsell, 1929) and more uniform in nature. There were examples where the stones were decaying, but not to the same extent as those on the balcony. Characteristically the stones exhibited surface weathering features specifically:

Table 2.3

Classification of weathering forms from VB and VQ samples

	VB1	VB2	VB3		VQ1	VQ2	VQ3
ASPECT							
NORTH		X			X		
WEST			X				X
SOUTH	X					X	
DESCRIPTIVE CLASSIFICATION							
FRESH (F1)		X	X		X	X	X
PATINA (P2)							
SCALING (C3)	X						
FISSURISATION							
U		X	X		X	X	X
FS	X						
W							
O							
DISCOLOURATION							
D	X	X	X		X	X	X
RD	X	X	X		X	X	X
GD							
B	X	X	X			X	X
DETACHMENT							
PS							
S							
G	X						
SG	X						
SP							

- exfoliation/contour scaling;
- fissures and back weathering emphasising natural weaknesses in the sediment such as (cross) bedding; and
- removal of the occasional clast.

The latter two features would be expected in such a material with a fluvial origin. However, the stone was less exposed to the direct effects of the coastal wind and rain and had been in place on the building for a shorter period of time than that used by Adam.

Due to its current preservation and the fact that there were no plans to touch the stonework of the west wing in the near future only three cores were sampled from this location. Each core had a different aspect to include both seaward and landward orientations (Table 2.3). These sites were fairly sheltered, being low down in the building and protected from the elements to a far greater extent than the balcony stones (Plate 16). Table 2.3 describes each core in turn, identifying variations in the appearance of the cores. VB1 core showed evidence of surface fissures/scaling. All three cores showed some minor discoloration on the exterior surface.

2.5.3 Original Building -The Late Medieval foundations of the 13th century

This stone has been part of a building for the longest period of time and was the best preserved of all the building stones. The material showed little to no inherent deterioration, no pattern of decay and This building stone formed the plinth of the castle, the foundations on which Adam built Culzean. As such it was partly protected from the elements by trees, but there was the possibility of fluid up-take from the ground. This stone showed no external evidence for deterioration, but exhibited a patina where it was colonised by microbiological growths.

the tooling marks were still visible (Plates 14 and 15). Its colour was fairly uniform ranging from *ivory buff* (8) to *silver grey* (23) on the Munsell colour charts.

Three core samples were obtained. This was a more difficult task than previously, the resistant nature of the stone being clearly evident. Cores were drilled from the three different faces as for the other stones (Table 2.4). Sampling restrictions were similar to those experienced on the west wing of the castle. The characteristics of the three cores are detailed in Table 2.4.

2.6 *The Quarries and their Locations*

Quarries believed to be the source of the stone for the Culzean building were located with a view to sampling them, to provide comparisons between the weathering

Table 2.4

Classification of weathering forms from OB AND OQ samples

	OB1	OB2	OB3		OQ1	OQ2	OQ3
ASPECT NORTH WEST	X	X	X		X	X	X
DESCRIPTIVE CLASSIFICATION FRESH (F1) PATTNA (P2) Organic	X	X	X		X	X	X
FISSURATION U FS W O	X	X	X		X	X	X
DISCOLOURATION D RD GD (MORE GREY) B	X	X	X		X	X	X
DETACHMENT PS S G SG SP				No visible expression deterioration			

characteristics on the building and the quarry. Differences, if they emerged, might suggest the prime decay mechanisms particular to the building. Descriptions of the quarry sites are recorded below, and where appropriate weathering features have been recorded.

An investigation with the help of the NTS was undertaken to locate these quarries. Unfortunately, the NTS possessed only a limited set of records on the history of the Culzean Estate, as it has only been owned by the NTS since 1945. The original records belong to the Estate Benefactor of Culzean who did not allow access to the records and did not provide any information on the building for the purposes of this research. Accordingly, contemporary Ordnance Survey maps in the University of Glasgow Library, dating back to the middle of the nineteenth century, were used to locate former quarry sites.

2.6.1 The Ballochnie Quarry

(Grid Reference 224 065)

After much investigation of possible quarry sites throughout the area, it was believed that material to build Adam's Culzean was obtained from a quarry at Ballochnie, near Girvan. Cores were sampled from the only accessible faces in the former quarry; now overgrown and filled with water.

The former quarry site was completely overgrown with trees and shrubs, nettles, ferns, mosses and other plants. There was evidence of very red soils. A lot of the stone had been weathered out to soil. Tree roots and soil creep had weakened the outcrop along bedding/layering and disturbed material loosened by quarrying to encourage extensive weathering. The thickness of the beds varied from 20 mm to 200 mm in width.

The only accessible outcrop of a 'reddy' surface colouration and surrounded by red soils was sampled 180 cm from the plant line/outcrop base from a strata facing West-North-West. There was evidence of leaching with whitening and reddening on the surfaces of the outcrop which exhibited horizontal bedding, and was well bedded. The sandstone itself was less well sorted with medium-large grains and a high carbonate content.

However the material obtained was no match in colour or mineralogy for that of the Adam's balcony stone. There could be two possible reasons for this:

1. the exposed area of the quarry which was sampled is geologically different to that from which the stone was originally taken; or
2. the stone was not taken from Ballochneil, i.e. it is the wrong quarry.

As a result, research undertaken on the balcony stone has not been compared with stone from the Ballochneil Quarry.

2.6.2 The Quarry used in 1879: St Murray's, Maybole

(Grid Reference 305 113)

The quarry used by Wardrop and Reid was far easier to locate from the list of alternatives. This distinctive red-brown micaceous sandstone has been used to build many of the houses in the local town of Maybole (Plate 10).

This was still quarried for small amounts of stone for restoration work until 1996 when it was turned into a driving range but many of the surfaces showed tool markings as if freshly cut. One of the surfaces, facing Eastwards, had not been cut, and was streaked with surface staining and also colonised by microbiological growth.

In order to ensure sampling of a range of lithologies, three cores were taken from strata on three different faces of the quarry, but not from the face where quarrying had been undertaken in recent years. One sample was taken from the South West face of the quarry, one facing South-South-East and one facing East-South-East, all the faces looked in on each other like three sides of a box.

The outcrops here were massively bedded with intermittent examples of thinner layering/bedding. The stone was medium grained and red in colour. There was some evidence of scaling but not as much as seen at the quarry on the Culzean Estate (see below) because the location was sheltered and not a coastal environment.

The face from which the first sample was taken had a patina of hematite, with super-reddening of the surface. It also showed evidence of leaching with white streaks of

carbonate on the surface. The core was taken from a massive lens 120 cm wide at a point 88 cm from its base. Above this lens there were a number of good examples of cross bedding, some slumping features, and some finer laminated sills, lichen growth inhabiting the sills as yellow and green patches.

The second sample was taken from an outcrop where the wall of the quarry faces South-South-East whilst the face of the outcrop faces East-North-East, in a bed 108 cm thick. The sample was taken from a spot 120 cm from ground level. There were extensive areas of lichen growth evident, yellow and white staining, but less leaching than on the previous face. The bed contained evidence of veins, fractures and fluid pathways. However, it appeared to be better cemented than the first sample.

The third sample was taken from another massive lens of sandstone facing East-South-East. The lens was 80 cm in width and 1m from the visible base of the outcrop. Above this lens there were examples of cross-bedding and leaching much the same as in the first sample. However the surface weathering appeared different, not as red in colour but more leaching, biological growth and carbonate weathering. There was evidence of the differential weathering of the iron nodules. There appeared a more readily weathered band of iron 20 cm from the location of the core sample. The classification of their weathering forms has been outlined in Table 2.3. This stone has been compared with that analysed from the West Wing.

2.6.3 Home Farm, Culzean Estate

(Grid Reference 234 104)

The original building was constructed using material retrieved from the cliffs beneath what was 'Home Farm' and is now the estate's Visitors' Centre. Although the shoreline consists of volcanic lavas, there are sandstone cliffs cut back not by the sea but by man. The samples here could be directly compared with those of the original building, resistant in nature and difficult to extract.

The outcrop, not recently quarried, was sheltered beneath foliage, now overgrown and much of the material colonised by moss and other higher plants.

The features evident were different to those seen at the Maybole quarry. The stone was medium grained and well sorted, but it was difficult to distinguish many lithological features on the weathered surface where considerable alteration had taken place. There was evidence of surface colouration, a reddening from iron mobilisation, and whitening from the immobilisation of carbonates, which, with the aid of fluids passing down the outcrop, had streaked the rock.

Microbiological growths were in abundance, including both white and black crusts of lichen, and greening, particularly along bedding planes and cracks. In addition there was the differential weathering of the iron nodules and some had been weathered out completely. These nodules were concentrated in major strata in near-horizontal bedding.

Three samples from adjacent faces were cored (Plate 11). Samples one and two were taken from a lens of massive sandstone. The first core was taken from the top of a massive lens of sandstone, a West-facing outcrop, 1 m from the base of the outcrop. The second core was also taken from this bed and again 1 m from the base of the exposed outcrop, but from the centre of the lens facing Westerly. The bed from which these two samples were taken was 120 cm in width to current ground level (which may not be the bottom of the bed but provides an estimate from what is exposed). The third core was taken from a North West facing block which showed evidence of spalling (3 to 5 mm pieces) but not on the sample itself, 1m from the outcrop base and in a more sheltered position under an overhang. This core represented a more bedded sample because it was higher up in the rock strata, although, at the same height from the present ground level. This was 130 cm above the other two samples in the succession. There was more carbonation between layers and surface staining.

There were variations in the weathering features of the three samples, particularly between the two taken from the massive lens and the other more bedded example. The more bedded/layered the rock, the greater the surface observation of weathering features/detail, especially carbonation and reddening but no differential of small-scale weathering could be made.

Classification of the weathering forms of the three cores has been outlined in Table 2.4. Although none of the three samples exhibited surface weathering features, all three samples were discoloured at the surface, particularly by organic matter due to their location at the base of the cliff.

2.7 Sampling summary

The sampling of the building and associated quarries was paramount to the success of the research. Despite the sampling constraints on the building, which allowed for only a small number of cores to be drilled, it was believed that a representative sample had been taken to accommodate for variations in stone type, weathering feature, aspect and microclimate. From these samples the following points are highlighted:

- the balcony walls showed the greatest deterioration on the building and the greatest variation in weathering features. As such twelve cores were taken in an attempt to provide a representative sample of the variations in aspect, stone colour and weathering type;
- there was some correlation between stone colour, aspect and weathering style of the balcony stones sampled. The reddy-brown stones exhibited no surface weathering features on the South and West facing parts of the balcony. The green-grey samples exhibited weathering features throughout but there was less variation in the weathering styles of the samples taken from the South facing blocks;
- the extent of weathering of the stone on the west wing, constructed in 1879, and original 13th century building faces was much less compared with the balcony

stone and showed little variability. As such aspect was more important when deciding where to take the three samples from each face;

- the quarry faces and their weathering features varied greatly from each other and from those of the building due to their aspect and use. The quarry at Balochneil, believed to be the source of Adam's building stone, showed no accessible material mineralogically similar to the building stone; and
- preliminary visual investigations gave an understanding of how the stone, especially the balcony stone, was breaking up but not why it was doing so. There were no visible surface salts, no visual immobilisation (e.g. iron and carbonate streaking as seen for example on the quarry faces), and no visible surface water retention.

Chapter Three

Analytical Methods

3.1 Introduction to analytical methods

This chapter provides a summary of the strategies for the laboratory work undertaken and a description of subsequent analytical methods used to study the core samples, described in the previous chapter. The methods were used in such a way as to achieve a maximum amount of knowledge with the scarce material available.

3.2 Investigative strategy for laboratory work

3.2.1 Previous Work

The principle aim of this research was the investigation and thus recording of degrees of weathering. Researchers in the past achieved this using simple criteria. For example, the use of colour or degree of colouration - hue, value, and chrom, as shown on Munsell colour charts and recorded for all the samples in *Chapter 2*. Soil Scientists, geomorphologists (Ruxton, 1968; Ollier, 1984) and engineering

geologists (Fookes & Horswill, 1969; Little, 1969); Fookes *et al.* 1971) have all adopted qualitative scales for classifying weathering profiles and degrees of weathering. However, these are generally inappropriate when looking at a building because there are far too many mechanisms involved to characterise the weathering process according to colour, loss of material and debris analysis.

It has already been hypothesised that there are a number of different mechanisms at work on the building stone, and as such, the approach required when looking at a building is that of a micro scale. As a result chemical and petrographical analyses are the dominant methods used.

Previous petrological approaches to weathering have often involved the microscopic analysis of thin sections and the evaluation of imagery from scanning electron microscopy; for example Pavia Santamaria (1994), in a petrographic study of the Antiguo de Logrono, Rioja. Associated X-ray diffraction and differential thermal analysis of materials have identified the minerals present in a weathered material, including the nature of clay minerals (Huggett & Uwins, 1994; Zhang & Wang, 1992). Chemical analysis, the use of atomic absorption and ion chromatography has illuminated the nature of weathering products in a sample, particularly in the case of atmospheric pollutants (Tennent *et al.*, 1993). Data from many rock properties may be used comparatively to reveal weathering changes.

3.2.2 Proposed analysis of the Culzean Stone

The following were highlighted as the anticipated weathering mechanisms. For each of these mechanisms, one or more appropriate methods of analysis were chosen from the experimental equipment available to best examine the principal deterioration mechanisms believed to be present:

- **salt weathering** (crystallisation and expansion) was believed to occur in the weathering of the stone at Culzean due to its exposure and the proximity of the building to the sea (and thus the accessibility of soluble salts from seaspray and wind-driven rain). Therefore, it was necessary to ascertain which salts species were present, the depth to which they had penetrated and their concentrations. X-ray diffraction analysis was required to examine salt species whilst ion chromatography and atomic absorption and emission were used to profile the quantity and depth of these salt species;
- **clay expansion** was also believed to be a likely factor in the breakdown of the stone possibly through hydration and ionic exchange. X-ray diffraction was again required to distinguish the different clay species and microscopy (particularly the scanning electron microscope) to examine the effect expansive clays were having on the other minerals present;
- associated with this and observed in the field was the **dissolution of minerals** particularly the loss of the stone's natural cement. Optical microscopy, the

scanning electron microscope, and cathodoluminescence were pinpointed as methods of analysis for this important process; and

- obtaining information on mineral, textural and chemical changes within the stone was paramount in understanding the depth to which fluids may be penetrating and the effect increased porosity and permeability at depth may be having on the stone. Therefore, in addition to specifically looking for evidence of salt crystallisation, clay expansion and cement dissolution, evidence for variations in porosity and mineral instability were also examined. SEM and optical microscopy were used as optical methods. X-ray fluorescence spectroscopy, the only bulk chemical analytical method available, was used to identify any changes in chemistry through the stones' profile.

3.3 Sub-sampling methodology

The core sample had to be divided so that different analytical techniques could be used to build up a profile for the stone. The cores were held in a clamp and cut by hand, using a hacksaw blade. They were divided into quarters lengthways (Plate 23) and then sliced horizontally as indicated in Table 3.1 so that each core could be prepared for analysis in the four ways as follows:

- X-ray diffraction (XRD) analysis;

Table 3.1
Division of cores for geochemical analysis - using AB1 as an example

	Number	Depth mm	
XRF	AB1/1	00-10	AA Atomic Absorption and Emission
IC	AB1/2	10-20	AAw Atomic Absorption and Emission of water extract
AA	AB1/3	20-30	CL Cathodoluminescence Microscopy
	AB1/4	30-40	IC Ion Chromatography
	AB1/5	40-50	ICw Ion Chromatography of water extract
	AB1/6	80-90	OM Optical Mineralogy
	AB1/7	120-130	SEM Scanning Electron Microscopy
SEM	AB1/1	00-30	XRD X-ray Diffraction
CL	AB1/2	30-60	XRF X-ray Fluorescence
OM	AB1/3	60-90	
	AB1/4	90-120	
	AB1/5	120-150	
XRD	AB1/1	00-30	
AAw	AB1/7	120-150	
ICw			

- to produce polished thin sections for use on the scanning electron microscope (SEM), cathodoluminescence microscopy (CL), and point counting on an optical microscope;
- X-ray fluorescence spectroscopy (XRF) & ion chromatography (IC); and
- Ion chromatography, Atomic Absorption (AA) and Atomic Emission (AE) to analyse material extracted from the stone using HPLC and rainwater.

It was imperative that sample preparation and the techniques used would in no way alter the chemical make-up of the stone to be analysed. It was important that no water was to be used in any of the preparation processes.

This presented many difficulties, as most of the techniques used in the laboratories require a lubricant such as water. As a result, at each step an alternative had to be found. Each technique has been described in Section 3.4.

3.4 Instrumentation

This section provides detailed information on the experimental techniques used, including sample preparation methods, experimental parameters and an indication of the perceived precision and accuracy of data collated.

3.4.1 XRD techniques

XRD analysis was undertaken using a Phillips PW 1050/35 vertical goniometer, Co K α radiation 1.7902X. 40 Kv 20X.

The XRD technique provides a profile dependent on atomic structure and to a lesser extent on chemical composition. The diffractometer printout consists of a number of peaks of different intensities. It was then necessary to identify the major peaks, and thus the main constituents of each sample (Hall, 1994).

To prepare samples for XRD analysis a small amount of the following were used:

- A* whole-rock sample;
- B* soluble salt-precipitate sample; and
- C* clay-fraction sample.

3.4.1.1 Type A

The whole rock samples were ground to a fine paste or slurry with acetone. They were then pasted onto a glass plate to form a 'smear mount' for analysis and allowed to dry before being loaded into the diffractometers.

Whole rock analysis is run at:

- 4° - 60° 2 θ

- $2^\circ 2\emptyset/\text{min}$
- Chart 1 cm/min
- Range 2×10^2

3.4.1.2 Type B

The soluble salt and carbonate content was analysed from a quarter-lengthways core, broken down into grain size fragments by crushing. This was placed in a beaker and rinsed through with deionized water to allow dissolution and settling for 12 hours. The remaining solution was then siphoned off, centrifuged for 30 minutes, before being evaporated on a hot plate at 50°C allowing the soluble salts and carbonates to reprecipitate. This process was repeated until all soluble matter had been extracted and the precipitate was then placed on a cavity mount, sitting in an aluminium 'window'; a technique which reduces the preferred orientation of the fine salt particles (Hall, 1994).

Clays are run at conditions of:

- $4^\circ - 16^\circ 2\emptyset$
- $1^\circ 2\emptyset / \text{min}$
- chart 1 cm/min
- range 4×10^2

3.4.1.3 Type C

The sample remaining after 'type *B*' extraction was divided between two, 100cm³ cylinders and filled with deionized water. 15 ml of calgon was added to each cylinder to allow the particles to disaggregate fully. The cylinders were shaken and the particulate matter allowed to settle over a period of 80 minutes (for clay 10 microns or less to be collected). The top 10 cm of solution were thus siphoned off and placed in a centrifuge for 30 minutes allowing the clay particles to settle. This process was repeated until all the clay of this particle size had been obtained. A concentrate of either <2 or <10 microns was obtained by centrifuging water containing the clay particles in suspension after a prescribed settling time (Stokes Law). The clay fraction was analysed on 'sedimentation mounts'. The slurry was pasted onto a ceramic slide and gently shaken to enhance the preferred orientation (Hall, 1994).

Analysis of the clays by diffractometer involved four stages. Initially, the sample was air-dried to give the basal spacings and to distinguish between the four principle clay mineral groups:

- Kaolinite 7Å

- Illite 10Å

- Smectite 12-15Å

- Chlorite 14Å

However to distinguish between smectite and chlorite minerals, the sample was treated with ethylene glycol and returned to the diffractometer. This treatment causes the smectite to expand from a basal spacing of 10Å to 17Å.

Following this treatment, the clay mineral samples were subjected to a heat of 300°C, a temperature that collapses smectites and illite-smectites to 10Å yet does not affect other clays. Finally, the sample was heated to 600°C, destroying the kaolinite and some chlorite species (Hardy & Tucker, 1988).

The main limitations of this method, especially when attempting to study clay characteristics are that mixtures of silicates proved difficult to characterise as many of the important peaks overlapped. Variations in chemical composition of, for example, illite, smectite, chlorite, and their intermediaries made identification difficult, as did variations in the compositions of the carbonate cements. Optical microscopy and SEM was also used to examine the clays.

3.4.2 Scanning Electron and Cathodoluminescence Microscopy

Initially a number of stained thin sections were made for use with the optical microscope, primarily for point counting. The remainder of the slides made were polished thin sections so that they could be used on the SEM and CL (Table 2.4).

3.4.2.1 Scanning Electron Microscopy

The SEM used was a leomicroscopy stereoscan 360 integrated link analytical AN10855 energy dispersive microanalyser, with resolution limits of a maximum of 4 nm, running at 7 nm. The X-ray microanalysis was undertaken at a probe size of 1 to 2 microns.

The SEM was used to examine both rock chips (sputter coated in gold) and polished thin sections at high magnification, to look at variations in the profile and to directly compare the exterior and interior of the sandstone cores. The 'rock chips' consisted of either the soluble salt-precipitate or the clay residues, also analysed by XRD. A large number of photographs were taken to provide pictorial evidence and to complement the chemical investigation undertaken.

These analyses and some of the thin section work involved the use of the EDS, or 'energy dispersive X-ray analysis system', allowing analysis of a particular point of around 1µm diameter for its chemical composition. A program was written to automate this process so that, for example, one hundred carbonate cement points could be stored and subsequently chemically analysed whilst the machine was not being utilised. This facilitated an investigation of compositional chemical variation within one mineral species to a reasonable degree of accuracy.

A major portion of work done on the SEM called for the use of BSE (back scattered electrons) processing. This involved atomic number contrast imaging, to produce a

grey-scale image corresponding to the varying atomic numbers of the minerals present in the stone. The use of such a method was dictated by the need to look at variations in the physical make-up of the stone e.g. an increase in mineral dissolution towards the surface of the stone. The method was used to achieve a modal analysis by image processing.

A profile through the core was created by cataloguing the proportions of mineral types present (much like optical point counting techniques but at a higher magnification and with greater accuracy). The following categorises (according to atomic number) were made:

- quartz;
- lithic fragments and feldspars;
- carbonate (cement);
- clay minerals; and
- pores.

Difficulties arose when analysing pores as a percentage of the sample. The nature of the stone caused it to crumble, often during the thin section preparation. Also, no clear distinction in atomic number could be made between feldspars and lithic fragments.

For each thin section, twenty frames were analysed for each of the above categories, an example of which is provided in Figure 3.1. A histogram was produced charting

Figure 3.1 An example of SEM BSE Imaging Atomic number contrast

An image from OB3 to show how SEM is used for measuring the compositional variation of a core sample



the relative quantities of the different variables (minerals of the same atomic number) in each frame. The process often required more than one histogram per frame. The information could then be transferred from the SEM and converted to 'adobe photoshop' on the Apple Macintosh from where Figure 3.1 was processed. Results demonstrated in the text are validated by the calculation of standard errors, which are represented by error brackets on the graphs.

3.4.2.2 Cathodoluminescence Microscopy

Carbonates were examined by looking at polished thin sections (mounted using heat-resistant epoxy resin and not cover-slipped) under a cathodoluminescent microscope. Cathodoluminescence (CL) results from "excitation by electrons" (Miller, 1988); a process which gives carbonate minerals, for example, a bright and stable luminescence. The CL instrument used is a Technosyn Model 8200 Mk II with an "Autohold" attachment. The microscope on which it was mounted is a Carl Zeiss Axioplan fitted with Leitz objectives in order to achieve the long working distances necessary for the vacuum chamber. It was run at 15-20 kV with a gun current of 250-300 μ A. Photographs were taken using a Zeiss MC100 automatic camera.

CL emission is generated only in the top few microns of a sample and it is responsive to certain minor compositional or structural contrasts at mineral or grain boundaries. CL can reveal growth zonation in otherwise clear minerals that give information on factors such as fluid movement, fluid composition, crystal growth rates and dissolution effects.

The presence of activator elements (i.e. luminescent colour triggered off by the presence of specific elements) can be linked to the geochemistry of precipitating fluids. CL can be used to determine cement stratigraphy and diagenetic history of the stone (Walkden, 1994).

CL was used to examine the carbonate cements within the building stones to build up a brief cement stratigraphy. It was important to identify the habit and overall structure of cement phases; to determine periods of crystallisation and growth history; and recent dissolution/reprecipitation and corrosion of other minerals if apparent. The CL was also used to identify the character and abundance of carbonate concretions (concentrations of carbonate cement), characteristic of many of the LORS sediments.

3.4.3 Optical Microscopy - Point counting

Point counting was undertaken from a number of the polished thin sections (impregnated with a dye-resin), as it is the most widely used technique for estimating quantitatively the composition of rock samples in thin section. In this case it was important to make distinctions between the sandstone types. The method used was the Glagolev-Chayes, the standard method (Stanton & Wilson, 1988). An orthogonal grid, which allows a linear traverse to be subdivided into short segments of equal length, was superimposed over the thin section. The traverse line is followed and a record of the composition of the constituent located at each grid intersection recorded. A Swift electronic counting system was used.

This consists of twelve data recording channels which tallies raw counts, computes percentages, and drives an electronically-triggered mechanical stage. Seven channels were used to record quartz, feldspar, lithics, calcite (and other carbonate material), micas, pore space, and unknowns. The grid size was selected by examining the thin section to ensure that the grid size was larger than the coarsest grain, to avoid correlated observations. This selection did not take into account the size of the carbonate concretions.

There were two principle drawbacks of the point counting method in this research:

- the mineral grains and cement, particularly near the surface, were so weathered that it was often difficult to distinguish between grains; and
- the friable nature of the samples, particularly near the surface of the stone, meant that some samples cracked during the thin section preparation, which could distort the pore space recording.

3.4.4 X-ray Fluorescence

X-ray fluorescence (XRF) analysis was undertaken using a Phillips PW1450/20 automatic X-ray fluorescence spectrometer equipped with a sixty position sample changer and on-line 'SuperBrain' microcomputer for data processing. The calibration of coefficients is established routinely from internal (departmental) standards with continual checks of accuracy against international standards. The

detection limits for the major and trace elements have been tabled in *Appendix 1*. Results presented in the text are validated by both standard errors and analytical errors, which have been combined and added to the graphs in the form of error brackets.

XRF analyses the quantities of individual elements and expresses them as oxide weight %. It does this by bombarding the sample with high energy X-rays that emit secondary radiation with intensities and wavelengths dependent on the elements present. Measurement of the intensity of the characteristic radiation for a particular element provides a concentration value (Fairchild *et al.* 1988). Standards are used for calibration purposes and the results are obtained as a percentage for the majors, and in parts-per-million (ppm) for the trace elements.

To prepare samples for XRF analysis the cores were sliced using a hand saw as shown in Table 3.1; seven slices from each core. Only a small amount of material was required for each analysis. Each sample was sliced to a width of 5 mm to allow enough material for major and trace elemental analysis:

- the fused beads for major elemental analysis; and
- the pressed powder pellets for trace element analysis.

Both methods of preparation required the sample to be crushed by hand (using a hammer so as not to contaminate the sample), and then placed in a ball mill to be

ground to a fine powder. Once this was done the individual samples were divided to evaluate major and trace elements from within that single sample.

3.4.4.1 Fused bead preparation for major elemental analysis

Once samples were prepared, individual glass bottles were placed in an oven for 24 hours to completely dry. Rock powder (0.3750g) and SPECTROFLUX 105 (2 g) were placed into numbered platinum crucibles and mixed. The crucible was then covered with a platinum lid, and placed in the furnace at a temperature of 1000°C for 30 minutes before being left to cool on an aluminium surface.

The first rock-flux mixture was then re-melted over a Bunsen burner, making sure that all bubbles were removed and no droplets remained on the sides of the crucible. The bead used in analysis was formed by first raising the plunger assembly on the first of two hot plates. Next molten glass was poured into the centre of a platen, and the plunger allowed to lower firmly. The plunger was then raised and the platen and bead placed onto the second hot plate in the centre of an asbestos block. The bead was then left on this hot plate for approximately 10 minutes before being allowed to cool on the aluminium surface. Finally the bead was trimmed using a pair of small blunt scissors and labelled ready for analysis. Each sample was made in duplicate.

3.4.4.2 Pressed powder pellets for trace elemental analysis

Rock powder (6g) and RO 214/1 (phenol formaldehyde) RESIN (1g) were weighed out and placed into clean vials. A small glass bead was added to each, the lid was replaced and the vial labelled. The two powders were then mixed for 30 minutes in a spexmixer. After mixing, the contents of the vials were emptied onto glossy paper, one at a time. The glass ball was removed using a spatula. The platens and former casing for the 30 tonnes press were then assembled. The base plate of the former casing was attached, and the bottom platen dropped into position. The powder was then poured into the former followed by the upper platens and the plunger. The complete former was then put into the centre of the press platform and the top of the plunger aligned with the plunger.

The pressure was then raised to 25 tonnes and maintained for approximately 1 minute before being slowly released. The pellet was then removed by taking away the base plate of the former and standing the rest of it on a customised plastic cylinder. The former was then put back on the press and pumped until the pellet fell from the casing. This was then labelled on its side and placed on an asbestos block in the oven for 20-25 minutes to cure the resin. On cooling the pellets could be analysed.

3.4.5 Ion Chromatography

This work followed on directly from the XRF profiling undertaken. The remaining rock powder was used for a quantitative and qualitative analysis of anions (water-soluble salts) present in the stone profile by ion chromatography.

This method of analysis is a form of ion exchange chromatography used for the separation and determination of inorganic anions and cations. A Dionex DX500 ion chromatography system was used, comprising an AS40 Autosampler, GP40 gradient pump, ED40 electrochemical detector in conductivity mode, and a data acquisition system using Dionex Peaknet software. An Ionpac AS11 (4 x 250 mm) separator column and AG11 guard column were used.

The most recent development in this form of analysis is the SRS or self regenerating suppresser (ASRA-1 suppresser running at 300 milliamps) which uses a combination of electrolysis and ion exchange membrane dialysis to remove the eluent ions, greatly improving the signal to noise ratio for conductivity detection.

In the anion SRS at the anode, H^+ ions are generated and pass through the cation exchange membrane into the eluent stream where they react with the hydroxyl ions to produce water. Sodium ions are attracted through the cation exchange membrane towards the cathode where they are paired with hydroxyl ions produced by electrolysis at the cathode and swept away to waste. This converts the anions in the

eluent to their hydrogen (acid) forms in a high quality water matrix with low background conductivity. The equivalent cation suppresser works in a similar way.

Simple inorganic anions were separated by gradient elution with sodium hydroxide (NaOH) where the order of elution was determined by the relative affinities of the ions for the resin, compared to the hydroxyl ion.

The elution conditions were as follows:

- a flow rate of 2 ml per minute;
- isocratic 5 mMolar NaOH for 1 minute;
- a linear gradient up to 30 mMolar NaOH in 9 minutes; and
- isocratic 5 mMolar NaOH for 5 minutes.

A low concentration of NaOH allows separation of ions such as fluoride, acetate and formate, with a low affinity for the resin. With increased NaOH concentration, sulphate, phosphate and citrate, which have a much greater affinity for the resin, are separated. The components calibrated for this experiment were 20 mg/litre fluoride, chloride, nitrite, bromide, nitrate, sulphate, and phosphate (Flowers, 1995).

The limits of detection and/or quantification vary with the method and how it is set up. The limit of quantification is perhaps the more useful. The method used for these samples was designed for chloride, nitrate and sulphate in the 0 to 20 mg/litre

range giving a limit of quantification for these macro constituents of the order of 1/200th of the highest standard, i.e. 0.1 mg/l Cl, nitrate-N and sulphate-S. The minor constituents (F, Br nitrite-N and phosphate-P) were also measured but the system was not optimised for these. As these were present at low concentrations a limit of quantification of 0.01 mg/litre is reasonable. Limits of detection for the system are approximately 0.002 mg/l for all except Br for which 0.01 mg/l is more reasonable. This refers only to the analytical step and does not make any allowance for extraction.

The sample preparation method used was adapted from a method described in a paper by Steiger *et al.* (1993).

Already reduced to a fine powder in a ball-mill, a 1g sample was weighed out and added to 100 ml of HPLC, high performance liquid chromatography (bidistilled) water for elution. The bottle was then mechanically shaken continuously for 1 hour before centrifuging. The solution was then filtered by sterile syringe through a 0.2µm cellulose acetate mesh into a 25 ml scintillation vial prior to injection into the chromatography column. All samples awaiting analysis were stored in a refrigerator and no sample was stored for more than 24 hours prior to injection.

The ion chromatography method was also used in the analysis of water samples from the water extraction experiment. In this instance core samples were split at a depth of seven cm from the surface of the stone. The further most ends of each half were then suspended in a 250 ml beaker in 25 ml of HPLC or rainwater (collected from the meteorological centre at Culzean) for 3 hours (this time was calculated to

be the most suitable period for analysis). After 3 hours, 5 ml of the solution was filtered by sterile syringe through 0.2 μm cellulose acetate meshes into scintillation vials for IC analysis, whilst the remaining solution was filtered by the same method into conical flasks for AA and AE analysis.

3.4.6 Atomic Absorption and Emission Spectrophotometry

The atomic absorption spectrophotometer used was a Smith-Hieftte 12, a double beam instrument with background correction facility.

Each element required different instrumental settings e.g. lamp current, wavelength, band pass and gas mix tube (See *Appendix 1*). Na^+ and K^+ were run on emission mode and as such do not require a lamp.

Atomic absorption (AA) and emission (AE) have been used as techniques for elemental analysis of the surface of the sandstone as well as water in the 'water-extraction' experiment. AE analysis involves passing light with the distinctive spectrum of an element through a flame in which the atoms are present. In AA a lamp is used to supply the radiation, with the cathode made of the element whose spectrum is required. Potassium and sodium do not require a lamp, as the flame itself is sufficient to excite the electrons. This is known as AE.

When the atoms are of the same element, there is a reduction in intensity (as absorption occurs), of a particular wavelength. According to Beer's law, the amount

of light absorbed depends on the concentration of the element in the vapour (Fairchild *et al.*, 1988). Samples must be in solution and the AA is calibrated using standards over a range of concentrations before injecting the unknown samples into the spectrophotometer.

For the analysis of rock powder, the samples were crushed using a hammer, and then crushed by hand with a pestle and mortar; because of the nature of the samples the ball mill was not required.

The samples were weighed (0.5g) and placed in PTFE beakers, since hydrofluoric acid etches glass. 70% ARISTAR grade nitric acid (5 ml), 70% ARISTAR grade perchloric acid (1 ml), and 40% ARISTAR grade hydrofluoric acid (10 ml) were added to each beaker, and swirled gently to ensure that all the powder was accommodated within the liquid. Three 'blanks' of the solution were also made up.

The beakers were then covered with a PTFE lid and placed on a hot plate at a temperature of 120°C for three hours to allow the resistant minerals to be attacked by the acid solution. Once the 3 hours had elapsed, the beakers were uncovered and heated for a further 3 hours at 160°C to allow the remaining hydrofluoric acid and nitric acid to evaporate. Following this, samples were left overnight at a temperature of 210°C to evaporate off the residual perchloric acid, resulting in a dry residue.

The next day, 50 ml of 5 % ARISTAR grade hydrochloric acid solution were added to the beakers which were then heated to 50°C for half an hour on a hot plate to

dissolve the solute. Once dissolved, the solutions were filtered through funnels with fine paper and made up in volume to 100 ml, ready for use in the AA process.

When analysing solutions from the water extraction experiment, no chemicals were required as no rock powder was involved (the stone was not powdered because the experiment was undertaken to see what could be extracted from the stone by water, not the total content of soluble material in the stone). The filtered solutions could thus be injected straight into the AAS for analysis, as outlined. The detection limits are tabled in *Appendix 1*. Results displayed in the text from the AA, AE and IC work are validated by triplicate errors i.e. variations in the results of three analyses of the same sample have been calculated and inserted in the form of an error bracket.

Chapter Four

The properties of the Culzean stones

4.1 Introduction

The weathering of building materials, as discussed in *Chapter 1*, is defined as a change in colour, the corrosion, or the degradation of a building material after exposure to rain, frost, pollution, salt air, ultra-violet etc. (Maclean & Scott, 1993). In geomorphological terms it is the breakdown and decay of rocks *in situ*, giving rise to a mantle of waste or loose debris that may be removed by the processes of transport (Small & Witherick, 1989). Processes involving the chemical action of air and rain water, of plants and bacteria and the mechanical action of changes of temperature, whereby rocks on exposure to the weather change in character, decay, and finally crumble to soil (AGI, 1960).

Therefore, when stone is exposed to the atmosphere, changes will inevitably occur, and the term 'weathering' will be used to refer to all such changes as a direct result of reactions between the stone and solutions entering the stone such as rainfall and runoff. Weathering reactions by this definition almost invariably result in the removal of constituents from the stone's profile (Nesbitt & Young, 1989). In specific cases where significant loss (deterioration) of substance or form occurs, the change is referred to as decay (Honeyborne, 1990). Decay results from 'weathering' and is the weakening of a material due to this attack (Maclean & Scott, 1993).

'The dissolution of minerals through the action of water and its solutes is an important feature of (any) hydrogeochemical cycle' (Biber *et al.*, 1994). The following factors combine to transform the stone from a hard, strong, coherent state to a completely disintegrated, weak state, and ultimately result in the destruction of the stone (*Plate 9*):

- endogenous (from the physical and chemical properties of the stone)
- exogenous (rainwater, runoff, pollutants, microbes, etc., from the surrounding environment); and
- the exchange of ions.

This chapter provides a description of the mineralogical properties of the different sandstones used to build Culzean before highlighting specific chemical and physical properties which have resulted in weakness, alteration, dissolution, redistribution, and the precipitation of new minerals within the stone. Both quantitative and qualitative analyses have been used to demonstrate what it is about the character of the stone that makes it so susceptible to decay. How and why the *Adam's Building stone* of 1777-1792 (AB) is deteriorating more quickly than *the Original Building stone* (OB) emplaced in the 1200s and the **V**ictorian **B**uilding stone (VB) of 1879.

Different constituents of the stone have been discussed in turn:

- the rock forming minerals;
- the role of clay content and distribution;
- the role of carbonate cement composition and distribution; and

- the role of soluble salts.

However before examining the microscopic properties of the stone, a description of the Old Red Sandstone (ORS) and the categories of clastic rocks are given to examine the complexity of sandstone classification.

4.2 Physical characteristics of sandstone

As explained in *Chapter 1*, sandstones, as a direct consequence of their secondary origin, are composed of the more resistant constituents of igneous rocks. They consist essentially of fragments of quartz, with subsidiary amounts of other minerals such as feldspar and mica.

The constituent grains may be large or small, angular or rounded, closely packed together or sparsely distributed in a matrix (cement) of some other material. It is these properties that will determine the stone's porosity and permeability, the strength of inter-granular bonds, and consequently serve to determine the compressive strength and other physical properties of the stone (Morton, 1926).

The weathering quality of sandstones is largely determined by the chemical stability of the mineral constituents and cementing properties of the material. However the essential feature of sandstone is that the quartz grains are relatively indestructible.

Sandstones may be classified as siliceous, ferruginous, calcareous or argillaceous, according to whether silica, iron oxide, calcium carbonate or clay is the predominant constituent of the matrix. The matrix may be of mixed constitution and different parts of the same deposit of stone may exhibit variations in the nature

of the cementing material. Siliceous sandstones are extremely durable because the intergranular silica possesses good cementing properties, and is not attacked by water and/or atmospheric pollution. Ferruginous sandstones are tolerably good weathering stones for the same reasons except where they contain other, less stable, constituents which make them less chemically stable. Calcite and dolomite have good cementing properties but are readily attacked by CO₂ and other acids in the air. The removal of quite a small amount of cementing material may loosen a relatively large number of the quartz grains. Thus these sandstones usually exhibit relatively poor weathering qualities, particularly when exposed to acid-polluted environments.

The argillaceous sandstones represent the poorest type of sandstone. Clay has no real cementing properties and any stone with a high clay content, whether it be the cementing agent or as a secondary mineral assemblage, will suffer rapid erosion as the clay is softened on wetting (Schaffer, 1950).

As indicated, the mode of aggregation of the grains varies widely. In some sandstones it is difficult to see any cementing material between grains, even under high magnification. In these cases the stone will exhibit low porosity and permeability. In other sandstones the cementing agent is present as irregular masses partially filling the pores, or forms a pellicle around the grains, or the grains are irregularly distributed in a more or less continuous cement. In these instances the stone will retain a relatively high permeability.

Therefore, it is the physical properties (size and shape) of the individual mineral grains, and their mode of aggregation that will determine the porosity, permeability, and strength of the inter-granular bonds, where present. Whereas the composition

of constituent grains and the chemical composition of the cementing agent in particular, will determine the reactivity of the constituents in the rock that determine how a particular stone is likely to weather on a building.

4.3 The ORS and characterisation of the stone

The Lower Old Red Sandstone (LORS) referred to in *Chapter 1*, is comprised of conglomerates, sandstones and siltstones. It has two outcrops in West-Central Ayrshire, centred on Maybole and Dalmellington (Anderton *et al.*, 1987).

In the Maybole area the lower sedimentary group is up to 1200 m thick and consists of a fairly uniform series of micaceous sandstone (mainly lithic arenites) with pebbly bands and marly partings. Conglomerates up to 20 m thick are developed near the top and there are also some thin tuffaceous beds in the upper part of the sequence. The latter may be derived from the large Lower Devonian volcanic vent at Mochrum Hill, 3 km west of Maybole (Mykura, 1991). The overlying volcanic rocks form the Carrick Hills as well as two smaller outcrops at Culzean Castle and Maidens (Geikie, 1897; Smith, 1909; Tyrrell, 1914).

Much provenance work has been attempted on the ORS. The paleogeographic interpretation of the area is largely based on work by Bluck (1978; 1983; 1984), Morton (1979), Wilson (1980) and Armstrong & Paterson (1970). However little work has been done on the petrography of the rock itself. Bluck (1983, 1984) and his co-workers studied the clasts in the ORS conglomerates, but only to consider

evidence for their derivation and paleogeographic origin. No further petrographic work has been published on these rocks.

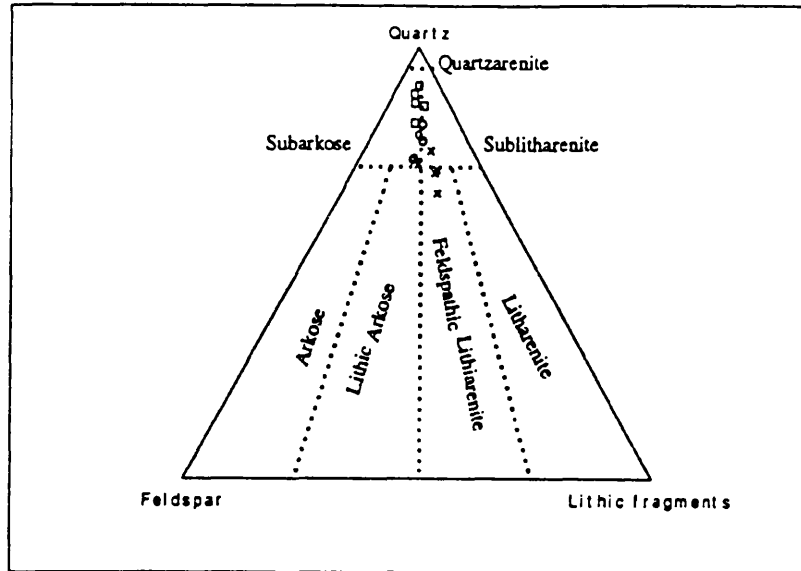
Two of the frequently used classification systems for clastic sedimentary rocks have been reproduced in Figure 4.1 to show where the Culzean sandstones lie within these classification schemes. The three sandstones used at Culzean fall on the border of the arkose/arenite boundary, however, it has been published (Bluck, 1983; 1984) that the sandstones of the area are lithic arenites, and this determination will have been undertaken from a wider sample of material. The sandstones can be defined quite differently, depending on which classification system is being used. For example, the OB samples show higher quartz contents and would be defined as quartz arenites under Gilbert's classification scheme (1953); whilst the AB stone could be described as a sublitharenite, subfeldspathic lithic arenite or a lithic subarkose, depending on which classification is utilised.

The name for the rock is derived from a classification system for clastic sedimentary rocks. Sedimentary rocks are classified according to the grain size, composition, sorting, origin, etc. In brief, the most commonly used method is based on the size of the clastic grains and on the mineral composition. There are three major subdivisions based on grain size:

- rudites;
- arenites; and
- lutites.

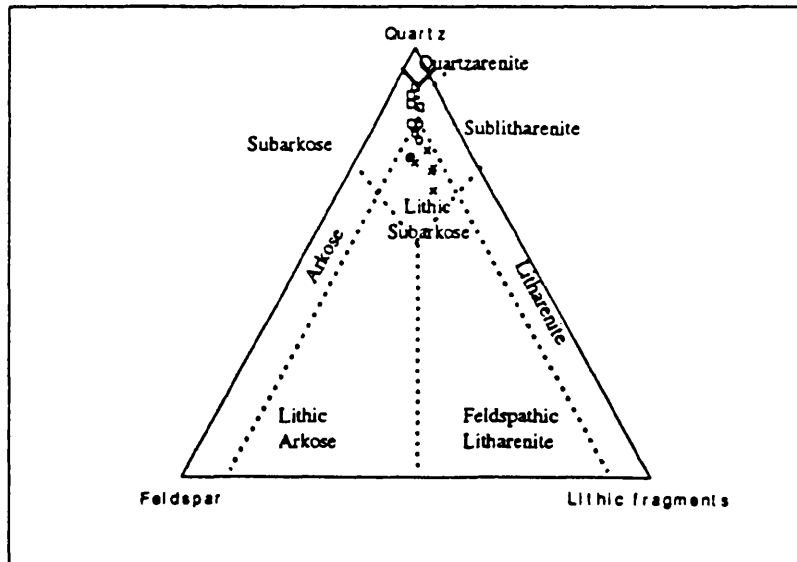
Figure 4.1 **Triangular plot to show compositional variations of AB (x), VB (o), and OB (□), both within and between stone types.**

Folk (1968)



4.1.1

McBride (1963)



4.1.2

Two of the most commonly used sandstone classification schemes are shown in this figure. In both examples, quartz or quartzose components occur at the upper apex, feldspars, and in some cases granitic fragments at the lower left apex, and rock fragments at the lower right apex.

Within the rudite and arenite groups the rock types range from those in which the rock has a dominant quartz composition to those in which the mineral content is varied and cements are of different compositions. The quartz-rich rudites are quartz conglomerates and quartz breccias. Those in which feldspar is relatively abundant are arkose conglomerates and arkose breccias, whilst those composed of a variety of minerals are termed wacke (ill-sorted) conglomerates and wacke breccia. Arenites also grade from pale sandstones, quartzites and orthoquartzites through feldspar-bearing sandstone (arkose), to ill-sorted sediment composed of a variety of mineral and rock fragments which are often angular (greywackes). The lutites comprise siltstone, mudstone, claystone and shale (Simpson, 1983).

Lithic arenites, a term proposed by Gilbert (Williams, Turner, and Gilbert in 1954), are sandstones which are rich in quartz, contain a substantial quantity of rock particles. They have little or no matrix materials, but have an empty pore system, or one which is filled with a precipitated mineral cement, in this case calcite.

Definitions vary:

- "A sandstone with over 25% rock particles and less than 10% feldspar" (McBride, 1963);
- "sandstones, with less than 10% matrix in which rock particles (unstable, fine grained) are an important constituent" (Williams, Turner, and Gilbert, 1954);
and
- "sandstone having 25% or more labile constituents but with rock particles exceeding feldspar" (Pettijohn *et al.*, 1987).

The arenites consist essentially of clastic grains, 0.5 to 2 mm in diameter, and are thus of sand-grade. Sandstones are formed by the consolidation of raw material of sand-grade size, mainly of quartz grains. The lithification of the sands can be by pressure welding, compaction and consolidation of the included clay products or by the introduction of cementing substances (authigenic mineral matter). The final character of these sediments is determined by the source of materials, the mode of transport, the environment of deposition and the ultimate diagenesis. In this case these sandstone are volcanigenic lithic arenites as there are shards or fragments of other rocks present in the stone which are of volcanic origin.

All the stones used to build Culzean have been defined as lithic arenites, containing volcanic fragments. This by no means implies that the different stones are petrographically or chemically similar, as lithic arenites show the greatest diversity of both mineralogy and chemical composition of all sandstones (Pettijohn *et al.*, 1987).

4.4 Mineralogical characteristics of the stones examined

The thin sections of the three building stone examples and two quarry stone samples provide evidence of distinct similarities and differences between the sandstones. As a result each of the stone sample groups will be described, in turn, highlighting the characteristics which make them distinctive and which may be the reason that stones have weathered the way they have on the building:

4.4.1 Building Stone used by Adam between 1777 and 1792 (AB)

The AB sandstone is a medium grained rock containing quartz, feldspar, lithic fragments, micas, clays and carbonate cement. Despite the abundance of cement, substantial porosity is apparent.

Many of the feldspars, lithics and micas appear altered and it is often difficult to distinguish between grains especially in crossed polarised light (XPL). *Plate 27* shows that alteration has taken place at the grain boundaries. Replacement is also evident within mineral grains, particularly along cleavage planes in feldspars and in fracture quartz (see *Plates 41 & 53*). In addition to diagenetic clay minerals, clays have been identified which result from feldspar and lithic alteration. Also, many of the minerals are coated with an iron-rich alteration product (see *Plate 26*) which stands out clearly in plane polarised light (PPL). The carbonate cement is distributed unevenly through the rock. The carbonate cement appears to play an important role in binding the rock together as often there are no clast boundary contacts, which is particularly evident in PPL (this could be a thin-section effect). In addition a number of small carbonate concretions rock (areas of high cement content) are evident.

The proportion of quartz in the AB stone is less than that of the OB and VB sandstones. The greater number of lithics and feldspars will mean it is less chemically stable than the other two samples. (Many of the lithics and feldspars will be chemical unstable and ions from these minerals will readily combine with ions of ingressing fluids to form new mineral assemblages e.g. clays.)

The rock can be described as mineralogically immature as it contains less stable grains including feldspars and rock fragments. The rock is texturally submature, the

sandstone contains <5% clay matrix. The grains are poorly-sorted and not well rounded (classification after Folk, 1951).

4.4.2 The Building Stone of 1879 (VB)

VB sandstone is a small to medium grained rock, also containing quartz, feldspars, lithics and clays and a higher proportion of micas, and micas undergoing alteration (*Plate 37*), compared with the other two building stones and respective quarry. There are fewer feldspars and lithic fragments but more examples of calcitic nodules/concretions in the stone when compared with the AB samples. Where these concretions are present there are seldom any grain boundary contacts. Clay minerals are again a prominent feature of the rock. The grains in the AB samples are of a more regular size than those of the VB samples i.e. the different mineral grains are of similar sizes whereas in the AB samples there were a range of sizes present. Again this rock is fairly porous, particularly in areas where the calcitic cement has undergone attack.

The rock can be described as mineralogically immature, it is texturally submature, and the grains are poorly-sorted and not well rounded.

4.4.3 Stone from the quarry used in 1879 (VQ)

VQ has similar properties to that of the VB samples, except that it appears to have a higher quartz content, and different cement composition. The latter is particularly noticeable under XPL where the birefringence colours are much brighter than those seen for the VB stone (Compare *Plates 29 & 31*). This is a reflection on their different chemical make-up as described in *Section 4.6* below.

Again the rock can be described as mineralogically immature, texturally submature, and the grains are poorly-sorted and not well rounded.

4.4.4 Building Stone used in 1200s for the original castle (OB)

The OB sandstone is a medium grained rock that contains quartz, feldspar, lithic shards, mica, clays and cement. The OB stone appears to have slightly more quartz than the other rocks. It is also much more compact, with more grain boundary contacts, and is thus the least porous; however there is still an abundance of calcitic cement, although there are less examples of carbonate concretions or nodules, and they tend to be less extensive than in the other rocks. There is a high proportion of feldspars and lithic shards. The lithics tend to be elongate and of a more vitreous nature than the fragments evident in the other two building stones. They show less alteration at the edges. Again clay is an important mineral and constitutes a large proportion of the rock, similar to that of VB, VQ and AB.

This sandstone can be described as mineralogically immature as it contains less stable grains including feldspars and rock fragments. It is texturally submature, the sandstone contains <5% clay matrix. The grains are moderately to poorly-sorted and not well rounded.

4.4.5 Stone from the quarry used in 1200s for the original castle (OQ)

OQ is similar to OB in its character, as might be expected. OQ is medium grained and compact containing quartz, feldspar, lithics, clays, micas, and carbonate cement. Again the rock appears to be less porous than AB, VB, and VQ, and there

are few carbonate concretions/nodules. It can be described as mineralogically immature and texturally submature. The grains are moderately to poorly-sorted and not well rounded.

4.4.6 Additional petrographic observations

As highlighted above, common to all the arenites used to build Culzean are their proportionately high quartz, clay and carbonate content, the large number of volcanic lithic fragments, and low feldspar content (*Plates 26-35*).

A notable constituent of these arenites are the lathes of detrital mica (*Plates 36 & 37*), both biotite and muscovite. These micas are orientated parallel to one another and are deformed as a result of compaction, often enveloping adjacent quartz grains. They are important because on alteration they expand and produce clays, e.g. illite, which can be detrimental to the stone. *Plate 66* for example shows expansion of mica and the resultant cracking of a mineral grain. Also of note, is the number of detrital carbonate grains hence the higher carbonate percentage in the point counting results (Table 4.1). These detrital grains are derived from pre-existing carbonate rocks which have subsequently undergone weathering, erosion and transportation. They are often replacement minerals for quartz, lithics, and more commonly feldspars (*Plates 40, 41, 50 & 51*). These carbonate grains have been included with the carbonate cement in the point counting analysis because interest here is not in provenance but in the sandstone's potential to decay.

Following on from this, and also of great importance, is the character of the calcite cement. This will be examined in depth later in the chapter. However, it is

Table 4.1
Mean and median point counting values for each building stone and quarry sample

	Quartz	Feldspar	Lithics	Clays & Micas	Carbonates	Others
mean AB	35.7	5.45	9.1	16.6	31.2	1.95
median AB	35.6	5.45	9	17.8	30.1	2.05
mean OB	37.7	3.6	4.5	19.8	29.4	5
median OB	36	3.6	4.3	19.6	27	9.5
mean OQ	33.65	5.65	5.5	20.7	33.3	1.2
median OQ	33.7	4.95	5.6	21.3	32.8	1.65
mean VB	42.5	3.3	2.5	13.3	36.2	2.2
median VB	40.9	2.4	3.2	14.6	34.8	4.1
mean VQ	35.7	4.7	4.1	22	33.2	0.3
median VQ	34.4	5.7	4.1	21.2	32	2.7

important to point out that there is evidence for diagenetic concretions and nodules (as defined by Pettijohn *et al.*, 1987) within these lithic arenites, from the chemical solution of detrital grains. In this case, the diagenetic concretions are a composite of pore-filling with replacement, and are formed by the greater deposition of grains in the nodule than in the surrounding matrix. As a result the grains in these diagenetic concretions are 'cement supported' (*Plates 38, 39, 42 & 43*) whilst the remainder of the minerals exhibit grain boundary contacts.

In order to determine the petrographic composition of the three building stones and the rocks from their respective quarries, XRD analysis and point counting using both a petrographic microscope and the SEM atomic number contrast (BSE processing), were undertaken. The latter, described in *Chapter 3*, is a relatively new method of compiling data and has only been referred to in the literature by a small number of researchers. Barrioulet *et al.* (1991) used this method whilst undertaking a quantitative structural study of fresh cement paste. It has also been used in France (Dan *et al.*, 1988) to examine moisture movement in a cement-polymer-glass composite (CCPV), and in Japan by Furukawa (1989) to examine the fracture surfaces of wood cell walls.

Whole rock XRD analysis was undertaken to isolate any major compositional differences between the stones. All samples contain quartz, K-feldspar, kaolinite, and mica. The majority also contain plagioclase feldspar and a calcium carbonate cement. Immediately, it became apparent that the AB samples contained more varied clay species including chlorite; the VB samples contain no plagioclase feldspar (confirmed by thin section); whilst the VQ core samples have no calcium carbonate diffraction peaks. Also some of the AB samples provided anhydrite

(CaSO₄) peaks, which could have been on the surface of the stone as gypsum. An attempt was made to compare peak intensities between samples (as described by Mausfield & Grassegger, 1994), particularly between AB samples at different stages of deterioration, to see if a pattern emerged. However the accuracy of such a method is debatable, and the SEM near surface (0 - 3 mm and 3 - 6 mm) profiling provides the same information.

Table 4.1 and Figure 4.1 present the point counting results for AB, OB, OQ, VB, and VQ. Greatest variation between samples is seen in the quantity of lithic fragments and the clay portion. The AB stone contains almost double the quantity of lithics found in the other samples (*Plates 26 & 27*), and incorporates the highest proportion of replacement calcite; thus a high proportion of its carbonate content is replacing feldspars and not binding the stone together. In the OB and OQ samples, a lot of the carbonate cement has been oxidised and has an iron oxide coating (*Plates 32 & 33*), but there appears to be less replacement calcite and so the mineral grains are more intact. In addition both OB and OQ contain the largest proportion of diagenetic clay, kaolinite (*Plates 34 & 35*), and the lithic fragments present are resistant volcanic shards (*Plates 54 & 55*).

The VB (*Plates 28 & 29*) and VQ stones (*Plates 30 & 31*) exhibit different characteristics, especially in the quantities of clay present. Furthermore, the VQ samples used for point counting were different from those cored for geochemical analysis, and show even greater variation, as is evident in the SEM Atomic Number Contrast results (Table 4.3).

The SEM atomic number contrast BSE processing was undertaken for two reasons:

- to establish the overall grain composition and compositional variation throughout an individual stone profile; and
- to compare the different building and quarry stones to look for grain compositional variations that might explain their propensity to deteriorate.

These results could then be used as reference points for the geochemical profiling, and as such will be referred to again in *Chapter 5*.

Table 4.2 provides the arithmetic mean and standard error of each slide through the core profile and demonstrates from the mineralogical variation found. Figure 4.2.1 to 4.2.10 illustrates this pictorially. These enrichment/depletion trends do not represent specific weathering features. The weathering categories detailed in Table 2.1 and Figure 2.4 have been referred to in assessing these profiles.

From these mineralogical compositional profiles it can be seen that although there appears to be some variation in the quantities of particular mineral species through the stone profiles, many of these variations tend to fall within the boundaries of the error brackets. This would be expected of a stone with such a heterogeneous composition. Despite this, there are some characteristic variations, particularly towards the outer surface of the stone. For example there is generally either an enrichment or depletion of clay, cement and feldspars/lithics at the surface of the stone.

AB2 is the only sample that records an increase in feldspar/lithic content towards the surface of the stone. AB1, AB4, AB8 and AB9 all record a decrease. AB1, AB4 and AB9 exhibit a surface contour scaling, and this reduction of feldspars and lithics near the surface of the stone may reflect loss of weaker material.

**Table 4.2 AB Samples
SEM Atomic Number Constrast
BSE Imaging percentage areas**

AM Arithmetic Mean
SE Standard Error

	Quartz minerals		Lithics+Feldspars		Carbonate Cement		Clays		Pore Space	
	AM	SE	AM	SE	AM	SE	AM	SE	AM	SE
AB1/a	46	2.8	10	1.2	6.7	3.1	25.1	2	9.9	1.4
AB1/b	45.6	2.6	10.7	0.8	8.9	1.5	27	1.5	6.8	0.6
AB1/c	47.7	1.4	16.6	1.2	10.1	0.7	17.5	1.1	6.9	2.2
AB1/d	42	1.6	16	1.6	11.5	1.2	18.7	0.9	10.6	1.4
AB1/e	40.5	1.7	15	1.1	9	0.8	25.1	1	9.6	0.6
AB2/a	40.9	1.7	19.8	1.7	9.4	1	20.2	0.9	9.1	0.7
AB2/b	44	2.4	16.3	1.8	5.8	0.8	24.5	1	9.7	0.8
AB2/c	42.2	1.9	17.3	1.3	8.6	1.8	24.1	2.4	7.3	0.6
AB2/d	39.6	2	20.4	1.9	8.8	0.9	22.7	2.2	8.4	0.8
AB2/e	40.3	1.3	21.5	1	8.3	1.2	23.6	1.6	6.9	0.3
AB3/a	44.3	1.9	16.4	1.3	12.6	1	16.6	0.9	8.3	1.1
AB3/b	44.3	1.9	18.2	0.9	15.3	0.9	13.6	0.7	7.4	0.9
AB3/c	37.4	1.1	19.1	1	17.8	0.8	13.3	0.6	10.1	0.4
AB3/d	35.3	1	20.3	0.9	19.7	1.2	13.3	0.5	10.1	0.6
AB3/e	46	1.5	17.5	1.2	12.9	1.2	12	0.9	11.3	0.5
AB4/a	39.5	2.8	11.5	1.5	14.1	1.8	19.1	0.9	15.6	1.5
AB4/b	40.7	0.9	13.7	1.1	7.9	0.9	16.4	0.7	21.3	1.5
AB4/c	38.2	1.4	13.9	1	9.6	1.2	19.2	1.2	17	1.5
AB4/d	40.3	2.1	17.4	1.3	10.3	0.8	18.6	1.1	13.3	1.1
AB4/e	38.6	2.6	22.5	1.5	14.4	2.2	20.3	1.2	3.8	0.6
AB5/a	38.7	1.7	8.8	0.6	11.5	0.9	19	1.1	18.3	1.8
AB5/b	38.1	1.3	9.2	1.8	10.6	1.3	22.4	1.6	17.7	0.8
AB5/c	48	2.7	6.5	1.1	12.6	1.1	20.6	1.8	8.3	1.4
AB5/d	48.1	1.8	8.2	1.1	11.3	1.6	21.2	1.5	9	0.7
AB5/e	41.8	2.7	10.7	1.4	11.3	1.4	22.3	1.8	8.6	1.1
AB6/a	44.5	1.3	20.4	1.5	6	1.2	22.9	1.2	5.7	0.6
AB6/b	34.5	2	20.9	1.2	10.1	1.3	24.7	0.9	7.4	1.4
AB6/c	34.9	0.9	22.9	2.9	9.2	2.6	22.2	2	10.5	2.1
AB6/d	43.6	1.1	17.4	1.8	6.2	1.9	22.7	1.7	9.9	1.7
AB6/e	40.8	1.9	21.2	1	5.8	1	23.6	1.1	8	0.8

Table 4.2 AB Samples Continued....

**SEM Atomic Number Constrast
BSE Imaging percentage areas**

**AM Arithmetic Mean
SE Standard Error**

	Quartz minerals		Lithics+Feldspars		Carbonate Cement		Clays		Pore Space	
	A M	S E	A M	S E	A M	S E	A M	S E	A M	S E
AB7/a	31.9	1.7	22.5	1	10.7	0.8	18.4	0.4	14.6	1.2
AB7/b	37.6	1.6	23.1	1.3	11.1	1.1	16.7	0.6	10.4	0.5
AB7/c	38.2	1.6	19.2	1	13.6	2	17.4	1.5	9.7	1.5
AB7/d	36.3	1.5	20.3	1.2	10.1	0.8	16.8	0.6	13.6	0.8
AB7/e	44.8	2.2	19.3	1.8	4.7	0.6	21	0.9	9.4	1.2
AB8/a	40.3	1.5	15.3	1.1	11.7	1.1	14.1	0.6	18	1.3
AB8/b	43.4	2.2	17.1	1.8	10.1	0.9	20	1	8.8	0.7
AB8/c	36.5	2.7	21	3.2	16.4	1.1	15.3	1.2	9.9	0.7
AB8/d	40.8	1.9	19.1	1.8	10.4	1.5	20.5	0.6	8.9	0.4
AB8/e	47.1	1.2	11.8	1.3	11.5	1	24.8	1.2	4.4	0.8
AB9/a	44.1	2.1	15	1.4	9.8	1.1	21.2	1.5	9.5	1.1
AB9/b	37	1.4	22.1	1.7	11.4	0.6	19	1	9.6	1.2
AB9/c	41.5	1.5	18.4	0.9	6.5	0.8	17.6	0.9	16	0.9
AB9/d	39.6	1.5	20.1	1	8.8	0.8	16.9	0.9	14.2	1.4
AB9/e	38.5	2.1	20.4	1.5	9	1.4	19.6	0.8	12.5	1.7
AB10/a	52.9	2.2	10.2	1.1	9.6	0.7	23.4	0.8	3.8	0.5
AB10/b	51.7	1.8	11.4	0.9	12.8	1.4	18.5	1.2	4.9	0.8
AB10/c	50.6	1.1	10.5	1.1	14.5	0.9	21.5	1.2	2.8	0.5
AB10/d	51.3	1.6	12.4	1.5	11.3	1.2	21.7	0.9	1.7	0.3
AB10/e	54.2	1.6	10.7	0.9	12.4	0.9	17.5	0.8	3.8	0.7
AB11/a	49.7	1.1	16.1	1.3	8	0.9	23.2	1	2.8	0.3
AB11/b	40.4	1.2	19.6	0.9	9.7	1.1	24.5	1.3	3.7	0.2
AB11/c	38.3	1.3	21.7	1.1	12.2	1.1	23	0.7	3.5	0.3
AB11/d	43.8	1.3	16.8	1.4	9	1.2	24	1.1	5.9	0.7
AB11/e	45.9	1.3	19	1.3	8.1	0.8	21.3	1.4	4.6	0.5
AB12/a	45.8	1	16.1	1.9	9.2	2.5	18.8	2.1	9.8	2.6
AB12/b	45.1	1.8	18.2	2.1	5.9	0.5	23.4	1.6	5.4	0.9
AB12/c	41.8	2.6	19.1	1.4	7.3	0.9	25.1	1.5	6.5	0.7
AB12/d	44	2.4	18	1.7	7.4	0.9	22.8	0.8	7.5	1.4
AB12/e	49.7	1.6	15.3	1	4.5	0.7	22.9	0.9	7.1	0.3

Figure 4.2 Mineralogical compositional profiles by SEM Atomic Number Contrast Imaging

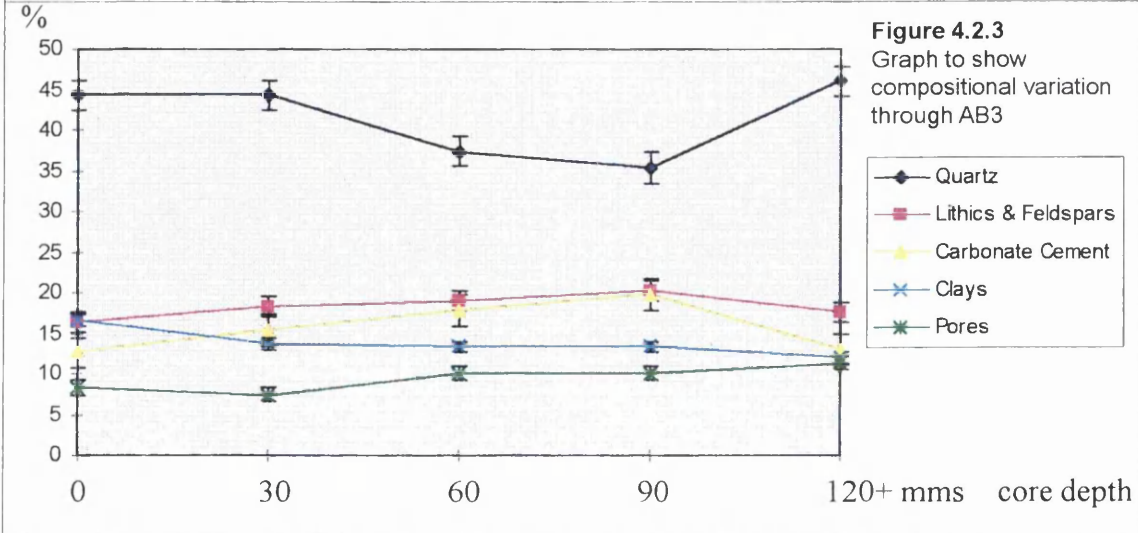
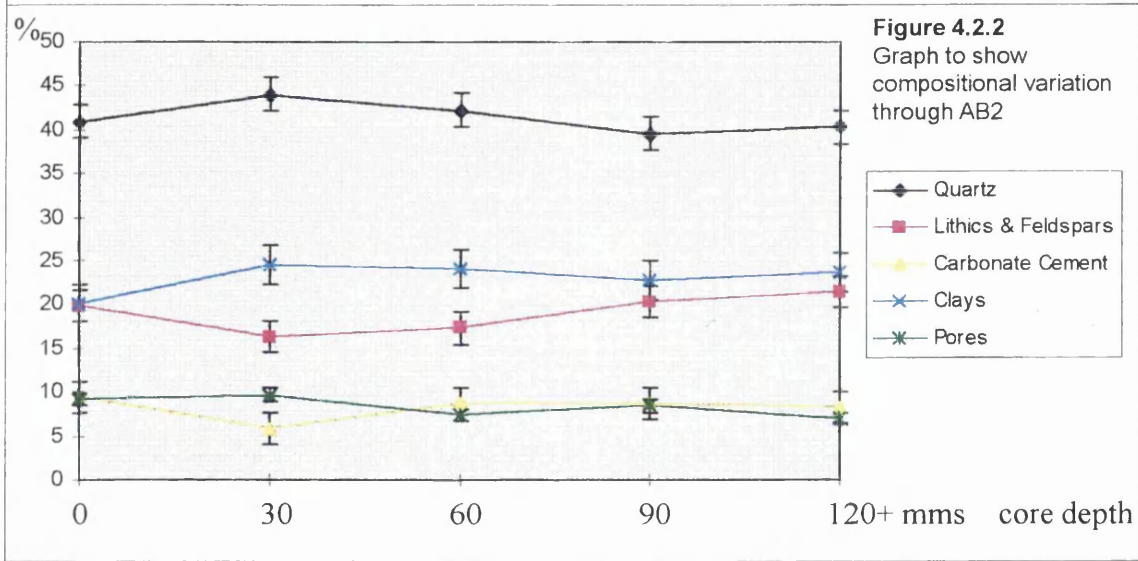
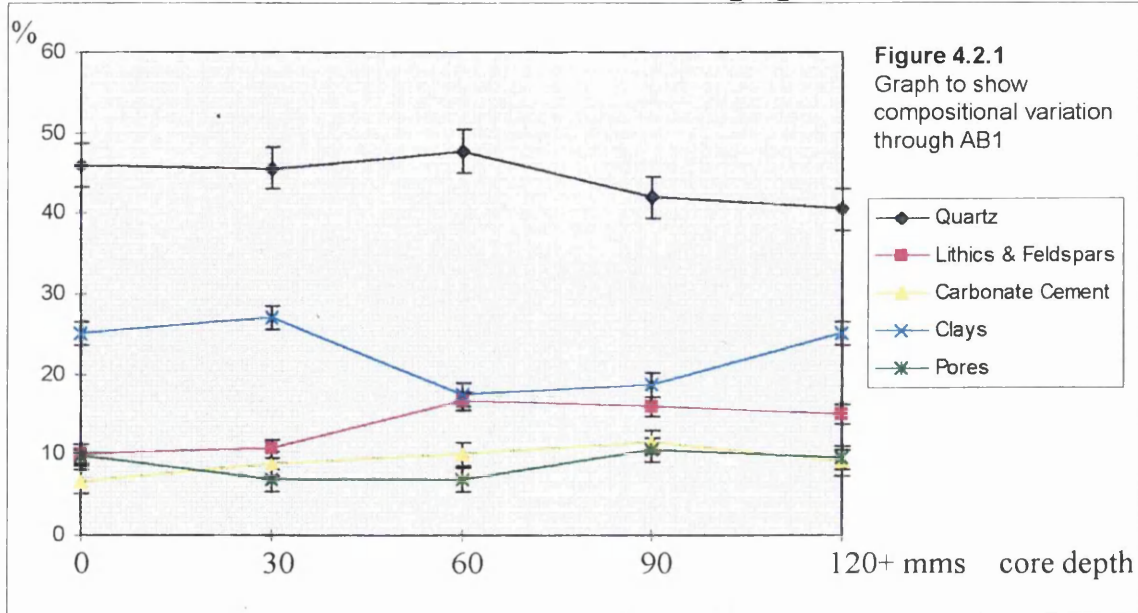


Figure 4.2 Mineralogical compositional profiles by SEM Atomic Number Contrast Imaging

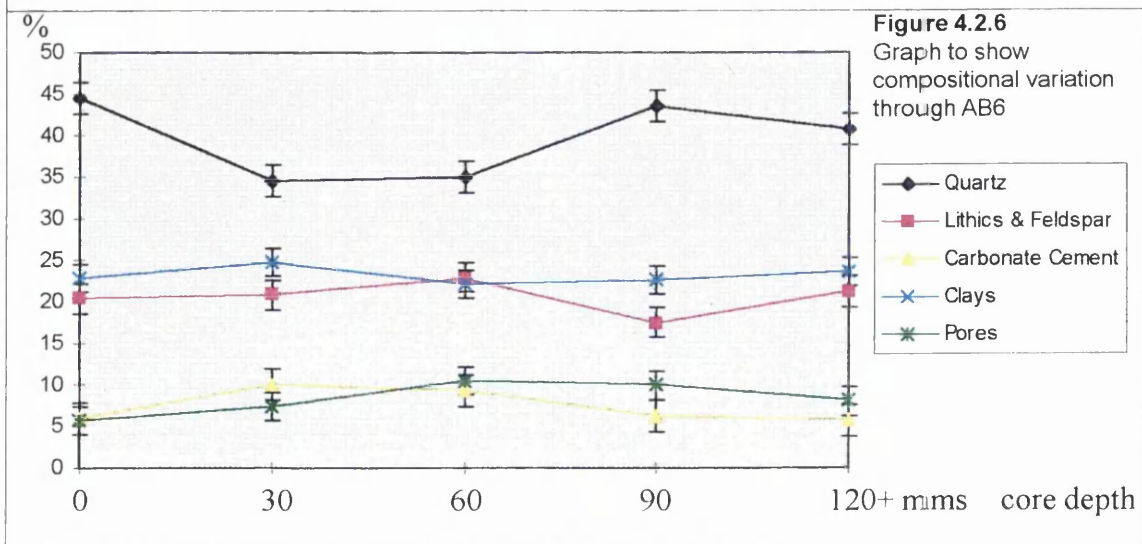
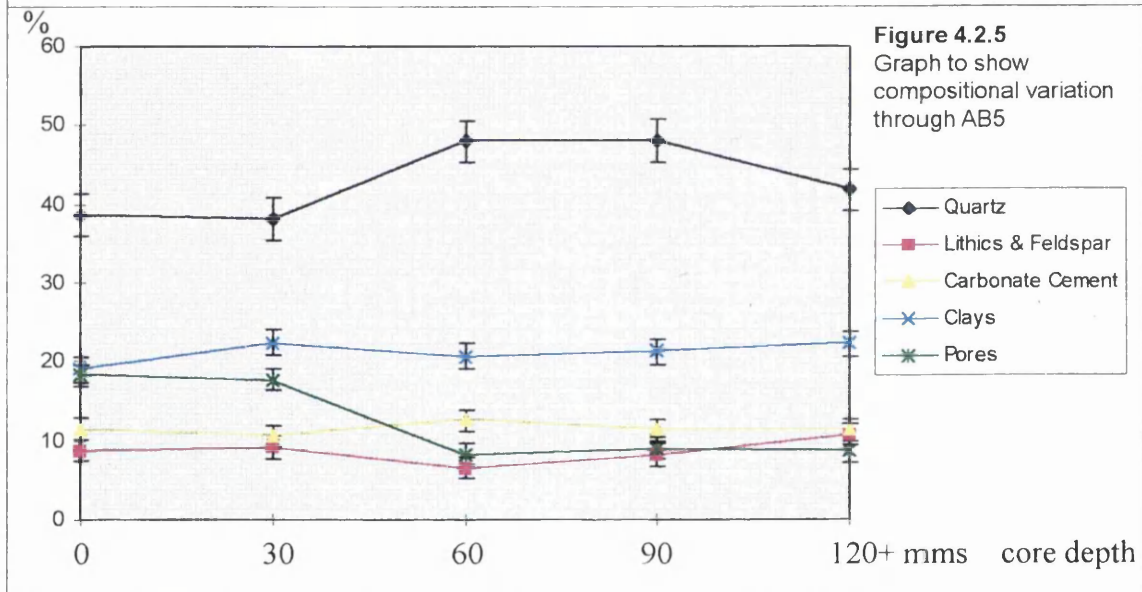
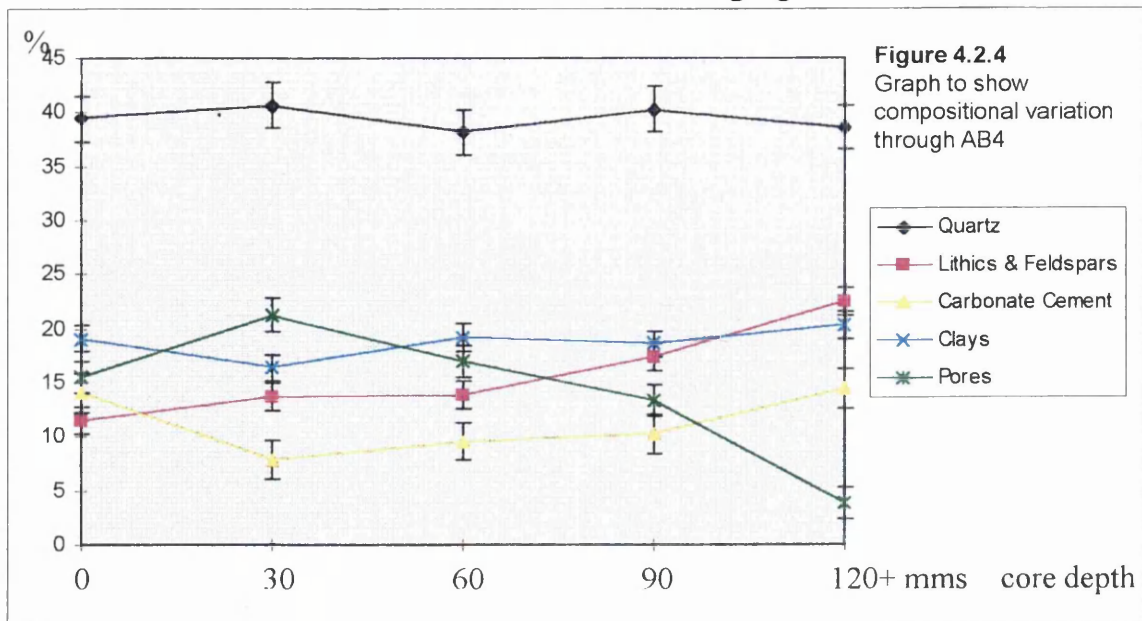


Figure 4.2 Mineralogic compositional profiles by SEM Atomic Number Contrast Imaging

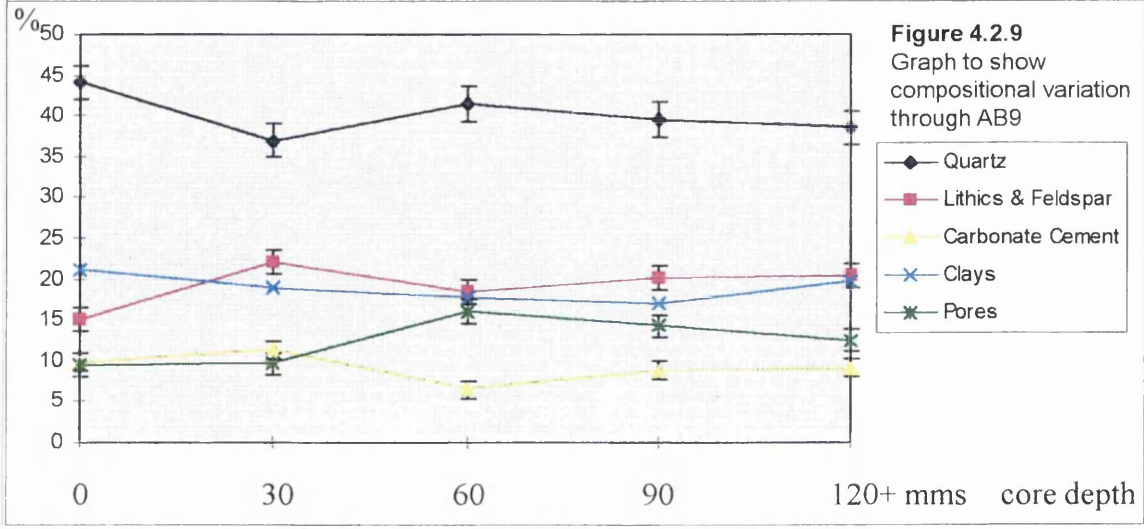
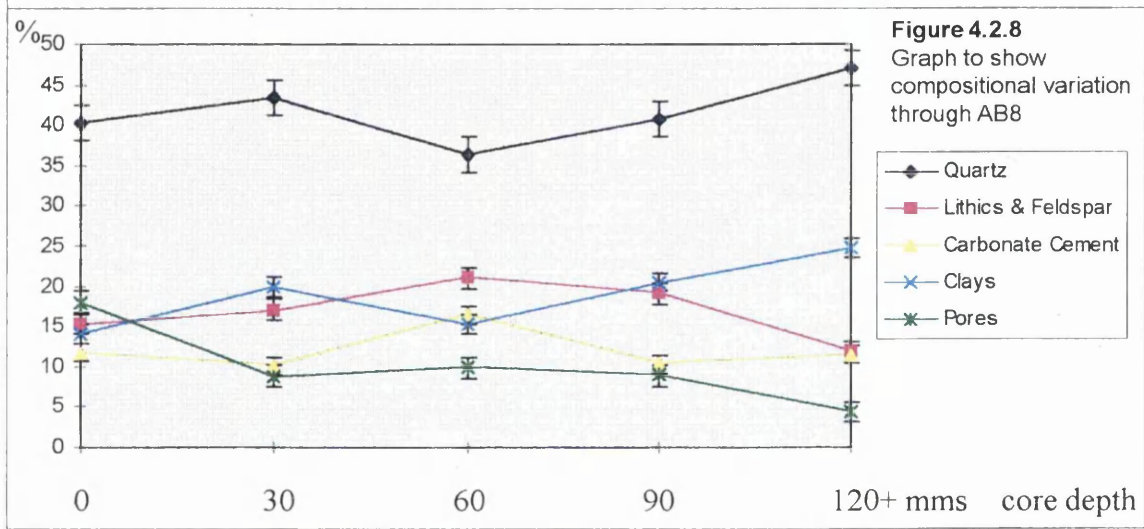
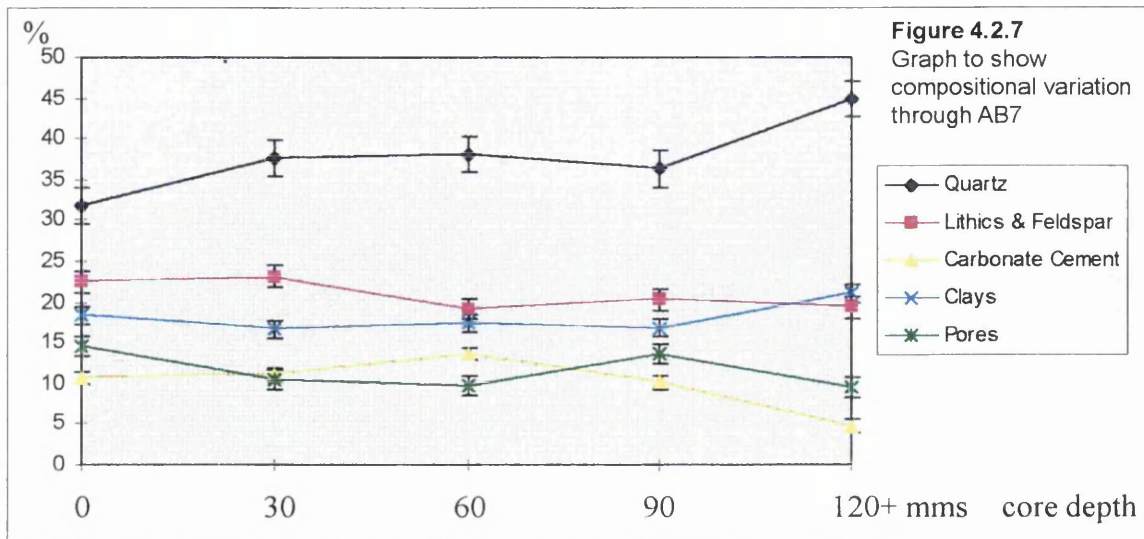
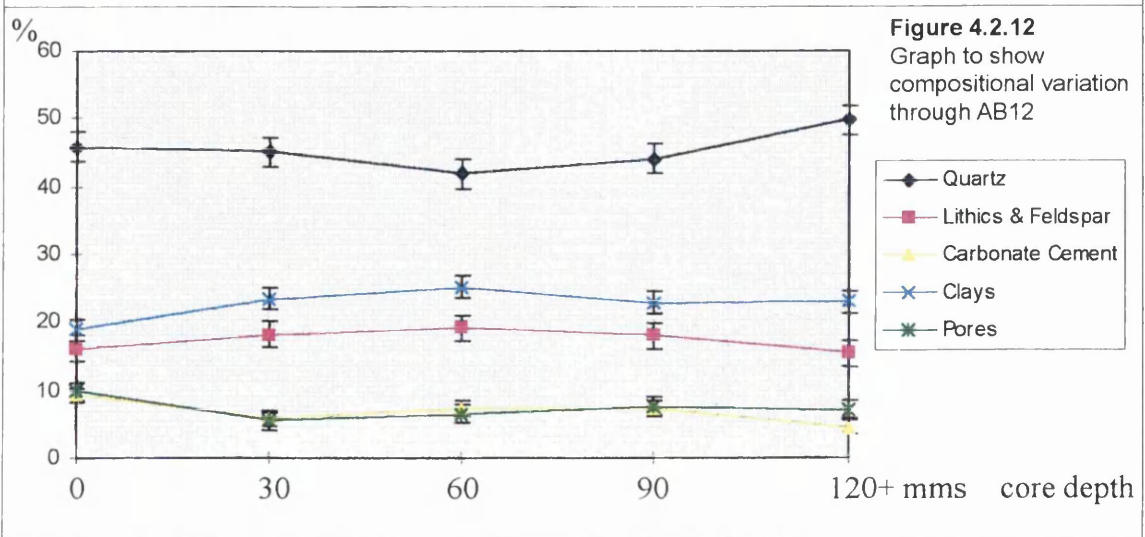
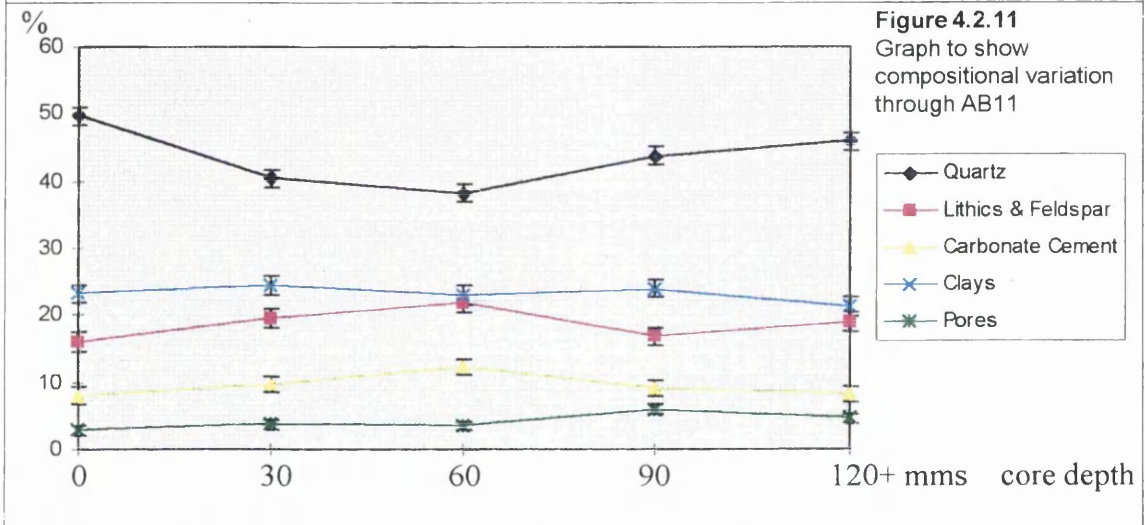
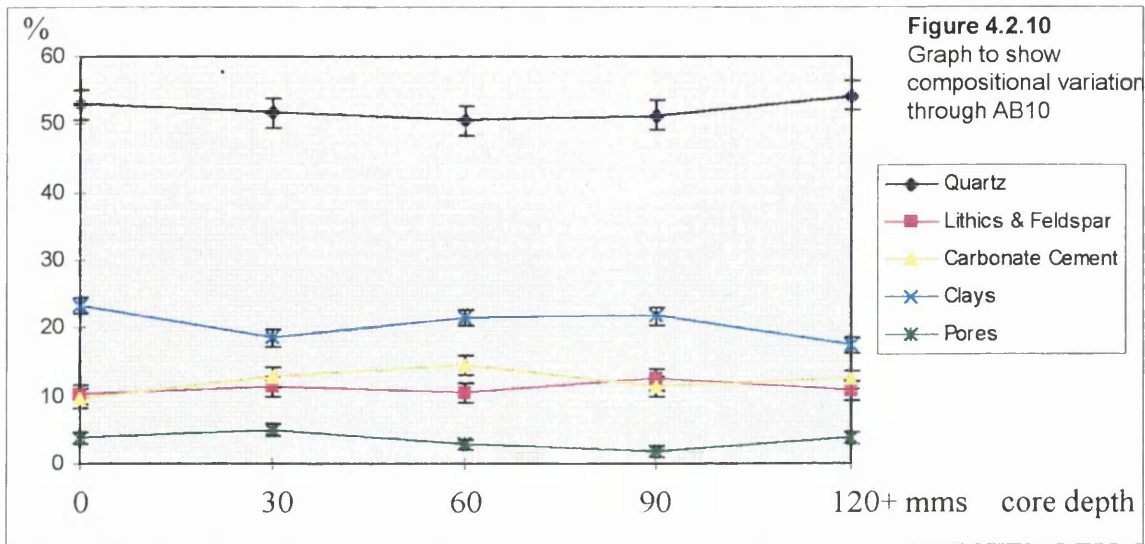


Figure 4.2 Mineralogic compositional profiles by SEM Atomic Number Contrast



AB5, AB7, AB8 and to lesser extent AB1 and AB12 show an increase in pore space at the surface of the stone. All of these samples exhibited granular disaggregation when visual assessment of the surface of the stone was undertaken.

AB4, AB6 and AB9 exhibit a reduction in pore space at the surface of the stone. AB6 retains a spalling patina and a reduction in pore space within this crust would be expected. However both AB4 and AB9 have surface scaling and this reduction in pore space may be indicative of the beginnings of a patina where ions in solution (externally or internally derived) are being reprecipitated in the pore space.

There is a distinctive increase in cement content at the surface of AB4, a stone with a contour scaling surface. Surface increases are also recorded in, AB2 and AB12. The remaining samples show a decrease in cement content at the surface of the stone.

Also it should be noted that quartz appears to show the greatest quantitative variation through the profiles, and often mirrors enrichments/depletions in the other minerals present. For example in AB4 and AB8, where a decrease in quartz content is mirrored by an increase in porosity; and AB6 and AB9 where a change in the quantity of quartz is mirrored by a change in amount of feldspar/lithics present.

Similar examinations were undertaken for OB, OQ, VB and VQ, and the results of these can be seen in Tables 4.3 and 4.4. Immediately, one can see greater similarities between OB and OQ when compared to VB and VQ (Figure 4.3.1 - 4.3.6, Figure 4.4.1 - 4.4.6). This is indicative of the extent of quarrying undertaken at St Murray's over the years, cutting through different horizons; compared with the Culzean cliffs, quarried only momentarily to construct the first part of Culzean. As

**Table 4.3 VB and VQ samples
SEM Atomic Number Constrast
BSE Imaging percentage areas**

AM Arithmetic Mean
SE Standard Error

	Quartz		Lithics+Feldspars		Carbonate		Clay		Pore space	
	AM	SE	AM	SE	AM	SE	AM	SE	AM	SE
VB1/a	43.3	2	5.3	0.8	11.6	1.3	34.5	1.7	4.5	0.5
VB1/b	44.1	2	4.65	1.1	12	1.2	30.3	1	7.8	0.5
VB1/c	47.8	1.9	4.7	1.1	14.6	1.5	29.5	1.9	3.1	0.4
VB1/d	49.3	1.3	4.5	0.9	10.7	1.6	30.2	0.8	4	0.5
VB1/e	45.2	1.5	4.8	1.2	15	2.6	27	1.9	8.7	1.3
VB2/a	45.7	1.5	4.2	1.1	12.4	1.1	30.3	1.3	7.7	1.1
VB2/b	41.6	1.1	7.1	0.9	12.9	0.7	31.1	0.5	7.4	0.4
VB2/c	50.2	1.5	4.8	0.6	9.4	1.7	28.4	2	7	0.5
VB2/d	43.8	1.5	7.7	1	8.6	0.6	37.1	1.4	2.7	0.5
VB2/e	46.4	1.2	7.2	1	9.9	1	35.1	0.9	1.6	0.2
VB3/a	43.2	1.6	5	1.5	15.4	0.9	23.1	1.4	13.3	1.3
VB3/b	49.2	1.5	3.3	1	10.7	0.7	29.7	1.7	7	1
VB3/c	48.5	1	2.8	0.9	11.9	1	28.6	1.2	8.1	0.9
VB3/d	50.1	1	5.8	1	11.6	1.4	27.1	1.4	5.2	0.8
VB3/e	50.9	1.4	5.6	0.7	9.1	0.8	28.3	1.1	6.1	0.5
VQ1/a	53.6	1.6	8	0.2	1.9	1.4	30.9	1.3	5.5	0.6
VQ1/b	52.5	0.8	7.8	1.2	2.8	1.3	27.3	1.2	3.4	0.9
VQ1/c	53.1	0.6	11.9	0.7	6.8	0.9	23.8	1	2.2	1
VQ1/d	52.8	1	10.4	1.6	5.4	0.7	24.3	0.9	5.7	0.8
VQ1/e	51.3	1.4	13.2	0.8	6.4	1	26	1.1	1.9	0.2
VQ2/a	54.9	1.6	8.3	0.7	2.9	1.1	24.8	1.7	8.7	0.9
VQ2/b	50.9	1	7.6	0.9	1.6	1.5	25	1.3	9.8	1.2
VQ2/c	41.7	1.2	13.1	0.3	5.4	0.7	26.8	1.2	12.8	0.9
VQ2/d	47.6	1.2	15.2	1.4	3.2	1.2	25.4	0.7	11.3	0.7
VQ2/e	42.9	1.5	14.7	0.9	5.5	1	27	1.2	9.6	0.5
VQ3/a	50.3	0.9	6.4	1.4	0.9	1.4	20.9	0.9	3.4	1.9
VQ3/b	52.3	0.5	5.9	0.9	1.7	1.5	21.2	1	4.6	1.5
VQ3/c	56.7	0.8	5.7	0.6	2.4	0.7	23	0.6	5.7	0.9
VQ3/d	51.3	1	3.6	0.6	3.4	0.7	23.5	1.8	3.6	1.1
VQ3/e	47.9	1.2	9.7	0.5	4.1	0.9	26.4	0.7	9	1.1

**Table 4.4 OB and OQ samples
SEM Atomic Number Constrast
BSE Imaging percentage areas**

AM Arithmetic Mean
SE Standard Error

	Quartz		Lithics+Feldspars		Carbonate		Clay		Pore space	
	AM	SE	AM	SE	AM	SE	AM	SE	AM	SE
OB1/a	50.4	1.1	9.2	0.9	10.9	1.4	26.7	1.3	3	0.5
OB1/b	50.7	2.7	7.5	1.1	8.8	2	27.2	1.4	5.5	0.9
OB1/c	47.2	1.2	9.4	0.5	9.9	1	30.1	1.3	3	0.3
OB1/d	48.3	1.4	8	0.9	12.5	1	28.8	1.1	2.1	0.2
OB1/e	46.6	1.4	11.1	1.1	11.5	1.2	24.9	0.8	3	0.3
OB2/a	48.5	1.4	15.3	1.5	14.8	1.4	20	1.4	1.5	0.2
OB2/b	47.2	1.3	19.8	1.6	16.1	1.8	16	0.8	1.2	0.1
OB2/c	50.9	0.6	13.1	1.2	14.6	1.3	21.1	1.4	1.1	0.1
OB2/d	47.4	1.5	11.4	1.2	15.8	1.4	23.56	0.7	2.3	0.7
OB2/e	47.3	1.3	13.8	0.7	14	0.9	21.2	1.5	1.6	0.1
OB3/a	41.1	2.3	15.6	1.3	12.4	2.1	16.7	1.7	13.7	1.3
OB3/b	45.4	1.3	15.7	1.3	8.5	1	17.8	1	12.3	1.1
OB3/c	43.1	1.9	14.8	1.7	13.5	1.8	19.9	1.3	8.9	0.8
OB3/d	44.1	1.4	14.1	1	14.5	0.8	17	1	10.2	0.8
OB3/e	37.7	1.7	17.8	1.1	13.8	0.9	19.6	1	10.3	0.6
OQ1/a	47.8	1.7	12.3	1.2	14.3	1.2	25.6	1.9	2.3	0.2
OQ1/b	46.5	1	9.4	2	15.2	2.1	23.3	1.5	3.2	0.4
OQ1/c	43.2	1.3	11.7	0.9	15.6	1.3	20.8	1.5	1.3	0.5
OQ1/d	42.1	1.6	12	0.8	17.6	1.3	20.8	1.3	1.8	0.1
OQ1/e	44.4	1.2	11.3	1.8	17.7	1	17.6	1.2	3.7	0.7
OQ2/a	49.8	1.9	12.4	1	14.3	1.3	22.9	1.5	0.7	0.1
OQ2/b	48.6	1.2	12.6	1	15.1	1	20.8	1.2	1.7	0.2
OQ2/c	43.2	1.8	13.4	1.4	18.1	1	16.7	1.3	8.1	1.3
OQ2/d	43.7	2.1	11.3	0.9	18.2	0.8	17.6	0.9	2.3	2.1
OQ2/e	45.9	1.6	15.3	1.5	17.8	0.7	19.8	0.9	6.5	1.2
OQ3/a	42.5	1.7	11.4	0.9	13.4	1.5	27.3	1.1	4.9	0.6
OQ3/b	46.7	1.5	10.7	0.8	13.8	0.9	27.3	1.7	2.6	0.2
OQ3/c	51.4	1.5	11.9	0.9	10.1	1	24.3	1.8	2.3	0.3
OQ3/d	49.8	1.2	11.8	0.8	14.5	1	22.5	1.2	1.9	0.9
OQ3/e	49.1	2.1	12	0.9	16.7	1.8	18.5	1.4	3.6	0.5

Figure 4.3 Mineralogic compositional profiles by SEM Atomic Number Contrast Imaging

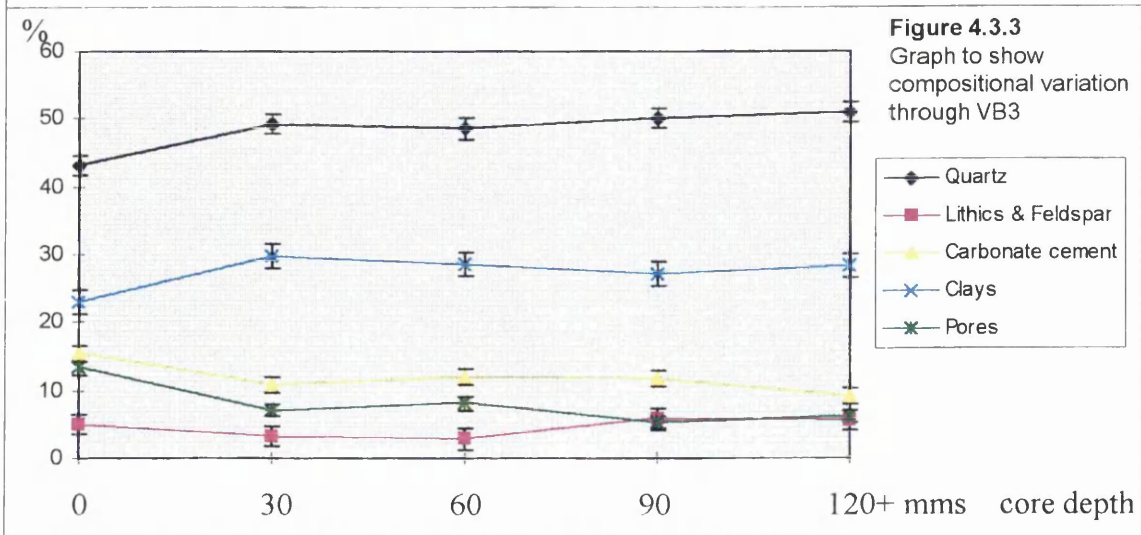
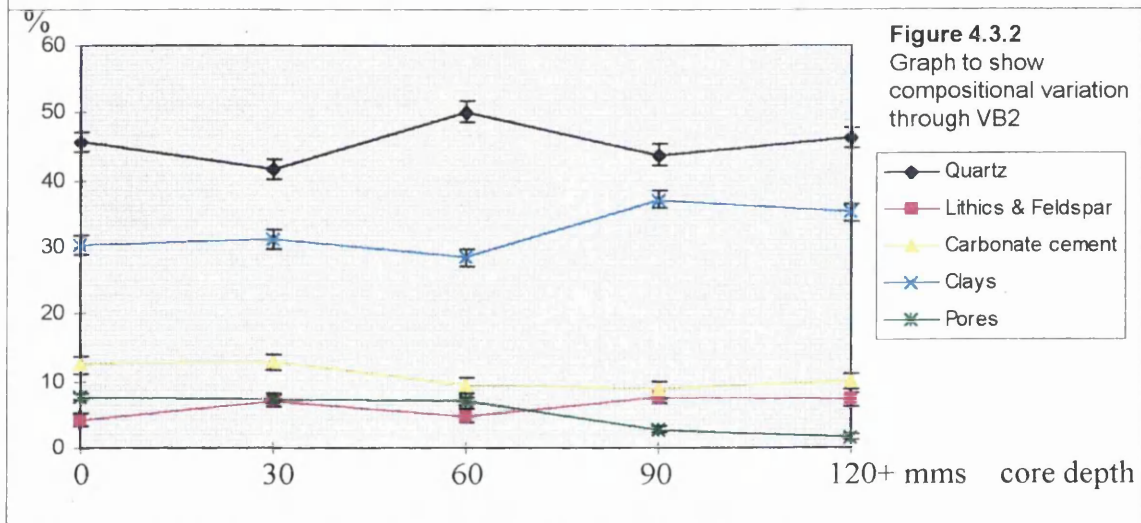
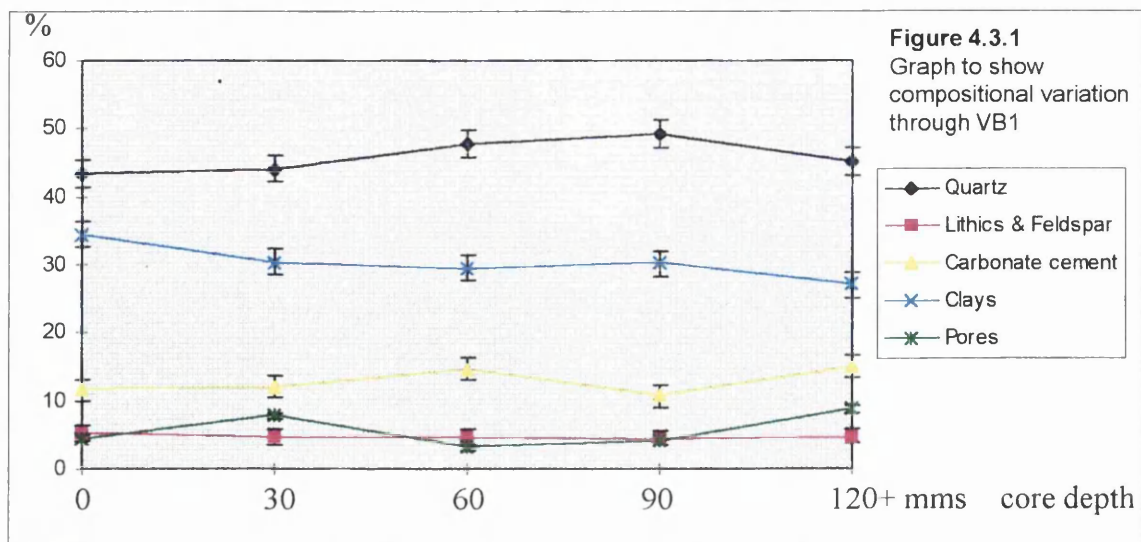


Figure 4.3 Mineralogic compositional profiles by SEM Atomic Number Contrast Imaging

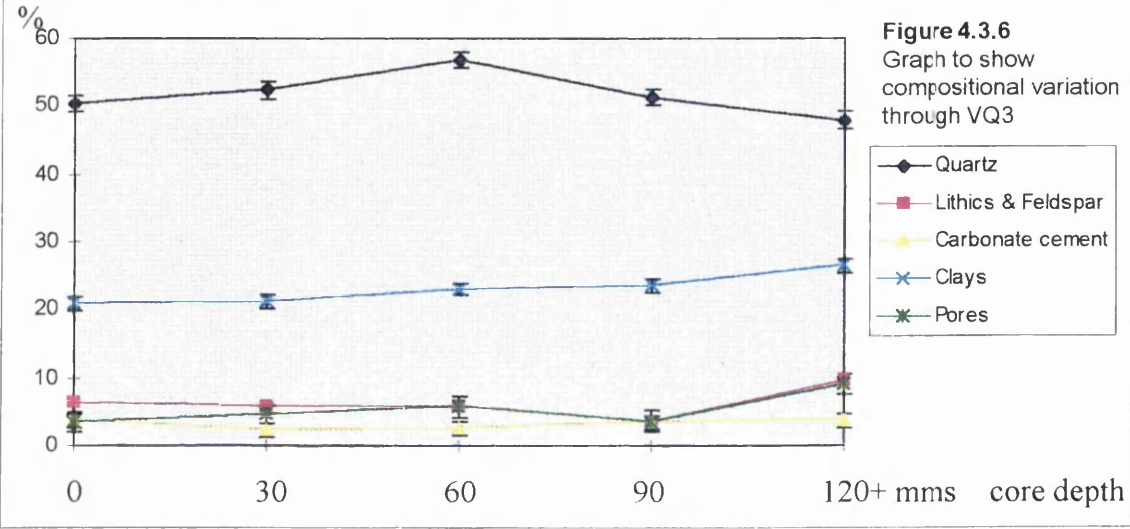
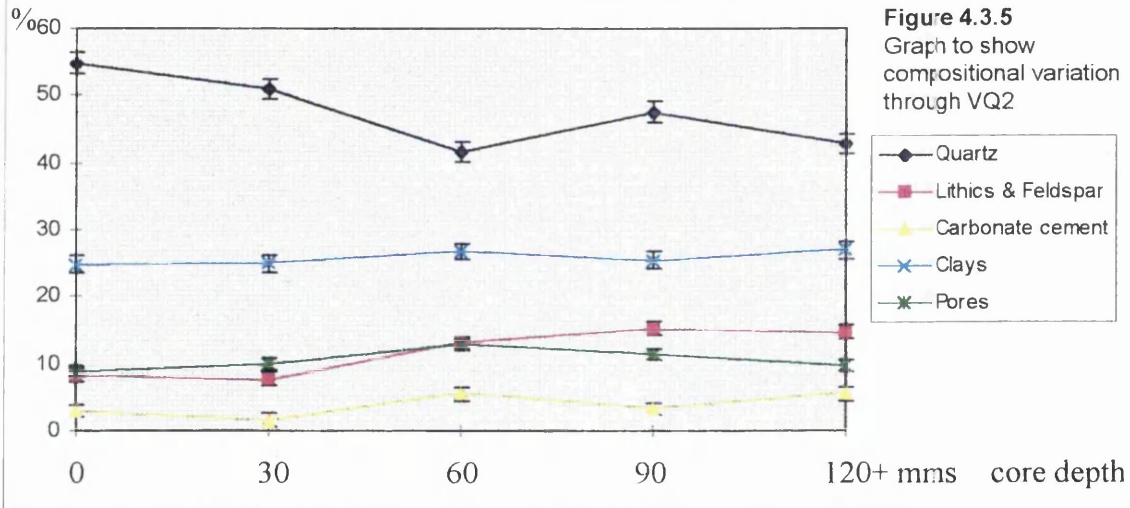
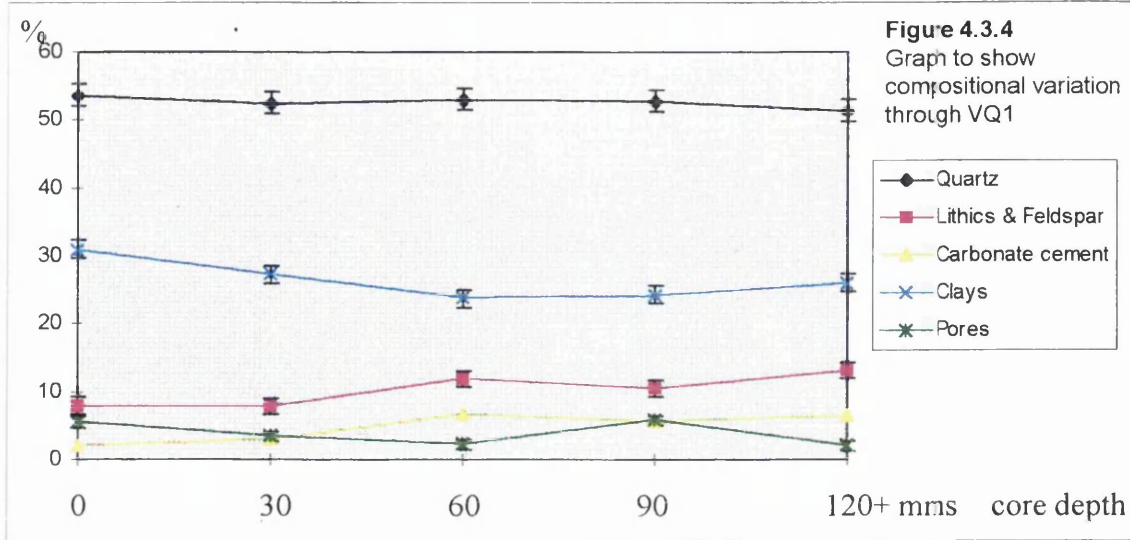


Figure 4.4 Mineralogic compositional profiles by SEM Atomic Number Contrast Imaging

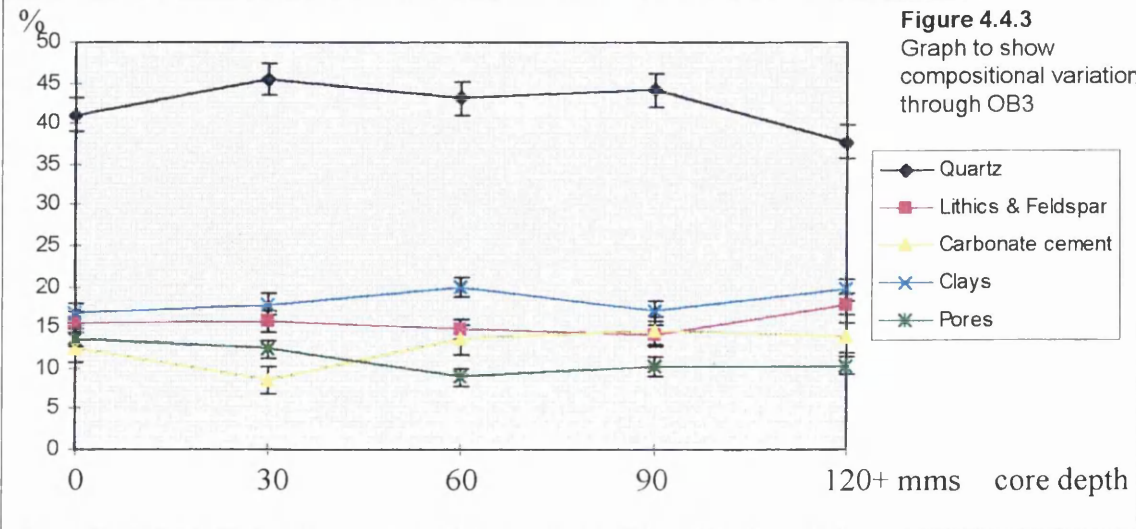
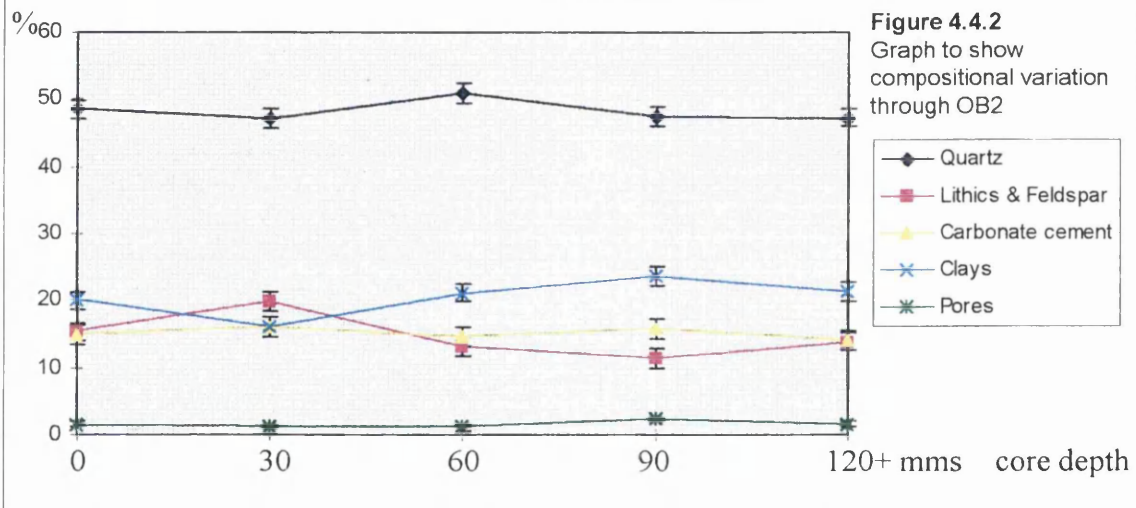
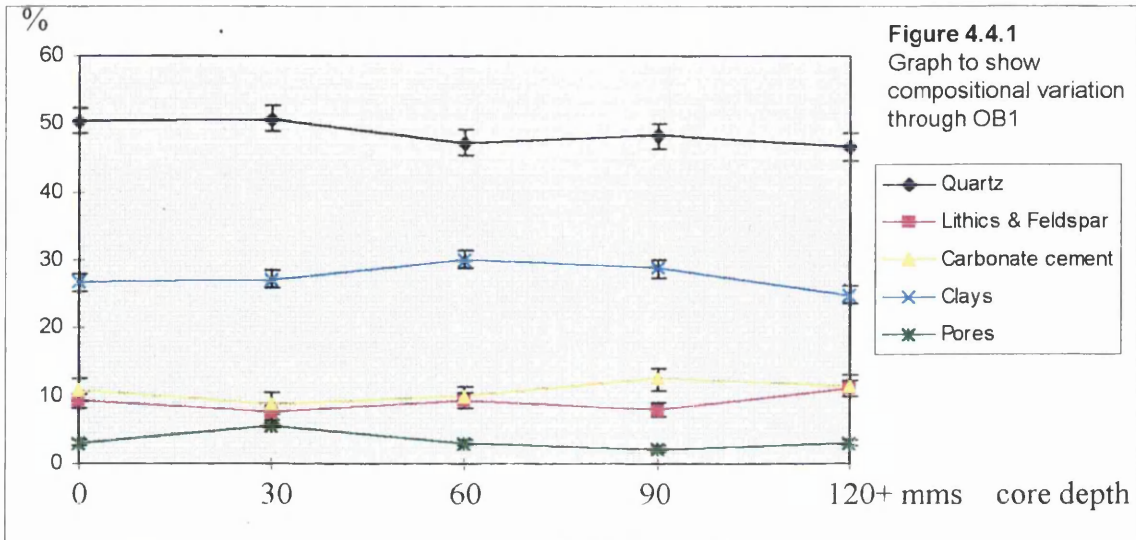
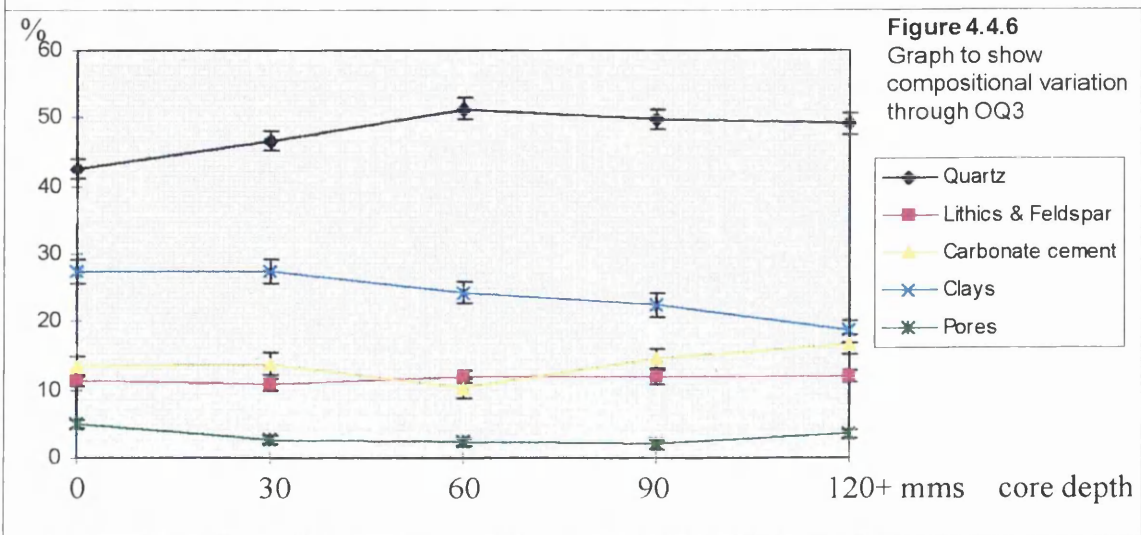
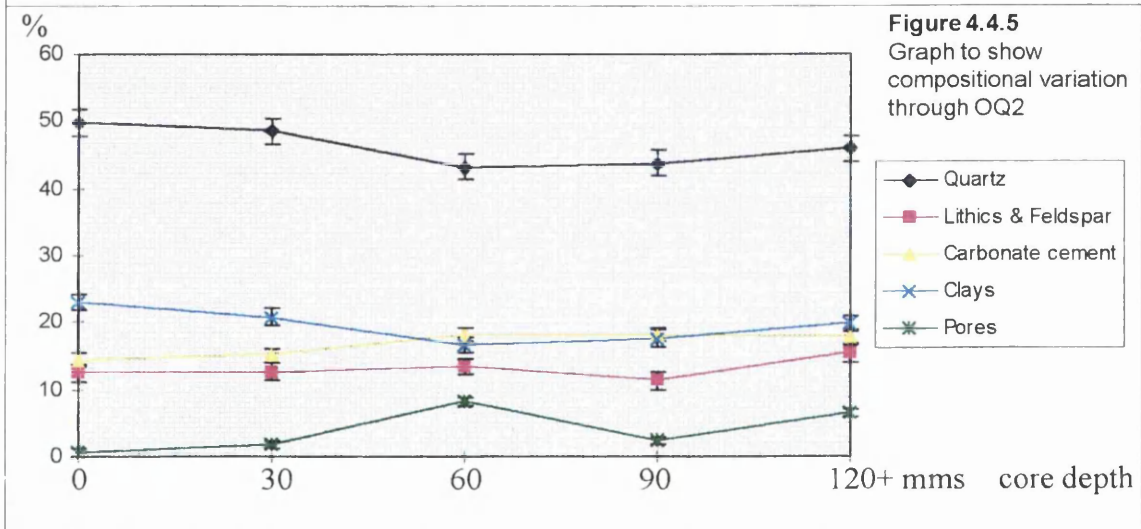
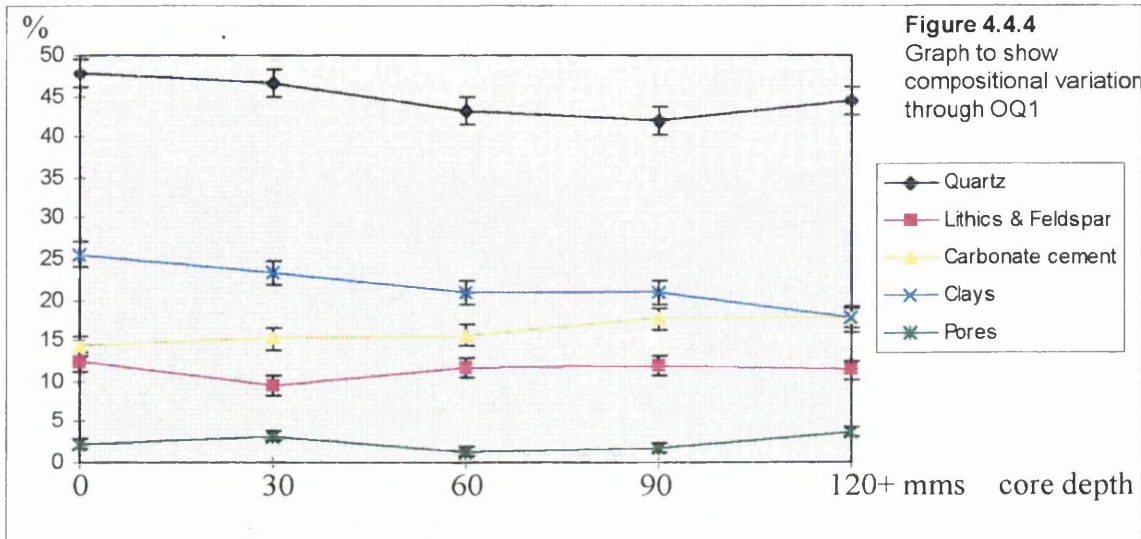


Figure 4.4 Mineralogical compositional profiles by SEM Atomic Number Contrast Imaging



mentioned briefly, the VQ material analysed contains no carbonate cement. The stone masons would almost certainly have only used stone with a high proportion of cement, as identified in the point counting results, and therefore a different stratigraphic horizon.

4.5 The alteration of rock forming minerals

For this investigation, it was necessary to look at the physical make-up of the stone, specifically for the following reasons:

- the weathering of a mineral depends upon its composition, structure and bonding;
- crystal size, shape, evolution, completeness, and faultlessness must be considered;
- minerals of the same chemical composition can deteriorate at different rates; and
- individual minerals will be subject to different quantities and concentrations of ingressing solutions, the primary agent of change.

Therefore, although chemistry may give some indication of weathering potential, more information is required.

However, the difficulty arises when attempting to look for more recent weathering features as opposed to those inherent in the stone (prior to their extraction for building purposes), which will include:

- kaolinitised feldspars and lithics (those which have been converted completely or partially to kaolinite);
- replacement of the same by calcite; and
- some grain dissolution.

As such it is sensible to point out the deterioration characteristics of the stone as points of weakness from which ions will be most easily removed in solution and either egress from the stone, or as is more likely, combine with other ions and remain in the stone.

4.5.1 Quartz

As one would expect, the AB samples provide an abundance of examples of mineral deterioration including quartz grains, the most resistant to chemical weathering of all rock forming minerals. Despite this fact, the quartz grains invariably exhibit eroded grain boundaries and textural features such as surface pitting (*Plates 52, 53 & 61*). Such surface morphology is indicative of dissolution (MacInnis & Brantley, 1993), and as quartz dissolution is not expected it may well be related to organic acids produced by the micro-organisms colonising on the stone (as reported by Ohse *et al.*, 1985). These processes are not confined to the exterior surfaces of the cores but are seen throughout the core profiles of all the samples analysed including the VB, VQ, OB and OQ cores.

4.5.2 Feldspars

Many feldspar grains throughout the samples have been either replaced partly by diagenetic calcite or kaolinite. As a result more micro-pore space is created, and the remaining mineral is much more susceptible to ingressing solutions and thus more readily dissolved (*Plates 50, 51 & 78*). More importantly, their cleavage allows rapid penetration by water through their structure, which will result in the gradual removal of ions such as K^+ , Ca^{2+} , Na^+ , and Mg^{2+} in solution (see *Chapter 5*). From SEM analysis one can establish many dissolution characteristics within and between different grains throughout the stone profiles. The feldspars from the surfaces of all the samples are highly weathered, and many of the grain surfaces have been completely destroyed by etching and pitting. The pits or fissures are always found on planes of weakness such as cleavages, twinning or perthite zones (*Plates 56 & 59*) and dissolve to develop elongated micro-cracks which vary in magnitude from grain to grain, although it would appear that plagioclase is the most susceptible to erosion. This is validated in the results of research undertaken by Oxburgh *et al.* (1994).

Many of these feldspars have already, and will continue to produce secondary minerals such as kandites, smectites and illites (Nesbitt & Young, 1989). The presence of these clays, particularly illites and smectites will induce instability, the importance of which will be discussed later.

4.5.3 Lithic fragments

Many of the lithic fragments in the AB samples show similar dissolution, particularly along lines of weakness and compositional changes. As a result dissolution features resemble those described for feldspars and indeed many former lithic fragments have virtually been transformed to clay throughout the AB samples.

However the lithic fragments for example in the OB (and OQ) samples show little corrosion as they are volcanic shards (*Plates 54 & 55*). They are inevitably more stable and thus of a higher resistance to ingressing fluids and chemical alteration than those in AB and VB. There are proportionately far fewer lithic fragments (and feldspars) in the VB and VQ samples (Table 4.3) and so their importance is immediately reduced.

4.5.4 Micas

Micas are basic alumina-silicate minerals but with a sheet structured crystal lattice, which make them relatively soft and easily attacked by fluids because of their cleavage. Thus it is simple for mica grains to break down into flakes and more importantly into chlorite, illite and other clays. Throughout the profiles of AB and VB there is much evidence of mica decay (*Plates 62 & 63*). Almost all micas examined displayed distinct exfoliation and transformation into clay (*Plates 64 to 67*) as a direct result of ion exchange. The creation of illite is the result of K^+ release from the lattice (Ohse *et al.*, 1985). The abundance of micas, particularly in

AB, are indicative of the variety of expansive clays present. Many of the photographs particularly *Plates 63 & 66* show the mechanical power of their expansion, as exhibited by the adjacent grains. There are fewer micas present in OB and OQ, however these, too, show expansion to some extent.

4.5.5 Pore Spaces

Pore space is discussed here as it was analysed by SEM at the same time as the rock forming minerals (see Tables 4.2 - 4.4). The individual pore characteristics of a stone will control the weathering behaviour. At the same time weathering processes modify the pore space, for example, mineral alteration can give rise to a change in porosity. The porosity is therefore one of the most important characteristics of the stone (Fitzner, 1994).

Pore space and permeability are of prime importance. The following must be considered in order:

- the availability of the mineral to an ingressing solution;
- saturation of that ingressing solution;
- the full or partial removal of the resultant solution from the stone; and
- the weathering product left behind.

A distinction can be made between primary porosity and secondary porosity. Primary porosity is porosity created by petrogenesis and secondary porosity is the modification of porosity after crystallisation or final deposition. The weathering porosity is a special case of the secondary porosity and is created by the weathering process and is very important for natural stones (Fitzner, 1994).

Of fundamental importance in this case is the pore structure of the stone and the need for connecting channels. There are examples of both open and closed porous systems. This controls the permeability of the stone. The open porosity being in connection with the atmosphere is divided in a through-flow porosity. The pore space consists of several cross-linked open pore channels. Isolated or non-through-flow porosity is formed by one-sided closed pores. These pores are not connected to any other pores and therefore do not add to the permeability of the stone. Porosity types identified in the stone can be divided into a number of categories (after Pittman, 1979):

- *intergranular* (i.e. between grains, often where the cement (and/or mineral edges) has been dissolved e.g. *Plate 61*);
- *dissolution* (e.g. *Plates 56 & 59* where dissolution has occurred along cleavage planes);
- *micro-porosity* ($< 5\mu$ - e.g. within the carbonate cement – see *Plate 89*); and
- *fracture* (e.g. *Plate 60* which provides an example of mineral cracking where cleavages have widened to enable porosity-channels to propagate through the grain).

The results obtained from SEM atomic number contrast show the undoubted importance of pore space in building stone deterioration. Those samples that exhibited the least sign of deterioration, OB and OQ, were indeed those samples with the lowest amount of visible pore space and exhibited many examples of isolated pores. Pore space in VB and VQ was higher, as would be expected and there were more open pore channels, but not as extensive as that exhibited by the AB samples, which were seen to contain lengthy pore structures, i.e. the pore spaces interconnected to allow through-flow and permeability. Micro-porosity, dissolution and fracture porosity, resulting from mineral alteration, are all visible. Examples of micro-porosity as a direct result of mineral dissolution were noted throughout the stone profiles; it is therefore not just a surface process. Results from further porosity and permeability tests undertaken by Napier University have been examined in *Section 4.9*.

In addition it should be recognised that all the samples examined under optical microscopy and SEM exhibit evidence of some surface material loss, even those samples with a 'fresh' exterior surface, which display micro-granular disintegration. This will produce an increase in surface porosity which enables greater penetration of fluids and consequently accelerates the production of micro-porous sites elsewhere. This has been captured in *Plate 58* which shows feldspar and cement dissolution at the surface of one of the AB samples (stone surface on LHS of photograph). An increase in porosity as the result of grain dislodgement (lower

LHS of photograph) and micro-porosity (as a result of dissolution and mineral cracking) can be identified.

4.5.6 Overview of mineral weathering

From this brief description of the state of deterioration of the major rock forming minerals, a number of key points can be established:

- overall there is no significant variation in the abundance of mineral weathering found through the sample profiles. Mineralogical attack is not just taking place at the surface of the stone. The mineral weathering processes discussed can be found at all points in the stones' profiles;
- the quantity of quartz present in AB is smaller than that exhibited by the others, and shows signs of dissolution;
- many of the feldspars in the AB samples have been partly replaced by diagenetic calcite increasing their susceptibility to the erosive powers of ingressing solutions. Many have previously been altered to clays;
- many of the lithic fragments in AB are already in a state of disintegration and contain clays. The fragments found in OB and OQ are highly resistant, showing few signs of alteration;
- there is an abundance of mica in AB and VB which have expanded and altered to clays;

- granular disintegration at the surface of the stone increases surface porosity; and
- the pore space available to/made available by ingressing and egressing fluids increases where fracture, dissolution and intergranular pore space have been identified (see *Section 4.7*).

4.6 Clay content composition and distribution

When looking at the clay portion of the stone it was important to look at the following factors in turn:

- relative quantities;
- compositional variations within and between the samples;
- the importance of clay minerals within the stone; and
- to understand why the presence of certain species may be more important than others.

There is an abundance of clay in the stone at Culzean. *Plate 49*, shows an example of clay coating minerals on the surface of AB4.

Clay minerals (sheet silicates), being subject to hydrolysis and volumetric changes are a key mineral in sandstone degradation and the complex nature of the clays found in AB cores are indicative of its fragile nature. The continual ingress and egress of fluids and the potential of the stone to retain moisture for long periods, provide the stone with water and other ions (such as Na^+) which allow the clays to

expand. When the rock is transformed into building stone, general conditions are altered (changes in mass, temperature and humidity). This results in expanding clay minerals, particularly smectites, to swell, which can place a force on adjacent mineral grains causing cracking along planes of weakness, making the mineral more susceptible to ingressing fluids and thus encouraging deterioration. This is particularly the case with clays. It is therefore necessary to evaluate the importance of clay minerals present in the stone, and the influence of their chemical alteration on its performance and longevity.

The presence and character of the clays in the sandstone have been assessed using the scanning electron microscope (SEM) and X-ray diffraction (XRD). SEM was used because the detection limits of other petrographic techniques were not sufficient for looking at clay in cement, within grains, and at the intergranular crevices. XRD was used to examine the residue from 6 hour sedimentations, to obtain the fraction $<2\mu\text{m}$ by centrifugation (as described in *Chapter 2* for 80 minutes sedimentations), to analyse the clay fraction in four stages (see *Section 3.4.1*).

The stone at Culzean is rich in clay. The clay minerals present in this case include transitional complex associations. Precise identification of the natural clay assemblages is difficult because as well as kaolinite, readily identified by both XRD and SEM, the neomorphic minerals are very small, poorly and diversely crystallised, and are associated with subamorphous compounds, particularly those silicates embedded within the carbonate cement (see *Section 4.7* below).

The XRD results (Table 5, Appendix 1) show an expanding mixed-layer clay identified as an illite-smectite. Random illite-smectite is the most common abundant mixed-layer clay in sandstones, which result from the progressive degradation on weathering and progressive diagenesis. Like all silicates, mixed layer silicates are hygroscopic, but have the additional ability to retain excess water in their interlayer sites (Hall, 1995).

The large chlorite peak identified at 14\AA is indicative of a non-expansive mineral (with a collapsing OH structure at 600°C). However, additional results obtained from SEM spot-analysis of silicates in the cement indicate chlorite-smectite compositions, with ions of Na^+ , K^+ , and Ti^{4+} in addition to Al^{3+} , $\text{Fe}^{2+/3+}$, and Mg^{2+} .

Due to their fine-grained nature, characterisation of chlorite grains is often difficult, and in many sedimentary rocks the chlorite present is in mixed-layer structures. Mixed-layer chlorites are derived from the aggregation of less organised sheet minerals by the degradation of pre-existing ferromagnesium minerals, and by the crystallisation from dilute solutions of their components, which will be highest where the fluid/stone contact is greatest. This would suggest the variations include chlorite-smectite, kaolinite-chlorite, and illite-smectite-chlorite. However, the chlorite-smectite present may not be a mixed layer clay species, as the two can coexist during alteration from chlorite to smectite. Preliminary SEM examinations were undertaken on interstitial silicates, both within the carbonate cement and at grain boundaries. It should be mentioned that these rudimentary results indicate that compositional variations in the interstitial clay fraction become more consistent with depth in the core profile. These findings are congruous with those of Mausfeld & Grassegger (1994), who also found depth-related changes in the clay mineralogy

of the building stone from the Romanesque Basilica of St. Vitus, Ellwangen, South West Germany. However further work is required to confirm this variation and no conclusion can be reached for the purposes of this research.

XRD and SEM have been used not only to identify the major clay mineral phases but also to pinpoint the occurrence of specific species and their chemical compositions. From these analytical methods three main clay groups have been established:

1. kaolinite formation surrounding minerals and thus lining the pore spaces. This is the main diagenetic process and constitutes the majority of clay formation in the stone;
2. the replacement of feldspars and lithic fragments with illites, smectites and chlorites (*Plate 59*), and the deterioration of micas to illite (initially diagenetic in origin) which may allow expansion and push against the framework grains (see *Plate 65*); and
3. the formation of additional sheet silicates within the carbonate cement (the white material shown in *Plates 96 & 97* and discussed in *Section 4.7*).

Groups 2 and 3 include the forms of illite-smectite, chlorite, and chlorite-smectite described, and these are the most significant in terms of current deterioration processes. They form in intergranular crevices where upon expansion due to the addition of water (hydration) they break down the cohesiveness of the stone (e.g. *Plate 63* which shows mica alteration to clay and the effect of the expansion of the mica on the surrounding mineral grains).

Following work done on the complex clay species present in the AB stone, analysis was repeated on the three cores from VB and OB and their respective quarries. The results for all six experiments proved to be similar and predominantly the clay kaolinite was identified (in accordance with the XRD results). OQ1 and VQ1 identify the kaolinite 7.21Å peak collapsing at 400°C when all kaolinite minerals decompose (Deer *et al.*, 1985).

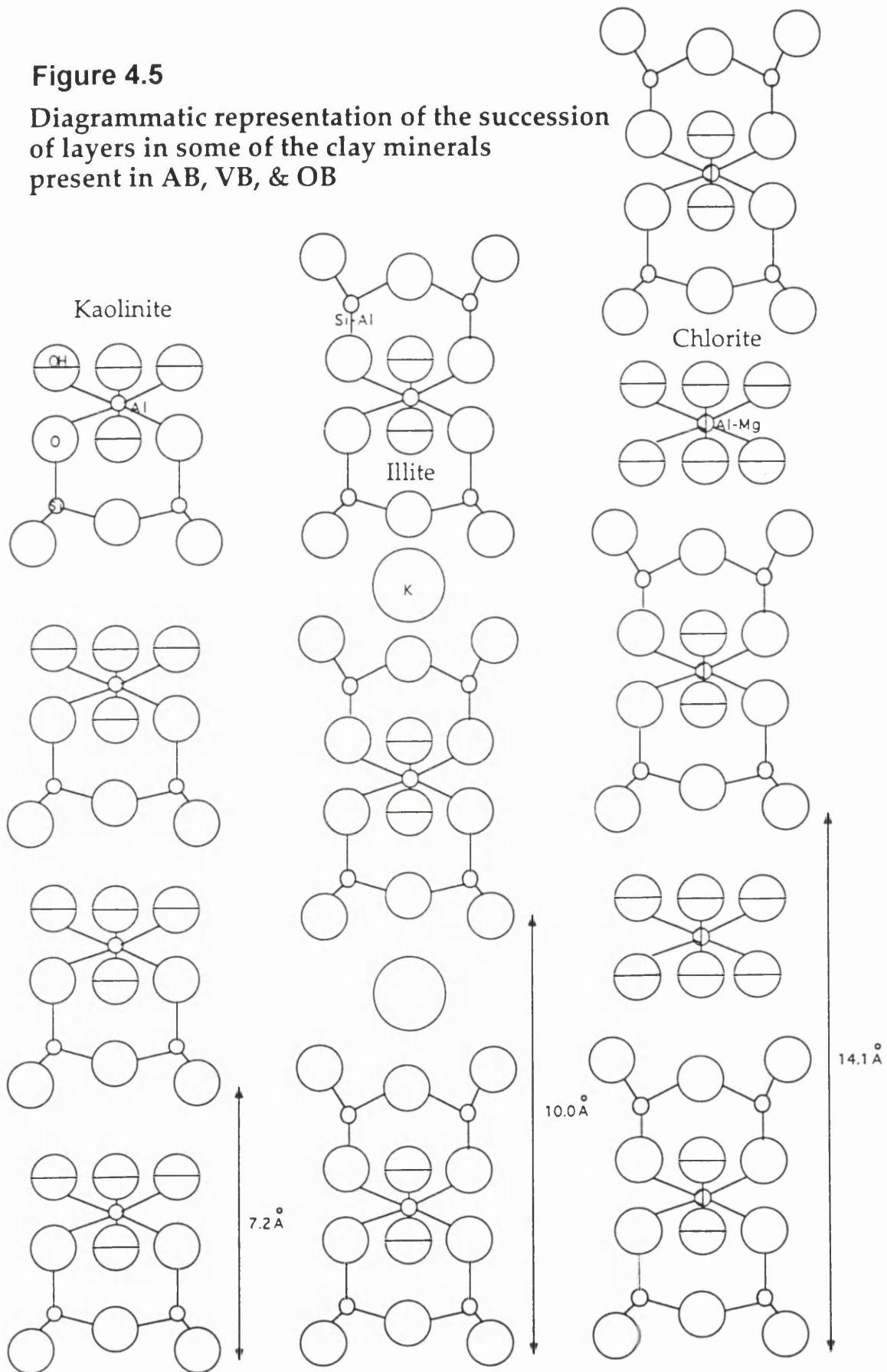
Therefore, the importance of the clays and their structures may be important in understanding the deterioration of the stone fabric on the balcony. Figure 4.5 provides an example of three of the clays identified and shows their basal spacing (distance between successive similar layers), as used in XRD to identify the mineral species. Smectite is not shown here, but has a similar structure to illite. Given that these clays have the capacity to expand their lattice by absorbing water, such a layer of oriented water molecules forms an extra sheet. The more finely divided the clay, the more water it can hold, and a greater volume can be reached.

Thus the swelling and shrinking of clays upon wetting and drying is of great consequence in weathering, and the more clay species present (especially those kaolinites, illites, smectites and chlorites produced from deteriorating feldspars and lithic fragments), the greater the effect will be (Hayles & Bluck, 1995).

In all the Culzean stones there is evidence for feldspars, lithics and mica mineral alteration through clay formation. As ingressing fluids enter the stone, particularly where the areas of micro-porosity are created by the dissolution of mineral grains, the rock will be further weakened. This will be more pronounced in the AB stones

Figure 4.5

Diagrammatic representation of the succession of layers in some of the clay minerals present in AB, VB, & OB



as they are more susceptible to ingressing fluids in their exposed location on the balcony. It is one of a number of weathering processes taking place in the stone.

4.7 Cement composition and distribution

Calcium carbonate is the most soluble of the common minerals. It is readily identified in thin section by its maximum interference colours (*Plates 70 & 71*). It is difficult to analyse the behaviour of the carbonate and its associated or accessory minerals despite their abundance.

4.7.1 Carbonate composition

Of importance when discussing the significance of cement is to look at the carbonate composition and compositional variation.

Although a number of divalent cations may partially replace Ca^{2+} , most calcite is free from other ions and is fairly close in composition to pure CaCO_3 (Deer *et al.*, 1985). SEM was used to examine chemical composition. It was often difficult to obtain recordings for the actual cement because frequently accessory or replacement material was analysed such that both calcite and, for example, feldspar were analysed simultaneously. Therefore a decision was made to take the results of material central to pore-infill and concretions at a very high magnification. These results can be seen in Tables 4.5 to 4.7.

Table 4.5 AB samples
To show compositional variation of calcium carbonate cement
Results given as percentages to 3 significant figures

Sample	CaCO ₃ + MgCO ₃ + MnCO ₃	CaCO ₃	MgCO ₃	MnCO ₃	FeCO ₃	FeCO ₃ + MnCO ₃
AB6/1						
mean	99.67	98.48	0.32	0.92	0.33	1.25
median	99.9	98.57	0.11	0.76	0.1	1.14
standard error	0.6	0.16	0.07	0.1	0.09	0.11
AB6/2						
mean	99.43	98.32	0.54	0.57	0.57	1.14
median	99.93	99.83	0.43	0.42	0.07	0.99
standard error	0.19	0.3	0.15	0.12	0.19	0.2
AB6/3						
mean	99.58	98.66	0.44	0.48	0.42	0.9
median	99.8	98.5	0.35	0.23	0.16	0.51
standard error	0.12	0.29	0.13	0.16	0.11	0.2
AB6/4						
mean	99.78	98.84	0.52	0.42	0.22	0.64
median	99.81	98.69	0.32	0.21	0.13	0.55
standard error	0.09	0.14	0.13	0.12	0.09	0.14
AB6/5						
mean	98.14	96.55	1.09	0.5	1.86	2.36
median	99.07	97.4	0.82	0.62	0.93	1.76
standard error	0.97	0.93	0.21	0.12	0.97	0.93
AB5/1						
mean	95.2	92.4	2.74	0.08	4.76	4.84
Median	98.1	95.5	2.41	0.08	1.56	1.86
standard error	2.19	2.52	0.58	0.03	2.19	2.21
AB5/2						
mean	92	90.3	1.73	0.74	7.96	8.01
median	95.3	94.3	1.87	0.03	4.71	4.71
standard error	2.13	2.25	0.22	0.69	2.13	2.13
AB5/3						
mean	92.3	95.4	1.89	0.56	6.78	2.7
median	96	93.2	2.1	0.1	3.8	2.5
standard error	2.04	1.87	0.33	0.24	2.24	0.16
AB5/4						
mean	95.3	92.6	2.06	0.14	5.67	6.7
median	98	95.7	1.9	0.1	3.01	5.6
standard error	1.98	2.32	0.4	0.33	2	0.11
AB5/5						
mean	95.8	93.5	2.18	0.11	5.24	4.36
median	97.9	94.8	1.88	0.08	2.23	2.34
standard error	2.04	2.11	0.33	0.42	1.97	2.01

Table 4.6 OB & OQ samples

To show the compositional variation of calcium carbonate cement
 Results given as percentages to 3 significant figures

Sample	CaCO ₃ + MgCO ₃ + MnCO ₃	CaCO ₃	MgCO ₃	MnCO ₃	FeCO ₃	FeCO ₃ + MnCO ₃
OB2/1						
mean	96.9	93.9	1.45	0.73	3.95	4.69
median	98.2	95.8	1.34	0.67	1.81	1.65
standard error	1.21	1.28	0.11	0.1	1.22	1.22
OB2/2						
Mean	98.2	96.3	1.05	0.85	1.77	2.62
median	98.8	97.3	1.02	0.84	1.05	1.91
standard error	0.72	0.78	0.1	0.12	0.72	0.74
OB2/3						
mean	97.1	95.6	0.98	0.5	2.91	3.41
median	99.1	97.8	0.28	0.56	0.9	1.63
standard error	1.3	1.77	0.35	0.17	1.4	1.47
OB2/4						
mean	98.9	97	1.34	0.6	1.09	1.69
median	99.2	97.1	0.8	0.69	0.85	1.65
standard error	0.19	0.25	0.03	0.07	0.19	0.21
OB2/5						
mean	98.7	96.2	1.63	0.91	1.29	2.2
median	99.5	97.5	1.09	0.77	0.43	1.06
standard error	0.71	0.91	0.28	0.16	0.72	0.77
OQ2/1						
mean	98.8	97.1	0.9	0.78	1.25	2.03
median	98.8	96.5	0.92	0.61	1.21	1.94
standard error	0.21	0.34	0.24	0.11	0.21	0.19
OQ2/2						
mean	98	96.3	1.33	0.45	1.93	2.38
median	98.6	96.8	0.93	0.1	1.43	1.83
standard error	0.37	0.44	0.26	0.25	0.36	0.44
OQ2/3						
mean	98.1	96.5	0.82	0.3	1.89	2.19
median	99.4	98	1.26	0.11	0.9	1.28
standard error	0.88	1.06	0.24	0.12	0.88	0.89
OQ2/4						
mean	95.4	94.1	1.22	0.43	4.59	5.02
median	97.4	95.3	0.87	0.37	2.56	2.56
standard error	1.53	1.64	0.32	0.17	1.53	1.48
OQ2/5						
mean	96.3	94.5	1.35	0.46	3.72	4.18
median	97.7	96.7	1.5	0.06	2.33	3.57
standard error	1.15	1.21	0.2	0.16	1.14	1.12

Table 4.7 VB & VQ samples**To show the compositional variation of calcium carbonate cement****Results given as percentages to 3 significant figures**

Sample	CaCO₃+ MgCO₃+ MnCO₃	CaCO₃	MgCO₃	MnCO₃	FeCO₃	FeCO₃+ MnCO₃
VB3/1						
mean	98.7	97.3	0.81	0.53	0.34	1.88
median	99.4	98.9	0.3	0.5	0.5	1.04
standard error	0.58	0.82	0.26	0.11	0.58	0.64
VB3/2						
mean	99.3	96.2	1.57	1.53	0.66	2.19
median	99.5	96.3	1.62	0.79	0.42	1.29
standard error	0.16	0.52	0.29	0.35	0.16	0.37
VB3/3						
mean	99.5	97	1.21	1.29	0.48	1.77
median	99.6	98.2	1.09	0.96	0.54	1.74
standard error	0.06	0.58	0.32	0.29	0.06	0.32
VB3/4						
mean	99.2	98	0.66	0.57	0.8	1.37
median	99.2	97.9	0.18	0.63	0.83	1.15
standard error	0.13	0.29	0.24	0.09	0.13	0.09
VB3/5						
mean	99.35	96.7	1.64	1.02	0.65	1.66
median	99.7	96.2	1.89	0.49	0.34	1.12
standard error	0.21	0.66	0.39	0.36	0.21	0.37

These tables provide concise results from SEM and have been calculated by the proportion of Ca^{2+} , Mg^{2+} , Fe^{2+} and Mn^{2+} carbonate present in the sixty samples analysed for each slide. The arithmetic mean and median values have been provided because in many cases there were consistently high CaCO_3 results brought down by a sudden increase in Fe^{2+} content. A number of AB samples were examined in this way. Table 4.5 provides information from profiles of AB5 (red-brown stone) and AB6 (green-grey stone):

1. AB5: The higher Fe^{2+} content would be expected in a stone of this colour. A primary diagenetic composition with high Fe^{2+} content was indicated by CaCO_3 and $\text{CaCO}_3 + \text{MgCO}_3 + \text{MnCO}_3$ figures; and
2. CaCO_3 totals for AB6 were higher than for all the other samples represented. The high proportion of Ca^{2+} has not decreased the solubility of the carbonate cement.

A higher Fe^{2+} content would have been expected in the VB3 cement, considering its dark red appearance. However, as indicated by Table 4.6 and 4.7 there was a greater Fe^{2+} content in OB2 and OQ2. Indeed, some of these results provided chemical formula equivalent to FeCO_3 or siderite, and hand specimens of the rock indicate its presence.

Profiles through the stone were produced to look for characteristic changes in overall cement composition throughout the cores, but particularly in the near surface regions. Variations across small sections of cement are so great that no overall change could be identified.

What are of importance are the quantities of MnO, MgO and especially FeO in the cement of the Culzean stones. This affects the solubility of this 'ferroan calcite' cement. This is highlighted in the fact that Fe-compounds are found in its decomposition i.e. the associated sheet silicates (see *Section 4.7.2*).

The calcium carbonate present in the Culzean samples exhibits three main textural sites. The importance of each of these will be discussed in turn:

- pore filler/cement;
- crystals replacing other rock forming minerals; and
- diagenetic nodules and concretions (c.f. Pettijohn *et al.*, 1987).

The amount of carbonate in and through the different stones has been quantified in Tables 4.2 - 4.4. Comparisons can be made between AB, VB, and OB. AB1, AB6, AB9, AB11 and AB12 samples exhibit comparatively low carbonate contents when compared to the VB and especially OB and OQ samples. There is no calcium carbonate cement in the VQ. The quarry faces exposed at the time of sampling must have been a different geological bed and therefore the VQ samples will not be discussed.

4.7.2 The pore-infill cement

This is the material filling the pore spaces between grains. Many of these grains have long-grain boundary contacts, so the cement fills in the other regions (*Plate 47*). OB and OQ samples tend to exhibit more long-grain boundary contacts than

the other samples (*Plate 46*), and thus the importance of this cement in binding the stone is less apparent.

The pore-infill cement in these lithic arenites, particularly AB and VB, appears to be most susceptible to dissolution by fluids penetrating the surface of the stone. As a result, many of the near surface cores, especially on the balcony stone, exhibit dissolution properties or textures, and more importantly tend to show enrichment or rather partial replacement of the calcium carbonate with other divalent cations. These properties can be readily seen on the SEM, and examples are shown here in *Plates 86 to 89* where dissolution occurs from the centre out towards the surrounding grains, such that cement still surrounds the mineral grains. These photographs show that it is often the white material that is left behind; indicating that it is less soluble. Its presence within the cement is exemplified in *Plates 96 & 97*.

An attempt has been made to identify this white material (under BSE processing) which can be found not only at grain boundaries but within the body of the cement (*Plate 87*), by analysing its composition under the SEM. The composition relates to that of an iron rich silicate, however it is also rich in titanium in places, and no fixed chemical pattern was found to tie it down to one mineral. This is to be expected, especially in the near surface regions of the stone where ions are being released into solution where they can readily bond. Calcium carbonate itself can readily substitute the Ca^{2+} in its lattice for other anions especially Mg^{2+} , $\text{Fe}^{2+/3+}$ and Mn^{+} (Deer *et al.*, 1985). For example a five percent proportion of Mg^{2+} will double the rate of dissolution of pure calcite (Kerr, 1977), of importance when looking at the

role of calcium carbonate dissolution in the deterioration of building stone (see Table 4.5).

There are complex relations between the many oxides and iron hydroxides, and determination of actual mineral species is not easy. However, as a result of this investigation and work using an optical microscope, it is believed that this iron-rich silicate is most probably related to hematite (opaque in thin section) and goethite (yellow to orange-red in thin section) and their alteration products.

Goethite contains a certain amount of SiO_2 , as identified in the SEM analysis, and commonly occurs as the weathering product of iron-bearing minerals, all appropriate under the circumstances. In addition it gives hematite on dehydration (Deer *et al.*, 1985). *Plates 96 & 97* show examples of the precipitation of silicates within the body of the cement.

Hematite is commonly found in sediments, providing their red coloration, and it may occur as a cementing medium, often coating grain boundaries. A small amount of FeO and MnO may be found, whilst SiO_2 and Al_2O_3 probably represent impurities (Deer *et al.*, 1985) which could be derived from the mobilisation of ions. Additionally, TiO_2 may occur, and when in large quantities is indicative of ilmenite, one of hematite's alteration products (FeTiO_3) and halfway to rutile (TiO_2), as identified in AB samples, a common detrital mineral.

The history of cement growth can be demonstrated by work undertaken using cathodoluminescent microscopy (CL). A representation from each of the sample locations and their quarries was looked at using CL, and it was from these investigations that the three categories of carbonate growth were identified. *Plates*

82 & 83 show examples of the carbonate cement where the pore-infill material appears to exhibit more than one growth stage.

Near the surface of samples AB2 and VB2, small brightly fluorescent carbonate appears to have formed in cracks or pores (*Plates 76 & 81*). This is complemented by optical microscopy which has shown cement growth in crevices in mineral grains (*Plates 72 & 73*) which is optically different from the surrounding cement and probably represents reprecipitated calcite, often compositionally richer in $\text{Fe}^{2+/3+}$ and Mg^{2+} when compared to surrounding carbonate. In addition there tends to be a difference in the fluorescence of the cement at grain boundaries (where the cement is in contact with a rock forming mineral e.g. quartz) and at the inter-cement grains (silicates) where infill has occurred (*Plates 84 & 85*). Therefore this provides evidence of the dissolution and reprecipitation of carbonate and its associated silicate material in pore spaces.

When the solutions in the stone become saturated in Ca^{2+} , no more will be dissolved. Values for CaCO_3 saturation are 0.0014g at 25°C, and 0.0018g at 75°C per 100ml of solution (Weast *et al.*, 1984). However the solubility of CaCO_3 changes in the presence of NaCl. Solubility increases from 0 to 1.5 moles per 100 ml due to the influence of NaCl on the activities of Ca^{2+} and the carbonate species. At a constant NaCl concentration and CO_2 pressure, the solubility of calcite decreases with increasing temperature (Wedepohl *et al.*, 1978). This validates the observed increase in cement solubility just beneath the surface of the stone in the AB samples where ingressing fluids are retained within the stone and NaCl is present in abundance.

4.7.3 Carbonate grains and mineral replacement

The replacement of rock forming minerals by carbonate can take on forms from complete replacement such that only a carbonate grain remains, to partial replacement where the former mineral is readily distinguished. Many of the carbonate grains are fluorescent to a greater extent when compared with the perceived original cement pore-infill (*Plate 74*). This suggests that their origin is post pore-infill but still pre-burial and probably originates during the same period from which the diagenetic concretions were formed. There are some grain-replacements that have subsequently been surrounded by cement.

The susceptibility to deterioration of the partially replaced minerals is dependent on their present-day habitat i.e. how deteriorated they already are and whether the carbonate provides a protection from ingressing fluids. Those alumina-silicates that have only been partly replaced will have weaknesses such as open cleavages and fractures that can be readily penetrated by solutions entering the stone. For example *Plates 57 & 60* show examples of feldspar and quartz which have been partially replaced with carbonate. These grains are not protected by the carbonate because dissolution of the carbonate has resulted in pore spaces (micro-porosity) around and between the carbonate and the mineral, exposing these minerals to ingressing fluids and further ionic exchange and/or dissolution.

4.7.4 Diagenetic nodules and concretions

This term, adopted from Pettijohn *et al.* (1985), has been used to describe the areas within all these samples where minerals appear to 'swim in a sea of cement'. Therefore unlike the pore-infill cement which binds already closely packed grains, the grains in this material are well spaced. *Plate 91* shows a large concretion within OB2, 3 mm by 4mm+ in size. These concretions are readily identified with CL and can be from nm to 6 mm⁺ in diameter. *Plates 82 & 83* show an example of part of a concretion in AB2, where carbonate cement can be seen to surround entire grains, particularly clear at lower magnification. At higher magnification (*Plate 83*), variations in the texture of the carbonate cement can be identified, particularly at cement edges. Their abundance is noted in AB and VB where concretion dissolution would accelerate the deterioration of the stone by removing the material that is in effect binding the stone together in this instance, especially with no confining pressures remaining. *Plate 94* exemplifies the lack of grain boundary contacts in a concretion in AB5.

4.8 Soluble salts

4.8.1 Soluble salts present

Externally derived soluble salts are believed to play an important role in both the physical breakdown and chemical decay of the stone at Culzean, particularly on the Drum Tower Balcony. It is here that the maximum effect of weathering by soluble salt has been studied by establishing the quantity and identity of soluble salts,

particularly in the outer few mm of the stone. Further reference to the analytical examination of these soluble salts will be made in *Chapter 5*.

XRD analysis was initially undertaken of the patinas removed by hand from the balcony and depicted in *Plates 20 to 22*. The soluble material (soluble salts and some of the carbonate cement) was dissolved and reprecipitated from these AB samples to identify halite (NaCl) and calcite (CaCO_3), with a number of additional smaller peaks including gypsum ($\text{CaSO}_4 \cdot 2\text{H}_2\text{O}$). The methodology was described in *Chapter 3*.

SEM analysis was undertaken on the reprecipitated salts (photographs of which can be seen in *Plates 100 & 101*) and revealed the presence of material indicative of thenardite/mirabolite ($\text{Na}_2\text{SO}_4 / \text{Na}_2\text{SO}_4 \cdot 10\text{H}_2\text{O}$). This would be feasible as it is possible that both Na^+ and Mg^{2+} sulphates will hydrate in the capillary fringe zone (as described by Evans, 1970). Some form of anhydrite/gypsum ($\text{CaSO}_4 / \text{CaSO}_4 \cdot 2\text{H}_2\text{O}$) was also present as indicated by the XRD traces. Small gypsum peaks were identified in XRD analysis near the surface of the stone on a number of the AB samples, and may result from the combining of SO_4^{2-} with Ca^{2+} from the carbonate cement at the surface (see *Chapter 5*). This is more common in urban regions, where sulphate values in the atmosphere are higher (Cooke and Gibbs, 1994; Pavia Santamaria, 1984; Pavia Santamaria, *et al.* (1994), but not unknown in marine locations as marine aerosols contain sulphate particles (Zezza & Macrì, 1995).

It may also be possible that sylvite (KCl) was present (as a result of K^+ ions either from rainwater or feldspar reacting with chloride ions), however this could not be confirmed.

4.8.2 Preliminary profiling of soluble salt content in core samples

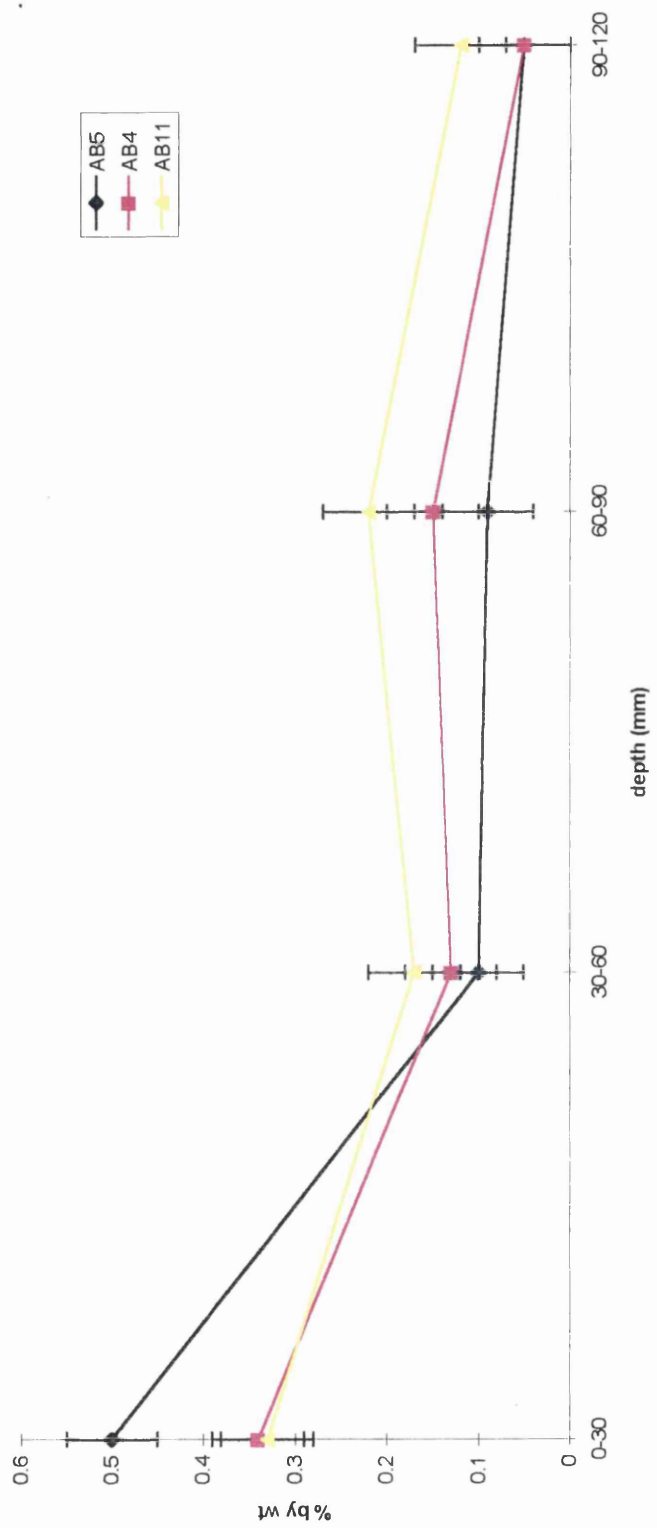
Results from the water soluble extracts (described in *Section 3.4.1.2*) show that soluble salt content generally decreases from the exterior to interior surface of the stone (Figure 4.6). The solute obtained on reprecipitation and examined by SEM contains halite (NaCl), calcite ($CaCO_3$), and gamma calcium sulphate, as in the analysis of the patinas. It can therefore be assumed that these mineral phases are likely to be present in the stone on the building, although recognising that under different temperature regimes the solutes could produce different mineral phases e.g. mirabolite/thenardite; anhydrite/gypsum etc.

By examining the weight percent of soluble material dissolved (and reprecipitated) from AB4, AB5, and AB11, the core profiles examined (Figure 4.6); it can be seen that:

- soluble salts are present up to at least 120 mm depth within the cores; and
- the highest concentrations of soluble material are in the outer 0 to 30 mm.

This indicates that where moisture has been drawn into the sandstone by capillary action the salts have precipitated out from solution. Ions in solution were both internally and externally derived (see *Chapter 5*).

Figure 4.6 Graph to show variation in soluble salt and carbonate content by % weight of sample



4.8.3 Soluble salt crystallisation, hydration and hygroscopy

Therefore a number of different possible soluble salt phases have been determined including halite, gypsum/anhydrite and thenardite/mirabolite. It is known that halite is hygroscopic, it has the ability to readily absorb water vapour from the atmosphere. Halite will therefore undergo continuous changes in volume dependent on its access to moisture. Sodium sulphate (thenardite/mirabolite) will undergo hydration readily. It will hydrate and dehydrate relatively easily in response to changes in temperature and humidity. As water is absorbed the volume of the salt will increase up to 300% (Goudie & Viles, 1997) and this can develop pressure against the pore walls in which the salts are located. Gypsum will produce a greater crystallisation pressure than mirabolite and the solubility of gypsum will increase in the presence of other soluble salts, lowering its deliquescence humidity (Zhender, 1996). The mixture of salts present is also important because salts will precipitate out at different times (Fitzner & Sneath, 1982). The order of crystallisation will depend on their hygroscopicities.

In addition to the deposition of soluble salts, as the solute has been concentrated, a number of chemical and biochemical reactions have taken place, attacking the mineral grains and calcium carbonate cementing agent, and allowing them to be dissolved (see *Sections 4.5 and 4.7*). SEM analysis provides evidence for the partial cracking of mineral grains, which provide a point of ingress for these soluble salt-rich solutions, many examples of which can be seen in the plates, particularly the examples in *Plate 56* through to *Plate 61*. This has enabled salt crystallisation

within micro fractures which is a pressure producing process (Cooke, 1981), and may well have encouraged mechanical as well as chemical break-up. According to Fitzner & Snethlage (1982) crystallisation in these micropores will only take place once the larger pores are saturated in salt solution. Evidence of cracking of micropores near the surface of the AB stone suggests that there are sufficient quantities of soluble salts present for this to happen.

The presence and influence of these soluble salts will be discussed in more detail in *Chapter 5* and *Chapter 7*.

Due to the initial number of cores available, no further work on dissolving and reprecipitating material was undertaken. Therefore, there are no comparative results from OB, OQ, VB, or VQ.

4.9 Engineering Tests

The following provides an overview of the engineering tests undertaken by John Fairhurst at Napier University as part of the Getty Grant Research Programme, and have been reproduced with his permission. The results of these tests have been outlined below rather than being placed in an appendix so that they could be considered with the geochemistry data. The engineering test results obtained from the Culzean samples have been reproduced in Appendix 1 (Table 17) and the average results for sandstones from tests previously undertaken have been recorded in Appendix 1 (Table 18).

4.9.1 Dry Mass Density

These results were reproducible $\pm 0.5\%$ for each sample and range from 2235 kg/m^3 for AB3 to 2312 and 2323 kg/m^3 for OB3 and VB3 respectively. The dry density for the AB samples being lower than for the VB and OB samples. The results are within the range expected for a sandstone (Fairhurst, 1995).

4.9.2 Absorption and Porosity

The absorption and porosity values are based on volume and use water, rather than mercury, as the test medium. These values were not calculated as a percentage of mass, and thus rock density is not a variable (Fairhurst, 1995).

The absorption values are all relatively high for the AB samples, particularly AB4 (16.6%) and AB6 (16%), which are the most decayed of the samples analysed here (see *Figure 2.4*). Absorption values are also high for both VB and OB and the corresponding porosities are low. These are unusual results. Absorption values are usually substantially lower than their corresponding porosity values. Therefore checks were undertaken on these samples. These checks showed that the samples could indeed absorb more water than the apparent pore space could contain.

Absorption tests involve prolonged immersion, usually 24 hours. Therefore the high values could be accounted for by the abundance of soluble salts present in the stone which will absorb water during prolonged immersion. Clays present in the

stone will also absorb water, but not to these volumes (Fairhurst, 1995), and will thus play a less important role.

The absorption test for samples with a high soluble salt and clay content is completely misleading as a measure of pore space accessed by water at atmospheric pressure. However, it is extremely useful in this instance for assessing the capacity of the stone to draw in solutions, such as rainwater and runoff.

As a result in Appendix 1 (Table 18) absorption and porosity have been renamed 'water absorbed' and 'indicative porosity' to avoid confusion with true measures of pore space. These may be more readily attained from the SEM atomic number contrast results as recorded in *Section 4.4.6*, where there is a far greater differential in pore space between AB, VB, and OB. The indicative porosity results shown in Table 18 are consistently higher than the porosity recorded by SEM atomic number contrast imaging except in AB4 and AB5, where the SEM records an increase in porosity towards the surface of the core.

The relationship between absorption and porosity is reversed in samples from OB and VB where porosity is often higher than absorption indicating that these stones have a lower water absorption capacity (relative to porosity) compared with the AB stone. However there is still an inconsistency here in the relative values of absorption and porosity as recorded in Table 19, Appendix 1.

4.9.3 Sodium Sulphate Test

The sodium sulphate test was not attempted on all the samples. This particular test is often criticised for its lack of scientific basis (Fairhurst, 1995), nevertheless the results produced in this instance are conclusive and can be seen in Table 18, Appendix 1.

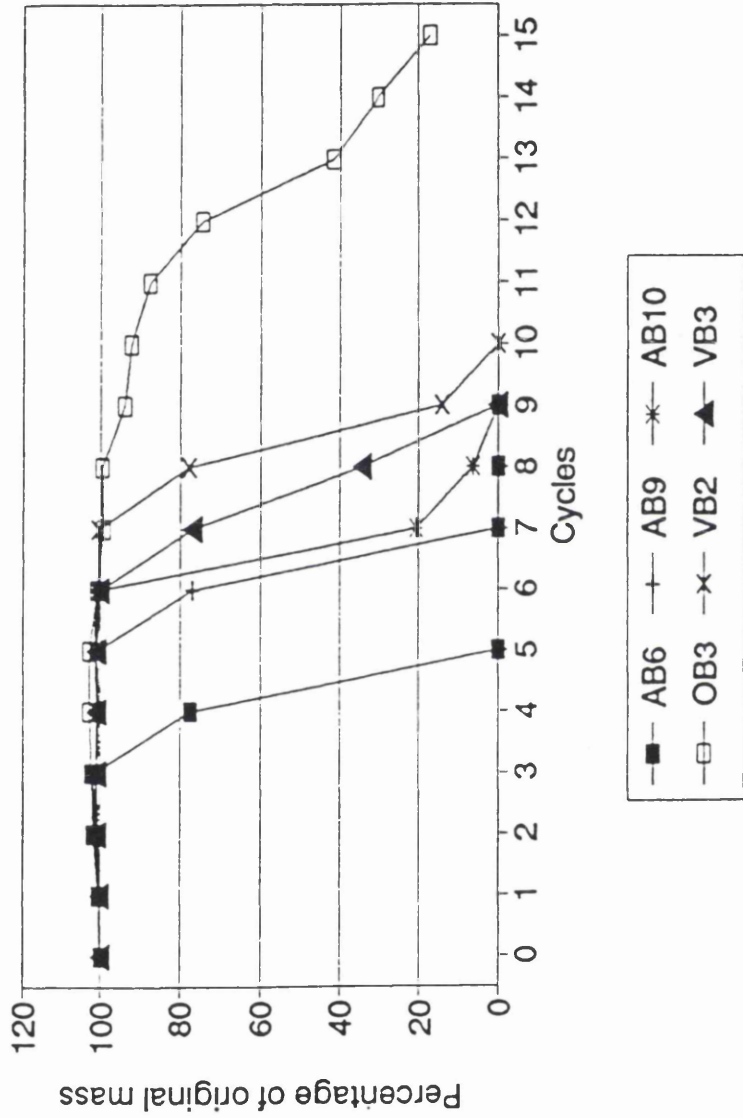
It is unusual for a sample to exhibit extensive failure before ten cycles, and even then decay is usually gradual, replicating the spalling/exfoliation of the weathering of a stone face (Fairhurst, 1995).

However, in this case all the AB samples failed between four (AB6) and six (AB10) cycles. VB failed after eight and nine cycles. Only OB3 behaved in a manner comparable with other acceptable building stones, reaching fifteen cycles, and replicating a spalling phenomenon (see Figure 4.7).

John Fairhurst reported that the failure of the AB samples was different to any he had previously observed (Fairhurst, 1995). The samples expanded until they cracked. To explain this it is necessary to refer to the absorption and porosity values.

The absorption and porosity values are unusually close and the reverse of those usually obtained. The expansion of soluble salts (and to lesser extent clay minerals) will result in a lack of pore space available for the growth of new minerals, namely sodium sulphate in this test. This would result in a relatively rapid increase in the internal stresses of the stone, which together with bond strengths, which are below

Figure 4.7 Graph to show the results from saturated sodium sulphate testing on selected AB, OB and VB samples



average (weakening of grain-to-grain boundaries exemplified in SEM observations), would lead to more rapid breakdown by weathering than is normal in sandstones.

4.9.4 Point-Load Strength

Although few values were obtained, most of the fractures were good, even and not affected by flaws in the stone. Overall the values were lower than average (1.9 MN/m²) but mostly within an acceptable range for a building stone (between 0.7 MN/m² and 3.8 MN/m², as shown in Table 19, Appendix 1).

4.10 Conclusions drawn from engineering tests

From these engineering tests one can assess the value of geochemical analysis without which the results from porosity and absorption would be unexplained. It is also important that the geochemistry can be substantiated by the engineering tests. These engineering tests can be used to compare the physical properties of the stone but cannot show why their deterioration rates differ. The two principal conclusions drawn from these tests are that:

- AB performs least well in the engineering tests in its present state; and
- whilst OB does have the capacity to absorb water as shown by the water absorption tests, it is physically stronger than AB and VB, and can withstand 15 cycles of the sodium sulphate test.

4.11 Conclusions drawn from petrographic & mineralogical data

Firstly it is important to summarise the petrographical characteristics of the sandstones used to construct Culzean. The three sandstones have very similar mineralogical and textural compositions. These can be summarised as follows:

- *AB sandstone*: A medium grained rock containing quartz, feldspar, lithic fragments, micas, clays and carbonate cement. AB contains almost double the quantity of lithics found in the other samples and incorporates the highest proportion of replacement calcite. Despite the abundance of cement, substantial porosity is apparent;
- *VB sandstone*: A small to medium grained rock, also containing quartz, feldspars, lithics and clays and a higher proportion of micas, and micas undergoing alteration. There are fewer feldspars and lithic fragments but more examples of calcitic nodules/concretions in the stone when compared with the AB samples; and
- *OB sandstone*: A medium grained rock that contains quartz, feldspar, lithic shards, mica, clays and cement. The OB stone appears to have slightly more quartz than the other rocks. It is more compact, with more grain boundary contacts, and thus has the lowest 'effective' porosity. There is an abundance of calcitic cement, although there are fewer examples of carbonate concretions and they tend to be smaller than in the other rocks.

The two quarry stones, as expected, are of similar composition. In addition, all the sandstones examined can be described as mineralogically immature as they contain

quantities of less stable grains, specifically feldspars and rock fragments. All the stones are texturally submature, containing <5% clay matrix. The grains are poorly-sorted and not well rounded.

The similarities in the composition and texture of the three sandstones make it difficult to understand how and why AB has deteriorated more rapidly than the others, in terms of its mineralogical make-up alone. Individual processes and reactions are taking place; the crystallisation, dissolution and reprecipitation of material within the stone is evolving simultaneously and the following processes can be highlighted:

- rock forming minerals of similar chemical composition are deteriorating in similar ways in the different sandstones (e.g. the erosion of quartz grain boundaries and surface pitting, the dissolution of feldspars along cleavage planes, and the expansion of micas). What is of importance therefore are the proportions of the various rock forming minerals found in AB, OB, and VB, and their state of decay, which combine to form the overall chemical make-up of the stone, and subsequently their states of decay;
- the porosity structure of the stone is of fundamental importance as interconnecting pore channels and micro-porosity will increase permeability. Porosity types include intergranular, dissolution, fracture and micro-porosity. The AB samples, with interconnecting pore-space structures near the surface of the stone, are susceptible to greater fluid ingress;
- clay minerals are abundant in the Culzean sandstones. Of greatest importance are the illites, smectites and chlorites found in the AB samples as they are the

most destructive for their size. Initial observations show these intermediary clay species to be more abundant in the surface regions of the stone;

- the calcium carbonate cement (ferroan calcite) can be dissolved, as is apparent in many of the AB samples analysed using the SEM. The solubility of the cement is affected by its composition; and often dissolves to leave micro-porosity around the silicate minerals embedded within it; and
- the presence of soluble salts plays an important role in both the physical breakdown and chemical decay of the stone. Halite (NaCl), gypsum ($\text{CaSO}_4 \cdot 2\text{H}_2\text{O}$), and thenardite (Na_2SO_4) are all present in the AB samples, with greatest concentrations in the outer 30 mm of the stone.

Inherent natural characteristics must and do play an important role here as exemplified by SEM and optical microscopy examination. However it is the chemical make-up of the stone and its interaction with natural and induced climates that allows salts to crystallise, clays to expand, cement to dissolve and minerals to alter.

The above processes may be at work throughout the stone, but they dominate in the near-surface regions, as many are dependent on pore spaces and channel outlets. Many of the weathering processes will have a knock-on effect, for example dissolution, as a result of the ingress of 'aggressive' solutions, will increase micro-porosity, release ions into solution, and provide spaces for salt crystallisation, and so on.

Chapter Five

Chemical Profiling of the Culzean stone

5.1 Introduction to chemical profiling

Chemical alteration and the mobility of ions are examined and discussed in this chapter. Interpretation of these results is supported by the petrographic analysis of the stones, specifically:

- the composition of the stones;
- their compositional variability; and
- evidence for alteration through soluble salt accumulation, mineral alteration (including the formation of clays), creation of micro-porosity and the dissolution/ reprecipitation of carbonate cement.

As a result close reference to *Chapter 4* has been made during the analysis of these results.

Three methods have been used to look at evidence for elemental and accordingly ionic mobility:

- atomic absorption and emission (AA & AE);
- ion chromatography (IC); and

- X-ray fluorescence (XRF).

The latter divides the major and minor (or trace) elements in the samples into single oxides such as SiO_2 , MgO , Fe_2O_3 , and trace elements such as Cu, Co, and Pb, whilst the other methods provide anion and cation data. Anions are negative ions, e.g. Cl^- (analysed by IC), and cations are positive ions, e.g. Na^+ (AA & AE). Therefore, by examining anions and cations one is not only looking at the character of the sandstone but its potential to interact with the surrounding environment and form new salts, which may be detrimental to the stone's life span.

The chapter has been divided into two sections:

- monitoring the solubility and extraction of material from the stone; and
- profiling of the stone using XRF and IC.

1. Monitoring the solubility and extraction of material from the stone

The mobility of anions and cations is best observed by attempting to simulate the effects of prolonged exposure of the surface of the stone to moisture from runoff and rainwater, the methodology for which has been described in *Chapter 2*. These results are considered first as they provide a good starting point for discussion of the overall chemical profile of the stones.

2. Profiling of the stone using XRF and IC

As weathering is an interaction between surface processes and the interior of the stone, throughout these experiments it has been important to examine the chemical profile through individual stone samples. As described in *Chapter 2*, cores were

sliced to the minimum thickness to allow these experiments to be undertaken. This was done so that the chemistry of the stone at each of these points could be obtained, particularly to identify any changes in chemical composition at or near the surface of the stone.

Section 1 Leaching experiments on stone cores

5.2 Anion and cation activity

5.2.1 Experimental approach to the leaching of ions

In comparing the quantity of soluble material leached from the surface (0-40 mm) of the core with material from a depth of 110-1450 mm, these experiments were approached with the following possibilities in mind:

- it was anticipated that ions could be mobilised more readily under surface conditions;
- there would be more soluble anions at the surface of the stone;
- there would be greater mobility with rainwater than HPLC (bidistilled water) as rainwater has a greater charge of ions present in solution and greater potential for ion exchange;
- there would be greater mobility in the AB samples when directly compared to VB and OB, as AB is a more exposed site and a chemically more complex stone; and

- the anion and cation data would correlate to fingerprint the presence of soluble salts such as halite and gypsum.

By undertaking this experiment an attempt was made to show how much material could be transported out from the stone into solution, and to determine which elements were most mobile. To test the validity of the results (because only one test could be undertaken on each core sample) a core was analysed in duplicate by cutting the two samples in half (60 mm from the exterior surface) and suspending each half in the beaker for 3 hours to compare the results. Results are given in Table 5.1.

Table 5.1 Comparative data for leaching experiments

Results given as ppm (mg/kg) of stone sample

		K ⁺	Al ³⁺	Fe ²⁺	Mg ²⁺	Ca ²⁺	Na ⁺
Core 1a	(outer surface)	12.60	0.12	0	39.0	84.9	448.5
Core 1b	(inner surface)	11.82	0.12	0	37.5	73.95	324.75
Core 2a	(outer surface)	9.04	0.09	0	22.50	43.65	281.25
Core 2b	(inner surface)	10.12	0.12	0	21.00	56.25	379.5

(5 significant figures)

Greatest variation was seen in the results for Ca²⁺ and Na⁺ because these cations have a greater solubility and they are in greater abundance.

Results have been given as ppm (mg/kg of stone sample accessible to the ingressing fluids). This has been calculated by knowing the volume of rock, its dry mass density and the ratio of rock material to fluid. The results are shown in Tables 6 and 7, Appendix 1. The HPLC and rainwater collected for the experiments have also been analysed and the mean values (from triplicates) for their analysis are outlined in Table 5.2:

**Table 5.2 Mean values for anion and cation contents
of HPLC and Culzean rainwater**

Results given as mg/litre of water

	Fluoride F ⁻	Chloride Cl ⁻	Nitrite NO ₂ ⁻	Nitrate NO ₃ ⁻	Sulphate SO ₄ ²⁻	Phosphate PO ₄ ³⁻
HPLC	0.025	0.328	0.012	0.019	0.051	0
CULZEAN H ₂ O	0.048	19.104	0	0.765	3.048	0
	Calcium Ca ²⁺	Sodium Na ⁺	Iron Fe ²⁺	Potassium K ⁺	Magnesium Mg ²⁺	Aluminium Al ³⁺
HPLC	0	0.17	0	0.05	0	0
CULZEAN H ₂ O	7.5	13	0	0.97	1.2	0.065

The results for AB2, AB6, AB9 and AB10; VB1, VB2 and VB3; and OB1, OB2 and OB3 have been produced graphically in Figures 5.1 and 5.2. Each of the AB samples represents one of the weathering categories predetermined in Chapter 2 (see Table 5.3), distinguished by their colour and surface deterioration properties:

**Table 5.3 Classification of weathering forms from
AB, VB and OB samples**

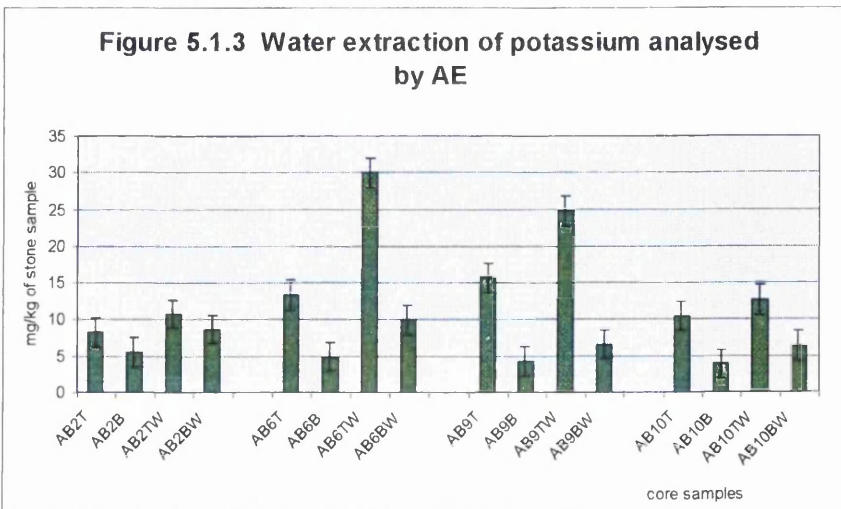
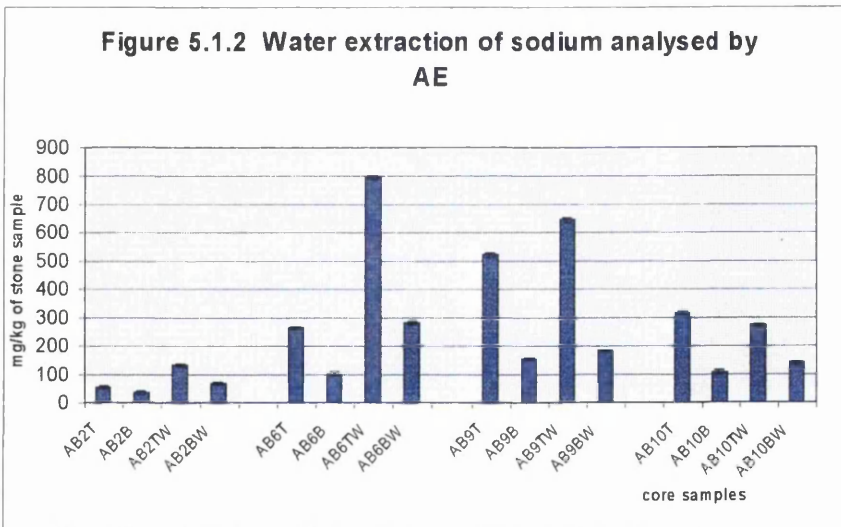
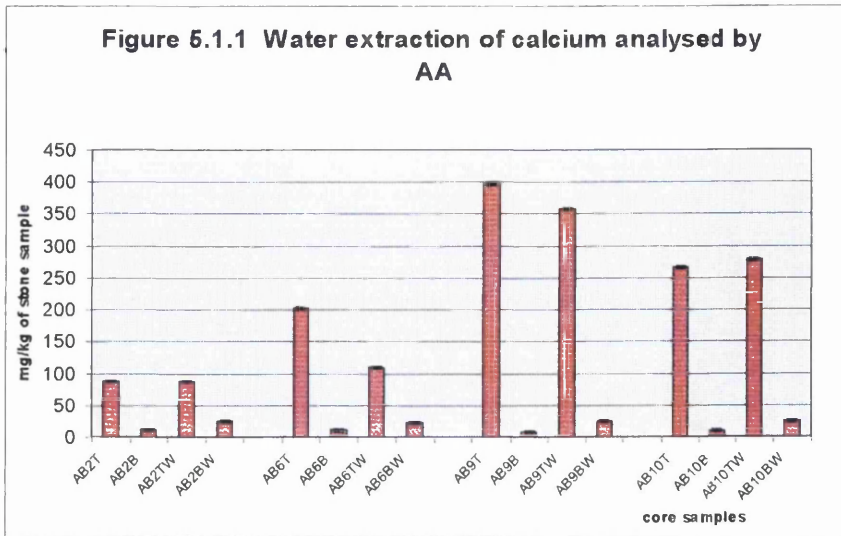
ASPECT	AB2	AB6	AB9	AB10	VB1	VB2	VB3	OB1	OB2	OB3
NORTH	X					X		X	X	
WEST		X					X			X
SOUTH			X	X	X					
DESCRIPTIVE CLASSIFICATION										
FRESH (F1)				X		X	X	X		X
PATINA (P2)		X							X	
SCALING (C3)	X		X		X					
COLOURATION										
RD	X			X	X	X	X			
GD		X	X					X	X	X
MINERAL ALTERATION	Yes	Yes	yes	yes	yes	yes	yes	yes	Yes	yes

Immediately from the results shown in Tables 6 and 7, Appendix 1, the extent of this difference between surface and subsurface soluble cation and anion contents can be seen. The surface consistently shows higher solution of cation and anion contents compared with the interior of the stone.

5.2.2 Sodium and chloride ions

As one would expect from samples directly exposed to seaspray and the prevailing offshore wind, Na^+ is the most abundant soluble cation. AB samples yield consistently high values of Na^+ , particularly the South facing samples. The majority of this Na^+ will have entered the stone as Na^+ -rich fluids, common sea salt (halite) raised by spray from the Clyde and present as a compound in both the atmosphere and rainwater (13 ppm of Na^+ was found in the rainwater analysis). However, a

Figure 5.1 AA and AE: Results from water extraction experiments
 Results from AB2, AB6, AB9 and AB10 given as concentrations of mg/kg of stone sample



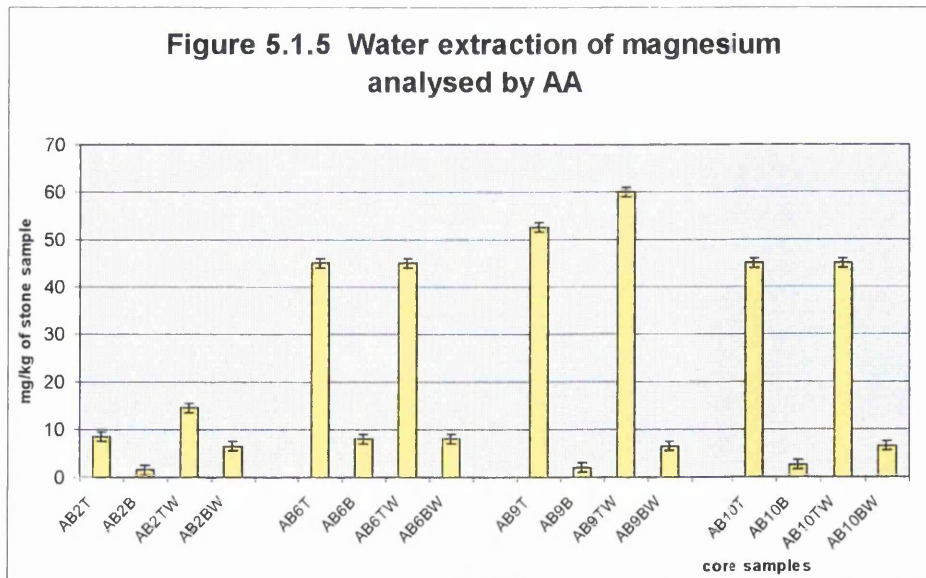
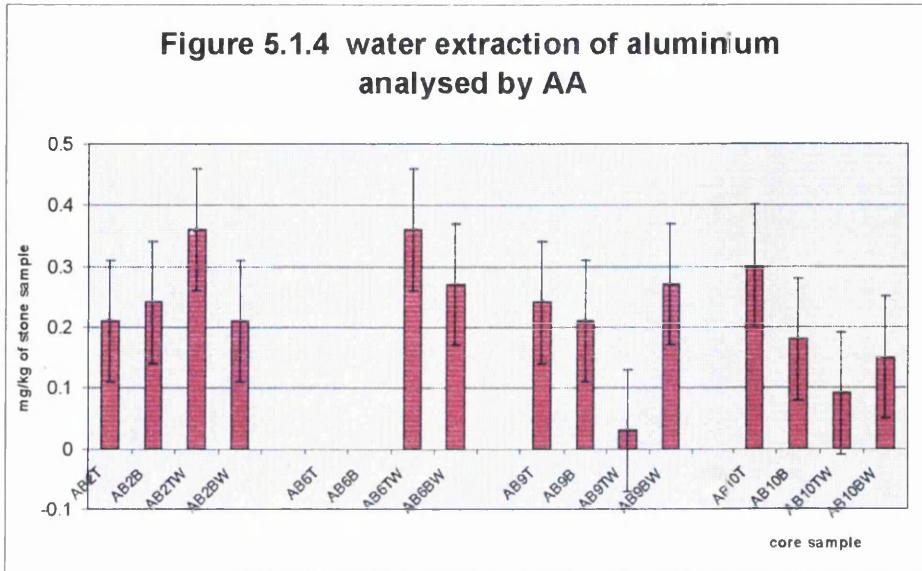
AB2T Sample AB2 at the surface (0-40mm) using HPLC
 AB2B Sample AB2 at 110-150mm depth using HPLC

AB2T Sample AB2 at the surface (0-40mm) using rainwater
 AB2B Sample AB2 at 110-150mm depth using rainwater

Figure 5.1 Continued...

AA and AE: Results from water extraction experiments

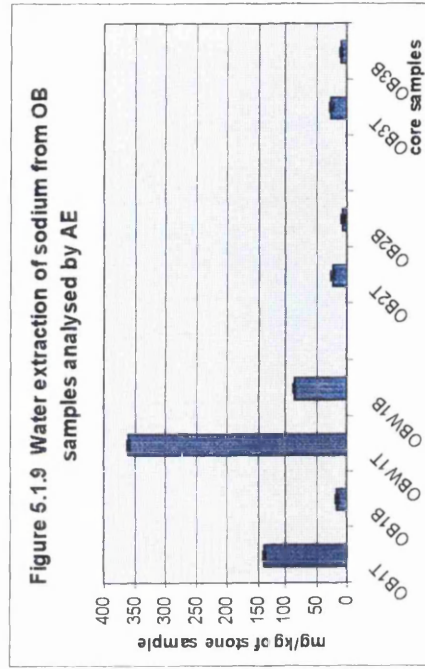
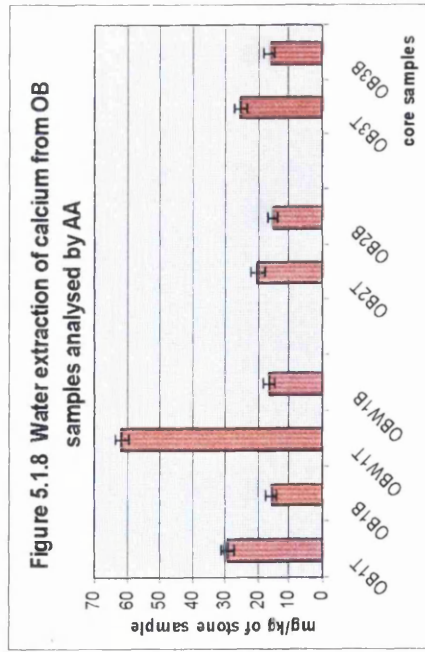
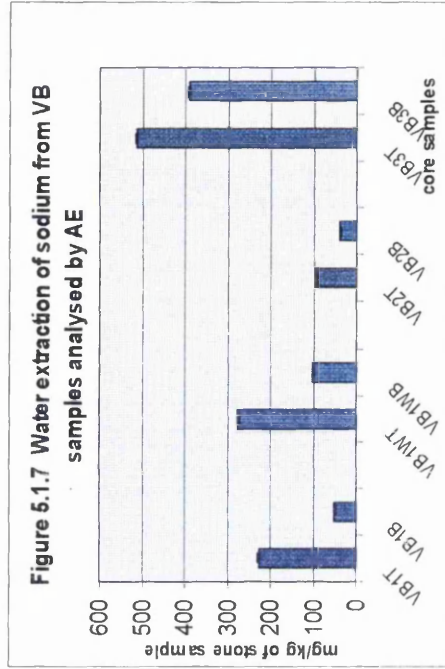
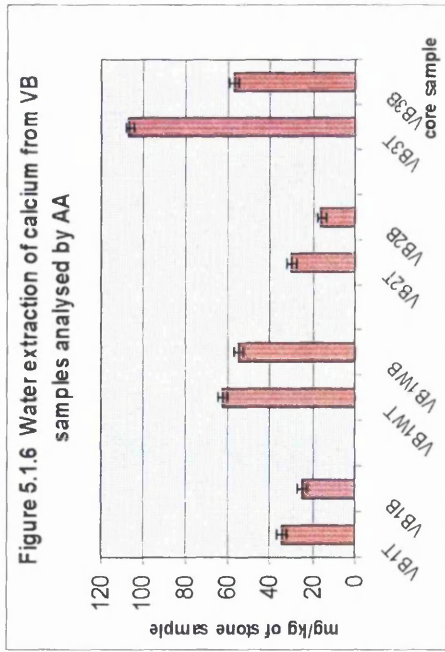
Results from AB2, AB6, AB9 and AB10 given as concentrations of mg/kg of stone sample



- AB2T Sample AB2 at the surface (0-40mm) using HPLC)
- AB2B Sample AB2 at 110-150mm depth using HPLC)
- AB2T Sample AB2 at the surface (0-40mm) using rainwater
- AB2T Sample AB2 at 110-150mm depth using rainwater

Figure 5.1 AA and AE: Results from water extraction experiments

Results from VB and OB given as concentrations of mg/kg of stone sample



small proportion of the Na^+ extracted from the stone could be from soluble precipitates produced during the weathering of feldspar and lithic fragments, and even some of the clays such as smectite.

The differences in the quantity of soluble material analysed using HPLC and Culzean rainwater are marked in AB6, the most deteriorated of all the samples analysed. In sample AB7 similar amounts of Na^+ are extracted from both the surface and interior of AB7, the sample with cement rendering attached. This sample shows reduced insolubility across all the ions analysed compared with the other AB samples.

There are marked increases in extraction quantities when using Culzean rainwater when compared with HPLC on OB1 and VB1 which are situated in more sheltered locations, due to the amount of Na^+ already in solution in the rainwater samples. In addition VB3 faces seawards and as expected there are higher quantities of soluble Na^+ present set against VB1 and VB2 (see Figure 5.1.7).

These results are mirrored in the Cl^- results. Larger quantities of soluble Cl^- are recorded at the surface of the stone than at depth, and with rainwater. More soluble Cl^- was removed from the AB samples facing South, than those facing North which recorded smaller values than the VB stones analysed. Rainwater already had 19 ppm Cl^- present (see Table 5.2), but these results show up to 1000 ppm (1 g/kg) of sample being dissolved from AB12. Many of the samples show significant levels of solubility at depth, AB6 records 378 ppm of chloride in solution, suggesting that salts are penetrating the stone a significant distance. The quantities of Cl^- extracted are higher than Na^+ but there is a trend in the relative extraction quantities between

the two ions indicating that much of the Na^+ and Cl^- in solution is from halite. Figure 5.2.8 provides a scatter graph of Na^+ plotted against Cl^- , to directly compare the two. Scatter graphs have also been produced to look for a correlation between Mg^{2+} and Cl^- to look for the presence of MgCl_2 . These are reproduced in Figures 5.2.10 and 5.2.11. The two scatter graphs demonstrate that plotting Cl^- against Mg^{2+} and Cl^- against Mg^{2+} and Na^+ do not produce a correlation.

5.2.3 Calcium and sulphate ions

Ca^{2+} is the other cation extracted from the stone in large quantities, and one can see similar trends to those established for Na^+ i.e. the is more soluble Na^+ extracted from the exterior surface of the stone than the interior.

Larger amounts of Ca^{2+} are extracted from the surface of the stone, than at depth, and larger amounts of soluble Ca^{2+} are found in the AB samples which retain a surface patina (e.g. AB3 and AB6) than samples with a 'fresh' surface (e.g. AB8 and AB12). This suggests that a large amount of soluble Ca^{2+} (the majority of which will be in the form of CaCO_3 cement) may be retained beneath the patina and found near the surface of the stone. Also, as with the Na^+ , there is particularly heightened solubility in surface samples AB9 and AB10 (see Figure 5.1.1) both located on the South-side of the Balcony.

There are significantly smaller amounts of Ca^{2+} being dissolved from the VB and OB samples. This may signify less soluble carbonate cement, particularly at the surface of the stone when compared directly with the AB samples. Also, there is

less variation between the interior and exterior of the stone as shown in Figures 5.1.6 and 5.1.8.

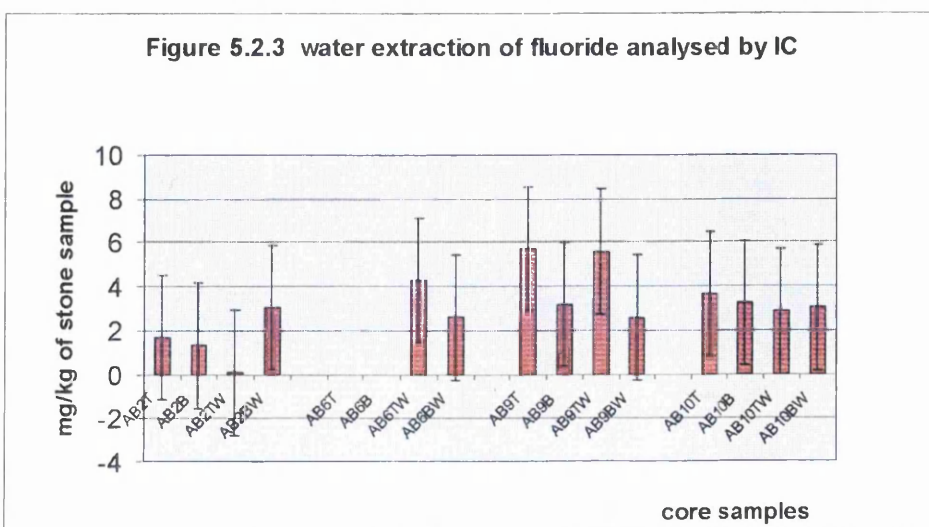
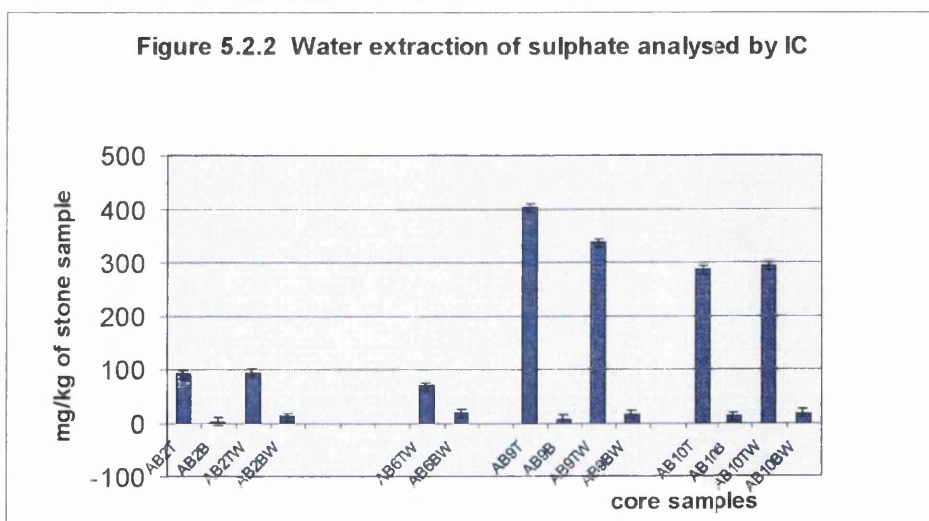
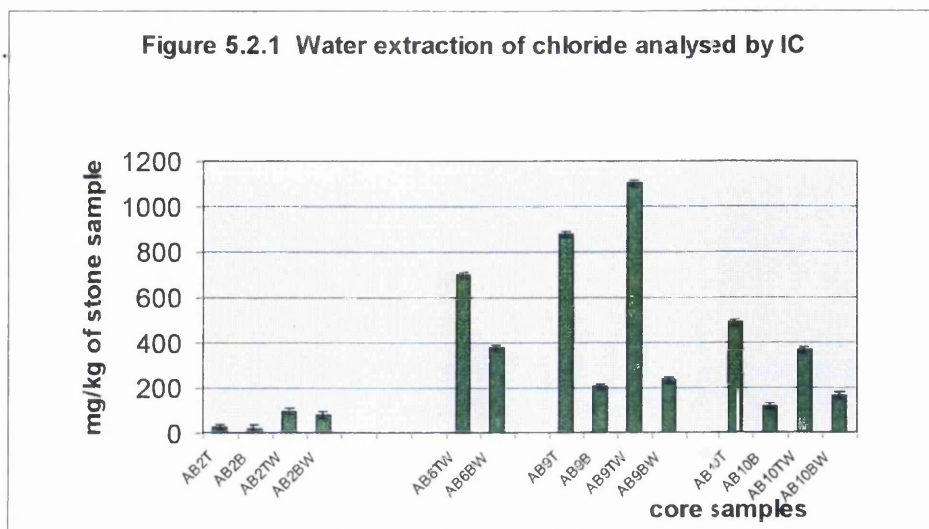
Many of the results, notably from AB3, AB6, and AB9 which, in contrast to those for Na^+ , demonstrate greater removal (and thus solubility) of Ca^{2+} using HPLC than Culzean rainwater. This is to be expected, as Culzean water may be almost saturated in Ca^{2+} (it already has dissolved in it 7.5 ppm of Ca^{2+} - see Table 5.2) which will be added to the total Ca^{2+} being removed from the stone.

Again there appears to be a relationship between the quantities of soluble Ca^{2+} and SO_4^{2-} extracted from the samples. Figure 5.2.9 plots the relationship between Ca^{2+} and SO_4^{2-} and provides a similar trend to that seen for Na^+ plotted against Cl^- . XRD analysis showed the presence of some anhydrite / gypsum in the AB samples, although the peak intensities were lower than those for halite. Therefore it is probable that a reaction is taking place, the Ca^{2+} cations from dissolved carbonate cement are combining with the SO_4^{2-} anions to form gypsum in the near-surface regions of the stone. It is noted that although Ca^{2+} may be extracted from the stone from soluble precipitates produced during the weathering of feldspar and lithic fragments, the proportion of Ca^{2+} derived from these reactions would be minimal. Gypsum (CaSO_4) crust formation on stone surfaces is a well-documented phenomenon (from Schaffer, 1932 to Pavia Santamaria *et al.*, 1994). The extent to which CaSO_4 is produced within the stone will depend on porosity, the penetration of solutions and the solubility of CaCO_3 in the stone.

SO_4^{2-} comes from sulphur compounds present in the atmosphere (in variable quantities which may be considered as contaminants), and to a lesser extent in

Figure 5.2 Ion Chromatography: Results from water extraction experiments

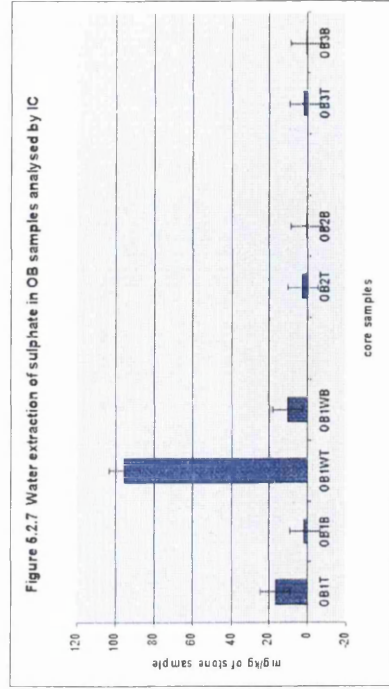
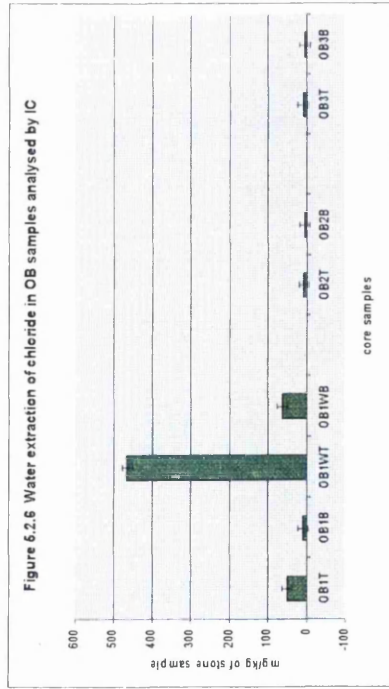
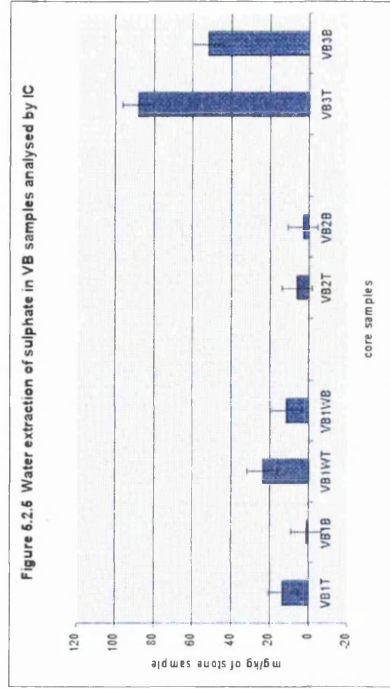
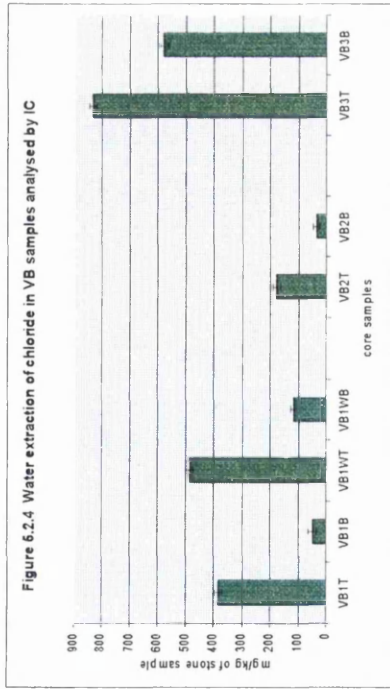
Results from AB2, AB6, AB9 and AB10 given as concentrations of mg/kg of stone sample



AB2T Sample AB2 at the surface (0-40mm) using HPLC
 AB2B Sample AB2 at 110-150mm depth using HPLC

AB2T Sample AB2 at the surface (0-40mm) using rainwater
 AB2B Sample AB2 at 110-150mm depth using rainwater

Figure 5.2 IC: Results from water extraction experiments
 Results from VB and OB given as concentrations of mg/kg of stone sample



marine aerosols (3 ppm were found in the Culzean rainwater derived from off-shore wind-driven rain). Sulphurous gases are temporary constituents of the air in so far as they are readily soluble in water and are washed out by rain. Since the Clean Air Act of 1956, there has been a vast decrease in sulphur emissions into the atmosphere. However, it is not known how much SO_4^{2-} is embedded in the stone, particularly as there was a gas house at Culzean which burnt coal to provide power for the castle from the late 1700s onwards. SO_4^{2-} is concentrated at or directly beneath the stone surface (Figure 5.2.2).

XRD results also indicate the formation of thenardite/mirabilite, Na_2SO_4 / $\text{Na}_2\text{SO}_4 \cdot 10\text{H}_2\text{O}$ an highly expansive and thus potentially damaging evaporite, related to halite.

5.2.4 Magnesium, potassium and aluminium ions

There are other cations and anions extracted from the core samples which react to form compounds including $\text{K}^+ + \text{Cl}^-$ (sylvite) and $\text{Mg}^{2+} + \text{SO}_4^{2-}$ (e.g. hexahydrate). These cations are drawn from the stone in much smaller quantities, but still show greater solubilities at the surface of the stone. Figures 5.1.4 and 5.1.5 show these cations, and there is a marked contrast in the extraction of Mg^{2+} from the stone surface compared with its interior.

Mg^{2+} exhibits a similar pattern to Ca^{2+} and Na^+ in that the largest amount is extracted from AB6 and from AB9, AB10, and AB12 using rainwater. Also of interest is the amount of Mg^{2+} removed from OB1 with rainwater. OB1W data is

repeatedly high compared with the other OB data, for all the cation extractions. In this experiment the rainwater will have greater access to the sub-surface material (beneath the organic patina-crust), extracting material more readily than it can on the building. K^+ behaves in a similar way, although concentrations are reduced.

Al^{3+} is present in minute concentrations and as a result there is no clear resulting pattern of dissolution. This is because the Al^{3+} present in the stone is in insoluble phases and rare in rainwater/seaspray.

5.2.5 Fluoride, nitrate, nitrite and phosphate ions

Fluoride, nitrate, nitrite, phosphate, and trace amounts of bromide are present in the core samples analysed. The halogen fluorine (F^-) is an industrial contaminant liberated by the burning of fuel and the calcination of material containing fluorine. It is possible that F^- has formed simple soluble salts in the stone with K^+ , or any other 2^+ cation, and is readily dissolved. F^- is also a common constituent of micas, and as many of the micas in all three stone types showed significant decay, it is likely that this is another source.

Nitrate (NO_3^-) is detectable in the stone, but in very small quantities (often < 1 ppm). Nitrite (NO_2^-) ions are not evident. NO_3^- and NO_2^- are both inorganic ions. NO_x compounds originate as motor vehicle emissions, (power station and refinery emissions). Since 1945 there has been a significant increase in UK NO_x emissions, chiefly due to increased oil consumption by the transport sector (BERG, 1989). In addition, ammonium ions (NH_4^+) occur in sheet silicates, therefore NO_3^- and NO_2^-

Figure 5.2 Continued...
IC, AA & AE: Results from water extraction experiments
Scatter graphs to show the relationship between
anions and cations in solution

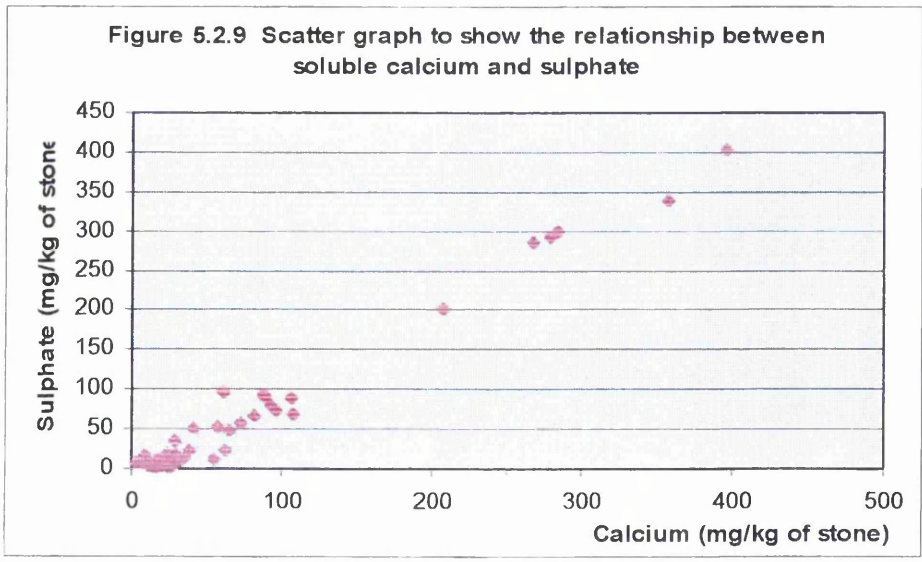
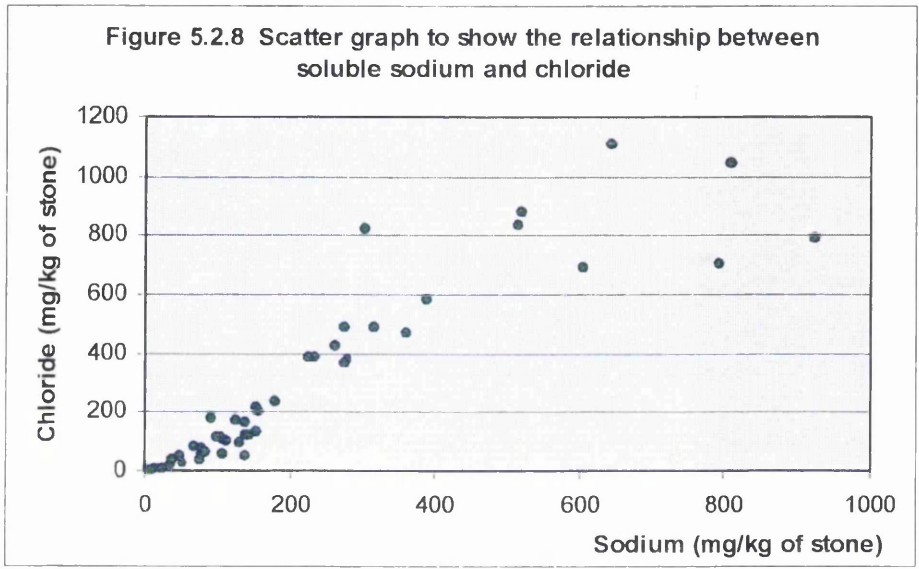
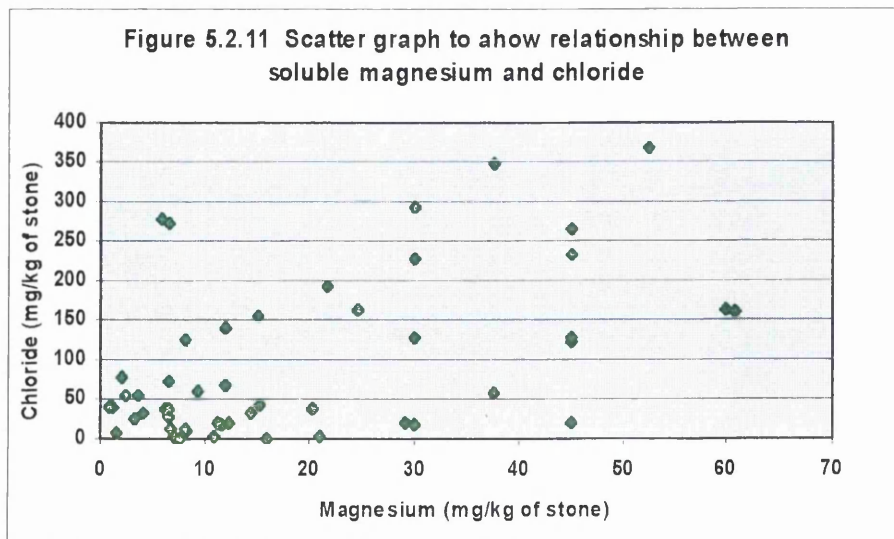
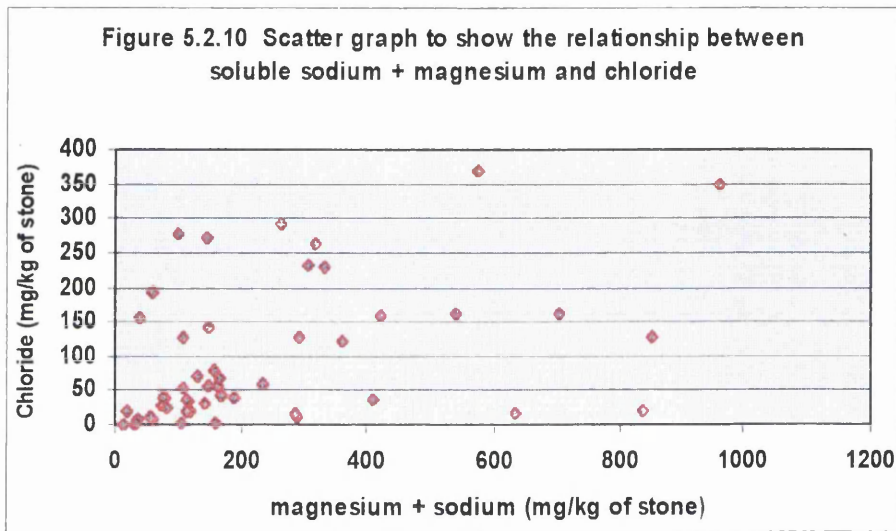


Figure 5.2 Continued...

IC, AA & AE: Results from water extraction experiments
Scatter graphs to show the relationship between
anions and cations in solution



may not be derived solely from an external source, but from e.g. clays, where NH_4^+ ions may be dissolved out.

It is believed that both SO_2 and NO_x can have synergistic effects on stone. A number of early investigations (Livingstone, 1985), dismissed the role of NO_x in stone decay because only small quantities of for example, NO_3^- , are found in stone surfaces and runoff water, as at Culzean. However, laboratory studies (Rosenberg & Grotta, 1980; Johansson *et al.*, 1986; 1988) suggest that NO_2^- can enhance SO_2 pick-up without producing nitrates (BERG, 1989). NO_3^- is more prevalent in the samples from Culzean than NO_2^- .

Phosphate (PO_4^{3-}) levels in the stone are as limited as NO_2^- . PO_4^{3-} are important nutrients for biological growth and their presence can nourish biological processes (eutrophication). This would explain the detectable levels of PO_4^{3-} in the OB samples (still < 1 ppm) compared to AB and VB, as the original building stone analysed is coated with organic material.

5.3 Section 1 summary and discussion

The most important points highlighted by the leaching experiments are:

- more soluble ions are removed from the exterior surface of all the stones than the interior;
- Na^+ is the most abundant soluble cation whilst Ca^{2+} is also extracted in large quantities;

- Cl^- and SO_4^{2-} are the most abundant soluble anions;
- the presence of halite and gypsum particularly in the near-surface regions of the samples, are characterised by the quantities of Na^+ , Ca^{2+} , Cl^- and SO_4^{2-} extracted from the stones;
- the South-facing part of the balcony yields more soluble material than the North or West as the stone has access to and draws in more soluble salts from seaspray and wind driven rain where it is more exposed;
- more Ca^{2+} is removed from the surface of the AB samples retaining a patina, suggesting that the patina and thus surface regions of these samples contain a larger quantity of more soluble CaCO_3 cement;
- fewer ions are drawn into solution from AB7 which has a cement rendered surface; and
- there is no relationship between AB stones of the same colour and extraction of soluble material.

The results of these leaching experiments can be compared with the profiles of anion concentrations through the cores outlined in *Section 2*.

Section 2 Chemical profiling of stone cores

5.4 Chemical weathering and compositional changes

From the petrography and mineralogy discussed in *Chapter 4* some of the processes taking place can be visualised and understood. It is now necessary to understand how the chemistry of the stone relates to the mineral properties of the stone. This involves an understanding of the following:

- the processes taking place;
- the chemistry of the stone; and
- any distinct variation in the chemistry of the stone.

5.4.1 The chemical composition of the stone in relation to mineralogy

The following presents the major element composition of minerals present in the Culzean Stones (*after* Brownlow, 1996). Lithics have not been included.

Quartz	SiO_2
Feldspar	
Orthoclase	KAlSi_3O_8
Microcline	KAlSi_3O_8
Plagioclase	$\text{NaAlSi}_3\text{O}_8 - \text{CaAlSi}_3\text{O}_8$
Micas	
Muscovite	$\text{KAl}_3\text{Si}_3\text{O}_{10}(\text{OH})_2$
Biotite	$\text{K}(\text{Mg, Fe})_3\text{AlSi}_3\text{O}_{10}(\text{OH})_2$
Clays	
Kaolinite	$\text{Al}_4\text{Si}_4\text{O}_{10}(\text{OH})_8$
Smectite	$(\text{Al, Mg, Fe})_4(\text{Al, Si})_8\text{O}_{20}(\text{OH})_4 \cdot n\text{H}_2\text{O}$
Illite	$\text{K}_{0.2}\text{Al}_4(\text{Al, Si})_8\text{O}_{20}(\text{OH})_4$
Chlorite	$(\text{Mg, Fe, Al})_3(\text{Al, Si})_4\text{O}_{10}(\text{OH})_2 \cdot (\text{Mg, Al})_3(\text{OH})_6$

Cementing agents

Calcite	CaCO_3
Aragonite	CaCO_3
Dolomite	$\text{CaMg}(\text{CO}_3)_2$
Siderite	FeCO_3

One can see from the formulae presented above that the chemical compositions of the mineralogical constituents of these sandstones are of relatively similar composition. There is a large proportion of the SiO_2 phase in the rock (as indicated by the large quartz content) highlighted in the SEM BSE point counting analysis. There are also significant amounts of Al_2O_3 , K_2O , Na_2O , and CaO .

Al_2O_3 , K_2O , Na_2O and CaO are constituents of feldspars, CaO is also found in CaCO_3 cement. The MgO , Fe_2O_3 and FeO come from the clay minerals and the carbonate cement. MnO is also present in the cement (see *Chapter 4*). The other major elements analysed by XRF are TiO_2 , P_2O and MnO , which may be present in the clay minerals, or from precipitation of other minerals, or from accessory detrital minerals.

5.4.2 Products of weathering

The rate of chemical weathering evident in the stone profiles will depend on both the amount and chemistry of the weathering fluids, and the texture and mineral compositions of the rock. When considering the XRF profiles, the following four products of the weathering process must be considered:

- soluble constituents removed from the weathering site;
- residual primary minerals unaffected by weathering reactions;

- any new stable minerals produced by these reactions; and
- organic compounds resulting from any organic decay reactions.

These were demonstrated visually in *Chapter 4*. It is now necessary to consider the effect these reactions have on the overall chemical profile of the stone.

5.5 Chemical profiling of Major elements by XRF and IC

The weathering processes described in *Chapter 4* are driving the movement of ions between mineral phases and into solution. XRF and IC analytical methods were used to see what scale of movement might be occurring and thus if this movement was detectable through the weathering profile. In order to do this it is necessary to understand the following:

- which elements are locked up in which mineral phases;
- which elements might have been introduced from outside; and
- how they may be moved into solution or to form additional mineral phases.

The importance of anions in the stone has been identified in *Section 5.2*. Specifically they combine with cations to form soluble salts in the stone, with dramatic effect. It was important to establish the anion concentration through the stone's profile. By identifying the profile an understanding of the depth of penetration of these anions (the majority of which would be from an external source) and the potential for deterioration through the penetration of rainwater and runoff solutions to greater subsurface depth can be gained. Due to lack of material for experimentation, only six of the AB cores, two from each aspect, were analysed for anion content (as described in *Chapter 2*), and the results have been recorded in Table 8, Appendix 1 and Figure 5.3 - 5.5.

XRF was used to provide a chemical profile for each of the stone samples under investigation, in order to show any distinct chemical variations through the stone samples, and similarities between samples from the same location and those of different origins.

Sandstone has an inhomogeneous composition, and there is natural chemical variation within the stone. This had to be taken into account when analysing the results. It was intended that the results of the XRF analysis could be used to assess changes in the composition through the core profile of the stone, which may indicate mobility.

In presenting the data, it was necessary to measure variations in chemistry against a 'fixed marker' point. As a result a number of different methods of representing the data were attempted. These are briefly described below:

1. *producing individual profiles for each element in turn as elemental wt. %.* This method artificially enhances variation towards surface of the stone due to nature of data acquisition process;
2. *producing individual elemental profiles showing enrichment and depletion with respect to the inner core value of each element (i.e. the value at greatest depth in the stone).* This method assumes that the wt. % recorded at a depth of 120-130 mm could be assumed to be the original or uniform wt. % of that element before weathering, and that plotted values should show enrichment/depletion with respect to this value. This cannot be justified due to the stones' inherent chemical variation; i.e. variation may be primary and not related to weathering.

3. *Plotting the results for the individual elements with respect to the corresponding Si^{4+} value.* Silica (Si^{4+}) is by far the greatest elemental constituent of sandstone. Also the majority of Si^{4+} is locked up in the most chemically and physically stable rock forming mineral i.e. quartz. Therefore plotting individual elements against Si^{4+} indicates the depletion /enrichment of individual elements relative to 'immobile' Si^{4+} . (In soil profiling this is usually done by plotting individual elements against Al^{3+} because Al^{3+} is known to be the most immobile element in a soil weathering profile (Brownlow, 1996)). However in this instance Si^{4+} is more appropriate as the most abundant stable element.

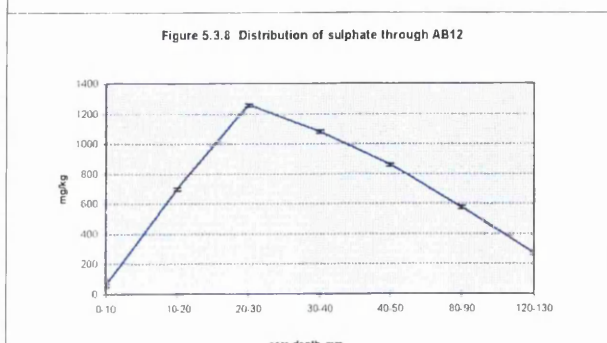
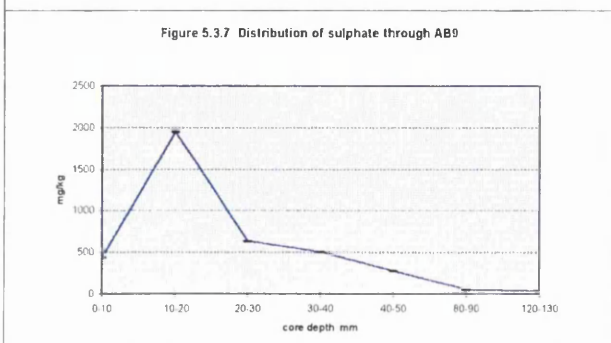
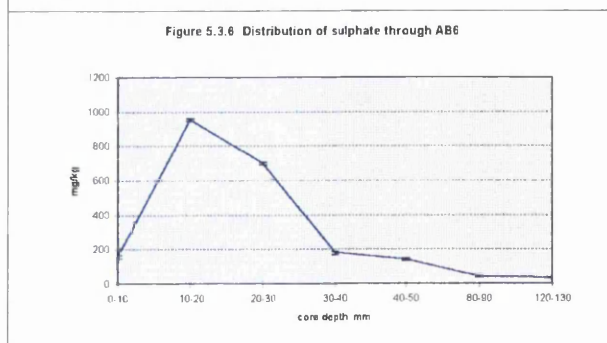
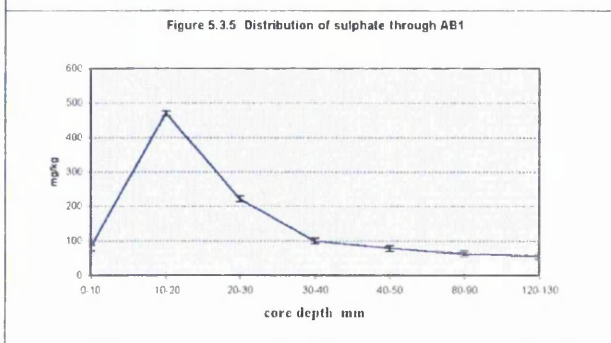
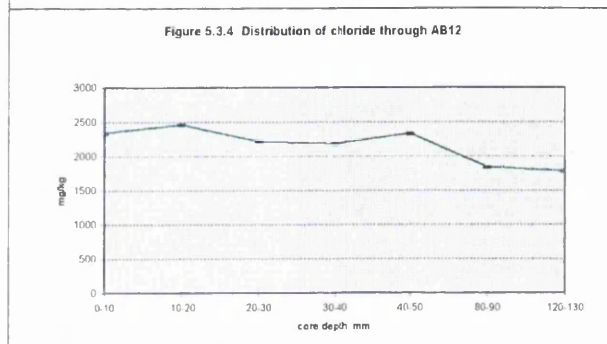
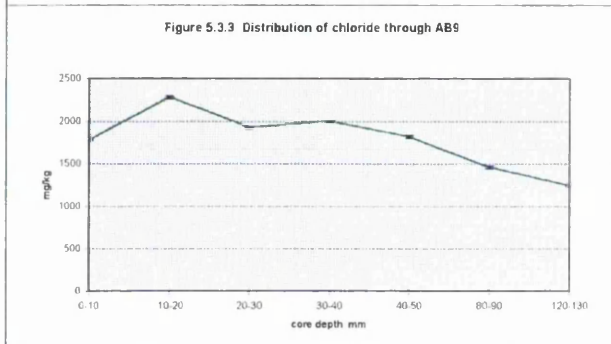
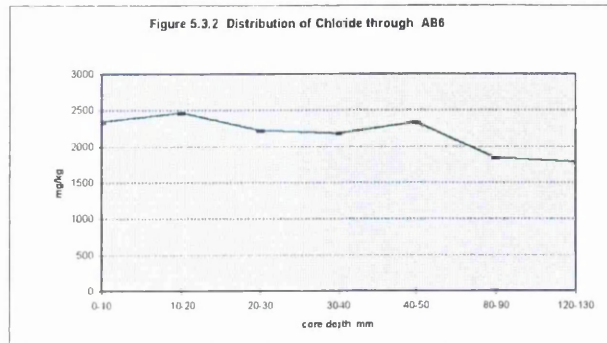
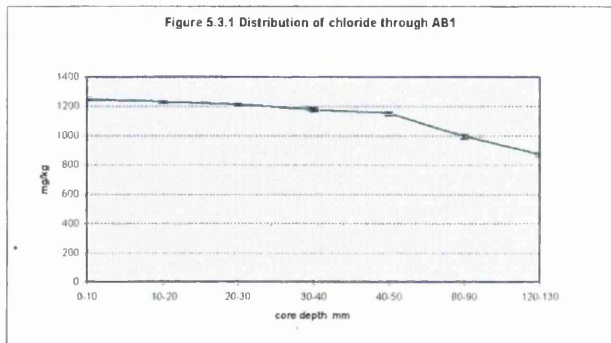
4. *As above, but plotting individual elements against the inner core Si^{4+} value (at 120-130 mm depth in the stone), on the basis that this is the least altered.* The problems with this method have been outlined above i.e. assumption that the inner core value can be used as a standard wt. %.

Initially all the AB samples were plotted using each of the methods outlined above. A decision was made to use the 3rd method, as it was believed that this took into account the natural chemical variation of the stone, whilst allowing, where possible, an assessment of any 'induced' chemical variations as a result of ion mobility. However this could only be attempted in close conjunction with the SEM atomic number contrast results detailed in *Chapter 4*, and the IC results.

An important consideration in the interpretation of the XRF and IC data, is the spacing of the analysed points. The close spacing of the data set towards the surface of the stone may give a first impression of greater variability. One would assume

Figure 5.3 Ion Chromatography: Results from OB and OQ core samples

Results given as concentration of mg/kg of stone



Continued...

Figure 5.3 Ion Chromatography: Results from OB and OQ core samples
Results given as concentration of mg/kg of stone

Figure 5.3.9 Distribution of fluoride through AB1

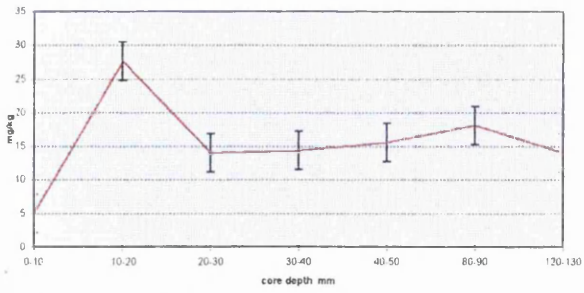


Figure 5.3.10 Distribution of fluoride through AB6

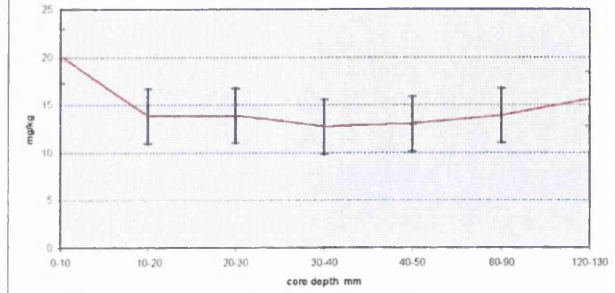


Figure 5.3.11 Distribution of fluoride through AB9

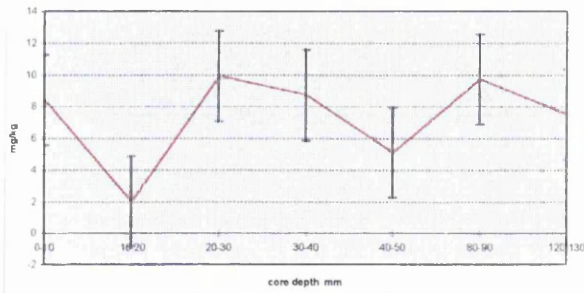


Figure 5.3.12 Distribution of fluoride through AB12

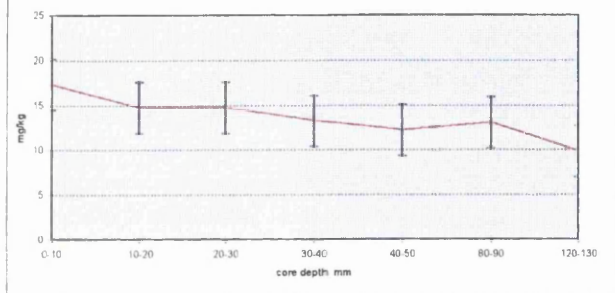


Figure 5.3.13 Distribution of nitrate through AB1

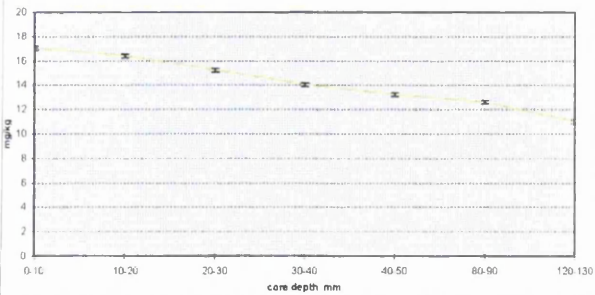
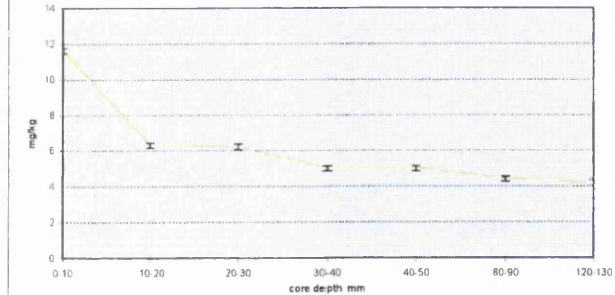


Figure 5.3.14 Distribution of nitrate through AB6



greatest variation nearer the surface of the stone, in the zone of weathering. However due to the nature of the stone and its variability, it is quite possible that there is as much variability at depth. There was no way of knowing if these variations seen towards the surface of the stone were repeated at depth. Therefore all assumptions made must be done relative to the information available from other analytical methods. The wider sampling space at greater depths in the stone may 'smooth out' variability.

Sampling was limited and it is possible that natural variability in the original composition of the stone samples could mask any variability due to weathering. The key to an accurate interpretation of the results is acceptance of the natural variations inherent in the stone. The individual cores have been dealt with for the AB samples, as it is in these that greatest variation would be expected. Outlined below are any variations seen through the XRF and IC results, and an explanation for these attempted.

5.5.1 AB profiles

The AB samples, as the most significant, have been summarised individually below, making reference to variations as illustrated in Figure 5.3 - 5.7.

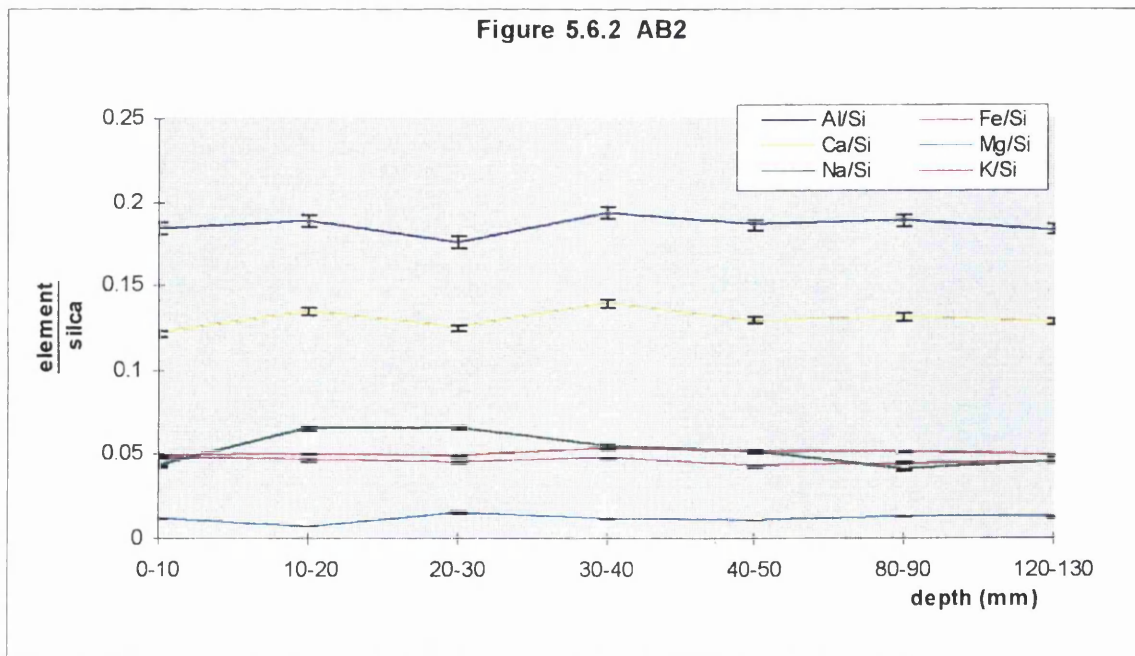
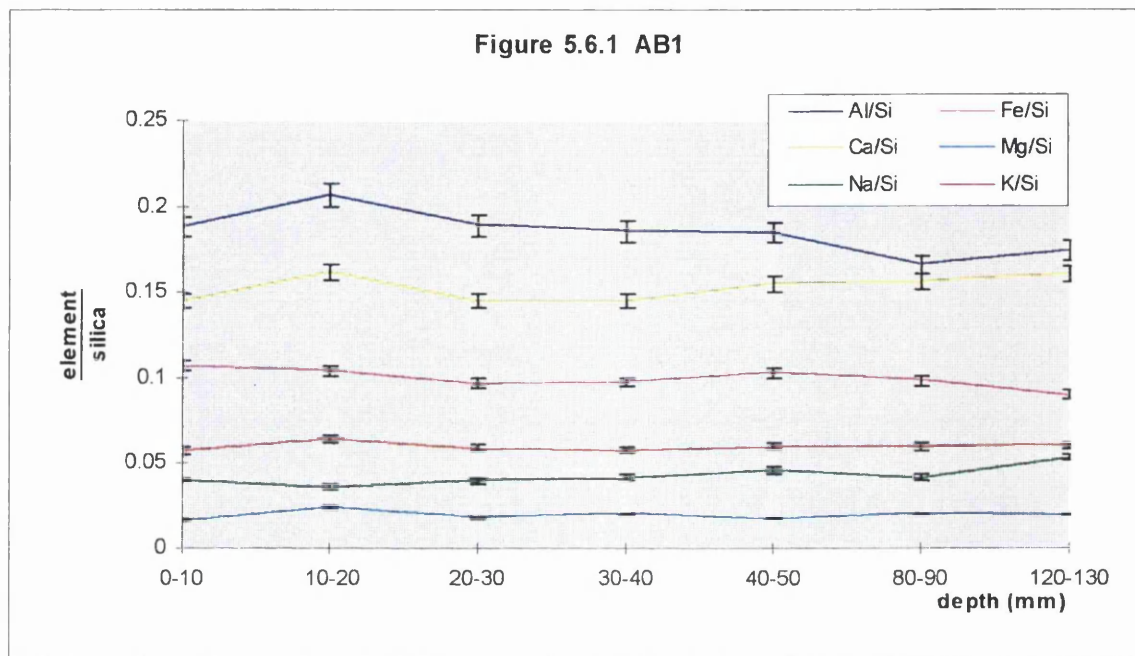
5.5.1.1 AB1

Colour <i>Red</i>	Aspect <i>North</i>
Description <i>Scaling</i>	Surface solubility <i>Medium</i>

Noticeably there is an increase in Al^{3+} relative to Si^{4+} just beneath the surface of the stone. This may be the result of the increased proportion of clay near the surface of the stone (portrayed by the SEM results), where there is also a reduction in feldspars

Figure 5.6

XRF: Results for AB samples
Based on wt% elemental values



and lithics (Section 4.4.6). This relative increase is also reflected in the Na^+ and K^+ profiles. There is an high level of Cl^- through the stone (around 1000 ppm (mg/kg of stone) to a depth of 50 mm). There is SO_4^{2-} enrichment recorded between the stone's surface and 30 mm depth (793 ppm).

Colour <i>Red</i>	Aspect <i>North</i>
Description <i>Scaling</i>	Surface solubility <i>Medium</i>

5.5.1.2 AB2

There is a marked increase in Na^+ levels just beneath the stone surface. This could be due to the presence of salts trapped within the stone. However there is no data for anion content in this sample to compare Cl^- values. Also there is a decrease in Ca^{2+} at 20-30 mm. This is duplicated by the dip in CaCO_3 cement present at that point on the SEM data (Figure 4.2.2), which could represent near-surface dissolution. High levels of Cl^- and SO_4^{2-} are extracted from the surface of this sample.

Colour <i>Green</i>	Aspect <i>North</i>
Description <i>Patina</i>	Surface solubility <i>Medium</i>

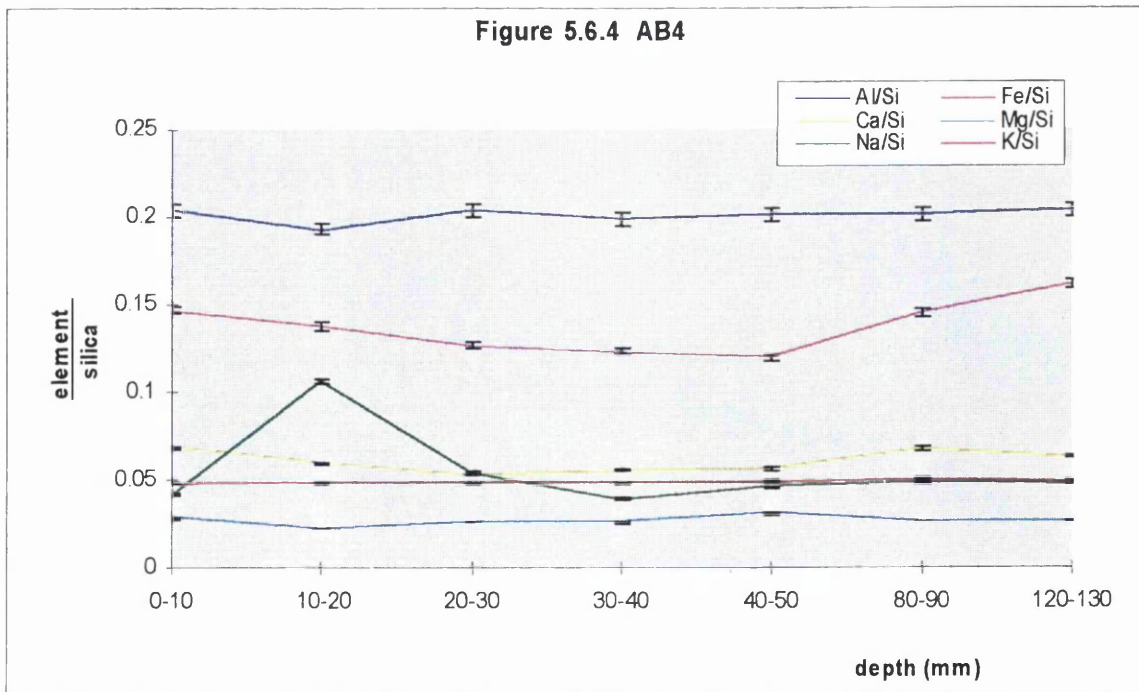
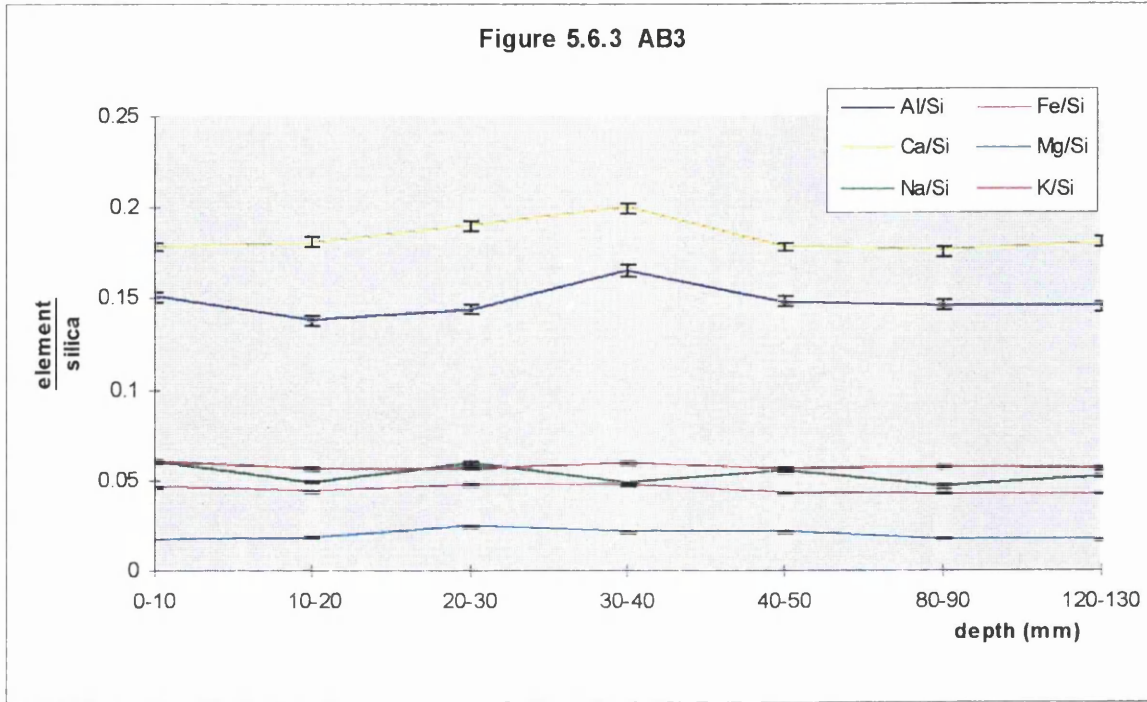
5.5.1.3 AB3

There is an increase in Al^{3+} and Ca^{2+} relative to Si^{4+} at 30-40 mm depth, which may indicate a reduction in quartz content at this point.

There is less variation in these anion profiles compared with AB1 and AB2. The Cl^- concentrations are fairly uniform through stone, around 350 ppm (as indicated in Table 8, Appendix 1), but there are increased SO_4^{2-} concentrations particularly in first 30 mm of stone (up to 1838 ppm).

Figure 5.6

XRF: Results for AB samples
Based on wt% elemental values



This sample had been rendered with cement, although none remained when the sampling was undertaken. This would account for its low Cl^- levels (protection from seaspray) and high surface SO_4^{2-} levels (sulphation reaction with cement rendering).

Colour <i>Green</i>	Aspect <i>North</i>
Description <i>Scaling</i>	

5.5.1.4 AB4

Due to the nature of the decay pattern exhibited by this sample i.e. contour scaling, where micro-fractures in the surface of the stone allow solutions to permeate more readily, greater movement of ions into solution at the surface of the stone would be expected. This may be reflected more in the increased porosity near the surface of the stone, greatest around 30 mm depth (Figure 4.2.4) than in the XRF profile. However it is at this point that Ca^{2+} content drops and so does Fe^{2+} , relative to Si^{4+} . This reflects the reduction in cement at this point, which again may have been dissolved. Na^+ rises and falls substantially in the outer 30 mm of the stone. It is known that Na^+ is readily mobilised in a weathering profile (Brownlow, 1996). This may reflect its combining in soluble salts, especially halite, rather than reactions taking place to form clays from e.g. feldspars, particularly as this increase in Na^+ is marked at a depth of 10-20 mm within the zone of contour scaling. There is no Cl^- data for AB4. However it would appear that halite is filling a porous zone left by the dissolution of CaCO_3 cement.

Colour <i>Red</i>	Aspect <i>West</i>
Description <i>Fresh</i>	

5.5.1.5 AB5

Na⁺ shows a similar pattern to that described in AB4, despite its different weathering features i.e. only exhibits surface granular disintegration. The reduction in Ca²⁺ and Fe²⁺ is not reflected in less cement present but rather an increase in Si⁴⁺ between 30 and 60 mm. Here the quantity of the original quartz content varies. Na⁺ content fluctuates towards the surface of the stone where there is a decrease. There is no Cl⁻ data for this sample.

Colour <i>Green</i>	Aspect <i>West</i>
Description <i>Patina</i>	Surface solubility <i>Medium</i>

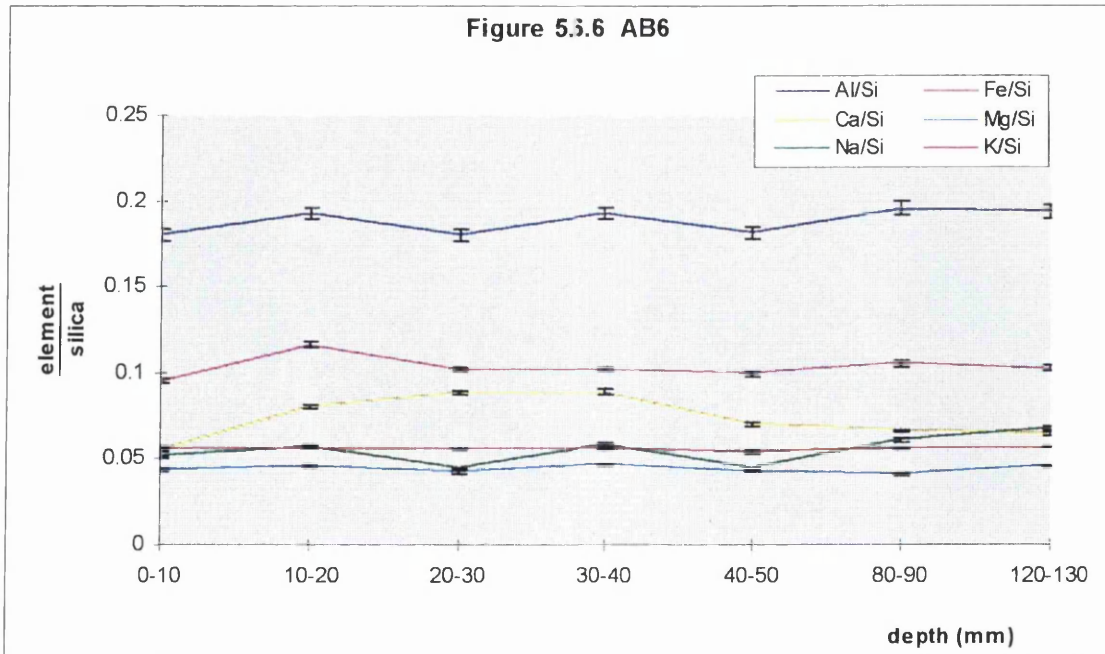
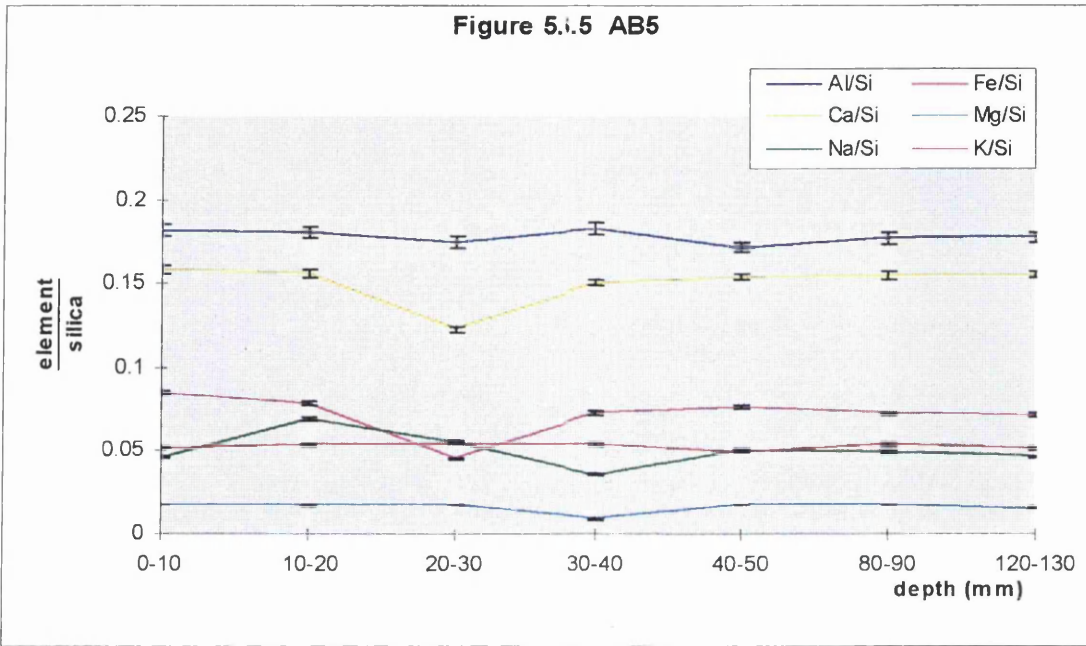
5.5.1.6 AB6

This stone, in appearance, is one of the most deteriorated, with a surface patina which is spalling to reveal contour scaling surfaces underneath. Looking at the SEM results, there is a depletion in quartz in the zone of contour scaling, with a decrease in clay and CaCO₃ cement content at the surface of the stone. The later is mirrored in the XRF results which show a dip in Ca²⁺ between 0-20 mm depth and then again from 50 mm inwards. The variability of Na⁺ is marked again, IC leaching experiments showing a large population of soluble salts present in this sample.

Both the Cl⁻ and SO₄²⁻ match a rise in Ca²⁺ (c.f. Figures 5.3.6 and 5.6.6). There are high Cl⁻ levels throughout the profile ranging from 1775 to 2456 ppm (also a large

Figure 5.6

XRF: Results for AB samples
Based on wt% elemental values



amount was extracted in the leaching experiments described in *Section 1*). SO_4^{2-} levels are fairly low except at 10-20 mm depth where increased to 952 ppm. AB6 is also highly enriched in an SO_4^{2-} phase at AB6/2 (Figure 5.3.6).

There are also variations in the Al^{3+} profile which may reflect the state of deterioration, as Al^{3+} is usually the least mobile of elements in a weathering profile (Brownlow, 1996). In addition there may be a concentration of Fe (total) behind the patina where the carbonate cement is reprecipitating after dissolution. This is reflected by the carbonate analysis discussed in Section 4.7.1.

Colour <i>Green</i>	Aspect <i>West</i>
Description <i>Cement</i>	Surface solubility <i>Low</i>

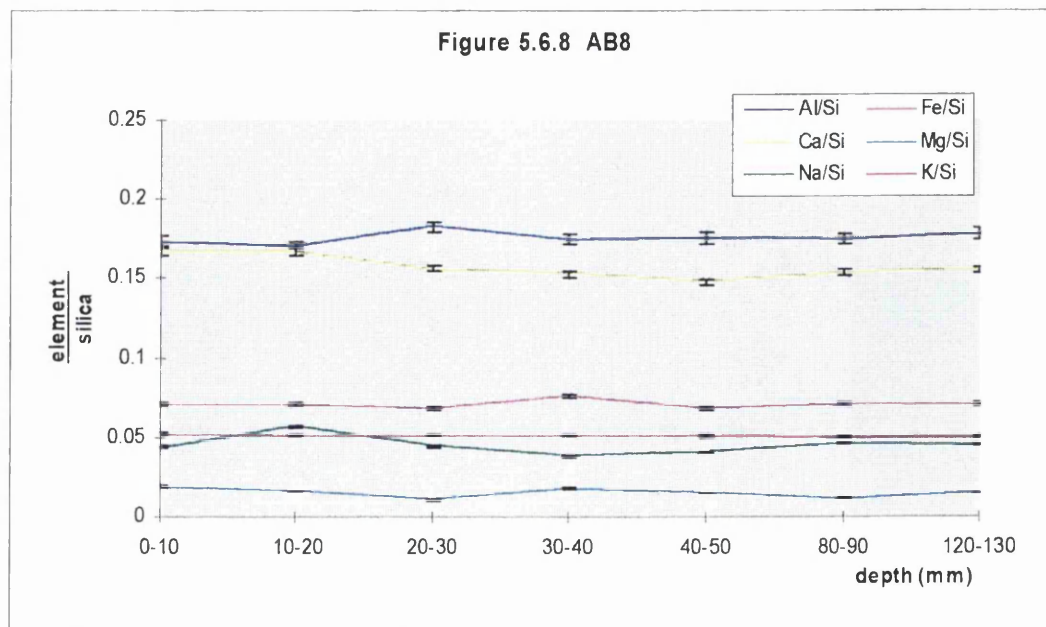
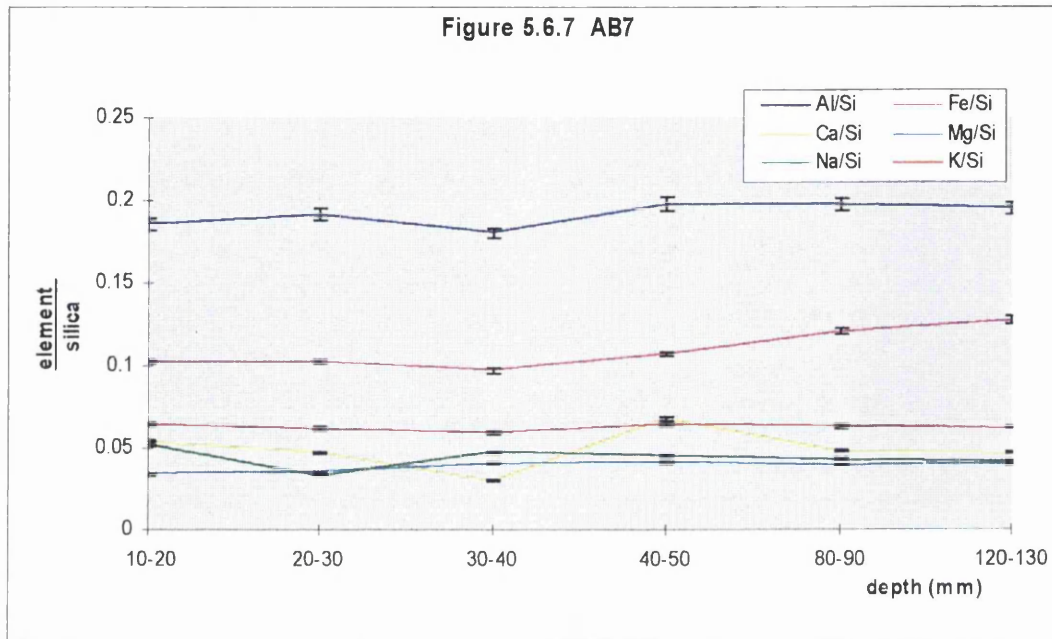
5.5.1.7 AB7

This sample has a contour scaling surface beneath its cement rendered surface. Ca^{2+} is the most variable major element in the profile with respect to Si^{4+} , reflected in the CaCO_3 cement patterns and concretions exhibited by the SEM data. There appears to be a general reduction in Fe (total) content in the first 40 mm of the stone which may also reflect variations in the cement. The remainder of the elemental profiles are unvarying with respect to Si^{4+} .

Cl^- concentrations extracted both from the surface and at depth in the stone varied by only 10 ppm compared with some variations of 130 ppm in other samples.

Figure 5.6

XRF: Results for AB samples
Based on wt% elemental values



Colour <i>Red</i>	Aspect <i>West</i>
Description <i>Fresh</i>	Surface solubility <i>High</i>

5.5.1.8 AB8

There is very little variation in the profile as one might expect of a stone showing few signs of decay. There are small variations towards the stone surface, for example increasing Ca^{2+} , decreasing Al^{3+} and Na^+ relative to Si^{4+} . This may indicate the beginning of patina formation. A lot of material was dissolved from this sample in the leaching experiments.

Cl^- concentrations are fairly stable throughout the profile between 1242 ppm and 2279 ppm (Table 8). These IC results show a slight increase in Cl^- towards the surface in sample (AB8/2). The SO_4^{2-} concentrations are fairly low. There is a fairly even distribution of SO_4^{2-} through the stone, only increasing slightly at 30-40 mm depths. There does not appear to be a relationship between the SO_4^{2-} and the Ca^{2+} , Na^+ and Mg^{2+} profiles, which may all combine with SO_4^{2-} to form soluble salts.

Colour <i>Red</i>	Aspect <i>South</i>
Description <i>Scaling</i>	Surface solubility <i>High</i>

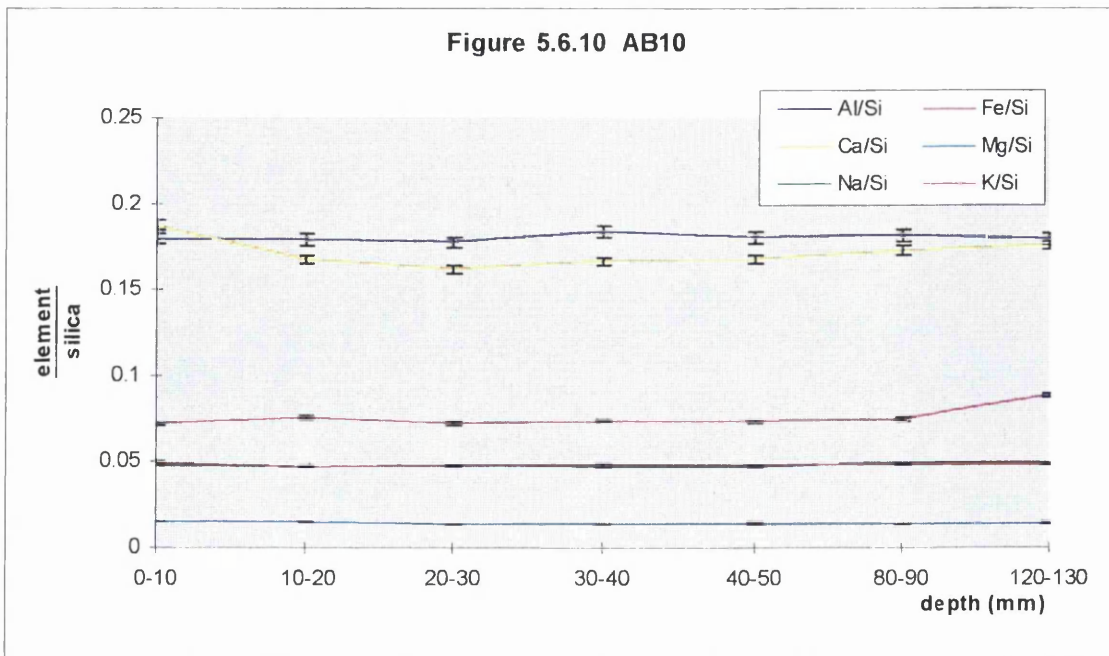
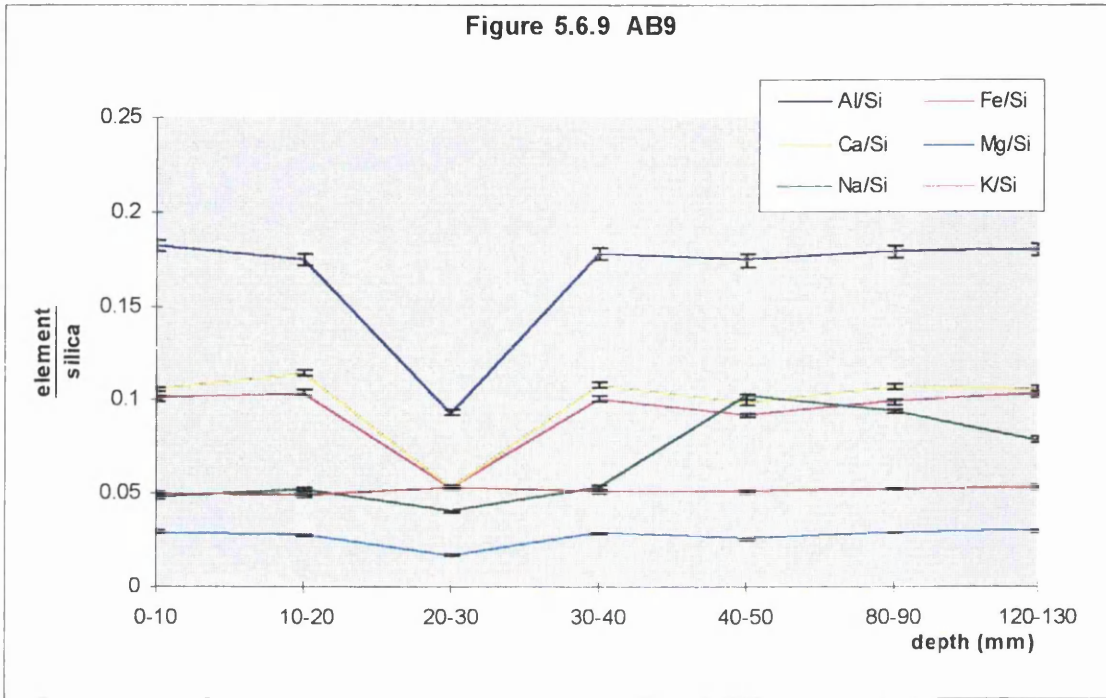
5.5.1.9 AB9

The XRF data for AB9 appears incomplete. There may be a problem with the XRF analysis of AB9/3 (analysed in duplicate). The very low Al^{3+} , Ca^{2+} and Mg^{2+} are suspect, and consequently the data set is skewed.

Again Cl^- concentrations are fairly stable (between 1784 and 2280 ppm in first 50 mm) through stone profile despite extraction levels at the surface being considerably higher (Figure 5.2.1). SO_4^{2-} content peaks just beneath the surface at

Figure 5.6

XRF: Results for AB samples
Based on wt% elemental values



1943 ppm. This concentration of SO_4^{2-} in the stone is the highest of all samples analysed. This will be due to the cement rendering on the surface of the stone and the subsequent formation of gypsum.

Colour <i>Red</i>	Aspect <i>South</i>
Description <i>Fresh</i>	Surface solubility <i>High</i>

5.5.1.10 AB10

The results are very similar to those described for AB8. This stone has an unweathered appearance. There is little evidence of chemical variability through the stone profile, but heightened solubility of the stone is reflected in the leaching experiments (Figures 5.1. and 5.2). There is a slight increase in Ca^{2+} at the surface of the stone, relative to Si^{4+} , which may indicate the beginning of cement reprecipitation as the stone begins to form a patina.

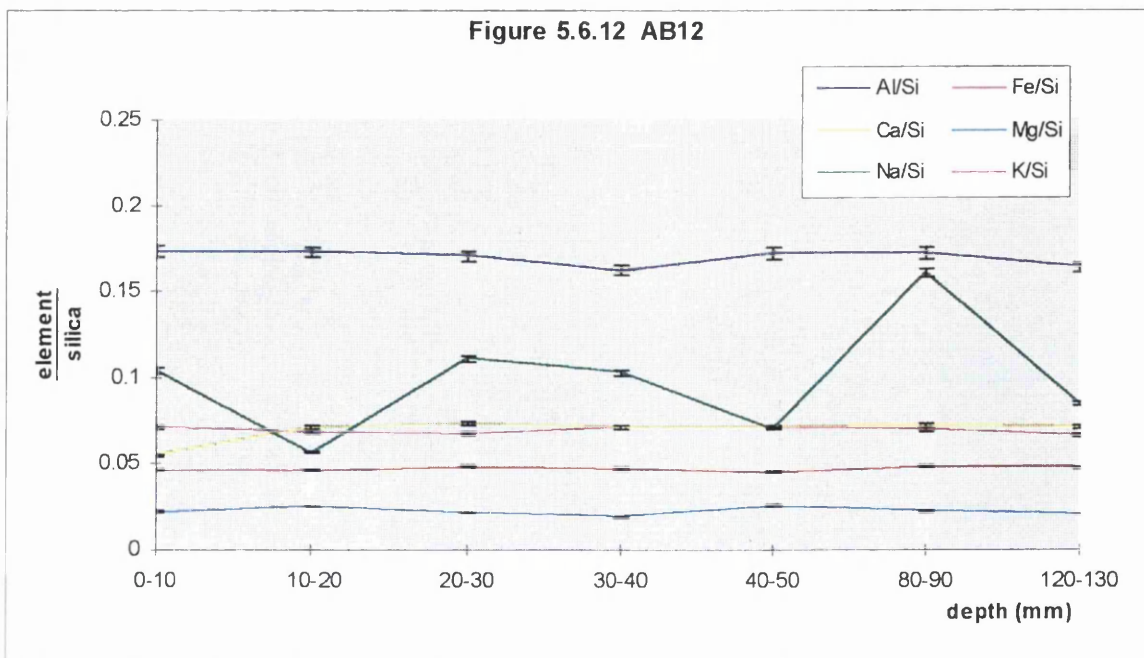
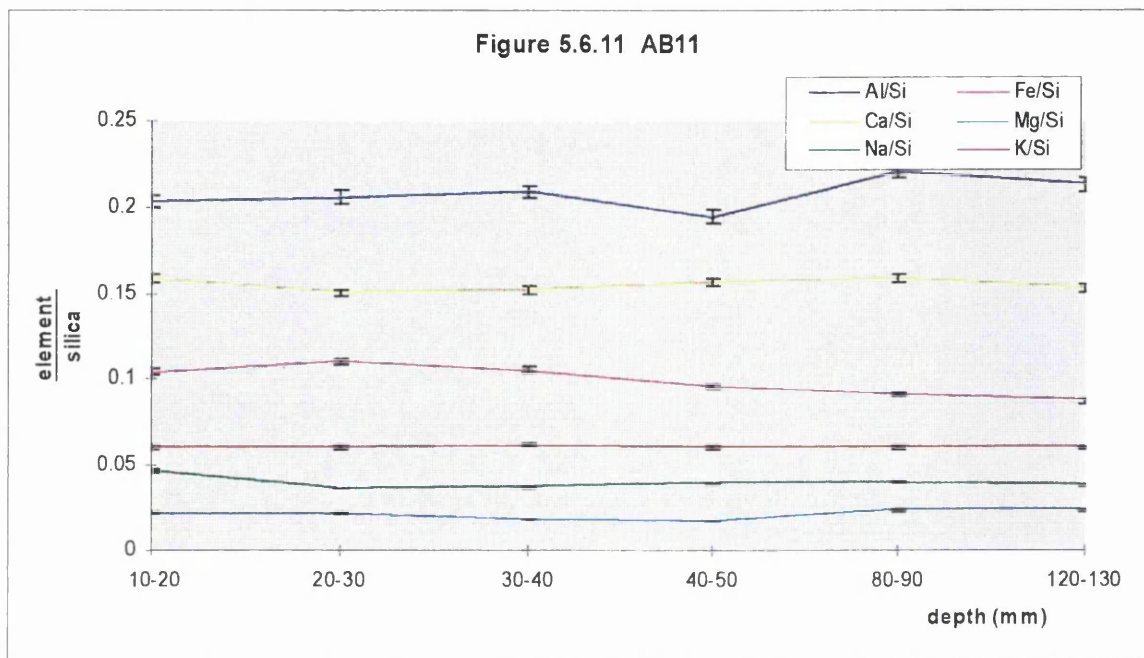
Colour <i>Green</i>	Aspect <i>South</i>
Description <i>Cement</i>	

5.5.1.11 AB11

There is little variation in the profile. This sample also had a cement rendered surface. There is also little variation in SEM compositional profile (Figure 4. 2.11) except an increase in quartz at the surface, which does not appear to be reflected in Figure 5.6.11. There is a slight increase in Na^+ and a slight decrease in Fe (total) relative to Si^{4+} at the stone surface. There is no IC data for this sample so these observations cannot be backed up by anion concentrations.

Figure 5.6

XRF: Results for AB samples
Based on wt% elemental values



Colour <i>Red</i>	Aspect <i>South</i>
Description <i>Fresh</i>	Surface solubility <i>High</i>

5.5.1.12 AB12

The most noticeable variation can be seen in the Na^+ profile, which is the only major element that varies significantly with respect to Si^{4+} . This reflects variation in the quantity of Na^+ present in the stone. Large quantities of soluble Na^+ were identified in the leaching experiments in *Section 1*. Ca^{2+} does decrease towards the surface of the stone and are highest where there is an increase in SO_4^{2-} content. Indeed there is a significant amount of SO_4^{2-} in the stone, particularly at the depths of 20-30 mm where concentrations of 1256 ppm were recorded. SO_4^{2-} may be combining with Ca^{2+} and Na^+ to form soluble salts.

Cl^- concentrations are consistent through the stone, with 2206 ppm the highest concentration, at the stone's surface. Cl^- extracted by rainwater was also high (1044 ppm from the surface compared with 686 ppm at depth).

5.5.2 Summary of cation & anion distribution variations through AB Profiles

The following section summarises the most significant variations brought out by XRF and IC analysis on the AB samples.

There were no great variations in the cation profiles examined above. Nevertheless, slight increases and decreases, particularly in both Na^+ and Ca^{2+} are seen at the surface and just beneath the surface at the contour scaling interface, where salt expansion is at its most prominent. This suggests that some soluble

phases are concentrated in the patina and depleted behind e.g. Ca^{2+} , whilst others like Na^+ might be concentrated behind the patina. These patterns are not always clear because often the patina has spalled, changing the dynamics of the stone's surface. In addition, these processes are occurring in the outer few mm of the stone. The remaining cations analysed (Figures 5.6.3 - 5.6.6) pinpoint few other variations between AB x/1 and AB x/2.

The presence of Cl^- ions is noted in large quantities throughout the stone's profiles (Figures 5.3.5 to 5.3.8). This is in contrast to the SO_4^{2-} concentrations through the cores, which show an enrichment at or near the exterior surface of the stone.

All but AB3 show a gradual decline in Cl^- concentrations from the surface to interior. AB3 has a low Cl^- content particularly AB3/1. This sample was formerly coated in cement rendering, although none remained when the sampling was undertaken. The protection provided by the render from seaspray, rainfall and runoff will account for its low Cl^- levels. AB6, AB8, and AB9 all show an increase in Cl^- in zone ABx/2 as identified above. This would suggest, with particular reference to AB6, that salt crystallisation is maximised behind an exterior patina (ABx/1), where contour scaling is prevalent (AB6), with up to 2500 ppm of Cl^- ions present.

The samples also show enrichment in SO_4^{2-} ions, and show increased concentration of SO_4^{2-} present in ABx/2 and ABx/3 except AB1, where it steadily declines. AB3 has a surface enrichment that steadily declines at a depth of 30 mm inwards. AB6 and AB9, both green-grey stone samples and more advanced in the deterioration process, were highly SO_4^{2-} enriched in zone ABx/2. AB8 and AB12, red-brown

stones (which both give the appearance of 'unweathered' surfaces), have a more even distribution, particularly AB12, which is the 'least' weathered of all the samples analysed on the balcony. Common to all the samples is the variation in SO_4^{2-} content within only 5 mm, particularly between AB3/2, AB3/3, and AB9/1, AB9/2. The high SO_4^{2-} values will be a direct result of the concrete rendering and mortar repairs undertaken on the stone in the 1970's. SO_4^{2-} could have been drawn into the near surface regions of the stone by capillary action. AB3 retains 18 ppm to a depth of 10 mm. This is the highest surface value recorded at Culzean. This block still has cement rendering in tact on much of its face.

SO_4^{2-} enrichment is not restricted to the more weathered stones. It is also present in high concentrations due to the cement rendering applied to the stones, most probably where it has combined with Ca^{2+} from the high CaO content of the cement. There is a greater correlation between Cl^- enrichment and weathering than SO_4^{2-} , although when both anions are present in large quantities, the deterioration is greatest.

As one would expect from the results in *Section 5.2*, there were only trace amounts of NO_2^- and PO_4^{3-} in the stone, and these were nearly always identified just beneath the surface in ABx/2, at a depth of 5 mm. This coincides with the results obtained in the water extraction experiment, as no NO_2^- or PO_4^{3-} was removed from any of the samples, either at the surface, or at depth, except AB12. Comparisons can be made with the distributions of both F^- and NO_3^- in the AB samples (Figure 5.3.9-5.3.14), although in diminished quantities. A decrease in NO_3^- content from exterior to interior is the common trend; only AB3 shows an increase towards the stone surface. The quantity of NO_3^- in the stone, however, was fairly insignificant,

and probably has little effect on the character of the stone as a whole. As discussed in Section 5.2.4, NH_4^+ (ammonium ions) occur in sheet silicates, therefore NO_3^- and NO_2^- may not be derived solely from an external source, but from e.g. clays, where NH_4^+ ions may be dissolved out.

5.5.3 Comparisons with VB, VQ, OB & OQ

It is also important to briefly compare the XRF results from VB, OB and the quarry samples. Less variation can be seen in the cores of the VB major elements (Table 15, Appendix 1) when compared with the AB samples, and even less when looking at OB (Table 13, Appendix 1), as one would expect from samples with more stable mineral compositions. The main exception being the Ca^{2+} values which one would expect to be variable due to the presence of the diagenetic concretions.

OB and OQ contain very similar proportions of elements to each other, as one would expect, whilst VB and VQ were significantly different chemically from each other as there is no CaCO_3 cement (as established by XRD and SEM) and thus very little Ca^{2+} in the VQ samples. One can also note the low Na^+ in the VB and VQ samples where there were no plagioclase feldspars.

Anion profiles have also been drawn up for OB, OQ and VB. All the results for OB and OQ have been reproduced in Figure 5.4 and VB results have been reproduced in Figure 5.5. (As can be seen in Table 10, Appendix 1, there was not enough sample remaining from the VQ cores; however as established in *Chapter 4*, they have different petrographic properties when directly compared with VB samples, and thus little geochemical significance here.)

Figure 5.4 Ion Chromatography: Results from OB and OQ core samples
 Results given as concentration of mg/kg of stone

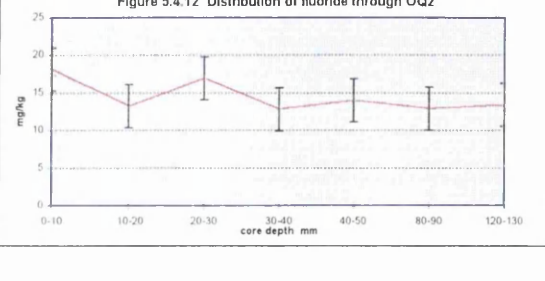
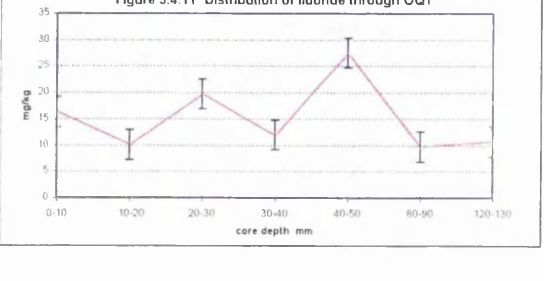
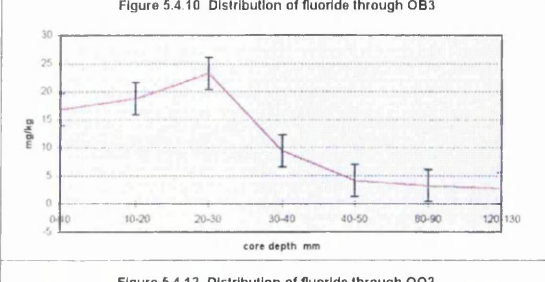
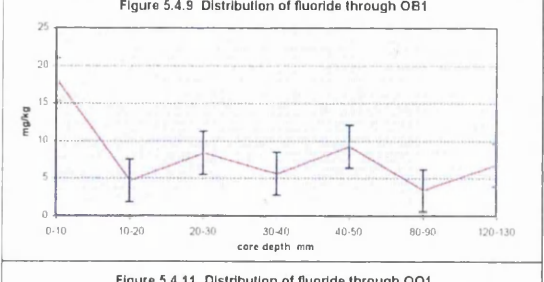
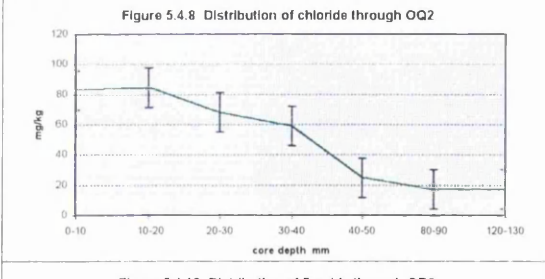
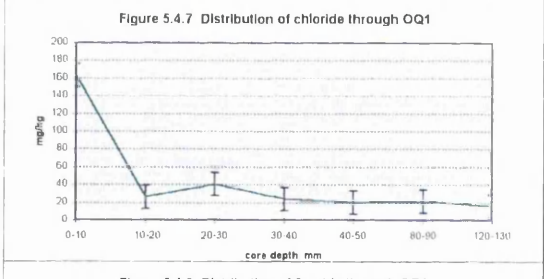
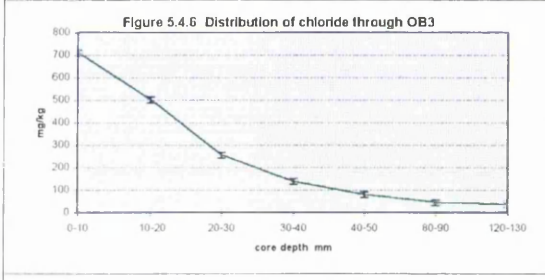
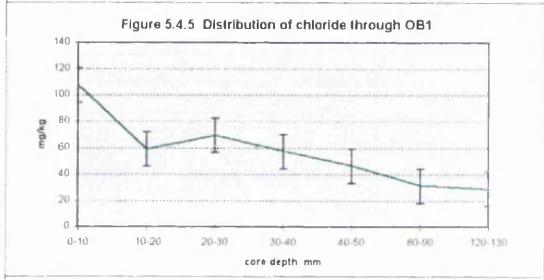
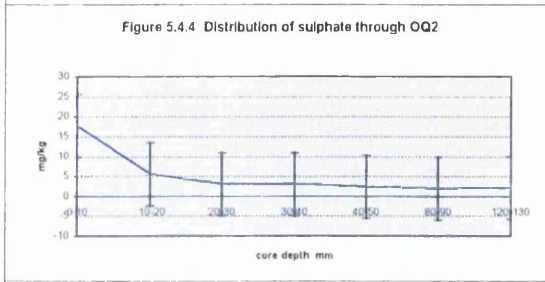
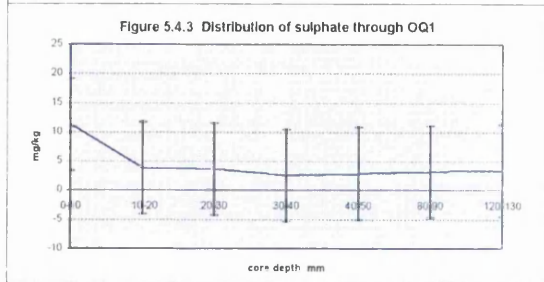
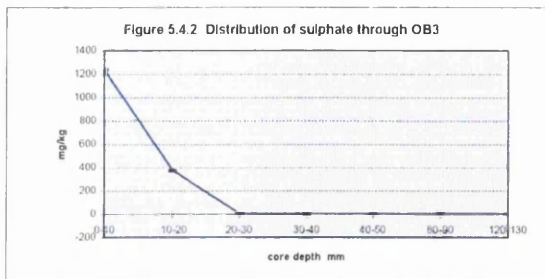
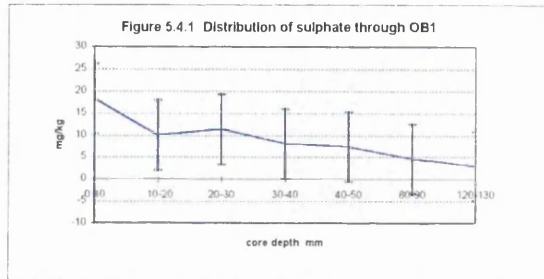
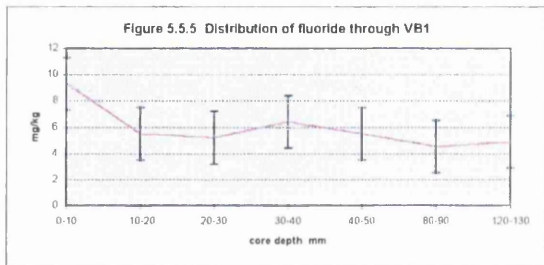
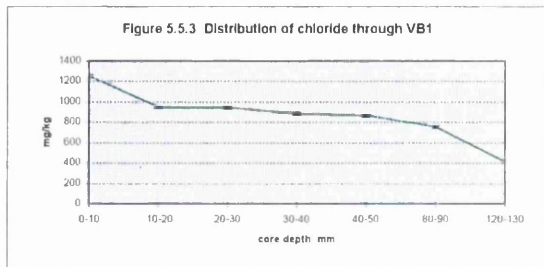
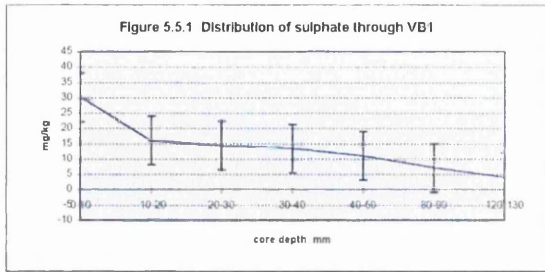


Figure 5.5 Ion Chromatography: Results from VB core samples
 Results given as concentration of mg/kg of stone



It is clear from the concentrations found in OB3 that this sample is taken from higher up and directly facing the sea, as the Cl^- and SO_4^{2-} figures were considerably higher compared with the other OB and OQ samples analysed. The F^- concentrations have also been reproduced, showing that trace amounts were present throughout the depth of the stone analysed. There is no indication of increased values att. The Cl^- concentrations in OB contrast with those shown in the AB samples; the highest figure being 710 ppm in comparison with 2500 ppm for AB and indeed 1251 ppm for the surface of VB1. The VB samples showed higher Cl^- concentrations than those exhibited by OB and OQ. SO_4^{2-} and F^- concentrations were significantly lower (particularly SO_4^{2-}) compared with the AB results. The low values of the OB samples reflect the low 'effective' porosity of the stone as well as its protected location in the foundations of the building. This highlights the importance of aspect (AB being most exposed, OB3 facing the sea, etc) and the strength of the rock matrix of the different stones in determining their response to salinity.

5.5.4 Trace elements

The mobility of trace elements is particularly hard to predict. A trace element released by the weathering of a primary mineral may behave in one of the following ways:

- become a structural part of a new secondary mineral;
- be adsorbed by clay minerals, organic matter, or iron and manganese oxides;
- be taken up by surface plants or other organisms growing on the surface of the stone; and

- be removed in solution as simple or complex ions or as adsorbed ions on colloidal particles (Brownlow, 1996).

Whilst numerous trace elements, specifically the rare earth elements (REE), are mobilised during weathering, they tend to be reprecipitated at the site of weathering (Nesbitt, 1979). Despite this, a number of trends can be seen in the trace element distribution patterns through the cores analysed, reflecting those demonstrated by the majors. Any enrichment/depletion tends to be marked in the outer 5 mm of the stone. Figures 5.7.1 and 5.7.2 highlight some of the most significant trends which are discussed below:

1. Sr is a mobile element, and high Sr levels are recorded particularly in the outer 0-10 mm of those stones which retain their exterior patina. This will reflect the higher calcium levels within this outer zone which occur as a result of the redistribution of calcium carbonate cement from within the stone, and the possible leaching of Ca and thus Sr from the surrounding mortar joints. Surface enrichment/depletion trends can be seen in Ni, Cu and Co. This distribution will be dependent on precipitation following oxidation or reduction, and reactions with organic matter (see Figure 5.7.1);
2. Ni is easily mobilised during weathering (Nesbitt, 1979) and is co-precipitated with Fe and Mn oxides. Thus any trends will be controlled by the Fe-Mn association;
3. Co occurs with Ni in a variety of minerals and can substitute for Mg^{2+} and Fe^{2+} cations. It is often depleted at the stone's surface reflecting its solubility and

Figure 5.7.1

XRF Trace Elements

Sr concentrations through AB4, AB5 and AB11

Results given in ppm

(Figure taken from Appendix2)

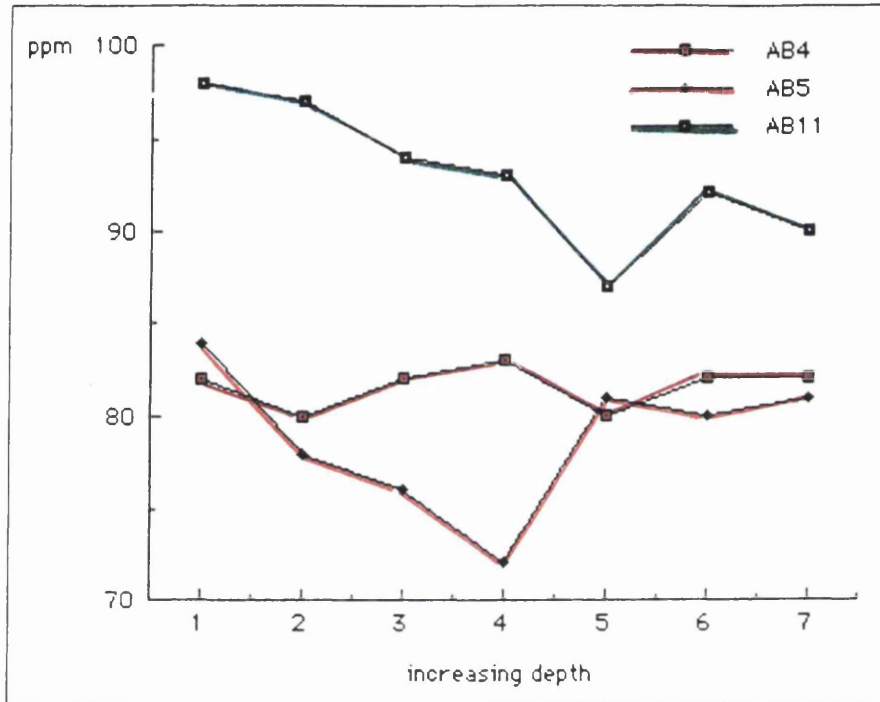


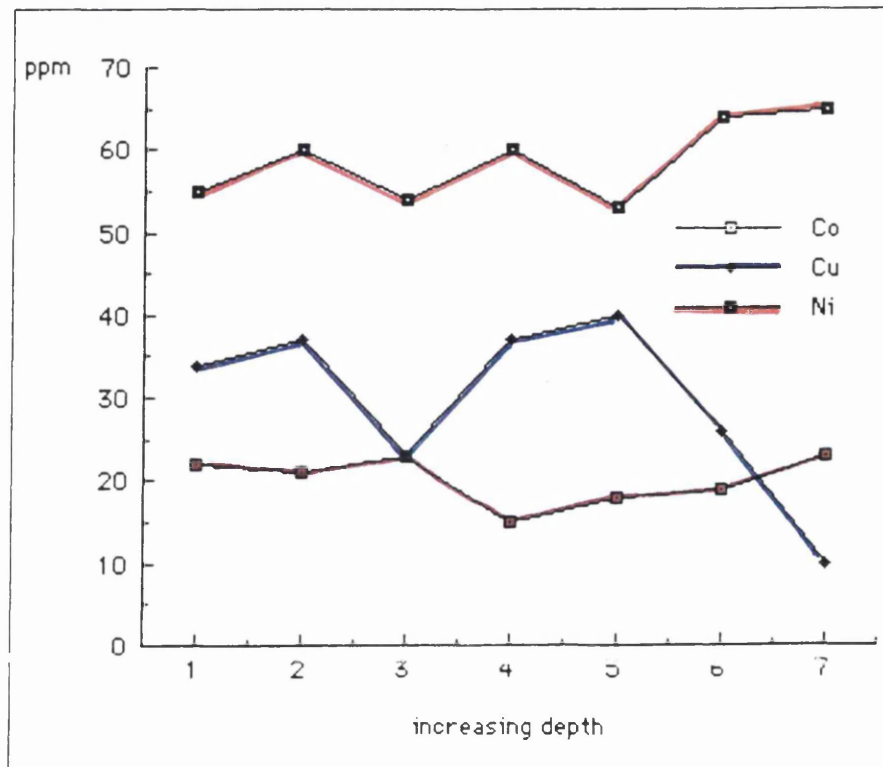
Figure 5.7.2

XRF Trace Elements

Co, Cu and Ni concentrations through core AB4

Results given in ppm

(Figure taken from Appendix2)



removal during weathering, as unlike Ni it does not form residual silicate minerals. Hence Co and Ni are both indicators of Fe^{2+} mobility;

4. Cu is present in some samples and below detectable levels in others. Wedephol (1964) showed a correlation between Cu and Fe_2O_3 in some red sandstones; however in this instance, there is no correlation between colour and quantity of Cu. Cu will be extracted from silicates, sulphides and oxides and has restricted mobility during chemical weathering, although fixation by organic matter and adsorption may occur. Where Cu occurs in these samples, there tends to be surface depletion (see Figure 5.7.2); and
5. Pb is frequently enriched at the surface. This is evident in most of the AB samples. Pb is primarily found in K-feldspars and micas and some mobilised Pb is absorbed on clay minerals. In addition, metal ions are commonly present in organic matter and therefore likely to concentrate at the stone's surface. Atmospheric Pb may also be absorbed, car exhaust fumes being the chief source.

The common trend running through the data is the variation in concentration (higher/lower) at the surface of the stone.

There has been much debate as to the mobility of the REE during chemical weathering (Fleet, 1986). Their importance in this instance, is however limited, as only Ce and La of the REE show any higher/lower concentration trends.

The results found in Tables 14 and 16, Appendix 1 are more consistent and display the trace elemental analysis for VB, VQ, OB, and OQ. Variations in concentrations

can still be seen at the surface of the stone in elements such as Cu, Ni, and Pb. The very high Pb values for OB2/1 could be accounted for by its proximity to lead guttering. However the high metal ion values for the surfaces of the OB samples may also be due to the concentration of organic matter on the surfaces of these samples.

The quarry samples, as one would expect, also show varying concentrations in the surface figures. Indeed often the greatest variation is seen between the OQx/1 and OQx/2 slices presumably due to the length of time that particular quarry face has lain dormant.

5.6 Section 2 summary

Despite the relationship between mineralogy and composition, sandstones cannot be interpreted using chemical analysis alone. The usefulness of XRF analysis can be recognised by its ability to process small amounts of material. However due to the naturally variable chemistry of sandstone, in this instance petrographical analysis is also required to interpret the results. Thus XRF results can only be interpreted once the mineralogy of the stone is known; as it is necessary, amongst other things to establish which minerals are detrital, authogenic, or cements, which components are mobile, and which are derived from external sources. All the major elements contribute to several different minerals, and microscopic analysis must be undertaken to establish which minerals are present. Also, the chemical composition of a sandstone is dependent on grain size (the larger the grains, the less variable the overall chemical composition), so this must also be defined.

The following comments are made for further research:

- XRF alone is not the best analytical method for looking for trends in the deterioration of the stone. However, combined with IC and SEM work variations in the compositional profile of the individual cores can be made;
- other than the major soluble salt phases identified, the wt % of material being transported into solution is very small. This method of analysis is not accurate enough to pick up these changes e.g. transfer of ions between mineral assemblages;
- the compositional variations identified may be the result of primary whole rock variation and not as a result of weathering.

By profiling the anion distribution from rock powders (IC), an understanding of depth of penetration of ingressing fluids containing contaminants could be established.

The following conclusions can be drawn:

- there is greater chemical variability in the AB sample profiles compared with those of the VB and OB and their respective quarries;
- there are slight increases and decreases, particularly in both Na^+ and Ca^{2+} at and near the surface of the stone;
- there is greater chemical variability towards the surface of the stones due to the presence of Cl^- and SO_4^{2-} phases;

- there is evidence for the surface enrichment in soluble salts (especially halite and gypsum), and subsequently a general decline in anion concentrations can be seen throughout the sample profiles;
- the most distinctive variations through the XRF profiles are the variations in Ca^{2+} due to the presence of concretions and cement dissolution; and
- trace elements (metal ions) may be used to trace the mobility of major elements through a weathering profile.

5.7 Chapter 5 summary

As expected, halite and sulphates e.g. gypsum can be found in abundance in the stone, particularly the AB samples. The principal source of the halite and a possible source of some of the SO_4^{2-} combined with e.g. Ca^{2+} to form sulphate salts is wind-driven marine aerosols. It is believed that the SO_4^{2-} may also be derived from other sulphurous gases in the air in addition to marine aerosols.

The occurrence of these and other soluble salts at depth in the stone provides important information on the composition of the solutions driven into the stone at Culzean and the depths to which they can penetrate according to porosity and permeability.

The chemical make-up of each individual stone is very complicated and unique. Only common trends can be accounted for and assumptions made in order to build on a model for stone decay. Key results taken from these geochemical experiments show that:

- more soluble ions are removed from the exterior surface of all the stones than the interior;
- there is greater chemical variability in the AB sample profiles compared with those of the VB and OB and their respective quarries;
- there is greater chemical variability towards the surface of the stones due to the presence of Cl^- and SO_4^{2-} phases;
- Na^+ is the most abundant soluble cation whilst Ca^{2+} is also extracted in large quantities;
- the presence of halite and gypsum particularly in the near-surface regions of the AB samples, are characterised by the quantities of Na^+ , Ca^{2+} , Cl^- and SO_4^{2-} extracted from the stones; and
- more Ca^{2+} is removed from the surface of the AB samples retaining a patina, suggesting that the patina and thus surface regions of these samples contain a larger quantity of more soluble CaCO_3 cement;

What is of significance is the evidence for the mobility of ions within the stone in relation to the natural chemical variation found in the stone, which will have produced the weathering styles identified.

Therefore, of greatest importance were the compositional variations seen within the profiles of the AB samples (whether due to natural variation and internal movement), when directly compared with those of the VB and OB.

The AB stone has a greater propensity to physical breakdown and chemical decay than the VB and OB stones because:

- exposure and access to ingressing solutions and soluble salts;
- pore structure, size, and form; and
- compositional instability (e.g. the variety of clay species and their propensity to exchange).

Chapter Six

Climate and the effect of temperature and humidity variations on building stone

6.1 Introduction to Chapter 6

This is a short chapter to provide an overview of previous research undertaken on meteorological conditions and their controls on the weathering mechanisms on buildings. This is followed by a brief look at the climate to which the buildings of Culzean are subjected, the thermal and humid properties of the stone including variabilities associated with rock properties, and a discussion of temperature and humidity data recordings undertaken at Culzean. A description of the shortcomings of the test methods and measurements has been provided at the end of the chapter with recommendations for future research. The information outlined below shows the potential for future research in this area.

6.2 Previous research

Many papers written on weathering in geomorphology concentrate on the importance of the environment and often attempt to replicate environmental conditions by laboratory simulation. Borovec & Nevzil (1966), McGreevy (1985), McGreevy & Whalley (1985), Velbel (1993), Warke & Smith (1994) and Brady &

Carroll (1994), all discuss weathering with respect to thermal properties, moisture content or frost weathering of stone under natural, or more commonly, experimental conditions. McGreevy and co-workers, attempted to simulate stone response to frost weathering in the laboratory, yet concluded that only by monitoring actual rock temperature and moisture regimes in appropriate climates, can their geomorphic effects be evaluated (see McGreevy & Whalley, 1985).

However, in the study of buildings, research has almost always concentrated on the effects of the anthropogenic environment; wet and dry deposition from atmospheric pollutants. This is in accordance with research undertaken in Italy, one of the centres of stone decay research. Here the majority of research on the effects of pollution has been initiated by Fassina, Camuffo and co-workers over the last 20 years, as discussed in Chapter 1 (e.g. Fassina, 1978, 1988; Camuffo, *et al*, 1982; Camuffo & Bernardi, 1989, 1993; Camuffo, 1984, 1989).

It is fully substantiated that the impact of particles and acidic gases from urban atmospheres leads to an acceleration of the weathering process (Fassina, 1988), Haneef *et al.*(1993), Camuffo *et al.* (1982). Hot arid environments provide excellent conditions to induce the weathering phenomenon in the development of cavernous weathering (Young, 1987), and to induce contour scaling (Smith & McGreevy, 1988). However research on more 'natural' decay processes on buildings is rare, particularly as most buildings studied are in an urban environment. However a number of these studies, which look at the effects of microclimate on both the preservation of monuments and the weathering rocks, can be used to examine the possible effects that climate may have on the as controlling mechanism on the stone decay taking place at Culzean. These studies fall into two categories,

those that deal with the thermal properties of the stone and those that deal with the effects of rainfall/moisture on the stone. The majority of these studies have been undertaken in either arid or polluted environments but their outcomes can be translated to considering the impact the microclimate may have on the weathering of the stone at Culzean.

One of the principal researcher in this field is Camuffo who has produced a number of papers in this area since the early 1980s. In an early paper Camuffo *et al.* (1982) show that the principal types of deterioration critically depend on the way the surface of the stone is wetted by rain. They conclude that the different ways in which the rainfall water hits the surfaces and spreads over them is related to the rain patterns of the observed stone deterioration features.

Following on from this, Camuffo & Bernardi (1988) looked at the thermal properties of stone and their relationship with other meteorological factors on the Orvieto Cathedral in Italy. They found that the thermal pattern of the stone is strongly influenced by solar radiation because the surface of the stone is warmed by direct radiation. They found that diurnal heating of the zones affected by direct solar radiation forces marked condensation/evaporation cycles. This effect was limited by the influence of surrounding buildings.

They also found that different materials juxtapose, possess a variety of albedos, which result in a range of thermal gradients and internal stresses. A series of measurements were made in different seasons to study the interactions between the atmosphere and the surface of the monument. Camuffo and Bernardi looked at:

- daily and seasonal environmental forcing cycles;
- exchange of heat and moisture;

- deposition processes;
- zones especially exposed to risk; and
- atmospheric stability.

December, February and August were chosen on the basis of the phase-lag between the thermal wave of the monument and the dew point of the atmosphere in relation to the condensation/evaporation processes. They found that at the beginning of winter, thick walls are still warmer than the air and therefore subject to less condensation. By February the situation is reversed. Condensation may occur in the micro-pores before the water vapour has reached saturation point in the free atmosphere i.e. relative humidity < 100% (Camuffo, 1984). When the temperature of the stone drops to the dew point, condensation also occurs on the surface. By August atmospheric forcing cycle are at a maximum, the atmosphere reaches both the maximum temperature and highest moisture content and the largest variation in the air temperature may play an important role in the condensation/evaporation cycles.

The position of the cathedral i.e. on a hill, causes the building to be exposed to free wind circulation. The walls cool slowly due to their low thermal diffusivity and vertical exposure.

On the NNW side, the largest amount of water is absorbed during the night whilst evaporation occurs during the dry days, resulting in a stationary maximum. In the early morning, when solar radiation causes soil evaporation, thus increasing the vapour content of the atmosphere, water is absorbed by the micro-pores of the still cool walls. This is shown by a local decrease in the specific humidity of the air in contact with the surface. The high relative humidity in proximity of the NNW wall shows that the micro-pores there are filled with water for a long period.

They conclude that in the case of Orvieto cathedral, the contribution of airborne pollutants is relatively modest in comparison with the action of the micro-physical processes induced by the meteorological conditions and the interaction between the stone and the atmosphere. Very low pollution levels and high moisture content allow lichens to flourish on the side walls and in particular on the NNW wall. The water absorbed by the rock favours the growth of biological life, especially lichens. Camuffo and Bernardi (1989; 1993) also studied the effect of microclimates on the Trajan Column. They describe the results of field surveys carried out to investigate the daily and seasonal meteorological factors, microclimates, various deposition processes of airborne pollutants and rainwater dissolution. The main factors influencing weathering that they come up with are:

- atmospheric pollutants;
- time duration;
- rate of deposition;
- time of wetness;
- rainfall; and
- run-off.

Camuffo (1989, 1995) also studied the meteorological nature of the precipitation i.e. showers or drizzle, which he found to be of great importance. He emphasises the importance of wind and rain and proposes that the problem of surface moisture and condensation is very complex and depends of the chemico-physical characteristics of both the atmosphere and the building.

Camuffo (1989) provides evidence to suggest that in Southern Europe the photo-oxidants and the dry deposited gases and particles are dominant especially in urban sites. The diurnal thermal cycles due to sunlight may mean that the monuments are

subjected to great ranges of temperature and condensation/evaporation cycles. The microclimate, as well as being responsible for mechanical stress, thermohygro-metric cycles and providing conditions suitable for biological degradation in low polluted areas, governs the rate of the dry deposition. Fresh westerly winds come freely from the Atlantic Ocean on the NW coasts where intense precipitation occurs.

The geographical distribution and seasonal variation of the air temperature can be interpreted on the basis of:

- conditioned by solar radiation;
- cloud cover and advection; and
- altitude at site.

He suggests that for yearly and diurnal frequencies of temperature, one should consider two parameters should be considered:

- seasonal variation (monthly averages); and
- diurnal with daily ranges.

In north and central Europe, the great frequency of rainfall makes the wet deposition important and the time of wetness is very long. He also suggests that in addition to the deposition due to precipitation, the wet surfaces of the monuments also have a greater captive efficiency for airborne gaseous and particulate pollutants, and there is more time for chemical reactions to occur in heterogeneous phase. Even low pollution levels do not necessarily ensure a situation ideal for stone preservation. Under certain microclimatic conditions biological degradation can develop e.g. algae, lichens, fungi and bacteria.

Pressure fluctuations associated with wind gusts may cause water to be trapped in the pores and rapidly penetrate towards the interior of the porous materials. Also therefore external pollutants may be trapped inside the material and continue the deterioration process each time micro-climatic factors are suitable.

The penetration of rainwater into the monuments while it is flowing over the surface also depends on climatic factors in addition to the nature of the material. Condensation/evaporation cycles occur on the surfaces or are triggered in the internal pores as a function of the environmental specific humidity and temperature of the building. Water supplied by condensation may cause dissolution of the matrix of the material. Condensation occurs not as a function of the relative humidity of the air, but when the building's temperature reaches the critical dew point of a flat surface or a curved meniscus, and this is determined on the micro-scale by the specific humidity of the air facing the surface.

Camuffo (1989) reports that solar radiation is largely responsible for the daily and seasonal forcing cycles. Examples of weathering caused by solar radiation include:

- Thermally induced mechanical stress, especially for coupling of materials with different heat diffusivity and thermal expansion;
- sugaring;
- cycles in the hygrometric balance;
- condensation/evaporation cycles with migration of the water-dissolved substances and recrystallisation; and
- freeze-thawing cycles.

Camuffo (1989) reports that air temperature as well as relative humidity are very important parameters for several purposes, but less convenient when studying weathering of outdoor objects.

He proposes that yearly air temperature averages are very little importance due to seasonal variations. Monthly averages and daily ranges are, he concludes, much more important.

Camuffo advises that it is necessary to understand both the temperature of the free air as well as the temperature of the stone, which may be a few or some tens of degrees different. This temperature variation will make the RH of the air different at the interface and in the micro-pores as a function of the solar radiation absorbed, the heat diffusivity of the material, the local wind speed, and other variables.

Other researchers working in this area include Jenkins & Smith (1990) and Warke & Smith (1994) who have concentrated on looking at the thermal properties of the stone in arid environments particularly the effects of insolation. Much of their work can also be directly related to the study of microclimates and the controls that meteorological conditions have on weathering.

Jenkins & Smith (1990) looked at summer and winter rock-surface temperature measurement from three sites along an altitudinal gradient in Tenerife. They found significant differences between and within site variables related to:

- insolation;
- cloud cover;
- air temperature differences;
- maritime influences; and
- time of year.

They found that superimposed upon diurnal patterns of heating and cooling are numerous short-term (3-15 minutes) and medium-term (1-2 hours) fluctuations related to wind-speed and cloud cover variations. Rates of surface temperature change were found to be very high during these fluctuations ($>3^{\circ}\text{C}/\text{minute}$) and it has been proposed that they may enhance the operation of a number of mechanical rock weathering mechanisms.

Jenkins and Smith propose that rock surface temperatures also vary in response to other factors. These can be divided into two categories, rock properties (albedo, thermal conductivity, specific heat capacity and moisture content) and climatic and meteorological controls (distribution of incoming solar radiation, cloud and wind conditions, air temperature and relative humidity).

All the above are influenced by time of day, year and altitude. Variations associated with rock properties must be superimposed upon any variability associated with climatic conditions.

Jenkins and Smith (1990) concentrate upon selected elements of rock temperature variability associated with climate and weather over seasonal and diurnal time-scales. In their observations, near the coast at El Palm-Mar, Tenerife, maximum temperatures and rates of background heating and cooling were suppressed by maritime influences to give a more symmetrical pattern of diurnal temperature change. Rock properties such as albedo were also said to influence maximum temperatures.

Hollermann (1975) recorded maximum surface temperatures and at coastal sites in adjacent Canary islands. Where maximum surface temperatures on black lapilli fragments of between $64\text{--}66^{\circ}\text{C}$, but considerably lower values for light sand (high

albedo) and black lava (high thermal conductivity). These results imply that rock surfaces are subject to a range of short-term temperature changes in addition to those associated with diurnal cycles of heating and cooling. They may be associated with greater levels of temperature-induced stress at the rock surface and should enhance fatigue failure and the operation of a number of mechanical weathering mechanisms.

The relatively short duration of these fluctuations suggests that their effects are restricted to a thin layer immediately beneath the rock surface and are not transmitted to any great depth. In many instances mechanisms of rock breakdown are restricted to this outer layer. Any surface micro-fracturing would in turn promote further weathering by allowing the ingress of moisture and/or salt in solution.

Jenkins & Smith (1990) suggest that weathering mechanisms could alternate as environmental conditions change between summer and winter and over diurnal or even shorter time-scales.

Also considering the thermal properties of stone decay in desert conditions, Warke & Smith (1994) subjected 5cm³ blocks of different types of stone to 30 minute cycles of heating and cooling in a laboratory experiment. Their experiment was designed to replicate short-term day time rock temperature fluctuations as experienced in hot deserts when insolation is interrupted. Their results show a marked difference in the surface and subsurface temperature responses of stones related to albedo and thermal conductivity.

All the rocks examined showed initial rapid near-surface rates of temperature change on heating and cooling. The results mean that the outer mm of rock will be

subject to numerous short-term thermally induced stress events. These can be superimposed over the longer-term cycles caused by diurnal temperature changes.

There are two issues in insolation related weathering, the control exerted on rock breakdown by external variables (latitude, altitude, aspect, time of year, cloud cover and air temperature) and diurnal temperature variability.

Intrinsic rock properties such as albedo, thermal conductivity, and heat storage capacity, have important effects upon the thermal response characteristics of different rocks (McGreevy, 1985).

In 1974, Peel suggested that there was a need for the systematic investigation of the controls exerted by different thermal properties on rock temperature variability. In recent years it has been possible to measure temperature changes to rock surfaces almost continuously. This has shown that rock surfaces are subjected to numerous short-term fluctuations in temperature of less than 15 minutes duration. These short term temperature changes can create conditions of 'thermal shock' where the rate of stress development is extremely rapid.

These fluctuations occur when insolation is interrupted by the passage of cloud or when rock surface temperatures are lowered by increases in wind speed or by the onset of rainfall. Whalley *et al.* (1984) and Jenkins & Smith (1990) have noted such factors, which are particularly evident when air temperatures are low and can cause rapid cooling of rock surfaces when placed in shadow.

The possible significance of these temperature changes has been demonstrated by Hall & Hall (1991) who reported high rates of rock surface temperature changed well in excess of $2^{\circ}\text{C min}^{-1}$ for short periods in simulation experiments performed

in subzero air conditions. Richter & Simmons (1974) also found that heating rates, when greater than $2^{\circ}\text{C min}^{-1}$ produced micro-cracking in igneous rock. Such temperature changes and the gradients established between the rock surface and substrate are restricted to the outer 1-2 cm of rock, but this, as noted by Jenkins & Smith (1990) is the zone in which rock breakdown by granular disintegration and flaking occurs.

The results of Jenkins & Smith (1990) study show that the effects of thermal conductivity are reflected in the surface/subsurface temperature gradients for the 5 rock types. Low thermal conductivity results in high surface temperatures when exposed to direct isolation, and therefore heat is only slowly conducted to subsurface layers a much steeper thermal gradient exists, resulting in corresponding high thermal stresses.

Research undertaken by Jenkins & Smith (1990) also shows that variations in the temperature gradients of different stones are also influenced by albedo. The darker the rock, the less incident radiation it reflects and when two rock types with similar albedo values are exposed to the same temperature fluctuations the resulting temperature curves reflect the differences in thermal conductivity. For example chalk and limestone have similar albedos but heat is more readily conducted through the chalk.

Under cool air conditions surface heat is rapidly lost by the passage of cooler air over the rock surfaces when shaded. Rock types with the highest unshaded surface temperatures should experience the greatest decrease in surface temperatures. Surface heating on coming out of shade is initially quite rapid, but gradually slows until re-entering shade. Once in the shade, the rate of cooling initially proceeds relatively rapidly, but then slows until the block moves out of shade.

Rocks with low thermal conductivities experience greatest surface/subsurface temperature gradients and thus will experience greater levels of thermally induced stress on sudden cooling or warming. This stress may be further enhanced if the rock also possesses a low albedo.

They found that under both warm and cool air conditions the subsurface temperature curves reflect more even rates of heating and cooling, resulting from the slower response of rock at depth to changes in external temperature conditions. In this way, subsurface temperature responses are seen to lag behind those at the surface. When heat supply is interrupted, rock surface temperatures immediately begin to fall at an initially rapid rate. Subsurface temperatures, however, continue to rise for a short period creating conditions in which the subsurface of the rock is warmer than the surface. During surface heating, tensile stresses arise between the rock surface and the cooler subsurface layers, but when the situation is reversed, compressive stresses will form as the rock surface contracts and the core tries to expand. Repeated reversals in temperature gradients and changes in the nature of the resulting thermally induced stresses will most readily affect the outer cm of rock where temperature gradients are steepest. Over a prolonged period such changes may possibly weaken the surface structure of the rock leading to the development of thermal stress fatigue. Rocks most prone are those with low levels of thermal conductivity and low albedos, the combination of which results in an increase in the thermal gradient between the surface and depth.

Jenkins & Smith (1990) conclude that although insolation may not cause sudden and dramatic rock breakdown, it probably acts by enhancing the effectiveness of other weathering mechanisms involving moisture and salts, through weakening outer layers of the rock. Expansion/contraction occurs in this outer zone where

many weathering mechanisms operate, and with a much greater frequency and at a greater rate than that induced by diurnal thermal cycles.

6.3 The climate at Culzean

The following quote comes from page 204 of Miller (1841). *"Some of the sandstone beds of the system are strongly saliferous; and these, however coherent they may appear, never resist the weather until first divested of their salt. The main ichthyolite bed on the northern shore of the Moray Firth is overlaid by a thick deposit of finely-tinted yellow sandstone of this character, which unlike most sandstones of a mouldering quality, resists the frosts and storms of winter, and wastes only when the weather becomes warm and dry. A few days of sunshine affect it more than whole months of high winds and showers. The heat crystallises at the surface and the salt which it contains; the crystals, acting as wedges, throw off minute particles of the stone; and thus, mechanically at least, the degrading process is the same as that to which sandstones of a different but equally inferior quality are exposed during severe frosts."*

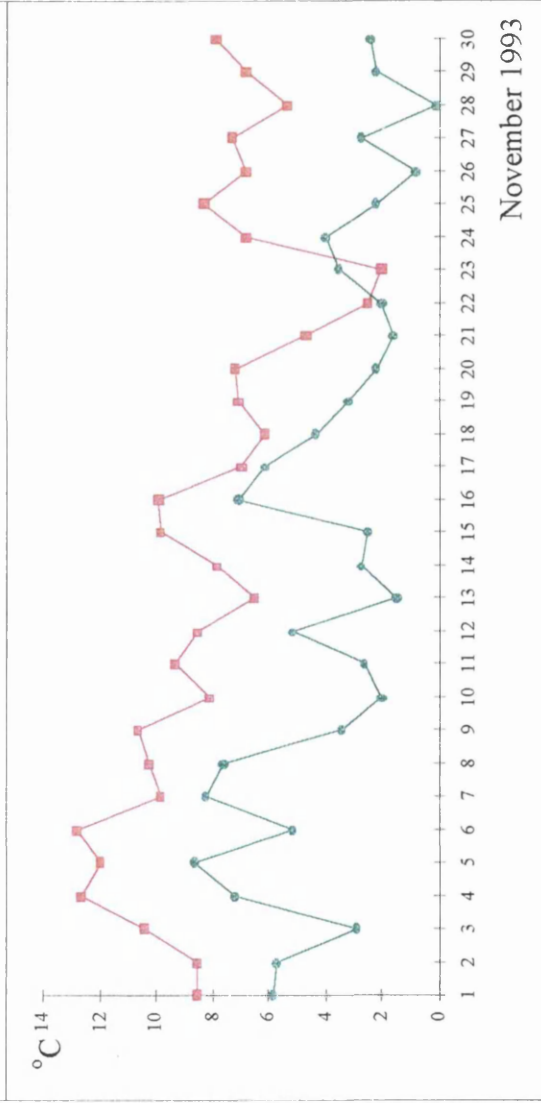
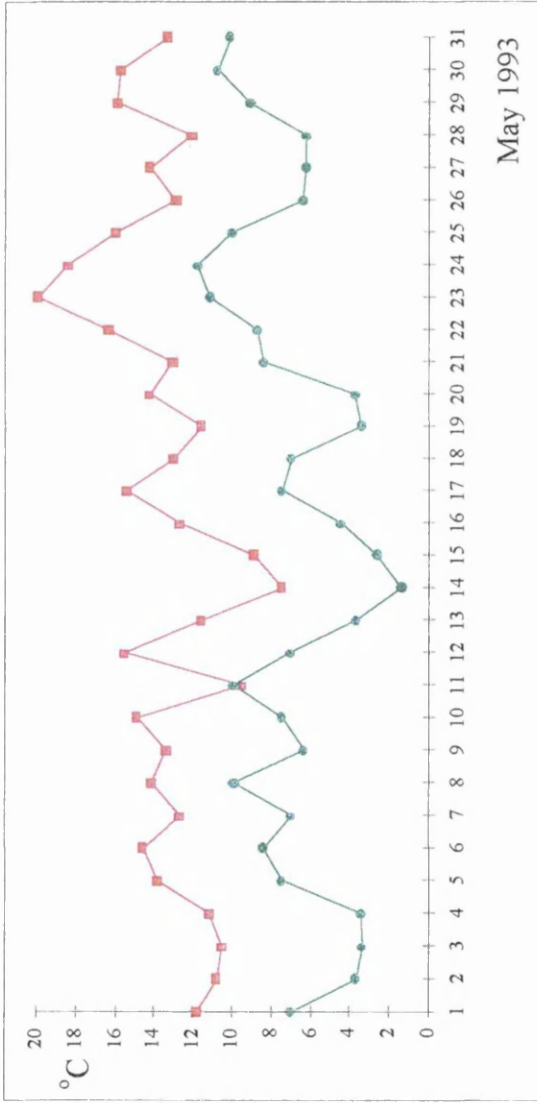
This well documented quote (Evans, 1970; Goudie, 1977) demonstrates observations not just of the mechanical processes endured by the ORS but more importantly combines this knowledge with observations of the climatic environment and its importance in the disintegration process.

The climate and microclimates experienced at Culzean are dominated by its cliff top position on the Firth of Clyde. It is subjected to cold (down to -7.3°C) and wet

weather (up to 36.5 mm in 24 hours) in the winter months amplified by the strong westerly winds. Table 19, Appendix 1, shows monthly temperature and rainfall characteristics over the 2 years period that the research at Culzean was carried out. The readings were taken at an official meteorological station (6526) within the 'walled garden' behind the castle. A pattern emerges from these results, with most rain falling in the months of December, January and March, and highest temperatures reached, as would be expected, from May to August. These results are congruous with those of the last ten years. Also of importance are the extremes of temperature reached (the highest and lowest of the maximum and minimum temperatures). These provide a measure of the diversity of temperature to which the stone will be exposed daily. In many cases, specifically in late Spring (May, June) and early Winter (October, November, December) within a month the maximum and minimum temperature will vary as much as 13°C, with day to day variations of between 3 and 9°C. The meteorological recordings for the months of May and November 1993 have been reproduced in Table 20 (Appendix 1) for comparison, and the temperature variations for these two months have been depicted graphically in Figure 6.1, to show the range of temperature experienced. These monthly variations are important and it has been shown by Camuffo (1989) and Jenkins & Smith (1990) that it is these variations alongside daily, hourly and even more rapid temperature variations that are most important when looking at the effect climate and specifically temperature has on the weathering process.

The wind that drives the rain is also important, especially at Culzean where its speed and direction vary greatly. Table 21 (Appendix 1) shows wind speed and direction recorded on the Drum Tower Balcony over three months during the spring

Figure 6.1 Maximum and minimum air temperature variations at Culzean during May and November 1993



of 1993. These exemplify the diversity of wind direction and particularly speed, recorded. Table 21 also shows the rainfall in mm for this recording period. Rainfall was recorded for a period of 9 consecutive days. During this time the stone will have been continually propagated by water from splash, run-off and capillary action, and will not have had an opportunity to 'dry out'. The stone will also undergo rapid changes in surface temperature as wind eddies set up local microclimates altering the surface temperature of the stone.

6.4 Temperature & humidity recordings from Culzean stone

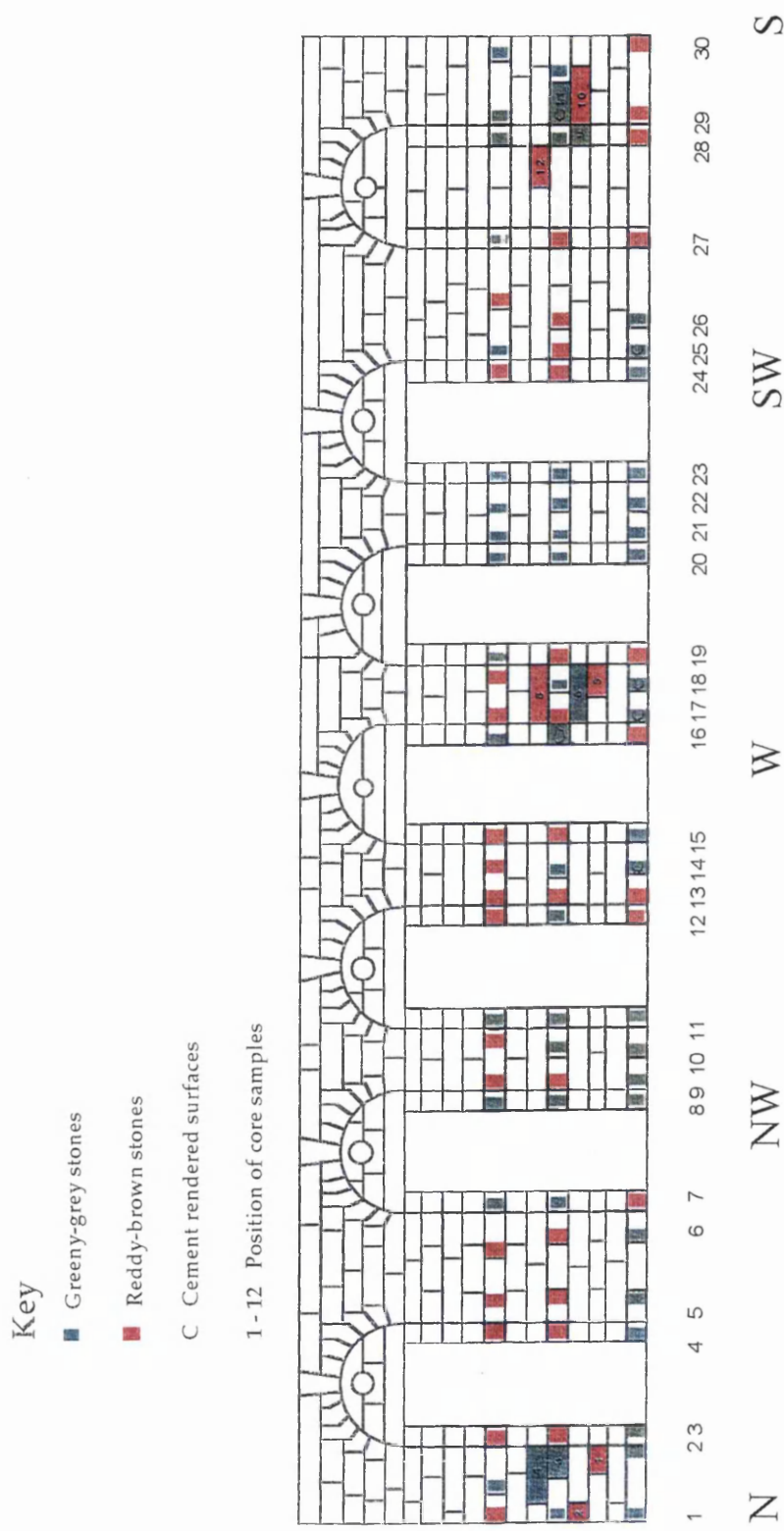
6.4.1 Surface temperatures

The range of temperatures to which the Culzean stone is exposed will have provided a control for the way in which the Culzean stone has deteriorated. At Culzean, observations and measurements were used as an aid to geochemical analysis and to the understanding of how and why these stones are deteriorating so rapidly.

The possible sources of variation in surface and sub-surface temperature exhibited at Culzean, other than those directly attributed to the climate, were perceived to be as follows:

- the nature of the stone - particularly its porosity and permeability;
- colour (absorptive potential - albedo);
- position on the balcony - high or low/sheltered or exposed;

Figure 6.2 Plan of Drum Tower Balcony to show where the recordings of surface temperature were undertaken



- aspect - facing North, Northwest, Southwest or South; and
- time of year (including angle of incident, length of daylight, air temperature, windspeed. For example, the North side of the balcony will be shaded from the sun for a large portion of the year compared with the South).

The first variable has been discussed at length in the preceding chapters. The remaining criteria can be examined by looking at the results of the monitoring undertaken on the balcony and correlated with the deterioration potential described in *Chapters 4 & 5*.

The Balcony stone consists of green-grey and red-brown blocks juxtaposed with one another (Plate 12). As a rule, the green-grey stones were more weathered than their red-brown neighbours (see *Chapter 4*). A simple experiment was undertaken to measure the surface temperature of a number of the blocks on the balcony to look for variations between orientation and colour. Surface temperature, specifically surface heating will draw moisture to the surface, and thus is a key factor in the evaporation of moisture retained at and near the surface of the stone.

An OMEGA OS91 infrared temperature scanner was used to record the surface temperature of the stone in the centre of each of the stone blocks used for recording. It is microprocessor-powered and computer calibrated with an automatic emissivity compensation system so that measurements may be taken within a close range, accurate to 0.01° resolution. Figure 6.2 is a plan of the balcony and indicates those blocks monitored.

6.4.1.1 Stone colour

Preliminary investigations show that the surface temperatures of the red-brown blocks are consistently higher than the green-grey. The red-brown and green-grey stones will have similar thermal conductivity values, but the red-brown stones have a higher albedo. This will influence the temperature gradient of these stones and they will reflect less incident radiation. Therefore surface evaporation of moisture from the red-brown stones is more likely. This is achieved because surface heating increases the immediate egress of moisture from the stone by capillary action. This will aid the overall 'drying out' of the stone.

6.4.1.2 Aspect

Further observation on variations in surface temperature have been identified and reproduced in Figure 6.3. Temperature variations between individual blocks were graphed for two days when air temperature was recorded as 8.3 °C using the infrared scanner. However, as the graph depicts, there was a large surface temperature variation around the balcony from North to South. The Northward-facing blocks showed little temperature variation. However, moving around the balcony from North to South, the temperature differences between these two days progressively increases. Despite the fact that on the days analysed, it was overcast and raining, there was still a significant surface temperature variation.

The results depicted in Figure 6.3 provide information on the importance of aspect with respect to the condensation/evaporation processes and consequently decay.

The South is more exposed to direct solar radiation and therefore it has the ability to adjust (to 'dry out'), and act as an open system. It will, however, be more affected by meteorological changes such as wind-speed and cloud cover which will frequently alter the surface temperature of the stones. The North of the balcony is sheltered from the direct effects of solar radiation due to its aspect. These stones remain cooler and consequently readily absorb moisture and are more likely to be affected by condensation/evaporation cycles. The pores are more likely to be filled with water and for longer; in effect there is no drying-out mechanism in place.

Therefore the North remains the part of the balcony which has the largest number of rapidly deteriorating stones (80% of stones here exhibit visual signs of decay). This is compared with the South where blocks are in much better condition (30% visual decay). This high moisture content of the North-facing stones is reflected in the humidity probe readings described below.

In addition, the visually unweathered stones monitored tend to produce higher temperature readings, indicating that they have a greater thermal conductivity will retain and absorb the heat more effectively than those blocks that exhibit for example contour scaling. This is probably because of the greater surface area associated with contour scaling. Larger surface areas create microclimates of variable temperature which reduce the temperature recorded by the scanner at the surface of the stone.

6.4.2 Surface and subsurface temperature and humidity

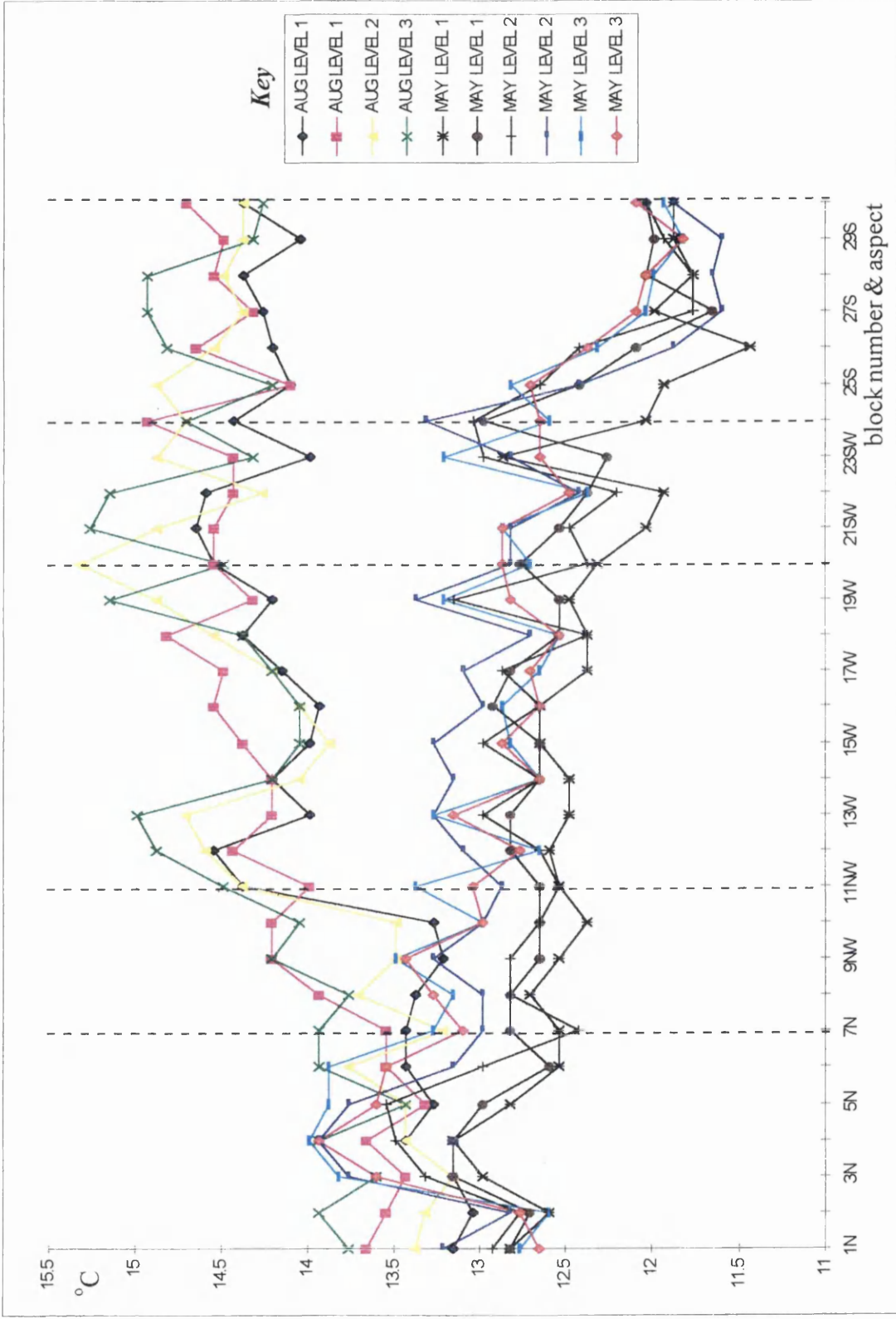
It is known that short term (3-15 minutes), medium term (1-2 hours) and daily fluctuating surface temperature of stone will influence a number of different processes within that stone (Jenkins & Smith, 1990). The temperature will influence moisture content. It has been suggested that it is the infiltrating fluids carrying soluble salts that have been a major source of decay within the stone at Culzean.

Galli & Serra (1976), discussed the influence of variable temperature conditions on water condensation in thick walls, and found that:

- water vapour condensation depends on the temperature field formed inside the wall and on the external conditions of relative humidity;
- the thermal properties of the wall do not influence the partial water vapour pressure but, by modifying the thermal field, influence the relative humidity; and
- daily oscillations of temperature only influence the thermal field in the outer layers of the wall where during the early hours of the morning they may cause a considerable increase in relative humidity.

The surface temperature of stone (a key variable in the evaporation of surface moisture retention) will influence near-surface water condensation and thus the relative humidity of the stone. Of greater importance is the effect of incidences of prolonged exposure to the sun, which will allow heat to be transmitted into the

Figure 6.3 Graph to compare Midday surface temperature variations of stone blocks around the balcony from North-to-West-to-South



stone. Heat retention in the stone as a whole can only be attained from the temperature within the stone. Moisture retention in the stone can only be attained from relative humidity within the stone. Thus two different physical phenomena due to temperature fluctuations can be recognised:

- stresses set up by the unequal expansion and contraction of the component minerals; and
- the expansion and contraction of the surface layers relative to the underlying stone.

These two phenomena have been recognised for some time (Schaffer, 1932) and are important when considering the stone's reaction to temperature.

The relative humidity (RH) of the stone is important as it controls the absorption of moisture, which in turn causes expansion, introduces O_2 into the stone, and transfers dissolved salts in fluids. Water is not just absorbed as a result of meteorological conditions e.g. the penetration of rainwater. It can be absorbed during the night as temperatures fall and in the early morning when solar radiation causes soil evaporation, increasing the vapour content of the atmosphere. It is at this stage that pores will fill with water. Condensation occurs not as a function of the RH of the air, but when the temperature of the building reaches the critical dew point, determined by the specific humidity of the air facing the surface of the stone. Therefore condensation/evaporation cycles on the surface of the stone or within the pores as a function of the environmental specific humidity and temperature of the building (Camuffo, 1995).

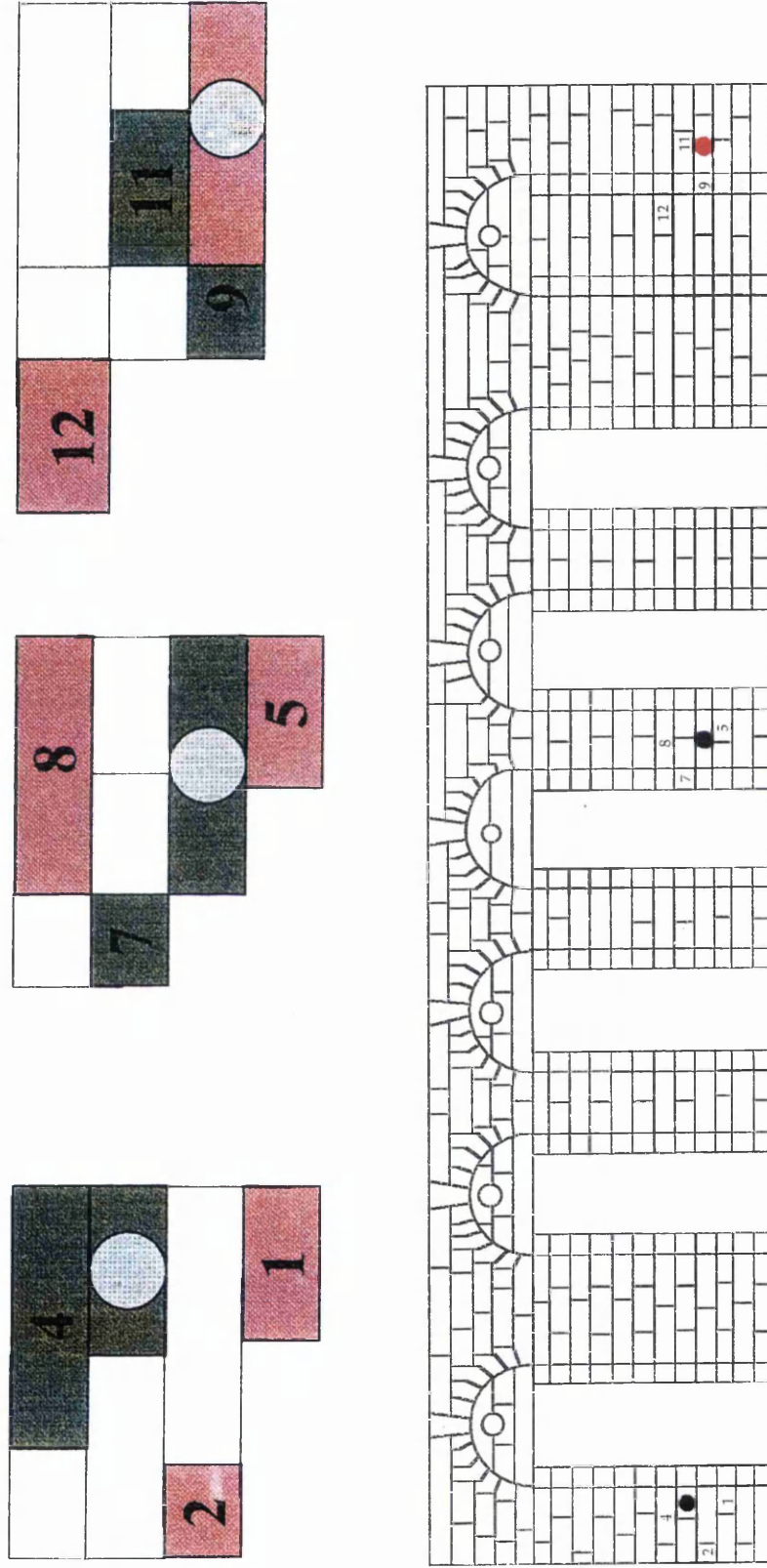
Any change in moisture content has the potential for stones to change in shape, especially when restraining forces have been removed, as is the case with quarried stone blocks, as discussed in *Chapter 4*.

However, in near-saturated conditions, direct physical damage is unlikely to occur for a long time and thus is difficult to determine. Consequently, in addition to observations and measurements undertaken with respect to the surfaces of the building stones, it was also considered important to attempt to monitor and compare the surface and subsurface variations in both temperature and humidity. This was done by making use of the bore holes left by the cores before they were permanently filled. Airtight plugs were made for five holes, three for each aspect of Adam's Balcony (Figure 6.4), and one each for cores drilled in the VB and OB building stones (although these were not monitored). A hole was drilled through the middle of each plug, and a piece of wire secured so that it would be easier to remove the plugs. This was then sealed with Akepox transparent resin which was also used to seal 5 mm foam around the stone plug so that it could be packed tightly into the hole (Plate 25). The bore holes were sealed to allow for as realistic an internal microclimate as possible, which could be monitored at depth in the stone.

Measurements were undertaken using a hand-held OMEGA HH205 microprocessor-driven thermometer and a VAISALA HMP35/0903 manual relative humidity and temperature probe. Measurements were undertaken at the surface of the bore hole and at a depth of 100 mm. The instrument was given time to settle before the reading was recorded. The measurements were taken daily and results from the monitoring on the balcony have been reproduced in Tables 22 and 23, Appendix 1.

Figure 6.4

A Plan of the Drum Tower Balcony to show location of plugged bore holes where temperature and humidity measurements were undertaken



6.4.3 Relative humidity and moisture retention

The results detailed in Table 22 suggest that moisture has been retained within the stone at depth. Of importance, and highlighted by the scatter graphs in Figure 6.5 (which provides recordings from the three bore holes monitored on the balcony) are the subsurface humidity readings. These show consistently higher RH at depth in the stone when directly compared with that of the surface of the stone and air RH. The RH recorded at the surface of the bore hole is consistently the lowest value recorded of the three. Little distinction could be made between the measurements taken from the different bore holes around the balcony (no emerging trend associated with aspect) as such similar patterns can be seen on all three scatter graphs.

These results suggest that there is moisture retention at depth in the stone, indicating that the depth of penetration of solutions into the stone is high, as verified by the geochemical results (particularly the anion profiles), discussed in *Chapter 5*.

Under the right environmental conditions, moisture will be drawn a short distance into the stone by capillary action. Surface evaporation of moisture will subsequently allow moisture to be removed from the face of the stone, which may encourage the development of the surface patina.

Beneath this drier surface layer, where humidity is greater, there will be a zone of high moisture up-take, at a depth of 10-30 mm. This zone of maximum moisture content and evaporation/condensation will encourage ionic mobility (the dissolution

Figure 6.5 Scatter graphs to show relationships between air relative humidity (RH), stone surface RH, and the RH of the inside of the bore holes for the North, West & South facing portions of the balcony

Figure 6.5.1
North

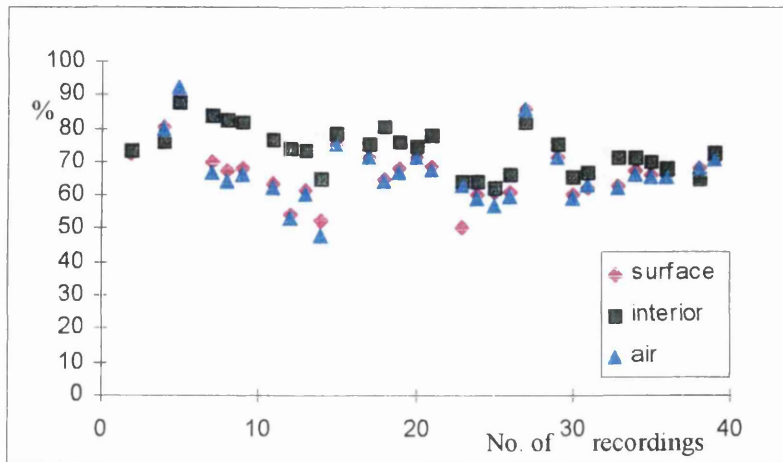


Figure 6.5.2
West

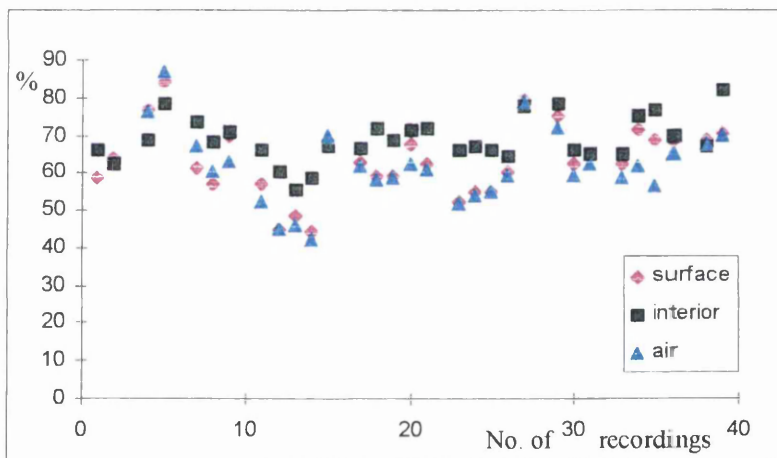
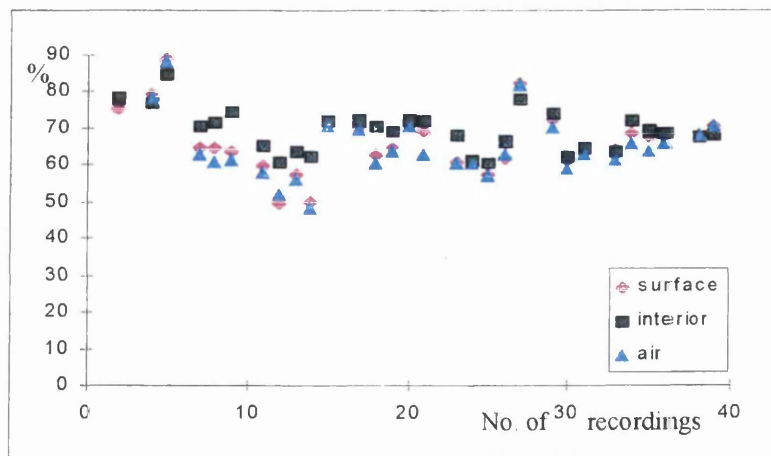


Figure 6.5.3
South



of mineral assemblages and matrix material, the swelling of clays and crystallisation/hydration of soluble salts) which results in exfoliation and eventually contour scaling.

6.4.4 Temperature variations

The results obtained from the temperature recordings show that there is little difference between air temperature, bore hole surface and interior temperature, or between the samples from different aspects.

Air temperature recordings are consistently higher than those recorded at the surface of the stone, and recordings for the bore holes at depth are slightly higher than those recorded at the bore hole surfaces. The temperature data recorded in the bore hole at depth and in the air are comparable.

Higher temperatures may have been expected on the surface of the stone when compared to its interior, and higher values may have been expected on the reddy-brown samples, facing south. This failure to record any significant difference between air temperature and those at the surface of the stone and at depth in the stone, although the surface of the stone may feel hotter to the touch, may be due to the method of data collection used. This is discussed further in *Section 6.6*.

When a material is exposed to the sun, the surface will become hotter than the underlying mass. Heating of the exterior surface of the stone will result in two processes which will aid its weathering processes. Firstly, the unequal expansion and contraction of the component minerals will set up stresses. Secondly, there will

Figure 6.6 Scatter graphs to show relationships between air temperature, stone surface temperature, and the temperature of the inside of the bore holes for the North-facing portion of the balcony

Figure 6.6.1

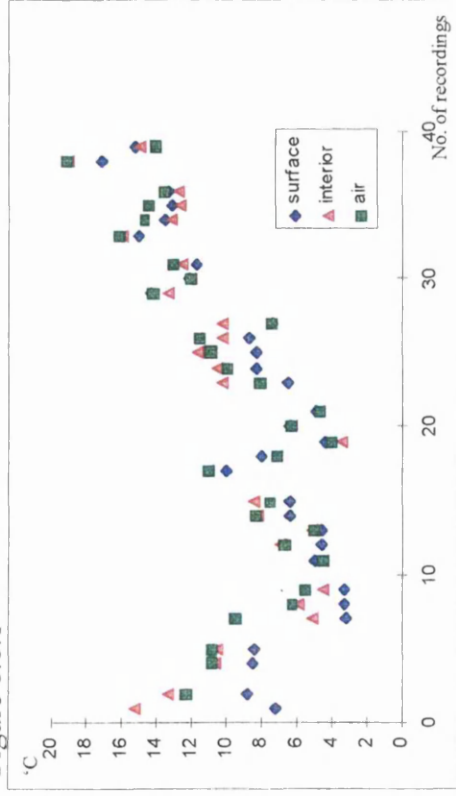


Figure 6.6.2

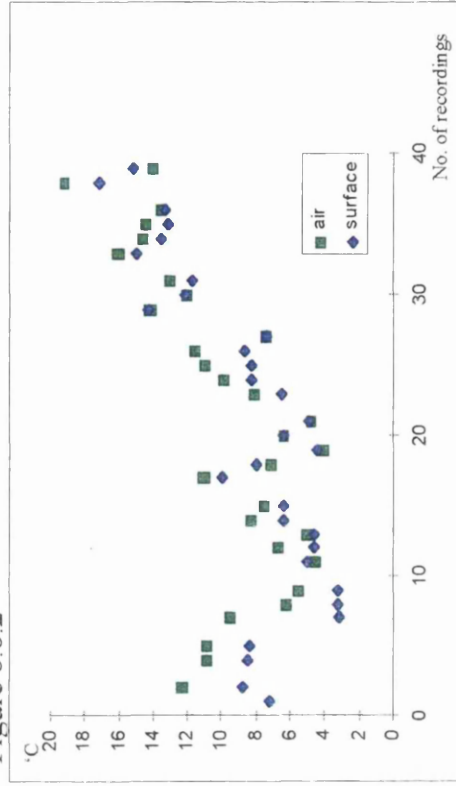


Figure 6.6.3

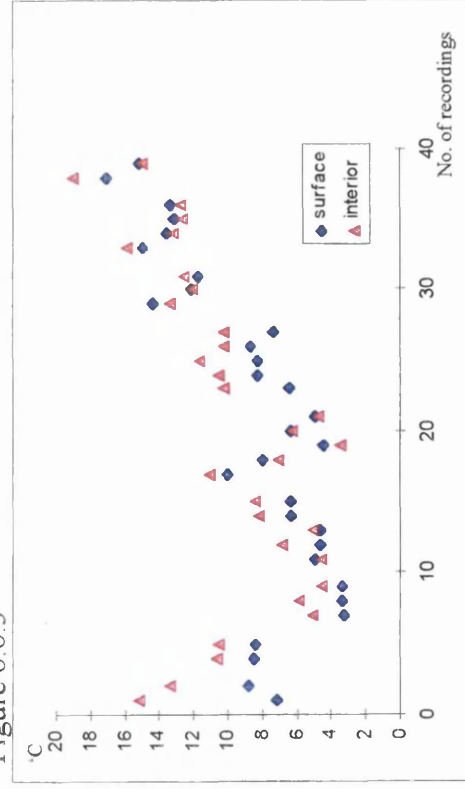


Figure 6.6.4

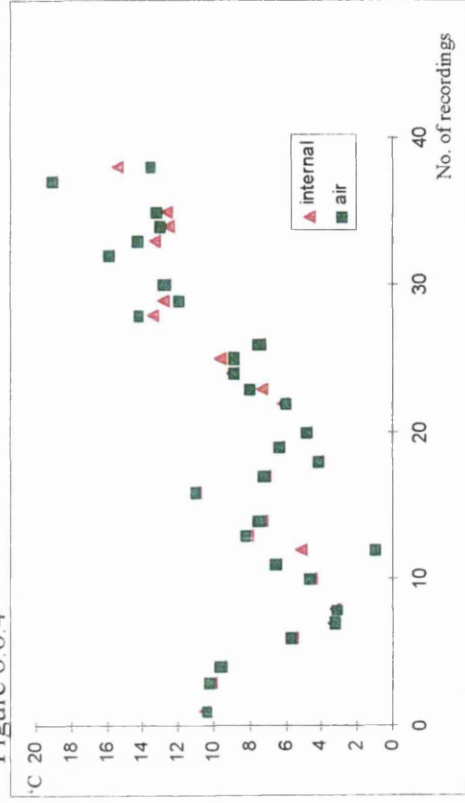


Figure 6.7 Scatter graphs to show relationships between air temperature, stone surface temperature, and the temperature of the inside of the bore holes for the West-facing portion of the balcony

Figure 6.7.1

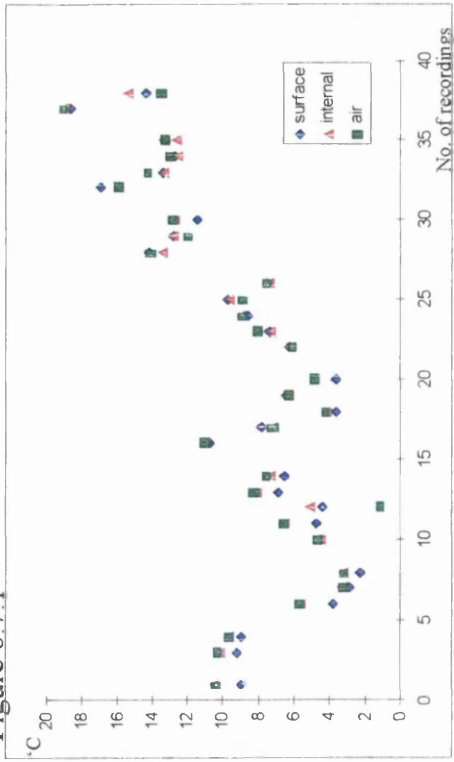


Figure 6.7.2

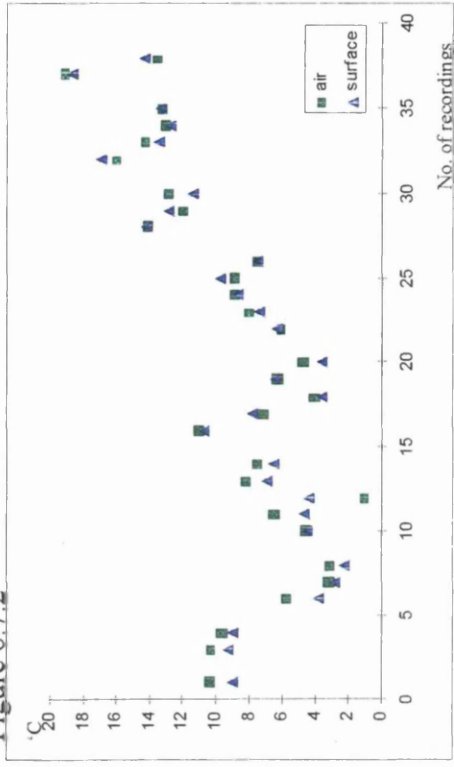


Figure 6.7.3

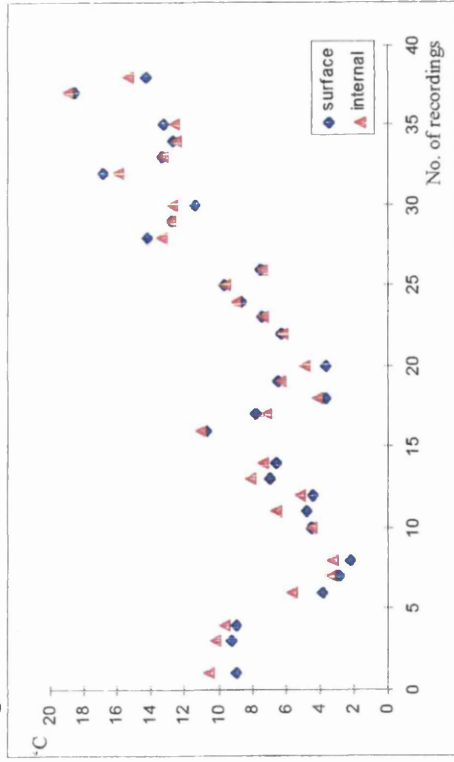


Figure 6.7.4

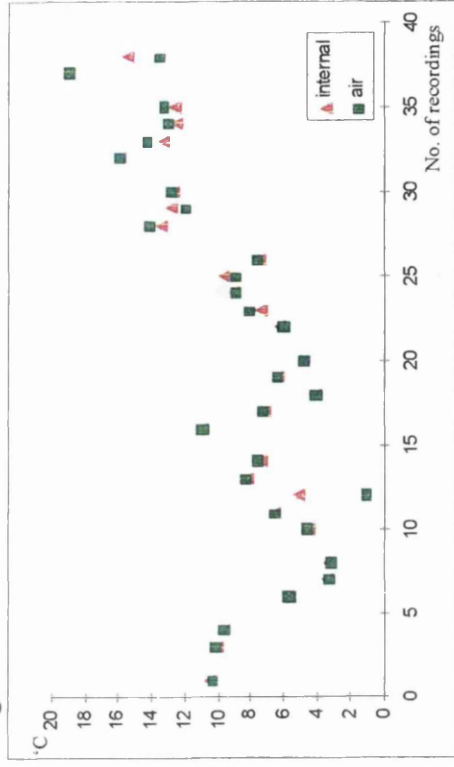


Figure 6.8 Scatter graphs to show relationships between air temperature, stone surface temperature, and the temperature of the inside of the bore holes for the South-facing portion of the balcony

Figure 6.8.1

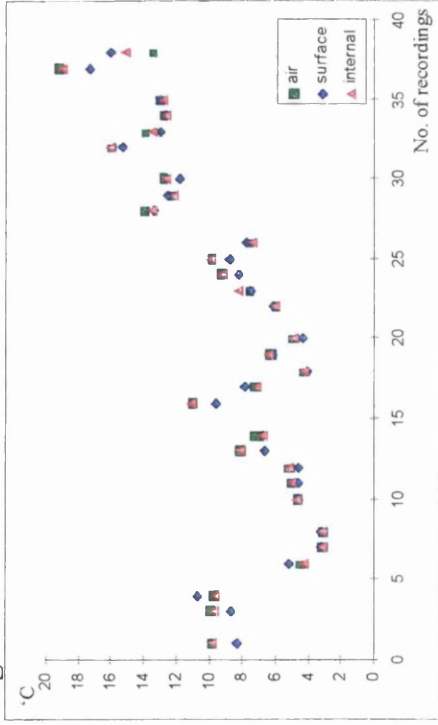


Figure 6.8.2

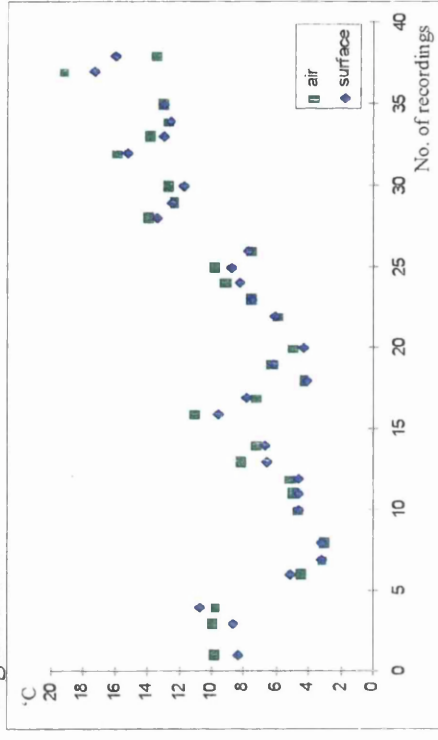


Figure 6.8.3

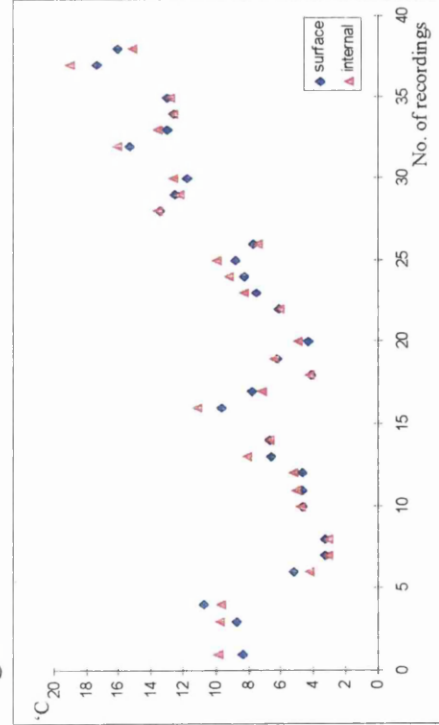
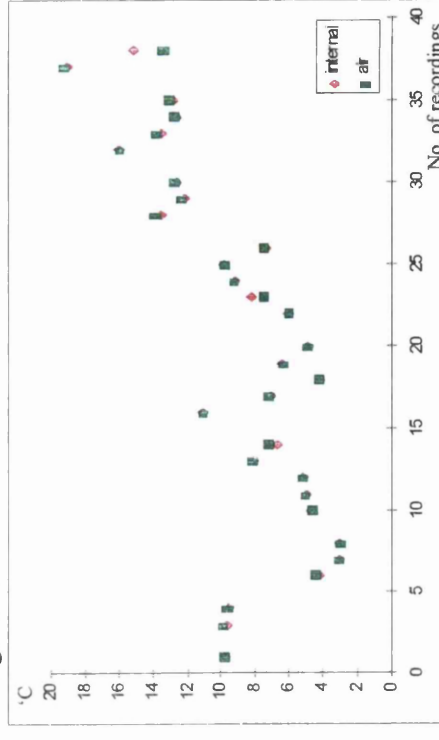


Figure 6.8.4



be expansion or contraction of the surface layers of the stone relative to the underlying stone. Also, at night, radiation causes the surface to become colder than the material beneath it.

These uneven temperature differences cause unequal expansion, and thus set up stresses in the material. Warke & Smith (1994) have shown that stones will initially show rapid near-surface rates of temperature change on heating and cooling. Thus the outer mm of the stone will be subject to numerous short-term thermally induced stress events. Stone has a low thermal conductivity and relatively high specific heat capacity, as such the diffusivity is low and the stresses are correspondingly higher than they would be in materials of higher diffusivity (Schaffer, 1932).

Similar temperatures between the interior and exterior of the stone are the result of the stone's relatively low thermal conductivity (compared with other building materials), whereby it is only the near surface regions of the stone that are affected by temperature fluctuations.

However, stresses which are set up in a stone with an uneven temperature distribution (one which is constantly being exposed to daily fluctuations in temperature) will encourage uneven expansion and differential moisture retention, especially within the first few mm of the stone surface.

6.4.5 Infrared video of the castle and its outbuildings

In addition to the work described above, an infrared video of the whole castle was undertaken by Napier University during March 1995. This time of year was chosen

Figure 6.9 Stills from the infrared video of the castle and its outbuildings



Figure 6.9.1 View of balcony West, high up



Figure 6.9.2 Wall adjacent to balcony North



Figure 6.9.3 Residential west wing, landward facing

Figure 6.9 Stills from the infrared video of the castle and its outbuildings



Figure 6.9.4 Far view of the castle from the cliffs



Figure 6.9.5 Balcony South

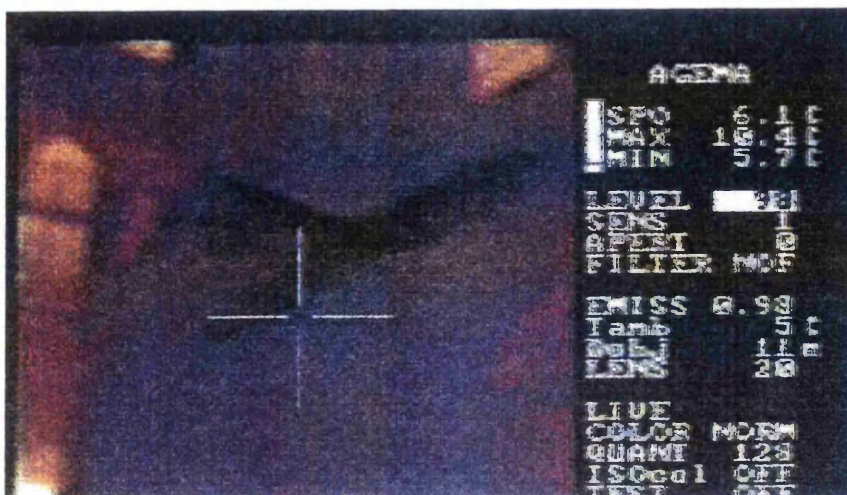


Figure 6.9.6 Residential west wing

Figure 6.9 Stills from the infrared video of the castle and its outbuildings



Figure 6.9.7 General view of the whole castle



Figure 6.9.8 View of the North face of the balcony North



Figure 6.9.9 The balcony North

by Napier University because it is the period when the colder weather has passed and there are still no trees to block and thus alter the output of the thermograph recordings. It is also after a period when there are no visitors to the castle and much of it has been uninhabited for five months.

Video stills taken from this recording have been reproduced in Figure 6.9. The blue represents the coldest regions; purple those stones reflecting some heating; and yellow, usually windows, where greatest heat loss is dissipated from inside, as would be expected. The area of the castle dissipating the greatest amount of heat is that of the West Wing. This area is inhabited all year round and thus regularly and substantially heated internally.

6.5 Summary of temperature, humidity and climate data

It is important to consider the influence of variable temperature conditions and their effect on moisture and relative humidity within thick blocks of stone such as those used at Culzean.

The climate at Culzean is harsh; strong winds, driving rain (up to 36.5 mm of rain in 24 hours), and extreme temperatures (as low as -7.3°C , with monthly variations of up to 13°C and daily variations of 6°C) recorded during the period of research. This climate will ultimately control the performance of the stone because the temperature and moisture content of the stone which will vary seasonally, diurnally

and over short-term periods, will be controlled by changes in precipitation, wind speed, cloud cover, solar radiation.

Surface temperatures varied according to the colour (albedo) of the stone and aspect, whether the stones were exposed to direct solar radiation. Blocks facing South and South-West were more exposed to solar radiation but also to direct changes in wind-speed and cloud cover, but responded to these climatic variations more readily, and were able to evaporate moisture and 'dry out'.

Sub-surface temperature and humidity recordings were also taken and compared with temperatures from the stone surface and the air. RH recordings provided evidence for moisture retention in the stone at depth; sub-surface RH being higher than that recorded at the surface of the stone or in the air.

Little variation was recorded between the air temperature, and surface or sub-surface temperature of the stone blocks. However they must exist. It is well documented that there will be variations in surface/subsurface temperature gradients and these.

Temperature conditions within stone are strongly influenced by thermal properties. Sandstone has a fairly low thermal conductivity, and will thus experience surface/subsurface temperature gradients (Jenkins & Smith, 1990).

Ultimately it is the amount of variation in temperature and humidity to which the stone is exposed that will increase its deterioration potential. Daily oscillations of temperature will influence the thermal field in the outer layers of the stone blocks, where zone of maximum moisture content will be situated.

Changes in volume due to the absorption and retention of moisture will always occur on the outer surface of a building wetted by rain. The crystallisation/hydration of salts, the differential movement produced by the expansion of near-surface regions on wetting/drying, and the subsequent development of planes of weakness, will be a contributory cause of exfoliation and contour scaling.

6.6 Analytical shortcomings

The work described in this chapter can help to provide an understanding of the processes at work with respect to the local climate, which in this case is a wet and exposed environment. It is however a preliminary investigation using observations made on site and by other researchers to draw conclusions.

Due to the tentative nature of the results, it is important to discuss the problems associated with the collection and processing of the data to provide the results detailed above. The following have been identified as the two principal shortcomings in the acquisition of the data:

- measurements should have been made over shorter time-scales to look at shorter term variations in temperature and RH. It would have been better if the equipment had been stabilised, with a permanent probe at each site and measurements recorded using a data logger; and
- the bore holes used for monitoring were the voids left by the cores cut for analysis (as no more cores were allowed). These were rather large for the

purposes of measuring temperature and humidity fluctuations, and thus the air temperature and moisture values may have been able to re-equilibriate with the external environment. It would have been more beneficial to drill a small core of 5 mm into the stone each time a recording was required. A thin probe could then have been inserted and a measurement taken.

Chapter Seven

Discussion, conclusions and recommendations for future research

7.1 *Aims of research and hypotheses tested*

When looking at the 'weathering', 'deterioration', or 'decay' of any material it is important to undertake research with a multidisciplinary approach. The objective of this research has been to look at the weathering of the stone on one building with such an approach in mind.

7.1.1 Research Aims

At the beginning of this work, a set of aims and objectives were established, these were as follows:

7.1.1.1 General Aims

- to determine the physical and chemical characteristics of the Culzean building stones in their fresh and weathered states, and to establish the factors causing stone decay;

- to consider the interrelationship between geological, environmental and time controls on decay, and the wider implications of this for building stones and weathering studies;
- to deduce, in the light of a simple model of aqueous ingress-egress, the physical and chemical weathering processes causing decay of the Culzean stones, and the relative tendencies of these stones to decay in the Culzean setting; and
- in the light of these findings, to advise the building owners on future conservation measures, including predictions of further decay patterns on existing stone and the choice of suitable stone for replacement.

7.1.1.2 Specific Objectives

- to establish the mineralogical and textural characteristics of the various Culzean stones in their unweathered state;
- to determine the physical patterns of decay in relation to stone type and aspect in both 'natural' and man-made environments;
- to measure the microclimatological parameters at the stone face and within the stone;
- to summarise the physical (engineering) properties of the Culzean stones;
- to describe the mineralogical, textural and chemical changes in the stone in the transition from unweathered to weathered material; and

- to undertake experiments to determine the reactivity of the stone under simulated natural conditions, and hence to deduce some of the chemical processes causing decay.

7.2 The variations in the character of the three stones

This section provides a summary of how the variations in the character and location of the three building stones are reflected in the weathering characteristics identified.

7.2.1 Adam's building stone

The AB stone is characterised by its natural variability and the high proportion of unstable minerals present. The stone contains quartz, feldspar, lithic fragments, micas, clays and carbonate cement. Despite the abundance of cement, the stone has a substantial effective porosity, identified by optical microscopy and SEM. Many of the feldspars, lithics and micas appear altered and replacement is evident. In addition to diagenetic clay minerals there are clays present as a result of feldspar and lithic alteration. Many of the minerals are coated with an iron-rich alteration product. In addition to the carbonate cement there are a number of small carbonate concretions evident in the rock. The proportion of quartz in the AB stone is less than that of the OB and VB sandstones. The greater number of lithics and feldspars make it is less chemically stable than the other two samples. When these characteristics are combined with the stone's unprotected exposure to wind-driven rain and seaspray loaded with soluble salts, there are a number of processes that take

place. The extent to which these affect the stone is dependent on the location of the samples, their exposure, their moisture retention and rate of drying. Weathering characteristics identified have been summarised below:

Table 7.1 A summary of the classification of weathering forms from AB samples

	AB1	AB2	AB3	AB4	AB5	AB6	AB7	AB8	AB9	AB10	AB11	AB12
ASPECT												
NORTH	X	X	X	X								
WEST					X	X	X	X				
SOUTH									X	X	X	X
DESCRIPTIVE CLASSIFICATION												
FRESH (F1)					X			X		X		X
PATINA (P2)			X			X	CEMENT				CEMENT	
SCALING (C3)	X	X		X					X			
FISSURATION												
L'					X			X		X		X
FS		X		X			X		X		X	
W	X	X		X			X		X		X	
O			X			X						
DISCOLOURATION												
D	X	X	X	X	X	X	X	X	X	X	X	X
RD	X	X			X			X		X		X
GD			X	X		X	X		X		X	
B			X		X	X		X				X
DETACHMENT												
PS			X			X	X				X	
S	X	X		X					X			
G	X	X		X	X	X		X	X	X		X
SG	X	X		X					X			
SP			X			X			X			

The weathering outcomes were:

- penetration of soluble salts into the stone, particularly chlorides and sulphates;
- salt crystallisation and hydration (halite, gypsum and thenardite) and to a lesser extent clay development and expansion (kaolinite, illite, smectite and chlorite) resulting in the removal of the stone's patina and exposure of contour scaling; and
- cement dissolution and reprecipitation reducing the cohesiveness of the stone.

These processes dominate the weathering of the AB samples because:

- there is inherent chemical instability and variation through the AB stone;
- high effective porosity;
- aspect (no protection);
- exposure to ingressing fluids; and
- inability of stones to dry out.

Therefore AB is a relatively poor building stone because of its chemical instability. It has a large proportion of unstable feldspars and lithic fragments. The instability of AB's rock forming minerals increases its potential for clay formation and subsequent modification by ionic exchange. AB is porous and has a high effective porosity that increases its permeability and thus susceptibility to ingressing fluids. This ingress of water exploits the hygroscopic nature of the stone and allows ionic mobility and chemical reactions to take place. These reactions are driven by the accessibility of the balcony stone to wind, rain, and runoff and the exposure to halite and formation

of gypsum/anhydrite, thenardite/mirabolite and their potential to crystallise within the stone.

7.2.2 Building stone used in 1879 for the west wing

The VB sandstone is a small to medium grained rock, also containing quartz, feldspars, lithics and clays and a higher proportion of micas compared with the other two building stones and respective quarry. There are less feldspars and lithic fragments but more examples of calcitic nodules/concretions in the stone to a larger extent than those seen in the AB samples. Where these concretions are present there are seldom any grain boundary contacts. Clay minerals are again a prominent feature of the rock. The stone is fairly porous, particularly in areas where the calcitic cement has undergone attack.

The only visible evidence of weathering on the building was surface contour scaling and granular disintegration. The weathering styles of the samples analysed are summarised in Table 7.2.

This has undergone less visible weathering than AB for a number of reasons:

- the stone is more stable and there is less chemical variability;
- there is a higher proportion of Si^{4+} present;
- the stone has a lower effective porosity;
- the stone is less exposed to soluble salts;
- soluble salts have not penetrated these samples to the same extent as the AB samples; and
- there is a more effective drying out of the stone.

Table 7.2 A summary of the classification of weathering forms from VB samples

	VB1	VB2	VB3
ASPECT EAST WEST SOUTH		X	X
DESCRIPTIVE CLASSIFICATION FRESH (F1) PATINA (P2) SCALING (C3)	X	X	X
FISSURATION U FS W O	X	X	X
DISCOLOURATION D RD GD B	X X X	X X X	X X X
DETACHMENT PS S G SG SP	X X		

7.2.3 Original Building Stone

The OB sandstone is a medium grained rock that contains quartz, feldspar, lithic shards, mica, clays and cement. The OB stone is much more compact than the other rocks with more grain boundary contacts, and is thus the least porous. There is still an abundance of calcitic cement. There are fewer examples of carbonate concretions or nodules, and these tend to be less extensive than in the other rocks. There are higher proportions of feldspars and lithic shards. The lithics tend to be elongate and of a more vitreous nature, and show less alteration at the mineral edges. Again clay is an important mineral and constitutes a large proportion of the rock, similar to that of VB, VQ and AB.

The OB samples exhibit no visual expression of weathering.

There are a number of external environmental factors that should have promoted the acceleration of the weathering of the OB stone over the years:

- emplacement in the building the longest;
- prolonged periods of wetting and drying; and
- proximity to the ground and thus exposure to groundwater percolation and capillary action.

Despite these factors, and although the bulk chemistry of the stone is similar to that of AB and VB, the OB stone exhibit least weathering problems because:

- the OB stone is less chemically unstable. It contains volcanic shards which are more stable than the lithic fragments found in AB and VB;
- the stone has a closed pore system and thus a reduced permeability and an organic patina which forms a skin and protects the stone from ingressing salt solutions;

- there is less exposure to the wind-driven rain and seaspray as this part of the castle is lower down and protected by the cliffs and trees; and
- there are lower soluble salts concentrations in the stone profiles due to position and thus less soluble salt penetration.

Table 7.3 A summary of the classification of weathering forms from OB samples

	OB1	OB2	OB3
ASPECT NORTH WEST	X	X	X
DESCRIPTIVE CLASSIFICATION FRESH (F1) PATINA (P2) Organic	X	X	X
FISSURATION U FS W O	X	X	X
DISCOLOURATION D RD GD (MORE GREY) B	X X	X X X	X X
DETACHMENT PS S G SG SP			

7.2.4 Quarry stone used in 1879

The VQ stone has similar properties to that of the VB samples, except that it has a higher quartz content and more importantly a different cement chemistry, which made it unfeasible to compare this directly with the VB stone.

7.2.5 Original Quarry

OQ is similar to OB in its character, as might be expected. Again the stone is less porous than AB, VB, and VQ, and there are few carbonate concretions/nodules.

The consequence of comparing the building stones with samples from their quarries to look for weathering patterns specific to the building was ineffective because the AB stones, which exhibited greatest deterioration, could not be directly compared.

7.2.6 Principal variations between the stones examined

7.2.6.1 Petrographic variations

Concentrating on compositional differences between the three building stones at Culzean, petrographic variation can be summarised as:

1. *the proportions of rock forming minerals found in AB, VB, and OB.* These combine to form the overall chemical make-up of the stone and consequently the state of decay;

2. *the porosity structure of the stone.* AB samples contain lengthy pores that interconnect to give a high effective porosity and thus increase permeability and its susceptibility to greater fluid ingress. The porosity of VB is less and the effective porosity of OB is very low;
3. *clay minerals.* The diagenetic clay kaolinite is present in all three samples. Illites, smectites, and chlorites are all present in AB, and are the most destructive for their size;
4. *calcium carbonate cement.* This can be readily dissolved particularly where more impurities are present as is seen in AB samples under the SEM. Dissolution is a near surface process and is dependent on pore space and channel outlets; and
5. *the presence of soluble salts, particularly halite.* Chlorides and sulphates play a very important role in both the physical and chemical break-up of the stone. The stone's susceptibility to salt crystallisation will depend on its physical and chemical make-up. The high sulphate values may be evidence of preventative measures taken to curb decay (i.e. cement rendering) and should not be repeated.

Ionic mobility and exchange are controlled by these petrographic and thus chemical variations. There is greater chemical variation in the carbonate cement and clay species towards the surface of the stone where ingressing fluids are at their most aggressive. Greater chemical variation is seen in AB because of the stone's naturally variable petrography; it has a greater potential to undergo chemical alteration.

7.2.4.2 Geochemical variations

The principle geochemical variations between the different sandstones identified by the leaching and experiments and chemical profiling of the stones showed that:

- there is greater chemical variability in the AB sample profiles compared with those of the VB and OB and their respective quarries;
- there is greater chemical variability towards the surface of the AB stones due to the presence of Cl^- and SO_4^{2-} phases;
- there are slight increases and decreases in cation content, particularly in both Na^+ and Ca^{2+} at and near the surface of the stone;
- there is evidence for the surface enrichment in soluble salts (especially halite and gypsum), and subsequently a general decline in anion concentrations can be seen throughout the sample profiles. Halite was often enriched just beneath the surface of the AB stones providing a potentially harmful situation where salt crystallisation/solution would result in the contour scaling phenomenon;
- more Ca^{2+} is removed from the surface of the AB samples retaining a patina, suggesting that the patina and thus surface regions of these samples contains a larger quantity of more soluble CaCO_3 cement; and
- the South-facing part of the balcony, which is the most exposed, yields more soluble material than the North or West, this may also indicate that more soluble

material has already been lost from the North and West, reducing the cohesiveness of the stone.

7.3 The key processes driving the variations examined

There are a number of key factors and subsequent processes driving the deterioration patterns and variation seen in the Culzean stones.

Principally there are two key prevalents, outlined in the model proposed in Figure 1.4.

7.3.1 Exogenous Factors: Environment/ Physical processes

7.3.1.1 External climate (Climate and microclimates)

That is the external climate and the exposure of the building to it. These include the physical properties of the wind, salt-laden rain & seaspray, and the aspect & exposure.

7.3.1.2 Internal climate

Driven by the external climate, these include the wetting and drying mechanisms of the stone, and the movement and retention of fluids migrating through the stone.

7.3.2 Endogenous factors: Lithology

7.3.2.1 Composition

The stone's porosity, mineralogical, petrographical, and thus overall chemical composition.

7.3.2.2 Chemical alteration

Controlled by the composition of the stone, the chemical deterioration processes of dissolution, hydrolysis, adsorption, oxidation & reduction. These factors were the driving forces that distinguish one building stone from another.

7.3.3 Key chemical weathering processes

The majority of ion mobility and thus exchange reactions took place where solutions penetrated the stone through pore throats and channels, where moisture was retained in the stone. These principle chemical weathering processes were deterioration mechanisms; namely crystallisation (which can also be described as a physical weathering process), dissolution, hydrolysis, adsorption, and redox (oxidation-reduction). These were discussed in *Chapter 1*. Examples of each are now put into the context of the Culzean stones. Examples of each of these processes are highlighted below.

7.3.3.1 Soluble salt crystallisation and hydration

Salt crystallisation and hydration is widespread at Culzean. Salts found in the stones include halite, gypsum/anhydrite, thenardite/mirabolite, and possibly sylvite.

Halite is hygroscopic; it has the ability to readily absorb water vapour from the atmosphere and is the most soluble of all the evaporite minerals. Halite will therefore undergo continuous changes in volume dependent on its access to moisture.

Sodium sulphate (thenardite/mirabolite) will undergo hydration readily. It will hydrate and dehydrate relatively easily in response to changes in temperature and humidity, changing in volume by up to 300%. Gypsum will produce a greater crystallisation pressure than mirabolite and the solubility of gypsum will increase in the presence of other soluble salts. The solubility of gypsum in a two molar solution of NaCl is five times that in a pure gypsum solution (Braitsch, 1971). Therefore the presence of these two soluble salts increases the frequency of gypsum/anhydrite dissolution/recrystallisation cycles (Livingstone, 1994).

All these salts react to changes in RH and temperature and thus will cycle more frequently from solution to solid with the more frequent RH and temperature changes experienced by the outer layers of the stone (Livingstone, 1994).

Thus evidence suggests that soluble salts are very mobile. They appear and disappear periodically. As they are transported by water, they move in and out of the stone, and along the surface of the stone. This dilation and contraction results in the build up of salt crystallisation and hydration pressures, which cause mechanical breakdown of the stone, in this instance by the mechanism of contour scaling, but only in strongly salt-enriched stones where the coarse pores can be filled up with salt crystals.

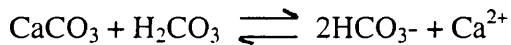
There are a number of parameters which control the nature and site of precipitation of salts, dependent on the cycle of ingress and egress of fluids. During the drying process, salts migrate into the part of a pore system that is still wet. They are enriched in the rest of the pore liquid and precipitate when all the remaining liquid has evaporated. Damage happens in the zone of the maximum moisture content, which is necessarily the zone of the salt precipitation. The actual location depends on the moisture transport coefficient of the stone and on the transition coefficient of the stone i.e. on the conditions of the building (Fitzner & Sneath, 1982).

The nature of the concentration gradient developed on the egress part of the cycle is believed to be particularly important (Lewin, 1982). If concentration to the point of precipitation occurs at the surface then efflorescence results.

On the balcony at Culzean salts have precipitated beneath the surface. There are several possible reasons for the zone of the maximum moisture and thus salts precipitation to be beneath the surface of the stone. Salts will crystallise where the fluid is saturated in the salts' components. A saturation front will exist at a position dependent on the concentration of soluble salts in solution. It can therefore be assumed that concentration gradients on the egress cycle are high and soluble salts concentrate and dilate/contract as they crystallise/hydrate beneath the surface of the stone. De-cementation and mineral expansion (and expansive clays) will further weaken the stone at this wetting/drying zone. Therefore contour scaling will form when the zone of the maximum moisture is situated in the interior of the stone.

7.3.3.2 Dissolution

The most common soluble mineral is halite (as discussed above). The solubility products of most rock forming minerals are very small. The most soluble constituents of rock are Na^+ , Ca^{2+} , K^+ , SO_4^{2-} , and Cl^- . Calcite, the main constituent of the calcium carbonate cement found in the Culzean stones suffers extensive solution as a result of the presence of dissolved CO_2 in the water ingressing into the stone, which forms weak carbonic acid (H_2CO_3), that reacts with the calcite:



The greater the ingress of CO_2 , the more calcite is attacked, and the greater the dissolution of the cementing material will be. Also the solubility of CaCO_3 increases from 0 to 1.5 moles per 100ml, due to the influence of NaCl on the activities of Ca^{2+} and carbonate species. Therefore there will be greater CaCO_3 dissolution where NaCl solutions are prevalent. In addition, the solubility of calcite decreases with increasing temperature (Wedepohl et al., 1978). Thus less calcite is dissolved at where the surface of the stone is heated.

There was even some visible evidence by SEM of quartz grain dissolution. Quartz is dissolved by a hydration reaction: $\text{SiO}_2 + 2\text{H}_2\text{O} \rightleftharpoons \text{H}_4\text{SiO}_4$. No new solid phase is produced as a result of this reaction.

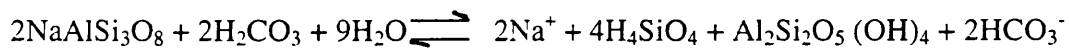
There are two dissolution reaction mechanisms:

- transport (diffusion) of a reactant or a weathering product through a leached layer at the surface of a weathered mineral; and
- chemical reactions at the surface involving the breaking of bonds and the formation of surface pieces that ultimately detach from the surface or break down into other products that detach from the surface. This tends to be the mechanism by which oxides and silicates are weathered (Strumm & Wollast, 1990)

The rate at which dissolution occurs is dependent on the rate of the surface reactions because these are generally slower than the rate of diffusion of reactants and products through the thin reaction layer that separates the mineral from the surrounding bulk solution.

7.3.3.3 Hydrolysis

These reactions involve compounds with H₂O where weak acids (e.g. H₂CO₃) or weak bases (e.g. NH₄OH) are formed. An example of this would be the weathering of feldspars, from which clays are produced. SEM examinations showed a number of examples of albite weathering to produce kaolinite:



At the same time as hydrolysis, clay formation results in the exchange of H⁺ ions for cations in the feldspar, with K⁺ and Na⁺ being released into solution:

- weathering rates of minerals are directly dependent on their atomic structure and bond strength; and
- these rates also depend on the nature of the weathering solution, especially abundance of hydrogen ions i.e. pH (see Casey *et al.*, 1998)

7.3.3.4 Adsorption

Adsorption is the attachment of a dissolved ion or molecule to the surface of a mineral, for example, sheet silicates. In this case it primarily involves the adsorption of H₂O molecules i.e. hydrogen bonding in clays such as smectites and chlorites.

The process evolves as follows:

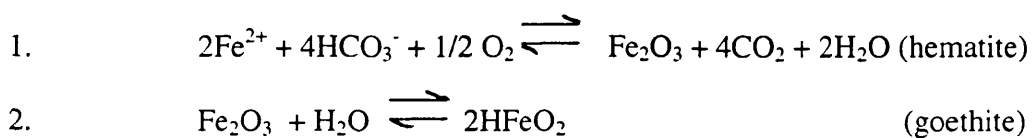
- the adsorption of water at the sites of Si-O bonds;

- the breaking of the Si-O bonds; and
- the formulation of other bonds involving the atoms of the water molecule as depolymerisation proceeds (Dove & Crerar, 1990).

7.3.3.5 Oxidation-reduction (Redox)

Redox reactions take place at the mineral-water interface and therefore are more common towards the surface of the stone, where ingress is maximised. The result is the oxidative and reductive dissolution of minerals (Hering & Stumm, 1990). There is an electron transfer between surface sites on minerals and multivalent aqueous species. For example, biotite undergoes a solid state oxidation reaction on contact with H₂O which is followed by a reductive solution reaction that releases Fe²⁺ into solution (White, 1990).

Redox reactions were common in other iron compounds, within the Culzean stone, especially AB samples. Ferrous iron from the weathering of iron-bearing silicates was oxidised by dissolved oxygen. Ferric iron often then occurred as goethite (see *Chapter 4*) HFeO₂.



7.3.4 Summary of chemical weathering processes

In the above, a number of the chemical reactions which have taken place in the stone are outlined. These involve a complex set of reactions incorporating and releasing many different major elements to produce a very complicated weathering profile.

These exchange reactions took place between cations and anions held in unbalanced charges at or near the surface of minerals. The exchange takes place with ions present in the surrounding mobile solution which have either been introduced to the stone by the penetrating solution or removed from other mineral species by these aggressive solutions.

Absorption by 'unsatisfied' valences forms an essential part of the ion-exchange processes. It was not possible to calculate ion exchange capacity of a given mineral or combination of minerals from the data collated.

Ion exchange will take place for the following reasons:

- unsatisfied valencies produced by 'broken bonds' at surfaces and edges particularly of clay particles;
- unbalanced charges caused by isomorphous substitution;
- the dissociation of OH^- radicals, the H^+ of which may be exchanged; and
- the accessibility of atoms in structural positions when brought to the exchange site as a result of a change in environment (the ingress of aggressive solutions).

The most significant environmental factors are:

- the ability for solutions to penetrate the stone i.e. porosity and permeability. Transport properties will vary significantly from one sample to another despite the fact that these belong to the same geological formation;
- the availability of exchangeable constituents in the mobile phase. The composition of the solutions penetrating the stone;

- pH-Eh relationships;
- the general chemistry of the environment, the mineralogy of the stone; and
- the pressure and temperature conditions to which the stone is subjected.

All these will allow soluble salts to crystallise, clay species to form and expand, and phenomena such as contour scaling to take place.

Ionic enrichment and depletion provides the primary driver for contour scaling. Mobility is the key to stone decay, as a stone will always deteriorate when it is in an open system where material can be readily introduced, redistributed, and removed from the stone. Ionic mobility was prevalent in the AB samples and resulted in the various weathering patterns seen on the balcony. This phenomena was reduced in the VB samples and non existent in OB because of the reduced porosity, differences in the mineralogy and geochemistry of these rocks, and variations in aspect of these two sites.

7.4 Formulation of model

The following observations have been made as a result of the experiments and analyses undertaken throughout the course of the research to show how the stone is altering and suggest the principal processes taking place. These are to be used to formulate a model for the weathering of the stone at Culzean and are as follows:

- 1. visually there were distinct zones of weathering in the AB stone, specifically surface patina with zones of contour scaling beneath. These were substantiated*

- by SEM analysis and experimentally by the IC profiles which often indicated distinct variations in soluble salt content, particularly at the surface of the stone;
2. a crust/patina was produced by the evaporation of moisture from the surface layers of the stone and through the precipitation of material at the surface of the stone (e.g. reprecipitated carbonate cement from deeper in the stone's profile and soluble salt precipitates);
 3. cement dissolution and replacement/reprecipitation did occur in the near surface regions;
 4. patina detachment/spalling was aided by soluble salt precipitation at a saturation front (zone of wetting/drying) where crystallisation pressures caused the contour scaling phenomenon;
 5. the process of contour scaling beneath the patina was dominated by the continued crystallisation and solution of soluble salts. The cohesiveness of the stone was also reduced by the loss of cementing agent (increased solubility of CaCO_3 in the presence of NaCl) and the expansion of clays;
 6. there were numerous examples of the near surface breakdown of minerals and the precipitation of new minerals (e.g. feldspars to produce clays), where a number of chemical weathering processes (outlined in Section 7.3) were prevalent; and
 7. the chemical alteration and expansion of clays occurred throughout the stones profile. However there was preliminary evidence for increased variation in the composition of clay species present towards the surface of the stone. This

highlighted greater chemical variation where moisture was retained for long periods of time.

7.5 Models

The intention of this work was also to bring together the analyses undertaken, subsequent results and interpretations of these results to produce a model for the decay processes examined.

The model produced is based on the deterioration processes seen on the Adam's balcony stone (although the other two have been referred to), and is thus based on a sandstone with a high effective porosity, a large proportion of unstable minerals, and a stone exposed to aggressive ingressing solutions.

7.5.1 Moisture movement models

Many problems in building materials are found to be moisture related. Indeed, many of the problems of building construction, building renovation and building use are related to the processes of water transport in porous building materials (Gummerson *et al.*, 1980).

One of the primary drivers for stone decay at Culzean is the availability of water, required by weathering processes to be effective:

- the ingress of solutions into the stone;
- the retention of that moisture within the stone; and

- ineffectiveness of the drying-out process.

In addition, the behaviour of moisture in the pore systems is complicated by the presence of salts in solution, in abundance at Culzean.

In putting together a model for the decay mechanisms studied at Culzean, it is necessary to take into account and build on models based on moisture movement, which have already been tested. One of the key processes that must be considered is the effect of evaporation and other drying mechanisms.

7.5.1.1 Drying out of the stone

Studies have shown that the drying process has several distinct phases. This is well established in the scientific literature of drying, and for building materials can be traced back at least to the paper of Cooling (1930) who put forward a model for different drying stages.

Sereda & Feldman (1970) put forward a concept for two stage drying, and Hall *et al* (1984) have found experimental evidence for the idea that drying could be categorised into at least two separate stages.

The idea is that drying under constant external conditions occurs in at least two distinct stages:

Stage one the constant drying rate period; and

Stage two the falling drying rate period.

In more detail, these can be described as follows:

Stage one involves evaporation from surface layers, dependent on environmental conditions.

Stage two is where a new drying process begins to take over. Here the rate of evaporation decays with time. The rate of drying is governed by the rate with which moisture can be transported from the interior of the material to the drying zone. This will be dependent on the liquid and vapour transport parameters and environmental conditions.

A third stage has been suggested in BRE digest 163 (1974) and by Platten (1985). (This stage is not relevant here as it involves the reaching of an equilibrium with the surrounding air and it can take several years before the material is considered dry.)

Van Brakel (1980) has discussed the evidence for stage one behaviour at length. He determines that there is considerable evidence that the stage one drying rate in a wide range of porous materials is equal to the evaporation rate of a free water surface under the same conditions (Van Brackle 1980).

The *stage one* appears to be essentially influenced by material properties, so it is generally accepted that free evaporation of liquid is occurring at the solid surface. Thus, the rate of drying is controlled by the vapour properties of the evaporating substance. The drying rate will be dependent on:

- relative humidity;
- air flow; and

- temperature.

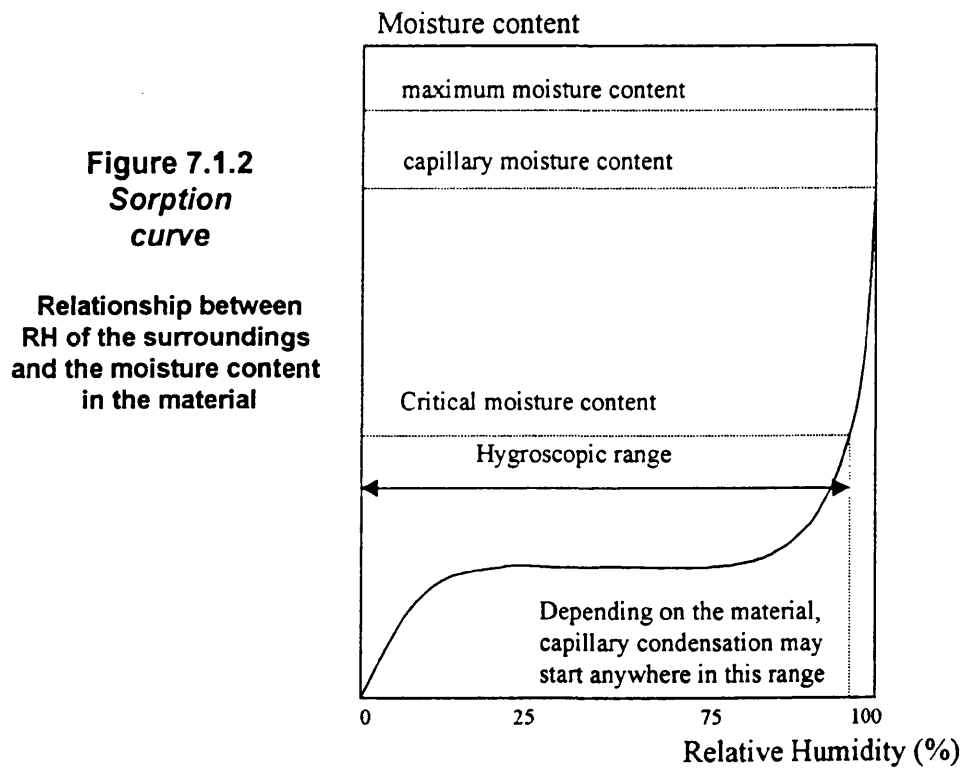
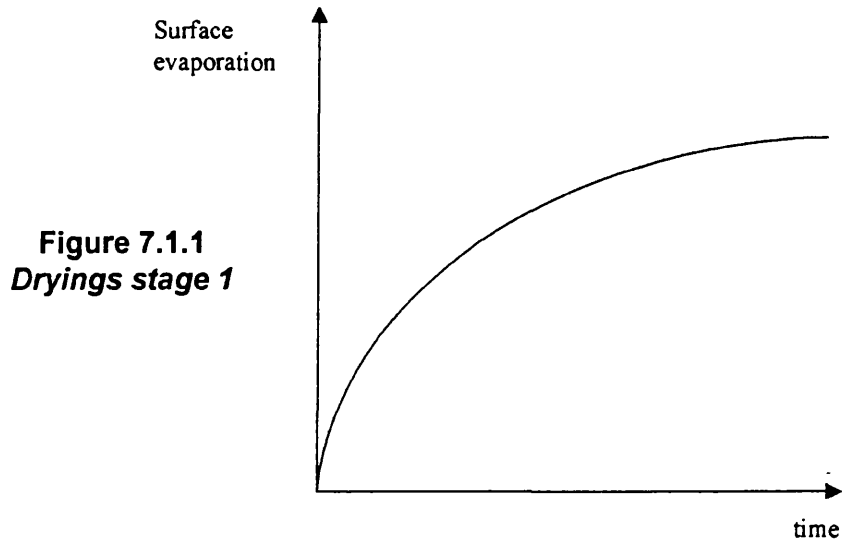
In Figure 7.1.1, the *stage one* drying diagram shows that the drying rate [r] eventually ceases to be constant and begins to fall. The change in [r] marks the beginning of stage two drying. In *stage two*, the rate of unsaturated flow within the porous solid, limits the drying rate.

The rate of unsaturated flow of the evaporating liquid towards the drying surface is determined by the material properties, which determine the *stage two* drying. A simple view of the transition from *stage one* to *stage two* based on the unsaturated flow theory of the surface water content during *stage one*.

Stage one drying is characterised by a constant rate of evaporation under constant drying conditions. The evaporating water is transported to the drying surface by unsaturated capillary flow, assuming the extended Darcy theory applies (Hall *et al*, 1984).

As drying proceeds the surface water content falls with time. Increases in airflow and temperature will result in more rapid drying during *stage one* (see balcony variations). Increases in the temperature of the wet material by 10°C approximately double the drying rate.

For any given material, the duration of the *stage one* drying varies inversely as the square of the drying rate and subsequently the drying rate falls with time. The terminal drying rate, like *stage one*, increases rapidly with temperature and surface heating.



Reproduced from the International Energy Agency Report Annex 24, task 3
'Material and Layer Properties' (1996)

7.5.1.2 Moisture transport and diffusivity

There are four phases of moisture transport; adsorption, condensation/vapour transport, liquid and vapour transport, and liquid transport (Rose, 1963).

Transport under saturated conditions requires the exertion of a pressure across the surface of the stone. This can occur where there is a continuous stream or film of liquid water across a surface exposed to a wind (Darcy's Law), Spooner (1982) details this. Water transport is proportional to the pressure gradient that is applied across it.

The diffusion component of moisture movement is assumed by many authors to be the dominant mechanism for moisture transport in building. It is important to consider both liquid phase transport and evaporation. The sorption curve, determined by the IEA (International Energy Agency), based on the relationship between the RH of the surroundings and the moisture content in the material has been reproduced in Figure 7.1.2.

7.5.2 Culzean sandstone models

To produce a model for the decay processes seen at Culzean it is necessary to combine the moisture movement theory and drying stage theory with the physical evidence for decay and the chemical weathering processes taking place at Culzean.

Figure 7.2 shows the perceived ingress of fluids, the retention of fluids in the stone and their subsequent egress. Solutions enter the stone by capillary and gravity action in one of the following phases:

- adsorption;
- condensation/vapour transport;
- liquid and vapour transport; and
- liquid transport.

A simple hypothetical equation can be drawn up to show the mechanism of moisture retention, where the egress of moisture is equal to the ingress of moisture minus that which is retained in the stone:

$$E_{gm} = I_{gm} + T_{m_i} - (T_{m_o} + K)$$

I_{gm} **Ingress of moisture**

Moisture entering the stone by condensation, adsorption, liquid and vapour transport

E_{gm} **Egress moisture**

Moisture being removed from the stone by surface evaporation and/or runoff

T_{m_i} **Transmitted moisture**

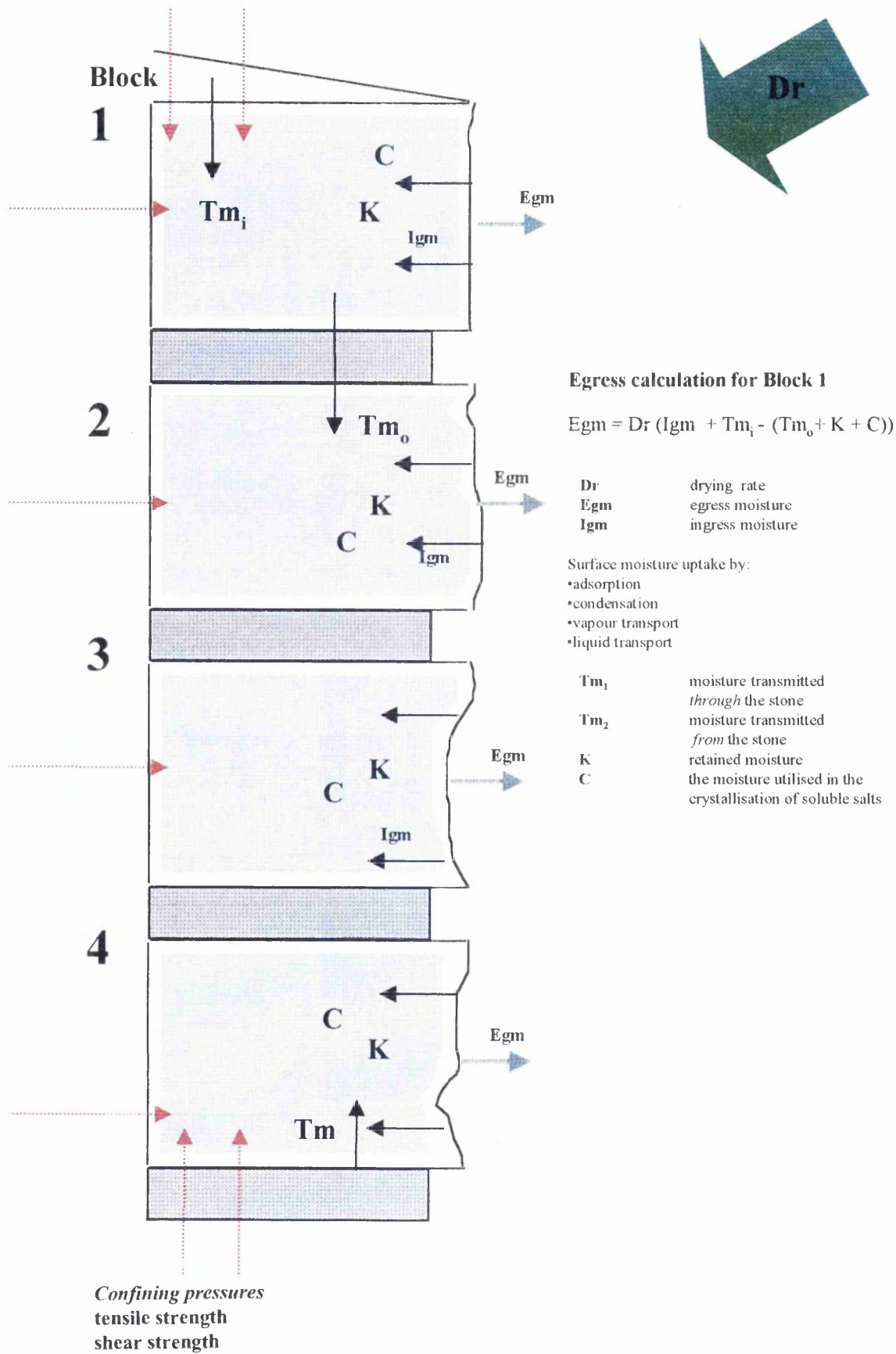
Moisture transmitted through the stone via other routes (e.g. through mortar joints)

T_{m_o} **Transmitted moisture**

Moisture transmitted from the stone (e.g. through mortar joints)

K **Retained moisture**

Figure 7.2 Diagram to show moisture ingress and egress and the mechanisms that drive them



Moisture retained in the stone in solution

Missing from this calculation is the mechanism controlling the E_{gm} , i.e. the drying mechanism that draws moisture from the stone to reduce the E_{gm} value. A value cannot be put on E_{gm} as it is dependent on external parameters. The external climatic conditions and the temperature and humidity characteristics of the stone will drive the drying process. Water penetration and thus chemical changes will be driven by temperature (see Figure 7.3):

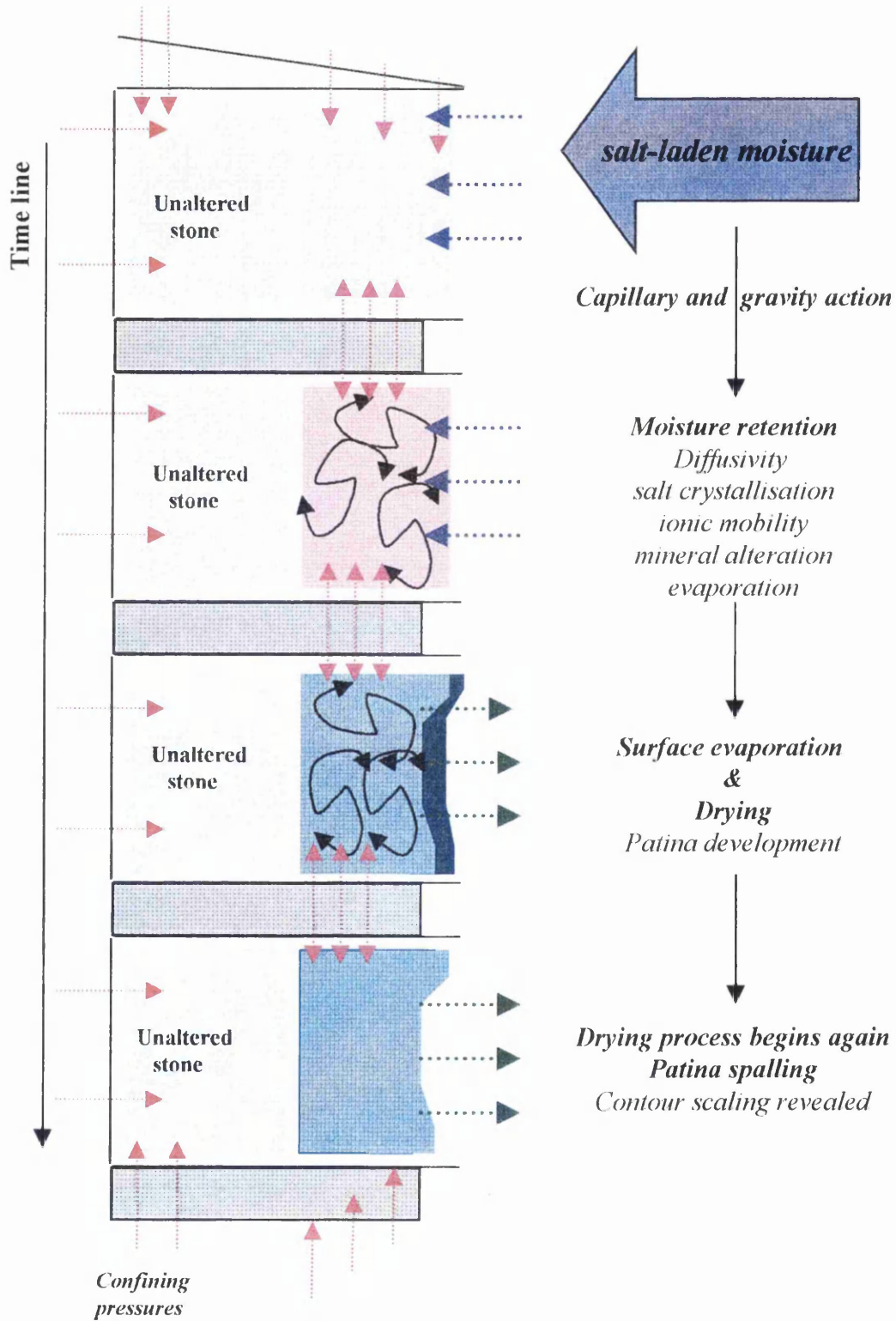
1. daily changes in the surface temperatures will influence near-surface water condensation and thus relative humidity of the stone;
2. extended insolation will allow heat to be transmitted into the stone and moisture to be drawn towards the surface of the stone; and
3. moisture retention in the stone can only be attained from the ineffective drying of the stone.

The drying rate (Dr) can be included in the equation as the factor or coefficient that will control all the other factors in the equation. Relative humidity, airflow and temperature control the drying rate coefficient.

$$E_{gm} = Dr (I_{gm} + Tm_i - (Tm_o + K))$$

The calculation can be complicated further as the behaviour of moisture in the pore systems is complicated by the presence of salts in solution. The weathering model here would be very different if soluble salts didn't play such a key role in the deterioration of the stone. Evidence suggests that the soluble salts are very mobile.

Figure 7.3 AB stone:
Development of current deterioration



They appear and disappear periodically. As they are transported by water, they move in and out of the stone, and along the surface of the stone.

Salts will crystallise when the fluid is saturated in the salt's components. In a drying or wetting rock with salts in solution, a saturation front will exist at a position depending on the concentration of the salts in solution. The front will move in and out during wetting/drying. There will be an increase in the hygroscopic moisture content of the stone at this point, and as a result, this solute deposition front is marked by a boundary.

As such, a wetting/drying zone has been established at a depth which varies between 5-45 mm depth. As the patina blisters off, as has been seen in a number of cases, a new equilibrium is obtained. In some cases, where the patina is in the process of blistering off, a second patina (further evaporation of retained moisture) can be seen behind it (Figure 7.3).

Therefore, with the repeated accretion and solution of salt crystals in this zone of wetting and drying, pressure is developed sufficient to produce a contour scaling effect behind the exterior patina. Visible surface alteration does not take place because ingress is greater than egress; there is no visible alteration to the stone surface. By the time the damage is noted, it is too late to save the exterior of the stone.

$E_{gm} = D_r (I_{gm} + T_{m_i} - (T_{m_o} + K + C))$ where C is the moisture utilised in the crystallisation of soluble salts (see Figure 7.2).

In addition, the mechanism by which salts become saturated and crystallise must be recognised. This is a critical stage for consideration, and should be the result of the balance between:

- salts carried by **Igm**;
- salts formed with ions from the mineral weathering of e.g. feldspars and lithics;
and
- **Egm**.

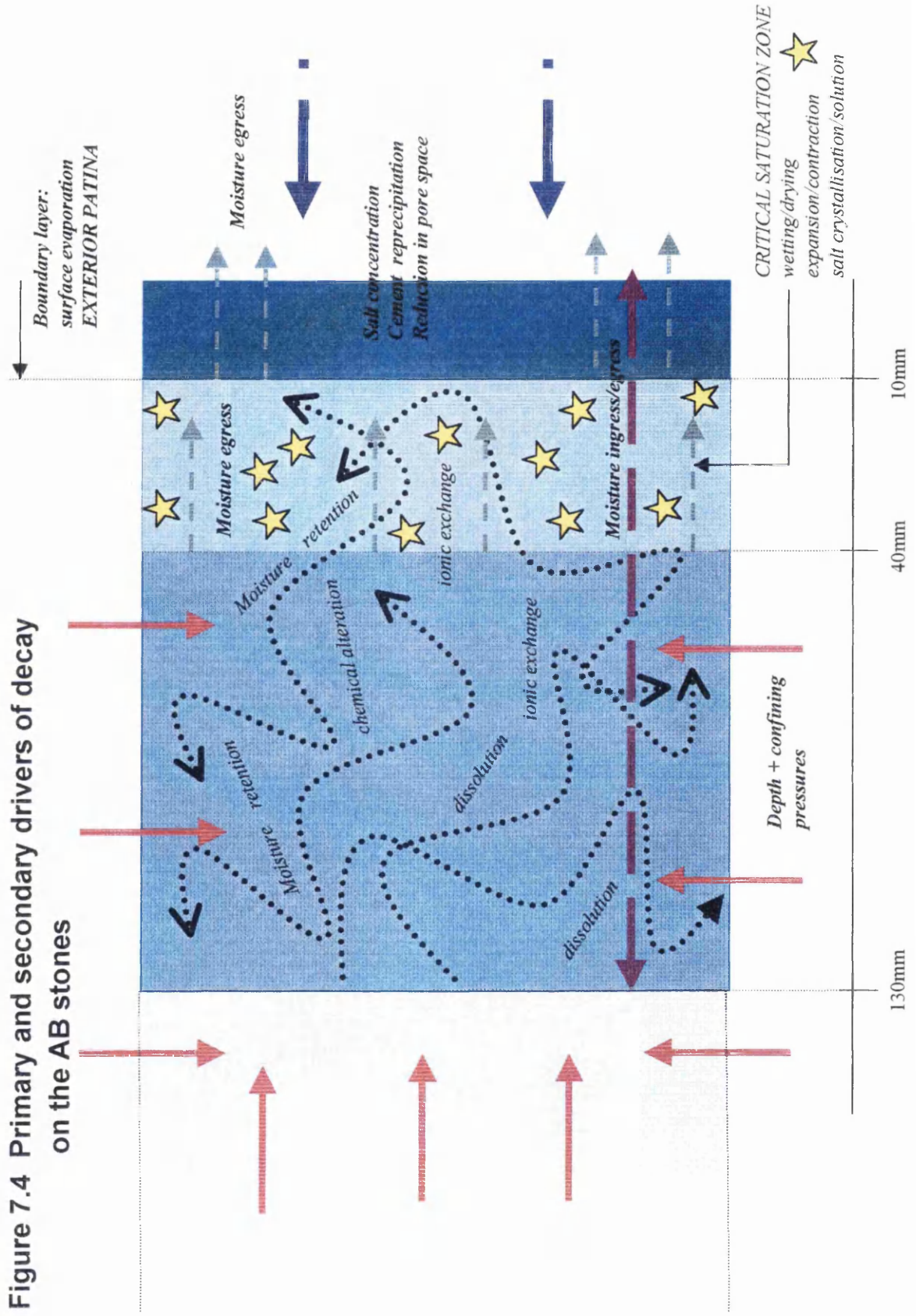
At some critical value of **Egm : Igm** a saturation front will form outside of which crystallisation takes place. This is part of the ingress/egress mechanism and is dependent on the quantity of soluble salts in the stone relative the quantity of solution. This is shown for the AB stones in Figure 7.4.

The importance of the ingress/egress model is dependent on the natural characteristics of the stone. It is here, that in addition to the increased exposure to solutions enriched with soluble salts, the petrographical and mineralogical characteristics of the AB stone explain the weathering phenomena seen on the balcony. To aid in this, models for the three stones have been drawn up, highlighting where the differences lie. These can be seen in Figure 7.5.

7.5.3 The *Egm* of the AB sandstone

The values of *K* and *C* will be highest for the balcony stones that are exposed to the largest amount of wind-driven rain and seaspray, and have been ineffective in drying

Figure 7.4 Primary and secondary drivers of decay on the AB stones



out. Thus *Egm* will be reduced. As such these stones retain solutions that harvest soluble salt crystallisation (on solution saturation), clay production and expansion; and the dissolution and precipitation of new and altered mineral species (Figure 7.3).

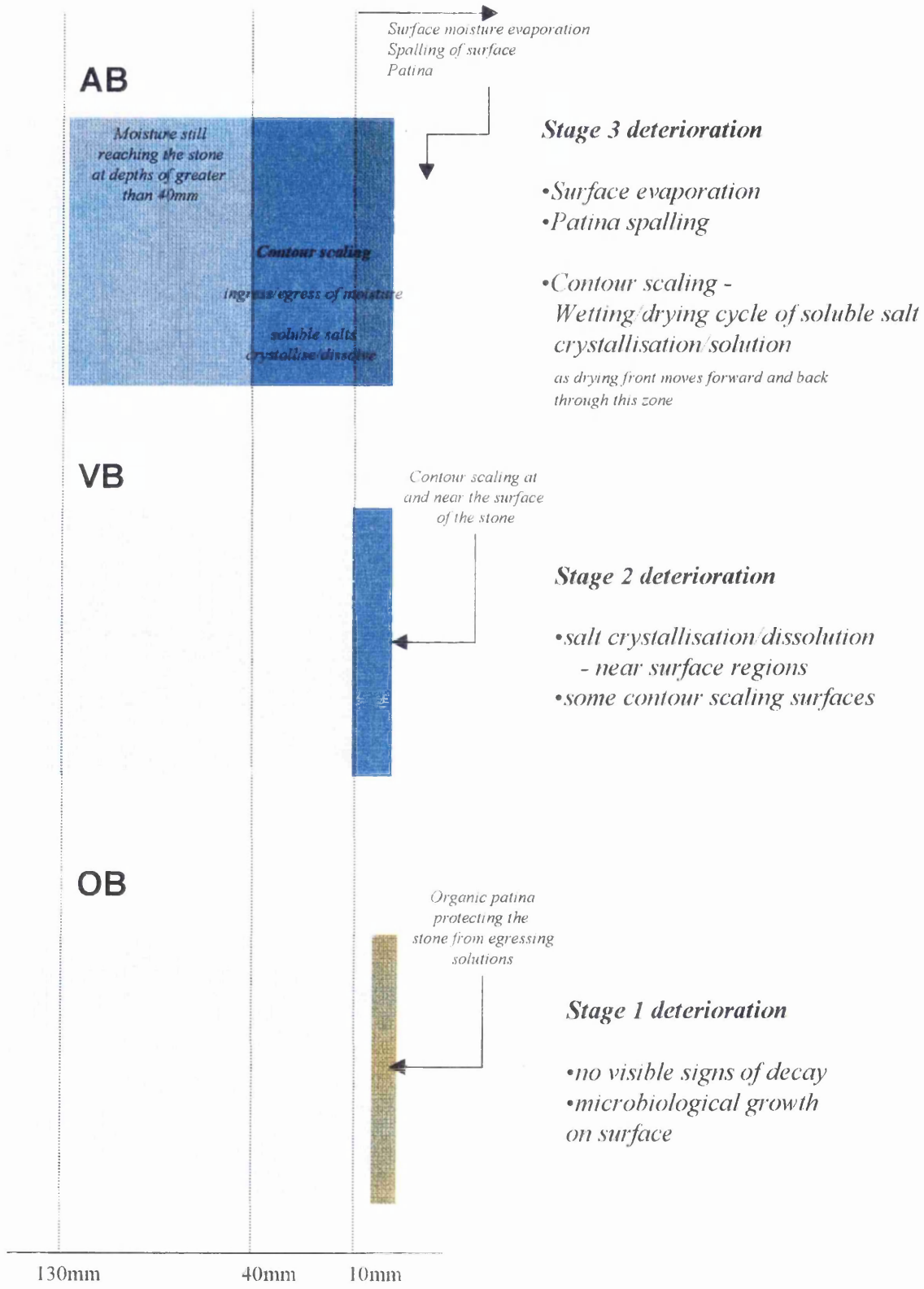
The variations seen in the weathering processes on the balcony are as a result of the temperature and humidity variations around the balcony. Some stones are able to dry out more readily than others. Where fluids are retained in the stone, salt crystallisation/solution cycles are more likely to develop.

The two primary characteristics of the balcony stones' weathering characteristics are the spalling of a surface patina and the contour scaling revealed beneath this. The formation of a patina can be explained by:

- the movement of reprecipitated carbonate cement from deeper in the stone's profile;
- new mineral precipitates; and
- soluble salts concentrations, particularly sulphates which were found to concentrate at the surface of the stone.

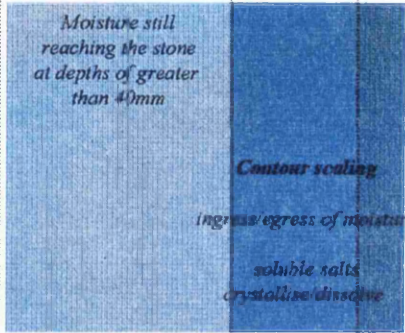
The patina formation can be explained by the two stage drying process described in section 7.5.1 (see figure 7.5). It results from the completion of *stage one* drying i.e. the evaporation of moisture from the surface layers of the stone, and the beginnings of *stage 2* drying, dependent on the microclimate of the stone. It appears that on the balcony North, it is only this surface patina that dries out, moisture is retained at depth beneath it. Here as wetting/drying behind the patina alternates, the saturation front moves in and out. The fluid becomes saturated/unsaturated in soluble salts

Figure 7.5 Comparison of visible stages of deterioration for the three Culzean stones



AB

Moisture still reaching the stone at depths of greater than 40mm



Surface moisture evaporation
Spalling of surface
Patina

Stage 3 deterioration

- Surface evaporation
- Patina spalling
- Contour scaling -
Wetting/drying cycle of soluble salt crystallisation/solution
as drying front moves forward and back through this zone

VB

Contour scaling at and near the surface of the stone



Stage 2 deterioration

- salt crystallisation/dissolution - near surface regions
- some contour scaling surfaces

OB

Organic patina protecting the stone from egressing solutions



Stage 1 deterioration

- no visible signs of decay
- microbiological growth on surface

130mm 40mm 10mm

which crystallise/dissolve. These changes in the state of the salts create differential pressures which induce the explosive effects of contour scaling and lead to the eventual mechanical breakdown of the stone, as the patina is forced off by pressures beneath it (see Figure 7.3 and 7.4). The balcony South has a different microclimate. Although soluble salts are present in concentrations throughout the stone, the different components of the process do not respond in the same way. Surface temperatures are higher, K is lower, fluctuations in soluble salt crystallisation/solution are reduced and deterioration of the stone does not take place to the same extent.

7.5.4 The E_{gm} of the OB sandstone

The value of E_{gm} for the OB stone will be much higher as the drying process is more efficient for these stones (Figure 7.2 and 7.5). This is because less water is entering the stone (lower I_{gm}), fewer soluble salts are entering the stone, fewer detrimental chemical reactions are taking place, and moisture is more readily drawn out of the stone. It has a different drying mechanism, primarily because fewer soluble salts are involved in the wetting/drying process.

7.5.5 The E_{gm} of the VB sandstone

The value of E_{gm} for the VB stones would fall between the OB and AB sandstones. The VB stones examined were taken from sheltered positions near the base of the west wing of the building. As such these stones were not exposed to the same

quantity of ingressing fluids as AB, although soluble salt extraction by IC did provide high values of halite at the surface of the stone. There was some evidence of contour scaling on the west wing of the building but no examples of patina spalling (Figure 7.5). In this instance the 'critical saturation zone' of wetting/drying and salt crystallisation/solution is at the surface. The stone is drying out more readily than the AB stone, preserving its weathering potential (see Figure 7.5).

7.6 Recommendations for the future

The balcony stone should be cut back to ensure safety, particularly where surfaces are spalling off. In addition, the contour scaling surfaces should be cut back, preferably by at least 50 mm+, to remove material highly enriched in soluble salts and to minimise the effects of contour scaling.

The weathering processes will continue and may be accelerated if the stone is not cut back to a suitable depth. Nothing can be done to prevent the decay cycle from reoccurring, such is the nature of the stone, climate, and exposure of the balcony at Culzean.

As the structural integrity of the building is not at risk, the NTS may consider cutting back the stone and leaving it to start building up another layer of surface salts once more. The other near surface weathering features of e.g. cement dissolution /reprecipitation, clay generation/expansion, will continue whether the stone is left or redressed.

However if the stone is to be redressed, the replacement stone should be chosen carefully with the following considerations in mind:

- *a similar mineralogical and textural composition.* When choosing a replacement stone it is advisable that a petrographic study is undertaken to prevent an unsuitable stone being used. This will prevent a mismatch with the surrounding stones, particularly with respect to porosity and permeability. If the stone is indented, a variation in porosity between the two stone types could make accelerate weathering by creating a deterioration zone between stone faces or at the original stone/indented stone boundary;
- *appearance of the stone – texture and colour.* It should be ensured that the stone replacing/indenting the current stone will ‘weather’ to a similar colour and in a similar textural manner with respect to the current stone. This will prevent a ‘patchwork’ effect resulting from the placing of stones of different colours and features side by side;
- *potential quarry supplies.* It is important to choose a stone which can be supplied in the future for further repairs i.e. a quarry with substantial supplies. It is also suggested that the source of the stone within the quarry is well documented as stone can vary significantly around a quarry; and
- *the consideration of cost.* It would be preferable to use local stone to ensure an appropriate match. Currently there are no suitable local stones quarried. The economics and logistics of reopening an old quarry might be unacceptable, especially if a large quantity of the stone will be required now and regularly in future years.

It is paramount that there is a reduction in moisture. There must be an attempt to put a dry stone on the building. No stone at Culzean should be rendered either with a cement coating or any non-breathable consolidant as this will seal moisture into the stone and decay will continue from the inside. Additionally, it may be suggested that the drainage system be altered to redirect and thus reduce the amount of runoff descending directly onto the balcony stone.

It should be appreciated that in a study such as this the recommendations given are case specific. If recommendations for newbuild on the same site were being given, the type of sandstone suggested would be very different.

Recommendations for the preservation/restoration of historic buildings and monuments must be case specific. More research should be undertaken on individual buildings to ascertain the causes of deterioration and the appropriate remedial action that should be taken to preserve the building. By undertaking mineralogical investigation on the properties of the stone and its deterioration mechanisms, it may be possible to prevent or reduce the acceleration of some of the decay processes. Where prevention is not possible, knowledge of the properties and decay mechanisms at work in the stone will provide the information required to make an informed choice for suitable indentation or replacement of the stone.

References

AGI (1960). "Glossary of geology and related sciences." The Am. Geol. Inst.: 365.

Alder, H. L. and E. B. Roessler (1964). Introduction to probability and statistics, W. H. Freeman.

Amoroso, G. G. and V. Fassina (1983). Stone decay and conservation. Venice.

Anderton, R., P. H. Bridges, et al. (1987). A dynamic stratigraphy of the British Isles: A study of crustal evolution. London, George Allen & Unwin.

Armstrong, M. and I. B. Paterson (1970). "The Lower Old Red Sandstone of the Strathmore region." Inst. Geol. Sci. Rep. **70**(12).

Arnold, A. (1976). Behaviour of some soluble salts in stone deterioration. 2nd International Symposium on the Deterioration of Building Stones, Athens.

Banfield, J. F. and R. A. Eggleton (1988). "A transmission electron microscope study of biotite weathering." Clays and Clay Minerals **36**: 47-60.

Barnhisel, R. I. (1982). Chlorites and hydroxy interlayered vermiculite and smectite. Minerals in soil environments. J. B. Dixon and S. B. Weed. Wisconsin, Madison, Soil Sci. Soc. Am. Inc. **Ch 10**: 331-355.

Barrioulet, M., R. Saada, et al. (1991). "A quantitative structural study of fresh cement paste by image analysis. Part 1: image processing." Cement and concrete research **21**(5): 835-843.

- Battle, W. R. B. (1936). Temperature observations in bergschrunds and their relationship to frost shattering. Norwegian Cirque Glaciers. W. V. Lewis. London, Royal Geographical Society. **Series 4**.
- Bell, F. G. (1993). "Durability of carbonate rock as building stone with comments on its preservation." Environmental Geology **21**: 187-200.
- BERG (1989). The effects of acid deposition on buildings and building materials in the United Kingdom. London, Building Effects Review Group.
- BGS (1867). Notes to accompany the Ayrshire Geological Map. Great Britain, Mem. Geol. Surv.
- Biber, M. V., M. D. Santos Afonso, et al. (1994). "The co-ordination chemistry of weathering: IV. Inhibition of the dissolution of oxide minerals." Geochimica et Cosmochimica Acta **58**: 1999-2010.
- Bluck, B. J. (1978). Sedimentation in a late orogenic basin: the Old Red Sandstone of the Midland Valley of Scotland. Crustal evolution in North Western Britain and adjacent regions. D. R. Bowes and B. E. Leake, Geol. J. Spec. Issue. **10**.
- Bluck, B. J. (1983). "Role of the Midland Valley of Scotland in the Caledonian orogeny." Trans. R. Soc. Edinburgh: Earth Sciences **74**: 119-136.
- Bluck, B. J. (1984). "Pre-Carboniferous history of the Midland Valley of Scotland." Trans. R. Soc. Edinburgh: Earth Sciences **75**(275-295).
- Bluck, B. J. (1992). The composition and weathering of sandstone with relation to cleaning. Proceedings of the International conference on stone cleaning and the nature, soiling and decay mechanisms of stone, Edinburgh, Bath Press.

Bluck, B. J. and J. Porter (1991). "Sandstone buildings and cleaning problems." Stone Industries **26**(2): 24-27.

Borovec, Z. and J. Neuzil (1966). "Experimental weathering of feldspars by hot water." Acta Universitatis Carolinae-Geologica **3**: 207-222.

Brady, P. V. and S. A. Carroll (1994). "Direct effects of CO₂ and temperature on silicate weathering: possible implications for climate control." Geochimica et Cosmochimica Acta **58**: 1853-1856.

Braitsch, O. (1971). Salt deposits: their origin and composition. Heidelberg, Springer-Verlag.

BRE (1974). Drying out buildings. Watford, Building Research Establishment.

Brownlow, A. H. (1996). Sedimentary rocks. Geochemistry. A. H. Brownlow. Boston, Prentice Hall. **1**: 347-414.

BS 7543 (1992). Guide to durability of buildings and building elements, products and components. London, BSI.

Butlin, R. N. (1991). Effects of air pollutants on buildings and materials. Proceedings of the Royal Society of Edinburgh.

Camuffo, D., M. Del Monte, et al. (1982). "Wetting, deterioration and visual features of stone surfaces in an urban area." Atmospheric pollution **16** (9): 2253-2259.

Camuffo, D., M. Del Monte, et al. (1983). "Origin and growth mechanisms of the sulfated crusts on urban limestone." Water, air, and soil pollution **19**: 351-359.

Camuffo, D. (1984). "Letter to the editor: The influence of run-off on weathering of monuments." Atmospheric environment **18** (10): 2273-2275.

Camuffo, D. and A. Bernardi (1988). "Microclimate and interactions between the atmosphere and Orvieto Cathedral." The science of the total environment **68**: 1-10.

Camuffo, D. (1989). Environment and microclimate. Science, technology and European cultural heritage: Proceedings of the European symposium, Bologna, Italy, 13-16 June 1989: 7-50.

Camuffo, D. and A. Bernardi (1989). Indoor and outdoor microclimate case studies: the Trajan Column and Sistene Chapel. Science, technology and European cultural heritage: Proceedings of the European symposium, Bologna, Italy, 13-16 June 1989: 295-305.

Camuffo, D. and A. Bernardi (1993). "Microclimate factors affecting the Trajan Column." The science of the total environment **128**: 227-255.

Camuffo, D. (1995). "Physical weathering of stones." The science of the total environment **167**: 1-14.

Carroll-Webb, S. A. and J. V. Walther (1988). "A surface complex reaction model for the pH-dependence of corundum and kaolinite dissolution rates." Geochimica et Cosmochimica Acta **52**: 2609-2623.

Casey, W. H., H. R. Westrich, et al. (1988). "Surface chemistry of labradorite feldspar reacted with aqueous solutions at pH=2, 3 and 12." Geochimica et Cosmochimica Acta **52**: 2795-2807.

Charola, A. E. (1987). "Acid rain effects on stone monuments." Journal of Chemical Education **64**(5): 436-437.

Charola, A. E. and S. Z. Lewin (1979). "Efflorescence on building stones - SEM in the characterisation and elucidation of the mechanisms of formation." Scanning Electron Microscopy **1**: 379.

Charola, A. E. and S. Z. Lewin (1979*). Efflorescence on building stones. Proceedings of the 3rd International Congress on Deterioration and Preservation of Stones, Venice.

Cooke, R. U. and I. J. Smalley (1968). "Salt weathering in deserts." Nature **220**: 1226-1227.

Cooke, R. U. (1979). "Laboratory simulation of salt weathering processes in arid environments." Earth Surface Processes and Landforms **4**: 347-359.

Cooke, R. U. (1981). "Salt weathering in deserts." Proc. Geol. Ass. **92**: 1-16.

Cooke, R. U. (1989). "Geomorphological contributions to acid rain research: studies of stone weathering." Geographical Journal **155**: 361-366.

Cooke, R. U. and J. C. Doornkamp (1990). Geomorphology in environmental management. Oxford, Clarendon Press.

Cooke, R. U. and G. B. Gibbs (1994). *Crumbling Heritage? Studies of stone weathering in polluted atmospheres*. Swindon, National Power Plc.

Cooling, L. F. (1930). "The evaporation of water from brick." Trans Ceram. Soc. **29**: 39-54.

Cooper, T. P. (1989). *The effect of air pollution on historic buildings and monuments: European Community R & D on Environmental Protection*.

Correns, C. W. (1949). "Growth and dissolution of crystals under linear pressure." Discussions of the Faraday Society, **5**, Crystal growth: 226-271.

Dan, W., D. Quenard, et al. (1988). "Moisture movement in a cement-polymer-glass composite (CCPV) and effect of moisture on its mechanical properties." CSTB Cahiers **295**: 2304-2319.

Deer, W. A., R. A. Howie, et al. (1985). *Framework silicates. An introduction to the rock forming minerals*. Hong Kong, Longman: 281-389.

Del-Monte, M. and O. Vittori (1985). "Air pollution and stone decay: the case of Venice." Endeavour **9**(3): 117-121.

Dove, P. M. and D. A. Crerar (1990). "Kinetics of quartz dissolution in electrolyte solutions using a hydrothermal mixed flow reactor." Geochimica et Cosmochimica Acta. **54**: 955-969.

Everett, D. H. (1961). "The thermodynamics of frost damage to porous solids." Transactions of the Faraday Society **57**: 1541-1551.

Evans, I. S. (1970). "Salt crystallisation and rock weathering: a review." Revue de Geomorphologie Dynamique **4**: 154-173.

Eyles, V. A., J. B. Simpson, et al. (1949). "Geology of Central Ayrshire." Mem. Geol. Surv. U.K. (Sheet 14).

Fairchild, E., H. Hendry, et al. (1988). Chemical analysis of sedimentary rocks. Techniques in sedimentology. M. Tucker, Blackwell Scientific Publications.

Fairhurst, J. (1995). Comments on results from the engineering tests undertaken on samples from Culzean Castle, Unpublished. Edinburgh, Napier University.

Fassina (1988). Air pollution in relation to stone decay. The deterioration and conservation of stone: studies and documents on the cultural heritage. M. T. Rubin de Cervin. Venice, UNESCO. **16**.

Fassina, V. (1978). "A survey on air pollution and deterioration of stonework in Venice." Atmospheric Environment **12**: 2205-2211.

Feilden, B. M. (1994). Conservation of historic buildings. Avon, Bath Press.

Fitzner, B. and R. Snethlage (1982). "Zum Einflub der Porenradienverteilung auf das Verwitterungsverhalten ausgewahlter sandsteine." Bautenschutz Bausan **3** (82): 97-102.

Fitzner, B., K. Heinrichs, et al. (1992). Classification and mapping of weathering forms. 7th International Congress on the Deterioration and Conservation of Stone, Lisbon, Portugal.

Fitzner, B. (1994). Porosity properties and weathering behaviour of natural stone – methodology and examples. Stone material in monuments: diagnosis and conservation.

F. Zezza : 43-54.

Fitzner, B., K. Heinrichs, et al. (1995). Stone deterioration of monuments in Malta. Preservation and Restoration of Cultural Heritage, Montreux, Switzerland, Ecole Polytechnique Federale de Lausanne.

Fleet, A. J. (1986). Aqueous and sedimentary geochemistry of the rare earth elements. Rare earth element geochemistry. P. Henderson. Amsterdam, Elsevier.

Flowers, H. (1995). Ion Chromatography - lecture notes. Unpublished. Glasgow, University of Glasgow.

Fobe, B., H. Sweevers, et al. (1993). "Weathering of Miocene ferruginous sandstone in ancient buildings in Northern Belgium." The Science of the Total Environment **132**: 53-70.

Folk, R. L. (1951). "Stages of textural maturity in sedimentary rocks." Journal of Sedimentary Petrology **21**: 127-30.

Fookes, P. G., W. R. Dearman, et al. (1971). "Some engineering aspects of rock weathering with field examples from Dartmoor and elsewhere." Quarterly Journal of Engineering Geology **4**: 139-85.

Fookes, P. G. and P. Horswill (1969). Discussion on engineering grade zones. Proceedings of Conference on in situ testing of soils and rocks, London, Institution of Civil Engineering.

Furukawa, I. (1989). "Three dimensional analysis of fracture surfaces of wood cell walls." Journal of Japan Wood Research Society **35**(1): 58-62.

Galli, G. and M. Serra (1976). Influence of variable temperature conditions on water condensation in thick walls. Proceedings of the 2nd Symposium on the Deterioration of Building Stones, Athens.

Geikie, A. (1897). The ancient volcanoes of Great Britain. London.

Ginell, W. S. (1994). The nature of change caused by physical factors. Durability and change: the science, responsibility, and cost of sustaining cultural heritage. W. E. Krumbein, P. Brimblecombe, D. E. Cosgrove and S. Staniforth. Berlin, John Wiley & Sons Ltd: 81-91.

Goudie, A. S. (1989). The nature of the environment. Oxford, Basil Blackwell Ltd.

Goudie, A. S. (1974). "Further experimental investigation of rock weathering by salt and other mechanical processes." Z. Geomorph. N. F. **21**.

Goudie, A. S. (1977). "Salt Weathering." School of geography research papers, Oxford **33**.

Goudie, A. S., R. Cooke, et al. (1970). "Experimental investigation of rock weathering by salts." Area **4**: 42-48.

Goudie, A. S. and H. A. Viles (1995). "The nature and pattern of debris liberation by salt weathering: A laboratory study." Earth surface processes and landforms. **20**: 437-449.

Goudie, A. S. and H. A. Viles (1997). Salt weathering Hazards. John Wiley & Sons. Chapters 2,3, 4 and 6.

Griggs, D. T. (1936). "The factor of fatigue in rock weathering." Journal of Geology **44**: 781-796.

Guidobaldi, F. (1981). Acid rain and corrosion of marble: an experimental approach. International Symposium on the Conservation of Stone, Bologna.

Guidobaldi, F. and A. M. Mecchi (1985). Corrosion of marble by rain: The influence of surface roughness, rain intensity and additional washing. 5th International Congress on the Deterioration and Conservation of Stone, Lausanne.

Guidobaldi, F., A. M. Mecchi, et al. (1988). Acid rain and the corrosion of marble. The influence of the frequency of rainfall. Proceedings of the 6th International Congress on the Deterioration and Conservation of Stone, Torun, Poland, University Press Department.

Gummerson, R. J., C. Hall, et al. (1980). "Capillary water transport in masonry structures: building construction applications of Darcy's Law." Construction Papers **1**(1): 17-27.

Haag, G. and G. Grassegger (1994). Evaluation and development of complex interactions of stone decay processes on historical monuments by using Neutral Networks. Simulation und Modelle von Umweltmarsnahmen. A. Diekmann, (in press).

Hall, K. and A. Hall (1991). "Thermal gradients and rock weathering at low temperatures: some simulation data." Permafrost and periglacial processes **2**: 103-112.

- Hall, A. J. (1994). Notes on the powder XRD technique as used in the Geology Department, Glasgow University. Unpublished. Glasgow, University of Glasgow.
- Hall, A. J. (1995). Clay mineralogy - layered silicates: Economic and environmental mineralogy notes. Glasgow, University of Glasgow.
- Hall, C., W. D. Hoff, et al. (1984). "Water movement in porous building materials-VI. Evaporation and drying in brick and block material." Building & Environment **19**(1): 13-20.
- Halsey, D. P., S. J. Dews, et al. (1995). "Real time measurements of sandstone deterioration: a microcatchment study." Building and Environment **30**(3): 411-417.
- Halsey, D. P., D. J. Mitchell, et al. (1995). The effects of atmospheric pollutants upon sandstone: evidence from real time measurements and analysis of decay features on historic buildings. Proceedings of the 10th World clean air congress, Espoo, Finland.
- Hammond, R. and P. S. McCullagh (1986). Quantitative techniques in geography: an introduction. Oxford, Clarendon Press.
- Haneef, S. J. (1993). "A laboratory simulation of degradation of Leinster granite by dry and wet deposition processes." Corrosion Science **34**: 511-524.
- Hardy, R. and M. Tucker (1988). X-ray powder diffraction of sediments. Techniques in sedimentology. M. Tucker, Blackwell Scientific Publications.

Hawkins, A. B. and B. J. McConnell (1992). "Sensitivity of sandstone strength and deformability to changes in moisture content." Quarterly journal of engineering geology **25**: 115-130.

Hayles, C. S. and B. J. Bluck (1994). Sandstone decay mechanisms under examination on the balcony of Culzean Castle, South West Scotland. Proceedings of the 3rd International Symposium on the Conservation of Monuments in the Mediterranean Basin, Venice, Sopintendenza ai Artistici e Storici di Venezia.

Hayles, C. S. and B. J. Bluck (1995). An examination of some of the causes of sandstone deterioration at Culzean Castle - Scotland. Preservation and restoration of cultural heritage, Montreaux, Switzerland, Ecole Polytechnique Federale de Lausanne.

Hering, J. G. and W. Stumm (1990). Oxidative and reductive dissolution of minerals. Mineral-water interface geochemistry. M. F. Hochella Jr. and A. F. White. Washington D. C., Mineralogical Society of America. **23**: 427-465.

Hollerman, P. (1975). "Formen kaevernosser verwitterung ("tafoni") auf Teneriffa." CATENA **2**: 385-410.

Honeyborne, D. B. (1982). The building limestones of France. London, HMSO.

Honeyborne, D. B. and P. B. Harris (1958). "The structure of porous building stone and its relation to weathering behaviour." Colston Papers **10**: 343-65.

Honeyborne, D. B. and C. A. Price (1980). "Decay mechanisms in porous limestones - Part 2." Society for the Protection of Ancient Buildings News **1(2)**: 23-31.

Hugget, J. M. and P. J. R. Uwins (1994). "Observations of water-clay reactions in water-sensitive sandstone and mudrock using an environmental scanning electron microscope." Journal of Petroleum Science and Engineering **10**: 211-222.

IEA (1996). Heat, air and moisture transport through building materials and components: symbols and terminology, International Energy Agency. Belgium, Laboratorium Bouwfysica.

Jaynes, S. M. and R. U. Cooke (1987). "Stone weathering in Southeast England." Atmospheric Environment **21**(7): 1601-1622.

Jenkins, K. A. and B. J. Smith (1990). "Daytime rock surface temperature variability and its implications for mechanical rock weathering: Tenerife, Canary Islands." CATENA **17**: 449-459.

Johansson, L. G., O. Lindqvist, et al. (1988). "Corrosion of calcareous stones in humid air containing SO₂ and NO₂." Durability of Building Materials **5**: 439-449.

Johansson, L. G., O. Lindqvist, et al. (1986). A study of the corrosion of calcareous stones exposed to humid air containing SO₂ and NO₂. Preprinted papers of the Air and Pollution Symposium, Rome.

Kerr, P. F. (1977). Optical mineralogy. New York, McGraw-Hill.

Krauskopf, K. B. (1982). Introduction to geochemistry, McGraw-Hill International Editions, Earth & Planetary Sciences.

Lal Gauri, K. (1978). "The preservation of stone." Scientific American **238**: 104-110.

Learmont, D. (1992). Culzean Castle and Country Park. Edinburgh, National Trust for Scotland Publications.

Leary, E. (1983). The building limestones of the British Isles. London, HMSO.

Lewin, S. Z. (1982). The mechanisms of masonry decay through crystallisation. Conservation of historic stone buildings and monuments., Washington, D.C., National academic press: 120-144.

Lewin, S. Z. and A. E. Charola (1978). "Scanning electron microscopy in the diagnosis of 'diseased' stone." Scanning Electron Microscopy **1**(1): 695-704.

Lewry, A. J., D. J. Bigland, et al. (1994). "The effects of sulfur dioxide on calcareous stone: a chamber study." Construction and Building Materials **8**(4): 261-265.

Lipfert, F. W. (1989). "Atmospheric damage to calcareous stones: comparisons and reconciliation of recent experimental findings." Atmospheric Environment **23**: 415-429.

Little, A. L. (1969). The engineering classification of residual tropical soils. Proceedings of the 7th International Conference on Soil Mechanics and Foundation Engineering.

Livingstone, R. A. (1985). The role of nitrogen oxides in the deterioration of carbonate stone. Proceedings of the 5th international congress on deterioration and

conservation of stone, Lausanne, Nicholas Copernicus University Press
Department, Torun, Poland.

Livingstone, R. A. (1994). Influence of evaporite minerals on gypsum crusts and alveolar weathering. Proceedings of the 3rd International Symposium on the Conservation of Monuments in the Mediterranean Basin, Venice, Sopintendenza ai Artistici e Storici di Venezia.

Loughnan, F. C. (1969). Chemical weathering of the silicate minerals. New York, Elsevier.

MacInnis and Brantley (1993). "Development of etch pit size distributions on dissolving minerals." Chem. Geol. **105**: 31-49.

Massey, S. W. (1992). Development of a theoretical model for the deterioration of stone samples on the NMEP. Watford, Building Research Establishment.

Mausfeld, S. A. and G. Grassegger (1994). The changing environment of pore solutions in natural building stones during immission accelerated weathering processes. Proceedings of the 3rd International Symposium on the Conservation of Monuments in the Mediterranean Basin, Venice, Soprintendenza ai beni artistici e storici di Venezia : 129-135.

Maclean, J. H. and J. S. Scott (1993). Dictionary of building. London, Penguin Books Ltd.

McBride, E. F. (1963). "The term greywacke (discussion)." Journal of Sedimentary Petrography **32**: 614-615.

McGreevy, J. P. (1982). "Hydrothermal alteration and earth surface rock weathering: a basalt example." Earth Surface Processes and Landforms **7**: 189-195.

McGreevy, J. P. and B. J. Smith (1982). "Salt weathering in deserts." Geogr. Annlr. **64A**: 161-170.

McGreevy, J. P. (1985). "Thermal properties as controls on rock surface temperature maxima, and possible implications for rock weathering." Earth Surface Processes and Landforms **10**: 125-136.

McGreevy, J. P. (1985*). "A preliminary scanning electron microscope study of honeycomb weathering of sandstone in a coastal environment." Earth Surface Processes & Landforms **10**: 509-518.

McGreevy, J. P. and B. J. Smith (1984). "The possible role of clay minerals in salt weathering." Catena **11**: 169-175.

McGreevy, J. P. and B. J. Smith (1985). "The spalling of quartz overgrowths during experimental salt weathering of a sandstone." Micron & Microscopia Acta **16**: 277-279.

McGreevy, J. P. and W. B. Whalley (1985). "Rock moisture content and frost weathering under natural and experimental conditions: a comparative discussion." Arctic and Alpine Research **17**: 337-346.

McMahon, D. J., P. Sandberg, et al. (1992). Deterioration mechanisms of sodium sulfate. Proceedings of the 7th International Congress on the Deterioration and Conservation of Stone, Lisbon, Laboratório Nacional de Engenharia Civil.

MCRG (1992). Stone cleaning in Scotland. Aberdeen, Masonry conservation research group, Robert Gordon University.

MCRG (1995). Biological growths, biocide treatment, soiling and decay of sandstone buildings and monuments in Scotland. Aberdeen, Masonry conservation research group, Robert Gordon University.

Miller, H. (1841). The Old Red Sandstone. Edinburgh.

Miller, J. (1988). Cathodoluminescence microscopy. Techniques in sedimentology. M. Tucker, Blackwell Scientific Publications.

Milne, J. (1927). "The evaporation of salt solution from surfaces of stone, brick and mortar." Proc. Royal Soc. of Edinburgh **47**: 52-68, 1926-1928.

Morton, D. J. (1979). "Paleogeographical evolution of the Lower Old Red Sandstone basin in the Western Midland Valley." Scottish Journal of Geology **15**: 97-116.

Morton, E. (1926). "The microscopic determination of the strength and durability of building stones." Engineering **122**(3167): 401-403.

Munsell, A. H. (1929). Munsell book of Colour - defining, explaining, and illustrating the fundamental characteristics of colour. Baltimore, Munsell Colour Company Inc.

Mykura, W. (1991). Old Red Sandstone. Geology of Scotland. G. Y. Craig. London, The Geological Society: 297-345.

- Nesbitt, H. W. (1979). "Mobility and fractionation of rare earth elements during weathering of a granodiorite." Nature **279**: 206-210.
- Nesbitt, H. W. and G. M. Young (1989). "Formation and diagenesis of weathering profiles." The Journal of Geology **97**: 129-147.
- NTS (1991). National Trust for Scotland - Culzean Appeal for the restoration of its landscape and buildings. Edinburgh, Waddie & Co.
- Ohse, W., G. Matthes, et al. (1985). Equilibrium and disequilibrium between pore waters and minerals in the weathering environment. The chemistry of weathering. J. I. Drever, D Reidel Publishing.
- Ollier, C. D. (1984). Weathering. London, Longman.
- Orshan, G. (1986). The deserts of the Middle East. Hot deserts and arid shrublands. M. Evenari, I. Noy-Meir and D. W. Goodall. Amsterdam, Elsevier,: 1-28.
- Oxburgh, R., J. I. Drever, et al. (1994). "Mechanism of plagioclase dissolution in acid solution at 25 degrees centigrade." Geochimica et Cosmochimica Acta **58**: 661-669.
- Pallecchi, P. and P. Pinn (1988). Alteration of stone caused by lichen growth in the Roman theatre of Firenze. Proceedings of the 6th International Congress on the Deterioration and Conservation of Stone, Torun, Poland, University press department.
- Paton, T. R. (1978). The formation of soil material. London, Allen & Unwin.

Pavia Santamaria, S. (1994). Material de construccion antiguo de logrono y la Rioja alta: petrografia, propiedades fisicas, geologia y alteracion. Gobierno de la Rioja. Logrono, Instituto de Estudios Riojanos: 247.

Pavia Santamaria, S., S. Caro Catalayud, et al. (1994). More about gypsum crusts on historic buildings. Proceedings of 3rd International Symposium on the Conservation of Monuments in the Mediterranean Basin, Venice.

Pearce, F. (1985). "Acid eats into Britain's stone heritage." New Scientist **26 September 1985**: 26-27.

Peel, R. F. (1974). "Insolation weathering: some measurements of diurnal temperature changes in exposed rocks in the Tibesti region, central Sahara." Zeitschrift fur Geomorphologie, Supplementband **21**: 19-28.

Pellant, C. (1990). Rocks, minerals and fossils of the World. London, Pan.

Pettijohn, F. J. (1985). Sedimentary rocks. New York, Harper & Row.

Pettijohn, F. J., P. E. Potter, et al. (1987). Sand and sandstones. New York, Springer-Verlag.

Pittman, E. D. (1979). "Recent advances in sandstone diagenesis." An. Rev. Earth Planet. Sci. **7**: 39-62.

Platten, A. K. (1985). A study of evaporation and drying in porous building materials. Department of Building. PhD Thesis, University of Manchester Institute of Science & Technology.

- Potter, R. M. and G. R. Rossman (1977). "Desert varnish: the importance of clay minerals." Science **196**: 1446-1448.
- Prentice, J. E. (1990). Geology of construction materials. London, Chapman and Hall.
- Price, C. A. (1975). The decay and preservation of natural building stone. Watford, Building Research Station.
- Proust, D., J.-P. Eymery, et al. (1986). "Supergene vermiculization of a magnesium chlorite: iron and magnesium removal processes." Clays and Clay Minerals **34**: 572-580.
- Pühringer, J., L. Berntsson., et al. (1985). Hydrate salts and degradation of materials. Proceedings of the 5th congress on deterioration and conservation of stone, Lausanne: 231-240.
- Reddy, M. M. (1988). "Acid rain damage to carbonate stone: A quantitative assessment based on the aqueous geochemistry of rainfall runoff from stone." Earth Surface Processes and Landforms **13**: 335-354.
- Richter, D. and G. Simmons (1974). "Thermal expansion behaviour of igneous rocks." International journal of rock mechanisms and mining sciences **11**: 403-411.
- Robinson, D. A. and R. B. G. Williams (1982). "Salt weathering of rock specimens of varying shape." Area **14**: 293-299.

Robinson, D. A. and R. B. G. Williams (1987). Surface crusting of sandstones in Southern England and Northern France. International geomorphology Part 2, John Wiley & Sons Ltd.

Robinson, D. A. and R. B. G. Williams (1994). Rock weathering and landform evolution. Chichester, John Wiley & Sons.

Rodriguez Navarro, C., S. E. Pardo, et al. (1994). Petrophysical mechanical parameters for decay evaluation of building stone: A case study - Jaen Cathedral, Andalusia, Spain. Proceedings of 3rd International Symposium on the Conservation of Monuments in the Mediterranean Basin, Venice.

Rose, D. A. (1963). "Water movement in porous materials: part 1. Isothermal vapour transfer." British Journal of Physics **14**(256-262).

Rosenberg, H. S. and H. M. Grotta (1980). "Laboratory studies of masonry exposed to SO₂ and NO₂." Env. Sci. and Tech **14**: 470-472.

Ross, G. J. and H. Kodama (1976). "Experimental alteration of chlorites into a regularly interstratified chlorite-vermiculite by chemical oxidation." Clays & Clay Minerals **24**: 183-190.

Rossi-Manaresi, R. and A. Tucci (1991). "Pore structure and the disruptive or cementing effect of salt crystallisation in various types of stone." Studies in Conservation **36**: 53-58.

Ruxton, B. P. (1968). "Measure of the degree of chemical weathering of rocks." Journal of Geology **76**: 518-27.

Rykwert, R. (1950). *The brothers Adam, the men and the style*. London, Collins.

- Sabbioni, C. and G. Zappia (1992). "Decay of sandstone in urban areas correlated with atmospheric aerosol." Water, Air and Soil Pollution **63**: 305-316.
- Sanchez Hernandez, R., J. N. Lopez-Cozar, et al. (1995). "Mapping of weathering forms in Burgos Cathedral." Ingenieria Civil **99**: 27-38.
- Sasaki, T., S. Kinoshita, et al. (1981). A study on water sensitivity of argillaceous rocks. Proceedings of the International Symposium on Weak Rock, Tokyo, Japan.
- Schaffer, R. J. (1932). The weathering of natural building stones. Watford, Building Research Establishment.
- Schiavon, N. (1992). Decay model for calcareous building stone. Proceedings of international conference on stone cleaning and the nature, soiling and decay mechanisms of stone, Edinburgh, Bath Press.
- Senkayi, A. L., J. B. Dixon, et al. (1981). "Transformation of chlorite to smectite through regular interstratified intermediates." Soil Sci. Soc. Am. Journal **45**: 650-656.
- Sereda, P. J. and R. F. Feldman (1970). Wetting and drying of porous materials, Canadian Building Digest.
- Sienko, M. J. and R. A. Plane (1974). Chemical principles and properties. Kogakusha, McGraw-Hill.
- Simmons, G. and D. Richter (1993). "Cracks in building stone." Int. J. Rock Mech. Min. Sci. & Geomech. Abstr. **30**(7): 1553-1557.

Simpson, B. (1983). Rocks and minerals. Exeter, Pergamon Press.

Simpson, J. W. and P. J. Horrobin (1984). The weathering and performance of building materials. Aylesbury, Medical and technical publications.

Singer, A. (1993). "Weathering patterns in representative soils of Guanxi Province, south-east China, as indicated by detailed clay mineralogy." Journal of Soil Science 44: 173-188.

Skoog, D. A., D. M. West, et al. (1994). Fundamentals of analytical chemistry. Fort Worth, Saunders College Publishing.

Small, R. J. (1987). The study of landforms: a textbook of geomorphology. Cambridge, Cambridge University Press.

Small, J. and M. Witherick (1989). A modern dictionary of geography, Edward Arnold.

Smith, B. J., B. Whalley, et al. (1992). Assessment of building stone decay: a geomorphological approach. Proceedings of the international conference on stone cleaning and the nature, soiling and decay mechanisms of stone, Edinburgh, Bath Press.

Smith, B. J., R. W. Magee, et al. (1994). Breakdown patterns of quartz sandstone in a polluted urban environment. Rock weathering and landform evolution. D. Robinson and R. B. G. Williams. Belfast, J. Wiley & Sons: 131-150.

Smith, B. J. and J. P. McGreevy (1988). "Contour scaling of a sandstone by salt weathering under simulated hot desert conditions." Earth Surface Processes and Landforms 13: 697-705.

Smith, B. J., J. P. McGreevy, et al. (1985). "Silt production by weathering of a sandstone under hot arid conditions: an experimental study." Journal of Arid Environments **12**: 199-214.

Smith, J. (1909). Upland fauna of the Old Red Sandstone formation of Carrick, Ayrshire. Kilwinning.

Snethlage, R. and E. Wendler (1996). Moisture cycles and sandstone degradation. Saving our architectural heritage : The conservation of historic stone structures. N. S. Baer & R. Snethlage. John Wiley & Sons: 7-24.

Sperling, C. H. B. and R. U. Cooke (1985). "Laboratory simulation of rock weathering by salt crystallisation and hydration processes in hot, arid environments." Earth surface processes and landforms **10**: 541-555.

Spooner, D. C. (1982). The practical relevance of mechanisms of water and water vapour transfer in porous building materials. RILEM International symposium on autoclaved aerated concrete, moisture and properties, Lausanne, Elsevier Scientific Publishing Company.

SSSA (1977). Minerals in soil environments. Madison, Wisc., Soil Science Society of America.

Stanton, P. T. and M. D. Wilson (1989). Measurement of independent variables - composition. Independent variables. P. T. Stanton, A. P. Byrnes and M. D. Wilson, SEPM short course notes.

Steeffel, C. I. and P. Van Cappellen (1990). "A new kinetic approach to modelling water-rock interactions: The role of nucleation, precursors, and Ostwald ripening." Geochimica et Cosmochimica Acta **54**: 2657-2677.

Steiger, M. and W. Dannecker (1994). The chemical composition and distribution of soluble salts in natural stone walls. Proceedings of 3rd International Symposium on the Conservation of Monuments in the Mediterranean Basin, Venice, Soprintendenza ai Artistici e Storici di Venezia.

Steiger, M., H.-H. Neumann, et al. (1993). "Chemische Zusammensetzung und Verteilung löslicher Salze in Natursteinmauerwerk." Jahresberichte Steinzerfall-Stein-Konservierung **3**: 21-33.

Steinforsk (1993). Norwegian Centre for Natural Stone Research Annual Report. Trondheim.

Stoch, L. and W. Sikora (1976). "Transformation of micas in the process of kaolinitization of granites and gneisses." Clay and Clay Minerals **24**: 156-162.

Stumm, W. and R. Wollast (1990). "Co-ordination chemistry of weathering: kinetics of the surface-controlled dissolution of oxide minerals." Rev. of Geophysics **28**: 53-69.

Swhaney, B. L. (1960). "Weathering and aluminium interlayers in a soil catena. Hollis-Charlton-Sutton-Leicester." Soil. Sci. Soc. Am. Journal **28**: 221-226.

Tamura, T. (1955). "Weathering of mixed layered clays in soils." Clay and Clay Minerals **4**: 413-422.

Tennent, N. H., B. G. Cooksey, et al. (1993). Simple monitors for carbonyl pollutants. Conservation science in the UK, Glasgow, Bell & Bain Ltd.

Trudgill, S. T. (1984). Weathering and erosion. London, Butterworth.

Trudgill, S. T., R. W. Crabtree, et al. (1989). "Remeasurements of weathering rates, St Paul's cathedral, London." Earth Surface Processes and Landforms **14**: 175-196.

Tyrrell, G. W. (1914). "A petrographic sketch of the Carrick Hills, Ayrshire." Trans. Geol. Soc. Glasg. **15**: 64-83.

Unknown. Atomic absorption preparation method. Glasgow, University of Glasgow.

Unknown. Preparation of pressed powder pellets and fused beads. Glasgow, University of Glasgow.

Unknown (1984). "Editorial." The Science of the Total Environment **36**.

Van Brackle, J. (1980). "Mass transfer in convective drying." Adv, Drying **1**: 217-267.

Van-Der-Molen, J., J. Garty, et al. (1980). "Growth control of algae and cyanobacteria on historical monuments by a mobile UV unit (MUVU)." Studies in Conservation **25**: 71-77.

Velbel, M. A. (1993). "Constancy of silicate-mineral weathering rate ratios between natural and experimental weathering: implications for hydrologic control of differences in absolute rates." Chemical Geology **105**: 89-99.

Velbel, M. A. (1993). "Temperature dependence of silicate weathering in nature." Geology **21**: 1059-1062.

Wakefield, R. D. and M. S. Jones (1998). "An introduction to stone colonizing micro-organisms and biodeterioration of building stone." Quarterly Journal of Engineering Geology **31**: 301-313.

Walkden, G. (1994). Cathodoluminescence and epifluorescence in petrography. Geochemical and allied techniques in earth science research: a one-day review seminar sponsored by the Geological Society of London, Edinburgh, Geological Society of London.

Wallace, R. C. (1916). "The corrosive action of certain brines in Manitoba." Geological Magazine **3**: 31-32.

Warke, P. A. and B. J. Smith (1994). Short-term rock temperature fluctuations under simulated hot desert conditions: some preliminary data. Rock weathering and landform evolution. D. A. Robinson and R. B. Williams. Belfast, John Wiley & Sons Ltd.

Warscheid, T. H., D. Barros, et al. (1992). Biodeterioration studies on soapstone, quartzite and sandstones of historical monuments in Brazil and Germany. Preliminary results and evaluation for restoration practices. Proceedings of the 7th International Congress on the Deterioration and Conservation of Stone, Lisbon, Portugal, Laboratorio Nacional de Engenharia Civil.

Warscheid, T. H., K. Petersen, et al. (1988). Physiological characterisation of chemoorganotrophic bacteria isolated from sandstones. Proceedings of the 6th International Congress on the Deterioration and Conservation of Stone, Torun, Poland, University Press Department.

Warscheid, T. H., K. Petersen, et al. (1990). "A rapid method to demonstrate and evaluate microbial activity on decaying sandstone." Studies in Conservation **35**: 137-147.

Weast, R. C., J. M. Astle, et al. (1984). Handbook of chemistry and physics. McGraw-Hill.

Webster, R. G. M. (1992). Stone cleaning and the nature, soiling and decay mechanisms of stone. Proceedings of the International conference on stone cleaning and the nature, soiling and decay mechanisms of stone, Edinburgh, Donhead Publishing, London.

Wedepohl, K. H. (1971). Geochemistry, Holt, Rinehart & Winston, Inc.

Wedepohl, K. H., C. W. Correns, et al. (1978). Handbook of geochemistry. Berlin, Springer-Verlag.

West, R. (1979). Discovering English Architecture, Longman.

Whalley, B., B. Smith, et al. (1992). Effects of particulate air pollutants on materials: investigation of surface crust formation. Proceedings of the International Conference on Stone Cleaning and the Nature, Soiling and Decay Mechanisms of Stone, Edinburgh, Bath Press.

Whalley, W. B. and J. P. McGreevy (1991). "The contribution of W. R. B. Battle to mechanical weathering studies." Permafrost and Periglacial Processes **2**: 341-346.

White, A. F. (1990). Heterogeneous electrochemical reactions associated with oxidation of ferrous oxide and silicate surfaces. Mineral-water interface

geochemistry. M. F. Hochella Jr. and A. F. White. Washington D. C., Mineralogical Soc. Am. **23**: 467-509.

Williams, H., F. J. Turner, et al. (1954). Petrography. San Francisco, Freeman.

Williams, R. B. G. and D. A. Robinson (1991). "Frost weathering of rocks in the presence of salts – a review." Permafrost and periglacial processes **2**: 347-353.

Wilson, A. C. (1980). "The Devonian sedimentation and tectonism of a rapidly subsiding semi-arid fluvial basin in the Midland Valley of Scotland." Scott. J. Geol. **16**: 291-313.

Wilson, M. D. (1989). Reservoir quality assessment and prediction in clastic rocks, SEPM (Society for Sedimentary Geology).

Wilson, M. J. and P. H. Nadeau (1985). Interstratified clay minerals and weathering processes. The chemistry of weathering. J. J. Drever, The Macaulay Institute for soil research: 97-118.

Wilson, P. (1992). "A European vision - Robert Adam's Glasgow." University of Glasgow Magazine **1992**.

Winkler, E. M. and P. C. Singer (1972). "Crystallisation pressure of salts in stone and concrete." Geological society of America bulletin **83**: 3509-3514.

Winkler, E. M. (1973). Stone: Properties, Durability in Man's Environment. Vienna, Springer-Verlag.

Winkler, E. M. (1975). Stone: Properties, Durability in Man's Environment. New York, Springer-Verlag.

Winkler, E. M. and E. J. Wihelm (1970). "Salt burst by hydration pressures in architectural stone in urban atmosphere." Geological Society of America Bulletin **81**: 567-72.

Wittenburg, C. and W. Dannecker (1992). "Dry deposition and deposition velocity of airborne acidic species upon different sandstones." Journal of Aerosol Science **23**(1): 869-872.

Yates, T. J. S., A. T. Coote, et al. (1988). "The effect of acid deposition on buildings and building materials." Construction and Building Materials **2**(1): 20-26.

Young, A. R. M. (1987). "Salt as an agent in the development of cavernous weathering." Geology **15**: 962-966.

Zehnder, K. (1996). Gypsum efflorescence in the zone of rising damp. Monitoring of slow decay processes caused by crystallising salts on wall paintings. Proceedings 8th International congress on deterioration and conservation of stone. J. Riederer. Berlin, Ernst und Sohn: 1669-1678.

Zeza, F. (1994). Marine spray and polluted atmosphere as factors of damage to monuments in the Mediterranean coastal environment. Proceedings of 3rd International Symposium on the Conservation of Monuments in the Mediterranean Basin, Venice, Sopintendenza ai Artistici e Storici di Venezia.

Zeza, F. and F. Macrì (1995). "Marine aerosol and stone decay". The science of the total environment **167**: 123-143.

Zhang, L.-F. and Q.-M. Wang (1992). "The electron microscopy study on the mixed layer of illite and chlorite." Chinese Science Bulletin **37**(24): 2066-2070.

Appendix One

- X-ray fluorescence calibration and detection limits

- Atomic absorption and emission calibration and detection limits

- Data from geochemical analyses:
 - X-ray diffraction
 - Atomic absorption and emission spectrophotometry
 - Ion chromatography
 - X-ray fluorescence

Appendix 1
XRF calibration and detection limits

Table 1
Count rate and calibration statistics
Major elements

Element	Count rate error %	Std. err of y in regression wt. %	Calibration Lower limit	Range Upper limit	Detection limits wt. %
SiO ₂	0.6	0.54	8	80.0	0.086
TiO ₂	0.8	0.03	0	3.2	0.018
Al ₂ O ₃	1.0	0.52	0	23.0	0.087
Fe ₂ O ₃	1.0	0.15	0	14.8	0.045
MnO	3.0	0.01	0	0.2	0.012
MgO	1.5	0.30	0	50.0	0.165
CaO	0.6	0.09	0	32.5	0.006
Na ₂ O	0.7	0.20	0	5.4	0.155
K ₂ O	0.6	0.07	0	5.0	0.002
P ₂ O ₅	1.6	0.01	0	0.6	0.008

Appendix 1
XRF calibration and detection limits

Table 2
Count rate and calibration statistics
Trace elements

Element	Count rate error %	Std. error of estimate ppm.	Upper limit ppm.	Detection limit ppm.	Precision c % G-TH
Zr	0.7	10	300	2.7	1.7
Y	0.9	4	150	1.4	2.4
Sr	0.9	14	800	1.5	0.9
U	4.0	1	100	9.4	55.9
Rb	0.9	9	600	1.7	4.3
Th	3.0	4	400	11.5	20.6
Pb	6.0	9	100	11.6	12.1
Ga	3.0	3	100	2.4	4.1
Zn	2.0	12	1400	1.8	1.6
Cu	1.5	8	400	4.4	10.9
Ni	1.5	12	2500	4.8	14.6
Co	0.5	3	250	3.2	4.9
Cr	1.2	22	3200	1.9	5.9
Ce	2.2	8	500	3.2	2.0
Ba	0.9	10	2500	12.3	2.7
La	2.5	6	250	3.9	6.1
Nb	2.5	4	890	7.3	-
S	2.5	75	5000	7.1	-

**Appendix 1
AA and AE Calibration and Detection Limits**

**Table 3
Instrument conditions**

Element	Wavelength nm	Signal current mA	Background current mA	Slit width nm	Gas mix	PM Voltage	Integ period secs	Integ Int. secs	Number of runs (integ)
Atomic Absorption									
Fe	346.6	8	530+	0.3	Air/Acetate	-	3	1	2
Ca	422.7	7	-	1.0	Air/Acetate	380	3	1	2
Al	309.3	8	-	1.0	N ₂ O/Acetate	380	3	1	2
Mg	285.2	1.5	-	1.0	Air/Acetate	380	3	1	2
Atomic Emission									
Na	330.2	-	-	0.5	Air/Acetate	1000+	3	1	2
K	769.9	-	-	1.0	Air/Acetate	1000+	3	1	2

**Appendix 1
AA and AE Calibration and Detection Limits**

**Table 4
Standards and calibration statistics**

Element	Standards ppm	Absorbance	Element	Standards ppm	Absorbance
Fe	100	0.026	Mg	1	0.449
	200	0.051		2	0.772
	300	0.075		3	0.975
	400	0.102		4	1.112
	500	0.124		5	1.196
Ca	2	0.098	Na	20	0.160
	4	0.190		40	0.322
	6	0.276		60	0.478
	8	0.356		80	0.611
	10	0.433		100	0.756
Al	10	0.067	K	2	2.098
	20	0.126		4	3.829
	30	0.184		6	5.215
	40	0.234		8	6.324
	50	0.286		10	7.320

**Appendix 1
Table 5**

**XRD Results from clay analyses
To show which clays were present in each sample analysed**

Samples	kaolinite	chlorite	illite-mica	illite/smectite	illite/smectite/chlorite
AB3	<input checked="" type="checkbox"/>	<input checked="" type="checkbox"/>			<input checked="" type="checkbox"/>
AB6	<input checked="" type="checkbox"/>	<input checked="" type="checkbox"/>			<input checked="" type="checkbox"/>
AB8	<input checked="" type="checkbox"/>				
AB10	<input checked="" type="checkbox"/>				
OQ1	<input checked="" type="checkbox"/>		<input checked="" type="checkbox"/>	<input checked="" type="checkbox"/>	
VQ1	<input checked="" type="checkbox"/>		<input checked="" type="checkbox"/>		

Appendix 1 AA and AE: Results from water extraction experiments
Table 6 Results given as mg/kg of stone sample (ppm)
5 significant figures

Sample	Calcium AA	Sodium AE	Potassium AE	Aluminium AA	Iron AA	Magnesium AA
AB1T	89.25	126.75	8.82	0.27	0	37.5
AB1B	28.5	112.5	5.28	0.27	0	4.2
AB2T	87	53.25	8.16	0.21	0	8.4
AB2B	10.74	36	5.43	0.24	0	1.5
AB2TW	87	130.5	10.71	0.36	0	14.4
AB2BW	25.5	69	8.61	0.21	0	6.6
AB3T	284.25	108.75	10.74	0.39	0	12.3
AB3B	17.25	79.5	4.92	0.27	0	3.3
AB3TW	207.75	155.25	11.43	0.12	0	15.3
AB3BW	29.25	107.25	6.69	0.18	0	6.3
AB6T	202.8	262.5	13.29	0	0	45
AB6B	10.53	102	4.83	0	0	8.1
AB6TW	108	793.5	30	0.36	0	45
AB6BW	23.25	281.25	9.9	0.27	0	8.1
AB7T	3.54	80.25	6.21	0.33	0	1.2
AB7B	2.4	78	4.62	0.45	0	0.9
AB7TW	29.25	138	9.75	0.27	0	12
AB7BW	8.31	144.75	7.47	0.18	0	3.6
AB8T	65.25	263.25	12.87	0.36	0	30
AB8B	23.25	126.75	5.01	0.27	0	6.6
AB8TW	72	234	13.08	0.27	0	30
AB8BW	39	153.75	8.31	0.21	0	12
AB9T	396.75	520.5	15.63	0.24	0	52.5
AB9B	6.81	156	4.26	0.21	0	2.1
AB9TW	357.75	643.5	24.75	0.03	0	60
AB9BW	25.5	181.5	6.57	0.27	0	6.6
AB10T	267.75	315.75	10.44	0.3	0	45
AB10B	10.35	106.5	3.87	0.18	0	2.4
AB10TW	278.25	274.5	12.6	0.09	0	45
AB10BW	24.75	138.75	6.33	0.15	0	6.6
AB12T	93	924	21	0.21	0	37.5
AB12B	41.25	303.75	7.44	0.18	0	30
AB12TW	96.75	808.5	21.75	0.15	0	45
AB12BW	81.75	604.5	15.9	0.03	0	30
VB1T	34.5	227.25	9.33	0.15	0	9.33
VB1B	24.75	50.25	6.75	0.36	0	6.75
VB2T	30	93.75	7.08	0.21	0	5.85
VB2B	15.75	39	5.85	0.36	0	21.75
VB3T	106.5	514.5	21.75	0.09	0	24.75
VB3B	57	390	24.75	0.18	0	20.25
VB1WT	62.25	276	20.25	0.24	0	11.64
VB1WB	54.75	100.5	11.64	0.18	0	7.08
OB1T	29.25	138.75	21	0.18	0	21
OB1B	15.75	16.5	16.02	0.36	0	16.02
OB2T	20.25	22.5	10.98	0.18	0	10.95
OB2B	15.36	6.78	7.56	0.06	0	7.56
OB3T	25.5	24.75	15.12	0.03	0	15.12
OB3B	16.38	9.03	11.22	0.03	0	11.22
OBWIT	61.5	360.75	60.75	0.21	0	60.75
OBWIB	16.5	84.75	29.25	0.27	0	29.25

T = stone surface B = stone at depth W = extracted with rainwater

Appendix 1 Ion Chromatography: Results for AB core samples
Table 8 Results given as concentrations of mg/kg of stone (ppm)
(to 5 significant figures)

	Fluoride	Chloride	Nitrite	Nitrate	Sulphate	Phosphate
AB1/1	5	1243	0	17	793	0
AB1/2	27.6	1228.2	16.1	16.4	468.9	9.1
AB1/3	14	1208.6	1.6	15.2	221.5	0
AB1/4	14.1	1175.6	0	14	99.2	0
AB1/5	15.6	1150.3	0	13.2	78	0
AB1/6	18.1	993	0	12.6	62.8	0
AB1/7	14	870	1	11	55	0
AB3/1	16.4	48	0	0	1838.1	0
AB3/2	16.7	323.4	3	0	182.1	2.8
AB3/3	14.9	325.9	0	1.8	385.4	0
AB3/4	14	370.7	0	2.1	86.2	0
AB3/5	13	365.2	0	3.6	47.8	0
AB3/6	11.4	344.2	0	3.2	42	0
AB3/7	11.4	306.3	0	2.8	27.9	0
AB6/1	20.1	2334.8	9.1	11.6	155.6	5.1
AB6/2	13.8	2456.7	0	6.3	951.9	0
AB6/3	13.9	2210.9	0	6.2	700	0
AB6/4	12.7	2174.3	0	5	177.7	0
AB6/5	13	2325.8	0	5	139.8	0
AB6/6	13.9	1834.9	0	4.4	42	0
AB6/7	15.6	1775.7	0	4.2	32.4	0
AB8/1	3	1814	0	5	118	0
AB8/2	25.3	1916	0.068	8.7	149.7	3.4
AB8/3	15.8	1788.5	0	5	764.6	0
AB8/4	14.5	1652.6	0	4.3	326.8	0
AB8/5	15.1	1602.5	0	3.8	108.3	0
AB8/6	11.4	1328.4	0	3	54.4	0
AB8/7	0	1134	0	3	50	0
AB9/1	8.4	1783.7	0	0	433.7	0
AB9/2	2	2279.9	0	0	1943.1	0
AB9/3	9.9	1924.8	0	0	632.2	0
AB9/4	8.7	2000.6	0	0	499.1	0
AB9/5	5.1	1819.5	0	0	273.6	0
AB9/6	9.7	1458.1	0	0	54.8	0
AB9/7	7.5	1242.5	0	0	32.2	0
AB12/1	17.3	2206.3	3.9	5.1	57.6	0
AB12/2	14.7	1845.8	0	0	697	0
AB12/3	14.7	1818.3	0	0	1256.1	0
AB12/4	13.2	1908.1	0	0	1077	0
AB12/5	12.2	1856.5	0	0	856.3	0
AB12/6	13	1797.9	0	0	572.9	0
AB12/7	9.8	1697.4	0	0	267.2	0

Appendix 1 Ion Chromatography:
Table 9 Results for OB and OQ core samples
Results given as concentrations of mg/kg of stone (ppm)
(to 5 significant figures)

	Fluoride	Chloride	Nitrite	Nitrate	Sulphate	Phosphate
OB1/1	18.1	107.6	3.3	0	18.3	3.4
OB1/2	4.7	59	0	0	10	0
OB1/3	8.4	69.3	0	0	11.3	0
OB1/4	5.6	57.4	0	0	8	0
OB1/5	9.2	46.3	0	0	7.3	0
OB1/6	3.4	31.2	0	0	4.6	0
OB1/7	6.8	28.5	0	0	2.9	0
OB3/1	16.8	710.4	0.02	0	1238.6	0
OB3/2	18.7	499.8	0	0	376.2	0
OB3/3	23.2	255	0	0	7.9	0
OB3/4	9.4	137	0	0	3.6	0
OB3/5	4.1	78.5	0	0	2.7	0
OB3/6	3.2	43.3	0	0	6.1	0
OB3/7	2.7	34.7	0	0	2.2	0
OQ1/1	16.3	162.7	0.044	0.044	11.3	4.6
OQ1/2	10.1	25.8	0	0	3.8	0
OQ1/3	19.7	40.3	0.007	0.007	3.6	0
OQ1/4	11.9	23.7	0	0	2.5	0
OQ1/5	27.5	19.9	0.006	0	2.9	0
OQ1/6	9.7	21.2	0	0	3.2	0
OQ1/7	10.7	15.6	0	0.007	3.4	0
OQ2/1	18.1	82.7	0.04	0.034	17.6	3.1
OQ2/2	13.2	84.4	0.008	0.008	5.5	0
OQ2/3	16.9	67.9	0	0	3	0
OQ2/4	12.8	58.9	0	0	3	0
OQ2/5	14	24.7	0	0	2.3	0
OQ2/6	12.9	17	0	0	1.9	0
OQ2/7	13.4	17.2	0	0	2.1	0

Appendix 1 Ion Chromatography:
Table 10 Results for VB and VQ core samples
Results given as concentrations of mg/kg of stone (ppm)
(to 5 significant figures)

	Fluoride	Chloride	Nitrite	Nitrate	Sulphate	Phosphate
VB1/1	9.3	1250.9	2.9	0	30.1	0
VB1/2	5.5	948.4	1.1	0	16	0
VB1/3	5.2	945.9	0	0	144.4	0
VB1/4	6.4	881.6	0	0	13.4	0
VB1/5	5.5	863.2	0	0	11.1	0
VB1/6	4.5	752.1	0	0	7	0
VB1/7	4.9	414.9	0	0	4.1	0
VB2/1	6.1	406.5	0	2.7	11.4	0
VB2/2	5.5	401.2	0	1.4	11.6	0
VB2/3	6.5	499.9	0	1.7	12.4	0
VB2/4	6	559.3	0	1.8	13.8	0
VB2/5	6	616.6	0	2	14.7	0
VQ1/1	9.8	97.5	6.7	0	7.7	3.9
VQ1/7	7	21.8	1	0	3.1	0
VQ3/3	3.8	444.8	0	0	2.3	0

Appendix 1
Table 11

XRF Major elements: Results from AB core samples
Results given by percentage weight of the total content

	SiO2	TiO2	Al2O3	Fe tot	MnO	MgO	CaO	Na2O	K2O	P2O5	Totals
AB1/1	66.12	0.46	10.96	4.73	0.07	0.85	6.25	1.67	2.13	0.08	93.32
AB1/2	60.95	0.44	11.1	4.23	0.08	1.15	6.47	1.38	2.22	0.08	88.1
AB1/3	65.18	0.43	10.87	4.2	0.08	0.91	6.18	1.65	2.16	0.09	91.75
AB1/4	66.05	0.43	10.81	4.31	0.1	1.03	6.25	1.72	2.15	0.09	92.94
AB1/5	65.18	0.4	10.64	4.47	0.09	0.88	6.6	1.89	2.2	0.08	92.43
AB1/6	65.58	0.4	9.62	4.3	0.11	1.03	6.69	1.71	2.21	0.09	91.74
AB1/7	65.03	0.4	10.02	3.9	0.11	0.99	6.82	2.18	2.21	0.08	91.74
AB2/1	70.19	0.44	11.42	2.23	0.07	0.63	5.58	1.91	1.93	0.1	94.5
AB2/2	67.02	0.45	11.21	2.1	0.07	0.38	5.91	2.79	1.89	0.21	92.03
AB2/3	69.39	0.45	10.8	2.11	0.07	0.84	5.69	2.86	1.91	0.2	94.52
AB2/4	68.35	0.45	10.9	2.03	0.07	0.6	5.82	2.23	1.93	0.1	92.48
AB2/5	68.18	0.49	11.27	1.98	0.08	0.57	5.81	2.24	1.97	0.14	92.73
AB2/6	68.63	0.48	11.39	2.04	0.07	0.69	5.88	1.75	1.97	0.16	93.06
AB2/7	68.69	0.48	11.26	2.11	0.07	0.66	5.83	1.98	1.92	0.12	93.12
AB3/1	68.82	0.26	9.18	2.12	0.1	0.92	8.03	2.61	2.35	0.09	94.48
AB3/2	69.91	0.27	8.54	2.06	0.09	1.02	8.29	2.16	2.22	0.09	94.65
AB3/3	67.49	0.31	8.6	2.14	0.09	1.28	8.4	2.53	2.16	0.07	93.07
AB3/4	63.69	0.29	9.33	2.02	0.1	1.05	8.33	1.94	2.15	0.15	89.05
AB3/5	68.66	0.3	9.04	1.99	0.09	1.15	8.06	2.39	2.2	0.06	93.64
AB3/6	68.31	0.28	8.82	1.95	0.09	0.94	7.86	2.01	2.21	0.07	93.35
AB3/7	69.43	0.29	8.94	1.98	0.08	0.91	8.23	2.27	2.21	0.07	95.13
AB4/1	65.23	0.8	11.76	6.39	0.05	1.42	2.91	1.7	1.75	0.13	92.14
AB4/2	68.39	0.81	11.66	6.29	0.04	1.19	2.67	4.57	1.85	0.13	97.6
AB4/3	68.13	0.87	12.27	5.75	0.05	1.4	2.35	2.32	1.87	0.13	95.14
AB4/4	67.29	0.83	11.8	5.53	0.06	1.34	2.44	1.64	1.83	0.13	92.89
AB4/5	66.56	0.85	11.86	5.34	0.06	1.6	2.45	1.91	1.83	0.12	92.58
AB4/6	65.44	0.83	11.61	6.34	0.05	1.32	2.88	1.99	1.86	0.12	92.44
AB4/7	68.06	0.85	12.22	7.34	0.05	1.41	2.8	2.05	1.87	0.13	96.78
AB5/1	71.87	0.47	11.53	4.06	0.09	0.99	7.45	2.09	2.1	0.07	100.72
AB5/2	63.22	0.4	10.1	3.35	0.09	0.84	6.46	2.76	1.9	0.08	92.2
AB5/3	67.59	0.39	10.44	2.05	0.09	0.92	5.44	2.34	2.07	0.1	91.43
AB5/4	67.67	0.41	10.93	3.27	0.08	0.46	6.67	1.52	2.06	0.08	93.15
AB5/5	66.57	0.47	10.1	3.41	0.08	0.91	6.71	2.11	1.87	0.08	92.31
AB5/6	66.6	0.42	10.41	3.21	0.1	0.92	6.76	2.07	2.02	0.08	92.59
AB5/7	66.47	0.43	10.44	3.16	0.1	0.82	6.76	1.95	1.93	0.08	92.14
AB6/1	71.41	0.52	11.32	4.55	0.05	2.41	2.55	2.31	2.28	0.09	97.49
AB6/2	63.6	0.53	10.81	4.93	0.06	2.26	3.32	2.29	2.02	0.08	89.9
AB6/3	68.49	0.5	10.91	4.66	0.06	2.25	3.93	1.92	2.14	0.08	94.94
AB6/4	68.01	0.5	11.54	4.63	0.06	2.46	3.95	2.51	2.13	0.08	95.87
AB6/5	69.72	0.51	11.17	4.62	0.05	2.33	3.17	1.96	2.12	0.09	95.74
AB6/6	67.02	0.5	11.57	4.7	0.04	2.12	2.89	2.58	2.11	0.09	93.62
AB6/7	68.45	0.52	11.68	4.69	0.04	2.42	2.87	2.91	2.18	0.09	95.85

Appendix 1

XRF Major elements: Results from AB core samples

Table 11 Cont.

Results given by percentage weight of the total content

	SiO2	TiO2	Al2O3	Fe tot	MnO	MgO	CaO	Na2O	K2O	P2O5	Totals
AB7/2	69.63	0.48	11.42	4.76	0.04	1.85	2.44	2.31	2.53	0.08	95.54
AB7/3	71.95	0.54	12.21	4.93	0.04	1.97	2.22	1.54	2.51	0.08	97.99
AB7/4	50.05	0.34	7.98	3.24	0.03	1.58	1.46	1.49	1.67	0.06	67.9
AB7/5	67.6	0.53	11.82	4.84	0.05	2.16	3	1.93	2.44	0.09	94.46
AB7/6	68.43	0.65	11.93	5.52	0.05	2.1	2.16	1.86	2.42	0.11	95.23
AB7/7	70.54	0.73	12.16	6.01	0.05	2.21	2.15	1.86	2.48	0.11	98.3
AB8/1	68.11	0.4	10.42	3.22	0.12	1.02	7.42	1.88	2.01	0.08	94.68
AB8/2	68.33	0.4	10.25	3.24	0.11	0.86	7.45	2.44	1.98	0.08	95.14
AB8/3	68.05	0.4	10.96	3.12	0.1	0.56	6.99	1.92	1.96	0.08	94.14
AB8/4	68.24	0.41	10.51	3.45	0.09	0.94	6.82	1.64	1.96	0.08	94.14
AB8/5	57.06	0.32	8.85	2.62	0.08	0.66	5.51	1.47	1.64	0.07	78.29
AB8/6	67.22	0.39	10.38	3.2	0.08	0.62	6.74	1.96	1.9	0.07	92.56
AB8/7	67.67	0.41	10.64	3.2	0.1	0.77	6.85	1.93	1.91	0.09	93.57
AB9/1	66.22	0.58	10.65	4.47	0.07	1.52	4.57	2.01	1.88	0.1	92.07
AB9/2	66.88	0.56	10.3	4.64	0.06	1.44	4.99	2.2	1.84	0.08	92.99
AB9/3	65.29	0.28	5.39	2.31	0.04	0.86	2.28	1.66	1.98	0.05	80.14
AB9/4	67.06	0.56	10.52	4.52	0.08	1.51	4.73	2.26	1.94	0.09	93.27
AB9/5	68.27	0.52	10.5	4.21	0.07	1.38	4.41	4.41	1.96	0.08	95.81
AB9/6	65.73	0.53	10.39	4.35	0.06	1.5	4.6	3.9	1.95	0.09	93.1
AB9/7	65.95	0.53	10.47	4.54	0.06	1.52	4.58	3.27	1.97	0.09	92.98
AB10/1	65.36	0.42	10.36	3.13	0.11	0.76	8.01	1.97	1.82	0.07	92.01
AB10/2	66.54	0.44	10.51	3.39	0.09	0.78	7.29	1.98	1.78	0.08	92.88
AB10/3	66.97	0.43	10.49	3.24	0.09	0.73	7.07	2.02	1.8	0.08	92.92
AB10/4	66.56	0.46	10.78	3.29	0.1	0.72	7.22	2	1.81	0.08	93.02
AB10/5	66.48	0.44	10.57	3.28	0.09	0.73	7.28	1.98	1.79	0.08	92.72
AB10/6	66	0.43	10.54	3.3	0.1	0.72	7.44	2.03	1.8	0.08	92.44
AB10/7	66.19	0.43	10.46	3.9	0.11	0.72	7.59	2.08	1.81	0.08	93.37
AB11/1											
AB11/2	64.81	0.45	11.61	4.52	0.09	1.11	6.71	1.92	2.2	0.09	93.51
AB11/3	64.38	0.44	11.7	4.75	0.08	1.09	6.32	1.48	2.2	0.08	92.52
AB11/4	63.3	0.44	11.68	4.46	0.07	0.9	6.29	1.49	2.19	0.08	90.9
AB11/5	66.09	0.48	11.36	4.24	0.08	0.86	6.76	1.65	2.25	0.09	93.86
AB11/6	65.17	0.42	12.69	3.99	0.08	1.19	6.75	1.66	2.22	0.09	94.26
AB11/7	65.14	0.44	12.26	3.81	0.07	1.2	6.53	1.59	2.21	0.09	93.34
AB12/1	73.77	0.57	11.26	2.45	0.04	1.28	2.64	3.58	1.93	0.1	97.62
AB12/2	71.69	0.55	10.93	2.32	0.05	1.39	3.33	1.9	1.87	0.09	94.12
AB12/3	71.88	0.53	10.82	2.27	0.05	1.21	3.47	3.73	1.96	0.08	96
AB12/4	72.92	0.54	10.44	2.41	0.04	1.08	3.39	3.51	1.93	0.09	96.35
AB12/5	72.26	0.52	10.97	2.4	0.04	1.42	3.37	2.38	1.83	0.09	95.28
AB12/6	73.12	0.48	11.12	2.38	0.02	1.28	3.46	5.49	2	0.09	99.44
AB12/7	74.01	0.46	10.69	2.31	0.04	1.2	3.45	2.94	1.99	0.08	97.17

Appendix 1 **Continued....**
Table 11 **XRF Major elements: Results from AB core samples**
Results given by percentage elemental weight
(conversion of data for graphs)

	Si	Al	Fe tot	Mg	Ca	Na	K
AB1/1	30.9	5.8	3.31	0.51	4.47	1.24	1.77
AB1/2	28.49	5.88	2.96	0.69	4.62	1.02	1.84
AB1/3	30.47	5.75	2.94	0.55	4.42	1.22	1.79
AB1/4	30.87	5.72	3.01	0.62	4.47	1.28	1.78
AB1/5	30.47	5.63	3.13	0.53	4.72	1.4	1.83
AB1/6	30.65	5.09	3.01	0.62	4.78	1.27	1.83
AB1/7	30.39	5.3	2.73	0.6	4.87	1.62	1.83
AB2/1	32.8	6.04	1.56	0.38	3.99	1.42	1.6
AB2/2	31.3	5.93	1.47	0.23	4.22	2.07	1.57
AB2/3	32.43	5.72	1.48	0.51	4.07	2.12	1.59
AB2/4	29.77	5.77	1.42	0.36	4.16	1.65	1.6
AB2/5	32.09	5.97	1.38	0.34	4.16	1.66	1.64
AB2/6	31.93	6.03	1.43	0.42	4.2	1.3	1.64
AB2/7	32.45	5.96	1.48	0.4	4.17	1.47	1.59
AB3/1	32.17	4.86	1.48	0.55	5.74	1.94	1.95
AB3/2	32.68	4.52	1.44	0.61	5.92	1.6	1.84
AB3/3	31.54	4.55	1.5	0.77	6	1.88	1.79
AB3/4	29.77	4.94	1.41	0.63	5.95	1.44	1.78
AB3/5	32.25	4.79	1.39	0.69	5.76	1.77	1.83
AB3/6	31.93	4.67	1.36	0.57	5.62	1.49	1.83
AB3/7	32.45	4.73	1.38	0.55	5.88	1.68	1.83
AB4/1	30.49	6.22	4.47	0.86	2.08	1.26	1.45
AB4/2	31.97	6.17	4.4	0.72	1.91	3.39	1.54
AB4/3	31.84	6.49	4.02	0.84	1.68	1.72	1.55
AB4/4	31.45	6.25	3.87	0.81	1.74	1.22	1.52
AB4/5	31.11	6.28	3.73	0.96	1.75	1.42	1.52
AB4/6	30.59	6.15	4.43	0.8	2.06	1.48	1.54
AB4/7	31.81	6.47	5.13	0.85	2	1.52	1.55
AB5/1	33.59	6.1	2.84	0.6	5.32	1.55	1.75
AB5/2	29.55	5.35	2.34	0.51	4.62	2.05	1.58
AB5/3	31.59	5.53	1.43	0.55	3.89	1.74	1.72
AB5/4	31.63	5.79	2.29	0.28	4.77	1.13	1.71
AB5/5	31.12	5.35	2.38	0.55	4.8	1.57	1.55
AB5/6	31.13	5.51	2.25	0.55	4.83	1.54	1.68
AB5/7	31.07	5.53	2.21	0.49	4.83	1.45	1.6
AB6/1	33.35	5.99	3.18	1.45	1.82	1.71	1.89
AB6/2	29.7	5.72	3.45	1.36	2.37	1.7	1.68
AB6/3	31.98	5.76	3.26	1.36	2.81	1.42	1.78
AB6/4	31.76	6.11	3.24	1.48	2.82	1.86	1.77
AB6/5	32.56	5.91	3.23	1.4	2.27	1.45	1.76
AB6/6	31.3	6.12	3.29	1.28	2.07	1.91	1.75
AB6/7	31.97	6.18	3.28	1.46	2.05	2.16	1.81

Appendix 1 Continued...
Table 11 XRF Major elements: Results from AB core samples
 Results given by percentage elemental weight
 (conversion of data for graphs)

	Si	Al	Fe tot	Mg	Ca	Na	K
AB7/2	32.54	6.04	3.33	1.12	1.74	1.71	2.1
AB7/3	33.63	6.46	3.45	1.19	1.59	1.14	2.08
AB7/4	23.39	4.22	2.27	0.95	0.71	1.11	1.39
AB7/5	31.6	6.26	3.39	1.3	2.14	1.43	2.03
AB7/6	31.98	6.31	3.86	1.27	1.54	1.38	2.01
AB7/7	32.97	6.44	4.2	1.33	1.54	1.38	2.06
AB8/1	31.83	5.52	2.25	0.61	5.3	1.39	1.67
AB8/2	31.94	5.43	2.27	0.52	5.32	1.81	1.64
AB8/3	31.81	5.8	2.18	0.34	4.96	1.42	1.63
AB8/4	31.9	5.56	2.41	0.57	4.87	1.22	1.63
AB8/5	26.68	4.68	1.83	0.4	3.94	1.09	1.36
AB8/6	31.42	5.49	2.24	0.37	4.82	1.45	1.58
AB8/7	31.63	5.63	2.24	0.46	4.9	1.43	1.59
AB9/1	30.95	5.64	3.13	0.92	3.27	1.49	1.56
AB9/2	31.26	5.45	3.25	0.87	3.57	1.63	1.53
AB9/3	30.52	2.85	1.62	0.52	1.63	1.23	1.64
AB9/4	31.34	5.57	3.16	0.91	3.38	1.68	1.61
AB9/5	31.91	5.56	2.94	0.83	3.15	3.27	1.63
AB9/6	30.72	5.5	3.04	0.9	3.29	2.89	1.62
AB9/7	30.82	5.54	3.18	0.92	3.27	2.43	1.64
AB10/1	30.55	5.48	2.19	0.46	5.72	1.46	1.51
AB10/2	31.1	5.56	2.37	0.47	5.21	1.47	1.48
AB10/3	31.3	5.55	2.27	0.44	5.05	1.5	1.49
AB10/4	31.11	5.71	2.3	0.43	5.16	1.48	1.5
AB10/5	31.07	5.6	2.29	0.44	5.2	1.47	1.49
AB10/6	30.85	5.6	2.31	0.43	5.32	1.51	1.5
AB10/7	30.94	5.54	2.73	0.44	5.42	1.54	1.5
AB11/2	30.29	6.15	3.16	0.67	4.8	1.42	1.83
AB11/3	30.09	6.19	3.32	0.66	4.52	1.1	1.83
AB11/4	29.59	6.18	3.12	0.54	4.5	1.11	1.82
AB11/5	30.89	6.01	2.97	0.52	4.83	1.22	1.87
AB11/6	30.46	6.72	2.79	0.72	4.82	1.23	1.84
AB11/7	30.45	6.49	2.66	0.72	4.67	1.18	1.83
AB12/1	34.48	5.96	2.45	0.77	1.89	3.58	1.6
AB12/2	33.51	5.79	2.32	0.84	2.38	1.9	1.55
AB12/3	33.6	5.73	2.27	0.73	2.48	3.73	1.63
AB12/4	34.08	5.53	2.41	0.65	2.42	3.51	1.6
AB12/5	33.77	5.81	2.4	0.86	2.41	2.38	1.52
AB12/6	34.18	5.89	2.38	0.77	2.47	5.49	1.66
AB12/7	34.59	5.66	2.31	0.72	2.47	2.94	1.65

Appendix 1
Table 12 **XRF Trace elements: Results for AB core samples**
Results given as concentrations in ppm

	Cr	Cu	Ga	Ni	Pb	Rb	Sr	Th	Y	Ga	Co	Zn	Zr	TiO2	Ba	La	Ce
AB1/1	105	2	13	29	6	62	88	9	17	13	25	28	156	1	474	18	34
AB1/2	78	4	12	28	7	61	87	13	15	12	19	26	155	2	457	20	26
AB1/3	91	1	13	25	5	64	78	5	20	13	23	26	146	2	420	20	36
AB1/4	78	2	13	29	7	62	77	4	19	13	17	27	150	0	445	19	35
AB1/5	73	b.d.l.	13	27	5	60	77	4	19	13	13	28	158	1	451	19	32
AB1/6	75	3	13	26	11	56	82	8	18	13	16	40	153	1	485	18	36
AB1/7	61	9	12	26	6	53	82	3	15	12	18	22	143	1	430	15	33
AB2/1	23	b.d.l.	7	9	225	32	53	2	15	7	b.d.l.	20	98	2	296	12	32
AB2/2	80	b.d.l.	11	14	7	49	82	4	20	11	6	13	137	2	474	20	37
VB2/3	72	b.d.l.	10	12	7	51	83	4	19	10	3	15	139	2	480	21	32
AB2/4	79	b.d.l.	11	10	5	49	81	3	21	11	5	13	139	1	466	20	47
AB2/5	77	b.d.l.	10	13	6	51	80	2	21	10	6	12	138	2	438	21	40
AB2/6	86	b.d.l.	10	11	8	55	78	4	20	10	4	15	132	2	470	22	39
AB2/7	137	b.d.l.	9	15	9	53	90	4	18	9	4	16	139	3	798	21	39
AB3/1	47	b.d.l.	9	18	28	59	109	1	23	9	14	21	121	2	357	24	54
AB3/2	67	b.d.l.	9	19	4	56	112	0	21	9	3	18	111	2	351	24	45
AB3/3	70	b.d.l.	8	17	7	56	101	b.d.l.	25	8	6	22	110	0	339	25	40
AB3/4	52	b.d.l.	9	18	9	60	104	0	25	9	12	22	116	2	361	19	32
AB3/5	44	b.d.l.	8	17	8	59	102	b.d.l.	24	8	11	22	112	2	343	18	36
AB3/6	89	b.d.l.	10	b.d.l.	10	55	114	b.d.l.	24	10	4	25	100	1	345	20	42
AB3/7	41	0	9	b.d.l.	9	55	117	b.d.l.	24	9	8	31	114	2	371	20	44
AB4/1	230	34	15	55	2	53	82	4	20	15	22	48	278	b.d.l.	317	22	70
AB4/2	252	37	16	60	4	51	80	6	20	16	21	46	295	b.d.l.	322	26	70
AB4/3	229	23	16	54	6	65	82	6	18	16	23	44	263	b.d.l.	309	28	75
AB4/4	249	37	16	60	6	62	83	3	22	16	15	44	269	b.d.l.	316	24	72
AB4/5	322	40	15	53	8	64	80	9	18	15	18	48	285	b.d.l.	311	29	77
AB4/6	248	26	15	64	7	60	82	4	17	15	19	49	289	b.d.l.	341	29	68
AB4/7	218	10	15	65	5	61	82	5	16	15	23	53	285	2	338	19	72

Appendix 1 XRF Trace elements: Results for AB core samples
Table 12 Cont. Results given as concentrations in ppm

	Cr	Cu	Ga	Ni	Pb	Rb	Sr	Th	Y	Ga	Co	Zn	Zr	TiO2	Ba	La	Ce
AB5/1	80	b.d.l.	13	24	32	61	84	2	16	13	18	29	128	b.d.l.	409	14	37
AB5/2	79	b.d.l.	11	21	5	66	78	3	16	11	12	21	143	b.d.l.	388	13	40
AB5/3	79	b.d.l.	11	21	11	66	76	6	16	11	9	20	144	0	413	13	37
AB5/4	77	b.d.l.	10	20	10	69	72	4	18	10	7	22	137	b.d.l.	370	18	48
AB5/5	84	b.d.l.	9	20	9	56	81	6	18	9	11	21	161	0	382	15	40
AB5/6	96	b.d.l.	11	28	9	57	80	5	21	9	9	21	168	0	405	14	42
AB5/7	98	b.d.l.	11	20	6	64	81	4	16	6	10	22	143	1	390	15	43
AB6/1	99	3	15	b.d.l.	25	64	93	0	18	15	17	65	140	2	521	27	44
AB6/2	96	4	16	33	44	60	86	b.d.l.	16	16	16	52	160	1	433	18	29
AB6/3	93	4	12	37	44	60	91	b.d.l.	17	12	18	50	147	1	398	22	35
AB6/4	101	1	15	36	51	65	85	1	15	15	16	51	142	1	409	23	39
AB6/5	100	4	12	45	48	65	86	1	17	12	16	50	153	1	578	18	34
AB6/6	11	2	15	47	20	62	82	0	16	15	12	48	147	1	451	18	32
AB6/7	94	7	14	35	11	61	86	1	15	14	17	52	150	1	397	20	36
AB7/1	308	23	8	21	32	19	265	4	16	8	7	28	130	3	169	12	30
AB7/2	109	43	17	43	11	66	86	7	17	17	12	60	167	1	402	28	61
AB7/3	101	26	14	26	8	66	81	2	17	14	13	54	150	0	380	29	62
AB7/4	103	38	16	38	8	70	88	7	17	16	13	55	151	2	426	22	45
AB7/5	119	41	16	41	10	67	90	6	18	16	15	57	167	1	401	19	43
AB7/6	161	45	16	45	8	57	87	5	21	16	18	58	219	2	427	27	55
AB7/7	191	49	18	49	8	56	84	6	22	18	20	60	232	1	421	34	68
AB8/1	68	b.d.l.	13	15	48	57	81	4	22	13	7	30	129	2	507	21	36
AB8/2	102	b.d.l.	10	20	7	54	80	7	21	10	10	22	143	1	443	18	36
AB8/3	75	b.d.l.	10	20	6	55	80	7	19	10	6	19	133	2	389	19	37
AB8/4	70	b.d.l.	11	18	9	56	80	0	18	11	12	21	132	1	401	18	34
AB8/5	72	b.d.l.	10	15	8	55	76	1	19	10	8	20	133	2	382	19	27
AB8/6	73	b.d.l.	11	23	6	54	74	1	20	11	8	20	143	1	397	20	31
AB8/7	66	b.d.l.	10	14	7	56	78	3	19	10	10	19	131	2	408	19	31

Appendix 1 XRF Trace elements: Results for AB core samples
Table 12 Cont. Results given as concentrations in ppm

	Cr	Cu	Ga	Ni	Pb	Rb	Sr	Th	Y	Ga	Co	Zn	Zr	TiO2	Ba	La	Ce
AB9/1	166	6	15	43	28	59	89	2	19	15	22	46	153	1	339	31	58
AB9/2	136	30	14	42	9	54	87	15	22	14	15	47	180	0	398	27	44
AB9/3	127	31	13	37	8	55	82	10	19	13	12	44	163	0	411	27	44
AB9/4	138	40	14	38	10	59	85	8	18	14	17	43	172	2	416	24	57
AB9/5	119	29	15	40	8	49	85	1	21	15	13	42	161	3	392	29	50
AB9/6	110	42	13	42	7	48	81	b.d.l.	22	13	15	43	160	1	402	30	61
AB9/7	112	31	13	39	8	48	81	b.d.l.	23	13	14	41	160	2	430	24	42
AB10/1	66	b.d.l.	11	22	24	50	90	b.d.l.	25	11	7	21	126	3	458	25	51
AB10/2	81	b.d.l.	12	24	7	52	83	b.d.l.	21	12	9	23	131	2	454	28	57
AB10/3	67	b.d.l.	13	18	5	52	87	b.d.l.	23	13	9	21	116	1	459	23	58
AB10/4	87	b.d.l.	11	21	8	53	87	b.d.l.	23	11	8	21	123	2	473	25	66
AB10/5	64	b.d.l.	12	19	9	51	83	b.d.l.	21	12	9	20	127	2	447	26	49
AB10/6	75	b.d.l.	11	15	9	50	84	b.d.l.	24	11	11	23	126	3	454	27	45
AB10/7	70	b.d.l.	11	17	7	51	84	b.d.l.	25	11	4	22	124	1	470	25	54
AB11/1	72	9	19	32	6	31	331	b.d.l.	15	19	11	19	83	2	223	10	34
AB11/2	87	15	14	32	14	76	97	9	18	14	22	34	145	1	384	15	49
AB11/3	80	10	13	33	11	77	94	7	18	13	21	29	140	0	424	15	52
AB11/4	80	1	13	35	9	77	93	9	17	13	24	33	131	4	419	16	48
AB11/5	109	b.d.l.	14	36	10	74	87	7	16	14	21	33	133	0	370	20	46
AB11/6	105	b.d.l.	15	32	11	78	92	14	20	15	21	32	134	0	405	18	38
AB11/7	85	0	14	31	13	78	90	7	17	14	17	30	132	b.d.l.	371	19	49
AB12/1	111	b.d.l.	13	27	37	57	82	13	21	13	10	30	211	1	309	25	44
AB12/2	111	b.d.l.	13	29	24	57	86	13	19	13	9	28	199	2	333	22	35
AB12/3	102	b.d.l.	12	25	15	56	89	5	17	12	12	28	184	2	336	17	40
AB12/4	105	b.d.l.	12	28	13	56	85	8	16	12	6	27	193	3	333	21	36
AB12/5	105	b.d.l.	10	26	10	54	84	7	19	10	7	26	198	2	328	20	35
AB12/6	90	b.d.l.	15	32	11	78	92	14	20	15	6	32	134	0	345	25	27
AB12/7	88	b.d.l.	11	28	10	58	74	6	19	11	6	26	193	2	359	24	36

Appendix 1 XRF Major elements: Results from OB and OQ core samples
Table 13 Results given by percentage weight of the total content

	SiO2	TiO2	Al2O3	Fe2O3	MnO	MgO	CaO	Na2O	K2O	P2O5	LOI	Totals
OB1/1	67.54	0.69	12.36	3.04	0.09	0.41	5.38	0.58	1.85	0.11	8	100.05
OB1/2	67.65	0.65	12.4	2.7	0.07	0.42	5.61	0.53	1.84	0.1	7.92	99.9
OB1/3	67.55	0.64	12.46	2.6	0.07	0.39	5.77	0.54	1.85	0.09	8	99.95
OB1/4	67.19	0.65	12.24	2.69	0.07	0.42	6.09	0.56	1.86	0.09	8.27	100.12
OB1/5	65.88	0.62	12.04	2.97	0.08	0.46	6.91	0.62	1.81	0.09	8.79	100.26
OB1/6	68.7	0.55	12.02	2.71	0.08	0.36	5.33	0.53	1.91	0.08	7.46	99.73
OB1/7	69.06	0.54	12	2.57	0.05	0.35	5.29	0.55	1.91	0.08	7.43	99.83
OB2/1	64.46	0.88	12.14	6.63	0.08	1.38	3.66	1.93	1.75	0.12	6.5	99.52
OB2/2	64.22	0.94	12.33	6.88	0.09	1.44	4.01	1.93	1.75	0.12	5.96	99.67
OB2/3	64.86	0.96	12.61	6.96	0.09	1.43	3.87	1.94	1.78	0.12	5.73	100.35
OB2/4	64.89	0.93	12.5	6.93	0.08	1.42	3.74	1.91	1.78	0.11	5.64	99.94
OB2/5	65.18	0.92	12.49	6.77	0.08	1.38	3.72	1.91	1.77	0.12	5.59	99.93
OB2/6	65.67	0.75	12.06	6.05	0.08	1.28	4.38	1.87	1.8	0.11	6	100.05
OB2/7	64.54	0.95	12.76	7.8	0.06	1.58	3.32	1.89	1.77	0.12	5.45	100.24
OB3/1	67.44	0.44	10.92	2.53	0.08	0.39	6.52	0.84	2.07	0.08	8.52	99.81
OB3/2	67.95	0.45	11.08	2.58	0.09	0.4	6.39	0.8	2.12	0.08	8.02	99.94
OB3/3	68.07	0.45	10.99	2.74	0.09	0.36	6.59	0.75	2.13	0.07	8.07	100.3
OB3/4	67.92	0.45	11.05	2.76	0.08	0.39	6.53	0.8	2.1	0.07	8.05	100.2
OB3/5	68.01	0.46	11.09	2.75	0.08	0.39	6.55	0.76	2.06	0.07	7.98	100.2
OB3/6	67.61	0.44	11.08	2.67	0.07	0.39	6.76	0.79	2.06	0.07	8.2	100.13
OB3/7	69.78	0.45	11.34	2.34	0.08	0.31	5.51	0.78	2.1	0.07	7.29	100.05
OQ1/1	69.88	0.78	12.97	2.16	0.05	0.39	4.05	1.31	2.02	0.11	6.16	99.87
OQ1/2	68.21	0.68	12.8	2.74	0.06	0.39	5.1	1.3	2.01	0.08	6.98	100.35
OQ1/3	70.19	0.68	13.54	2.14	0.05	0.37	4.11	1.24	2.07	0.08	6.38	100.84
OQ1/4	70.85	0.69	14.04	1.89	0.04	0.32	3.48	1.2	2.11	0.09	5.99	100.7
OQ1/5	70.66	0.68	14.1	1.87	0.04	0.35	3.57	1.18	2.07	0.09	6.12	100.73
OQ1/6	67.11	0.73	12.42	2.83	0.08	0.44	5.96	1.2	1.93	0.09	7.7	100.49
OQ1/7	66.21	0.6	11.93	3.28	0.1	0.49	6.52	1.19	2.02	0.06	8.04	100.45
OQ2/1	66.96	0.47	10.54	2.79	0.07	0.49	7.6	1.21	1.81	0.03	8.53	100.49
OQ2/2	67.98	0.49	10.88	2.73	0.07	0.42	6.6	1.25	1.85	0.03	7.78	100.07
OQ2/3	68.35	0.5	10.86	2.71	0.07	0.43	6.68	1.23	1.83	0.03	7.81	100.48
OQ2/4	67.82	0.51	10.86	2.82	0.07	0.46	7.12	1.26	1.85	0.04	8.11	100.92
OQ2/5	67.61	0.55	11.23	3.09	0.08	0.41	6.87	1.28	1.83	0.07	7.87	100.89
OQ2/6	68.88	0.52	11.05	2.73	0.08	0.4	6.5	1.29	1.86	0.08	7.43	100.83
OQ2/7	66.44	0.58	11.21	2.86	0.08	0.42	7.34	1.2	1.84	0.08	8.33	100.38
OQ3/1	66.07	0.62	11.61	2.53	0.07	0.54	7.31	1.29	1.64	0.08	8.71	100.48
OQ3/2	68.18	0.62	12.07	2.63	0.06	0.49	5.92	1.27	1.73	0.07	7.4	100.44
OQ3/3	68.49	0.61	12.21	2.48	0.06	0.47	5.49	1.29	1.79	0.07	7.13	100.09
OQ3/4	69.68	0.6	12.3	2.37	0.06	0.46	5.27	1.28	1.79	0.07	6.95	100.83
OQ3/5	68.62	0.61	11.94	2.63	0.06	0.51	5.72	1.28	1.79	0.07	7.4	100.62
OQ3/6	67.37	0.69	12.14	2.51	0.06	0.51	5.9	1.31	1.74	0.1	7.61	99.92

Appendix 1 XRF Trace elements: Results from OB and OQ core samples

Table 14 Results given as concentrations in ppm

	Cr	Cu	Ga	Nb	Ni	Pb	Rb	Sr	Th	V	Y	Ga	Cb	Zn	Zr	TiO2	Ba	La	Ce	Nd	Cl	S	P2O5	TiO2	U
OB1/1	130	b.d.l.	16		37	111	52	118	6	24	16	20	29	199		217	27	77							2
OB1/2	134	b.d.l.	16		39	17	53	122	2	22	16	18	15	185		289	29	79							2
OB1/3	141	b.d.l.	16		34	14	51	115	b.d.l.	23	16	21	15	189		272	24	75							2
OB1/4	110	b.d.l.	16		34	17	51	116	0	23	16	20	16	190		270	23	72							3
OB1/5	115	b.d.l.	17		39	16	47	107	b.d.l.	22	17	23	17	183		266	27	78							3
OB1/6	116	0	15		32	16	53	120	b.d.l.	21	15	12	14	165		294	24	75							2
OB1/7	94	b.d.l.	15		33	19	54	117	b.d.l.	20	15	12	13	172		262	28	73							2
OB2/1	229	0	17		47	2039	50	70	10	20	17	18	302	275		288	24	112							2
OB2/1	268	b.d.l.	18		51	17	45	82	b.d.l.	24	18	22	57	255		410	27	45							3
OB2/3	255	b.d.l.	18		53	9	45	81	b.d.l.	24	18	25	54	231		394	28	47							1
OB2/4	287	b.d.l.	20		54	7	50	85	b.d.l.	23	20	26	58	240		394	34	67							0
OB2/5	270	b.d.l.	20		49	7	58	81	0	22	20	22	50	203		376	24	55							3
OB2/6	188	b.d.l.	17		50	7	56	84	b.d.l.	21	17	24	47	183		370	33	71							1
OB2/7	263	b.d.l.	21		60	9	55	74	11	21	21	24	64	220		373	30	53							1
OB3/1	37	b.d.l.	10		23	58	49	117	8	24	10	11	20	149		239	10	50							3
OB3/2	65	b.d.l.	12		25	15	52	123	1	22	12	17	10	146		263	15	69							2
OB3/3	63	b.d.l.	14		25	20	51	116	0	21	14	14	28	143		270	16	65							2
OB3/4	61	b.d.l.	14		31	12	47	116	b.d.l.	22	14	15	14	138		272	14	65							3
OB3/5	62	b.d.l.	13		28	17	43	120	b.d.l.	23	13	14	11	144		275	16	63							3
OB3/6	67	b.d.l.	15		31	14	43	114	b.d.l.	23	15	15	13	138		245	21	78							3
OB3/7	64	b.d.l.	19		32	16	49	121	6	23	19	18	17	139		291	24	70							2
OQ1/1	133	8	18	8	29	26	63	156	4	105	17	17	22	170	1.03	350	39	76	28	876	108	0.14	0.88		
OQ1/2	115	7	16	8	39	27	60	128	2	109	18	18	25	148	0.89	373	27	75	24	195	67	0.1	0.76		
OQ1/3	109	6	17	7	25	24	61	137	2	93	15	15	22	162	0.84	363	27	63	30	203	72	0.1	0.71		
OQ1/4	120	5	18	7	23	23	63	153	1	99	16	16	19	166	0.93	361	33	70	21	172	74	0.11	0.78		
OQ1/5	126	6	18	8	23	24	62	155	4	100	15	15	19	179	0.98	363	39	79	29	135	73	0.11	0.85		
OQ1/6	132	8	17	8	33	25	59	128	4	124	19	19	28	166	1.02	402	39	73	32	185	78	0.12	0.88		
OQ1/7	119	7	14	8	42	27	60	110	4	156	20	20	30	156	0.88	445	27	63	25	236	80	0.09	0.75		
OQ2/1	70	4	13	5	26	23	57	102	0	74	15	15	28	128	0.6	401	18	35	19	597	115	0.06	0.51		
OQ2/2	67	1	13	5	27	22	57	91	1	75	14	14	26	118	0.6	341	5	49	23	444	78	0.05	0.52		
OQ2/3	68	2	14	6	28	24	57	93	0	82	15	15	27	128	0.62	349	13	28	14	462	78	0.06	0.52		
OQ2/4	76	2	12	6	28	24	58	93	0	79	16	16	27	126	0.64	334	12	50	19	437	75	0.07	0.54		
OQ2/5	82	3	16	6	34	23	57	104	1	92	17	17	31	130	0.74	374	21	35	19	209	79	0.1	0.64		
OQ2/6	85	3	11	5	27	22	55	106	0	79	15	15	27	129	0.69	395	21	37	19	191	79	0.1	0.6		
OQ2/7	93	4	14	7	32	23	56	113	1	74	19	19	31	153	0.81	386	21	45	18	191	75	0.11	0.69		
OQ3/1	110	3	14	6	23	18	55	136	2	100	15	15	24	164	0.76	436	24	55	34	654	135	0.11	0.69		
OQ3/2	103	4	14	6	24	15	57	110	1	108	16	16	25	143	0.83	325	27	72	23	481	88	0.1	0.7		
OQ3/3	100	1	14	6	24	18	57	112	1	111	15	15	24	150	0.85	342	18	79	32	338	76	0.1	0.73		
OQ3/4	108	1	14	6	21	17	58	111	0	107	14	14	24	142	0.82	342	21	54	28	323	76	0.1	0.72		
OQ3/5	108	2	15	6	23	17	58	110	1	109	16	16	27	157	0.81	338	24	50	17	204	76	0.1	0.71		
OQ3/6	113	3	15	7	23	21	57	132	1	110	16	16	26	154	0.93	315	30	70	30	295	79	0.12	0.79		

Appendix 1 XRF Major elements: Results from VB & VQ core samples
Table 15 Results given by percentage weight of the total content

	SiO2	TiO2	Al2O3	Fe2O3	MnO	MgO	CaO	Na2O	K2O	P2O5	LOI	Totals
VB1/1	72.1	0.69	11.65	3.25	0.09	0.3	3.79	0.04	1.55	0.11	6.47	100.03
VB1/2	73.09	0.64	11.72	3.23	0.09	0.29	3.46	0	1.54	0.11	6.19	100.35
VB1/3	72.8	0.61	11.71	3.24	0.09	0.28	3.43	0	1.56	0.1	6.2	100.01
VB1/4	72.75	0.64	11.57	3.3	0.09	0.29	3.57	0.02	1.51	0.1	6.26	100.12
VB1/5	72.57	0.61	11.72	3.21	0.09	0.29	3.48	0.02	1.55	0.1	6.25	99.89
VB1/6	72.52	0.61	11.58	3.33	0.1	0.27	3.72	0.02	1.52	0.11	6.35	100.11
VB1/7	72.69	0.64	11.52	3.2	0.09	0.27	3.6	0	1.52	0.1	6.15	99.78
VB2/1	73.26	0.42	10.99	2.74	0.12	0.27	3.98	0	1.44	0.06	6.49	99.76
VB2/2	73.85	0.4	11.05	2.81	0.12	0.28	3.9	0	1.45	0.06	6.44	100.34
VB2/3	73.79	0.41	11.15	2.77	0.12	0.28	3.77	0.01	1.47	0.06	6.31	100.15
VB2/4	73.49	0.42	11.1	2.89	0.12	0.28	3.93	0	1.48	0.06	6.39	100.15
VB2/5	74.1	0.41	11.27	2.77	0.11	0.29	3.63	0	1.48	0.06	6.25	100.36
VB2/6	70.04	0.44	10.66	4.25	0.12	0.35	5.57	0.01	1.47	0.06	7.55	100.51
VB2/7	71.47	0.44	10.8	3.7	0.1	0.32	4.56	0.01	1.46	0.06	7.01	99.94
VB3/1	67.99	0.45	9.83	3.96	0.3	0.62	6.84	0.07	1.44	0.07	8.74	100.3
VB3/2	67.96	0.49	10.22	3.89	0.27	0.56	6.27	0.09	1.41	0.06	8.42	99.65
VB3/3	70.79	0.5	10.48	3.66	0.23	0.49	5.33	0.05	1.4	0.06	7.62	100.61
VB3/4	70.64	0.5	10.25	3.65	0.22	0.51	5.24	0.05	1.34	0.06	7.58	100.05
VB3/5	70.91	0.53	10.32	3.48	0.2	0.47	4.98	0.08	1.36	0.07	7.35	99.75
VB3/6	72.23	0.45	10.14	3.67	0.2	0.37	4.62	0.01	1.36	0.06	7.05	100.16
VB3/7	72	0.42	10.09	3.36	0.26	0.38	5.16	0.05	1.38	0.06	7.34	100.5
VQ1/1	76.81	0.5	12.63	3.36	0.07	0.22	0.11	0	2.14	0.08	4.03	99.94
VQ1/2	77.64	0.52	12.66	3.42	0.1	0.2	0.09	0.01	2.14	0.08	3.83	100.7
VQ1/3	77.09	0.53	12.1	3.95	0.11	0.19	0.08	0	1.93	0.08	3.86	99.93
VQ1/4	76.94	0.56	12.06	4.08	0.09	0.2	0.08	0	1.94	0.08	3.87	99.91
VQ1/5	77.16	0.55	12.63	3.62	0.08	0.21	0.09	0	2.09	0.08	3.88	100.39
VQ1/6	76.66	0.54	12.62	3.69	0.08	0.21	0.09	0	2.19	0.09	3.86	100.03
VQ1/7	76.39	0.57	12.51	3.82	0.09	0.26	0.08	0	2.11	0.08	3.87	99.78
VQ2/1	73.42	0.76	13.22	5.43	0.06	0.28	0.12	0	1.83	0.13	4.92	100.16
VQ2/2	73.83	0.73	13.33	5.35	0.14	0.28	0.12	0	1.85	0.13	4.45	100.22
VQ2/3	73.6	0.7	13.17	5.45	0.16	0.26	0.11	0	1.87	0.12	4.42	99.85
VQ2/4	73.49	0.71	13.23	5.57	0.16	0.26	0.11	0	1.88	0.11	4.31	99.83
VQ2/5	73.83	0.69	13.21	5.52	0.15	0.28	0.11	0	1.9	0.11	4.27	100.09
VQ2/6	73.85	0.69	13.19	5.61	0.15	0.25	0.12	0	1.91	0.11	4.26	100.14
VQ2/7	74.14	0.54	12.85	5.41	0.14	0.28	0.09	0	1.97	0.09	4.15	99.66
VQ3/1	73.54	0.59	12.05	3.84	0.06	0.32	0.7	0.4	1.75	0.09	6.38	99.73
VQ3/2	76.47	0.61	12.72	3.97	0.08	0.22	0.08	0.01	1.79	0.09	4.08	100.12
VQ3/3	76.92	0.61	12.79	3.93	0.09	0.23	0.07	0.02	1.79	0.09	4.14	100.67
VQ3/4	76.43	0.58	12.73	4.07	0.1	0.21	0.07	0	1.81	0.09	4	100.08
VQ3/5	76.98	0.6	12.73	3.92	0.09	0.21	0.07	0	1.78	0.09	4.04	100.51
VQ3/6	76.36	0.6	12.59	3.8	0.08	0.2	0.08	0.01	1.76	0.08	4.06	99.62

Appendix 1 XRF Trace elements: Results from VB and VQ core samples
 Table 16 Results given as concentrations of ppm

	Cr	Cu	Ga	Nb	Ni	Pb	Rb	Sr	Th	V	Y	Co	Zn	Zr	TiO2	Ba	La	Ce	Nd	Cl	S	P2O5	TiO2	U
VB1/1	93	3	15	9	21	61	52	288	1	53	18	20	29	236	0.74	259	27	82	27	5141	190	0.13	0.63	2
VB1/2	92	2	12	8	20	19	52	282	1	55	17	18	22	252	0.7	271	33	69	35	2591	92	0.13	0.6	2
VB1/3	93	2	15	8	18	20	52	283	2	59	18	21	25	248	0.71	261	33	62	32	3017	98	0.13	0.6	2
VB1/4	95	1	13	9	24	21	51	280	3	54	18	20	23	250	0.69	272	27	67	23	2132	85	0.12	0.59	3
VB1/5	84	2	15	9	19	20	51	283	2	58	17	23	23	243	0.7	275	33	69	30	3306	96	0.13	0.6	2
VB1/6	91	1	12	8	21	17	51	273	1	59	18	12	24	243	0.69	267	30	66	32	2532	79	0.12	0.60	2
VB1/7	101	1	15	8	19	18	52	273	1	67	18	12	23	246	0.7	256	30	68	29	1784	71	0.12	0.59	2
VB2/1	57	2	11	5	20	91	47	188	0	54	14	18	32	124	0.46	234	15	53	34	1857	83	0.08	0.38	2
VB2/2	54	1	14	5	18	15	47	188	0	54	14	22	32	124	0.46	231	21	49	25	1138	75	0.08	0.37	3
VB2/3	52	1	13	5	19	16	47	188	0	54	14	25	21	123	0.45	261	15	40	21	1918	80	0.08	0.37	1
VB2/4	54	2	14	5	20	15	47	185	0	56	14	26	22	121	0.47	255	18	47	19	2616	91	0.08	0.39	0
VB2/5	53	2	12	5	20	15	49	189	0	52	14	22	19	124	0.48	268	18	42	21	2245	89	0.09	0.41	3
VB2/6	72	4	14	6	27	18	47	176	0	68	16	24	27	123	0.49	217	21	36	19	2838	95	0.08	0.42	1
VB2/7	68	3	11	6	27	18	48	183	0	59	17	24	24	130	0.47	228	15	44	25	2174	81	0.08	0.4	1
VB3/1	60	7	13	6	23	20	52	197	0	92	18	11	31	120	0.56	207	21	56	23	8054	262	0.1	0.45	3
VB3/2	68	3	11	6	22	16	50	161	0	87	19	17	31	127	0.56	201	8	38	17	9473	390	0.09	0.48	2
VB3/3	67	2	13	5	20	17	49	154	0	76	17	14	24	122	0.57	202	15	37	13	5671	225	0.09	0.49	2
VB3/4	65	3	12	6	19	14	46	151	0	87	16	15	23	122	0.58	196	18	40	13	6953	278	0.09	0.49	3
VB3/5	66	2	13	6	18	16	46	158	0	82	17	14	22	125	0.62	200	21	50	28	6038	279	0.1	0.53	2
VB3/6	61	2	13	5	20	15	47	175	0	88	18	15	24	1216	0.48	218	7	49	19	8119	419	0.09	0.42	3
VB3/7	61	2	12	4	20	18	47	179	0	87	17	18	22	117	0.47	299	18	42	17	6330	334	0.09	0.4	2
VQ1/1	60	10	15	6	42	17	73	240	1	82	15	33	33	134	0.61	485	27	65	28	1739	182	0.12	0.52	
VQ1/2	63	5	14	6	34	17	70	228	0	96	17	37	37	137	0.61	612	27	59	29	645	74	0.11	0.52	
VQ1/3	80	3	14	7	44	16	67	210	2	101	20	44	44	148	0.66	590	18	57	30	330	74	0.11	0.57	
VQ1/4	78	3	15	6	47	18	65	230	0	104	22	42	42	148	0.67	522	27	55	26	157	72	0.1	0.56	
VQ1/5	69	1	15	6	36	17	73	238	0	92	18	34	34	145	0.64	523	27	59	28	105	66	0.11	0.55	
VQ1/6	62	4	14	7	33	20	74	293	1	91	16	35	35	147	0.64	566	36	69	36	124	75	0.11	0.55	
VQ1/7	76	5	17	7	31	18	79	230	0	99	19	38	38	145	0.73	599	30	70	27	211	78	0.12	0.63	
VQ2/1	149	4	17	9	36	19	68	243	5	157	20	54	54	186	0.95	547	58	112	41	470	119	0.17	0.82	
VQ2/2	142	8	16	9	64	19	69	241	5	160	33	54	54	185	0.9	708	52	126	51	190	86	0.14	0.76	
VQ2/3	139	5	13	9	66	16	68	243	4	160	28	52	52	175	0.86	702	55	105	42	205	78	0.13	0.73	
VQ2/4	136	5	16	9	61	17	68	244	5	161	30	55	55	182	0.87	736	58	118	45	267	80	0.14	0.74	
VQ2/5	129	5	14	9	60	17	69	247	5	157	29	54	54	184	0.82	704	58	113	43	190	75	0.13	0.7	
VQ2/6	132	4	16	9	58	18	68	252	4	157	30	56	56	181	0.86	716	49	104	36	167	77	0.13	0.73	
VQ2/7	86	6	14	7	57	19	71	248	3	149	27	57	57	149	0.65	700	55	99	45	163	71	0.11	0.57	
VQ3/1	98	3	14	7	26	19	63	269	0	90	16	37	37	164	0.69	481	24	69	29	8783	439	0.11	0.58	
VQ3/2	99	2	15	7	31	17	67	266	1	105	17	33	33	172	0.72	521	39	76	50	2057	91	0.11	0.62	
VQ3/3	96	4	15	6	33	16	66	260	1	100	17	33	33	161	0.71	517	27	85	42	1496	82	0.11	0.6	
VQ3/4	88	1	13	7	34	17	68	260	3	99	16	34	34	149	0.69	528	27	61	28	1654	81	0.11	0.61	
VQ3/5	94	3	16	7	33	16	65	256	1	107	18	33	33	161	0.7	515	30	65	34	432	80	0.11	0.6	
VQ3/6	98	3	14	7	32	17	64	254	1	98	17	32	32	163	0.7	495	27	71	36	2294	81	0.11	0.61	

Appendix 1
Table 17

Dry mass density, absorption, porosity
saturated sodium sulphate crystallisation and point-load strength tests

Sample	Dry density kg/cu m	Water absorbed %	Indicative porosity %	NaSO4 No. of cycles	Point-load strength (range) MN/sq m
AB1	2297	11.9	13.6		1.5 1.8
AB2	2252	13.9	14.1		0.4
AB3	2235	14.8	15.5		1.2
AB4	2286	16.6	15.4		0.9
AB5	2266	14	13.5		1.3 2.1
AB6	2234	16	14.6	4	0.9 1.2
AB9	2285	13.5	13.7	6	0.9
AB10	2291	13.1	13.1	7	1.4 1.8
OB1	2308	13.5	14.6		1.4 1.3
OB3	2312	12.6	12.4	15	
VB2	2287	13.2	14.3	9	1.1 2.2
VB3	2323	12	13.1	8	1.3 1.4

**Appendix 1
Table 18**

**Dry mass density, absorption, porosity
saturated sodium sulphate crystallisation and point-load strength tests**
Values from tests on mainly Lower Carboniferous rocks but some Permian and ORS

Average Values	Dry density kg/cu m	Water absorbed %	Indicative porosity %	NaSO4 No. of cycles	Point-load strength (range) MN/sq m
Minimum	1990	2.6	2.6	10*	0.7
Maximum	2630	15.9	22.7	15+	3.8
Median	2180	11.2	17	15+	1.9

Appendix 1 Table 19
Monthly Climatic Data from Culzean
All information at 0900 GMT

Date	Temperature in degrees Centigrade				Greatest Rainfall		Rainfall mm		
	Maximum		Minimum		In 24 hours		Number of days with rain		
	highest	lowest	highest	lowest	in mm	> 0.2 mm	> 1.0 mm	> 5.0 mm	
Feb-93	10.3	3.6	7.9	-0.7	6.1	12	5	1	
Mar-93	12.3	4.3	7.3	2.2	22.9	15	10	2	
Apr-93	13.4	8.6	9.4	2.3	18.5	19	17	9	
May-93	19.9	7.4	11.8	1.4	45.2	15	10	5	
Jun-93	22.4	12.3	16.1	6.2	18.4	10	9	4	
Jul-93	17.9	13	14.5	2.5	10.3	23	20	7	
Aug-93	18.9	12.5	13.1	7.4	14	12	8	5	
Sep-93	20.9	12.6	13.4	3	7.9	12	12	3	
Oct-93	15.3	7.9	8.1	-0.6	23.2	9	9	3	
Nov-93	12.8	2	8.6	-4	21.8	12	12	8	
Dec-93	12.4	3.2	7.6	-4	16.8	26	22	13	
Jan-94	10	4	7.2	-1.5	33.2	25	22	14	
Feb-94	8.6	1.5	5.3	-7.3	13	13	12	5	
Mar-94	11.9	4.9	8.4	0.1	16.7	30	27	12	
Apr-94	16.5	5.7	6.8	-0.4	8.7	18	18	4	
May-94	22.5	9.9	10.4	-0.3	5.7	5	4	1	
Jun-94	19.7	11.5	12	6	8.9	19	15	3	
Jul-94	23.4	14.8	14.8	7.7	18.8	14	12	5	
Aug-94	21.5	13.7	13.9	6.4	12.9	14	9	6	
Sep-94	19	12.6	12	4.5	15	15	10	4	
Oct-94	17.2	8.8	10.5	-3.5	19.6	20	14	4	
Nov-94	14.7	8.5	9.8	-2.5	15.2	23	19	8	
Dec-94	11.7	2.1	8.1	-2	36.5	24	21	10	
Jan-95	11.6	3.1	7.5	-3.3	15.5	23	17	10	
Feb-95	10.9	2.9	7	-1.7	15	25	23	8	

Appendix 1 Table 20
 Culzean Meteorological recordings at 0900 GMT for May & November 1993

1993		Temperature			Rainfall			Wind				
		Maximum degrees centigrade	Minimum degrees centigrade	(mm)	Direction 10 X degrees	Speed knots		Maximum degrees centigrade	Minimum degrees centigrade	Rainfall (mm)	Direction 10 X degrees	Speed knots
May-01	Nov-01	11.8	6.9	0	7	5	8.5	5.8	0	0	0	0
May-02	Nov-02	10.7	3.6	0.5	29	5	8.5	5.7	0	0	0	0
May-03	Nov-03	10.5	3.3	0	29	9	10.4	2.9	6.2	23	13	13
May-04	Nov-04	11.1	3.4	0	25	2	12.6	7.2	0	23	2	2
May-05	Nov-05	13.8	7.4	0	25	2	11.9	8.6	0	23	2	2
May-06	Nov-06	14.5	8.4	0	25	9	12.8	5.1	2.6	0	0	0
May-07	Nov-07	12.7	6.9	5.3	36	2	9.8	8.2	5	18	9	9
May-08	Nov-08	14.1	9.9	0	29	2	10.2	7.6	21.8	18	2	2
May-09	Nov-09	13.4	6.3	0	2	15	10.6	3.4	4.2	23	24	24
May-10	Nov-10	14.8	7.4	0	25	19	8.1	2	0	0	0	0
May-11	Nov-11	9.5	9.9	0	7	19	9.3	2.6	1.1	0	0	0
May-12	Nov-12	15.5	7	0	25	19	8.5	5.1	6.6	18	5	5
May-13	Nov-13	11.5	3.6	20.9	0	0	6.5	1.5	0	0	0	0
May-14	Nov-14	7.4	1.4	28.2	7	13	7.8	2.7	0	5	19	19
May-15	Nov-15	8.9	2.6	1.1	27	24	9.8	2.5	16.1	14	19	19
May-16	Nov-16	12.7	4.4	45.2	27	5	9.9	7.1	1	18	9	9
May-17	Nov-17	15.4	7.4	11.2	20	19	7	6.1	0	18	19	19
May-18	Nov-18	13	6.9	3.5	25	19	6.1	4.3	0	18	19	19
May-19	Nov-19	11.5	3.4	4.4	11	5	7.1	3.2	0	14	2	2
May-20	Nov-20	14.2	3.7	1.8	14	5	7.2	2.2	0	9	5	5
May-21	Nov-21	13.1	8.4	0.1	0	0	4.7	1.6	0	7	2	2
May-22	Nov-22	16.4	8.7	0	18	19	2.5	2	0	9	5	5
May-23	Nov-23	19.9	11.1	0	1	9	2	3.5	0	0	0	0
May-24	Nov-24	18.4	11.8	0	5	19	6.8	4	5.7	0	0	0
May-25	Nov-25	16	10	0	14	19	8.3	2.2	0	23	19	19
May-26	Nov-26	12.9	6.4	0	9	19	6.8	0.8	0	0	0	0
May-27	Nov-27	14.2	6.2	0	7	13	7.3	2.7	0	23	9	9
May-28	Nov-28	12.1	6.2	0.2	14	2	5.3	0.1	10.3	16	13	13
May-29	Nov-29	15.9	9.1	3.6	23	9	6.8	2.2	6.1	16	24	24
May-30	Nov-30	15.7	10.7	0.5	23	19	7.9	2.4	0	16	16	16
May-31		13.3	10.1	0.5	25	5						

Appendix 1 Table 21
Wind and Rain Recordings on the Adam's Balcony

1993				1993				1993			
Speed Knots	Beaufort Scale	Direction Degrees	Rainfall (mm)	Speed Knots	Beaufort Scale	Direction Degrees	Rainfall (mm)	Speed Knots	Beaufort Scale	Direction Degrees	Rainfall (mm)
9	3	5	trace	9	3	25	0	9	3	25	0
13	4	5	trace	5	2	16	0	5	2	16	0
5	2	7	0	19	5	20	6.3	19	5	20	6.3
2	1	14	0.1	2	1	20	9.2	2	1	20	9.2
2	1	14	0	19	5	18	8.7	19	5	18	8.7
5	2	23	0.4	13	4	18	0.2	13	4	18	0.2
2	1	18	trace	5	2	18	0.8	5	2	18	0.8
19	5	11	0	13	4	18	5.1	13	4	18	5.1
5	2	5	0.4	5	2	18	2.7	5	2	18	2.7
9	3	5	3.7	5	2	18	0	5	2	18	0
13	4	18	trace	5	2	36	trace	5	2	36	trace
9	3	14	4	9	3	16	3	9	3	16	3
13	4	23	0	5	2	18	0	5	2	18	0
13	4	23	0	5	2	18	0	5	2	18	0
19	5	20	1.8	5	2	23	1.6	5	2	23	1.6
13	4	23	10.9	9	3	25	3.6	9	3	25	3.6
19	5	23	4.2	5	2	27	6.7	5	2	27	6.7
19	5	23	2.2	0	0	0	18.5	0	0	0	18.5
24	6	25	0	5	2	18	7.5	5	2	18	7.5
13	4	20	0.7	19	5	25	2.8	19	5	25	2.8
2	1	23	0	19	5	25	1.3	19	5	25	1.3
9	3	25	4.1	9	3	18	2.2	9	3	18	2.2
24	6	25	0.6	0	0	0	1.2	0	0	0	1.2
2	1	29	1.8	5	2	20	0	5	2	20	0
2	1	36	0	2	1	5	5.2	2	1	5	5.2
2	1	36	0	9	3	5	trace	9	3	5	trace
24	6	18	0	5	2	5	0	5	2	5	0
19	5	18	2.7	9	3	34	0	9	3	34	0
19	5	16	22.9	9	3	7	0	9	3	7	0
5	2	18	trace	5	2	9	0	5	2	9	0
9	3	20	0.2								

Wind speed given both in Knots and as its position on the Beaufort Scale

Wind direction measured in tens of degrees

Rainfall collection in millimetres per day

Appendix 1 Table 22
Midday Relative Humidity as a percentage

Surface < 10 mm depth
Interior >100 mm depth

1995	North (green)		West (green)		South (red)		Air Relative Humidity		
	surface	interior	surface	interior	surface	interior	North	West	South
Feb-95	58.8	65.9							
Feb-03	63.7	62.2	75.2	78.3	72.5	73			
Feb-27	76.7	68.5	79.1	76.9	80.1	75.5	76.1	78.2	80
Feb-28	84.3	78.5	88.8	84.8	89.7	87.5	86.8	87.8	92
Mar-01	61.5	73.5	64.5	70.2	70.2	83.8	67.3	62.8	66.4
Mar-02	56.8	68	64.5	71.5	67.5	82.2	60.4	60.8	64.2
Mar-03	69.5	70.6	63.7	74.5	68	81.5	62.8	61.1	65.8
Mar-06	56.9	66.1	59.7	65	63.4	76.3	52.2	57.5	62.1
Mar-07	44.7	60.3	49.2	60.7	54.4	73.8	44.6	51.7	52.8
Mar-08	48.2	55.5	57.2	63.8	61.2	73.2	45.7	56	60.4
Mar-09	44.2	58.4	49.8	61.9	52.5	64.8	42.2	48.1	47.7
Mar-10	68.9	67.1	72.1	72.1	75.1	78.6	69.6	70.4	74.9
Mar-14	62.9	66.7	70	72.3	71.5	75	61.9	69.5	71.2
Mar-15	59	72.1	62.8	70.5	64.6	80.2	58.2	60.2	64
Mar-16	59	68.5	64.8	68.9	67.9	76.1	58.5	63.5	66.5
Mar-17	67.8	71.6	70.8	72.2	71.5	74.7	62.5	70.4	71.1
Mar-18	62.2	71.9	69	71.9	68.9	77.8	60.8	62.5	67.4
Mar-20	52.1	65.8	60.6	67.8	50.4	64.3	51.8	60.2	62.9
Mar-21	54.7	67	60.3	60.9	60.2	64.1	53.7	60.2	58.8
Mar-22	55.1	66	57	60.2	60.7	62	54.8	56.6	57.1
Mar-23	60.2	64.3	61.5	66.5	60.6	65.8	59.3	62.7	59.6
Mar-24	79.2	77.9	82.1	77.9	85.6	81.8	79	81.5	85.3
6-Jun	74.9	78.5	72.4	74.1	71.4	75.2	72	70	71.1
8-Jun	62.3	66.2	61.2	62.2	60.1	65.6	59.3	58.9	58.9
9-Jun	64.5	65.2	63.2	64.6	61.9	66.6	62.2	62.8	62.8
12-Jun	62.4	64.8	64.2	63.6	62.9	71.1	58.8	60.9	62.1
13-Jun	71.6	75.3	68.6	71.8	67.4	71.2	61.8	65.5	66.3
14-Jun	68.9	76.6	67.5	69.5	66.3	70.2	56.2	63.6	65.1
15-Jun	68.8	69.8	67.8	68.3	66.2	67.9	65.2	65.7	65.6
19-Jun	68.6	66.9	68.1	67.6	67.9	64.8	67.5	67.8	67.7
27-Jun	70.4	81.9	70.3	67.8	70.7	72.5	69.7	70.2	70.4

Appendix 1 Table 23
Midday temperature in degrees Centigrade

Surface < 10 mm depth

Interior >100 mm depth

1995	North (green)		West (green)		South (red)		Air Temperature		
	surface	interior	surface	interior	surface	interior	North	West	South
Feb-02	7.2	15.2							
Feb-03	8.8	13.3	8.9	10.5	8.3	9.8	12.3	10.3	9.8
Feb-27	8.5	10.6	9.2	10.1	8.7	9.7	10.8	10.2	9.9
Feb-28	8.4	10.5	8.9	9.6	10.7	9.6	10.8	9.6	9.7
Mar-01	3.2	5.1	3.8	5.6	5.2	4.2	9.5	5.7	4.4
Mar-02	3.3	5.9	2.8	3.3	3.2	3.1	6.2	3.2	3.1
Mar-03	3.3	4.5	2.2	3.2	3.2	3.1	5.5	3.1	3
Mar-06	5	4.5	4.5	4.5	4.6	4.7	4.5	4.6	4.6
Mar-07	4.6	6.9	4.7	6.5	4.6	5	6.7	6.5	5
Mar-08	4.6	5.1	4.4	5.1	4.6	5.2	5	1	5.2
Mar-09	6.4	8.2	6.9	8.1	6.6	8.1	8.3	8.2	8.1
Mar-10	6.4	8.4	6.5	7.3	6.7	6.7	7.5	7.5	7.2
Mar-14	10	11	10.7	11	9.6	11.1	11	11	11
Mar-15	8	7.1	7.8	7.1	7.8	7.1	7.1	7.2	7.2
Mar-16	4.4	3.4	3.6	4.1	4.1	4.2	4	4.1	4.2
Mar-17	6.4	6.3	6.4	6.3	6.2	6.4	6.3	6.3	6.3
Mar-18	4.9	4.7	3.6	4.8	4.3	4.9	4.7	4.8	4.9
Mar-20	6.5	10.2	6.3	6.2	6.1	6	8.1	6	5.9
Mar-21	8.3	10.5	7.4	7.3	7.5	8.2	9.9	8	7.5
Mar-22	8.3	11.6	8.6	8.9	8.2	9.2	10.9	8.8	9.2
Mar-23	8.7	10.2	9.7	9.6	8.8	9.9	11.5	8.8	9.8
Mar-24	7.4	10.2	7.5	7.4	7.7	7.4	7.4	7.5	7.5
6-Jun	14.3	13.3	14.2	13.4	13.4	13.5	14.2	14.1	13.9
8-Jun	12.1	12	12.8	12.8	12.5	12.2	12	11.9	12.3
9-Jun	11.7	12.5	11.4	12.7	11.8	12.6	13	12.8	12.7
12-Jun	15	15.9	16.9	15.9	15.3	16	16.1	15.9	15.9
13-Jun	13.5	13.1	13.4	13.3	13	13.5	14.6	14.2	13.8
14-Jun	13.1	12.6	12.7	12.5	12.6	12.6	14.4	13	12.7
15-Jun	13.3	12.7	13.3	12.6	13	12.8	13.5	13.2	13
19-Jun	17.1	19	18.6	19	17.3	19	19.1	19	19.2
27-Jun	15.2	14.9	14.3	15.4	16	15.1	14	13.5	13.4

Appendix Two

***Sandstone decay mechanisms under examination on the
balcony stone of Culzean Castle, South West Scotland***

**III International Symposium on the Conservation of Monuments in the
Mediterranean Basin**

Sandstone decay mechanisms under examination on the balcony stone of Culzean Castle, South west Scotland

Carolyn S Hayles & Brian J Bluck
Department of Geology & Applied Geology
Lilybank Gardens Glasgow University
G12 8QQ Scotland

Abstract

The decay of a lithic arenite (sandstone) building on the South West Coast of Scotland is being examined using XRF, XRD, and SEM analyses. We have identified cement dissolution/re-precipitation, mineral disintegration, and salt crystallisation as the prominent causes of stone decay. The ingress of solutions exceeds egress. As such the exterior patina of the stone is allowed to dry out whilst solutions retained within the stone increase its hygroscopic moisture content prohibiting drying and inducing rapid salt out-crusting. Growth, volume change, and thermal expansion of soluble salts, carbonates, and clays at depths of up to 10 centimetres are resulting in destruction of the stone.

Keywords

Weathering, lithic arenite, salt crystallisation, calcium carbonate, swelling chlorite, hygroscopy.



Figure 1 - View of Culzean Castle from the sea

Introduction

Culzean Castle, property of the National Trust for Scotland, lies forty five miles South of Glasgow on the West Coast of Scotland (Figure 1). The main Castle building and a number of outbuildings, which were designed by Robert Adam and completed between 1777 and 1792, are of international importance. A majority of the stonework has suffered from prolonged exposure to the elements in their cliff-top setting above the salt waters of the Firth of Clyde.

Culzean has been constructed from at least four differ-



Figure 2 - Erosion of the Castle

ent sandstone which have been added to the building at different times and from a number of different sources. Whilst the degree of weathering is a function of age it is also clear that each sandstone type exhibits a different pattern of decay. In addition, the complex shape of the buildings, with their infinite number of micro climates impose yet another set of variables which affect the weathering of small individual parts of the building (Figure 2). The outcome of such diversity, is an inconsistency in the resistance of the building to decay.

The nature of the stones and their sources

The older parts of the Castle have been constructed from three different sandstones (volcanigenic lithic arenites) over three main periods. The basal structure was built during the Twelfth Century from stone which was quarried beneath Home Farm, facing the sea, on the Culzean Estate (grid reference 234 104). This is a quartz-rich lithic arenite, consisting of approximately 50% quartz. This stone has fared well on the Castle, presently exhibiting very little inherent decay. Adam's Georgian additions to the Castle, for which the Estate is renown, was built from a lithic arenite consisting of 33% quartz quarried at Ballochneil, near Girvan, grid reference 224 065. This stone is decaying rapidly, particularly on the sea-ward facing balcony (Figure 3), and it is the disintegration of this stone on which this paper will concentrate. The final part of the building was constructed during the Nineteenth Century from an arenite with 22% quartz, 30% feldspar, and 16% lithic fragments, quarried a few miles North of Maybole, grid reference 305 113. This younger stone also decaying, but not to the extent of the Eighteenth Century stone. More recently, replacement stone has been taken from quarries in the North East of England and Derbyshire.

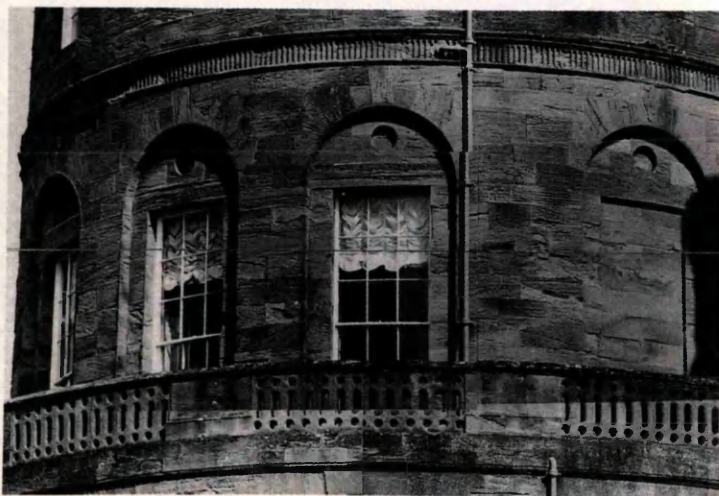


Figure 3 - The Eighteenth Century 'Adam Balcony'

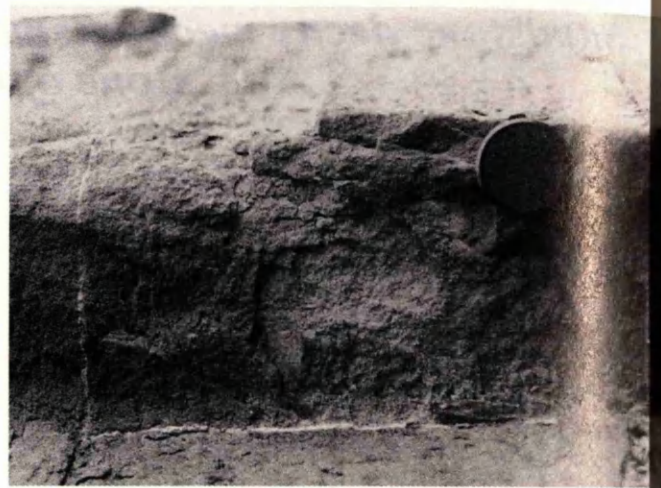


Figure 4 - Exfoliated block of sandstone from the North Face of the Balcony

Experimental work in analysing the nature of the weathering of the stone

Only the most decayed sandstones are analysed at this stage as they illustrate the maximum effects of weathering. For that reason, research at Culzean has concentrated on the Eighteenth Century 'Adam Balcony', where the stonework is in a variable state of decay from completely exfoliated blocks to blocks still intact (Figure 4). In order to determine the extent of damage and understand the mechanism causing it, selected parts of the building were drilled to a depth of 12 centimetres using a dry drill, six centimetres in diameter. Twelve cores were taken from the balcony, four from each aspect. A slow drill, without a lubricant, was used so that soluble salts within the stone would not be washed out during the drilling process. These cores were then quartered and subsequently used for (1) a quantitative measure of soluble salt, carbonate, and clay composition, (2) SEM and probe work, (3) XRF analyses, and (4) run-off assimilation.

Decay by carbonate dissolution and salt crystallisation

The amounts of soluble salt and carbonate was assessed from quartered-lengthways core which was then broken down into grain size fragments, placed in a beaker and rinsed through with deionized water allowing the dissolution and settling for 12 hours. The remaining solution was then siphoned off, centrifuged for thirty minutes, before being evaporated on a hot plate at 50 degrees centigrade allowing the soluble salts & carbonates to re-precipitate. This process was repeated until all soluble mater had been extracted and the precipitate was then analysed by XRD to establish compositions.

The remaining sample was divided between two, one hundred centimetre cubed cylinders and filled with ionized water. Fifteen millilitres of calgon were then added to each cylinder to allow the particles to disaggregate. The cylinders were shaken and the particulate matter allowed to settle over a period of eighty minutes (clay size of ten microns or less to be collected). The ten centimetres of solution were thus siphoned off and placed in a centrifuge for thirty minutes allowing the fine particles to settle. This process was repeated until all the clay of this particle size had been obtained. On drying, the clays were weighed and identified by XRD, chemical and SEM examination.

Soluble salt content generally decreases from the exterior to interior surface of the stone (Figure 5). The material obtained, on re-precipitation, contains halite (sodium sulphate), calcite (calcium carbonate), and gamma calcium sulphate. We therefore conclude that these mineral phases are likely to have been present in the stone on the building, although recognising that under different temperature regimes the solutes could produce different mineral phases.

From XRD examination, it can be seen that salts are present up to a 12 centimetre depth within the cores. Moisture has been drawn into the sandstone by capillary action and salts have precipitated out from solution. Ions in solution were both internally and externally derived. As the solute has been concentrated, a number of chemical and biochemical reactions have taken place, including the calcium carbonate cementing agent, and allowing it to be dissolved. SEM analysis provides evidence

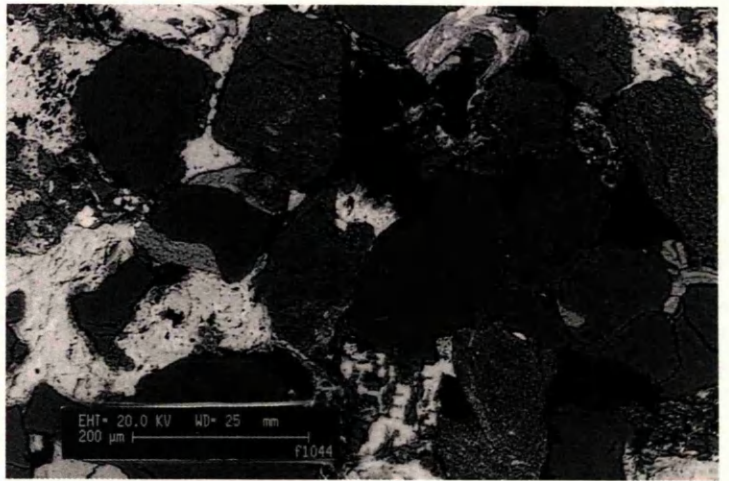


Figure 6 - SEM thin section of the sandstone examined

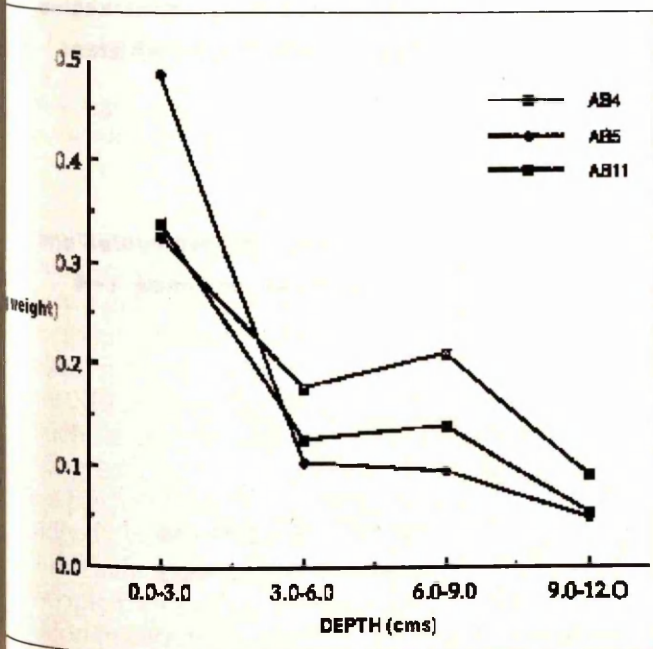


Figure 5 - Graph to show soluble salt and carbonate content by percentage weight of sample

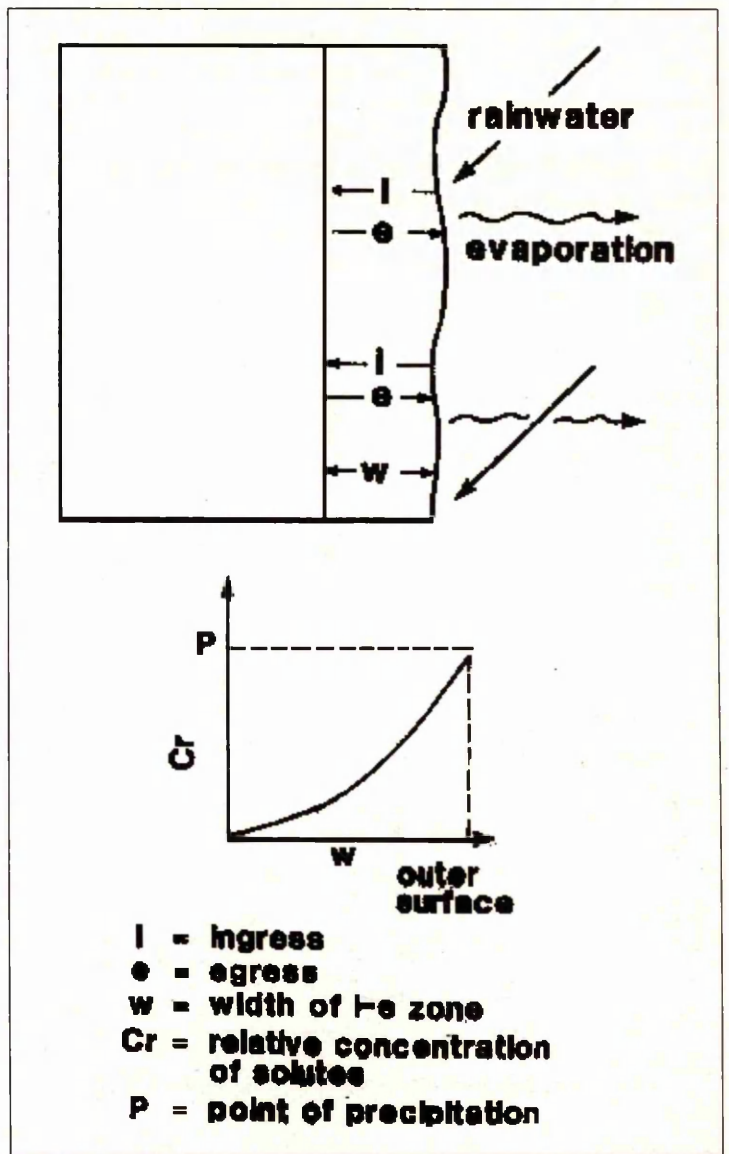


Figure 7 - Diagram to show the ingress/egress cycle of solutions at and beneath the surface of the stone

dence for the partial cracking of mineral grains, which provide a point of ingress for these solutions (Figure 6). This has enabled salt crystallisation within micro fractures which is a pressure producing process (Cooke, 1981), and may well have encouraged mechanical as well as chemical break-up.

Although there are a number of parameters which control the nature and site of precipitation of salts in the cycle of ingress and egress of fluids into the stonework of prime importance is the nature of concentration gradient developed on the egress part of the cycle (Lewin, 1982). Of particular significance is the concentration acquired by an egress of solution with respect to the stone surface: if concentration to the point of precipitation occurs at the surface then efflorescence results. At Culzean, on the Balcony, salts have precipitated beneath the surface (Figure 7) so we can assume that concentration gradients on the egress cycle were high.

There are many possible reasons for the salts precipitating beneath the surface. (I) That the ingress fluid is already concentrated in salts, or is of such a composition that it effects much solutioning of the rock constituents. In both these cases there is a greater than usual salt concentration in the fluids. (II) That the solutions, although having free access to the external (evaporating)

surface, reach precipitation point before getting there (III) The fluids did not ingress and egress through the same route. The ingress fluids were transmitted down the surface of the building, getting access to the interior through the surface fractures; and egress is limited because in the patina of the weathering front capillary

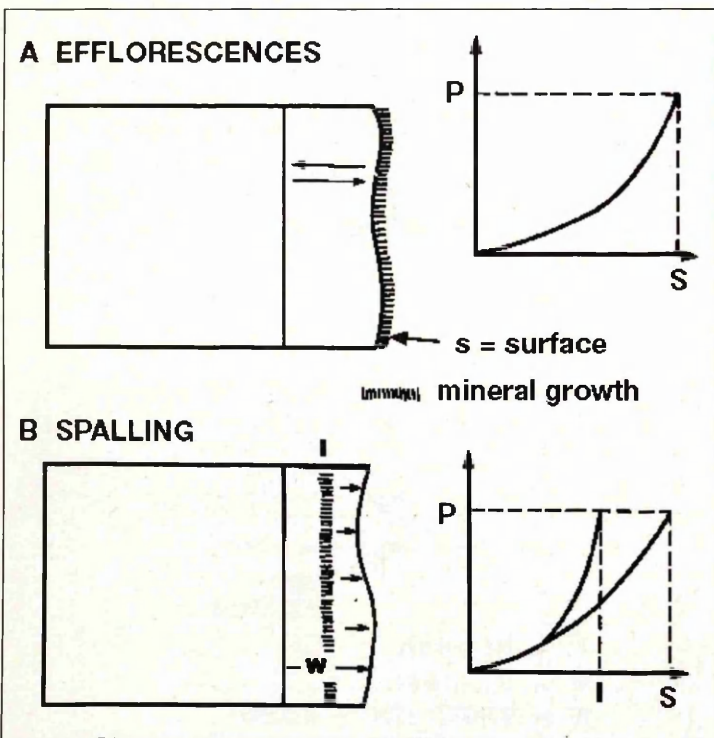


Figure 8 - Diagram to show the concentration of salts on the egress cycle

S = surface
 I = some level below the surface where precipitation may occur
 P = point of precipitation
 w = width of ingress/egress zone

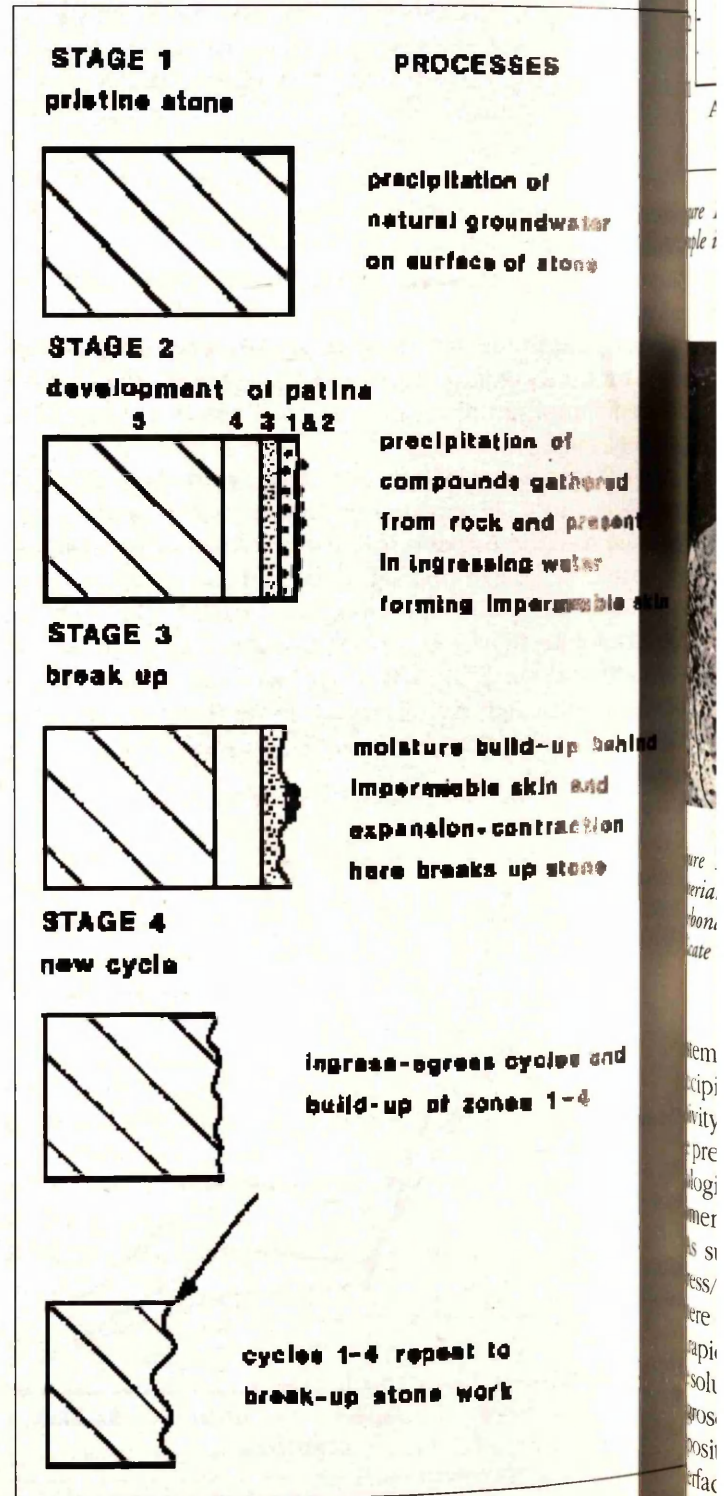


Figure 9 - To show the four stages of stone break-up

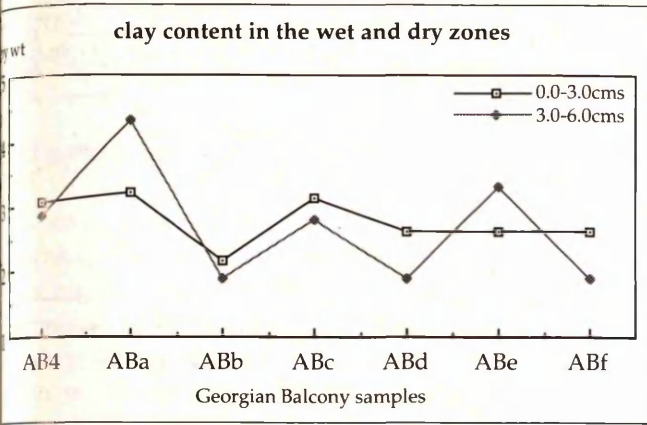


Figure 10 - Graph to compare clay content by percentage weight of sample in the outer 'dry' and inner 'wet' zones

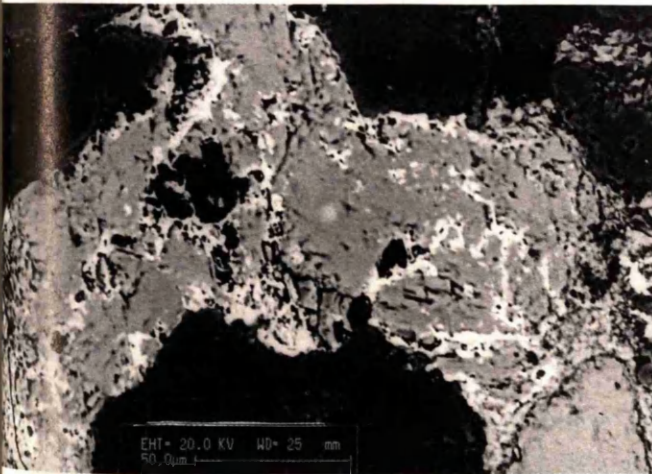


Figure 11 - Infilling of cracks in the carbonate cement by silicate material
Carbonate = grey material
Silicate = white material

Systems have been clogged by cement produced on re-precipitation. (IV) There was a level of micro biological activity at a given distance within the stone which caused precipitation of the salts there. The presence of micro biological activity is possibly indicated in the trace element XRF results (see below).
As such, a steady state has been established and an ingress/ingress balance is achieved at 5-45 mm depth, where a fresh solution is not being brought to the surface as rapidly as vapour is departing from it. In this instance, insoluble salts are trapped within the stone, increasing the hygroscopic moisture content, and as a result, this solute position front is marked by a boundary, a wet/dry stone surface; the depth of which varies over the balcony. As the wet zone blisters off, as has been seen in a number of cases, a new equilibrium is obtained. In some cases, where the dry

patina is in the process of blistering off, a second dry zone can be seen to be forming (Figure 8).

Therefore the growth of salt crystals in the wet zone are developing sufficient pressure to produce a contour scaling effect behind the dry zone. Visible surface alteration does not take place because ingress is greater than egress; there is no visual alteration to the stone surface. By the time the damage is noted, it is too late to save the exterior of the stone. Thus, unlike the process described by Rossi-Manaresi and Tucci, 1991, it is not the outer surface on the balcony at Culzean that is effected by contour scaling and crumbling, but the wet zone behind it. The outer dry, well cemented, crust will eventually spall because of the zone of decementation and mineral expansion behind it. This outer crust is strengthened by the possible activity of micro-organisms and the re-precipitation of calcite cement, whilst the wet stone behind it is weakened by salt production (and expansive clays) whose hygroscopic nature results in contour scaling (Figure 9).

Clay composition and distribution

The clay concentration through the profile remains fairly constant throughout (Figure 10). Clays present are

	Turekian & Wedepohl	Sample AB4 Balcony	Sample AB5 Balcony	Sample AB11
Ba	10-100	322	394	396
Ce	92	72	41	47
Co	0.3	20	11	21
Cr	35	250	85	91
Cu	1-10	30	5	
Ga	12	15	11	14
La	30	25	15	17
Ni	2	59	22	33
Pb	7	5	12	11
Rb	60	59	63	77
Sr	20	82	79	92
Th	1.7	5	4	9
U	0.45			
Y	40	19	17	18
Zn	16	47	22	32
Zr	220	280	146	136

Turekian & Wedepohl, Table 2
Geological Society of America Bulletin, Volume 72. pp175-191.

Table 1 - Table to show average concentrations of Trace Elements in core samples from Adam's Balcony, Culzean Castle, in comparison with average figures provided by Turekian & Wedepohl, 1961. (expressed in parts per million)

CATIONS	(ZiWi)	ANIONS	(ZiWi)
Sodium	1.84±0.003	Sulphate	6.48±0.06
Calcium	4.82±0.64	Chloride	0.46±0.006
Potassium	0.26±0.06	Acetate	0.11±0.002
Magnesium	0.70±0.20	Nitrate	0.13±0.002
TOTAL (ZiWi)	7.62±0.67	TOTAL (ZiWi)	7.18±0.07

Where:
 Zi charge on the ion
 Wi weight of ion in terms of the number of moles

Table II - Results to show balancing ion equivalences obtained by ion chromatography from the runoff assimilation experiment after 10 days

chlorite, kaolinite, illite, and an iron-rich silicate not yet identified. The chlorite is a magnesium rich expansive clay which swells when immersed in ethylene glycol (Chamley, 1990), and thus will expand in a hygroscopic environment such as has already been described. The kaolinite, which can be seen in association with illite, formed after the generation of the calcite cement, and is itself being replaced by the iron-rich silicate material of varying composition.

The iron-rich silicate can also be seen to have formed in micro fractures within the calcite cement. Silicate-rich solutions have entered these fractures (cf. Smith et al, 1985), have crystallised there and weakening the natural cement of the stone (Figure 11).

Iron enrichment at the surface

The iron enrichment seen will be the result of the dissolution of ferrous compounds under reducing conditions at the stone's surface (common in the presence of organic matter), by rain and runoff water, which will subsequently be oxidised (Krauskopf, 1982). With an exposed surface such as we have on the balcony at Culzean, these reactions will occur rapidly and the amount of iron 2+ present at one time will be undetectable.

XRF analyses of trace element distribution

Whilst numerous trace elements, specifically the rare earth elements are mobilised during weathering, they tend to be re precipitated at that site of weathering (Nesbitt, 1979). Despite this, a number of trends can be seen in the trace element distribution patterns through the cores analysed, which can be attributed indirectly to decay mechanisms. Sr is a mobile element, and high Sr levels are recorded particularly in the first few outer centimetres of those stones which retain their exterior

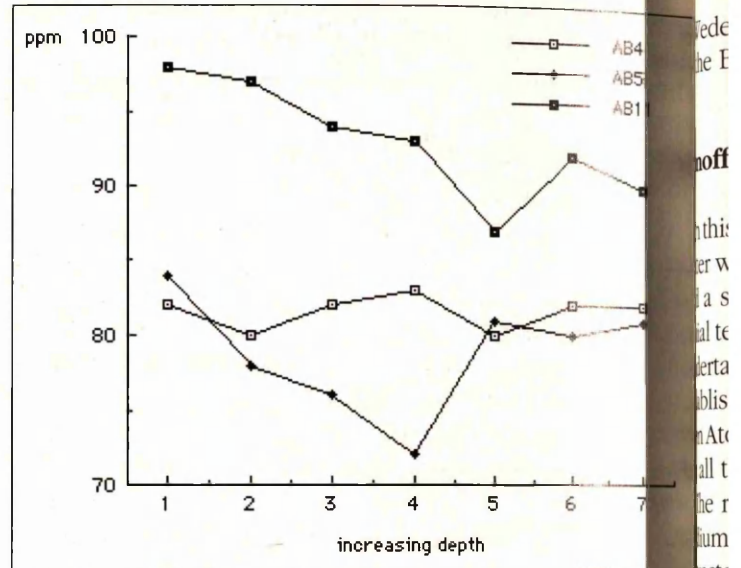


Fig. 12 - To show Sr concentration through 3 cores.

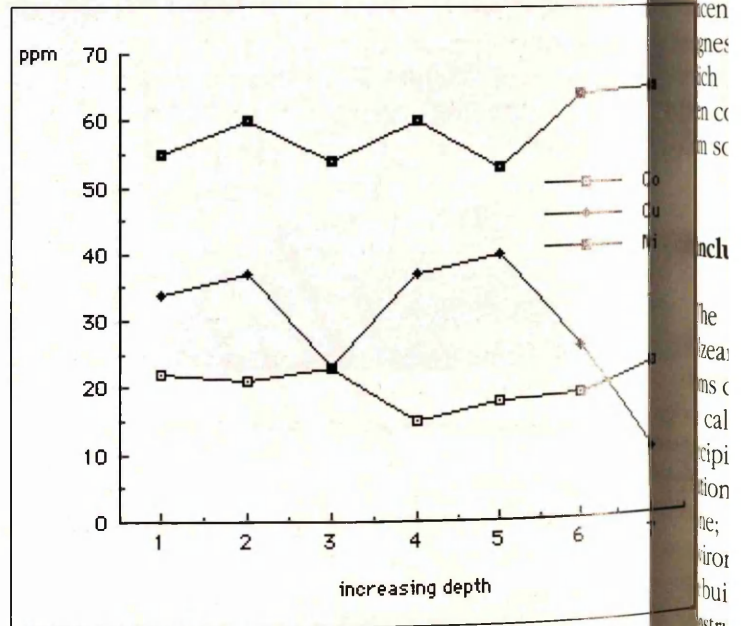


Fig. 13 - Co, Cu and Ni data from core AB4/1-7.

patina. This probably reflects the higher calcium levels in this outer zone which occur as a result of the redistribution of calcium carbonate cement from within the stone (Table 1), and the leaching of Ca and thus Sr from the surrounding mortar joints (Figure 12).

Enrichment trends in Ni, Cu and Co, which are commonly present in organic matter, can clearly be seen (Figure 13). Distribution will be dependent on precipitation following oxidation or reduction, and reactions with the organic matter (Krauskopf, 1982). Table I compares the average concentrations of these minor elements (Turkian, Sc

Wedepohl, 1961), to those found in the surface regions of the Balcony stone at Culzean.

Soil assimilation experiment

In this experiment, using a peristaltic pump, deionized water was continually flushed through a circular system, and a sample of water collected once a week after an interval of ten day period. Analyses of the water extract were undertaken using an ion chromatograph in order to establish which anions and cations were present, and Atomic Absorption was used to assess the time taken for all the mobile ions to be extracted.

The results, which can be seen in Table II show that sodium and calcium were the dominant cations to be extracted, with small amounts of potassium and magnesium present. It was mainly sulphate anions that were extracted, with evidence of chloride, nitrate, phosphate, and acetate at lower concentrations. The high sulphate concentrations result from the conversion of calcium and magnesium carbonate into the more soluble sulphates, which form several hydrates readily. This has already been confirmed by XRD analysis on salts reprecipitated from solution.

Conclusions

The research undertaken on the balcony stone of Culzean Castle shows that the most important mechanisms controlling decay rates on this part of the building are calcium carbonate dissolution and subsequent reprecipitation at the ingress/egress interface; salt crystallisation at this interface and within the wet portion of the stone; and swelling clays within such a hygroscopic environment. These factors are prevalent on this part of the building because of the material with the balcony was constructed and the harshest of wet weather conditions which the balcony is exposed. as a result the stone is inhibited from drying out and decay mechanisms are accelerated.

This is the study of only a small part of a great building. The prevalent mechanisms described only refer to the balcony stone at Culzean; much of the Castle and its captured stone is decaying quite differently and requires separate investigation.

Acknowledgements

We are very grateful to the offices of the National Trust in Scotland, Neal Sharp, Bob Heath, and the staff at

Culzean for all their assistance in the collection of material; and to the Getty Conservation Institute for funding the research program.

References

- Chamley, H. (1990) *Sedimentology*. Berlin, London.
- Cooke, R. U. (1981) Salt weathering in deserts. *Proceedings of the Geological Association.*, 92, 1-16.
- Krauskopf, K. B. (1982) *Introduction to Geochemistry*. McGraw-Hill International Editions, Earth and Planetary Sciences.
- Kunzel, H. (1991) The drying process blockage. *Bautenschutz und Bausanierung.*, 14, 63-66.
- Lewin, S. Z. (1982) The mechanisms of masonry decay through crystallisation. *National research council-conservation of historic stone buildings and monuments*.
- Nesbitt, H.W. (1979) Mobility and fractionation of rare earth elements during weathering of a granodiorite. *Nature.*, 279, 206-210.
- Rossi-Manaresi, R. and Tucci, A. (1991) Pore structure and the disruptive or cementing effect of salt crystallisation in various types of stone. *Studies in Conservation.*, 36, 53-58.
- Smith, McGreevy, and Whalley (1985) Silt production by weathering of a sandstone under hot arid conditions: an experimental study. *Journal of Arid Environments.*, 12, 199-214.
- Turekian, K. K. and Wedepohl, K. H. (1961) Distribution of the elements in some major units of the Earth's crust. *Bulletin of the Geological Society of America.*, 72, 175-192.

Appendix Three

***An examination of some of the causes of sandstone
deterioration at Culzean Castle - Scotland***

1995 LCP Congress: Preservation and Restoration of Cultural Heritage

Preservation and restoration of cultural heritage

**Stone Materials
Air Pollution
Murals
Scientific research work and case studies**

**Proceeding of the 1995 LCP Congress
Montreux 24-29 September 1995**

**Edited by Renato Pancella
Laboratoire de Conservation de la Pierre
Département des matériaux
Ecole Polytechnique Fédérale de Lausanne**

An examination of some of the causes of sandstone deterioration at Culzean castle - Scotland

C. S. Hayles, B. J. Bluck

Department of Geology and Applied Geology - University of Glasgow - Scotland

Abstract

The sandstone used by Robert Adam to build part of Culzean castle in the eighteenth century is decaying by exfoliation due to salt burst, clay growth, cement redistribution, and mineral dissolution. Using XRF, XRD and SEM, a redistribution of carbonates, silicates, sulphates and chlorides have been identified, and this has resulted in a loss of binding within the stone and a partial reprecipitation of material on the exterior.

Introduction

Whilst there has been much research into the deterioration of sandstone buildings involving close examination of the characteristics of the exterior surface of the stone, there has been less work directed towards the understanding of the decay process on buildings in the light of what is known about weathering processes of sandstone generally. Using mineralogy and geochemistry we begin by establishing the weathering profile for the Culzean sandstone, and then discuss some of the mechanisms which may be responsible for the profile.

The buildings at Culzean are situated on a cliff-top above the Firth of Clyde and are exposed to westerly winds which bring salt water onto the sandstone surface. Halite crystal growth pressures in the stone at Culzean and their effect on its decay have been discussed by Hayles & Bluck, (1994).

Fluids ingress and egress through the pore-space of the stone as a consequence of wetting and drying. This activates an important means of stone deterioration with the movement and redistribution of ions at depth in the stone. The fluids which ingress into the stone have dissolved ions from the atmosphere and on the stone surface; but on egress, ions dissolve from the minerals and increase in concentration as they are drawn by capillarity towards the surface where evaporation takes place. The chemical reactions that arise are on the whole straight forward and involve ionic dissociation, addition of H₂O and CO₂, hydrolysis, and oxidation of, for example, unstable aluminosilicates.

At these low temperatures and with fluids of variable ionic composition and degrees of supersaturation, minerals with complex composition and mixed mineral phases are precipitated out, with different mineral phases forming depending on the ionic medium and the pH of the ingressing fluids. This is further complicated by the potential for different solid phases to form from a supersaturated solution making the interpretation of data and the description of crystallisation mechanisms complicated. For this reason it is necessary to discuss the geochemical processes working through the stone profile and the chemical solid phases produced in order to assess the resulting deterioration propensity.

Data Acquisition

Cores for analysis were obtained from the balcony of the Drum tower at Culzean castle, South West Scotland. Culzean was built over three main periods, the most architecturally important of which was designed and constructed by Robert Adam. The Drum Tower is part of Adam's Eighteenth Century additions to the castle (1777-1792). Adam used a locally quarried volcanogenic lithic arenite which has since suffered from its prolonged exposure in a cliff top location overlooking the Firth of Clyde, weathering to varying degrees according to position, architectural design, exposure and mineralogical properties.

In order to determine and understand the processes at work in the stone, cores have been drilled to a depth of fifteen centimetres using a dry drilling method. Details of the cores and their division for analysis are recorded in Tables 1 and 2. Current findings have been reported in three sections; clay characterisation, mineral dissolution: feldspar and lithic fragment instability, and cement composition and mobility:

	Surface Colour		Surface Properties			Aspect		
	Green	Red	Fresh	Patina	Scaling	North	West	South
Cores								
AB1		+			+			+
AB2		+			+			+
AB3	+			+				+
AB4	+				+			+
AB5		+	+					+
AB6	+			+				+
AB7	+			0				+
AB8		+	+					+
AB9	+				+			+
AB10		+	+					+
AB11	+			0				+
AB12		+	+					+
+ denotes property of stone								
0 denotes cement rendered surface								

Table 1 : Core properties.

	number	cms depth
XRF	AB1/1	00.0-01.0
	AB1/2	01.0-02.0
	AB1/3	02.0-03.0
	AB1/4	03.0-04.0
	AB1/5	04.0-05.0
	AB1/6	08.0-09.0
	AB1/7	12.0-13.0
SEM	AB1/1	00.0-03.0
	AB1/2	03.0-06.0
	AB1/3	06.0-09.0
	AB1/4	09.0-12.0
	AB1/5	12.0-15.0

Table 2 : Core slices.

Clay characterisation

Clay minerals (sheet silicates), being subject to hydrolysis and volumetric changes are a key mineral in sandstone degradation. The continual ingress and egress of fluids and the potential of the stone to retain moisture for long periods, provide the water and other ions (such as sodium) which allow the clays to expand. Within a rock mass under conditions of high confining pressures and sometimes elevated temperatures the clays are unable to expand, even when they contain an appreciable proportion of expansive minerals.

When the general conditions are altered, (change in mass, temperature and humidity) as when they are used in numerous small slabs for building; clay minerals, particularly smectites, prove explosive, and trigger 'rapid' decay in geological terms. It is therefore necessary to evaluate the importance of clay minerals present in the stone, and the influence of their chemical alteration on its performance and longevity .

The presence and character of the clays in the sandstone have been assessed using the scanning electron microscope (SEM) because the detection limits of other petrographic techniques would not be sufficient when looking at the clay present in the cement, within the grains, and at the intergranular crevices; and X-ray diffraction (XRD) by undertaking six-hour sedimentations (to obtain the fraction $<2\mu\text{m}$ by centrifugation) and analysing these sediments in four stages: the sediment; sediment + glycol; sediment + glycol + 300°C heat; sediment + glycol + 600°C heat.

The stone at Culzean is rich in clay. Surface and subsurface depletion/enrichment is not uncommon where the ingress/egress of penetrative solutions has been the most aggressive.

The clay minerals present in this case include transitional complex associations and precise identification of the natural clay assemblages is difficult because besides the kaolinite, readily identified by both XRD and SEM, the neomorphic minerals are very small, poorly and diversely crystallised, and are associated with subamorphous compounds, particularly those silicates embedded within the carbonate cement.

The XRD results show an expanding mixed-layer clay identified as illite-smectite. Random illite-smectite is the most common abundant mixed-layer clay in sandstones, which result from the progressive degradation on weathering and progressive diagenesis. Like all silicates, mixed layer silicates are hygroscopic, but have the additional ability to retain excess water in their interlayer sites.

The large chlorite peak identified at 14A' is indicative of a non expansive mineral (with a collapsing OH structure at 600°C). However, additional results obtained from SEM spot-analysis of silicates in the cement indicate chlorite-smectite compositions, with ions of Na, K, and Ti in addition to Al, Fe, and Mg.

Due to their fine grained nature, characterisation of chlorite grains is often difficult, and in many sediments the chlorite present is in mixed-layer structures. Mixed-layer chlorites are derived from the aggregation of less organised sheet minerals by the degradation of pre-existing ferromagnesium minerals, and by the crystallisation from dilute solutions of their components, which will be greatest where the fluid/stone contact is at its most intense. This would suggest the variations include chlorite-smectite, kaolinite-chlorite, and illite-smectite-chlorite.

However, the chlorite-smectite present may not be a mixed layer clay species, as the two can coexist during alteration from chlorite to smectite. SEM analysis of interstitial silicates within the carbonate cement and at grain boundaries indicate that compositional variations of the interstitial clay fraction decreased with depth in the core profile; these findings are congruous with those of Mausfeld & Grassegger, 1994 who also found depth-related changes in the clay mineralogy of the building stone from the Romanesque Basilica of St. Vitus, Ellwangen, S.W.Germany.

Thus these results show that the chlorite/smectite/illite clay composition in the deeper regions of the cores are more regular indicating that it is the current weathering phenomenon causing such compositional variations in the stone profile as a direct result of the ion exchange capacity of the stone activated by the migration of fluids through the stone.

XRD and SEM have been used not only to identify the major clay mineral phases but also pinpoint the occurrence of specific species and their chemical compositions. From these analytical methods three main clay groups have been established:

1. Kaolinite formation in pore spaces, which is the main diagenetic process and constitutes the majority of clay formation in the stone;
2. The replacement of feldspars and lithic fragments, and the deterioration of micas, initially diagenetic in origin;
3. The formation of additional sheet silicates within the carbonate cement.

Groups 2 and 3 include the forms of illite-smectite, chlorite, and chlorite-smectite described, and are the most significant in terms of current deterioration processes because they form in intergranular crevices where upon expansion due to hydration, they break down the cohesiveness of the stone.

Mineral dissolution

From the character of the clays and their distribution, one is aware how important it is to look at the effect of the mobility of ions in all of the stone. This has been done by slicing the cores as indicated in Table 2 and analysing the material by X-ray Fluorescence (XRF). The results obtained are shown in Table 3.

The variability of the chemical composition of the stone is immediately apparent in near-surface regions where fluid ingress/egress is at its most intense. Of foremost importance therefore is to recognise trends associated with mineral compositions. K, Al, Na, and Ca are all constituents of feldspar:

Feldspar = X (Al, Si)₄ O₈ where X = Na, K, Ca, Ba

KO, AlO and NaO exhibit a significant mobility potential in the outer 5 cms of the stone profile. (Figure 1: Core profiles from XRF data). In accordance with this, SEM analysis has established that the amount of altered feldspars and lithic rock fragments exhibiting dissolution features and associated clay increases exponentially towards the surface of the stone, whilst the proportion of fresh feldspars and lithic rock fragments decreases. Combined with the data on clay composition and distribution, this would suggest that aluminosilicates dissolve under weathering conditions during time spans of, in this case, 200 years.

Carbonate cement composition and distribution

Carbonate as a pre-diagenetic cementing agent plays a very important role in the current stone deterioration because carbonates are subject to acid attack as the carbonate group CO₃⁻ combines with a hydrogen ion to form HCO₃⁺, a stable bicarbonate ion.



The cement in this case is a ferroan calcite, a calcium carbonate invariably rich in Fe, Mg, and to a lesser extent Mn. The composition of the cement changes through the core. This variation may result from the dissolution of the cement and its components by aggressive solutions and the subsequent reprecipitation of the material, often enriched in Fe and Mg. Goethite (FeOOH), a common weathering product of Fe-bearing minerals and silicates, is intermixed with the cement.

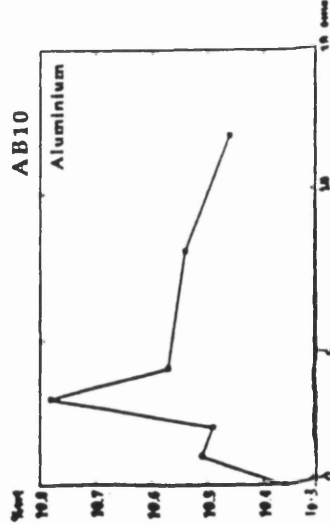
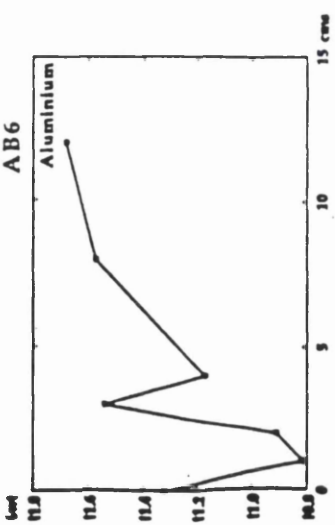
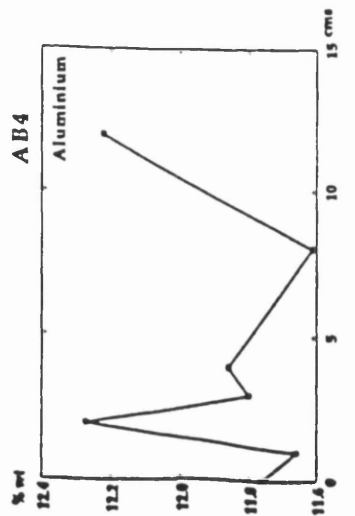
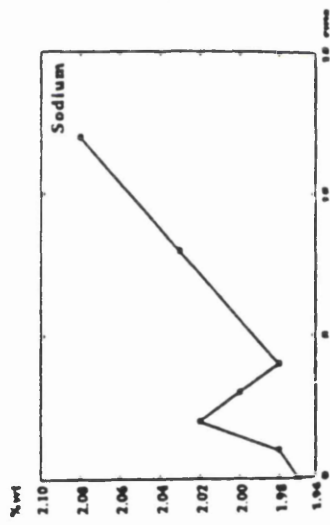
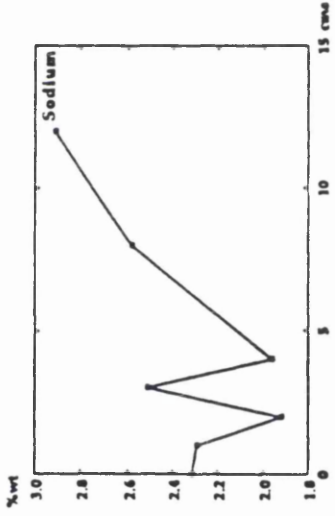
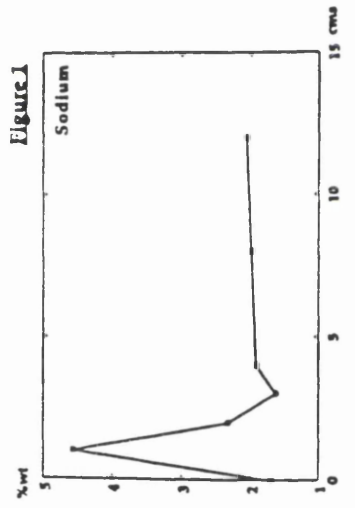
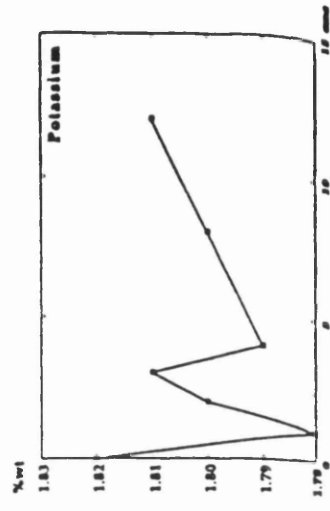
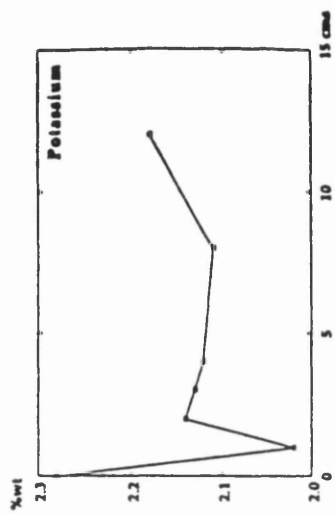
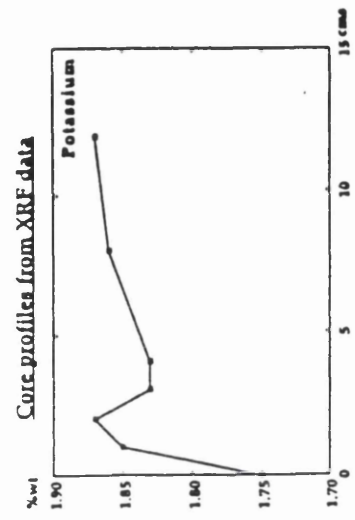
Migrating fluids are driven into the stone by capillarity and gravity through micropores and the cracking of near surface minerals, dissolving the calcium carbonate, and transporting it towards the surface during solution egress when the surface dries. This cement does not reach the surface because the capillary tubes are blocked (hard patina surface) preventing egress=ingress, and thus deposition occurs at depth. Most activity of this kind occurs within mms of the stone surface where the greatest number of variables are at work.

In some cases enrichment of the outer surface in the elements discussed is apparent. This occurs in sample AB4 where the hard outer casing of the stone has fallen away and the underlying contour scaling surface, now exposed, still retains some of its enrichment character relating to its former profile. In such cases the ingress/egress balance has been disturbed as the outer layer which completed the profile has been lost. Eventually the zone of enrichment will shift so that the surface of contour scaling will become the zone of mobile element enrichment.

For example AB1 and AB2, exposed contour scaling surfaces, where ingress > egress and reprecipitation occurs at depth. It is not yet known whether a further hard, 'biogenic' patina will be formed, indeed the rotten stone is hydrated and structurally weak and unlikely to withstand the exterior processes to which it is being exposed. A number of mullion edges suggest new zonal formation beneath the contour scaling, however this too is likely to be a continuation of the contour scaling phenomenon.

	SiO2	NO2	Al2O3	Fe2O3	MnO	MgO	CaO	Na2O	K2O	PTOS	Total
AB1/1	66.12	0.46	10.86	4.73	0.07	0.88	6.25	1.67	2.13	0.08	83.32
AB1/2	66.86	0.44	11.1	4.23	0.08	1.15	6.47	1.38	2.22	0.08	88.1
AB1/3	65.18	0.43	10.87	4.2	0.08	0.81	6.18	1.65	2.16	0.08	81.75
AB1/4	66.06	0.43	10.81	4.31	0.1	1.03	6.25	1.72	2.15	0.08	82.84
AB1/5	65.18	0.4	10.84	4.47	0.08	0.88	6.6	1.88	2.2	0.08	82.43
AB1/6	65.58	0.4	8.82	4.3	0.11	1.03	6.68	1.71	2.21	0.08	81.74
AB1/7	66.03	0.4	10.02	3.8	0.11	0.88	6.82	2.18	2.21	0.08	81.74
AB2/1	70.18	0.44	11.42	2.23	0.07	0.83	5.58	1.81	1.83	0.1	84.3
AB2/2	67.02	0.45	11.21	2.1	0.07	0.38	5.91	2.78	1.88	0.21	82.03
AB2/3	68.38	0.45	10.8	2.11	0.07	0.84	5.88	2.86	1.81	0.2	84.52
AB2/4	68.35	0.45	10.8	2.03	0.07	0.8	5.82	2.23	1.83	0.1	82.48
AB2/5	68.18	0.48	11.27	1.98	0.08	0.57	5.81	2.24	1.87	0.14	82.73
AB2/6	68.83	0.48	11.38	2.04	0.07	0.88	5.88	1.75	1.87	0.18	83.08
AB2/7	68.88	0.48	11.28	2.11	0.07	0.88	5.83	1.88	1.82	0.12	83.12
AB3/1	68.82	0.28	9.18	2.12	0.1	0.82	8.03	2.81	2.35	0.08	84.48
AB3/2	68.31	0.27	8.54	2.04	0.08	1.02	8.28	2.18	2.22	0.08	84.85
AB3/3	67.48	0.31	8.8	2.14	0.08	1.28	8.4	2.53	2.16	0.07	83.07
AB3/4	68.88	0.28	8.33	2.02	0.1	1.05	8.33	1.84	2.15	0.15	88.05
AB3/5	68.88	0.3	8.04	1.88	0.08	1.15	8.08	2.38	2.2	0.08	83.84
AB3/6	68.31	0.28	8.82	1.85	0.08	0.84	7.88	2.01	2.21	0.07	83.35
AB3/7	68.43	0.28	8.84	1.88	0.08	0.81	8.23	2.27	2.21	0.07	85.13
AB4/1	65.23	0.8	11.78	6.38	0.05	1.42	2.81	1.7	1.75	0.13	82.14
AB4/2	68.38	0.81	11.88	6.28	0.04	1.18	2.87	4.57	1.85	0.13	87.8
AB4/3	68.13	0.87	12.27	5.75	0.05	1.4	2.35	2.32	1.87	0.13	85.14
AB4/4	67.28	0.83	11.8	5.53	0.06	1.34	2.44	1.84	1.83	0.13	82.88
AB4/5	68.58	0.85	11.88	5.34	0.06	1.8	2.45	1.81	1.83	0.12	82.58
AB4/6	65.44	0.83	11.81	6.34	0.05	1.32	2.88	1.88	1.84	0.12	82.44
AB4/7	68.38	0.85	12.22	7.34	0.05	1.41	2.8	2.35	1.87	0.13	84.78
AB5/1	71.87	0.47	11.53	4.06	0.08	0.88	7.45	2.88	2.1	0.07	100.72
AB5/2	63.22	0.4	10.1	3.35	0.08	0.84	6.48	2.78	1.8	0.08	82.2
AB5/3	67.88	0.38	10.44	2.05	0.08	0.82	5.44	2.34	2.07	0.1	81.43
AB5/4	67.87	0.41	10.83	3.27	0.08	0.48	6.87	1.52	2.08	0.08	83.15
AB5/5	66.57	0.47	10.1	3.41	0.08	0.81	6.71	2.11	1.87	0.08	82.31
AB5/6	66.8	0.42	10.41	3.21	0.1	0.82	6.78	2.07	2.02	0.08	82.58
AB5/7	66.47	0.43	10.44	3.18	0.1	0.82	6.78	1.85	1.83	0.08	82.14
AB6/1	71.41	0.52	11.32	4.55	0.06	2.41	2.55	2.31	2.28	0.08	87.48
AB6/2	63.8	0.53	10.81	4.83	0.06	2.28	3.32	2.28	2.02	0.08	88.8
AB6/3	66.48	0.5	10.81	4.68	0.08	2.25	3.83	1.82	2.14	0.08	84.84
AB6/4	66.01	0.5	11.54	4.83	0.08	2.48	3.85	2.51	2.13	0.08	85.87
AB6/5	68.72	0.51	11.17	4.82	0.05	2.33	3.17	1.88	2.12	0.08	85.74
AB6/6	67.02	0.5	11.57	4.7	0.04	2.12	2.88	2.58	2.11	0.08	83.82
AB6/7	68.45	0.52	11.88	4.88	0.04	2.42	2.87	2.81	2.18	0.08	85.85
AB7/1	68.83	0.48	11.42	4.76	0.04	1.85	2.44	2.31	2.53	0.08	85.54
AB7/2	71.85	0.54	12.21	4.83	0.04	1.87	2.22	1.54	2.51	0.08	87.88
AB7/4	50.05	0.34	7.88	3.24	0.02	1.88	1.48	1.48	1.87	0.08	87.8
AB7/5	67.8	0.53	11.82	4.84	0.05	2.18	3	1.83	2.44	0.08	84.48
AB7/6	68.43	0.45	11.83	5.52	0.05	2.1	2.18	1.88	2.42	0.11	85.23
AB7/7	70.54	0.73	12.18	8.01	0.05	2.21	2.15	1.88	2.48	0.11	88.3
AB8/1	68.11	0.4	10.42	3.22	0.12	1.02	7.42	1.88	2.01	0.08	84.88
AB8/2	68.32	0.4	10.25	3.24	0.11	0.88	7.45	2.44	1.88	0.08	85.14
AB8/3	68.05	0.4	10.88	3.12	0.1	0.58	6.88	1.82	1.88	0.08	84.14
AB8/4	68.24	0.41	10.51	3.45	0.08	0.84	6.82	1.84	1.88	0.08	84.14
AB8/5	67.08	0.32	8.85	2.82	0.08	0.88	5.51	1.47	1.84	0.07	78.28
AB8/6	67.22	0.38	10.38	3.2	0.08	0.82	6.74	1.88	1.8	0.07	82.58
AB8/7	67.87	0.41	10.84	3.2	0.1	0.77	6.85	1.83	1.81	0.08	83.57
AB9/1	66.22	0.58	10.85	4.47	0.07	1.52	4.57	2.01	1.88	0.1	82.07
AB9/2	68.88	0.58	10.3	4.84	0.08	1.44	4.88	2.2	1.84	0.08	82.88
AB9/3	65.28	0.28	5.38	2.31	0.04	0.88	2.28	1.88	1.88	0.05	48.43
AB9/4	67.08	0.58	10.52	4.52	0.08	1.51	4.73	2.28	1.84	0.08	83.27
AB9/5	68.27	0.52	10.5	4.21	0.07	1.38	4.41	4.41	1.88	0.08	85.81
AB9/6	65.73	0.53	10.38	4.35	0.08	1.5	4.8	3.8	1.85	0.08	83.1
AB9/7	65.85	0.53	10.47	4.54	0.08	1.52	4.58	3.27	1.87	0.08	82.88
AB10/1	65.28	0.42	10.38	3.13	0.11	0.78	8.01	1.87	1.82	0.07	82.01
AB10/2	66.54	0.44	10.51	3.38	0.08	0.78	7.28	1.88	1.78	0.08	82.88
AB10/3	66.87	0.43	10.48	3.24	0.08	0.73	7.07	2.02	1.8	0.08	82.82
AB10/4	66.58	0.48	10.78	3.28	0.1	0.72	7.22	2	1.81	0.08	83.02
AB10/5	66.48	0.44	10.57	3.28	0.08	0.73	7.28	1.88	1.78	0.08	82.72
AB10/6	66	0.43	10.54	3.3	0.1	0.72	7.44	2.02	1.8	0.08	82.44
AB10/7	66.18	0.43	10.48	3.8	0.11	0.72	7.58	2.08	1.81	0.08	83.37
AB11/1	64.81	0.48	11.81	4.52	0.08	1.11	6.71	1.82	2.2	0.08	83.51
AB11/2	64.38	0.44	11.7	4.75	0.08	1.08	6.32	1.48	2.2	0.08	82.52
AB11/4	63.3	0.44	11.88	4.48	0.07	0.8	6.28	1.48	2.18	0.08	80.8
AB11/5	66.08	0.48	11.38	4.24	0.08	0.88	6.78	1.85	2.25	0.08	83.88
AB11/6	65.17	0.42	12.88	3.88	0.08	1.18	6.75	1.84	2.22	0.08	84.28
AB11/7	65.14	0.44	12.28	3.81	0.07	1.2	6.53	1.58	2.21	0.08	83.34
AB12/1	73.77	0.57	11.28	2.45	0.04	1.28	2.84	3.58	1.83	0.1	87.82
AB12/2	71.88	0.55	10.83	2.32	0.05	1.38	3.33	1.8	1.87	0.08	84.12
AB12/3	71.88	0.53	10.82	2.27	0.05	1.21	3.47	3.73	1.88	0.08	88
AB12/4	72.82	0.54	10.44	2.41	0.04	1.08	3.38	3.81	1.83	0.08	86.35
AB12/5	72.28	0.52	10.87	2.4	0.04	1.42	3.37	2.38	1.83	0.08	85.28
AB12/6	73.12	0.48	11.12	2.38	0.02	1.28	3.48	3.48	2	0.08	88.44
AB12/7	74.81	0.48	10.88	2.31	0.04	1.2	3.45	2.84	1.88	0.08	87.17

Table 3 : XRF results for core samples taken from the Drum tower, Culzean castle. Results given by percentage weight of the total content.



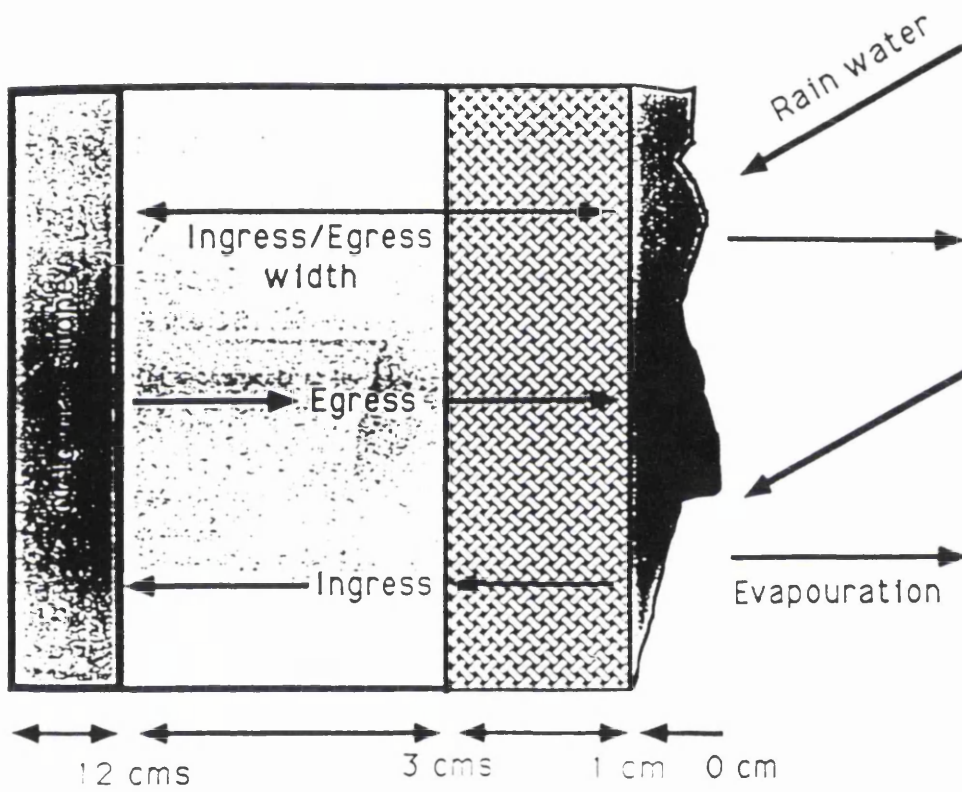


Figure 2a

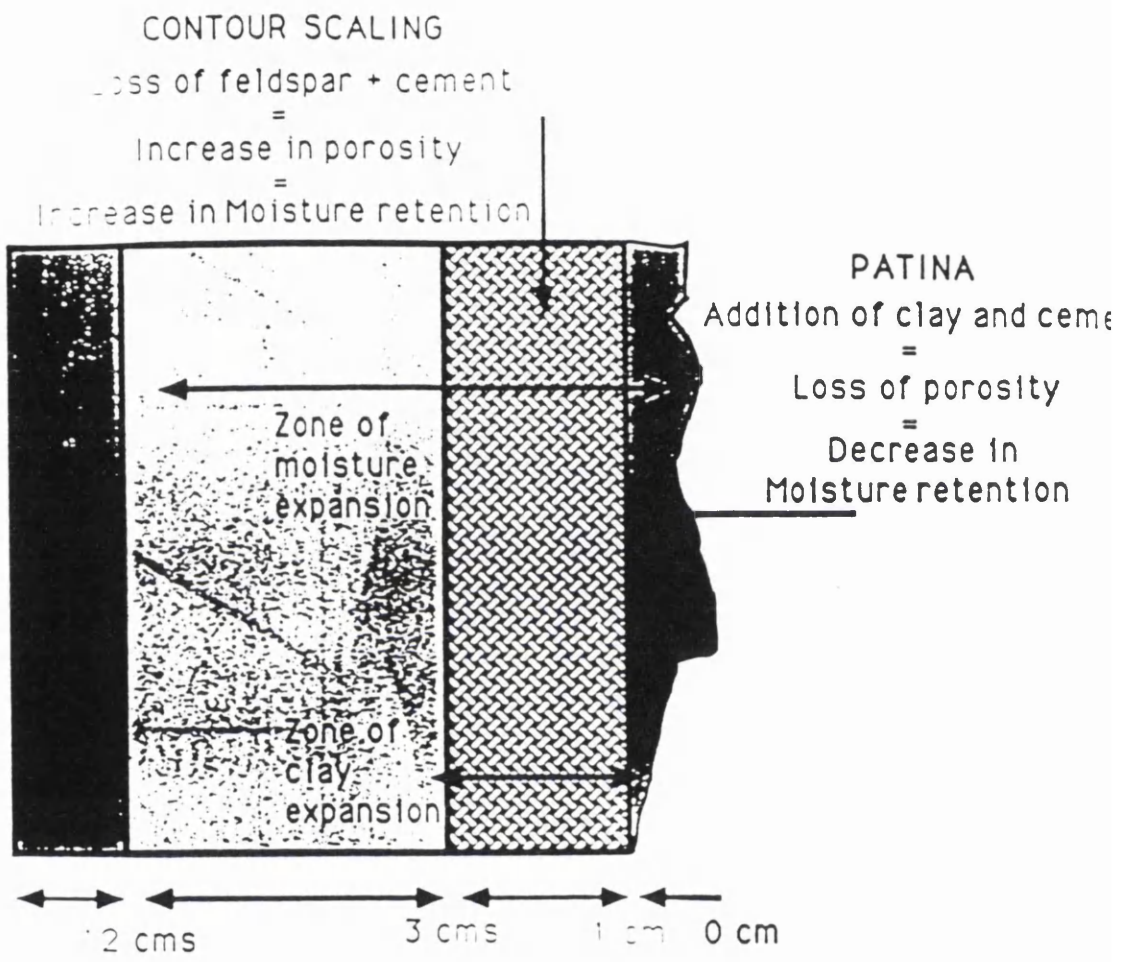


Figure 26

Summary

We present a genetic model of stone decay by re-distribution of mobile elements, mineralogical changes and clay expansion. This model must now be used to predict the fate of other buildings constructed of similar stone. The model has been produced using the data obtained from stone samples (all at various stages of weathering). Analysis of core slices show that beneath the outer, 'biogenic' patina, at a depth of > 0.3 cms, there is the zone of maximum fluid movement where ion mobility potential is greatest. This is the zone of contour scaling/spalling where ingress > egress and where solutions retained within the stone increase its hygroscopic moisture content and prohibiting drying (Figure 2a).

It is in this zone of weakness that certain ions in solution, such as CaO, MnO, MgO, and FeO are enriched, whilst K₂O, SiO₂, Na₂O, and Al₂O₃ are depleted. Of particular importance is the quality of the intergranular cementation, with the redistribution of calcium through the core as a result of cement dissolution and reprecipitation (Figure 2b).

The processes at work within the stone from its emplacement in the castle are controlled by the elimination of confining pressures, the ingress and egress of fluids, and the enhanced temperature and humidity variations controlling the fluid movement, resulting in a series of deterioration features.

References

- Hayles, C. S. & Bluck, B. J.
Sandstone decay mechanisms under examination on the balcony stone of Culzean Castle, South West Scotland.
The conservation of monuments in the Mediterranean Basin, (ed Fassina, V., Ott, H., & Zezza, F.), Proceedings of the 3rd international symposium, Venezia, 1994, 729-735.
- Krauskopf, K. B.
Chemical weathering, Chapter 4, Introduction to geochemistry,
Ed. K. B. Krauskopf, McGraw-Hill International Editions, Earth & Planetary Sciences, 79-97.
- Lewin, S. Z. & Charola, A. E.
Scanning Electron Microscopy in the diagnosis of 'diseased' stone,
Scanning Electron Microscopy, 1, 1978, 695-704.
- Mausfield, S. A. & Grassegger, G.
The changing environment of pore solutions in natural building stones during immission accelerated weathering processes,
The conservation of monuments in the Mediterranean Basin, (ed Fassina, V., Ott, H., & Zezza, F.), Proceedings of the 3rd international symposium, Venezia, 1994, 129-134.
- Reddy, M. M.
Physical-chemical mechanisms that affect regulation of crystallisation,
Chemical aspects of regulation of mineralization, Ed. Sikes & Wheeler, 1988.

Résumé

Le grès utilisé par l'architecte Robert Adam pour construire une partie du château de Culzean au XVIII^e siècle est actuellement en train de se détruire principalement à cause de:

1. l'augmentation du volume des sels
2. l'expansion des argiles
3. la redistribution du ciment
4. la dissolution des minéraux constituants.

A l'aide de XRF, XRD et SEM, nous avons identifié une redistribution des carbonates, des silicates, des sulfates et des chlorures qui peuvent être à la cause d'une perte de la cohérence intérieure de la roche et de la re-précipitation de ces composés à l'extérieur.

Appendix Four

***Culzean Castle Project: Microbiological examination of
sandstone construction material***

Pollution Research Unit

Napier University

By

J H Kinross & N Christofi

Microbiological examination of sandstone construction material

This is a report produced in conjunction with the work presented in this thesis to describe and explain the processes of microbiological degradation.

It is important to note that all the samples analysed produced algae and in some cases undamaged stone contained higher microbial populations when directly compared with decayed stone. This is in accordance with observations on the OB samples reported in the thesis.

It is suggested that carbonates are being converted into insoluble sulphate with an increase in volume. However results show no S-oxidisers, therefore the sulphate produced may be the result of geochemical reactions and not microbiological/ biochemical. There is no geochemical evidence for this conversion, and this will not account for the higher sulphate levels seen in the AB samples.

It is also possible that organic acids will increase the solubility of some cations (chelation), particularly Al and Fe. However there is no evidence for organisms producing mineral acids, no oxalates were found in the AB, VB, and OB samples analysed by XRD, and there is an inverse relationship between lichen activity (growth) and stone degradation. Therefore cation

chelation and not acidification by mineral acids will be responsible for dissolving the stone's matrix.

It is unlikely that mineral acids of microbial origin are important in the ashlar stonework degradation at Culzean.

CULZEAN CASTLE PROJECT :
Microbiological Examination of Sandstone
Construction Material

Authors: John H Kinross and Nick Christofi

**Pollution Research Unit
Napier University
10 Colinton Road
Edinburgh EH10 5DT**

February 1993

CONTENTS

	Page
Introduction	1
Materials and Methods	2
Results	2
Discussion	3
Conclusion	4
Recommendations for further work	4
References	5

INTRODUCTION

Culzean Castle is located in an exposed position on the Ayrshire coast. The castle and various outbuildings on the estate are built of sandstone and some parts are showing serious deterioration, with the stones spalling or crumbling.

The owners, the National Trust for Scotland, wish to preserve or repair the structure and therefore seek to understand the cause(s) for the deterioration. The patchy nature of the deterioration offers an opportunity to study variation in the influence of potential agents of damage.

Damage is in some places associated with lichen growth, and it is possible that these, through the production of organic acids, may damage the stonework (Bech-Andersen, 1987). Other microorganisms may also be present which can produce mineral acids such as sulphuric or nitric acid from nutrients present in airborne pollution. Algae growing on the stonework can cause discolouration but more importantly may produce the organic carbon necessary to support the growth of bacteria and fungi producing the damaging acids (Lyalikova and Petushkova, 1991; Sand and Bock, 1991).

It is presumed that the action of organic or mineral acids would be to destroy the cementation between the sand grains, reducing the mechanical strength of the stone and ultimately causing it to crumble. In such a state it will be more susceptible to physical agents such as wind erosion and freeze-thawing.

Differences in the degree of stone damage on different parts of Culzean Castle may be due to differences in the nature of the stone, its exposure to weather, differences in the chemical nature of precipitation (e.g. content of sea-spray), degree and type of microbial contamination, extent of lichen growth, and length of exposure period.

A preliminary survey was carried out to ascertain the degree of microbial contamination at different sites on the stonework of Culzean Castle and its immediate environs.

MATERIALS AND METHODS

The structure of Culzean castle was built in three distinct phases. The oldest part was built during the 16th or 17th century, while the most recent dates from the Victorian period, completed in 1870, and has relatively little stonework damage.

The intermediate period was completed in about 1780 and contains stonework which is in places deeply eroded or spalling. In order to eliminate the variable of exposure time, all samples were taken from the intermediate building period, which also provides the greatest variety of locations with damaged stonework.

Samples were taken from deteriorated and native stonework (Fig. 1) by scraping the surface with a sterile scalpel and collecting the scrapings into a sterile tube. Samples were also taken of any loose surface layer, including lichen material for identification, and from beneath this layer (i.e. on the newly exposed surfaces) (Table 1). These samples were used to inoculate growth media for sulphur-oxidising and nitrifying bacteria, total heterotrophic bacteria, fungi and algae. The methodology used for detecting these groups of microorganisms is shown in Table 2.

RESULTS

All samples produced algae in culture, however this is not surprising considering the ubiquity of organisms such as *Chlorella* and *Desmococcus*. The ability of the algae found in the culture to grow on native stonework, utilising only nutrients present in rainfall and run-off, would need to be demonstrated in tests before it could be assumed that sufficient fixed carbon was available to heterotrophs.

There is no evidence for the presence of sulphur-oxidising bacteria in these samples, and only samples from Site 1 contained nitrifying bacteria capable of producing nitric acid. It therefore appears unlikely that mineral acids of microbial origin are important in the stonework degradation.

The total counts of heterotrophic bacteria and fungi are within the range generally reported for soil (Palmer *et al.*, 1991) but higher than those found in degraded sandstone in Germany (Palmer *et al.*, 1991). It appears from this study that total bacterial counts are not related to damage. Site 8 sample was scraped from a completely undamaged portion of stone yet contained a higher microbial population than samples 2, 3 and 9 which were from crumbling stone. Damage may not be a function of the number of organisms and heterotrophic activity is probably unimportant in the degradation process in these samples at least over short time periods.

The relationship between damage and lichen growth is also equivocal. Samples 4, 5 and 6 are all from damaged portions of the same stone, 4 and 5 being associated with lichen growth, while 6 is from a face devoid of lichen growth.

DISCUSSION

It has been assumed that degradation of sandstone may result from the action of acids dissolving the cementing matrix between sand grains. Mineral acids could result from air pollution or from microbial activity or both. Strong mineral acidity would certainly dissolve carbonates; even carbonic acid would achieve this in time. However, another action of sulphuric and nitric acid on stone is to convert carbonates into insoluble sulphates with a net increase in volume, causing splitting and spalling (Lyalikova and Petushkova, 1991).

Organic acids produced by microbes or lichens could also cause deterioration of the matrix, by chelating and rendering soluble polyvalent cations such as Aluminium and Iron. Lichens are known to produce such acids and cause damage to stonework (Bech-Andersen, 1987). However, in this study little evidence has been found of organisms producing mineral acids, nor any relationship between lichen growth and degradation of stone. The involvement of mineral acids resulting from air pollution cannot be ruled out at this stage, but Culzean is not in a notably polluted location. Long-term monitoring of the chemistry of rainfall and run-off from the walls may be necessary in order to determine this.

It has been shown that acidification by organic acids is not necessary for the dissolution of the cementing matrix by chelation (Palmer *et al.*, 1991), and indeed dissolution may be more rapid under neutral or alkaline conditions.

In the sandstone studied by Palmer *et al.* (1991)) the cementation was mainly silicate, which is practically insoluble at neutral or acidic pH but becomes soluble above pH 9. Consideration should therefore also be given to physical, chemical or biological processes which can cause a rise in pH. Elevated pH values occur in eutrophic water as a result of photosynthetic activity, and may occur on a micro-scale within lichen associations.

CONCLUSIONS

The involvement of biological activity in the deterioration of the stonework of Culzean Castle has not yet been demonstrated. The involvement of mineral acidity from aerial contamination cannot be ruled out, but organic acid chelation is a more likely cause of deterioration, and need not be linked to acidification.

If this is the case then differences between different locations in the degree of damage must also be related to qualities inherent in the stone, such as porosity, grain size, nature of cementation and permeability, as well as exposure.

RECOMMENDATIONS FOR FURTHER WORK

Further work should be carried out along the following lines:

1. determine whether physical/chemical differences exist between types of stone showing greater and lesser degrees of damage;
2. determine whether chemical differences (e.g. precipitation of sulphates, oxalates, etc.) have been produced in damaged stone;

3. attempt to weaken stone artificially by treatment with dilute mineral and organic acid solutions, to determine the susceptibility of different stones to such acid attack;
4. isolate and characterise the heterotrophic organisms found on the stones;
5. culture the isolates under realistic conditions, e.g. on pulverised sandstone, to determine which are capable of growth rather than merely being present as contaminants. This may require an analysis of rainfall and run-off to determine the content and concentration of the medium to be used;
6. inoculate isolates onto stones under environmentally realistic conditions to determine which can cause deterioration;
7. investigate physical conditions or biocide treatments which can inhibit the growth of organisms, or prevent damage being caused.

REFERENCES

- Allen, M.M. (1973). Methods for Cyanophyceae. Chapter 11 in Handbook of Phycological Methods: Culture methods and growth measurements. Ed. J.R. Stein. C.U.P.
- Bech-Andersen, J. (1987). Oxalic acid production by lichens causing deterioration of natural and artificial stones. The biodeterioration of construction materials. Biodeterioration Society Occasional Publication No. 3. pp 9-13. Ed. L.H.G. Morton.
- Francis, A.J., Dodge, C.J., Rose, A.W. and Ramirez, A.J. (1989). Aerobic and anaerobic microbial dissolution of toxic metals from coal wastes. Mechanism of action. Environmental Science and Technology 23 (4), 435-441.

- Gode, P. and Overbeck, J. (1972). Untersuchungen zur Heterotrophen Nitrifikation im See. *Z. Allg. Mikrobiol.* 12, 567-574.
- Kinross, J.H. (1991). The effects of acidification on epilithic algae in the Loch Ard catchment. PhD Thesis, Napier University, Edinburgh.
- Lyalikova, N.N. and Petushkova, Y.P. (1991). Role of Microorganisms in the Weathering of Minerals in Building Stone of Historic Buildings. *Geomicrobiology Journal* 9, 91-101.
- Palmer, R.J. Jr., Siebert, J. and Hirsch, P. (1991). Biomass and organic acids in sandstone of a weathering building: production by bacterial and fungal isolates. *Microb. Ecol.* 21, 253-266.
- Sand, W. and Bock, E. (1991). Biodeterioration of Mineral Materials by Microorganisms - Biogenic Sulfuric and Nitric Acid Corrosion of Concrete and Natural Stone. *Geomicrobiology Journal* 9, 129-138.

Table 1. Details of Culzean Castle stonework samples

Site no.	Location	Aspect	Observations
1	Balcony	North facing	Spalling green sandstone; sub-surface sample
2	Balcony	North facing	Same stone as 1; surface sample
3	Balcony	South-West facing	Crumbling pink sandstone; surface sample
4	Castle gateway	Arch face of gateway, South facing	Loosened flake of stone associated with lichen <i>Ochrolechia parella</i>
5	Castle gateway	Arch face of gateway, South facing	Loosened flake of stone associated with lichen <i>Pertusaria lactea</i>
6	Castle gateway	Outer face of gateway, South-east facing	Stone flake from same stone as samples 4 and 5, but not associated with lichen growth
7	Eastern garden gateway	Interior of gate building, South facing	Crumbling stone
8	Eastern garden gateway	Exterior of gate building, South-West facing	Same stone as 7; non-crumbling face
9	Pre-Victorian back of Castle, near rear door	West facing	Crumbling yellow-red stone

Table 2: Methods used in Microbiological Investigations of Culzean Castle stonework

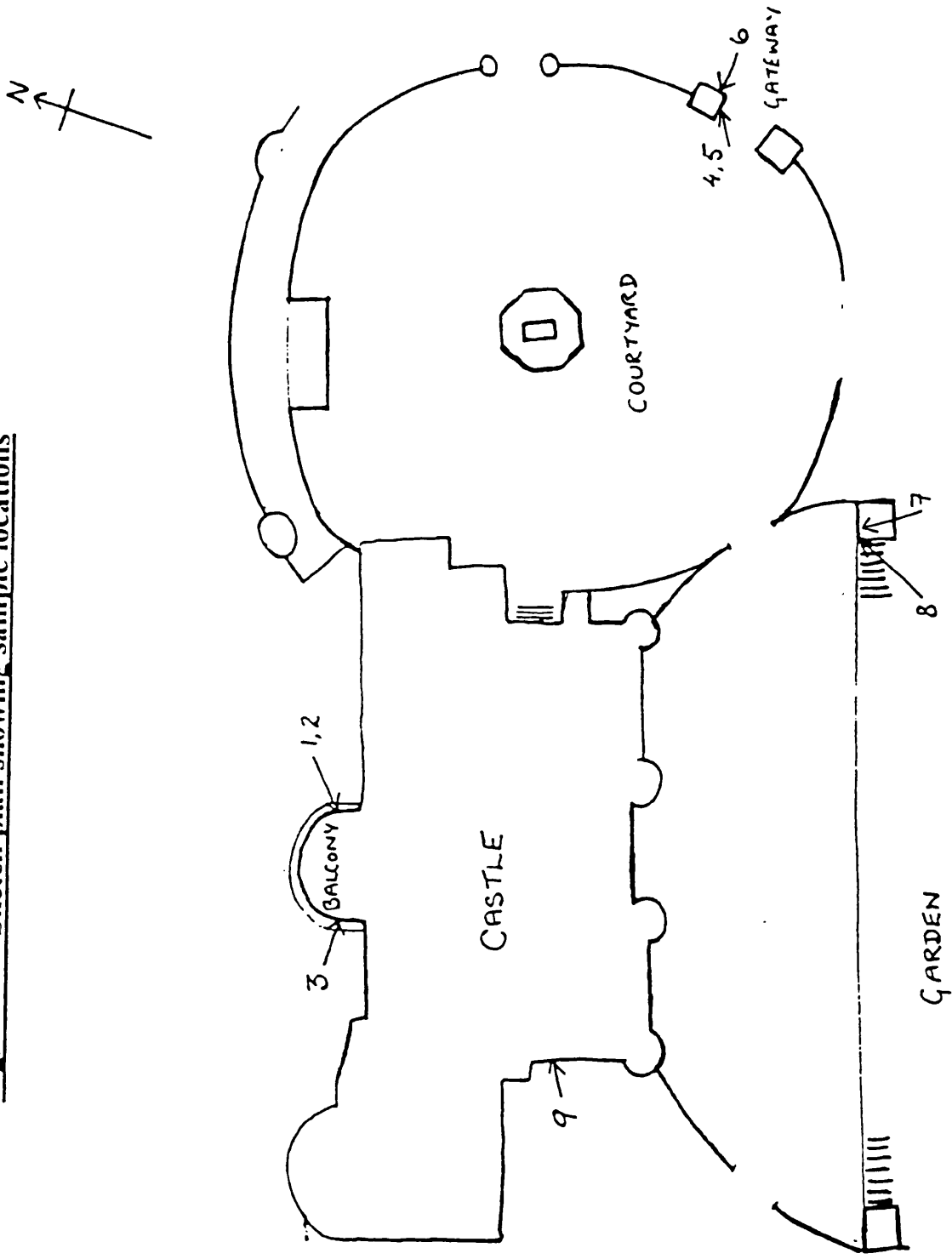
Type of Organism	Medium	Incubation time	Temperature	Light	Inoculum size
Total heterotrophs	Oxoid Plate Count Agar	7 days	20°C	dark	0.1 ml of 10 ⁻¹ to 10 ⁻⁴ dilutions
Sulphur oxidising bacteria	SOX medium, (Francis <i>et al.</i> , 1989)	100 days	20°C	dark	0.1 ml of 10 ⁻¹ dilution
Nitrifying bacteria	NH ₄ OX medium, (Gode and Overbeck, 1972)	100 days	20°C	dark	0.1 ml of 10 ⁻¹ dilution
Algae	Mineral Medium #11, (Allen, 1973)	21 days	20°C	30µEm ⁻² s ⁻¹	0.1 ml of 10 ⁻¹ dilution
Algae (& moss)	Corrie (Kinross, 1991)	>100days	20°C	30µEm ⁻² s ⁻¹	0.1 ml of 10 ⁻¹ dilution

Table 3: Results of microbiological investigations of Culzean Castle Stonework.

Sample	Total Heterotrophic count (cfu.g ⁻¹ material)	S-oxidisers	Nitrifiers	Algae
	Fungi Bacteria			
1	4,000 27,500	negative	positive	<i>Chlorella, Rhizoclonium*</i>
2	2,150 1,400	negative	negative	<i>Chlorella, Desmococcus, Rhizoclonium*</i>
3	200 175	negative	negative	<i>Chlorella, Rhizoclonium*</i>
4	68,000 160,000	negative	negative	<i>Geminella, Desmococcus, Oscillatoria.</i>
5	1,828 139,800	negative	negative	<i>Desmococcus</i>
6	12,100 46,600	negative	negative	<i>Chlorella, Desmococcus, Chlorococcum.</i>
7	4,000 595,000	negative	negative	<i>Chlorella, Geminella.</i>
8	25,000 15,000	negative	negative	<i>Chlorella, Chlorococcum, Hormidium.</i>
9	4,400 1,400	negative	negative	<i>Chlorella, Rhizoclonium*</i>

* Extended incubation may reveal this to be a moss.

Fig. 1 Sketch plan showing sample locations



Plates

Back Pocket

The back pocket contains a series of photographs taken both in the field and the laboratory that are referred to in the text.

They also provide a graphical bibliography of the investigation as required for all research projects funded by the Getty Grant Programme.



Plates

A series of photographs taken both in the field and the laboratory to substantiate details described in the text



Plate 1 Landward face of Culzean Castle. Stone replaced in 1970's



Plate 2 Seaward face of the castle

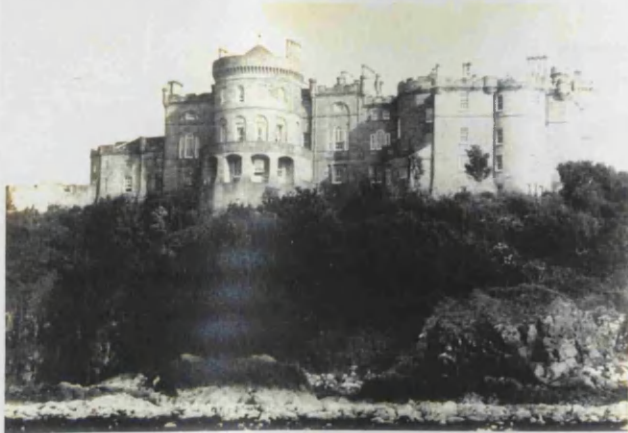


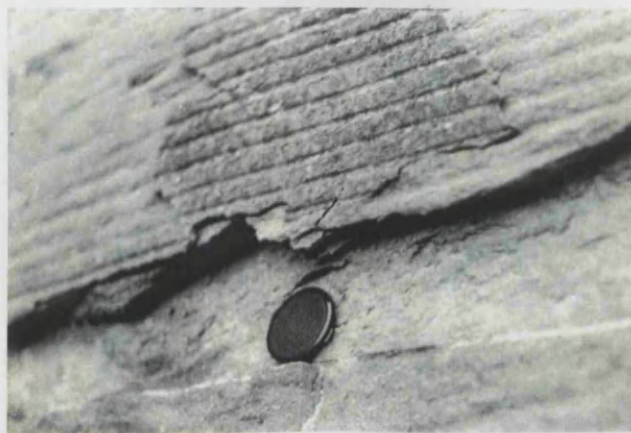
Plate 3 Surface spalling



Plate 4 Contour scaling on the balcony



Plate 5 Surface spalling and contour scaling on balcony



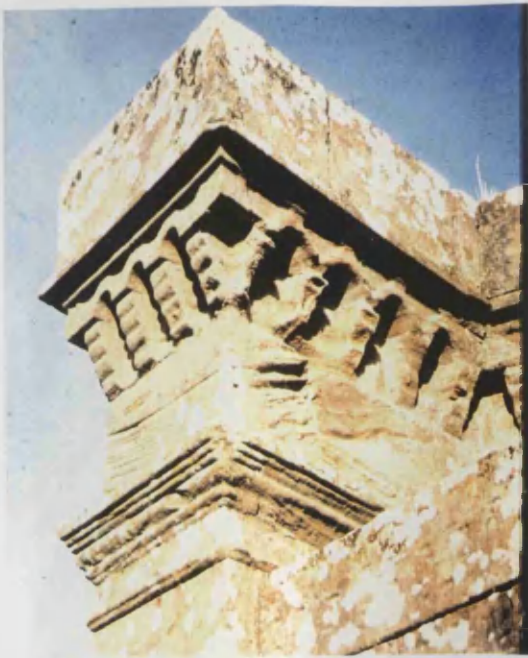


Plate 6 Cavernous weathering



Plate 7 Differential weathering

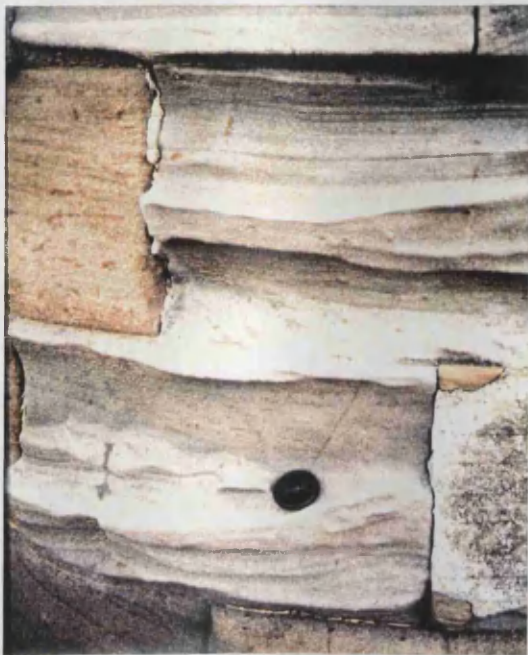


Plate 8 Weathering along planes of Weakness

Plate 9 Exfoliation surfaces exposed

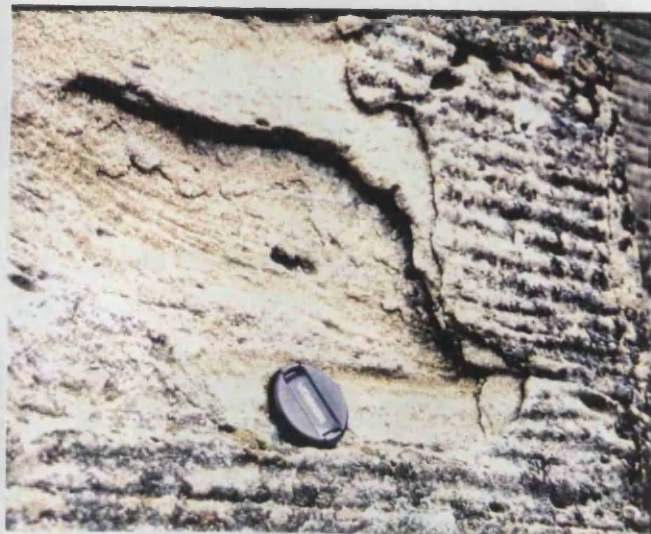


Plate 10 St Murray's Quarry

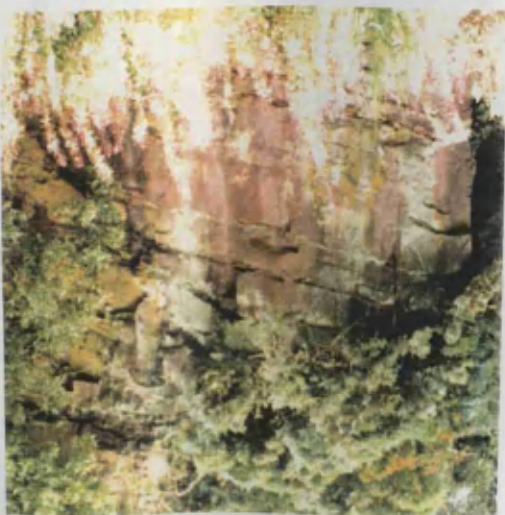


Plate 11 Home Farm Quarry



Plate 12 Coring the balcony

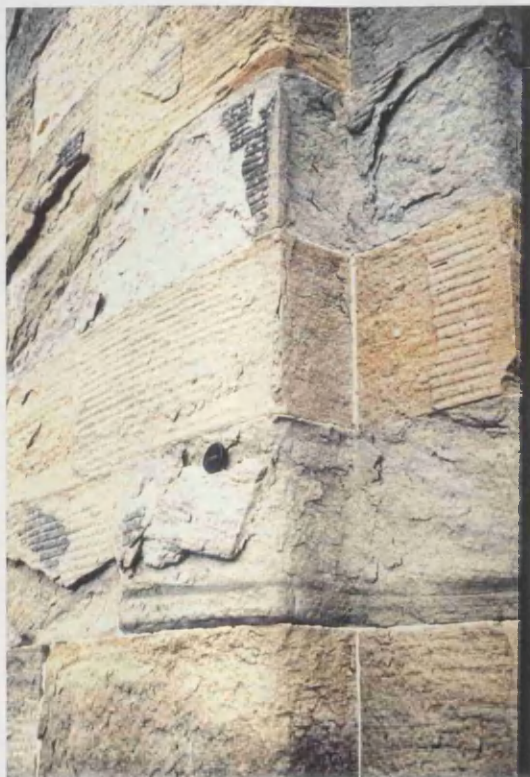


Plate 13 A second set of cores for the engineering tests

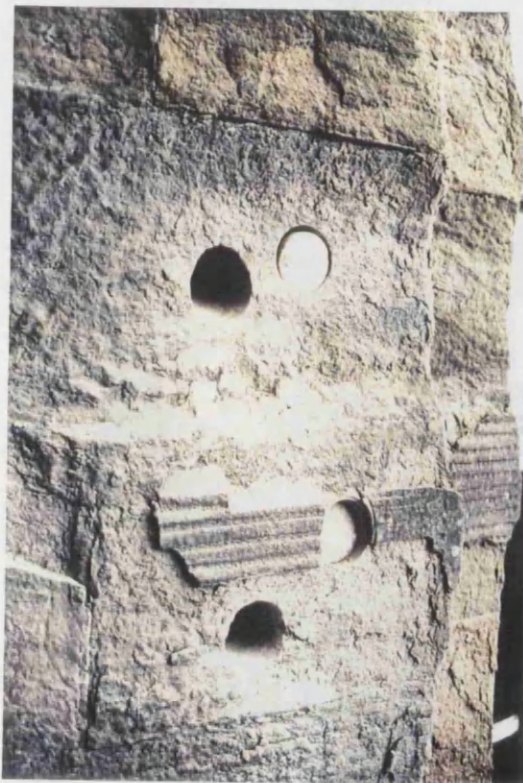


Plate 14 Core OB1

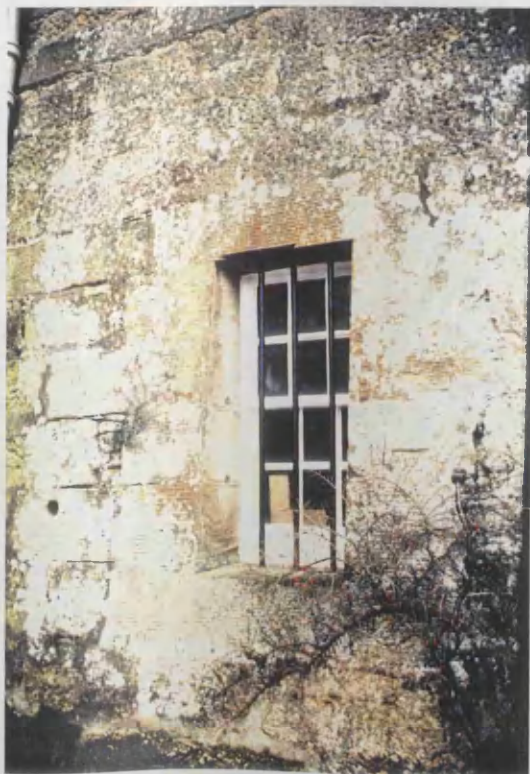


Plate 15 Core OB2

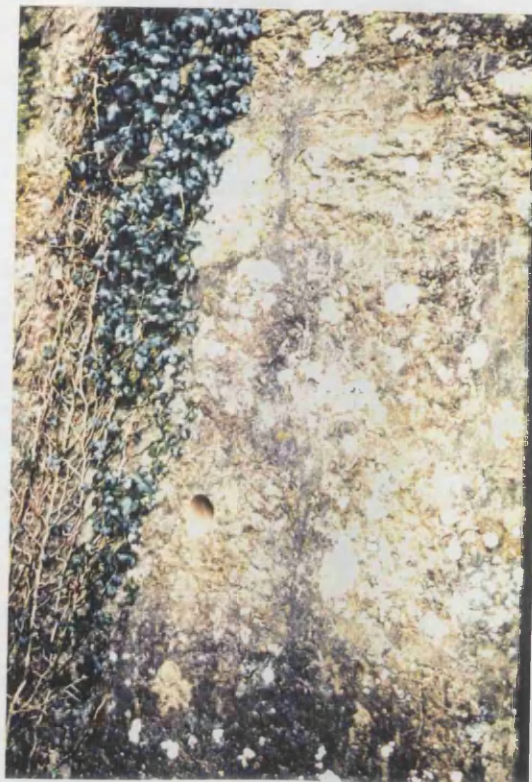


Plate 16 Victorian Building cores holes

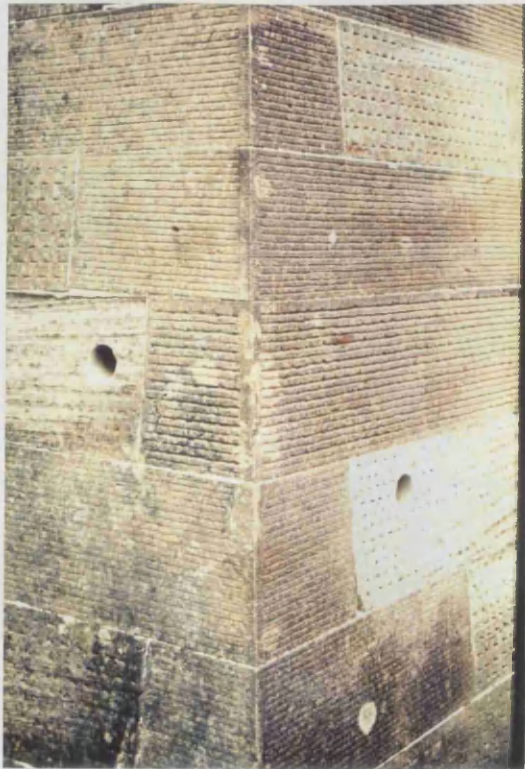


Plate 17 The three building stones
Upper RHS VB stone
Upper LHS AB stone
Lower OB stone

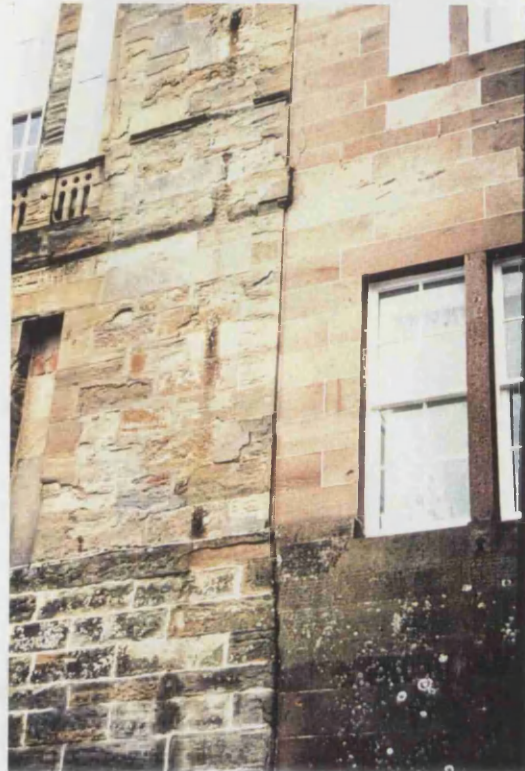


Plate 18 Lower OB stone
LHS AB stone
RHS VB stone

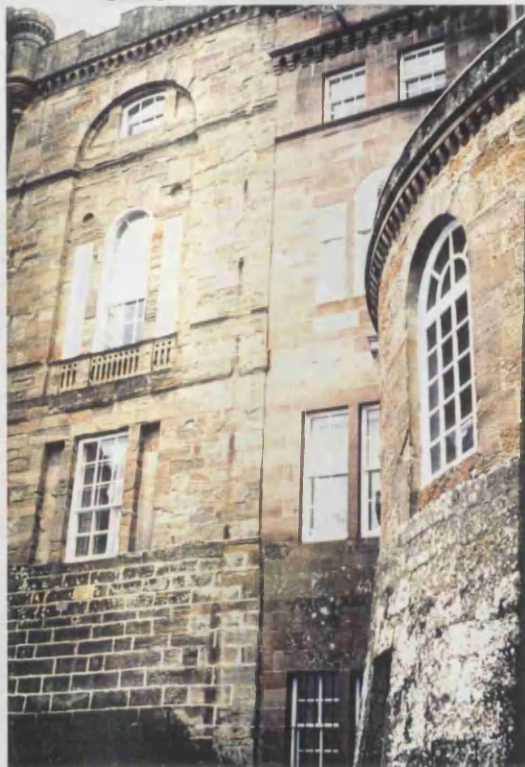


Plate 19 Replacement stone on chimney pots

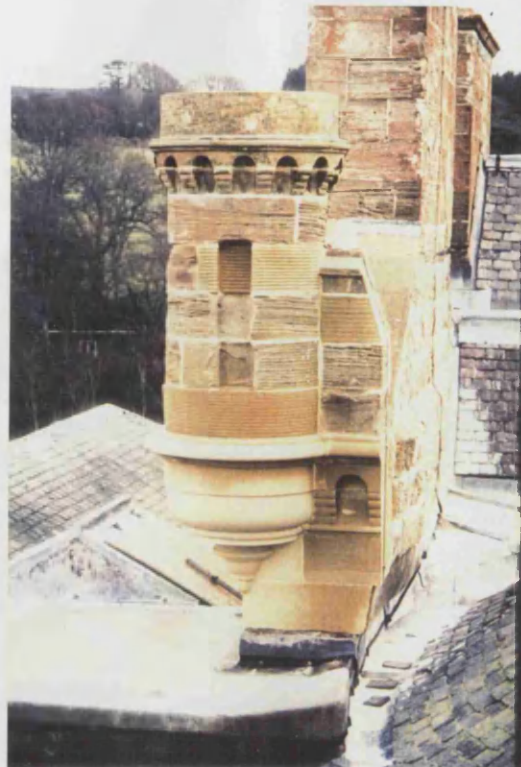


Plate 20 Surface tooling and patina



Plate 21 Exfoliation surface



Plate 22 Core quarters from Each sample site

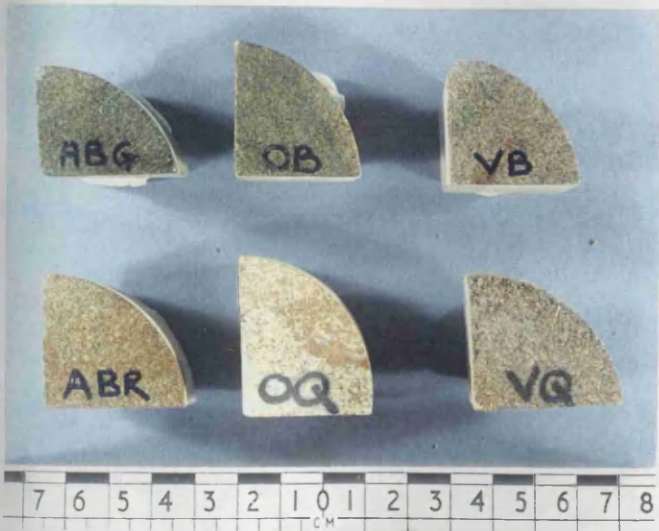


Plate 23 Cross section of surface layers



Plate 24 Hand-held dry Drilling method

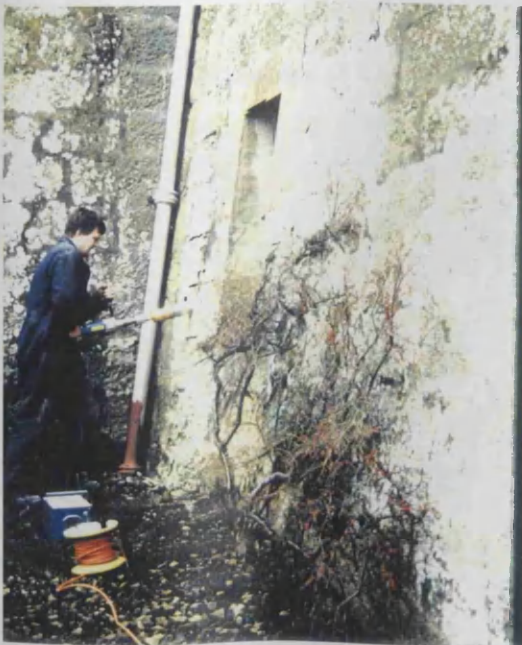


Plate 25 Preparation of plugs



Plate 26 Example of AB in PPL

Plate 27 AB in XPL

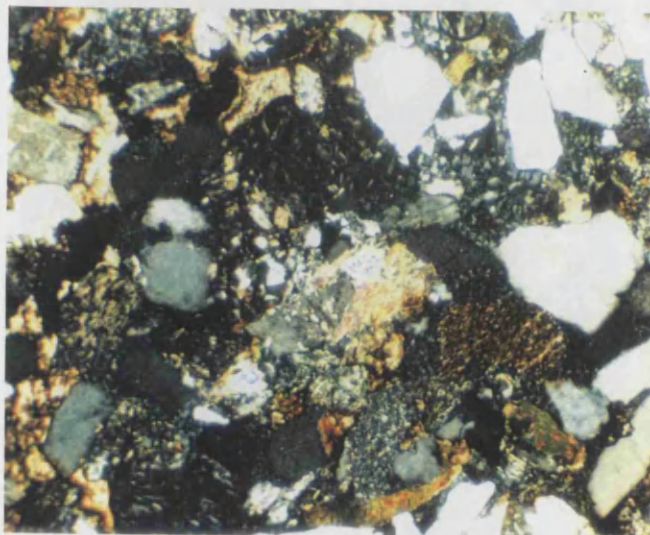
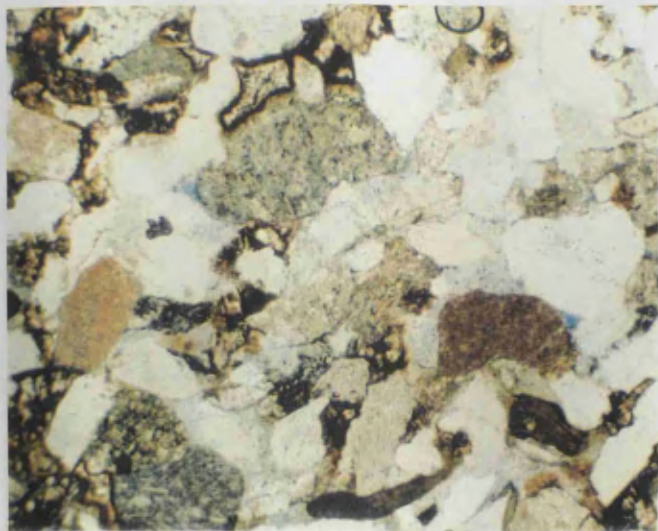


Plate 28 Example of VB in PPL

Plate 29 VB in XPL

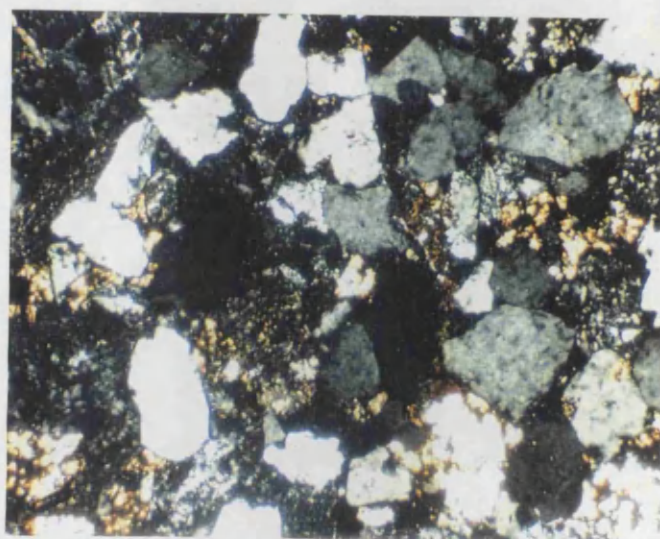
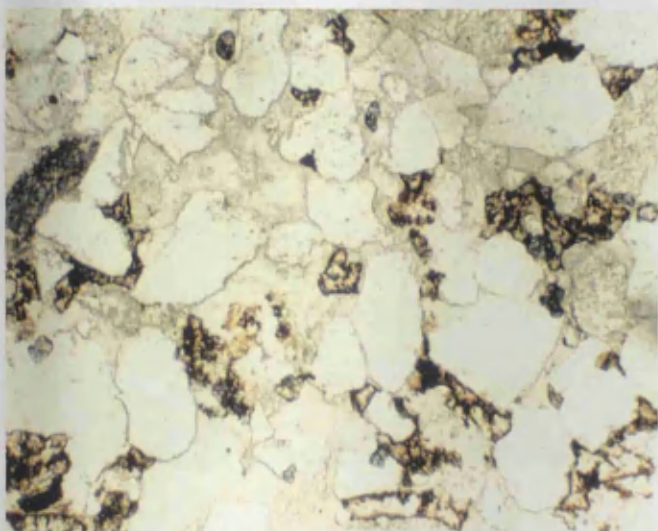


Plate 30 Exmaples of VQ in PPL

Plate 31 VQ in XPL

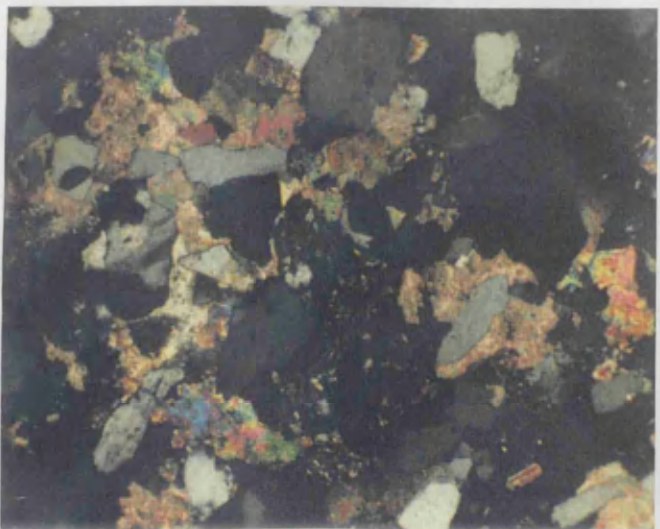
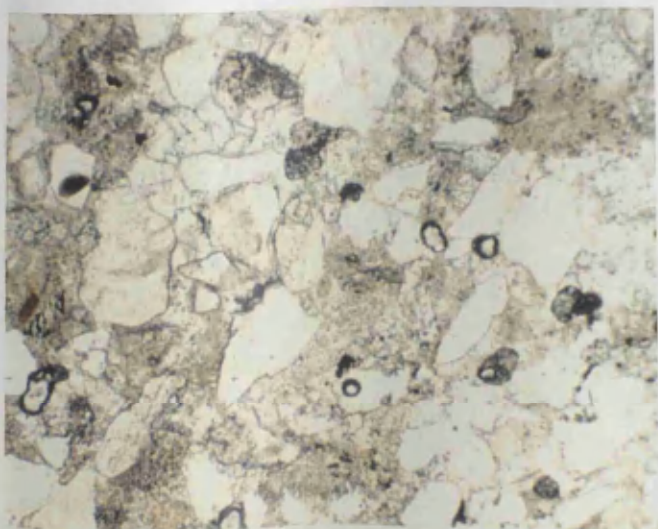


Plate 32 Example of OB in PPL

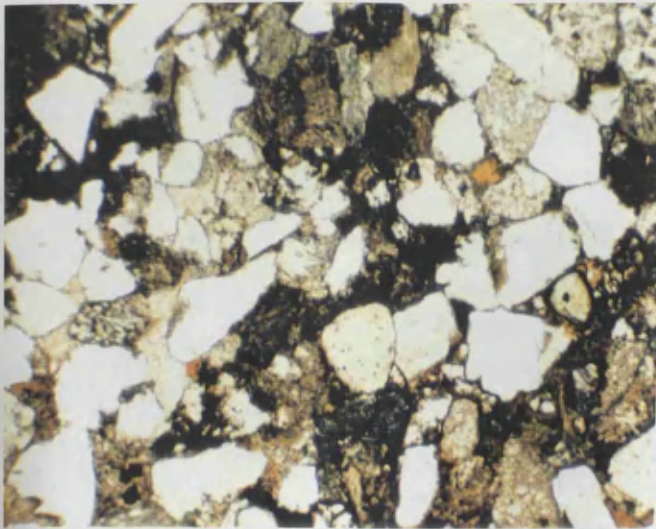


Plate 33 OB in XPL

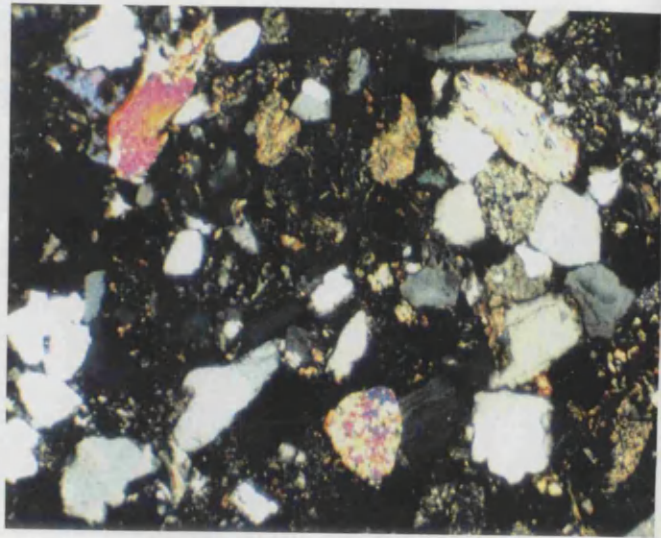


Plate 34 OQ in PPL

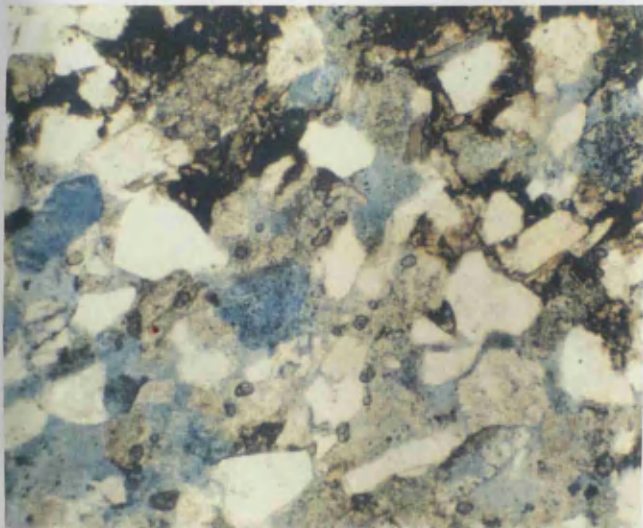


Plate 35 OQ in XPL

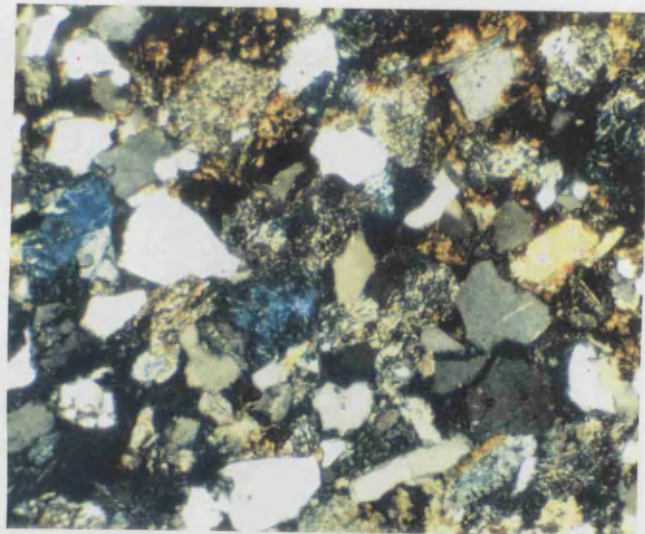


Plate 36 Mica in VB sample (PPL)

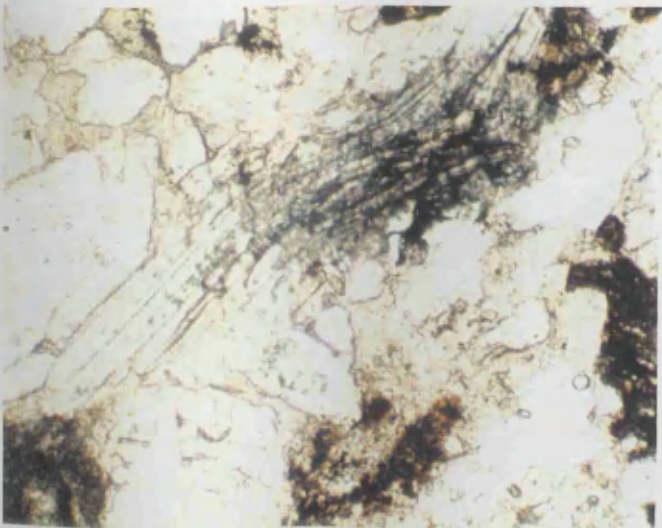
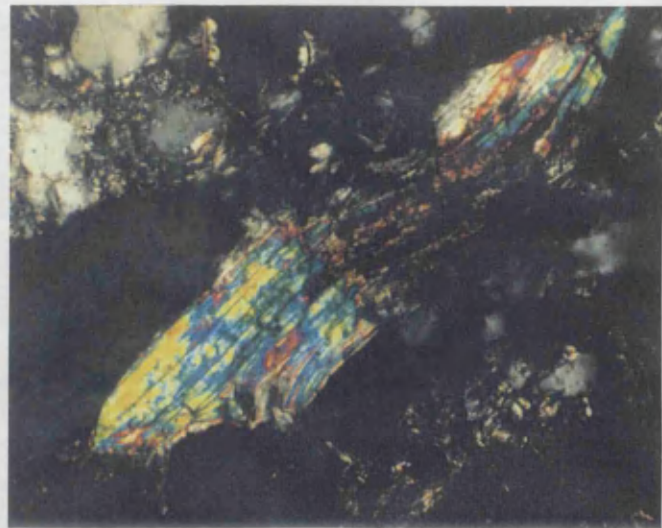
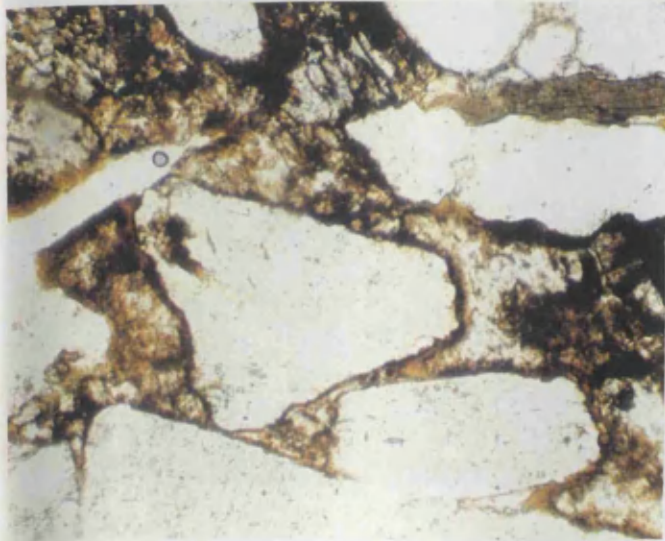
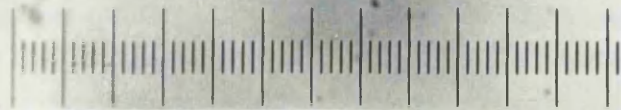


Plate 37 Mica in VB sample (XPL)





**Plate 40 Calcite replacement
AB in PPL**

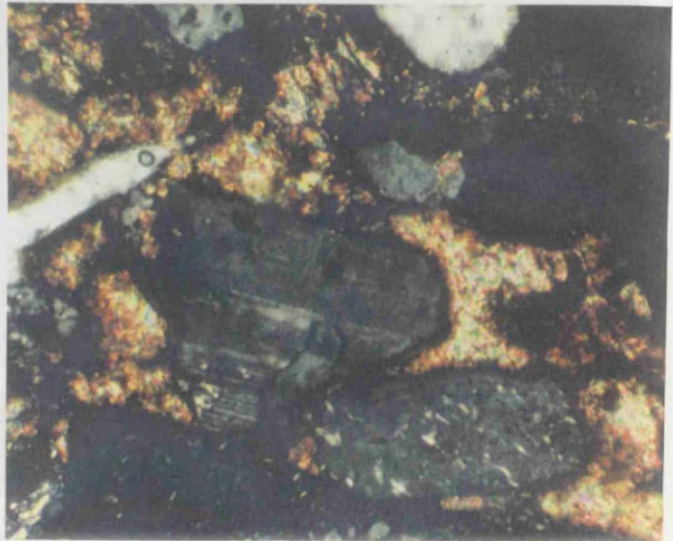


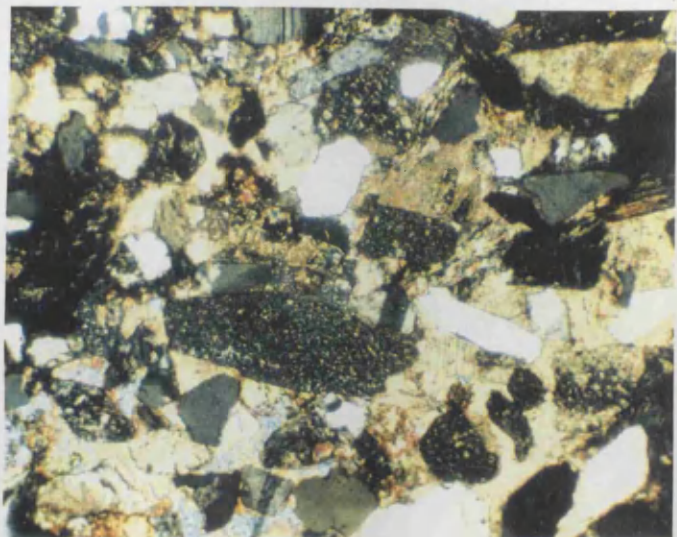
Plate 41 XPL



**Plate 42 example of diagenetic
concretion in AB (PPL)**



Plate 43 AB sample in XPL



SEM Images

Plate 44 SEM image from VQ sample

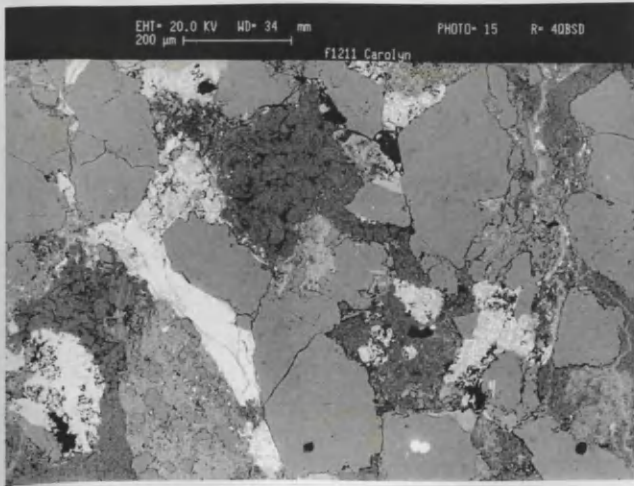


Plate 45 SEM image from VB sample

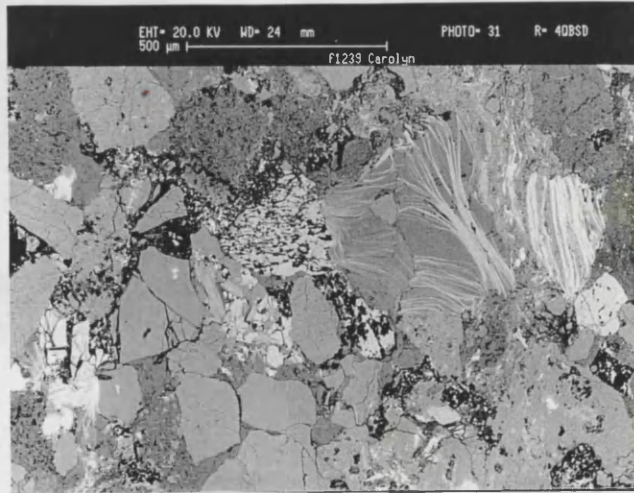


Plate 46 SEM image from OQ sample

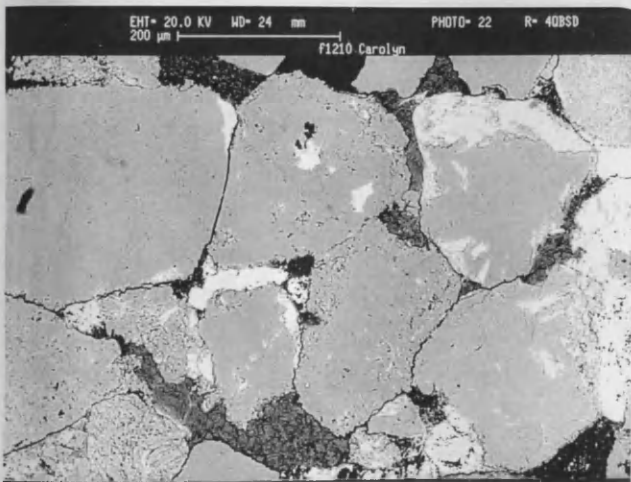


Plate 47 SEM image from OB sample

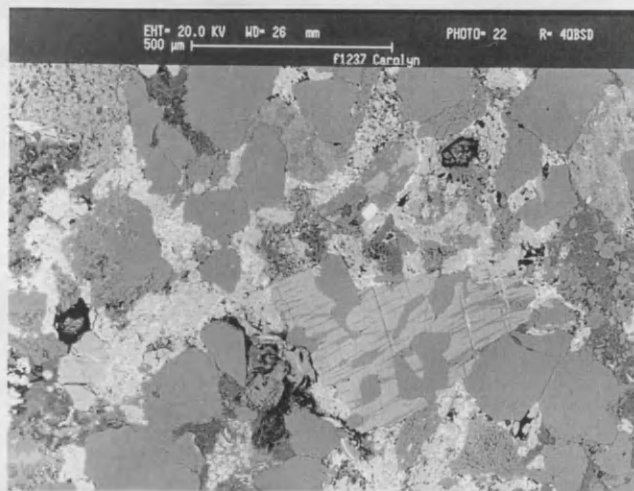


Plate 48 Clay precipitation from sedimentations

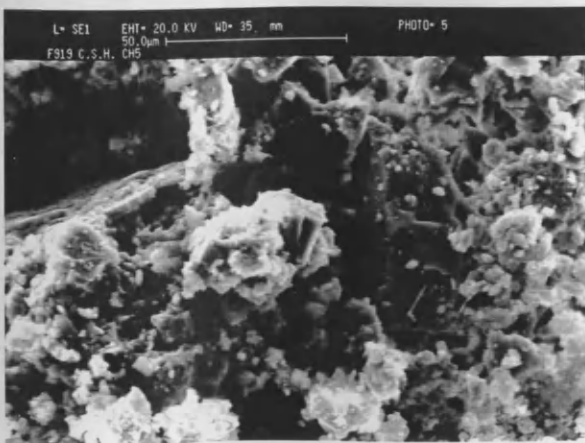


Plate 49 Clay growth on mineral surfaces of AB samples



**Plate 50 Partial calcite replacement
In feldspar**



Plate 51 Feldspar replacement

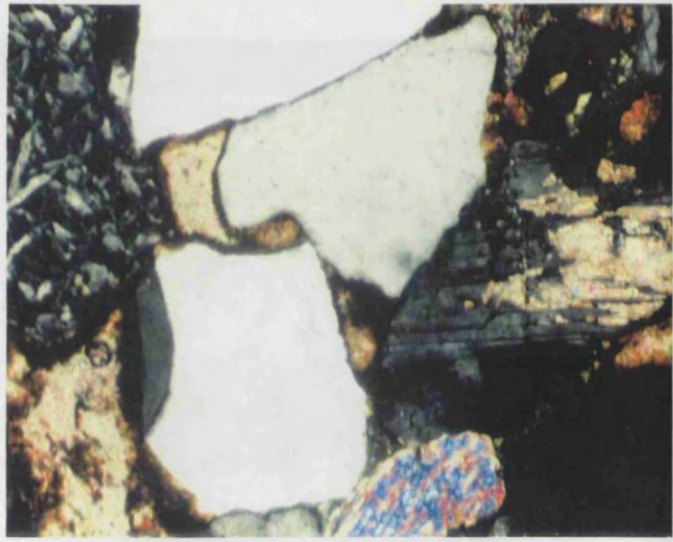
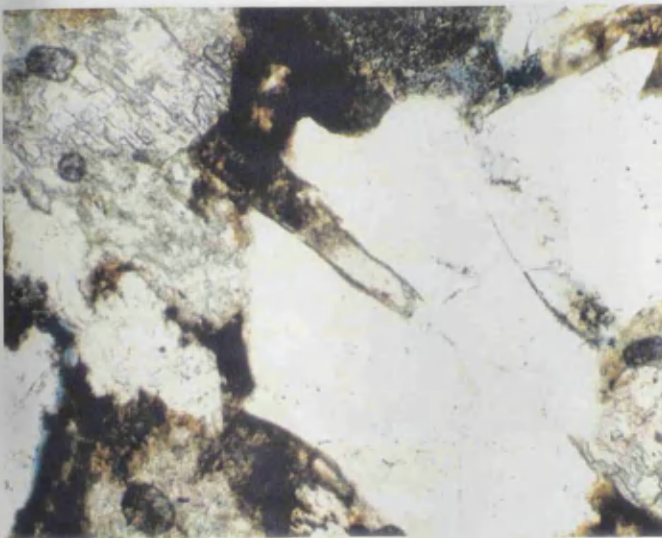


Plate 52 AB sample in PPL



**Plate 53 Calcite replacement in
Quartz (XPL)**



Plate 54 Lithic fragment in OB3



Plate 55 Lithic clast in OB2

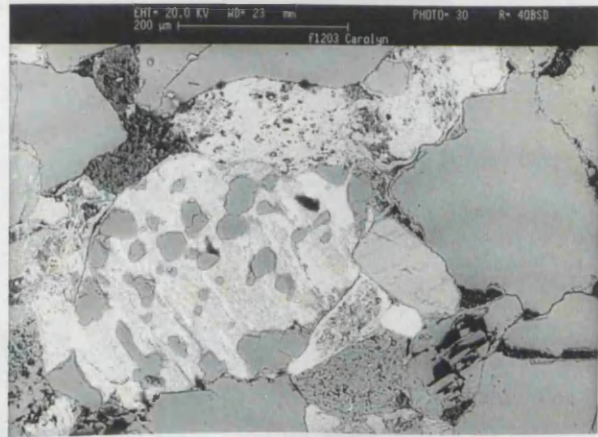


Plate 56 Dissolution along cleavages in AB

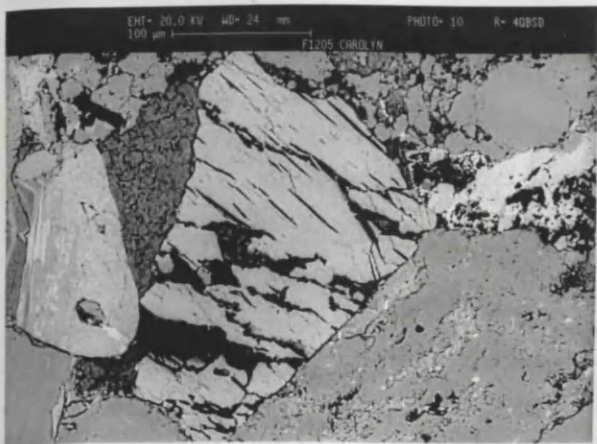


Plate 57 Near surface dissolution in VB sample



Plate 58 Surface dissolution of feldspar and cement

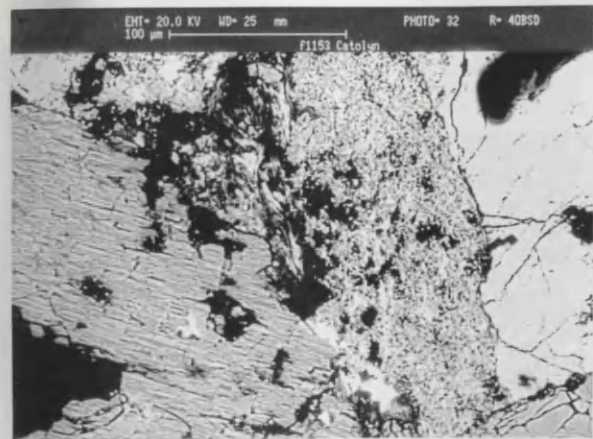


Plate 59 Feldspar dissolution and breakdown

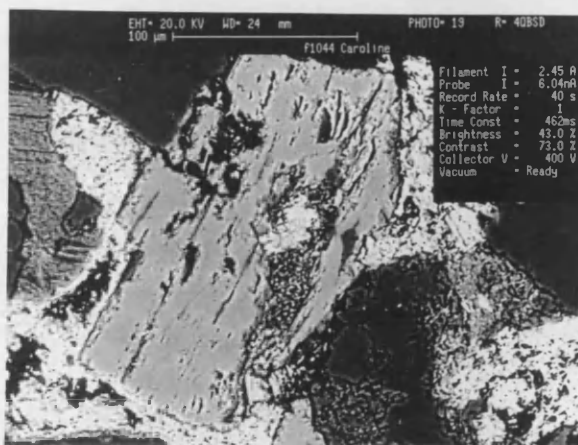


Plate 60 Partial replacement and dissolution

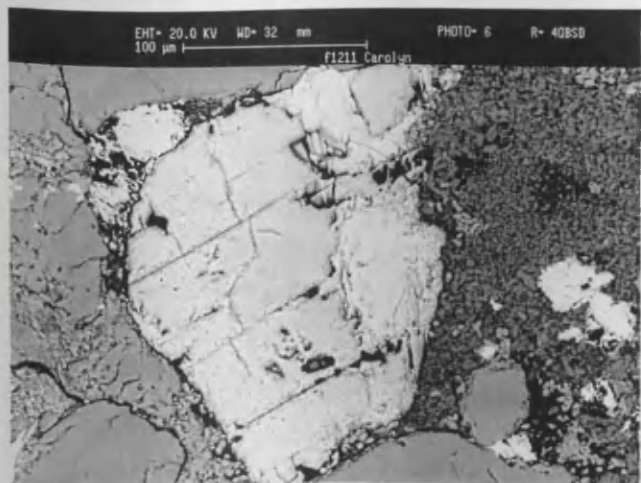
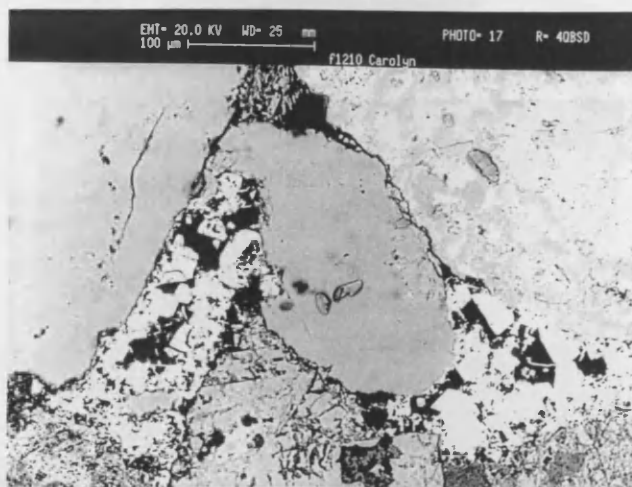
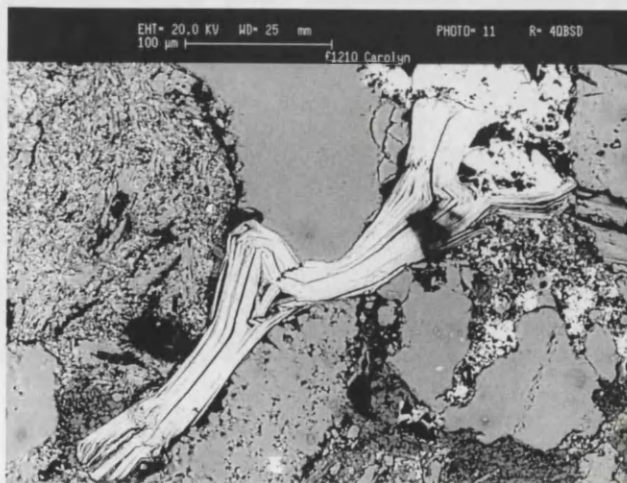
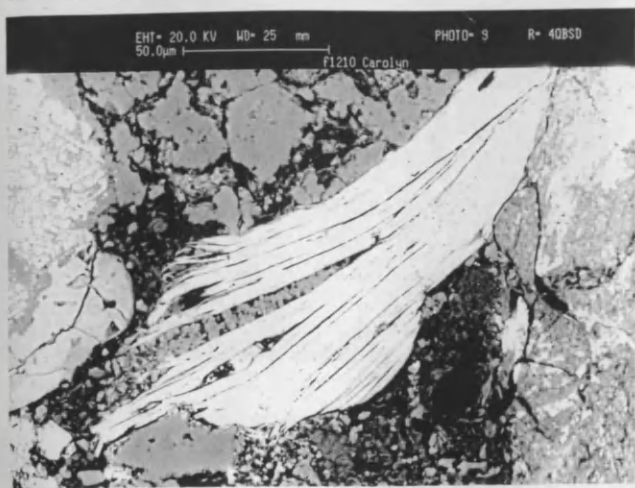


Plate 61 Surface pitting of minerals



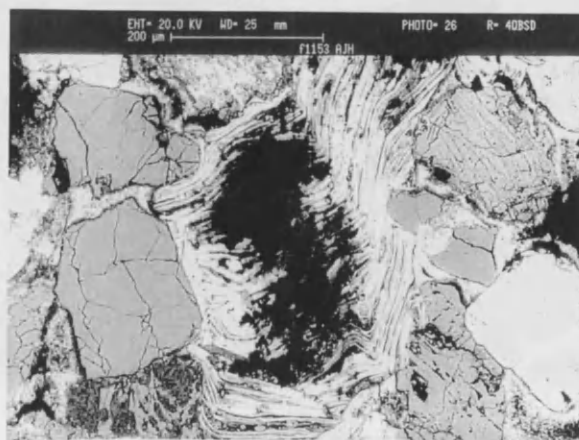
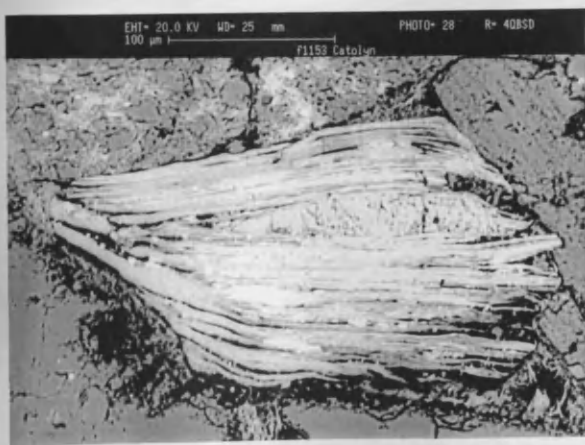
Mica expansion and weathering

Plates 62 and 63 show the importance of the role of mica in the breakdown of the stone



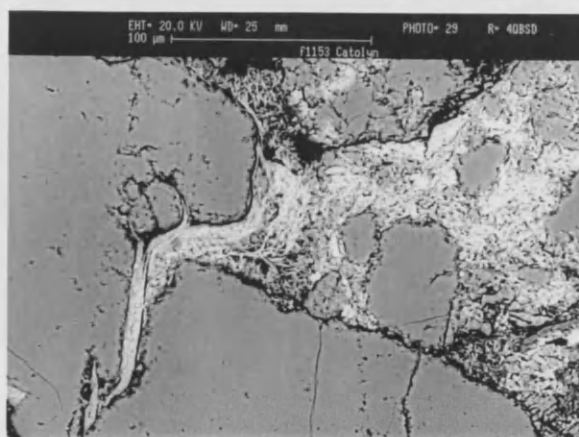
**Plate 64 Mica growth and cement
Precipitation**

Plate 65 Mica growth and clays



**Plate 66 Mica expansion
Mechanical effects**

**Plate 67 mica expansion between
mineral grains**



Calcium carbonate cement under the optical microscope

Plate 68 OQ in PPL

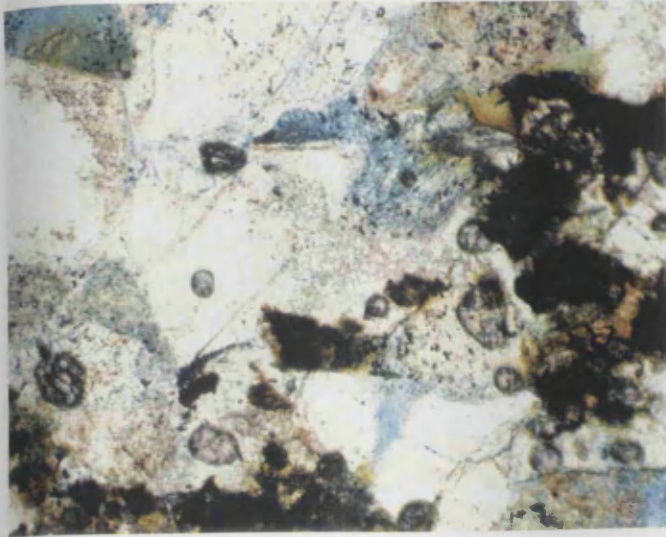


Plate 69 XPL high magnification



Plate 70 Cement pore-fill
OQ in PPL

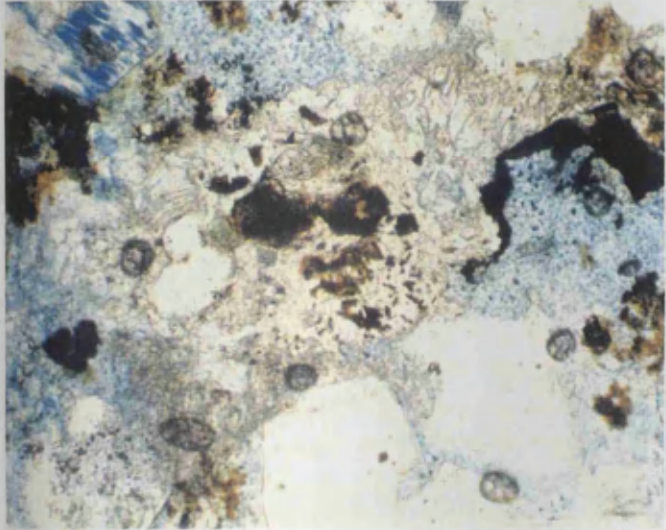


Plate 71 High interference colours
OQ in XPL

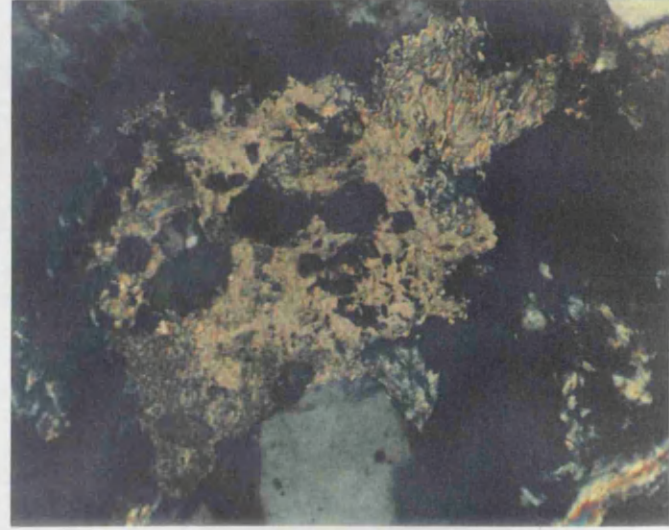


Plate 72 Recent cement precipitation
AB sample under PPL

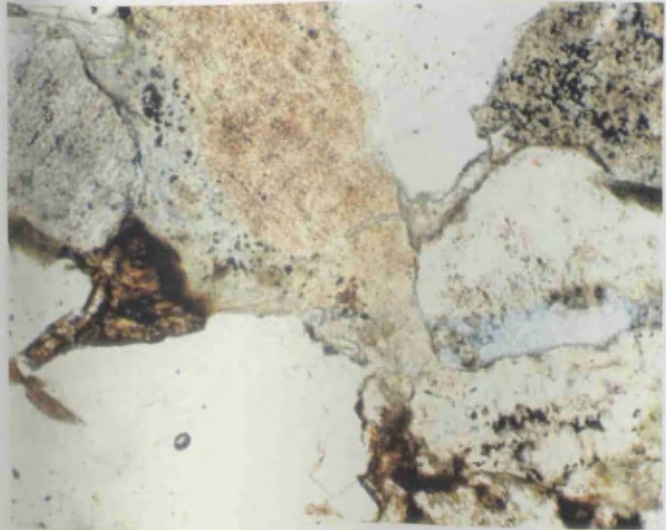
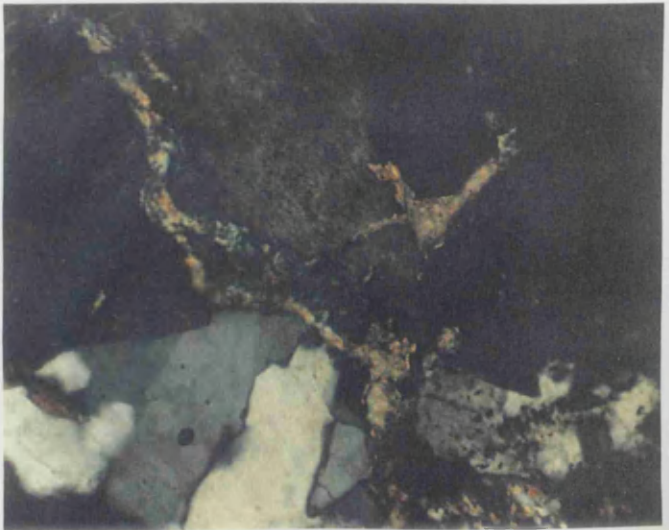


Plate 73 Growth in cracks between
mineral grains in XPL



Cathodoluminescence images of cement and carbonate mineral replacement

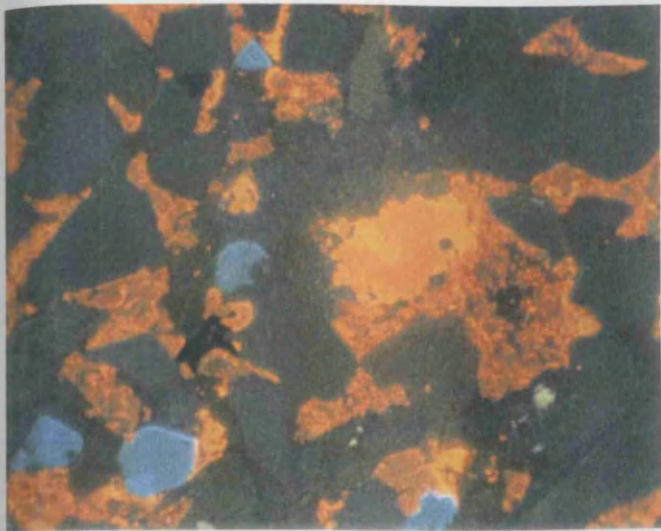


Plate 74 AB11 Bright cement areas most recent precipitation

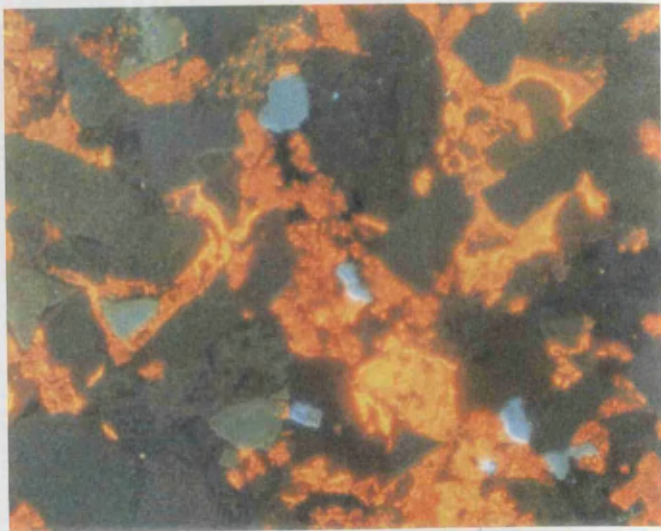


Plate 75 AB11 scale = 1.7mm diameter



**Plate 76 VB calcite rhombs
Plate 78 Calcite replacement of feldspar**



**Plate 77 A cluster of rhombs in VB
Plate 79 0.8mm diameter scale**



Cathodoluminescence images
Periods of cement precipitation represented by different brightnesses



Plate 80 Concretions in VB2

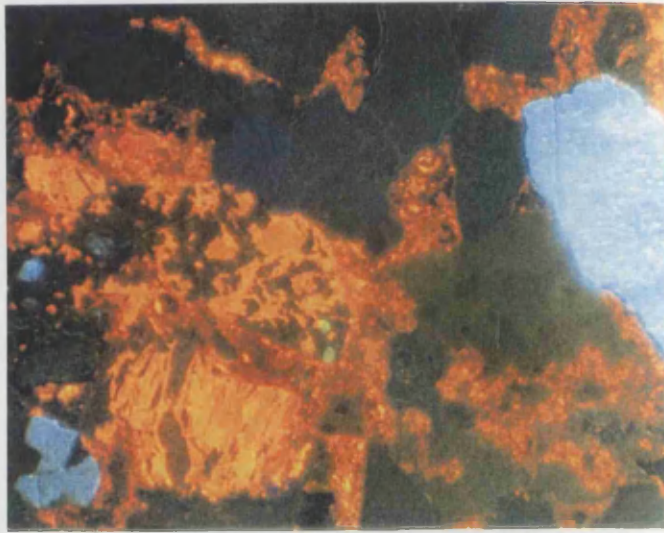


Plate 81 AB2



Plate 82 Concretion in AB2



Plate 83 At higher magnification

Plate 84 OQ sample (1.7mm diameter)



Plate 85 At 0.8mm diameter



SEM images

Plate 86 Cement dissolution



Plate 87 Silicate precipitation in Cement

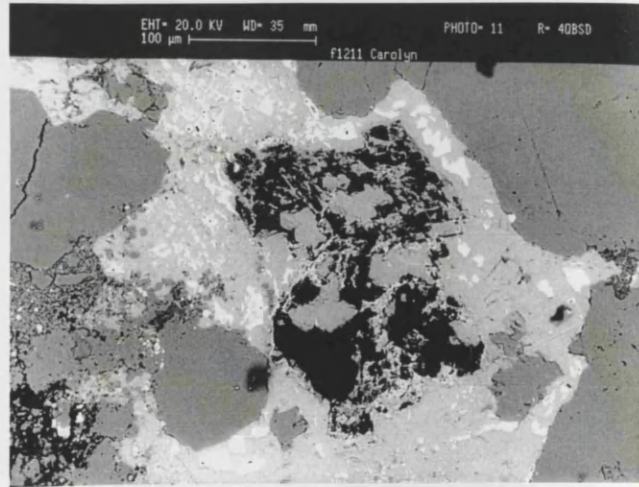


Plate 88 Cement dissolution

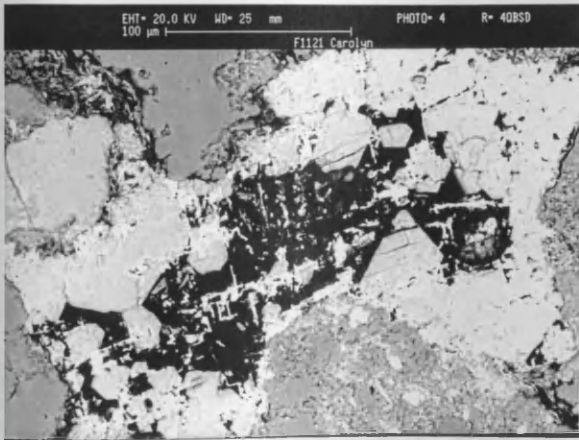


Plate 89 Cement dissolution in OB

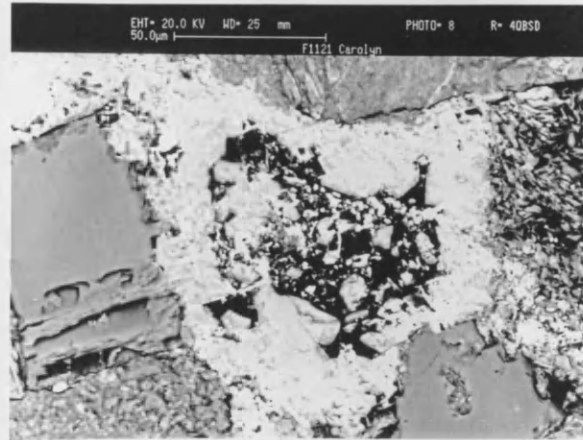


Plate 90 Cement pore infiller

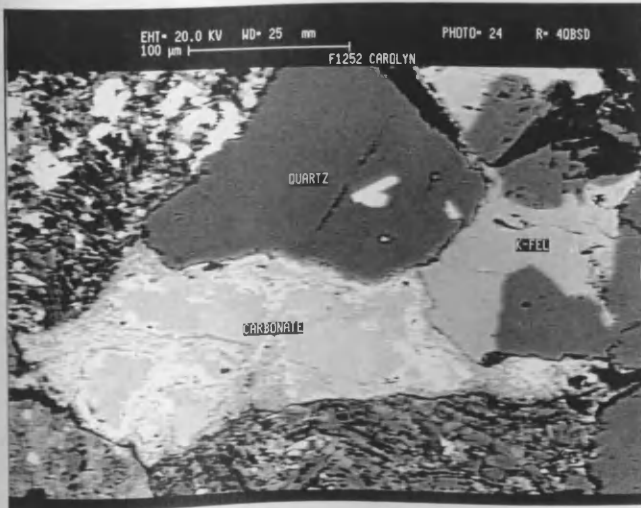
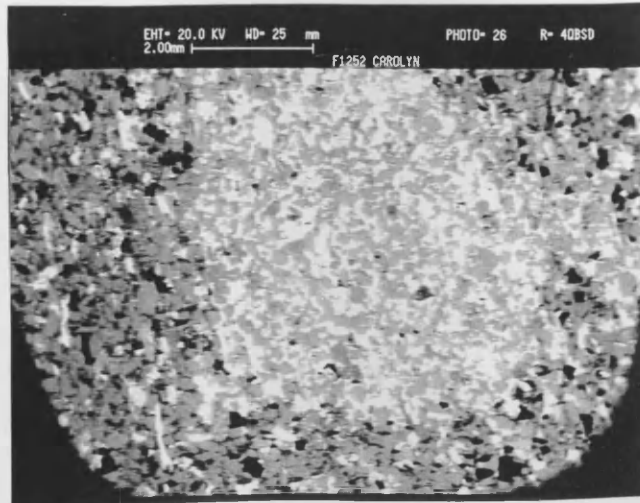


Plate 91 Diagenetic concretion



SEM images

Plate 92 Concretion

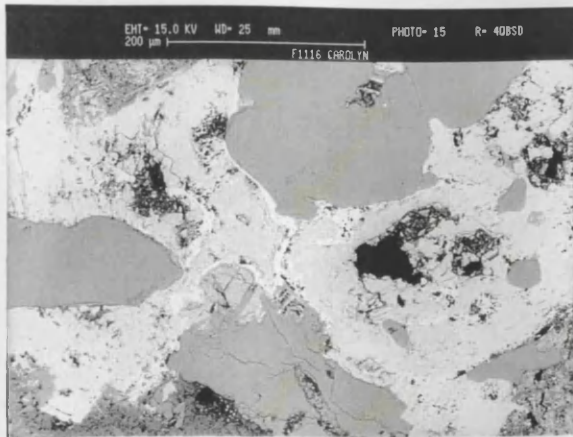


Plate 93 Cement supported AB3

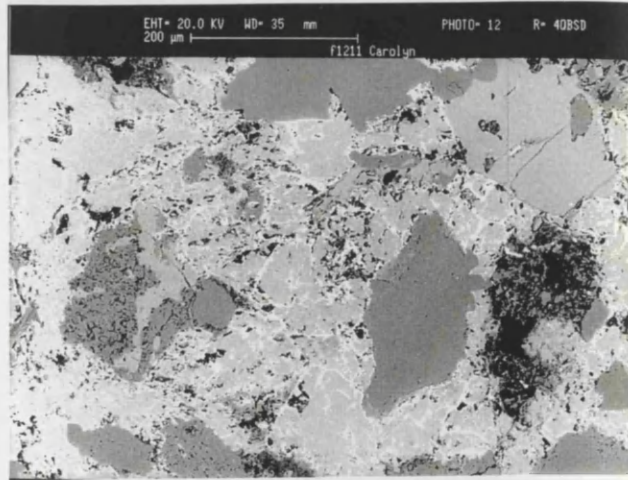


Plate 94 Diagenetic concretion in AB5

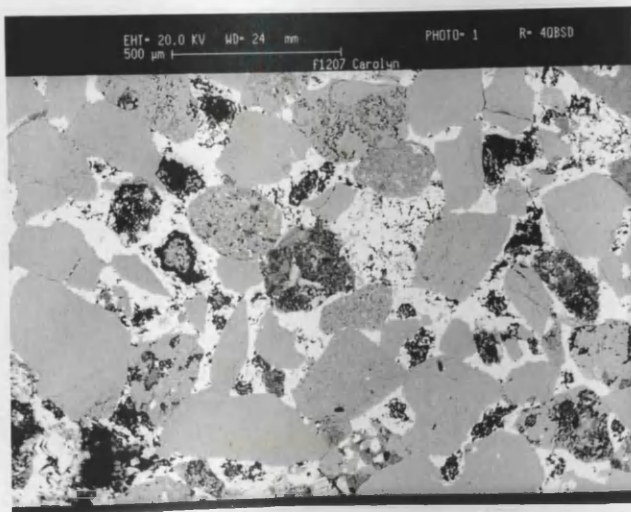


Plate 95 Concretion in VB3

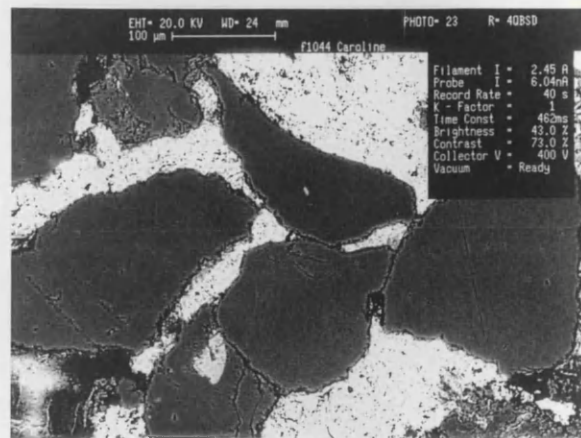


Plate 96 AB2 silicates precipitated Within cement

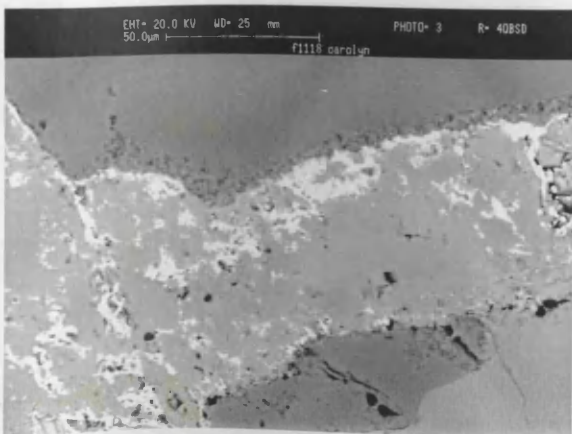
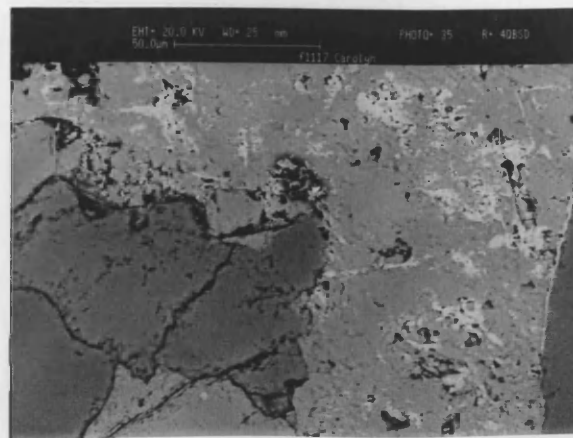


Plate 97 White area is silicate material



Analysis of carbonate cement surface pitting and dissolution at high magnification

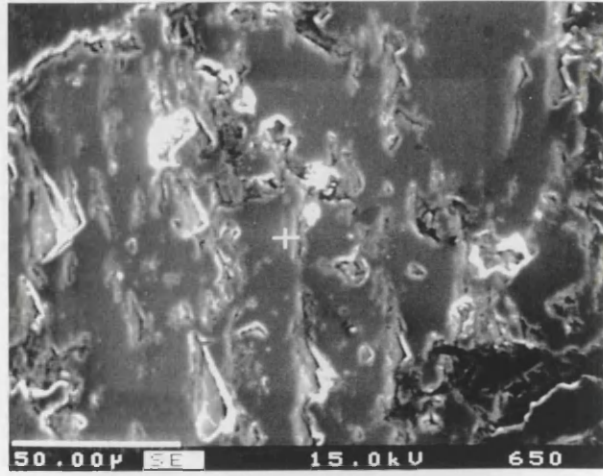
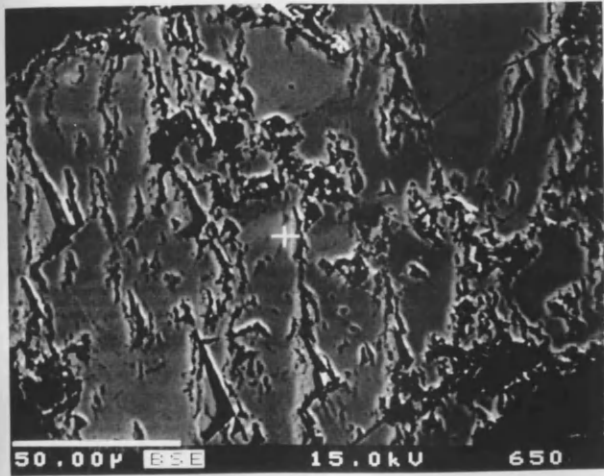
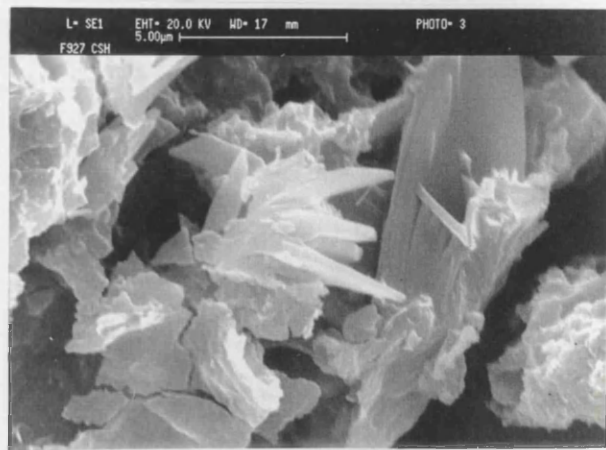
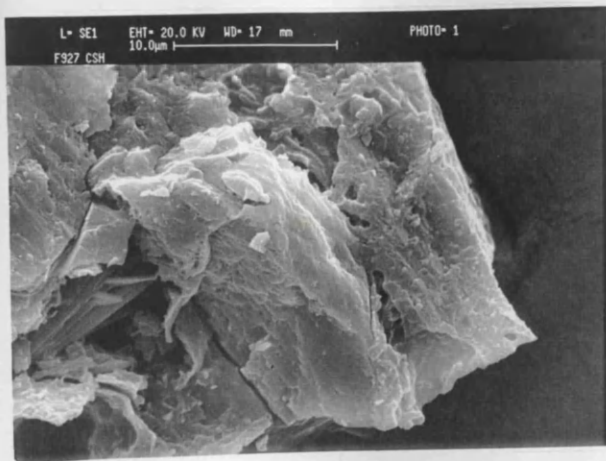


Plate 98 Back scattered image

Plate 99 Secondary image



SEM analysis of salt crystals

Plate 100 Halite crystals from AB5

Plate 101 Reprecipitated salts present in AB5